Investigation of pancreatic beta cell differentiation and function, and global profiling analysis of diabetes serum for the identification of disease biomarkers

Erica Hennessy

Ph.D. Thesis 2012

Investigation of pancreatic beta cell differentiation and function, and global profiling analysis of diabetes serum for the identification of disease biomarkers

A thesis submitted for the degree of Ph.D.

January 2012

By

Erica Hennessy B.Sc.

School of Biotechnology

Dublin City University

The research described in this thesis was performed under the supervision of

Dr. Finbarr O'Sullivan,

Prof. Martin Clynes

And

Dr. Lorraine O'Driscoll

I hereby certify that this material, which I now submit for assessment on the programme of study leading to the award of Ph.D. is entirely my own work, and that I have exercised reasonable care to ensure that the work is original, and does not to the best of my knowledge breach any law of copyright, and has not been taken from the work of others save and to the extent that such work has been cited and acknowledged within the text of my work.

Signed:_____ ID number:_____ Date: _____

Acknowledgements

First and foremost I would like to thank my supervisors, Prof. Martin Clynes, Dr. Finbarr O'Sullivan and Dr. Lorraine O'Driscoll, your patience, guidance and encouragement has been invaluable over the past few years, and I deeply appreciate your support through all the tough times when science was not my friend.

To our clinical collaborators in Connolly Hospital Blanchardstown, Prof. Seamus Sreenan and Dr. Ana Rakovac Tisdall, without which this biomarker study could not have been performed. I would also like to extend my gratitude to Dr. Paul Dowling for overseeing the proteomics study, and for sharing his wealth of information in all protein related issues.

A big thank you to Dr. Niall Barron for all his help and never-ending patience on all molecular biology related issues. To Dr. Derek Walsh for teaching me the ropes when it came to virus manipulations. To Dr. Padraig Doolan, Dr. Sinead Aherne and Dr. Colin Clarke for all their help with the microarray data, especially under such time constraints, I really appreciated it. A big thank you also to Carol, Yvonne, Mairead, Mick and Ken who keep the center running so smoothly.

To all the amazing friends I've made since I started in the NICB, they've made the NICB a great place to work, especially Martina, Kathy, Fiona, Trish and Karen, I owe you guys my sanity. An especially huge thanks to Dr. Sandra Roche who's been there since we both started our PhDs together, thanks for being such a great friend and partner in crime! Thanks also to all the lab members past and present, Justine, Kishore, Clair, and Sweta for the great company through the long days and nights in cell culture.

A very special thanks to my family, especially my mum and sister Louise, for their never-ending love, support and encouragement, I couldn't have done it without you guys.

Abbreviations

-RT	No reverse transcriptase enzyme control
1,5-AG	1,5-anhydroglucitol
2D DIGE	2-dimensional gel electrophoresis
3'UTR	3 prime untranslated region
αSMA	Alpha smooth muscle actin
ABCG2	ATP-binding cassette, sub-family G (WHITE), member 2
ADP	Adenosine diphosphate
am-neg	Anti-mir negative control
ANOVA	Analysis of variance
ATP	Adenosine triphosphate
BCAA	Branched chain amino acids
bFGF	Basic fibroblast growth factor
BiPs	Beta cell derived induced pluripotent stem cells
BMI	Body mass index
BSA	Bovine serum albumin
C_t	Cycle threshold
cDNA	Copy deoxyribonucleic acid
CK-3	Cytokeratin 3
CK-12	Cytokeratin 12
CM	Conditioned media
CMPF	3-carboxy-4-methyl-5-propy-2-furanpropanoate
c-myc	v-myc myelocytomatosis viral oncogene homolog
CoA	Coenzyme A
Control new	Controls for newly diagnosed type 1 diabetes mellitus samples
Control old	Controls for type 1 diabetes mellitus established disease samples
Cxcr4	Chemokine (C-X-C motif) receptor 4
DMSO	Dimethyl sulfoxide
DNA	Deoxyribonucleic acid
dNTP	Deoxyribonucleotide triphosphate
EDTA	Ethylenediaminetetraacetic acid
EGF	Epidermal growth factor
ELISA	Enzyme linked immunosorbent assay

FACS	Fluoresence activated cell sorting
FCS	Fetal calf serum
FFA	Free fatty acids
FGF	Fibroblast growth factor
Foxa2	Forkhead box A2
FPA	Fibrinopeptide A
GFP	Green fluorescent protein
GLUT4	Glucose transporter 4
GSIS	Glucose stimulated insulin secretion
HbA1c	Glycated hemoglobin
HDL	High density lipoprotein
hES	Human embryonic stem cells
Hes1	Hairy and enhancer of split 1
Hlxb9	Motor neuron and pancreas homeobox 1
HMDB	Human metabolome database
Hnf4a	Hepatocyte nuclear factor 4, alpha
Hnf6	Hepatocyte nuclear factor 6
IAPP	Islet amyloid polypeptide
iMEF	Irradiated mouse embryonic fibroblasts
iPS	Induced pluripotent stem cells
IR	Immediately releasable
$K_{(ATP)}$	ATP sensitive potassium channel
Kir6.2	Potassium inwardly-rectifying channel, subfamily J, member 11
Klf4	Kruppel-like factor 4
LDL	Low density lipoprotein
Lipofect	Lipofectamine
MafA	v-maf musculoaponeurotic fibrosarcoma oncogene homolog A
MEF	Mouse embryonic fibroblasts
mES	Mouse embryonic stem cells
miRNA	MicroRNA
MMLV	Moloney Murine Leukemia Virus
MOI	Multiplicity of infection
mRNA	Messenger ribonucleic acid
NeuroD	Neurogenic differentiation 1

Ngn3	Neurogenin 3
Nkx6.1	NK6 homeobox 1
NSCLC	Non small cell lung cancer
NTC	No cDNA template control
Oct4	POU class 5 homeobox 1
OD	Optical density
ORF	Open reading frame
Pax6	Paired box 6
PBS	Phosphate buffer solution
PCA	Principal component analysis
PCR	Polymerase chain reaction
Pdx1	Pancreatic and duodenal homeobox 1
pm-neg	Pre-mir negative control
PP	Pancreatic polypeptide
Prox1	Prospero homeobox 1
Ptf1a	Pancreas transcription factor 1 subunit alpha
qRT-PCR	Quantitative reverse transcription polymerase chain reaction
RNA	Ribonucleic acid
ROCK	Rho kinase
RR	Readily releasable
RT-PCR	Reverse transcription polymerase chain reaction
Shh	Sonic hedgehog
Sox2	SRY (sex determining region Y)-box 2
Sox9	SRY (sex determining region Y)-box 9
TAE	Tris base, acetic acid and EDTA buffer
TCA	The citric acid cycle
TGFβ	Transforming growth factor beta
T1DM old	Type 1 diabetes patients with established disease
T1DM new	Newly diagnosed type 1 diabetes mellitus
T2DM	Type 2 diabetes mellitus
TLDA	TaqMan low density array
tRNA	Transfer ribonucleic acid
Txnip	Thioredoxin interacting protein
ViP	Lentivirus induced pluripotent-like cells

Abstract

This study aimed to investigate the molecular mechanisms of glucose stimulated insulin secretion (GSIS), specifically the role of microRNAs (miRNAs) in this process. TaqMan low density miRNA arrays identified a panel of 10 miRNAs down-regulated in glucose non-responsive compared to glucose responsive MIN6 cells. Functional investigations involving knockdown of mir-200a, mir-130a and mir-410 in MIN6 cells exhibiting GSIS resulted in reduced GSIS. This suggested that these three miRNAs functioned in supporting the capability of MIN6 cells to secrete insulin in response to stimulatory glucose levels i.e. they are "pro-GSIS" miRNAs, presumably down-regulating "anti-GSIS" mRNAs/protein. Over-expression studies of mir-410 supported the idea that it may enhance levels of GSIS.

However, the MIN6 system was somewhat unpredictable. The advent of iPS technology represented a possible route for generation of human pancreatic beta cells for the study of regulated insulin secretion. Attempts were made to generate iPS cells from the MiaPaCa2 pancreatic adenocarcinoma cell-line, normal human epidermal keratinocytes, and normal human limbal epithelial cells. Alterations in cell morphology and marker expression were observed, possibly representing partially reprogrammed cells, but fully reprogrammed iPS cells were not identified. Directed differentiation of an established iPS cell line was performed in 2D and 3D culture, with improved efficiency of definitive endoderm formation in 3D cultures (a step on the differentiation route towards beta cells).

In parallel, serum from diabetes patients was examined to identify new disease biomarkers in a collaborative clinical study with Connolly Hospital, Blanchardstown. MiRNAs identified as being potentially involved in GSIS from the MIN6 study were measured in serum from type 1 and type 2 diabetes patients. Proteomic and metabolomic profiling were performed on type 1 diabetes samples. These studies demonstrated the importance of stringent criteria for control sample selection, as evidenced by altered caffeine and lipid metabolism in control samples in this study.

1.0 Introduction

1.1 Diabetes Mellitus

Diabetes Mellitus is a metabolic disorder, in which insulin is either not secreted in sufficient amounts or does not efficiently stimulate its target cells. Despite high blood glucose levels cells starve due to impaired glucose entry into cells, as it is insulin which stimulates movement of the GLUT4 glucose transporters for translocation of glucose into cells.

Currently, there are more than 346 million people worldwide affected by diabetes. In 2004, an estimated 3.4 million people died from consequences of high blood sugar, with this figure estimated to double by 2030 (Organization 2011). There are three main types of diabetes mellitus, type 1 (also known as insulin-dependent diabetes mellitus), type 2 (known as non-insulin dependent diabetes mellitus) and gestational diabetes.

1.1.1 Type 1 diabetes

Type I diabetes (T1DM) accounts for approximately 10% of diabetes cases (Organization 2011). In T1DM, insulin is absent or nearly so because the pancreas lacks or has defective beta cells, which are responsible for the production of insulin and regulation of blood glucose levels. This condition results from an autoimmune response that selectively destroys the pancreatic beta cells (Atkinson and Maclaren 1994). Individuals with T1DM require daily insulin injections to survive. T1DM typically brews for several years before being diagnosed, as the immune system slowly destroys the beta cells of the pancreas. Only when greater than 80% of beta cells are destroyed do the symptoms of diabetes arise (Kloppel, Lohr et al. 1985). T1DM develops in an individual due to a combination of genetic predisposition and environmental factors.

The normal endogenous insulin secretory profile consists of a basal component along with short-lived prandial surges of insulin secretion, released in response to meals. Daily insulin injections are unable to match these release profiles, due to the pharmacokinetic properties of pharmaceutical insulin preparations, leading to episodes of hyper- and hypo-glycemia.

1.1.2 Type 2 diabetes

Type 2 diabetes accounts for approximately 90% of diabetes cases (Organization 2011), with 55% of patients also suffering clinical obesity. Type 2 diabetes is characterised by impaired beta cell function as well as insulin resistance. Insulin resistance is characterised by reduced insulin-mediated glucose uptake in insulin target tissues such as muscle, liver and adipose.

In an attempt to maintain euglycemia, the pancreas compensates by secreting increased amounts of insulin. When insulin secretion can no longer compensate for insulin resistance then hyperglycemia develops. Hyperglycemia can cause impaired insulin secretion as consistently high glucose levels desensitize beta cells, leading to beta cell dysfunction or failure (Hosokawa, Hosokawa et al. 1996).

1.1.3 Gestational diabetes

Gestational diabetes is a condition in which women without previously diagnosed diabetes exhibit high blood glucose levels during pregnancy. Pregnancy related hormones can block insulin from effectively signalling its target tissues, thereby resulting in symptoms similar to type 2 diabetes. Patients with gestational diabetes tend to have larger birth weight babies, which increases the chances of delivery related complications. Gestational diabetes is routinely screened for in pregnancy by an oral glucose tolerance test, with blood glucose levels returning to normal soon after the birth (U.S. Preventative Services Task Force recommendation statement 2008).

1.1.4 Secondary complications of diabetes

Patients with diabetes can develop a number of potentially serious complications including cardiovascular disease, retinopathy, nephropathy and neuropathy (Nathan 1993). The possibility of developing these complications can be reduced by tight glycaemic control (The Diabetes Control and Complications Trial Research Group 1993), this is difficult to achieve with current diabetes treatments, and risks episodes of hypoglycaemia, which can be dangerous for the patient. Replacement of the damaged

insulin-producing beta cells is the only treatment likely to achieve a constant normoglycemic state. Transplantation of the pancreas or preparations of islet tissue have been shown to achieve insulin-independence in type 1 diabetes patients (Ricordi and Strom 2004), but due to major problems in obtaining donor tissue and in preventing immune rejection of the graft, other cell sources need to be considered. Renewable beta cell lines need to be established which secrete insulin in a glucose dependent manner.

1.2 The Pancreas

The pancreas plays a central role in nutrient regulation and energy balance through two distinct types of tissue, exocrine and endocrine. The exocrine function of the pancreas is carried out by centroacinar and basophilic cells. Centroacinar cells secrete bicarbonate ions which neutralize stomach acid in the duodenum (Slack 1995), while basophilic cells produce the digestive enzymes. Pancreatic juices drain into the pancreatic duct and from there travel to the duodenum, their site of action (figure 1.1). When partially digested food from the stomach reaches the duodenum, the pancreatic juices are released via the pancreatic duct and mix with the food. The enzymes in this juice help break down the fats and protein into smaller fragments which can be absorbed into the body through the small intestine.

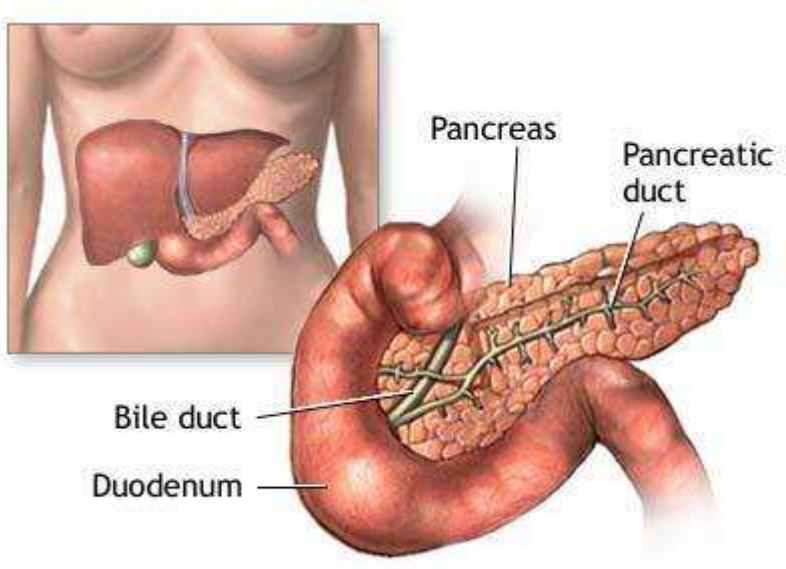

Figure 1.1 Location of pancreas within the body (www.ncbi.nlm.nih.gov/pubmedhealth)

The cells with endocrine function of the pancreas are clustered in groups called islets of Langerhans which are scattered around the pancreas and make up 1-2% of the total cell mass. These islets are composed of four major cell types, alpha (α), beta (β), delta (δ) and PP cells (figure 1.2). Beta cells produce and secrete insulin and amylin. Insulin controls the level of glucose in the blood by regulating glucose uptake in target tissues, and amylin, also known as IAPP (islet amyloid polypeptide), is co-secreted with insulin, and regulates glucose influx into the bloodstream (Weyer, Maggs et al. 2001).

Alpha cells are responsible for producing and secreting the peptide hormone glucagon. Glucagon is a 29 amino acid polypeptide with a molecular weight of 3485 Da. Glucagon is released in response to hypoglycaemia (Dunning and Gerich 2007; Gromada, Franklin et al. 2007) and elevates blood glucose levels by regulating breakdown of glycogen to glucose in the liver. Elevated blood glucagon levels are seen in diabetes patients, contributing to diabetic hyperglycaemia (Muller, Faloona et al. 1973). Additionally, diabetes patients exhibit blunted α-cell suppression in response to hyperglycaemia (D'Alessio 2011).

Delta cells secrete somatostatin. There are two active forms of somatostatin, ss-14 and ss-28, reflecting their amino acid chain length (Florio and Schettini 2001). The ss-14 variant is produced in the pancreas and functions as an inhibitor of insulin and glucagon release, and can also suppress exocrine pancreas secretions (Alberti, Christensen et al. 1973; Mortimer, Tunbridge et al. 1974; Gerich, Charles et al. 1976). Somatostatin inhibition of insulin secretion is associated with a reduction in cAMP generation and hyperpolarization of the plasma membrane, leading to decreased intercellular Ca^{2+} concentration, and hence decreased exocytosis (Pipeleers 1987; Nilsson, Arkhammar et al. 1989). In addition to the pancreatic delta cells, somatostatin is also produced in the stomach, intestine, brain and central nervous system.

PP cells secrete pancreatic polypeptide, a 36 amino acid polypeptide. Pancreatic polypeptide is secreted after ingestion of a meal and functions to inhibit the exocrine pancreas, as well as playing a role in appetite (Adrian, Besterman et al. 1977). Altered pancreatic polypeptide secretion has been observed in a number of disorders associated with abnormal eating behaviour, such as Prader-Willi syndrome (Zipf, O'Dorisio et al.

1981), morbid obesity (Lieverse, Masclee et al. 1994) and anorexia nervosa (Alderdice, Dinsmore et al. 1985; Fujimoto, Inui et al. 1997).

A fifth endocrine islet cell type, the ε cell, has recently been identified (Wierup, Svensson et al. 2002; Prado, Pugh-Bernard et al. 2004), which secretes the 28 amino acid peptide hormone ghrelin (Kojima, Hosoda et al. 2001). Ghrelin functions to increase secretion of growth hormone from the pituitary gland and also has a role in stimulating appetite and promoting food intake (Date, Kojima et al. 2000; Ariyasu, Takaya et al. 2001; Kojima, Hosoda et al. 2001).

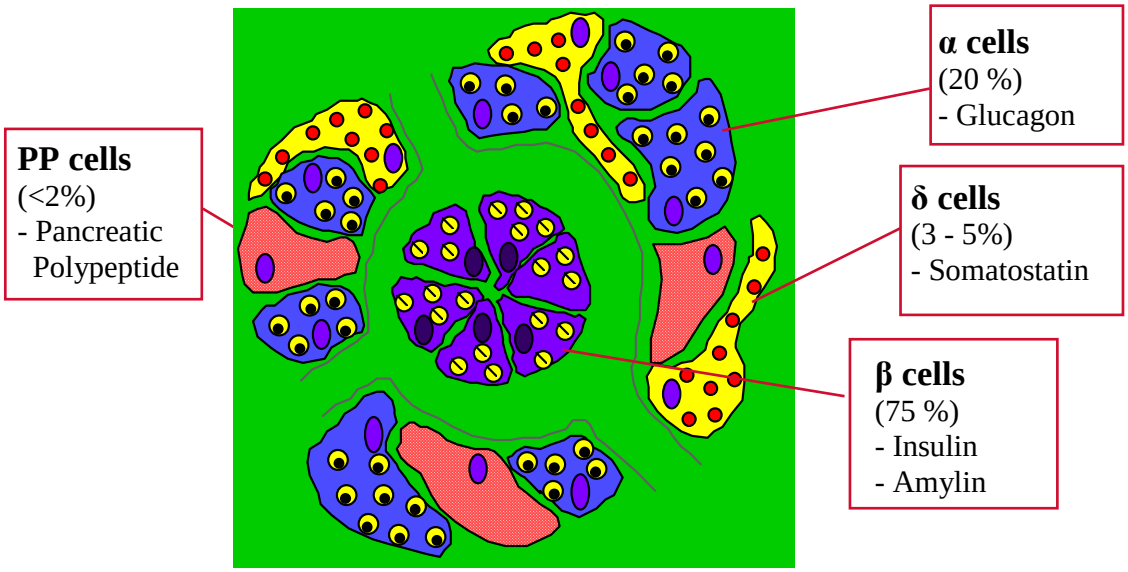

Figure 1.2 Schematic representation of islet of Langerhans cell composition.

1.2.1 Insulin

Beta cells were first identified as the source of insulin in 1938 (Richardson and Young 1938). Insulin is synthesized by beta cells as a single chain precursor molecule called preproinsulin, preproinsulin is discharged into the cisternal space of the rough endoplasmic reticulum, where the signal peptide is cleaved, leaving proinsulin (figure 1.3). Proinsulin is then transported to the Golgi apparatus by microvesicles (Orci 1984), where it is packaged into secretory granules. Proinsulin consists of three domains, an amino-terminal B chain, a carboxy-terminal A chain, and a connecting C-peptide chain. Conversion of proinsulin to insulin begins in the golgi and continues within the maturing secretory granule, where it is exposed to several specific endopeptidases (prohormone convertases 2 and 3, and carboxy peptidase H) (Hutton 1994). These enzymes remove the C-peptide chain, liberating two cleavage dipeptides, connected by two disulphide bridges, finally yielding insulin (figure 1.3). These secretory granules containing mature insulin remain within the cytoplasm until the cell is stimulated to release.

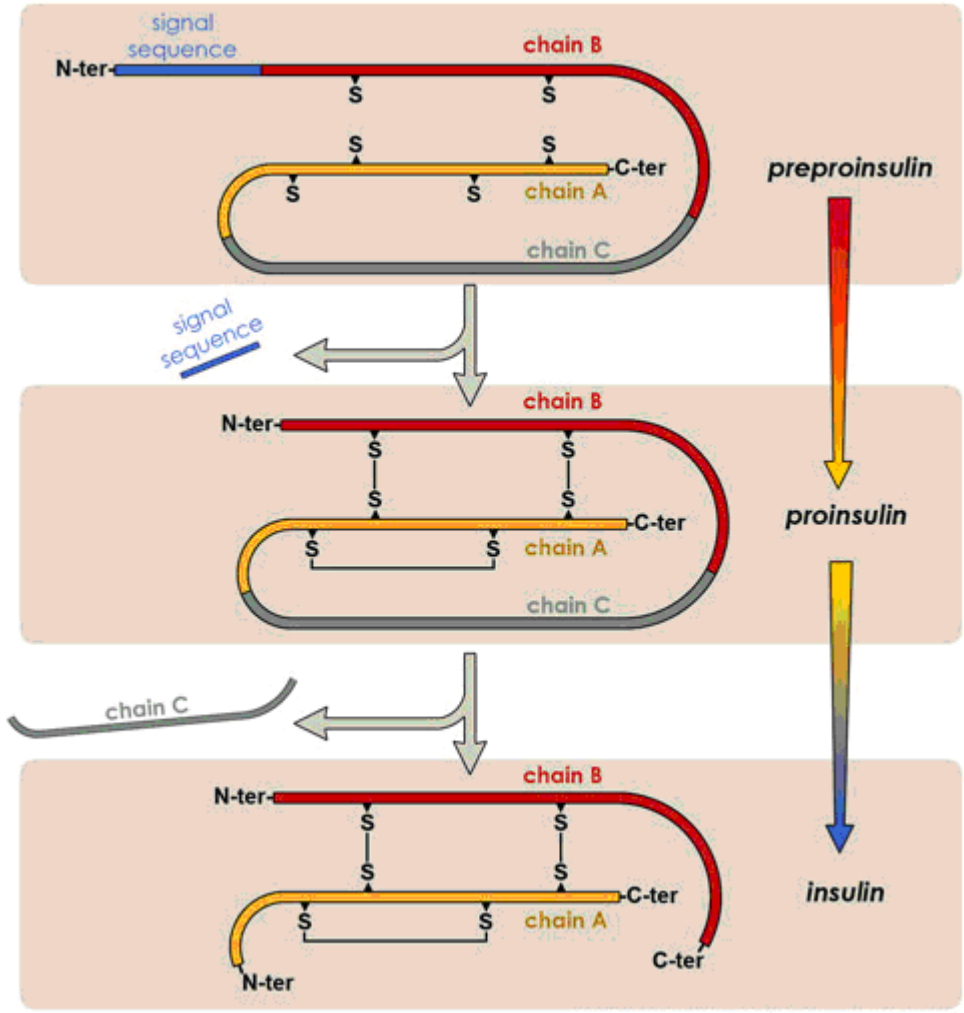

Figure 1.3 Processing of preproinsulin to insulin. Signal sequence of preproinsulin in cleaved, generating proinsulin. Disulphide bonds are formed between A and B chain, C chain is cleaved generating mature insulin (www.betacell.org).

1.2.2 Glucose Stimulated Insulin Secretion

Mature insulin granules are transported to the cell surface via cytoskeleton filaments. On reaching the plasma membrane, the insulin granules become docked in the membrane (Bratanova-Tochkova, Cheng et al. 2002; Olofsson, Gopel et al. 2002; Straub and Sharp 2002), and are considered to be in different states of readiness for secretion. They may be primed and capable of being released, termed the 'immediately releasable' (IR) pool, or they may be un-primed and incapable of being released, termed the 'readily releasable' (RR) pool (Barg, Ma et al. 2001; Barg, Eliasson et al. 2002; Bratanova-Tochkova, Cheng et al. 2002; Straub and Sharp 2002).

When beta cells are exposed to an increase in glucose concentration, insulin is released in a biphasic response. The first phase consists of a rapid burst of release which reaches its maximum four minutes after stimulation followed by a low secretion rate, the second phase shows an increasing rate of secretion to a plateau at thirty minutes (Cerasi and Luft 1963). The first phase is due to the release of granules from the IR pool, while the second phase is due to the release of granules that have to be prepared for immediate release, *i*.e. converted from the RR pool to the IR pool.

Glucose is the major stimulator of insulin secretion in mammalian beta cells. Beta cells have an active glucose transporter – GLUT2, which maintains the intracellular glucose concentration at the same level as the plasma (Thorens, Sarkar et al. 1988). The rate of insulin secretion is dependent on the rate of glucose metabolism; the rate-limiting step being its phosphorylation to glucose-6-phosphate, which is catalyzed by glucokinase. Glucokinase acts a glucose sensor in insulin secreting cells (Matschinsky 1990).

Following phosphorylation, glucose-6-phosphate is metabolised within the cell generating ATP via glycolysis. The change in ATP/ADP ratio stimulates the ATP sensitive K-channel (K_{ATP}) to close, preventing potassium ions from leaving the cell. Due to the action of the K^+ ions trapped within the cell, the plasma membrane becomes depolarized, which in turn opens voltage-gated calcium channels allowing an influx of Ca^{2+} (figure 1.4). This increase in Ca^{2+} results in a spike in exocytosis of insulin granules (the first phase) in a concentration dependent manner (Grodsky 1972; Grodsky

1972; Nesher and Cerasi 2002). At the low secretion stage between the first and second phases, the IR pool is depleted (Olofsson, Gopel et al. 2002) and must be resupplied. Granules from the RR pool are primed for conversion to the IR pool before they can be released by exocytosis, leading to the second phase of the response. The rate of exocytosis during the second phase increases over time until it plateaus out at a higher level.

The overall rate of insulin secretion is controlled by the concentration of glucose to which the beta cell is exposed, the interaction of glucose with glucokinase and the physiological state of the beta cell (Matschinsky 1996).

The capillaries which serve the insulin producing beta cells are permeable to peptides; therefore, after exocytosis from beta cells, insulin molecules can readily enter the bloodstream for transport to target cells elsewhere, mainly in liver, muscle, and adipose tissue.

Insulin signals these tissues that blood glucose is higher than necessary, as a result, cells take up excess glucose from the blood and convert it to the storage compounds glycogen and triacylglycerol.

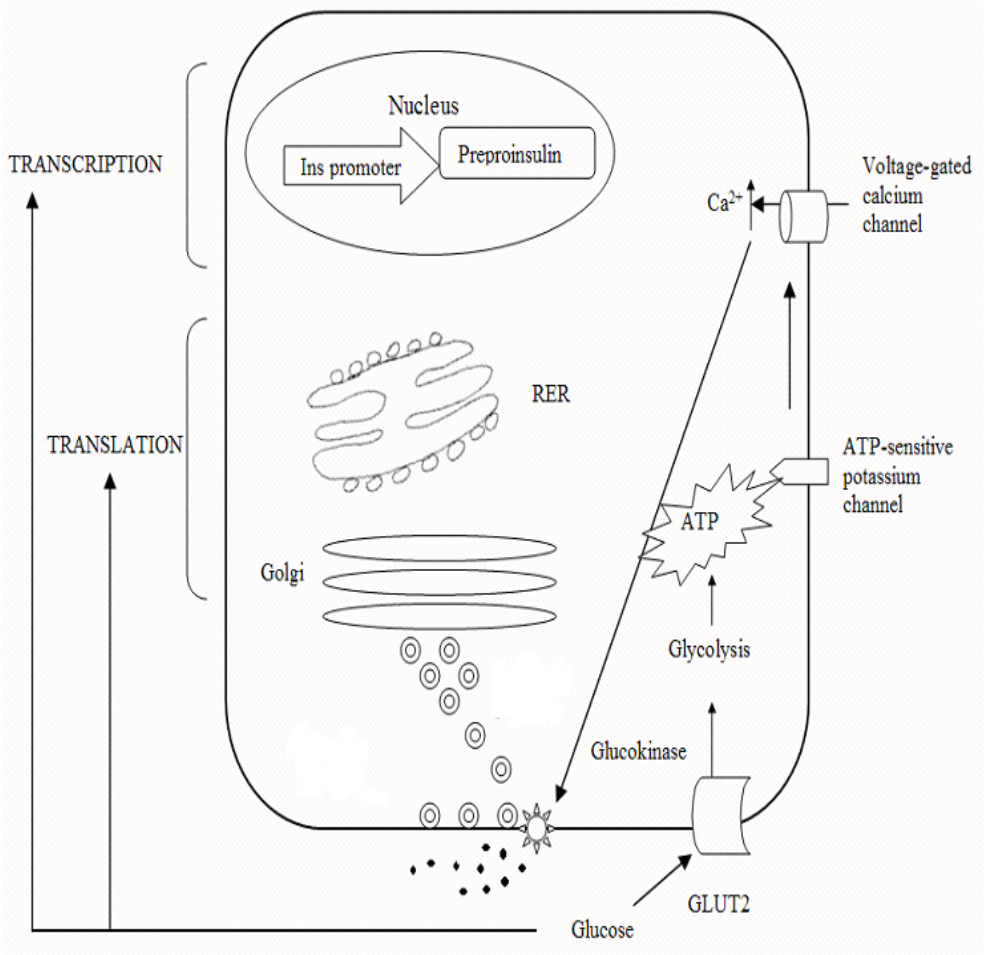

Figure 1.4 Regulated insulin secretion. Rising blood glucose levels trigger insulin secretion from beta cells. Starting with the uptake of glucose by the GLUT2 transporter, the glycolytic phosphorylation of glucose causes a rise in the ATP:ADP ratio. This rise inactivates the potassium channels that depolarise the membrane, causing the calcium channel to open up allowing calcium ions to flow inward. The ensuing rise in levels of intracellular calcium leads to the exocytotic release of insulin from their storage granules (Rani 2008).

1.2.3 Cell models for studying GSIS

Due to the limited availability and restricted culture potential of primary pancreatic tissue for the study of the molecular mechanisms of GSIS, much work has been put into the development of pancreatic beta cell lines. Various transformation approaches have been employed to overcome the replicative senescence associated with primary pancreatic beta cells in attempts to generate immortalised pancreatic beta cell lines (Gazdar, Chick et al. 1980; Santerre, Cook et al. 1981; Newgard 1994). These experiments have proven difficult as the differentiated phenotype and the proliferative phenotype are mutually exclusive cell processes. Many of the cell lines generated exhibit some degree of de-differentiation and loss or reduction of mature beta cell function.

A number of pancreatic beta cell lines have been generated, such as MIN6, β which produce significant amounts of insulin, up to one third of that found in normal beta cells, and also maintain a normal glucose response within the physiological range (Asfari, Janjic et al. 1992; Ishihara, Asano et al. 1993; Radvanyi, Christgau et al. 1993; de la Tour, Halvorsen et al. 2001). MIN6 cells are the most widely used of these cell lines, as the mature differentiated phenotype of these cells is thought to be most stable compared to other cell lines available. However, with increasing time in culture hormone secretion, and the glucose responsiveness in all these cell lines is reduced (Skelin, Rupnik et al. 2010). Previous studies in our lab on the MIN6 cell line indicate that loss of GSIS associated with increasing time in culture is not due to a decrease in insulin production (O'Driscoll, Gammell et al. 2004), but is more likely caused by de-differentiation coupled to an altered capacity of these cells to successfully fold, modify and secrete proteins and to respond to problems associated with oxidative stress (Dowling, O'Driscoll et al. 2006; O'Driscoll, Gammell et al. 2006).

MIN6 cells which have been maintained in culture for an extended period, and exhibit a reduced GSIS phenotype may represent a potential model for the study of beta cell dysfunction associated with type 2 diabetes, as beta cell dysfunction in these patients has also been suggested to occur through a de-differentiation mechanism (Prentki and Nolan 2006).

1.3 Pancreas Development

Much of what we already know about pancreatic development is based on experiments with nonhuman organisms (McKnight, Wang et al. 2010), as limited biological material exists for experiments with human development. Knowledge of human pancreas development can be utilised for generation of replacement cells for type 1 diabetes. *In vitro* methods attempt to recapitulate the sequence of endogenous signalling pathways that first create progeny cells resembling definitive endoderm, then primitive gut tube epithelium, foregut pancreatic progenitors, islet progenitors and in the final step hormone positive progeny producing insulin positive cells.

1.3.1 Specification of Pancreatic Fate

Gastrulation occurs at embryonic day 6.5 (E6.5) in the mouse. During gastrulation, embryonic reorganisation occurs to form three germ layers, endoderm, mesoderm and ectoderm, with endoderm and mesoderm arising from a common cluster of mesendoderm. Wnt signalling is required for primitive streak formation and differentiation of mesendoderm cells (Liu, Wakamiya et al. 1999). Subsequent nodal signalling determines mesoderm or endoderm fate of mesendoderm cells, with high nodal levels leading to endoderm and low levels leading to mesoderm (Conlon, Lyons et al. 1994; Brennan, Lu et al. 2001; Vincent, Dunn et al. 2003).

At E7.5, gastrulation is complete, definitive endoderm cells roll up to form the gut tube. The dorsal endoderm is adjacent to the notochord and the ventral pancreatic endoderm is adjacent to the hepatic diverticulum and the cardiogenic mesoderm (figure 1.5).

By E9.5 the first sign of pancreatic buds appear, on the dorsal and ventral side of the primitive gut tube (Edlund 2002). The dorsal mesenchyme condenses and through signalling from the adjacent mesoderm, the endoderm region evaginates to form the dorsal bud (figure 1.6) (Munger 1958; Kallman and Grobstein 1964; Pictet, Clark et al. 1972). As the stomach and duodenum rotate, the ventral bud comes into contact with the dorsal bud and they fuse at approximately E12.0-13.0. The ventral bud goes on to

form the posterior part of the head of the pancreas, while the dorsal bud forms the remainder of the organ.

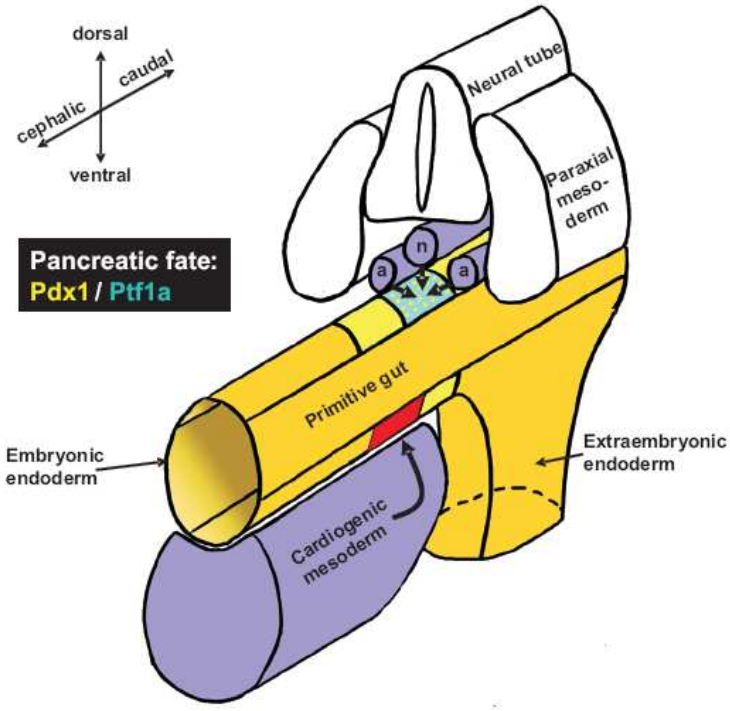

Figure 1.5 Endodermal junction of an E8.5 mouse embryo (Bonal and Herrera 2008). Dorsal endoderm develops towards the pancreatic fate in response to mesodermal factors (secreted from the notochord and aortae, in purple). Dorsal endoderm is characterised by co-expression of *Pdx1* (yellow) and *Ptf1a* (blue). Ventrally the cardiomesoderm defines the presumptive liver (red) in the ventral endoderm. Adjacent to it, at the leading edge of the embryonic endoderm, the ventral pancreatic primordium, which only expresses *Pdx-1*, is specified by unknown mechanisms. n-notochord, a-aortae.

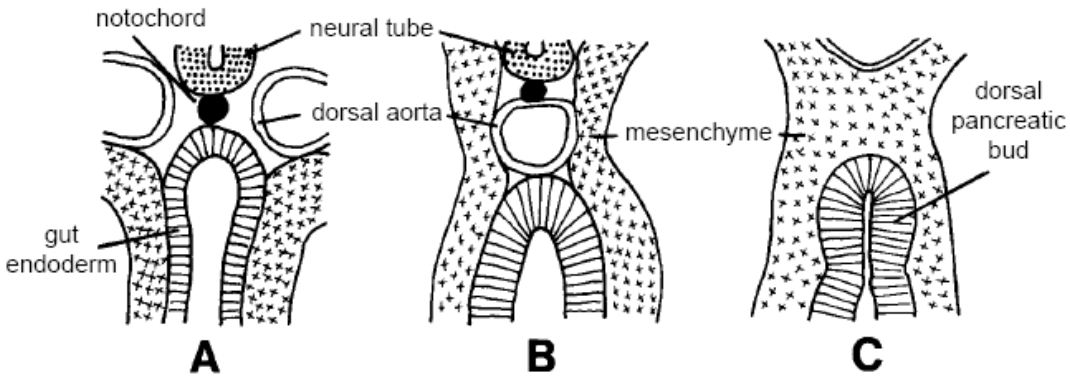

Figure 1.6 Development of dorsal pancreas in rodents. (A) Close proximity of dorsal aspect of gut endoderm and notochord at E8. (B) The two dorsal aortae fuse, separating the gut endoderm from the notochord, E8.75-9.0. (C) The mesenchyme proliferates separating the dorsal endoderm from the dorsal aortae E9.0-9.5 (Slack 1995).

1.3.1.1 Hedgehog signalling

Sonic Hedgehog *(Shh)* is expressed in regions of the gut endoderm except where the dorsal and ventral buds form and almost defines the boundary where the pancreas develops. Shh inhibition using cyclopamine can lead to ectopic pancreatic development in the stomach and intestine (Kim and Melton 1998). Inhibition of *Shh* expression in the dorsal bud is mediated by notochord signalling via FGF2 and Activin (Hebrok, Kim et al. 1998). Inhibition in the ventral bud is mediated by release of factors from the cardiac mesoderm, the factors released from the cardiac mesoderm are less well known (Kim, Hebrok et al. 1997). Inhibition of Shh allows expression of the transcription factor pancreatic and duodenal homeobox 1 (Pdx1), which is a marker of pancreatic and duodenal progenitor cells. This initial induction of *pdx1* expression is triggered by hepatocyte nuclear factor 6 (Hnf6) transcription factor. Hb9 and Isl1 are also required in the dorsal bud for pdx1 expression, while Hex1 is required in the ventral bud.

1.3.1.2 Influence of notochord, aorta and mesenchyme

The notochord is in contact with the dorsal prepancreatic endoderm up until E8, removal of notochord from early chick embryos prevented correct dorsal pancreas formation (Kim, Hebrok et al. 1997), possibly through lack of activin and FGF2 signalling. At E8.75-9.0 the two dorsal aortae fuse, separating the notochord from the pancreatic endoderm. The aortic endothelium is involved in the induction of pancreatic

differentiation from the early endoderm. Removal of the aorta in *Xenopus* endoderm prevents pancreas development, however co-culture with other endothelial cells allowed correct pancreas development (Lammert, Cleaver et al. 2001). It is unknown what signalling molecules contribute to aortic endothelium promotion of pancreas development.

At E9.0-9.5 the mesenchyme proliferates separating the dorsal endoderm from the dorsal aortae (figure 1.3). Dorsal mesenchyme, in response to signals from the aorta, secretes FGF10, which promotes dorsal pancreas development. FGF10 promotes accumulation of Pdx1+ pancreatic progenitor cells, but at the expense of cellular differentiation (Elghazi, Cras-Meneur et al. 2002). Disruption of FGF signalling can lead to under-development of the pancreas, while over-expression of *FGF10* leads to excessive accumulation of pancreatic progenitor cells and formation of over-sized pancreas (Jacquemin, Yoshitomi et al. 2006). Further differentiation of these expanded progenitor cells into endocrine or exocrine cells may be also modulated by FGF signalling.

Mesenchyme is critical for acinar development. Contact of pancreatic epithelial cells to mesenchyme leads exclusively to acinar differentiation, while absence of direct contact of mesenchyme with pancreatic epithelium leads exclusively to endocrine differentiation (mainly beta cell differentiation) (Li, Manna et al. 2004). FGF signalling from pancreatic mesenchyme apparently favours exocrine differentiation. Exogenous FGF enhances the presence of amylase positive cells, while a pdx1-FGF4 transgenic mouse, with *FGF4* expressed in all early pancreatic epithelial cells, had ductal degeneration of the pancreas with persistent acini and severe destruction of the endocrine tissue (Dichmann, Yassin et al. 2006). In addition, FGF10 and FGF7 lead to enhanced proliferation of pancreatic epithelium with reduced endocrine differentiation (Elghazi, Cras-Meneur et al. 2002; Hart, Papadopoulou et al. 2003; Norgaard, Jensen et al. 2003). Mesenchyme suppression of endocrine differentiation due to contact of mesenchyme with pancreatic epithelium may be mediated by enhanced notch signalling-induced hairy enhancer of split 1 *(hes1)* expression and inhibition of neurogenin 3 (*ngn3*) expression (Duvillie, Attali et al. 2006).

1.3.1.3 Activin

Activins are members of the TGFβ family of signalling molecules. They signal through a large family of receptors to activate smads and other intracellular pathways to initiate specific cell responses.

Activin A and B are present in endocrine cells of the developing pancreas (Furukawa, Eto et al. 1995; Maldonado, Kadison et al. 2000) and enhance differentiation of endocrine cells while suppressing differentiation of exocrine/acinar cells. Addition of activin to embryonic pancreas explant cultures inhibits branching morphogenesis associated with ductal and acinar differentiation (Ritvos, Tuuri et al. 1995). Inhibition of activin activity using follistatin (which is present in early pancreatic mesenchyme), was sufficient to replace the pro-exocrine/anti-endocrine effect of mesenchyme (Miralles, Czernichow et al. 1998). Exogenous activin has also been shown to increase the number of insulin-positive cells as well as insulin content in cultured human fetal pancreas (Demeterco, Beattie et al. 2000). Activin may mediate its effects on insulin positive differentiation by reducing expression of pre-proglucagon and Arx (transcription factor vital for α-cell differentiation) (Mamin and Philippe 2007), and by inducing expression of neurogenin3 (ngn3: a key determinant of pancreatic endocrine lineage selection) (Zhang, Mashima et al. 2001).

1.3.1.4 Hepatocyte nuclear factor 6 (Hnf6)

Hnf6 is a transcription factor, expressed at E8 in early pre-pancreatic endoderm, it is subsequently expressed in early pancreatic epithelium at E9.0-10.0 (Rausa, Samadani et al. 1997; Jacquemin, Lemaigre et al. 2003; Maestro, Boj et al. 2003). Hnf6 is a key determinant of pancreatic specification, and is an inducer of *pdx1* expression. Hnf6 null mice exhibit reduced size of pancreas-specified endoderm and are born with hypoplastic pancreas (Jacquemin, Durviaux et al. 2000; Jacquemin, Lemaigre et al. 2003). The effects observed in Hnf6 null mice may be mediated through a lack of induction of *pdx1* expression. Hnf6 is also an inducer of *ngn3* expression. Hnf6 null mice also show a reduction in ngn3 positive cells (Jacquemin, Durviaux et al. 2000). Following Hnf6 induced *pdx1* expression in pancreatic progenitors; *Hnf6* expression becomes limited to ductal and acinar cells from E18.

1.3.1.5 Pancreatic and duodenal growth factor 1 (Pdx1)

Pdx1 is first expressed at E8.5 in all epithelial cells of the developing pancreas following induction by Hnf6, and represents the earliest marker of endocrine and exocrine progenitors. *Pdx1* expression is suppressed in cells as they commit to endocrine (Jensen, Heller et al. 2000) or ductal lineages (Jonsson, Ahlgren et al. 1995; Gu, Dubauskaite et al. 2002). As endocrine cells begin to differentiate towards the insulin positive β-cell lineage, *pdx1* expression reappears. Low *pdx1* expression also persists in 20% δ-cells, acinar and ductal cells (Guz, Montminy et al. 1995; Wu, Gannon et al. 1997).

Pdx1 null mice exhibit limited dorsal bud formation with no ventral bud formation (Ahlgren, Jonsson et al. 1996). The dorsal bud contained a few insulin and glucagon expressing cells, but without expansion of these cells (Ahlgren, Jonsson et al. 1996), indicating that pdx1 expression is not required for early budding of dorsal pancreas, or for formation of early endocrine cells, but is required in later steps of pancreas development. Pdx1 null mutations in humans were also associated with pancreas agenesis (Stoffers, Zinkin et al. 1997).

The number of pdx1 positive progenitors formed between E8.5-12.5 is thought to determine the size of the adult pancreas. The pool of pdx1 positive progenitors depends on the proper commitment and proliferation of early endodermal cells into pdx1 positive cells. Disruption of Notch, FGF or Wnt/β-catenin signalling leads to a reduced pool of pdx1 positive progenitors, and hence pancreatic hypoplasia (Stanger, Tanaka et al. 2007).

Pdx1 expression is required for growth and maturation of acinar cells (Holland, Hale et al. 2002; Hale, Kagami et al. 2005), with inhibition of *pdx1* from E13.5-14.0 leading to reduction of acinar cells, and the cells that were present were immature (Hale, Kagami et al. 2005). *Pdx1* expression is necessary for correct glucose regulated insulin synthesis in β-cells (MacFarlane, Read et al. 1994; Marshak, Totary et al. 1996). Pdx1 inhibition in β-cells leads to β-cell depletion and increased numbers of α-cells, due to the loss of normal β-cell inhibition of α-cell development (Ahlgren, Jonsson et al. 1998; Lottmann, Vanselow et al. 2001; Thomas, Devon et al. 2001; Holland, Hale et al. 2002; Gannon, Ables et al. 2008).

1.3.1.6 Pancreas specific transcription factor 1a (PTF1a)

PTF1a is first expressed at E9.5 in the cells of the foregut endoderm which give rise to ventral and dorsal pancreas, its induction in dorsal pancreas is mediated by pdx1, while factors mediating its induction in ventral pancreas are unknown (Krapp, Knofler et al. 1998; Burlison, Long et al. 2008). *PTF1a* and *pdx1* are co-expressed in pancreatic progenitor cells from E9.5 to E12.5. Expanding the field of *pdx1/PTF1a* co-expressing cells in *Xenopus* foregut leads to oversized pancreas, suggesting that *pdx1/PTF1a* co-expression induced formation of increased numbers of pancreatic progenitor cells (Afelik, Chen et al. 2006). 100% acinar cells, 95% ductal cells, 75% alpha cells, and 100% of non-alpha endocrine cells are derived from PTF1a positive progenitor cells. By E16 *PTF1a* expression becomes restricted to acinar cells, with low expression remaining in some early endocrine progenitor cells (Kawaguchi, Cooper et al. 2002; Chiang and Melton 2003; Lin, Biankin et al. 2004; Zecchin, Mavropoulos et al. 2004; Zhou, Law et al. 2007). In PTF1a null mutant mice, exocrine pancreas is absent, while endocrine cells locate within the spleen (Krapp, Knofler et al. 1998; Lin, Biankin et al. 2004) and PTF1a mutations in human led to pancreas agenesis (Sellick, Barker et al. 2004), indicating a role for PTF1a in both endocrine and exocrine lineage development.

1.3.2 Maintenance of uncommitted pancreatic progenitors

Notch signalling and sox9 activity prevent commitment of pancreatic progenitors into endocrine or exocrine cells by promoting progenitor self-renewal. TGFβ and Prox1 mediate commitment to endocrine and exocrine fates following sufficient expansion of progenitor cell pools.

1.3.2.1 Notch signalling

Notch is a cell membrane bound receptor. When bound by notch ligands such as jagged, serrate, or delta-like molecules, progenitor cells are maintained in an undifferentiated state, allowing expansion of pdx1 positive progenitors up to E12.5. Notch signalling stimulates up-regulation of hes1 (a member of notch signalling pathway), which in turn leads to ngn3 suppression, maintaining the undifferentiated state. Hes1 null mice exhibit severe pancreas hypoplasia due to inappropriate commitment of early precursor cells to endocrine lineages (Jensen, Pedersen et al. 2000). Notch may also be involved further downstream in specification of endocrine cell types; as mutations in notch ligands such as deltaA lead to increased number of β-cells, and jagged 1B mutants have increased α-cell population (Zecchin, Filippi et al. 2007).

1.3.2.2 Sox9

Sox9 is a transcription factor involved in the maintenance of undifferentiated progenitor cells, and is thought to mediate the transition from pancreatic progenitor to endocrine committed cells through ngn3. *Sox9* is expressed from E9.5 in pdx1 positive progenitors; following progenitor cell specification *sox9* expression is restricted to acinar cells and a small number of ductal cells (Seymour, Freude et al. 2007). *Sox9* displays a similar expression pattern to *hnf6* and possibly functions in conjunction with hnf6, as conditional deletion of sox9 displayed similar phenotype to hnf6 null mutants, with formation of ductal structures and lack of endocrine cells (Seymour, Freude et al. 2007). Sox9 can interact with the regulatory elements of *hnf6* and *ngn3* genes (hnf6 is an inducer of ngn3 expression) (Lynn, Smith et al. 2007; Seymour, Freude et al. 2007). Hes1 positive cells are likely precursors of ngn3 positive cells, sox9 co-localises with hes1 indicating a possible role for sox9 in mediating transition of hes1 positive/ngn3

negative endocrine progenitors to hes1 negative/ngn3 positive endocrine committed cells (Seymour, Freude et al. 2007).

1.3.3 Specification of endocrine progenitors

Pancreatic hormone expression is first detected in the first wave of endocrine cell generation (E9.5 – E10.5); however, these early hormone-expressing cells do not contribute to the mature endocrine cell population. Mature pancreatic endocrine cells arise from neurogenin 3 expressing progenitor cells (Bonal and Herrera 2008).

1.3.3.1 Neurogenin 3 (ngn3)

The transcription factor *Ngn3* is first expressed in early pancreatic endoderm at E9.0, peaking at E15.5, and decreases substantially by E17.5 (Apelqvist, Li et al. 1999). Ngn3 positive cells represent endocrine progenitor cells which can give rise to cells expressing the islet transcription factors neuroD, nkx6.1 and pax6 (Jensen, Heller et al. 2000). All pancreatic endocrine cells derive from ngn3 positive cells (Gu, Dubauskaite et al. 2002). Ngn3 expression is repressed by notch signalling. Inactivation of notch signalling leads to premature expression of *ngn3* and endocrine development (Apelqvist, Li et al. 1999). *Ngn3* expression is also modulated by Hnf6 (Jacquemin, Durviaux et al. 2000).

1.3.3.2 Nkx transcription factors

Nkx are a family of homeodomain transcription factors. Three family members – nkx2.2, nkx6.1 and nkx6.2 are involved in regulation of endocrine pancreas development.

Nkx2.2

Nkx2.2 is first expressed at E9.5 in *pdx1* co-expressing cells (Sussel, Kalamaras et al. 1998; Chiang and Melton 2003); by E12.5 *nkx2.2* expression is restricted to ngn3 positive cells. Nkx2.2 null mice develop with no β-cells, 80% reduction in α-cells and slight reduction in PP-cells, indicating that nkx2.2 is required for commitment and differentiation of endocrine precursors to α-cells, β-cells and PP-cells, with expression remaining in these mature cell types (Sussel, Kalamaras et al. 1998). Nkx2.2 can bind and activate *mafA* and *insulin* gene expression (Cissell, Zhao et al. 2003; Raum, Gerrish et al. 2006), its effect on endocrine commitment and differentiation may be mediated though these factors.

Nkx6.1 and nkx6.2

Nkx6.1 and *nkx6.2* expression become detectable in the pancreatic epithelium by E10.5. Pdx1 null mice have reduced nkx6.1 positive cells, while nkx6.2 positive cells are unaffected, indicating that pdx1 acts upstream of nkx6.1, but not nkx6.2 (Pedersen, Nelson et al. 2005). Nkx6.1 expression becomes restricted to β-cells by E15, and expression continues in mature β-cells (Sander, Sussel et al. 2000). Nkx6.2 becomes restricted to α- and acinar cells by E15, but is turned off by E15.5 (Sander, Sussel et al. 2000). Nkx6.1 plays an important role in β-cell generation. Nkx6.1 null mice have 85% reduction in β-cells due to inability of insulin-positive cells to self-renew beyond E13 (Sander, Sussel et al. 2000; Henseleit, Nelson et al. 2005). There is some evidence that nkx6.1 and nkx6.2 may exhibit functional compensation when expression of one is knocked down. Transgenic expression of nkx6.2 is capable of rescuing the nkx6.1 null phenotype when expressed in pdx1 positive cells, but not ngn3 positive cells, indicating that nkx's function upstream of ngn3 (Nelson, Schaffer et al. 2007). Nkx6.2 null mice develop normal pancreas, while nkx6.1 and nkx6.2 double null mice have 65% reduction in α-cells, suggesting that nkx6.1 compensates lack of nkx6.2 expression in

the nkx6.2 null mutant to allow correct α-cell development (Henseleit, Nelson et al. 2005).

1.3.3.3 Pax4 and Arx

Pax4 is first expressed in the pancreatic epithelium from E9.5 (Sosa-Pineda, Chowdhury et al. 1997; Brink, Chowdhury et al. 2001), with expression peaking from E13-E15 (Wang, Elghazi et al. 2004). Pax4 is a marker of endocrine progenitor cells which give rise to α-, β-, δ- and PP-cells (Greenwood, Li et al. 2007). As endocrine cells mature *pax4* expression diminishes (Smith, Ee et al. 1999). Pax4 null mice lack β- and δ- cells. Some early embryonic insulin-positive cells were detected in these null mutants, but fully mature β-cells did not develop, indicating that pax4 is not required for the initial formation of β-cells, but for the proliferation and maturation of these cells (Sosa-Pineda, Chowdhury et al. 1997; Wang, Elghazi et al. 2004). In these null mutants, the number of α-cells was greatly increased (Heller, Jenny et al. 2005).

Arx is an enhancer of α-cell differentiation, and is directly target for inhibition by pax4. Arx null mice develop no α-cells, the α-cell precursors become directed towards β- and δ-cell lineages due to *pax4* expression (Collombat, Mansouri et al. 2003; Collombat, Hecksher-Sorensen et al. 2005). Over-expression of *arx* is also capable of redirecting β- and δ-cell precursors to α- and PP-cell lineages (Collombat, Hecksher-Sorensen et al. 2007).

1.3.4 Maintenance of islet cell identity

Pax6 expression is required for the proliferation and maturation of all endocrine cells, while MafA, pdx1 and beta2/neuroD are required for insulin gene expression in β-cells, and Brn4 required for glucagon expression in α-cells.

1.3.4.1 Pax6

Pax6 is expressed in early embryonic pancreas from E9.0 (Turque, Plaza et al. 1994). *Pax6* expression is induced in endocrine committed cells which also express *neuroD* and *isl1* (Jensen, Heller et al. 2000). NeuroD in conjunction with E47 can induce *pax6* expression (Marsich, Vetere et al. 2003). These pax6 positive cells then initiate hormone expression possibly through pax6 binding sites in the promoter regions of the preproglucagon, insulin and somatostatin genes (Sander, Neubuser et al. 1997). Pax6/glucagon double positive cells are detected by E9.5, and pax6/insulin double positive cells are detected at E12.5 (Sander, Neubuser et al. 1997; St-Onge, Sosa-Pineda et al. 1997; Heller, Stoffers et al. 2004). Pax6 is involved in the expansion of endocrine cell types; pax6 null mutants have 75-100% reduction in α-cells and 65% reduction in β-cells (Sander, Neubuser et al. 1997; St-Onge, Sosa-Pineda et al. 1997).

1.3.4.2 MafA

MafA is expressed in mature β-cells; it binds to enhancer elements of the insulin gene, in response to glucose and stimulates insulin gene expression. *MafB* is expressed in α-cells and stimulates glucagon expression. MafA acts downstream to pax4 and pax6 to maintain mature β-cell identity. MafA inactivation does not effect the early stages of pancreas development, but leads to reduced expression of β-cell markers such as insulin1, insulin2, pdx1, beta2/neuroD and glut2 (Zhang, Moriguchi et al. 2005).

1.3.4.3 NeuroD

NeuroD expression is first detected in pancreatic epithelium from E9.5, and from E14.5 in *ngn3* expressing cells, following birth *neuroD* expression is limited to β-cells. Ngn3 stimulates *neuroD* expression by binding enhancer regions of the neuroD promoter

(Huang, Liu et al. 2000). Expression of *neuroD* represents a transition from proliferative ngn3 positive progenitor cells, to post-mitotic committed cells (Jensen, Heller et al. 2000; Gu, Dubauskaite et al. 2002). NeuroD is involved in formation and maturation of β-cells; it is an activator of insulin gene expression. NeuroD null mice still form endocrine cells, but at reduced numbers, due to increased apoptosis from E17 (Naya, Huang et al. 1997).

1.3.4.4 Other factors required for β-cell identity

As mentioned above, pdx1 is also an activator of insulin gene expression (MacFarlane, Read et al. 1994; Marshak, Totary et al. 1996). Pdx1 is required for expression of a number of β-cell markers, including glut2 and glucokinase (Serup, Petersen et al. 1995). Pdx1 expression is limited to β-cells and 20% α-cells from E19.

Conversely to its function in pancreatic endoderm specification, hedgehog signalling is required for maintenance of mature β-cell identity (Thomas, Rastalsky et al. 2000). Hedgehog signalling activates *pdx1* expression, which in turn activates insulin gene expression (Thomas, Lee et al. 2001).

1.3.4.5 Specification of exocrine lineages

Acinar cells develop from the tips of ductal branches from E14.5; by E16.5 zymogen granules are present for storage of digestive enzyme. *Pdx1* expression is required from E13.5 for commitment and maturation of exocrine cells. Pdx1 is necessary for induction of *PTF1a*, which in turn stimulates expression of acinar specific genes such as elastase1, chymotrypsinogen B and α-amylase2 (Cockell, Stevenson et al. 1989). Mist1 transcription factor is not required for early exocrine development, but is necessary at later stages for correct organisation and maturation of acini, indicated by mist1 null mice (Pin, Rukstalis et al. 2001). Expression of srf transcription factor is also critical of maintenance of exocrine identity postnatal (Miralles, Lamotte et al. 2006). Notch signalling is required for exocrine commitment, while wnt/β-catenin and TGFβ signalling are required for differentiation and expansion of exocrine committed cells.

1.4 *In vitro* differentiation of pancreatic cells

In vitro models for differentiation of human ES cells to pancreatic phenotypes are mainly based on knowledge of mouse pancreas development. However, differences exist between mouse and human pancreas development, such as duration of embryogenesis, organ morphology and islet organisation.

Mouse embryonic stem cell lines (mES cells) were developed a number of years before the establishment of the first human embryonic stem cell lines (Evans and Kaufman 1981; Martin 1981; Thomson, Itskovitz-Eldor et al. 1998), therefore initial *in vitro* pancreatic differentiation protocols were designed for use with mES cells. Initial attempts at differentiation of mES cells were based on spontaneous differentiation of embryoid bodies (Shiroi, Yoshikawa et al. 2002) or over-expression of pancreas-specific genes (Levinson-Dushnik and Benvenisty 1997; Blyszczuk, Czyz et al. 2003; Vincent, Treff et al. 2006). While some insulin positive cells were detected in these initial studies, this limited success prompted the use of more developmental-biology based approaches, to mimic the natural development of the pancreas *in vivo* for differentiation of both human and mouse ES cells *in vitro* (D'Amour, Bang et al. 2006; Jiang, Au et al. 2007; Jiang, Shi et al. 2007; Phillips, Hentze et al. 2007; Shim, Kim et al. 2007; Zhang, Jiang et al. 2009).

Differentiation of pancreatic beta cells from ES cells can be broken into four specific developmental stages- endoderm formation, pancreas specification, endocrine specification and beta-cell maturation (Murtaugh 2007; Spence and Wells 2007; Gittes 2009). Definitive endoderm is the first step ES cells must achieve for differentiation towards pancreatic cells types, *in vivo* this step is achieved during gastrulation, during which ES cells are specified for ectoderm, endoderm or mesoderm formation. *In vivo* experiments have shown that nodal signalling is required for endoderm specification (Conlon, Lyons et al. 1994; Brennan, Lu et al. 2001; Vincent, Dunn et al. 2003). To mimic this signalling process *in vitro* another member of the TGFβ family- Activin A is used as it binds and activates the same receptors as nodal (de Caestecker 2004). The use of Activin A and low serum conditions can achieve cultures of up to 80% definitive endoderm cells, as measured by percentage of sox17 expressing cells (D'Amour,

Agulnick et al. 2005). These efficiencies can be increased further still with the use of Wnt3a (D'Amour, Bang et al. 2006), stimulating Wnt signalling which is an important regulator of mesendoderm and primitive streak formation (Liu, Wakamiya et al. 1999).

Following formation of definitive endoderm cells, removal of Activin A allows formation of cells resembling gut-endoderm (D'Amour, Bang et al. 2006). Pancreas specification of posterior foregut-like cells is initiated by inhibition of hedgehog signalling (Hebrok, Kim et al. 1998; Lau, Kawahira et al. 2006), which can be mimicked *in vitro* using FGF2 (bFGF) (Jiang, Au et al. 2007). Expansion of PDX-1 positive pancreatic progenitor cells can be induced by FGF10 signalling (Bhushan, Itoh et al. 2001; Ye, Duvillie et al. 2005). Noggin has also been shown to enhance differentiation of definitive endoderm into pancreatic endoderm (Jiang, Au et al. 2007; Kroon, Martinson et al. 2008; Zhang, Jiang et al. 2009).

The next stage of pancreas formation involves endocrine versus exocrine specification; endocrine cells are marked by *ngn*3 expression. EGF signalling plays a role in expansion of endocrine specified cells *in vivo* (Miettinen, Huotari et al. 2000), this effect of EGF can also be mimicked in *in vitro* differentiation protocols (Jiang, Au et al. 2007; Zhang, Jiang et al. 2009).

The final stages of beta-cell directed differentiation protocols employ factors such as extendin-4 (D'Amour, Bang et al. 2006), NGF (Navarro-Tableros, Fiordelisio et al. 2007), nicotinamide (Jiang, Au et al. 2007) and IGF11 (Jiang, Au et al. 2007) to induce the maturation and terminal differentiation of pancreatic beta cells. The final steps of pancreatic maturation remain the least well understood. Using protocols and signalling molecules similar to those discussed above, many groups have achieved insulin producing cells, however many of these cells are polyhormonal and do not represent fully mature pancreatic beta cells (D'Amour, Bang et al. 2006; Jiang, Au et al. 2007). Pancreatic progenitor cells transplanted into mice undergo a maturation process *in vivo* and exhibit functions of mature pancreas which cannot yet be replicated *in vitro* (Jiang, Shi et al. 2007; Kroon, Martinson et al. 2008). Much work remains to be performed to understand the *in vivo* molecular and signalling processes responsible for the maturation of transplanted progenitor cells.

1.5 Induced pluripotent stem cells

The generation of induced pluripotent stem cells (iPS cells) represents a significant advancement in stem cell research. iPS cells can be generated from somatic cell types by forced expression of stem cell related genes- *oct4, sox2, c-myc* and *klf4* (Takahashi and Yamanaka 2006; Takahashi, Tanabe et al. 2007), this technology overcomes the ethical and political concerns associated with human embryonic stem cell research, and also represents a potential avenue for the generation of autologous transplantation material.

At the time of undertaking this study, lentiviral based reprogramming techniques were the gold standard of reprogramming technologies, due to increased transduction efficiency compared to the original retroviral methods (Blelloch, Venere et al. 2007; Yu, Vodyanik et al. 2007). However, concerns remained about genomic modifications of iPS cells containing viral genes insertions at random integration sites. Since this work was completed a number of newer techniques using non-integrating plasmids, recombinant proteins and mRNAs have been developed to overcome these problems associated with viral based methods (Okita, Nakagawa et al. 2008; Kim, Kim et al. 2009; Zhou, Wu et al. 2009; Warren, Manos et al. 2010).

Initially, fibroblasts were typically the cell type selected for iPS reprogramming, as they had been previously shown to be capable of reprogramming via nuclear transfer and cell fusion techniques (Wakayama, Perry et al. 1998; Tada, Takahama et al. 2001; Cowan, Atienza et al. 2005). However, keratinocytes showed faster reprogramming rates and improved efficiency compared to fibroblasts (Aasen, Raya et al. 2008; Maherali, Ahfeldt et al. 2008). Cells with a progenitor or adult stem cell phenotype generally reprogram with increased efficiency compared to mature cell types, as these cell types already endogenously express at least one of the reprogramming factors (Kim, Zaehres et al. 2008). Factors which are endogenously expressed in the starting population cell type can be removed from the reprogramming cocktail, however this leads to a reduction in reprogramming efficiency compared to reprogramming with all four factors (Kim, Zaehres et al. 2008).

Molecular characterisation of colonies formed following treatment with reprogramming cocktail is vital to identify truly reprogrammed iPS cells, as semi-reprogrammed cells may exhibit morphology similar to ES cells (Takahashi, Tanabe et al. 2007). Nanog is the marker of choice for such applications, as is routinely used to differentiate truly reprogrammed from semi-reprogrammed cells, as this marker is exclusively expressed in true pluripotent cells (Maherali and Hochedlinger 2008). Oct4, sox2, c-myc and klf4 expression is also monitored during iPS cell generation, as viral expression of these genes should be detectable for the duration of the reprogramming protocol, however, once reprogrammed has occurred, viral transgene expression should be silenced and endogenous expression of these markers should begin.

iPS cells have been shown to possess similar if not equal differentiation potential as hES cells (Takahashi and Yamanaka 2006; Takahashi, Tanabe et al. 2007). A number of studies have demonstrated differentiation of iPS cells into pancreatic phenotypes, with similar efficiencies as that achieved with ES cells (Tateishi, He et al. 2008; Maehr, Chen et al. 2009; Zhang, Jiang et al. 2009), these differentiated iPS cells also exhibit insulin secretion properties, however, this insulin secretion profile more closely resembles that of fetal islets rather than mature pancreatic beta cells (Tateishi, He et al. 2008).

Progress in the understanding of normal pancreatic development, specifically the late stages of beta cell maturation will allow the design of more efficient directed differentiation protocols, which will bring the potential use of iPS derived pancreatic beta cells closer to the clinic.

1.6 MicroRNAs

MicroRNAs (miRNAs) are endogenous small non-coding RNAs of 19-28 nucleotides in length that regulate gene expression at the post-transcriptional level by binding to complementary sites in the 3' untranslated region (3'UTR) of target mRNAs. Based on the level of complementarity, miRNAs can direct mRNAs for degradation or translational repression (Bartel 2004). MiRNA biogenesis, function, and mechanisms of action is reviewed in full in appendix E (Hennessy and O'Driscoll 2008).

Of particular interest to the area of diabetes, miRNAs have been implicated to play a role in regulation of insulin secretion (Poy, Eliasson et al. 2004; Plaisance, Abderrahmani et al. 2006; Baroukh, Ravier et al. 2007; Lovis, Gattesco et al. 2008), pancreatic islet development and β-cell differentiation (Joglekar, Parekh et al. 2007; Joglekar, Parekh et al. 2007; Kloosterman, Lagendijk et al. 2007; Lynn, Skewes-Cox et al. 2007; Correa-Medina, Bravo-Egana et al. 2009; Joglekar, Joglekar et al. 2009; Poy, Hausser et al. 2009), insulin resistance (Teleman, Maitra et al. 2006; He, Zhu et al. 2007; Huang, Qin et al. 2009; Ling, Ou et al. 2009), and have been associated with secondary complications of diabetes, such as diabetic nephropathy (Kato, Zhang et al. 2007; Wang, Wang et al. 2008) and cardiovascular disease (Xiao, Luo et al. 2007; Wang, Qian et al. 2009). A number of miRNAs have been shown to be directly involved in glucose stimulated insulin secretion (GSIS); indicating potential therapeutic targets for enhancement of GSIS and β-cell function in type 2 diabetes patients.

1.6.1 miRNAs associated with β-cell insulin secretion

MiRNAs are critical for pancreatic beta cell function. MiRNA inactivation in adult murine beta cells resulted in establishment of a diabetic phenotype, as a result of dysfunctional insulin synthesis (Melkman-Zehavi, Oren et al. 2011). Mir-375 is, apparently, an important miRNA which negatively regulates GSIS in the murine insulinoma cell line, MIN6, and is thought to act at the late stages of exocytosis through its target myotrophin (Poy, Eliasson et al. 2004). Glucose is a negative modulator of mir-375 expression. Mir-375 also negatively regulates insulin gene expression in INS-1E cells by directly targeting PDK1, thereby glucose induced reduction of mir-375 ultimately leads to increased insulin gene expression (El Ouaamari, Baroukh et al. 2008). Mir-30d expression is also glucose modulated in MIN6 cells and mouse pancreatic islets; with up-regulation of mir-30d levels induced by high glucose concentrations. Over-expression of mir-30d in MIN6 cells leads to increased insulin gene expression, while knockdown leads to reduced expression (Tang, Muniappan et al. 2009), although it is unknown whether the effect of glucose-induced mir-30d, on insulin expression, is also mediated through PDK1. Mir-19b was also shown by luciferase reporter assay to directly target neuroD1 and hence regulate insulin 1 expression in MIN6 cells (Zhang, Zhang et al. 2011).

Another miRNA mir-124a, targets transcription factor foxa2, which in turn regulates PDX-1 (which regulates insulin transcription) and potassium channel subunits Kir6.2 and sur1. Overexpression of mir-124a leads to increased Ca^{2+} levels within MIN6 cells, possibly due to dysregulation of Kir6.2 and sur1 subunits (Baroukh, Ravier et al. 2007). Overexpression of mir-124a in MIN6 B1 cells led to increased insulin secretion in response to basal glucose concentrations and reduced secretion in response to stimulatory glucose concentrations (Lovis, Gattesco et al. 2008). Mir-124a affects the expression of a number of other exocytosis related proteins in MIN6 B1 cells including SNAP25, Rab3A, synapsin-1A, Rab27A and Noc2; although only Rab27A is a direct target of mir-124a (Lovis, Gattesco et al. 2008). These exocytosis-related proteins also have predicted binding sites for regulation by other miRNAs, but these still remain to be experimentally validated (Abderrahmani, Plaisance et al. 2006).

Mir-9 negatively regulates GSIS in INS-1E cells by directly targeting transcription factor onecut2, which in turn regulates granuphilin, a negative modulator of exocytosis (Plaisance, Abderrahmani et al. 2006). Mir-96 mediated reduction of GSIS in MIN6 B1 cells is also associated with reduced expression of granuphilin and Noc2 exocytosis related proteins.

High levels of mir-34a are observed in islets from diabetic db/db mice. Over-expression of mir-34a in MIN6 B1 cells leads to reduced GSIS, possibly through its target protein VAMP2 which plays a role in β-cell exocytosis (Lovis, Roggli et al. 2008). As each miRNA can target multiple mRNAs, regulation of insulin secretion may be controlled by a small network of miRNAs co-ordinately targeting the extensive range of proteins involved in regulation of exocytosis.

A more comprehensive understanding of the function of miRNAs in regulated insulin secretion could potentially identify miRNA targets which could be manipulated in order to maintain or enhance GSIS of replacement beta cells for treatment of type 1 diabetes, or for treatment of beta cell dysfunction associated with type 2 diabetes.

1.6.2 MiRNAs as therapeutic targets

Until recently, miRNAs had not been considered as classical therapeutic targets, as they do not code for proteins. Initial studies aimed at exploiting miRNAs as a form of therapy have shown promising results. Following intravenous injection of modified antisense oligonucleotides (termed antagomirs) into mice, *in vivo* inhibition of four miRNAs – mir-16, mir-122, mir-192 and mir-194 – has been successfully demonstrated (Krutzfeldt, Rajewsky et al. 2005). This approach resulted, not only in blockage of target miRNAs, but also in their degradation in most organs analysed, including liver, kidney, heart, lung, intestine, bone marrow, muscle, skin, fat, ovaries and adrenals. Lack of effect observed in brain is possibly due to restricted diffusion of charged nucleic acids across the blood–brain barrier. Alternative approaches to targeting miRNAs therapeutically by inhibiting Drosha, Dicer or other miRNA pathway components are being investigated as alternative approaches to targeting miRNAs directly. Conversely, where reduced miRNA expressed is associated with a disease phenotype and increased expression of relevant miRNA could be of potential therapeutic relevance to rescue disease phenotype, introduction of miRNA mimics is being investigated. However, suitable expression vectors have yet to be identified for the safe delivery and maintenance of such effects long-term (Esau and Monia 2007).

1.7 Biomarkers in diabetes

Type 1 diabetes typically brews for a number of years before symptoms become evident and the condition is diagnosed, by this stage approximately 80% of pancreatic cells are destroyed (Kloppel, Lohr et al. 1985). Once diagnosed, patients are on insulin treatment for the remainder for their life. Therefore, there is a great need to identify predictive biomarkers for type 1 diabetes, so that autoimmune attack of the pancreatic beta cells can be treated before the damage becomes irreparable.

1.7.1 MiRNAs as serum biomarkers

Serum microRNAs are highly stable, being resistant to RNaseA digestion and other harsh conditions (low/high pH, boiling, extended storage and freeze/thaw cycles) making them ideal for use in the clinical setting as biomarkers (Chen, Ba et al. 2008).

Serum miRNA expression profiling has demonstrated the presence of different miRNA expression patterns in pathological conditions such as NSCLC (Chen, Ba et al. 2008), colorectal cancer (Chen, Ba et al. 2008), diffuse large B-cell lymphoma (Lawrie, Gal et al. 2008), prostate cancer (Mitchell, Parkin et al. 2008), ovarian cancer (Resnick, Alder et al. 2008) and type 2 diabetes (Chen, Ba et al. 2008), as well as physiological conditions such as pregnancy (Chim, Shing et al. 2008; Gilad, Meiri et al. 2008).

A recent study of serum from pregnant females identified three miRNAs- mir-132, mir-29a and mir-222 associated with development of gestational diabetes and represent potential biomarkers for prediction of this pregnancy complication (Zhao, Dong et al. 2011). Distinct miRNA profiles have also been identified in patients with type 2 diabetes (Chen, Ba et al. 2008; Zampetaki, Kiechl et al. 2010), pre-diabetes, and patients with normal glucose tolerance but at risk of developing type 2 diabetes (Kong, Zhu et al. 2011). Table 1.1 details patient populations and main findings from these biomarker discovery studies. These miRNA profiles may represent potential biomarkers for prediction of type 2 diabetes and allow patients to make the relevant lifestyles changes required before establishment of the disease.

The scope for miRNA serum biomarkers spans a wide range of diseases and physiological conditions. Together with their stability, resistance to RNase degradation, and non-invasive procurement techniques would make them an ideal tool for disease diagnosis.

1.7.2 Protein biomarkers in diabetes serum

Proteins also represent a potentially useful class of serum biomarkers, as specific protein levels can be easily and sensitively measured in the clinical setting using ELISA technology. A range of proteomic profiling experiments on diabetes serum have been published in the literature, these studies identify specific protein profiles associated with type 1 diabetes (Metz, Qian et al. 2008), type 2 diabetes (Zhang, Sun et al. 2010), metabolic disease (Matsumura, Suzuki et al. 2006), as well as secondary complications of diabetes (Otu, Can et al. 2007; Gianazza, Mainini et al. 2010; Madan, Gupt et al. 2010), these studies are detailed in table 1.1. The promising results from these studies indicate the potential for protein biomarkers for prediction, diagnosis and management of diabetes.

1.7.3 Metabolite biomarkers in diabetes serum

Recent advances in mass spectrometry technologies in combination with data processing software for large scale metabolite profiling (Ryals, Lawton et al. 2007; Evans, DeHaven et al. 2009) has prompted a surge in metabolomic profiling experiments and biomarker studies which were previously unachievable. Metabolomic profiling of diabetes serum gives an insight into the extent of metabolomic dysregulation characteristic of diabetes. Distinct metabolite profiles have been identified for type 1 diabetes (Oresic, Simell et al. 2008; Lanza, Zhang et al. 2010), type 2 diabetes (Li, Xu et al. 2009; Suhre, Meisinger et al. 2010), pre-diabetes (Zhang, Wang et al. 2009; Gall, Beebe et al. 2010; Lucio, Fekete et al. 2010; Tsutsui, Maeda et al. 2010; Zhao, Fritsche et al. 2010), as well as secondary complications of diabetes (Xia, Liang et al. 2009; Zhang, Yan et al. 2009). The main findings of these studies are detailed in table 1.1. Metabolite biomarkers have been used extensively over the years for monitoring disease, e.g. glucose for diabetes, cholesterol for heart disease, the use of straight forward, rapid biochemical assays for metabolite quantification also makes metabolites an ideal candidate for biomarker identification.

Condition	Biomarker Type	Study Population	Findings	Reference
Gestational Diabetes	miRNA	68 gestational diabetes patients and 68 controls	Decreased levels of mir-29a and mir-222 associated with gestational diabetes.	(Zhao, Dong et al. 2011)
Type 2 diabetes	miRNA	Study population not detailed in publication	Identified a miRNA fingerprint for type 2 diabetes, including 3 diabetes specific miRNAs (not named in the publication).	(Chen, Ba et al. 2008)
Type 2 diabetes	miRNA	18 newly diagnosed type 2 diabetes patients (n-T2D), 19 pre-diabetes patients, 19 type 2 diabetes susceptible patients with normal glucose tolerance (s-NGT)	Increased levels of mir-9, mir-29a, mir-30d, mir-34a, mir-124a, mir-146a and mir-375 during disease progression.	(Kong, Zhu et al. 2011)
Type 2 diabetes	miRNA	80 type 2 diabetes patients and 80 controls	Decreased levels of mir-20b, mir-21, mir-24, mir-15a, mir-126, mir-191, mir-223, mir-320 and mir-486, while increased levels of mir-28-3p in type 2 diabetes serum.	(Zampetaki, Kiechl et al. 2010)
Type 1 diabetes	Protein	10 type 1 diabetes patients, 4 type 1 diabetes patients with diabetic nephropathy and 9 controls	Increased levels of fibrinopeptide A in type 1 diabetes serum, while decreased levels of fibrinopeptide A fragments in patients with type 1 diabetes alone and type 1 diabetes with nephropathy.	(Gianazza, Mainini et al. 2010)
Diabetic nephropathy	Protein	31 type 2 diabetes patients with diabetic nephropathy and 31 type 2 diabetes patients without nephropathy	Identified a 12-peak proteomic signature which predicts type 2 diabetes patients who will subsequently develop diabetic nephropathy.	(Otu, Can et al. 2007)
Diabetic microvascular complications	Protein	Type 2 diabetes patients with (n=40) and without (n=20) diabetic microvascular complications, and 30 control healthy samples	PAI-1, fibrinogen, vWF increased in T2D compared to healthy controls. Diabetic retinopathy associated with decreased protein S and vWF levels. Diabetic nephropathy associated with increased PAI-1 and vWF levels.	(Madan, Gupt et al. 2010)

Type 2 diabetes	Protein	Serum from rat model of type 2 diabetes, and control heathy rat (n=1)	Differential expression of apolipoproteins and α2-HS-glycoprotein in serum from type 2 diabetes rat compared to non diabetic control.	(Matsumura, Suzuki et al. 2006)
Type 2 diabetes	Protein	10 type 2 diabetes rats, and 10 healthy control rats	Decreased levels of apolipoprotein E, apolipoprotein A-1, Ig gamma-2A chain C region, and increased levels of transthyretin, haptoglobin, serum amyloid P-componen, prothrombin were identified in type 2 diabetes compared to control healthy rats.	(Zhang, Sun et al. 2010)
Type 1 diabetes	Protein	10 newly diagnosed type 1 diabetes patients, and 10 healthy controls	Increased levels of α-2-glycoprotein 1, corticosteroid-binding globulin, lumican, and decreased levels of clusterin and serotransferrin in type 1 diabetes compared to control samples.	(Metz, Qian et al. 2008)
Type 1 diabetes	Metabolite	56 patients who subsequently progressed to type 1 diabetes, and 73 non-diabetic controls	Increased levels of succinic acid and phosphatidylcholine at birth in patients who would later develop type 1 diabetes. Reduced levels of triglycerides and antioxidant ether phospholipids, and increased levels of proinflammatory lysoPCs before seroconversion to autoantibody positivity.	(Oresic, Simell et al. 2008)
Type 1 diabetes	Metabolite	Type 1 diabetes patients during insulin treatment and acute insulin deprivation (n=9), and non-diabetic controls (n=9)	Increased levels of lactate, acetate, allantoin and ketones identified during insulin deprivation. Protein synthesis and breakdown, gluconeogenesis, ketogenesis, amino acid oxidation, mitochondrial bioenergetics and oxidative stress pathways altered during insulin deprivation.	(Lanza, Zhang et al. 2010)
Type 2 diabetes	Metabolite	48 type 2 diabetes patients and 31 healthy controls	2-hydroxyisotubyric acid, linoleic acid, palmitic acid and phosphate levels correctly distinguished type 2 diabetes and control specimens.	(Li, Xu et al. 2009)
Type 2 diabetes	Metabolite	40 type 2 diabetes patients and 60 healthy controls	Alterations in pathways related to kidney dysfunction (3-indoxyl sulphate), lipid metabolism	(Suhre, Meisinger et

			(glycerophospholipids, free fatty acids), and interaction with the gut microflora (bile acids) were identified in type 1 diabetes patients.	al. 2010)
Pre-type 2 diabetes	Metabolite	399 non diabetes subjects with a range of insulin sensitivities and glucose tolerance	Identified α-hydroxybutyrate as an early marker of both insulin resistance and impaired glucose regulation.	(Gall, Beebe et al. 2010)
Pre-type 2 diabetes	Metabolite	48 non-diabetic subjects exhibiting high to low insulin sensitivities	Identified alterations in lipid-related pathways (arachidonic acid metabolism, essential fatty acid metabolism, and biosynthesis of unsaturated fatty acids), steroid hormone biosynthesis and bile acid metabolism associated with changes in insulin sensitivity.	(Lucio, Fekete et al. 2010)
Pre-type 2 diabetes	Metabolite	Diabetic mice and normal control mice (number of mice in each group not specified in the publication)	Alterations in metabolites related to lysine biosynthesis and degradation were identified in diabetic compared to control mice, before onset of type 2 diabetes.	(Tsutsui, Maeda et al. 2010)
Pre-type 2 diabetes	Metabolite	39 subjects with normal glucose tolerance, and 12 subjects with impaired glucose tolerance	Alterations in fatty acid, tryptophan, uric acid, bile acid and lysophosphatidylcholine metabolism, and TCA cycle associated with pre-diabetes state. Decreased levels of gut flora-associated metabolites (hippuric acid, methylxanthine, methyluric acid and 3-hydroxyhippuric acid) identified in subjects with impaired glucose tolerance.	(Zhao, Fritsche et al. 2010)
Pre-type 2 diabetes	Metabolite	Subjects with normal glucose tolerance (n=80), impaired glucose tolerance (n=77) and type 2 diabetes (n=74)	Alterations in choline, glucose and amino acid metabolism, and TCA cycle identified in type 2 diabetes and impaired glucose tolerance subjects compared to normal glucose tolerance subjects. Alterations in glucose, fatty acid, protein/amino acid metabolism identified in impaired glucose tolerance subject compared to type 2 diabetes subjects.	(Zhang, Wang et al. 2009)

Type 2 diabetes and diabetic nephropathy	Metabolite	8 diabetic nephropathy patients, 33 type 2 diabetes patients and 25 healthy controls	Alterations in leucine, dihydrosphingosine and phytoshpingosine were identified in type 2 diabetes patients with and without diabetic nephropathy compared to healthy control specimens.	(Zhang, Yan et al. 2009)
Diabetic nephropathy	Metabolite	88 subjects with diabetic nephropathy and 50 healthy control subjects	Altered levels of adenosine, inosine, uric acid, xanthine and creatinine in diabetic nephropathy subjects compared to healthy controls.	(Xia, Liang et al. 2009)

Table 1.1 MiRNA, proteomic and metabolomic profiling studies for the identification of biomarkers for type 1 diabetes, type 2 diabetes, pre-diabetes and secondary complications of diabetes.

Aims

MicroRNAs involved in glucose stimulated insulin secretion in MIN6 cells:

- To investigate the mechanisms of regulated insulin secretion, in particular, the role of miRNAs in this process.
- To profile miRNA expression in glucose responsive and glucose non-responsive MIN6 cells, to identify miRNAs differentially expressed in these cell populations.
- To determine if these differentially expressed miRNAs have a direct effect on regulated insulin secretion by over-expression and knockdown of miRNA targets, while monitoring GSIS response.

Attempt to generate iPS cells and differentiation of an established iPS cell line towards pancreatic phenotypes:

- To generate iPS cells using retroviral and conditioned media reprogramming techniques, followed by subsequent testing of reprogramming status by analysis of pluripotency marker expression.
- To compare directed differentiation of iPS cells in 3D and 2D culture systems. To evaluate differentiation efficiency by PCR analysis of differentiation and pluripotency marker expression.
- To determine transdifferentiation potential of human limbal stromal cells towards pancreatic phenotypes, measured by PCR analysis of pancreatic marker expression.

Biomarker discovery in diabetes serum specimens:

- To determine if GSIS related miRNAs are differentially expressed in serum specimens from type 1 and type 2 diabetes patients.
- To perform proteomic, metabolomic and miRNA profiling on serum from diabetes patients to identify potential disease biomarkers.
- To validate potential protein, metabolite and miRNA markers in a larger cohort of patients to evaluate if expression trends were maintained in larger sample size study.

2.0 Materials and Methods

2.1 Culture of cell lines

2.1.1 Cell lines

The cell lines used during the course of this study are listed in table 2.1. Cell lines were maintained under standard culture conditions, 5% CO_2, at 37ºC and fed every 2-3 days, except iPS cells which were fed every day.

Cell Line	Cell Type	Source
MIN6	Murine pancreatic beta cells	Dr. Per Bendix Jeppesen*
iPS (hFib2-iPS4)	Human induced pluripotent stem cells	Dr. George Daley**
MEF	Mouse embryonic fibroblasts	ATCC
293	Human embryonic kidney cells	Stratagene
MiaPaCa2	Human pancreatic carcinoma cells	ATCC
NHEK	Normal human epidermal keratinocytes	ATCC
L-epi	Limbal epithelial cells	Mr. Kishore Reddy***
Stromal	Limbal stromal cells	Mr. Kishore Reddy***
ESD3	Mouse embryonic pluripotent stem cells	ATCC

Table 2.1. Cell lines used in this study

*Dr. Per Bendix Jeppesen, Aarhus University, Denmark.

****Dr. George Daley, Howard Hughes Medical Institute and Children's Hospital Boston.

***Limbal epithelial and stromal cells were isolated from donor cornea-sclera ring by Mr. Kishore Reddy, NICB. Donor cornea retrieved by Dr. William Murphy at The Royal Victoria Eye and Ear Hospital, Dublin.

2.1.2 Preparation of cell culture media

DMEM for culture of MIN6 cells was purchased pre-made at 1X concentration (Gibco 21885). DMEM/F12 (D8437), DMEM (D5671), MEM (M5650) and RPMI (R8758) for culture of additional cell-lines used in this thesis were also purchased at 1X concentration from Sigma Aldrich. Basal media was stored at 4^{o}C up to their expiry date as specified on each individual container. Working stocks of culture media were prepared as 100mL aliquots and supplemented as required (table 2.2). These were stored for up to 3 weeks at 4^{o}C, after this time, fresh culture medium was prepared.

Cell Line	Basal Media	FCS (%)	Additives
MIN6	DMEM	10	880µL of 45% glucose solution (Sigma G8769) / 100mL media
iPS (hFib2-iPS4)	DMEM/F12		20% Knockout serum, 1mL L-Glutamine, 1mL Non-essential amino acids, 3.5µL β-mercaptoethanol, 10ng/mL bFGF
MEF	DMEM	10	4mM L-Glutamine
293	DMEM	5	4mM L-Glutamine
MiaPaCa2	DMEM	5	4mM L-Glutamine
NHEK	KBM (Lonza CC-3103)		KGM SingleQuots (Lonza CC-4152)
L-epi	DMEM+HAM F12 (3:1)	10	5ug/mL insulin, 10ng/mL rhEGF, 100ng/mL cholera toxin A subunit, 0.4µg/mL hydrocortisone, 2nM triiodothryonine
Stromal	DMEM	10	N/A
ESD3	DMEM	10	0.1mM 2-mercaptoethanol, 2000U LIF / 100mL media

Table 2.2 Media requirements for cell lines used in this study (N/A- non applicable).

2.1.3 Subculture of cell lines

Prior to subculture, cells were monitored for contamination and were subcultured when cells reached 70-80% confluency. The cell culture medium was removed from the tissue culture flask and discarded into a sterile waste bottle. The flask was then rinsed with 10mL pre-warmed 1X Ca^{2+}/Mg^{2+}- free PBS (Gibco, 14200-067). 1.5mL trypsin/EDTA solution (0.25% trypsin, 0.01% EDTA in PBS) was then added; the flask was given a gentle swirl to coat the surface (for MIN6 cell-line, trypsin-EDTA solution was then removed). The flask was then incubated at 37^{o}C for 5 minutes. 10mL culture media was added to inactivate the trypsin and the cell suspension was removed and placed in a sterile universal container. Cells were centrifuged at 1000 rpm for 5 minutes. The supernatant was discarded from the universal and the pellet re-suspended in pre-warmed culture medium, media was aspirated up and down a number of times to ensure a single-cell suspension. A cell count was performed and cells re-seeded to flasks or assay plates at the required density.

2.1.3.1 Subculture of iPS cells

IPS cells were subcultured as per protocol from Harvard Stem Cell Institute. Cells were washed with PBS before addition of 1mL collagenase (200 units/mL) per well of a 6-well plate and incubated at 37ºC for 10 minutes. When visible curling and thickening of colonies around the edges was seen, collagenase was removed and 1mL of iPS media was added. iPS cell clusters were scraped from the plate using a Pasteur pipette. The solution containing loosened cell clusters was placed into a universal tube, the well was rinsed with an additional 1mL iPS media, and this was also transferred into the universal tube. The cell suspension was centrifuged at 1000 rpm for 2 minutes, supernatant was removed and cell clusters were resuspended in fresh media, avoiding excess pipetting to maintain cell clusters. iPS clusters were then plated in 6-well plate pre-coated with gelatin and irradiated MEF feeder layer, at the ratio of 1:6.

2.1.4 Cell counting

Cell counting and viability determinations were carried out using a trypan blue (Gibco, 15250-012) dye exclusion technique.

Cells were trypsinised, pelleted and resuspended in media. An aliquot of the single-cell suspension was then added to trypan blue at a ratio of 5:1. After 3 minutes incubation at room temperature, a sample of this mixture was applied to the chamber of a haemocytometer over which a glass cover slip had been placed. Cells in the 16 squares of the four outer corner grids of the chamber were counted microscopically. The average cell numbers per 16 square corner grid was calculated taking into account the dilution factor, and multiplied by a factor of 10^4 to determine the number of cells per mL in the original cell suspension. Non-viable cells stained blue, while viable cells excluded the trypan blue dye as their membranes remained intact, and remained unstained. On this basis percentage viability could be calculated.

2.1.5 Cryopreservation of cells

Freezing media was prepared as described in table 2.3 and then placed on ice until required. Appropriate number of cryogenic vials (Greiner, 122 278) were labelled with the cell line name, passage number, date and placed on ice at this point. Cells were trypsinised and counted as outlined in section 2.1.3 and 2.1.4. The supernatant from the centrifuged cells was removed and the cell pellet resuspended in freezing media to a cell density of $5x10^6$ cells/mL. 1mL of cell suspension in freezing media was then added to each pre-cooled cryovial. Cryovials were placed on ice for 10 minutes, and then transferred to a -80^oC freezer overnight in a Boehringer Mannheim enzyme box, and then placed in liquid nitrogen for storage.

Cell Line	Freezing Media 1X
MIN6	Complete media + 10% DMSO
iPS (hFib2-iPS4)	50% complete media + 40% FCS + 10% DMSO
MEF	FCS + 10% DMSO
293	FCS + 5% DMSO
MiaPaCa2	FCS + 5% DMSO
Stromal	80% DMEM + 10% FCS + 10% DMSO
ESD3	FCS + 20% DMSO

Table 2.3 Freezing media composition

2.1.6 Thawing of cryopreserved cells

Prior to thawing 8mL of culture media was added to a tissue culture flask and allowed to equilibrate in a 37°C, 5% CO_2 humidified incubator overnight. A sterile universal tube containing 5 mL growth medium was pre-warmed before thawing cells. This allowed for the rapid transfer and dilution of thawed cells to reduce their exposure time to the DMSO freezing solution (DMSO is toxic at room temperature). For thawing iPS cells, media was supplemented with 10mM ROCK inhibitor Y27632 (Calbiochem, 688000). The cryovial taken from the liquid nitrogen storage and immediately diluted with media using a Pasteur pipette, and its contents were transferred to the universal. The suspension was centrifuged at 1000 rpm for 5 minutes (2 minute for iPS cells), the DMSO-containing supernatant was removed and the pellet was then resuspended in fresh growth medium, ensuring a single-cell suspension was achieved (minimal pipetting was used for iPS cells to maintain cell clusters). Viability counts were carried out (section 2.1.4) to determine the efficacy of the freezing/thawing procedures. Thawed cells were placed in tissue culture flasks with the appropriate volume of medium and allowed to attach overnight. The following day cells were fed with fresh warmed medium to remove any residual traces of DMSO.

2.1.7 Irradiation of cells

Mouse embryonic fibroblasts (MEF) were routinely maintained in DMEM, 5% FCS. To harvest for irradiation, cells were trypsinised at 60-70% confluency, washed and transported in HBSS (Ca^{2+} and Mg^{2+} free) to the cell irradiator, which was a MDS Nordion Gammacell 3000. Inactivation of MEFs was achieved by treatment with a 30 gray radiation dose. Irradiated MEF were stored in liquid nitrogen in freezing media containing 10% DMSO, at a cell density of 500,000 cells per vial, sufficient for seeding 3 wells of 6-well plate.

2.1.8 Sterility checks

Sterility checks were routinely carried out on all media and supplements used for cell culture. Samples of basal media were inoculated into columbia blood agar plates (Oxoid, CM331), sabauraud dextrose (Oxoid, CM217) and thioglycollate broths (Oxoid, CM173) which enable detection of most contaminants including bacteria, fungus and

yeast. All cell lines used in this study were mycoplasma-free, testing was carried out in-house every four months.

2.2 Specialised techniques in cell culture

2.2.1 Glucose stimulated insulin secretion (GSIS) assay of cultured cells

The GSIS profile of MIN6 cells was examined at glucose concentrations of 3.3 and 16.7 mmol/L. MIN6 cells were seeded at 2×10^5 cells/well in a 24-well plate and allowed to grow for 72 hours prior to the GSIS assay. Following this, 1X KRB (Krebs–Ringer Bicarbonate) was prepared from an aliquot of frozen 10X stock (36.525g NaCl, 2.2g KCl, 0.941g $CaCl_2.2H_2O$ and 1.22g $MgCl_2.6H_2O$ dissolved in 500mL H_2O), BSA and HEPES were added to a final concentration of 0.1% and 25mM respectively. The KRB–BSA was adjusted to pH 7.4 with 1M NaOH. This solution was incubated for 30 minutes at 37°C and 5% CO_2. Glucose concentrations of 3.3 and 16.7mmol/L were prepared with conditioned 1X KRB and placed at 37°C and 5% CO_2 for 30 minutes. MIN6 cells to be analysed were rinsed twice in 1X KRB and were equilibrated with 1X KRB for 15 minutes at 37°C. After equilibration, the glucose-containing media was added (1mL/well), incubated at 37°C and 5% CO_2 for 60 minutes. The GSIS assay was then terminated by placing the plate on ice. Conditioned medium (300µL) was removed from each well, placed in an ice-cold eppendorf tube, centrifuged at 1000 rpm for 2 minutes and 200µL supernatant was removed for analysis by (pro)insulin ELISA (Mercodia, AB, Sylveniusgatan, Uppsala, Sweden 10-1124-10) (see section 2.2.2). A volume of 200µL of 0.1M NaOH was added to each well to lyse cells for protein assay normalisation (section 2.2.3). Plates were then stored at -20ºC until required.

2.2.2 ELISA Analysis for Insulin and Proinsulin

Analysis of conditioned media was carried out using an insulin ELISA kit (Mercodia, 10-1124-10). The kit was supplied with reagents, standards and pre-coated ELISA plates. Standard protocol was followed as per manufacturer's instructions. In brief, standards and samples (25µL) were added directly to the coated plate (mouse monoclonal anti-insulin) in triplicate. 50µL conjugate solution (enzyme conjugate 11X in enzyme conjugate buffer) was then added to the samples and standards. The plate was wrapped in foil (to prevent debris falling into the wells) and incubated at room temperature for 2 hours on a belly dancer set to maximum speed. Following this, the conjugate/sample mixes were tapped off into the sink and the wells were washed 6 times with washing solution (wash buffer 21X diluted with UHP). After washing, the plate was tapped firmly on absorbent tissue to remove the excess wash solution. At this point 200µL peroxidase substrate was added to each well. As it is light sensitive, this reaction was allowed to develop in the dark (the plate was wrapped in tinfoil) for 15 minutes and stopped by adding 50µL stop solution per well. The plates were mixed gently and read at 405nm on a plate reader (BIO-TEK®, Synergy HT).

2.2.3 Protein quantification

Lysed samples were removed from the freezer and placed on ice. A BSA stock solution of 1mg/mL was prepared in UHP. Diluted BSA standards of 0, 0.2, 0.4, 0.6 and 0.8mg/mL were prepared and 5µL of standards or sample were placed in triplicate wells on a 96-well plate (Costar, 3596). The Biorad D_c Protein Assay was used for protein quantification. 25µL of Reagent A (Bio-Rad, 500-0113) followed by 200µL of Reagent B (Bio-Rad, 500-0114) were added to each test well. The plate was kept in the dark at room temperature for 15 minutes prior to reading absorbance at 750nm on a plate reader.

2.2.4 MiRNA transfection for monitoring GSIS

MIN6 cells were transfected with Ambion® Pre-miR™ miRNA precursors and Ambion® Anti-miR™ miRNA inhibitors). Ambion® Pre-miR™ miRNA precursors are chemically modified dsRNA molecules designed to mimic mature miRNA molecules. They enable functional analysis of individual microRNAs via "gain-of-function" experiments. Ambion® Anti-miR™ miRNA inhibitors are chemically modified, single stranded nucleic acids designed to specifically bind to and inhibit mature miRNA molecules. They enable detailed study of miRNA biological effects via "reduction-of-function" experiments. Pre-mir negative was used as a negative control for pre-mir experiments. Anti-mir negative was used as a negative control for anti-mir experiments.

Cell suspensions were prepared at a cell density of $4x10^5$ cells/mL. Solutions of pre/anti-mirs and negative controls were prepared in optiMEM (final concentration 50nM). 2μL lipofectamine was diluted in 50μL optiMEM per well to be transfected, mixtures were incubated at room temperature for 5 minutes. After incubation diluted lipofectamine was added to each pre/anti-mir and negative control mix and incubated for a further 20 minutes. 100μL of pre/anti-mir/lipofectamine mix was added per well of 24-well plate. 500μL cell suspension was then added to each well to achieve a final concentration of $2x10^5$ cells/well, with 50nM pre/anti-mir and 2μL lipofectamine per well. Plates were gently mixed and incubated at 37ºC for 24 hours. At 24 hours the transfection media was removed and replace with complete growth media. Cells were allowed to grow for a further 48 hours until GSIS assay was performed (section 2.2.4) to determine effect of transfection on GSIS capacity of MIN6 cells.

2.2.5 Differentiation towards pancreatic cell types

Cells were differentiated in either 2D or 3D culture. For 2D cultures 6-well plates were pre-coated with 1:20 dilution of matrigel (BD Biosciences, 354230) in DMEM for 30 minutes prior to seeding cells. Cells to be differentiated were then added directly to the pre-coated plates and allowed to attach for 24 hours before addition of differentiation media. For 3D cultures, 24-well plates were percolated with 1.5mg/mL collagen type 1 for 30 minutes. Cells to be differentiated were suspended in 600μL of media containing 1.5mg/mL collagen type 1 and 200μL of matrigel. 800μL was then added to each well of a 24-well plate. 3D cultures were allowed to gel for 2 hours, then 350μL of media was added per well. Cells were allowed to proliferate for up to 3 days in 3D culture before initiation of differentiation.

2.2.5.1 Directed differentiation protocol

Cells in 2D and 3D culture were treated with either differentiation media or control media. For iPS differentiation experiments control media consisted of iMEF conditioned iPS media. For stromal cell differentiation experiments control media consisted of standard stomal media - DMEM 10% FCS. Directed differentiation consisted of four stages, summarised in figure 2.1.

Stage 1: Definitive endoderm induction

Cells were treated with RPMI media supplement with 1X B27 (Invitrogen, 0080085-SA), 4nM Activin A (R&D Systems, 338-AC), and 1mM Sodium Butyrate (Sigma, B5887) for 24 hours. Media was changed to RPMI, B27, 4nM Activin A and 0.5mM sodium butyrate, cells were cultured in this for 6 days. On day 8 cells were harvested for RNA to check expression of definitive endoderm markers.

Stage 2: Pancreatic endoderm induction

Cells in 2D culture were treated with 200units/mL collagenase IV and each well of a 6-well plate was transferred to a well of an ultra-low attachment 6-well plate, while cells in 3D culture were maintained in the original 24 well plate. Media was changed to RPMI/B27 supplemented with 20ng/mL EGF (R&D systems, 236-EG), 2ng/mL bFGF (Invitrogen, 13256-029) and 100ng/mL noggin (R&D systems, 1967-NG). Cells were maintained in this media for 2 weeks. On day 22 cells were harvested for RNA to check expression of pancreatic endoderm markers.

Stage 3: Endocrine induction

Cells were cultured in RPMI/B27 media supplemented with 20ng/mL EGF and 100ng/mL noggin for 1 week. On day 29 cells were harvested for RNA to check expression of endocrine markers.

Stage 4: Islet maturation

Cells were cultured in RPMI media supplemented with 0.5% BSA (Sigma, A7888), 10mM nicotinamide (Sigma, N0636) and 50ng/mL insulin-like growth factor (R&D systems, 292-G2) for 5 days. Media was then changed to RPMI, 0.5% BSA and 10mM

nicotinamide for a further 2 days. On day 36 cells were harvested for RNA to check expression of mature islet markers.

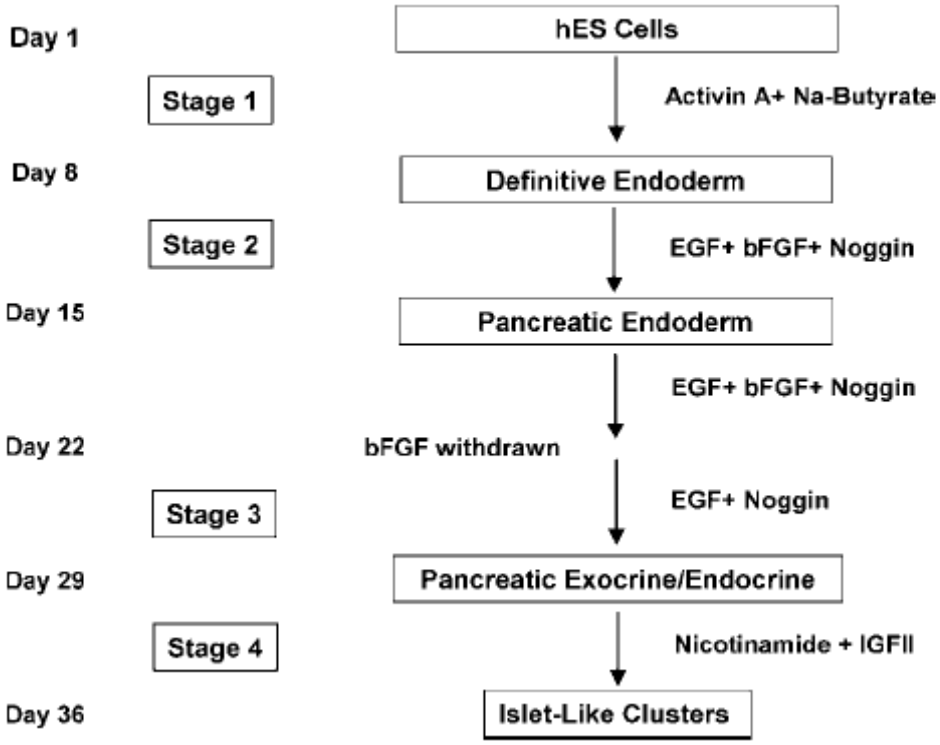

Figure 2.1 Summary of directed differentiation protocol used in this study for generation of pancreatic cells from iPS cells (Jiang, Au et al. 2007).

2.2.6 Generation of hanging drop cultures

Stromal cells were trypsinised and a cell count performed. Cells were centrifuged at 1,000 rpm for 5 minutes. Cell pellet was resuspended at a cell density of $1x10^6$ cells/mL. 20μL drops of cell suspension were placed of the inside lid of a petri dish, the lid was covered with drops and then placed on the petri dish base, 10mL water was added to the petri dish base to prevent evaporation of media. Hanging drops were incubated for 48 hours, and then transferred to suspension culture in petri dish coated with 2% agar. Cell clusters were maintained in suspension culture for 48 hours before seeding 2D, 3D or monolayer differentiation studies (section 2.2.5).

2.3 Lentivirus Techniques

2.3.1 Generation of Lentiviral Particles

Lentiviral particles were generated by co-transfecting the lentiviral ORF expression clone containing oct4 [EX-T2820-Lv07], sox2 [EX-T2547-Lv07], c-myc [EX-Z2845-Lv07] or klf4 [EX-Z2836-Lv07] gene together with the lentiviral packaging plasmids (GeneCopoeia PLv-PK-01). The lentiviral ORF plasmid contains the elements required for packaging, transduction and stable integration of the viral construct into the host genomic DNA. While the lentiviral packaging plasmids contain the elements required for transcription and packaging of an RNA copy of the ORF construct into active viral particles.

2.3.1.1 Transformation of ORF expression clones

ORF expression clones were supplied by Genecopoeia on filter paper discs. To reconstitute the plasmids the filter paper discs were placed in 1.5mL centrifuge tubes containing 50µL TE buffer. Tubes were then incubated for 60 minutes at room temperature to allow resolubilisation of plasmids.

To perform the transformation OneShot Max Efficiency DH5α T1 competent cells (Invitrogen 12297-016) were allowed to thaw on ice. 50µL of competent cells were added to 3µL of the reconstituted plasmids, or 3µL of pUC19 plasmid as a control transformation. Tubes were flicked to ensure even mixing of plasmid with cells and placed on ice for 5 minutes. Cell/plasmid mixtures were then heat-shocked for 30 seconds at 42ºC, and then placed back on ice for 2 minutes. 500µL of pre-warmed SOC media (supplied with competent cells) was added to the cells/plasmid mix and incubated in a shaking incubator at approximately 250rpm at 37ºC for 45 minutes to allow cells to recover from the heat-shock. 100µL of transformation mixture was spread onto LB agar plates and incubated at 37ºC overnight.

2.3.1.2 Generation of ORF expression clone plasmid stocks

Transformation colonies were picked and a single colony was seeded into 5mL LB broth cultures and incubated in a shaking incubator overnight. 1.5mL of culture media was then used to seed a 250mL large scale culture. After overnight incubation in a shaking incubator at 37ºC, plasmid DNA was harvested using Endofree Plasmid Maxi Kit (Qiagen 12362) as per manufacturer's instructions. DNA concentration was assessed using the Nanodrop (section 2.4.4) and then stored at -80ºC until required.

2.3.1.3 Plasmid transfection to generate viral particles

293 cells were seeded in 90mm tissue culture dishes at a density of $4x10^6$ cells/plate approximately 6 hours before performing transfection. DNA mix was prepared by adding 1µg of each of the packaging plasmids with 2µg of the ORF expression clone plasmid, made up to 15µL with TE buffer. Fugene was prepared by adding 18µL Fugene 6 (Roche, 11814443001) to 200µL opti-MEM reduced-serum media (Invitrogen, 11058-021) and allowed to stand for 5 minutes. DNA mix was added to diluted fugene mix and incubated at room temperature for 15 minutes. Media was removed from pre-plated 293 cells and replaced with 8mL fresh DMEM, the fugene/DNA mix was then added dropwise to the culture, swirled and incubated at 37ºC. At 24 hours post transfection media containing Fugene was removed and fresh low serum media (DMEM 2% FCS) was added. Conditioned media was harvested at 48 and 72 hours post-transfection and filtered with 0.45µM low protein binding filter. Conditioned media containing active viral particles was then aliquoted and stored at -80ºC until required.

2.3.2 Lentivirus transduction for generation of iPS cells

Cells to be transduced were seeded at a density of $5x10^4$ cells/well in a 6-well plate one day before transduction. Media was removed and replaced with 1mL of fresh media per well. 250µL of each of the 4 viruses (oct4, sox2, c-myc and klf4) were mixed with 1µL of 8mg/mL polybrene, added dropwise to the well and incubated at 37ºC. After 24 hours, media was removed and 1mL of fresh media added per well. 250µL of each of the viruses were mixed with 1µL polybrene, added drop wise to the well and incubated at 37ºC. After 24 hours, virus containing media was removed and replaced with fresh media. Five days after virus treatment, cells were trypsinised and cells from a single well of a 6-well plate were seeded into a 90mm tissue culture dish pre-coated with irradiated MEF cells. 24 hours after trypsinisation media was changed to iPS media. Colonies should appear approximately 10 days after trypsinisation.

2.3.3 Conditioned media generation of iPS cells

Conditioned media induction of reprogramming was performed using limbal epithelial cells, using a protocol adapted from Balasubramanian *et al*., (Balasubramanian, Babai et al. 2009). Limbal epithelial cells were isolated from donor corneal-sclera ring using the explant technique. This involved growing of cells from explants on a transwell membrane with 3T3 feeder layers in the lower chamber. Once limbal epithelial cells began to emerge from the explants, cells were treated with enriched media (1X B27, 20ng/mL EGF, 10ng/mL bFGF and 100ng/mL noggin) for 7 days, followed by treatment with ESD3 conditioned media (50% ESD3 conditioned media, 48% ES media and 2% FCS) for 10 days. In this study B27 supplement was used in the enriched media instead of N2 supplement used by Balasubramanian *et al.,* 2009.

2.3.3.1 Collection of ESD3 conditioned media

ESD3 cells were grown on 0.1% gelatin coated flasks. Conditioned media was collected once cells reached 60% confluency. Conditioned media was centrifuged at 1,800rpm for 5 minutes, filtered using 0.45μm filter and stored at -20ºC until required.

2.4 RNA Analysis

2.4.1 RNA isolation cells using MirVana kit

To analyse levels of RNA in cells, cell pellets of $1x10^5$ cells were prepared. Cell pellets were washed twice with PBS and then stored at -80ºC until required. MirVana miRNA isolation kit (AM1560, Applied Biosystems) was used for all RNA analysis studies in section 3.1. MirVana miRNA isolation kit contains all wash buffers, lysis buffer and reagents required for the procedure, standard protocol was performed as per manufacturer's instructions. In brief, 600µL lysis buffer was added to cell pellets, pipetting up and down to ensure complete lysis of cells. 1/10 volume of miRNA homogenate additive was added; mixed by vortexing and allowed to stand on ice for 10 minutes. A volume of acid-phenol:chloroform (equal to the volume of lysis buffer added i.e. 600µL) was added, vortexed for 60 seconds and centrifuged for 5 minutes at maximum speed. The aqueous (upper) phase was carefully removed without disturbing the lower phase, and transferred to a fresh tube, taking note of the volume removed. 1.25 times the noted volume of 100% ethanol was added to the aqueous phase and transferred to the filter cartridge in a collection tube. Up to 700µL was applied at a time, for larger samples larger the mixture was applied in successive applications to the same filter. Mixture was centrifuged for 15 seconds at 10,000 rpm, the eluent was discarded, and this was repeated until all of the lysate/ethanol mixture was through the filter. 700µL miRNA wash solution 1 was applied to filter and centrifuged for 10 seconds. Flow-through was discarded. 500µL wash solution 2/3 was applied and centrifuged for 10 seconds. Flow-through was discarded and wash step repeated with wash solution 2/3. Flow-through was discarded and filter cartridge was centrifuged for 1 minute to remove residual fluid from the filter. Filter cartridge was transferred to fresh collection tube; 25µL RNase free water (pre-heated to 95ºC) was applied to the filter cartridge, taking care to cover the entire surface of the filter. This was centrifuged for 30 seconds at maximum speed to recover RNA, and repeated with 25µL RNase free water and centrifuged for a further 30 seconds at maximum speed, the eluent was collected and store at -80ºC until required.

2.4.2 RNA isolation from cells using TriReagent

RNA isolation using TriReagent was used for RNA analysis in section 3.2. 1mL TriReagent was added per well of 24-well plate for RNA isolation. These samples were allowed to stand for 5 minutes at room temperature to allow complete dissociation of nucleoprotein complexes. 0.2mL of chloroform was added per mL of TriReagent. Samples were shaken vigorously for 15 seconds and allowed to stand for 15 minutes at room temperature. The resulting mixtures were centrifuged at 13,000 rpm in a microcentrifuge for 15 minutes at 4ºC. The colourless upper aqueous phase (containing RNA) was removed into a fresh tube. To this 0.5mL of ice-cold isopropanol (Sigma, I9516) was added. The samples were mixed and incubated at room temperature for 10 minutes, and then centrifuge at 12,000 rpm for 30 minutes at 4ºC to pellet the precipitated RNA. Taking care not to disturb RNA pellet, the supernatant was removed and the pellet was subsequently washed by the addition of 750µL of 75% of ethanol and vortexed. The samples were centrifuged at 7,500 rpm for 5 minutes at 4ºC. The supernatant was removed and the wash step was repeated. The RNA pellet was allowed to air-dry for 10 minutes and then re-suspended in 50µL of RNase free water. To facilitate dissolution the sample was repeatedly pipetted.

2.4.3 RNA isolation from serum using TriReagent

Frozen serum samples were allowed to thaw on ice, and 250µL was aliquoted into labelled eppendorf tubes. To each 250µL serum aliquot 750µL TriReagent was added. TriReagent/serum samples were allowed to sit for 5 minutes to ensure complete dissociation of nucleoprotein complexes. 0.2mL of chloroform was added to each tube and shaken vigorously for 15 seconds, then allowed to stand for 15 minutes at room temperature. The resulting mixture was then centrifuged at 13,000 rpm in a microcentrifuge for 15 minutes at 4^{o}C. The colourless upper aqueous phase (containing RNA) was removed into a fresh RNase-free eppendorf tube. Glycogen (Sigma, G1767) 1.25 µL (final concentration 120 µg/mL) and 0.5 mL of ice-cold isopropanol (Sigma, I9516) were added. The samples were mixed by inverting, incubated at room temperature for 10 minutes and stored at -20^{o}C overnight, to ensure maximum RNA precipitation.

Tubes were then centrifuge at 12,000 rpm for 30 minutes at 4^{o}C to pellet the precipitated RNA. Taking care not to disturb RNA pellet, the supernatant was removed and the pellet was subsequently washed by the addition of 750µL of 75% of ethanol and vortexed. Centrifugation was followed at 7,500 rpm for 5 minutes at 4^{o}C. The supernatant was removed and the wash step was repeated. Each RNA pellet was allowed to air-dry for 10 minutes and subsequently re-suspended in 5µL of RNase free water. To facilitate dissolution repeated pipetting was done (figure 2.2)

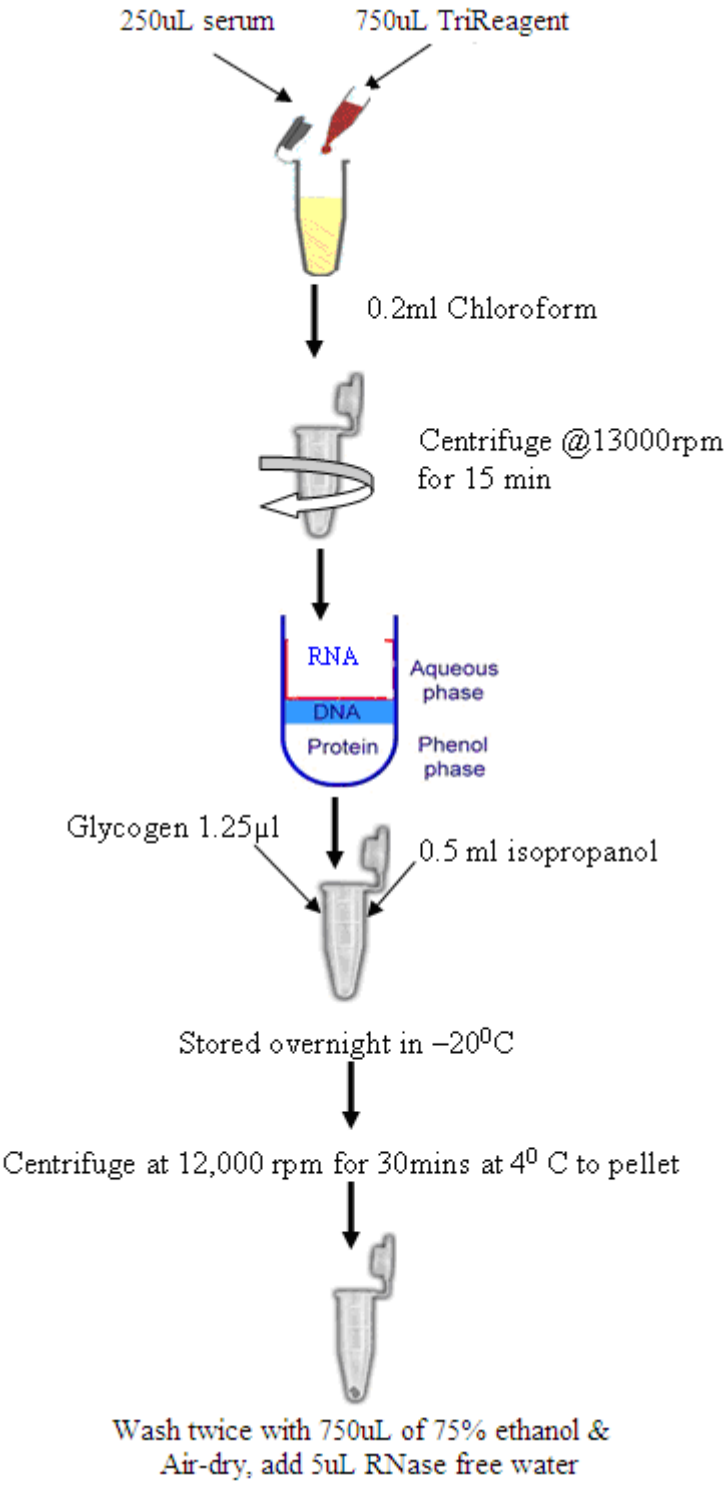

Figure 2.2 RNA isolation using TriReagent from serum

2.4.4 RNA Quantification using NanoDrop

RNA was quantified spectrophotometrically at 260nm and 280nm using the NanoDrop® (ND-1000 spectrophotometer). A 1µL aliquot of RNA was placed on the nanodrop pedestal. The ND-1000 software automatically calculated the quantity of RNA in the sample based on an OD_{260} of 1 being equivalent to 40mg/mL RNA. The software simultaneously measured the OD_{280} of the samples allowing the purity of the sample to be estimated from the ratio of OD_{260}/OD_{280}. This was typically in the range of 1.8-2.0. A ratio of <1.6 indicated that the RNA may not be fully in solution.

2.4.5 Total RNA Analysis using the Bioanalyser

The Agilent 2100 Bioanalyser is a microfluidics-based platform for the analysis of proteins, DNA and RNA. The miniature chips are made from glass and contain a network of interconnected channels and reservoirs. The RNA 6000 Nano LabChip kit was used for this study.

RNA 6000 Nano Labchip kit contains all components required for the procedure, standard protocol was performed as per manufacturer's instructions. In brief, RNA Gel Matrix was vortexed and 550µL added into top receptacle of spin filter and centrifuged at 4,000 rpm for 10 minutes. RNA dye concentrate was vortexed for 10 seconds and 1µL added to 65µL of RNA gel matrix, and then vortexed to mix, gel-dye mix was then centrifuged for 10 minutes at 14,000 rpm. RNA samples to be analysed and RNA ladder were heat denatured at 70°C for 2 minutes.

9µL gel-dye mix was added to the appropriate wells; the plunger was then pressed to allow gel-dye mix to enter channels. 5µL of fluorescent dye marker was added to each well, followed by 1µL of denatured RNA sample per well. 1µL RNA ladder was added into the well marker ladder to allow for size comparison of RNA samples. The chip was then vortexed at 2,400 rpm for 1 minute.

The Agilent Bioanalyser instrument is fully automated and electrophoretically separates the RNA samples. The resulting data is represented as an electropherogram (figure 2.3).

The fluorescence was measured on the Y-axis and the time in seconds is measured on

the X-axis. The first peak on the graph at 22.5 seconds represents the RNA marker, which acts as a control for each well. The second peak at approximately 25 to 28 seconds represents the small RNA fraction; including miRNAs. The third and fourth peak at approximately 41 and 47.5 seconds represent the 18S and 28S ribosomal RNA. The height of peaks represents the quantity of RNA in each fraction. Figure 2.2 shows an example of good quality cell RNA, the 18S and 28S ribosomal RNA peaks are quite sharp. As RNA degrades, the 28S RNA peak decreases and smaller fragments are visible.

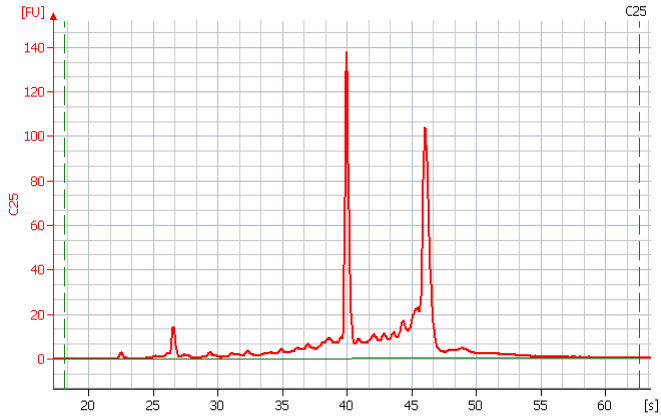

Figure 2.3 Electropherogram generated using the Agilent Bioanalyser.

2.4.6 End-Point RT-PCR analysis

2.4.6.1 DNase treatment of RNA

Total RNA was pre-treated with RNase-free DNase to remove any contaminating genomic DNA. 1µg of RNA was treated with 1U of RNase-free DNase enzyme (Promega, M6101) according to table 2.4. RNA was incubated at 37ºC for 30 minutes.

Reagent	Volume
RNA in water	1-8µL
RQ1 RNase-free DNase 10X reaction buffer	1µL
RQ1 RNase-free DNase	1U/µg RNA
Nuclease-free water to a final volume of	10µL

Table 2.4 Preparation of master mix for DNA digestion reaction

To this mixture 1µL of RQ1 DNase Stop Solution was added to terminate the reaction, and mixture was incubated at 65ºC for 10 minutes to inactivate the DNase.

2.4.6.2 Reverse transcription of DNase-treated RNA

Messenger RNA was copied to cDNA by reverse transcriptase (Sigma, M1302) using an oligo dT primer. Reverse transcription reaction was performed in two steps. Step one involved incubating 1µg RNA with the oligo dT primer and dNTPs for 10 minutes at 70ºC according to table 2.5. The reaction mixture was then placed on ice and the remaining components for step two of the reverse transcription reaction were added according to table 2.6.

Reagent	Volume
DNase-treated RNA	1µg RNA in 11µL
10mM dNTPs (Sigma, DNTP100)	1µL
50µM oligo dT (MWG)	1µL

Table 2.5 Preparation of reaction mix for step 1 of reverse transcription

Reagent	Volume
10X MMLV Reverse Transcriptase Buffer	2µL
MMLV	1µL
RNase Inhibitor (40U/µL) (Sigma, R2520)	0.5µL
Nuclease-free water	3.5µL

Table 2.6 Preparation of reaction mix for step 2 of reverse transcription

Reaction mixtures were allowed to stand at room temperature for 10 minutes, and were then incubated at 37ºC for 50 minutes to allow first stand synthesis, followed by 10 minutes at 80ºC to denature the MMLV reverse transcriptase. The resultant cDNA was stored at -20ºC until required. Minus RT negative controls were also prepared for each set of reactions, water was added instead of MMLV enzyme for the reverse transcription reaction. The resultant mix was then used as template for the PCR reaction. No amplification should be detected from the –RT controls. If a band is amplified this indicates that there is genomic DNA contamination in the isolated RNA.

2.4.6.3 PCR

The cDNA was analysed for the expression of genes of interest by PCR. Table 2.7 lists the standardised PCR mix which did not change significantly throughout this thesis. 2.5µL cDNA was added to the following reaction mixture (table 2.7). The samples were mixed and centrifuged before being placed on the thermocycler (Biometra).

Reagent	Volume
10X PCR buffer	2µL
25mM $MgCl_2$	2.8µL
10mM dNTPs (Sigma, DNTP100)	1.6µL
10mM Forward primer (MWG)	1µL
10mM Reverse primer (MWG)	1µL
Taq DNA polymerase (Sigma, D4545)	0.2µL
Nuclease-free water	8.9µL

Table 2.7 PCR reaction mixture

A typical PCR protocol is outlined below. However annealing temperatures can vary from primer set to primer set therefore a full list of the primers used in this thesis and the annealing temperatures are listed in table 2.8.

95°C for 3 min (Denaturation step)
Followed by
30 cycles of:
95°C for 30 seconds (Denaturation)
52-60°C for 30 seconds (Annealing)
72°C for 1 minute (Extension)
And
72°C for 7 min (Extension)

Resultant PCR products were stored at -20ºC until they were analysed by gel electrophoresis.

Target	Forward & Reverse Primer 5'-3'	Annealing Temperature	Product Size (bp)
Oct-4	GTAAGCTGCGGCCCTTGCTG GGCACTGCAGGAACAAATTCT	54ºC	165
c-myc	GGCGGGCACTTTGCACTGGA CGCGGGAGGCTGCTGGTTTT	60ºC	190
Klf4	GCAGCCACCTGGCGAGTCTG CCGCCAGCGGTTATTCGGGG	62ºC	130
Sox2	TAAATACCGGCCCCGGCGGA GGCGCCGGGGAGATACATGC	59ºC	520
Nanog	TGAACCTCAGCTACAAACAG TGGTGGTAGGAAGAGTAAAG	52ºC	154
Amylase	GATGGCGCCAAATAAGGAAC GACATCACAGTATGTGCCAG	53ºC	197
Sox17	CTCGACGGCTACCCGTTGCC TCCTTAGCTCCTCCAGGAAGTGTG	62ºC	674
Cxcr4	AGTTGATGCCGTGGCAAACTGGTA CAGGATAAGGCCAACCATGATGT	58ºC	346
Foxa2	GAGGACAAGTGAGAGAGCAAGTGG AGGAGTCTACACAGTAGTGGAAAC	59ºC	235
Hnf4α	AGATTGCCAGCATCGCAGATGTG TGCCGAGGGACAATGTAGTCATT	58ºC	224
Pdx1	CGGACATCTCCCCGTACGAGGT TCATCCATGGGAAAGGCAGCTGG	57ºC	180
Hlxb9	ACTGCTCCTCGGAGGACGACTC CCAGCAGTTTGAACGCTCGTGAC	57ºC	587
Ngn3	CACTCGCACACGGGGGAACT TGGTGAGCTTCGCGTCGTCT	56ºC	245
Nkx6.1	TGGCCTGTACCCCTCATCAAGGA ACTTGGTCCGGCGGTTCTGGA	57ºC	216
Ptf1a	TCCATCAACGACGCCTTCGAGG GGGAGGGAGGCCATAATCAGGGT	56ºC	294
Nkx2.2	GTCCAGGCCCAGCAGTGGACTT AACGCTGGGACGGTTTGGTCC	58ºC	348

Pax4	TTGCCTGGCCCTGCCTCGAT TTTTTGGGGATGCATGCTGGAAGATTT	56ºC	446
Insulin	AGCCGCAGCCTTTGTGAACCAACA TTCCATCTCTCTCGGTGCAGGAGGCG	57ºC	326
Ghrelin	GAATCAAGCTGTCAGGGGTTC CTAAACTTAGAGAGAGGTGAGTAAG	52ºC	145
Somatostatin	TTTGACCAGCCACTCTCCAGCTC TGCAGCCAGCTTTGCGTTCTCG	57ºC	357
Glut2	CTCACTATAGACATGTTTTGGGTGT AGTCCTGATATGCTTCTTCCAGC	52ºC	370
Glucagon	AGGCAGCTGGCAACGTTCCCTTCA GCCAAGTTCTTCAACAATGGCGACC	57ºC	382
N-cadherin	GTGCCATTAGCCAAGGGAATTCAGC GCGTTCCTGTTCCACTCATAGGAGG	62ºC	370
CK-12	GAAGAAGAACCACGAGGATG TCTGCTCAGCGATGGTTTCA	54ºC	146
CK-3	CGTACAGCTGCTGAGAATGA CTGAGCGATATCCTCATACT	53ºC	261
ABCG2	GGTTTCCAAGCGTTCATTCAAA TAGCCCAAAGTAAATGGCACCTA	54ºC	112
ΔNp63	CTGGAAAACAATGCCCAGAC GGGTGATGGAGAGAGAGCAT	55ºC	198
β-actin	CGGGAAATCGTGCGTGACAT GGAGTTGAAGGTAGTTTCGTG	55ºC	228

Table 2.8 List of primers used in this study.

2.4.6.4 Gel Electrophoresis of PCR products

1% agarose (Sigma, A9539) gels were used for PCR gel electrophoresis, which were prepared and run in 1X TAE prepared with 10X TAE stock (121g Tris base, 9.3g EDTA, 28.5mL glacial acetic acid and made up to 500mL with UHP). The gel was then poured into an electrophoresis unit and supplemented with 5µL ethidium bromide (10mg/mL) per 50mL gel. Ethidium bromide is a dye that binds to double stranded DNA by interpolation (intercalation) between the base pairs. Here it fluoresces when irradiated in the UV part of the spectrum. Sample wells were formed by placing a comb into the top of the gel prior to hardening.

To prepare the PCR product samples for electrophoresis, 2µL of 10X loading buffer (30% Glycerol, 0.1M EDTA, 0.25% bromophenol blue made up to 10mL with water) was added to 20µL PCR product and the mixture was loaded to the gel with an appropriate size marker (Sigma, P1473). The gels were electrophoresed at 100V for 45 minutes. The gel was viewed with a gel analyzer (an EpiChemi II Darkroom, UVP Laboratory Products) and photographed using Labworks software (UVP).

2.4.7 Quantitative real time miRNA RT-PCR (qRT-PCR)

2.4.7.1 Reverse Transcription of miRNA (cDNA Synthesis)

For reverse transcription of miRNAs, cDNA was reverse transcribed from total RNA samples using specific miRNA primers from the TaqMan MicroRNA Assays and reagents from the TaqMan MicroRNA Reverse Transcription kit (Applied Biosystems) (figure 2.4).

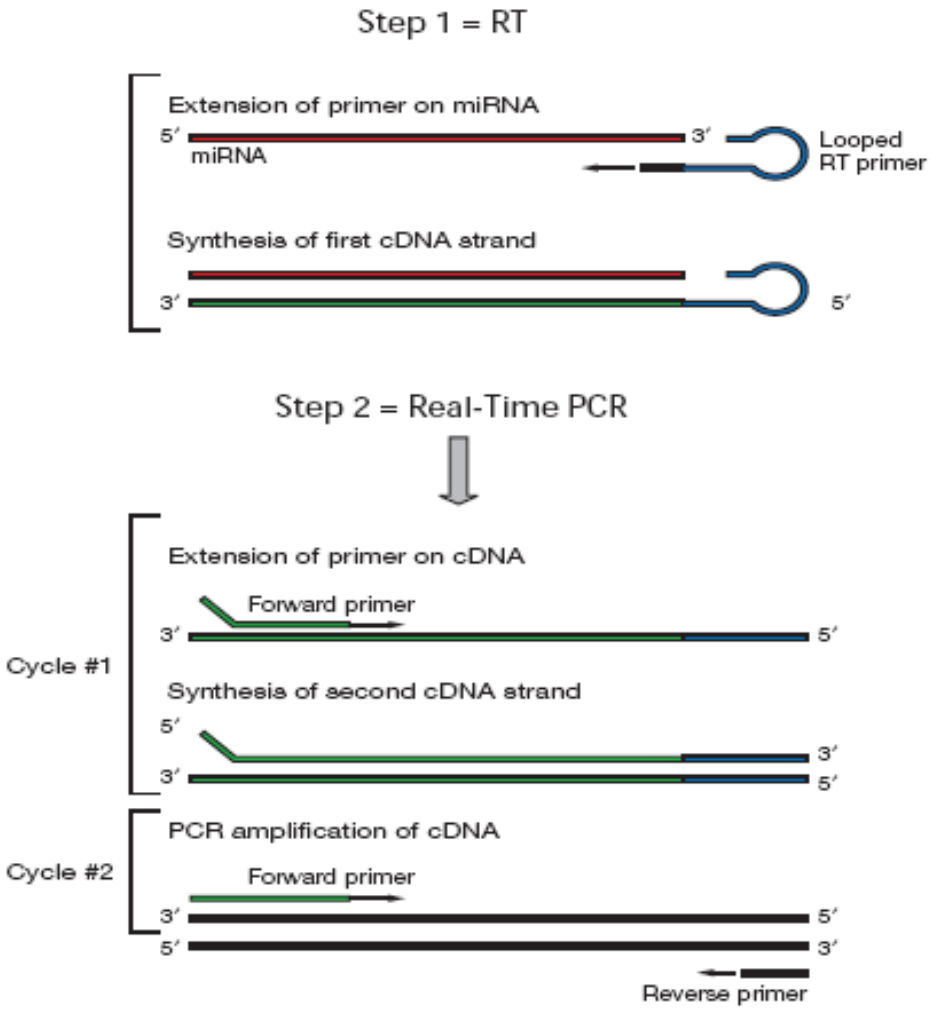

Figure 2.4 Two-step reverse transcription PCR of miRNAs (image from www.appliedbiosystems.com).

For each miRNA to be reverse transcribed a specific looped RT primer was used to reverse transcribe that specific miRNA (figure 2.4). For multiple miRNAs to be reverse transcribed from the same RNA sample, multiple reactions needed to be performed, as only a single miRNA species was reverse transcribed per reaction.

Based on the nanodrop concentration reading, total RNA was diluted to 2ng/µL in RNase free water. 5µL of diluted RNA was added to an eppendorf tube. The RT-primer for the specific miRNA to be reverse transcribed, and the components of the TaqMan microRNA reverse transcription kit were allowed to thaw on ice. Once thawed, reverse transcription master mix was prepared as per table 2.9. Volumes from table 2.9 were scaled up when multiple reverse transcription reactions were performed, plus an extra 10% excess was made up to allow for pipetting losses.

Reagents	Master Mix Volume / 15µL reaction
100mM dNTPs	0.15µL
MultiScribe Reverse Transcriptase, 50U/µL	1.00µL
10x Reverse Transcription Buffer	1.50µL
RNase Inhibitor, 20U/µL	0.19µL
Nuclease-free water	4.16µL
Total	**7.00µL**

Table 2.9 miRNA reverse transcription master mix

For each 15µL reverse transcription reaction, 5µL RNA (diluted to 2ng/µL), 7µL master mix and 3µL TaqMan RT-primer were added to a tube, mixed by vortexing, and centrifuged to bring mixture to the bottom of the tube. Reaction tubes were incubated on ice for 5 minutes before loading onto BioMetra T3 thermocycler, thermocycler parameters are outlined in table 2.10.

Step Type	Time (minutes)	Temperature (ºC)
Hold	30	16
Hold	30	42
Hold	5	85
Hold	∞	4

Table 2.10 Thermocycler parameters for microRNA reverse transcription reaction

2.4.7.2 TaqMan real-time miRNA PCR

TaqMan probes are oligonucleotides that have fluorescent reporter dyes attached to the 5' end and a non-fluorescent quencher coupled to the 3' end. These probes are designed to hybridize to an internal region of a PCR product. In the unhybridized state, the proximity of the fluorophore and the quencher molecules prevents the detection of fluorescent signal from the probe. During PCR, when the polymerase replicates a template on which a TaqMan probe is bound, the 5'- nuclease activity of the polymerase cleaves the probe. This decouples the fluorescent dye, thus, increasing the fluorescence in each cycle proportional to the amount of probe cleavage.

TaqMan microRNA assays and TaqMan universal PCR master mix (Applied Biosystems) were used for miRNA PCR analysis in this study. cDNA synthesised as per section 2.4.7.1. was used as the template for PCR reactions. Each PCR reaction was performed in triplicates. In order to exclude any amplification product derived from genomic DNA or any other contaminant that could contaminate the RNA preparation, total RNA without reverse transcription was used as a negative control. As an additional control, water on its own was amplified as a negative control to rule out presence of any contaminating RNA or DNA.

PCR master mix was prepared as described in table 2.11, and were scaled up when multiple PCR reactions were performed, plus an extra 10% excess was prepared to allow for pipetting losses.

Reagents	Master Mix Volume / 20µL reaction
TaqMan Universal PCR master mix	10.00µL
RNase-free water	7.67µL
Total Volume	**17.67µL**

Table 2.11 miRNA PCR master mix

For each 20µL PCR reaction, 1.33µL cDNA (prepared from section 2.4.7.1), 17.67µL master mix and 1µL TaqMan miRNA assay mix (containing PCR primers and TaqMan probe) were added per well of a MicroAmp fast optical 96-well reaction plate (Applied Biosystems). Plates were then sealed with optical adhesive film (Applied Biosystems)

and run on the 7500 Fast Real-time PCR system according to the cycling parameters in table 2.12, on the 9600 emulation mode.

Step	AmpliTaq Gold® Enzyme Activation	PCR	
	Hold	Cycle (40 cycles)	
		Denature	Anneal/Extend
Time	10 min	15 sec	60 sec
Temp (°C)	95	95	60

Table 2.12 Thermocycling parameters for miRNA PCR

MiRNA real-time PCR analysis in this study was preformed using the TaqMan miRNA assays outlined in table 2.13.

Real-time PCR data was analysed using the comparative cycle threshold (C_t) method, which involves comparison of the C_t values of the samples of interest with a control or calibrator sample (such as an untreated sample). The C_t values of both the calibrator and the samples of interest are normalised to an appropriate endogenous control, generating a ΔC_t for both the sample of interest and the control/calibrator samples.

$$\Delta C_t = C_t \text{ [target]} - C_t \text{ [endogenous control]}$$

$\Delta\Delta C_t$ is then calculated as the difference between ΔC_t for the sample and calibrator.

$$\Delta\Delta C_t = \Delta C_t \text{ [sample]} - \Delta C_t \text{ [calibrator]}$$

Relative quantification (RQ) of target expression is calculated from the equation below as a difference of one C_t is equal to 2 fold change in expression level.

$$RQ = 2^{-\Delta\Delta Ct}$$

RQ values greater than one indicate an increase in expression, while RQ values between zero and one indicate a reduction in expression levels.

Target miRNA	Supplier	Assay ID
hsa-mir-376a#	Applied Biosystems	4378104
mmu-mir-369-5p	Applied Biosystems	4378118
hsa-mir-130a	Applied Biosystems	4373145
hsa-mir-27a	Applied Biosystems	4373287
hsa-mir-410	Applied Biosystems	4378093
mmu-mir-124a	Applied Biosystems	4373295
hsa-mir-200a	Applied Biosystems	4378069
mmu-mir-337	Applied Biosystems	4373338
hsa-mir-532	Applied Biosystems	4380928
hsa-mir-320	Applied Biosystems	4373055
mmu-mir-192	Applied Biosystems	4373308
mmu-mir-379	Applied Biosystems	4373349
hsa-mir-375	Applied Biosystems	4373027
hsa-mir-9	Applied Biosystems	4373285
hsa-let-7b	Applied Biosystems	4373168
hsa-mir-140	Applied Biosystems	4373138
hsa-mir-21	Applied Biosystems	4373090
hsa-mir-24	Applied Biosystems	4373072
hsa-mir-29a	Applied Biosystems	4373065
hsa-mir-29c	Applied Biosystems	4373289
hsa-mir-30d	Applied Biosystems	4373059
hsa-mir-345	Applied Biosystems	4373039
hsa-mir-28	Applied Biosystems	4373067
hsa-mir-16	Applied Biosystems	4373121

Table 2.13 TaqMan miRNA assays used for analysis of miRNA expression in MIN6 cells and diabetes serum study.

2.4.8 TaqMan Low Density miRNA arrays (TLDAs)

TaqMan low density miRNA arrays (TLDAs) consist of a 384-well microfludic card used for performance of 384 simultaneous real-time PCR reactions (figure 2.5). Each well contains a different set of TaqMan primers and probes, for detection of a single miRNA target. One RNA sample is used per card, to allow for profiling of 384 targets.

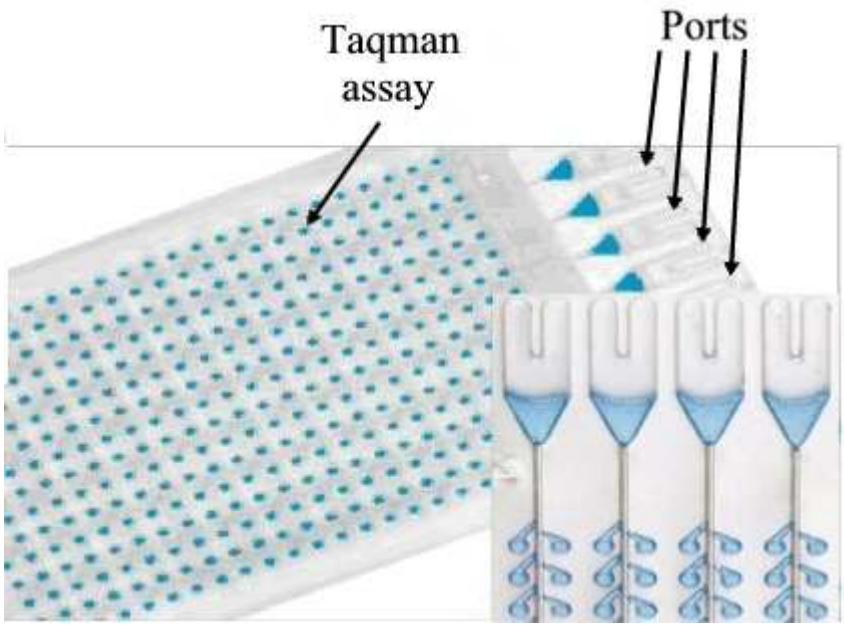

Figure 2.5 TaqMan Low Density miRNA array format (image from www.appliedbiosystems.com).

Reverse transcription of miRNAs for use on TLDA cards were performed using TaqMan Multiplex RT-primer pools. These Multiplex pools consisted of 8 separate primer pools, and each pool containing 48 different RT-primers allowing for reverse transcription of 48 different miRNAs per pool. Each primer pool corresponds to a port on the TLDA card, therefore 8 different primer pools allowed for reverse transcription of the 384 targets to be detected by the TLDA.

RNA was isolated (as per section 2.4.1 for MIN6 TLDAs, and section 2.4.3 for diabetes serum TLDAs) and quantified (as per section 2.4.4), according to quantification reading RNA was diluted to 50ng/µL with RNase-free water. 2µL RNA was required per RT-reaction, as 8 RT-reactions were required to run each TLDA card, therefore 16µL of diluted RNA was required.

Each RT-reaction master mix was prepared as per table 2.14. For each samples 8 RT-reactions were prepared, plus and extra 10% excess to allow for pipetting losses.

Reagent	Volume for one RT-reaction	Volume for one sample (8 RT-reactions)
100mM dNTPs	0.20µL	1.6µL
MultiScribe reverse transcriptase, 50U/µL	2.00µL	16.0µL
10X reverse transcription buffer	1.00µL	8.0µL
RNase Inhibitor, 20U/µL	0.125µL	1.0µL
RNase-free water	3.675µL	29.4µL
Total	**7.00µL**	**56.0µL**

Table 2.14 MultiPlex miRNA reverse transcription master mix

Eight tubes were prepared per sample, for 8 multiplex reverse transcription reactions, to each tube 7µL master mix, 2µL diluted RNA, and 1µL of the appropriate MultiPlex RT-primer pool were added. Tubes were mixed gently and centrifuged to bring solution to the bottom of tube and stored on ice for 5 minutes before loading thermocycler. Thermocyler parameters are outlined in table 2.15.

Step Type	Time (minutes)	Temperature (°C)
Hold	30	16
Hold	30	42
Hold	5	85
Hold	∞	4

Table 2.15 Thermocycler parameters for MultiPlex miRNA reverse transcription.

The generated cDNA was then diluted 62.5 fold by adding 615µL of RNase-free water to each of the 8 RT-reactions. 8 PCR master mixes per sample were prepared, as outlined in table 2.16, for each RT-reaction.

Reagent	Volume per fill reservoir
Diluted RT-reaction	50µL
TaqMan universal PCR master mix	50µL
Total	**100µL**

Table 2.16 PCR master mix for miRNA TLDA

Tubes were mixed and centrifuged to bring solution to the bottom of tube. 100µL of master mix from table 2.16 was loaded into the corresponding port on the TLDA card, i.e. RT-reaction mix generated from MultiPlex primer pool 1 was loaded into port 1 (figure. 2.5). Once all the ports were loaded the TLDA card was centrifuged at 1,200 rpm for 2 consecutive 1 minute spins. TLDA cards were then sealed and the ports removed, cards were then loaded onto the 7900HT Fast Real-Time PCR instrument on standard mode, with thermocycling parameters outlined in table 2.17.

Step	AmpErase UNG Activation	AmpliTaq Gold® Enzyme Activation	PCR	
	Hold	Hold	Cycle (40cycles)	
			Denature	Anneal/Extend
Time	2 min	10 min	30 sec	60 sec
Temp (°C)	50	94.5	97	59.7

Table 2.17 Thermocycler parameters for miRNA TLDA analysis

2.5 Collecting Serum from blood

Diabetes and control serum specimens were collected by Dr. Ana Rakovac Tisdall, Connolly Hospital Blanchardstown. Two blood specimens of approximately 10mL were taken with consent from each patient recruited for the diabetes and control serum study. From the collected blood samples, the red blood cells were allowed to clot naturally. These specimens were processed within 3-4 hours of blood draw. Serum specimens from control volunteers (no history or symptoms of diabetes) were also collected and processed the same way.

Blood specimens were processed by removing the serum from the clotted blood and placing into a 10mL centrifuge tube. The tubes were then centrifuged at room temperature for 15 minutes at 400 rcf (relative centrifugal force). After centrifugation the cleared serum was carefully removed and passed through a 0.45µm filter to further ensure no particles / platelets were retained. The serum was then aliquoted into 1mL aliquots and stored at -80°C until required. Serum specimens were coded according to the order they arrived in DCU at e.g. DCU serum 1 (DS-1), DCU serum 2 (DS-2) *etc*.

2.6 Label-free LC-MS serum proteomics

Proteomic analysis was performed on serum samples from newly diagnosed type 1 diabetes (T1DM new), established diabetes (T1DM old), matched controls (control new and control old) and autoimmune samples. Serum samples were prepared using the ProteoMiner™ Protein Enrichment Kit (BioRad, 163-3007). ProteoMiner™ is a column-based technique, with the column containing a highly diverse bead-based library of peptide ligands. High abundance proteins saturate their high affinity ligands and excess protein is washed away, while low abundance proteins are concentrated on their specific ligands. ProteoMiner™ columns were prepared according to manufacturers instructions, 1mL of serum was then applied to column and rotated end-on-end for 2 hours to allow binding of protein to ligand. Column was then washed and proteins eluted in 300µL of elution buffer.

50µL of elute was then processed using the ReadyPrep 2D Cleanup Kit (BioRad, 163-2130) according to manufacturers instructions. This kit allows for precipitation of protein leaving behind salts, detergents and nucleic acid contaminants. Precipitated protein was resuspended in 100µL of MS grade water. Protein concentration was assessed using Quick-Start Bradford Dye Reagent 1X (BioRad, 500-0205). Protein samples were diluted 1:4 with water, then 5µL diluted sample was added per well of a 96 well plate. Each sample was analysed in triplicate. 200µL of Bradford reagent was added to each sample and incubated for 15 minutes. The absorbance was then read at 595nm. Using the concentration calculated from the Bradford assay, 20µg of each sample was used for the digestion steps.

To prepare protein samples for digestion, samples were first incubated with 1µL 5mM dithiothreitol reducing agent for 30 minutes at 37ºC. 1µL of 25mM iodoacetamide was then added to each sample and incubated in the dark for 20 minutes at room temperature. Digestion of protein samples was performed with Endoproteinase Lys-C (Promega, V1071) at a ratio of 100/1, protein/enzyme w/w, i.e. 20µg of protein was digested with 0.2ug of Endoproteinase Lys-C. Samples were incubated at 37ºC for 3 hours to allow the digestion to occur. Samples were subsequently digested with trypsin (sequence grade, Promega). 7.5µL of trypsin and 80µL of 50mM ammonium

bicarbonate was added to each sample and incubated overnight at 37ºC. Following overnight incubation 2% trifluoroacetic acid (TFA) and 20% acetonitrile were added to each sample to stop the trypsin digestion.

To prepare the samples for MS analysis, digested peptides were processed using PepClean C-18 Spin Columns (Pierce, 89870) according to manufacturer's instructions to remove interfering contaminants and chemicals. Peptide samples were eluted in 80µL of 80% ACN/water v/v, dried down using a speed-vac (MAXI dry plus) and stored at -20ºC until required. Samples were resolubilised in 80µL of LC-MS grade water with 0.1% TFA and 2% ACN. 40µL was then transferred to glass vials. Mass spectrometry was performed by Dr. Paul Dowling. Peptides were first submitted to the nano-LC-MS/MS using an Ultimate 3000 system (Dionex) coupled to an LTQ-Orbitrap XL mass spectrometer (Thermo Fisher Scientific) operating in positive mode with a spray voltage of 1.6kV. 6.5µL of each sample was injected onto a C18 precolumn (300µm inner diameter x 5mm; Dionex) at 25µL/min in 5% ACN, 0.05% TFA. After a 3 minute desalting step, the precolumn was switched on line with the analytical column (75µm inner diameter x 25cm PepMap C18; Dionex) equilibrated in 98% solvent A (2% ACN, 0.05% TFA) and 2% solvent B (98% ACN. 0.04% FA). Peptides were eluted using a 10-35% gradient of solvent B during 150 minutes at a 300nL/min flow rate. Data were acquired with Xcalibur software version 2.0.7 (Thermo Fisher Scientific). The mass spectrometer was operated in the data-dependent mode and was externally calibrated. Survey MS scans were acquired in the Orbitrap in the 300-2000m/z range with the resolution set to a value of 60,000 at m/z 400. Up to seven of the most intense multiply charged ions (1+, 2+ and 3+) per scan were CID fragmented in the linear ion trap. A dynamic exclusion window was applied within 40s. All tandem mass spectra were collected using a normalized collision energy of 35%, an isolation window of 3m/z, and one microscan.

2.6.1 Validation of proteomics targets

ELISAs were used for validation of targets identified from proteomic profiling study (section 2.5). Validation was performed on the same 8 newly diagnosed type 1 diabetes (T1DM new), established diabetes (T1DM old), and matched controls (control new and control old) serum specimens used for the profiling experiment, as well as an additional 22 T1DM old and control old specimens

2.6.1.1 Vitronectin

A vitronectin ELISA kit was sourced from American Diagnostica GmbH (803). Serum specimens to be analysed were diluted by a factor of 4,000 using dilution buffer. Standards were reconstituted as per manufacturer's instructions using dilution buffer. 100µL of diluted samples or standards were added to each well, and incubated for 1 hour at room temperature on a shaker at 250rpm. The plate was then washed 4 times using wash buffer and excess liquid was removed from the plate by tapping on absorbent paper 4-5 times between each wash step. 100µL of detection antibody was added to each well and incubated for 1 hour at room temperature on a shaker at 250rpm. The plate was then washed 4 times using wash buffer, and excess liquid was removed after each wash step by tapping plate on absorbent paper. 100µL of substrate was added and incubated for 5 minutes at room temperature. 50µL stop solution was added and plate was read at 450nm. A polynomial standard curve was plotted using the absorbance of the standards, using the equation of the line the vitronection concentration was calculated for each sample.

2.6.1.2 Clusterin

A clusterin ELISA was sourced from Phoenix Pharmaceuticals (EK-018-35). Serum specimens to be analysed were diluted by a factor of 6,000 using assay buffer. Standards were reconstituted as per manufacturer's instructions using assay buffer. 300µL assay buffer was added to each well of the ELISA plate and allowed to stand for 5 minutes, buffer was then removed and plate tapped on absorbent paper to remove excess liquid. 100µL of diluted samples or standards were added to each well and incubated for 2 hours at room temperature on a shaker at 350rpm. Plate was washed four times using assay buffer, plate was tapped on absorbent paper to remove excess liquid between each wash step. 100µL of detection antibody was added to each well and

incubated for 2 hours at room temperature on a plate shaker at 350rpm. Plate was washed four times, tapping on absorbent paper between each wash. 100µL substrate solution was added and incubated for 30 minutes at room temperature on a shaker at 350rpm. 100µL stop solution was added and absorbance was read at 450nm on a plate reader. Standard curve was plotted as log concentration versus log absorbance. Equation of the line was used for calculation of clusterin concentration in serum specimens.

2.6.1.3 Vitamin K-dependent protein S

A vitamin K-dependent protein S ELISA was sourced from USCN Life Science Inc. (E1971h). Serum specimens to be analysed were diluted by a factor of 10 using sample diluent. Standards were reconstituted as per manufacturer's instructions using sample diluent. 50µL of diluted samples or standards were added to each well, followed by 50µL of detection reagent A, and incubated for 1 hour at 37ºC. The plate was washed three times using wash buffer, and tapped on absorbent paper after the last wash to remove excess liquid. 100µL detection reagent B was added and incubated for 45 minutes at 37ºC. The plate was washed five times with wash buffer, and tapped on absorbent paper after last wash. 90µL of substrate solution was added to each well and incubated at 37ºC for 30 minutes. 50µL of stop solution was added and absorbance read at 450nm on a plate reader. A 4-parament logistic standard curve was plotted and using the equation of the line vitamin K-dependent protein S concentration in serum specimens was calculated.

2.6.1.4 Apolipoprotein L1

An apolipoprotein L1 ELISA kit was sourced from USCN Life Science Inc. (E9374Hu). Serum specimens to be analysed were diluted by a factor of 5 using PBS. Standards were reconstituted as per manufacturer's instructions using standard diluent. 100µL of diluted samples or standards were added to each well and incubated for 2 hours at 37ºC. Liquid was removed from wells, and without washing, 100µL of detection reagent A was added and incubated for 1 hour at 37ºC. The plate was washed three times using wash solution and tapped on absorbent paper after each wash to remove excess liquid. 100µL of detection reagent B was added to each well and incubated for 30 minutes at 37ºC. The plate was washed five times using wash solution, and tapped on absorbent

paper after each wash. 90µL of substrate solution was added to each well and incubated for 15 minutes at 37ºC. 50µL stop solution was added to each well and absorbance read at 450nm on a plate reader.

2.7 Serum metabolite profiling

Overnight fasting whole blood specimens were collected from newly diagnosed type 1 diabetes patients (n=8) and age/BMI/gender matched healthy controls (n=8). Samples were processed as outlined in section 2.5 and resulting serum specimens were stored at -80ºC until required. Serum specimens (500µL) were shipped on dry-ice to Metabolon Inc., North Carolina, USA, where the metabolomic profiling was performed.

Metabolon incorporates three independent complimentary analysis platforms to maximise the number of small molecules and metabolites that the combined systems can identify and measure. Two independent ultra-high performance liquid chromatography / tandem mass spectrometry (UHPLC/MS/MS2) injections (one optimised for basic compounds, and the other for acidic compounds) and one GC/MS injection per sample are performed.

Firstly, small molecules were extracted from serum specimens using methanol to allow precipitation of proteins. The extract supernatant was then split into four equal aliquots; two for UHPLC/MS, one for GC/MS and one reserve aliquot. Aliquots were then dried overnight to remove solvent.

For the UHPLC methods, one aliquot was reconstituted in 50µL 0.1% formic acid and the other in 50µL 6.5mM ammonium bicarbonate pH 8.0. For GC/MS analysis, aliquots were derivatized using equal parts N,O-bistrimethylsilyltrifluoroacetamide and a solvent mixture of acetonitrile:dichloromethane:cyclohexane (5:4:1) with 5% triethylamine at 60ºC for 1 hour. All reconstitution solvents contained instrument internal standards used to monitor instrument performance.

UHPLC/MS was carried out using a Waters Acquity UHPLC coupled to an LTQ mass spectrometer equipped with an electrospray ionization source. Two independent UHPLC/MS injections were performed on each sample. The acidic injections were monitored for positive ions and the basic injections were monitored for negative ions. The derivatized samples for GC/MS were analyzed on a Thermo-Finnigan Trace DSQ fast-scanning single-quadrupole MS.

The resulting MS/MS^2 data was then searched against Metabolon's reference standard library. This library was generated from 1500 standards and contains the retention time/index, mass to charge (m/z), and MS/MS spectral data for all molecules in the library, including their associated adducts, in-source fragments, and multimers. The library allows identification of experimentally detected metabolites based on a multi-parameter match basis. All identifications and quantifications were subjected to QC to verify the quality of the identification and peak integration.

2.7.1 Validation of metabolomics target – Fibrinopeptide A

Validation of metabolite target was performed on the same 8 T1DM new and control samples as well as 30 T1DM old and control old samples. Fibrinopeptide A ELISA was sourced from Hyphen BioMed (catalogue number RK016A). Serum specimens to be analysed were diluted by a factor of 1,500 using sample diluent. Standards were reconstituted as per manufacturer's instructions using sample diluent. 100µL of anti-FPA antibodies were added to 1mL diluted samples or standards in an eppendorf tube, and incubated at 37ºC for 1 hour. 200µL of sample/antibody or standard/antibody mix was added to each well of ELISA plate, and incubated for 1 hour at room temperature. The plate was washed five times using wash solution. 200µL antibody conjugate solution was added to each well and incubated for 1 hour at room temperature. The plate was washed five times using wash solution. 200µL substrate solution was added to each well and incubated for 5 minutes at room temperature. 50µL stop solution was added and incubated for 10 minutes, and then absorbance was read at 450nm. Standard curve was plotted as log concentration versus log absorbance, and FPA concentration of samples was calculated using the equation of the line.

3.0 Results

3.1 MicroRNAs involved in glucose stimulated insulin secretion in MIN6 cells

This study set out to investigate the mechanisms of regulated insulin secretion; in particular the role miRNAs might play in this process. As no human pancreatic beta-cell lines are currently available, a murine insulinoma cell line which exhibits regulated insulin secretion was used. However, with increasing time in culture MIN6 cells lose their glucose responsiveness. To investigate any possible role that miRNAs might play in regulated insulin secretion, miRNA analysis was performed on low passage glucose responsive and high passage glucose non-responsive cells.

3.1.1 Identification of glucose responsive and non-responsive MIN6 cells

The responsiveness of pancreatic β cells to glucose is measured as a fold change in insulin secretion (protocol outlined in section 2.2.1, 2.2.2 and 2.2.3). This fold change indicates the increase in insulin secreted in response to stimulatory concentrations of glucose (16.7mM glucose) compared to basal insulin secretion (3.3mM glucose). With increasing time in culture, this GSIS fold change decreases (figure 3.1.1).

MIN6 cells were continuously cultured while monitoring GSIS at each passage to determine at which passage GSIS reached a minimum level. Insulin secretion was measured by ELISA, and data was normalised using protein assay to determine insulin secretion per mg of protein.

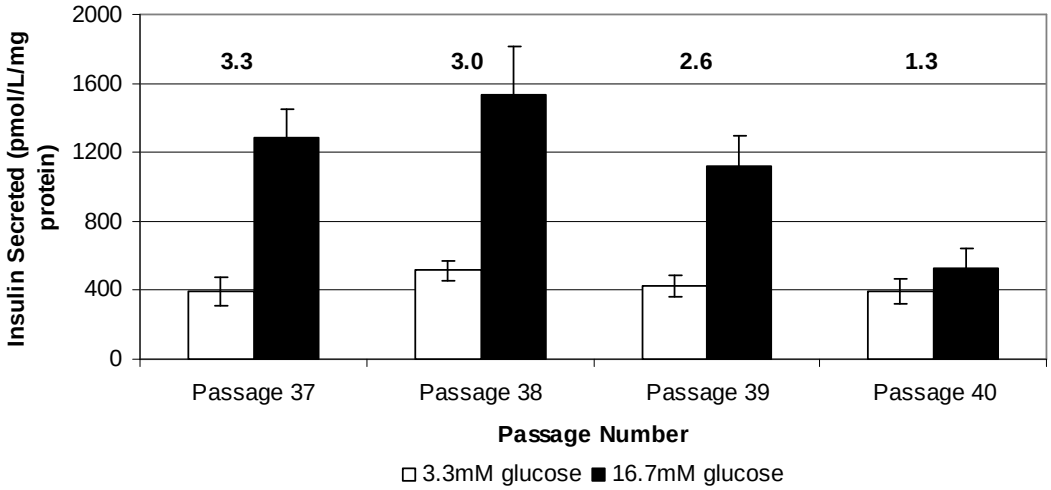

Figure 3.1.1 Increasing time in culture led to reduction of glucose stimulated insulin secretion (numbers above bars indicate fold change of insulin secretion in response to 16.7mM glucose compared to 3.3mM glucose) (n=3). Error bars represent standard error (except passage 39, error bars represent range, n=2).

Biological triplicate flasks were prepared and GSIS monitored at each passage, cell pellets for RNA extraction were also prepared at each passage. With increasing passage number average fold change decreases. Fold change variations between biological triplicates are seen due to the sensitive nature of the MIN6 cells. Passage 37 represents the most reproducibly glucose responsive cells, with an average GSIS fold change of 3.3 (figure 3.1.1). Passage 40 represents the most non-glucose responsive cells, with an average GSIS fold change of 1.3 (figure 3.1.1). Therefore, passage 37 cell pellets were chosen as the glucose responsive sample and passage 40 cell pellets were chosen as the non-glucose responsive sample for miRNA profiling analysis. These passages are also sufficiently close to limit other changes in the cells, which could contribute to differential miRNA expression.

3.1.2 RNA quality control

RNA was isolated from biological triplicate cell pellets of MIN6 glucose responsive and glucose non-responsive pellets (using technique outlined in section 2.4.1). Total RNA quality was assessed on the Agilent Bioanalyser, to ensure sufficient quality for miRNA profiling analysis (section 2.4.5).

All traces show good quality RNA, with no signs of degradation (figure 3.1.2). Height of 18S and 28S peaks indicate high yield of isolated RNA. RNA appears to be of sufficient quantity and quality to proceed with miRNA profiling analysis.

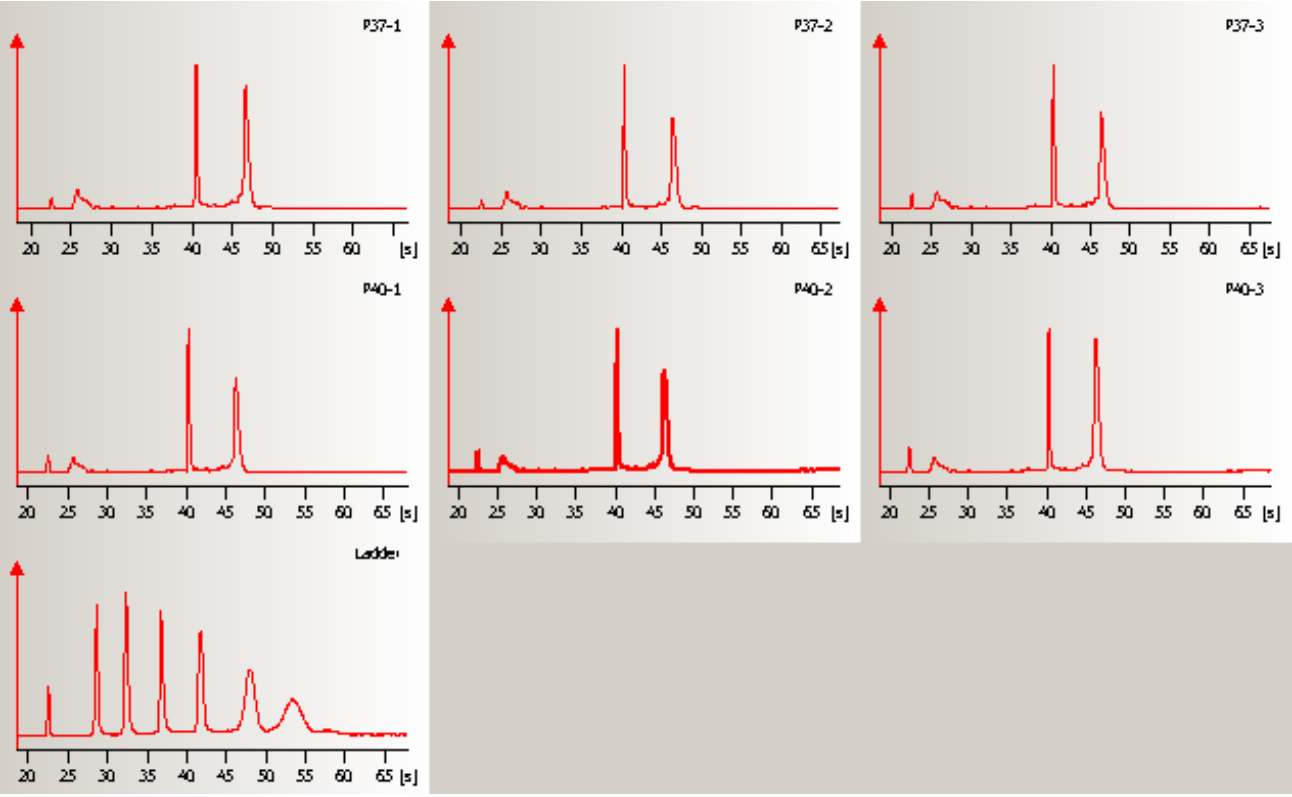

Figure 3.1.2 RNA traces of isolated RNA from Agilent Bioanalyser

3.1.3 TaqMan Low Density MicroRNA Arrays

TaqMan Low Density microRNA arrays (TLDAs), available from Applied Biosystems, are 384-well micro fluidic cards used for performance of 384 microRNA real time PCR reactions simultaneously (protocol outlined in section 2.4.8). Each well contains a different TaqMan primer and probe set, detecting a different microRNA.

At the time of experimentation TLDAs were only available in human format. Therefore, the human specific TLDAs were assessed for their suitability to be used with murine RNA. TLDAs are 384 well cards, 19 wells of which are controls containing either endogenous control assays or blank wells. The 365 remaining wells represent 365 different human miRNAs. The sequence of each was retrieved from the miRNA database - miRBase (www.mirbase.org/) (Griffiths-Jones 2004; Griffiths-Jones, Grocock et al. 2006; Griffiths-Jones, Saini et al. 2008) and the human sequence was compared against the murine equivalent sequence to assess homology (figure 3.1.3). 242 of 365 sequences were found to be conserved between human and mouse. For a further 121 sequences there was no murine equivalent registered in miRBase. The remaining 2 miRNA sequences represent what are now described as “dead” miRNAs *i.e.* sequences which were initially thought to be miRNAs but have more recently been described as potential tRNA fragments.

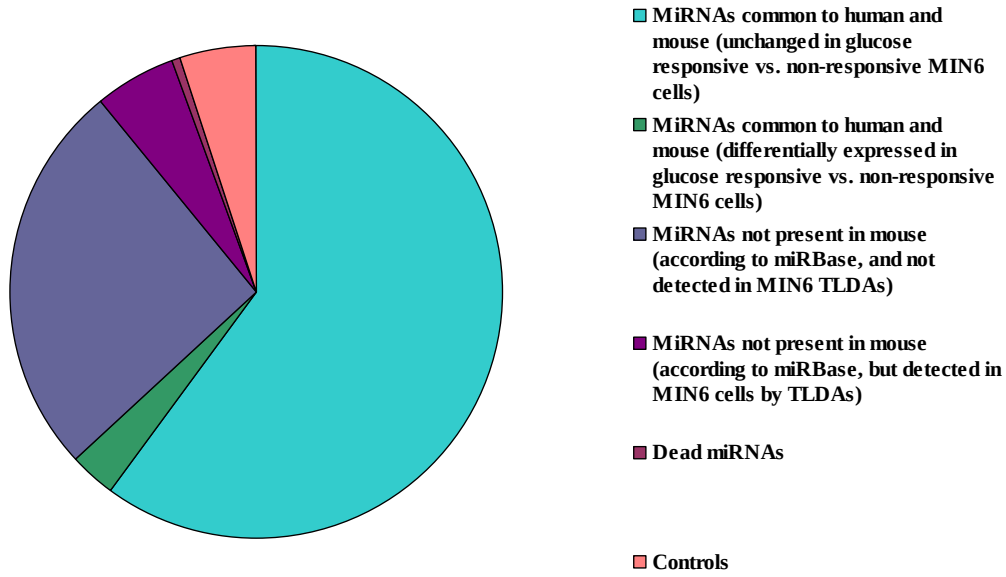

Figure 3.1.3 Pie chart representation of 384 well human TLDA card. 242 miRNAs were found to be common to human and mouse, 12 of which were identified as differentially expressed in glucose responsive MIN6 cells compared to glucose non-responsive cells. A further 121 of the 384 miRNAs are not known to be present in mouse according to the miRBase (release 18, November 2011), 21 of which were detected by TLDA in MIN6 cells (table 3.1.1). 2 miRNAs (i.e. mir-594 and mir-565) are now known to be dead miRNAs, and 19 wells constitute control wells.

3.1.3.1 Novel murine miRNAs

121 of 365 human miRNAs have no murine equivalent registered in miRBase. However, 21 of these 121 miRNAs were reproducibly detected in all 6 TLDA cards run with the murine MIN6 RNA samples, indicating that these human miRNA sequences may have a conserved murine homolog (table 3.1.1).

MiRNA	Average CT
mir-515-3p	32.33
mir-517a	33.64
mir-517b	32.68
mir-517c	33.46
mir-518c	32.61
mir-518d	32.22
mir-518e	32.88
mir-520f	34.88
mir-521	33.96
mir-518f	31.59
mir-519c	32.53
mir-519e	32.09
mir-564	33.43
mir-596	29.97
mir-597	33.86
mir-617	31.94
mir-646	31.68
mir-650	31.56
mir-572	31.84
mir-512-3p	34.05
mir-659	31.96

Table 3.1.1 Human miRNAs not previously known to have an equivalent homolog in mouse but detected by TLDA in MIN6 murine pancreatic β cells during the course of this study (n=6).

3.1.3.2 MiRNA profiling of glucose responsive compared to glucose non-responsive MIN6 cells

In order to identify miRNAs which may be responsible for the loss of GSIS in MIN6 cells, miRNA profiling was performed on glucose responsive MIN6 cells and glucose non-responsive MIN6 cells using TaqMan Low Density miRNA arrays (protocol outlined in section 2.4.8). Endogenous controls RNU44, RNU48 and RNU6B were incorporated onto each plate; however, none of these transcripts were detected in the samples used. Therefore, miRNA let-7b was chosen as endogenous control for normalisation, as levels of this miRNA were unchanged in all samples. Fold changes were calculated using the comparative C_t method detailed in section 2.4.7.2. Following application of Student's *t*-test, differentially expressed targets were identified as miRNAs with p-value < 0.05. Using this criterion 10 differentially expressed miRNAs were identified (table 3.1.2). Mir-376a and mir-124a, although just beyond the level of statistical significance, were also added to this list for further investigation as (section 1.5.1) these miRNAs are known to be highly expressed in pancreatic islets. All differentially expressed miRNAs were down-regulated in glucose non-responsive compared to glucose responsive MIN6 cells.

Of the 246 miRNAs on the human TLDA panel which were present in mouse (including miRNAs not thought to have a murine homolog, but detected in this study in MIN6 cells), 4.9% were differentially expressed in glucose responsive compared to non-glucose responsive cells (table 3.1.2). Fold changes shown in table 3.1.2 are changes in glucose non-responsive cells compared to glucose responsive cells. All 12 differentially expressed miRNAs were down-regulated in non-GSIS cells compared to GSIS cells (table 3.1.2). This data was presented at RNAi 2008 (see poster appendix E).

Target miRNA	Fold Change Glucose non-responsive Vs. glucose responsive MIN6 cells	P-value
mir-376a	-2.6	0.055
mir-369-5p	-2.56	0.014
mir-130a	-2.53	0.037
mir-27a	-2.21	0.021
mir-410	-2.19	0.018
mir-124a	-1.87	0.056
mir-200a	-1.79	0.037
mir-337	-1.79	0.013
mir-532	-1.43	0.017
mir-320	-1.41	0.033
mir-192	-1.35	0.015
mir-379	-1.23	0.015

Table 3.1.2 MiRNAs differentially expressed in glucose responsive and glucose non-responsive MIN6 cells. Fold change indicates expression levels in glucose non-responsive MIN6 cells compared to glucose responsive MIN6 cells.

3.1.3.3 Validation of TLDA targets

All 12 TLDA targets from table 3.1.2 were validated using single-plex RT-PCR (protocol outlined in section 2.4.7). Each miRNA target is reverse transcribed in a singleplex reaction. Table 3.1.3 shows results of single-plex experiments. For the TLDA experiment, let-7b was used as endogenous control in validation experiments, and glucose responsive, P37 cells were designated as calibrator. Fold changes indicated are for glucose non-responsive compared to glucose responsive cells.

Target	TLDA results		Single-plex Results	
	Fold change Glucose non-responsive Vs. glucose responsive	P-value	Fold change Glucose non-responsive Vs. glucose responsive	P-value
mir-376a	-2.6	0.055	-1.86	0.0029
mir-369-5p	-2.56	0.013	-1.5	0.001
mir-130a	-2.53	0.037	1.15	0.45*
mir-27a	-2.21	0.02	1.3	0.15*
mir-410	-2.189	0.018	-1.1	0.7*
mir-124a	-1.87	0.056	3.03	0.058*
mir-200a	-1.79	0.037	-2.69	0.0005
mir-337	-1.79	0.01	-2.49	0.0018
mir-532	-1.43	0.017	-1.88	0.0044
mir-320	-1.41	0.03	-1.38	0.127*
mir-192	-1.35	0.015	-1.63	0.069*
mir-379	-1.23	0.0149	-1.56	0.038

Table 3.1.3 Comparison of TLDA and single-plex validation results. Fold changes were calculated using the comparative C_t method. Fold changes indicate changes in non-glucose responsive cells compared to glucose responsive cells. (*indicates non-statistically significant result).

According to the single-plex validation experiment mir-130a, mir-27a, mir-410, mir-124a, mir-320 and mir-192 were not statistically significantly differentially expressed in glucose responsive compared to glucose non-responsive cells, as p-values are greater than 0.05 (table 3.1.3). These results are conflicting with TLDA results, where all targets chosen were significantly differentially expressed between the two populations.

Mir-124a was 1.56 fold down-regulated according to TLDA results, conversely, single-plex validation experiments showed mir-124a up-regulated 3.03 fold (table 3.1.3). The p-value of mir-124a result from TLDA experiment is on the border of being statistically significant; this miRNA was chosen as a target regardless, as it had previously been shown to be involved in regulation of exocytosis related proteins (Plaisance, Abderrahmani et al. 2006). P-value for mir-124a from validation experiment remained on the border of statistical significance for single-plex validation experiments.

Single-plex validation experiments showed reduced fold changes for mir-376a and mir-369-5p, and improved fold changes for mir-200a, mir-337 and mir-532 compared to TLDA results (table 3.1.3).

3.1.3.4 Putative miRNA targets

Microarray and proteomic studies performed in house identified mRNAs (Gammell 2002; O'Driscoll, Gammell et al. 2006; Rani 2008) and proteins (Dowling, O'Driscoll et al. 2006) differentially expressed in glucose responsive compared to glucose non-responsive MIN6 and MIN6 B1 cells. Here, bioinformatic analysis was performed on these mRNA and protein targets using the miRanda algorithm (http://www.microrna.org/microrna/home.do) to determine if they could potentially be regulated by the miRNAs identified as of interest in this study. A large number of these mRNAs were found to contain putative binding sites for the target miRNAs, including several mRNAs of which could potentially be targeted by more than one of the identified miRNAs. Table 3.1.4 shows mRNAs and proteins which were up-regulated in glucose non-reponsive cells, representing potential targets for the miRNAs down-regulated in this cell population.

MicroRNA	mRNA (Gammell 2002; O'Driscoll, Gammell et al. 2006; Rani 2008)	Protein (Dowling, O'Driscoll et al. 2006)
mir-376a	Faf1	N/A
mir-130a	Egr1, neuroD1, gap 43, txnip, Rgs4, Mxi1, IVNS1abp, meox2 (x2), ccna2, smn (x2), BMP6	N/A
mir-27a	Isl1, Bhlhb9, ube2g1, Pnrc1, meox2, FGF12, btg2	DUT
mir-410	Pld1, Rgs4, Serf1, eya2	Hmgb1 (x2)
mir-124a	Egr1, Trib1, eif4b, meox2, ccna2, btg2, eya2	N/A
mir-200a	Ceacam1, txnip, Jun, Rgs4, IVNS1abp (x2), smn, Faf1	Hmgb1
mir-320	Mxi1 (x2), bri3, FGF12 (x2), gnas, btg2 (x2), BMP6	Ppp1cb
mir-192	N/A	Hmgb1 (x2)
mir-379	Dusp1	N/A

Table 3.1.4 mRNAs and proteins previously identified in our laboratory as up-regulated in glucose non-responsive compared to glucose responsive MIN6 and MIN6 B1 cells (Gammell 2002; Dowling, O'Driscoll et al. 2006; O'Driscoll, Gammell et al. 2006; Rani 2008) with putative binding sites for miRNAs identified here by TLDAs (x – multiple putative binding sites in target mRNA, N/A – non-applicable, no putative binding sites found in these mRNA sequences).

3.1.4 Functional Validation of microRNA targets

Functional validation of miRNA targets was performed in order to evaluate miRNA effect on GSIS, using the protocol outlined in section 2.2.4. Pre-mir and anti-mirs were used for over-expression and knockdown of miRNAs respectively. All target miRNAs were down-regulated in non-glucose responsive cells, following from this knockdown of miRNA targets in glucose responsive cells would be expected to lead to a reduction in GSIS. While over-expression of miRNA targets in glucose non-responsive cells would be expected to lead to an increase in the GSIS response. However, as is often observed in science, functional validation studies may not always follow the trend observed in the profiling study. To allow for this possibility, functional validation over-expression studies were performed in cells with a GSIS response to ensure that 'unexpected' reductions in GSIS may also be observed.

A time course assay was performed to determine how long the effect of anti-mir was present in the cell. As an example, cells were transfected with anti-mir-532 to knockdown expression of mir-532; anti-mir-negative was transfected into cells as a control. RNA was collected at several time points from anti-mir-532 and control transfected cells and assessed for mir-532 levels (table 3.1.5) (section 2.4.7). 96% knockdown of miRNA levels was achieved after only 24 hours, with knockdown only decreasing slightly to 80% by 144 hours (figure 3.1.4).

Time	Treatment	C_t Mir-532	C_t let-7b	ΔC_t	$\Delta\Delta C_t$	RQ	% mir-532 knockdown
24hrs	**am-neg**	30.463	26.186	4.277	0	1	0
	am-532	34.588	25.549	9.039	4.762	0.037	96.3
48hrs	**am-neg**	30.029	25.649	4.38	0	1	0
	am-532	33.484	25.722	7.761	3.381	0.096	90.4
72hrs	**am-neg**	29.798	25.214	4.584	0	1	0
	am-532	32.319	24.669	7.65	3.066	0.119	88.1
96hrs	**am-neg**	28.92	24.373	4.548	0	1	0
	am-532	32.603	24.844	7.759	3.211	0.108	89.2
120hrs	**am-neg**	28.53	24.111	4.419	0	1	0
	am-532	31.716	24.206	7.51	3.091	0.117	88.3
144hrs	**am-neg**	28.391	24.169	4.222	0	1	0
	am-532	30.418	23.788	6.629	2.407	0.189	81.1

Table 3.1.5 Time course assay for knockdown of mir-532. Cells were transfected with anti-mir-532 (am-532) or anti-mir-negative (am-neg), and levels of mir-532 measured at set time-points. Let-7b was used as endogenous control for normalisation of PCR data.

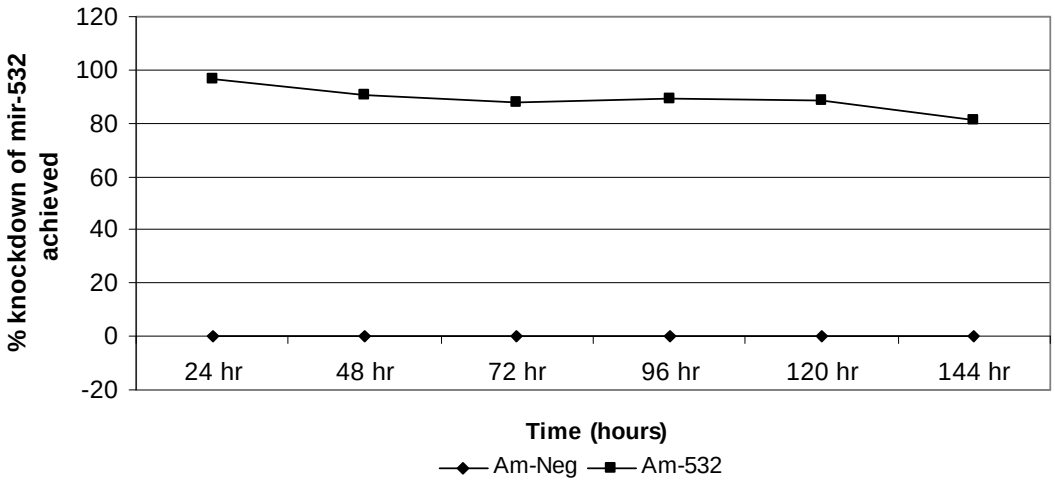

Figure 3.1.4 Percentage knockdown of mir-532 levels in MIN6 cells treated with anti-mir-532 (am-532) and control anti-mir-negative (am-neg). Data normalised to endogenous control let-7b.

A time point of 72 hours post-transfection was chosen for determination of GSIS response following manipulation of miRNA expression as anti-mir still exhibiting approximately 90% knockdown of miRNA expression at this stage (figure 3.1.4). Also, 72 hours post transfection potentially allows time for manipulated miRNA to effect the target mRNA and allow any downstream effect on GSIS to be detected.

Knockdown and over-expression experiments were performed for each target miRNA. For miRNAs which exhibited an effect on GSIS, experiments were carried out a large number of times to establish if these effects were reproducible or just a random variation in GSIS of MIN6 cells. Results of individual assays can be seen in appendix A. Biological triplicate experiments were then chosen from the large number of individual assays as representatives of manipulation of each specific miRNA, the Student's *t*-test was then applied to determine if such changes were of statistical significance.

For miRNAs which did not exhibit effects on GSIS, experiments were performed at least in biological duplicate. Anti-mir negative, pre-mir negative and untreated controls were performed with each experiment to prove that effect on GSIS was due to manipulation of specific miRNA, rather than a more general or non-specific event.
According to our TLDA analysis, each of the 12 miRNAs had reduced expression in glucose non-responsive MIN6 cells (table 3.1.2); therefore, pre-mir over-expression of miRNA would be expected to improve GSIS function, while anti-mir reduction of miRNA would be expected to reduce GSIS function. Functional validation experiments were designed to perform pre-mir over-expression experiments in low or non-GSIS cells, as pre-mir transfection was expected to improve GSIS, and anti-mir knockdown experiments in GSIS-competent cells, as anti-mir transfection was expected to reduce GSIS based on the TLDA results. However, due to the variable nature of the GSIS response in MIN6 cells sometimes cells which were expected to exhibit low or non-GSIS response showed a good GSIS, while cells expected to exhibit good GSIS response were low or non-GSIS response.

3.1.4.1 Mir-410

Mir-410 expression was reduced in non-GSIS MIN6 cells (table 3.1.2), therefore knockdown of this target with mir-410 inhibitors was expected to reduce GSIS function of MIN6 cells, while mir-410 mimics were expected to improve GSIS function.

(a) Knockdown of mir-410

Anti-mir-410 (am-410) was transfected into MIN6 cells (section 2.2.4). GSIS response of cells was then measured following 72 hours post transfection to test the effects of miRNA manipulation on GSIS (section 2.2.1).

Transfection controls can be inconsistent with large differences in the GSIS fold change of control cells, therefore triplicate experiments (appendix A, figure 3, 10 and 11) where the GSIS of controls was consistent were taken as representatives of the effect of knockdown of mir-410 levels in MIN6 cells. Knockdown of mir-410 in GSIS-competent cells using am-410 led to a reduction in GSIS, from 2.3 fold GSIS in am-neg treated cells to 1.6 fold GSIS in am-410 treated cells. The Student's *t*-test showed that the decrease in GSIS of these triplicate experiments was statistically significant (figure 3.1.5).

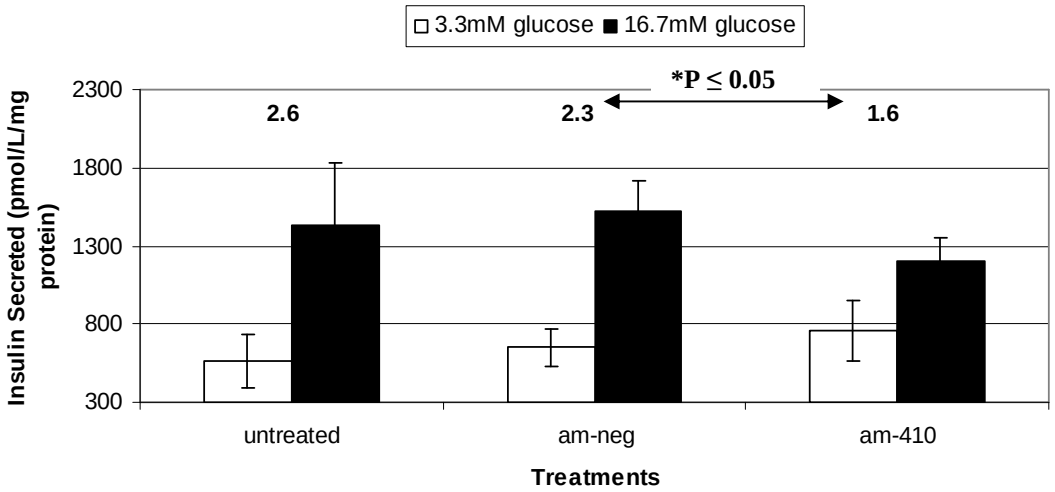

Figure 3.1.5 Knockdown of mir-410 levels in GSIS-competent MIN6 cells (error bars indicate standard error of biological triplicates).

(b) Over-expression of mir-410

Pre-mir-410 (pm-410) was used for over-expression of mir-410 levels in MIN6 cells (section 2.2.4). GSIS response of cells was then measured 72 hours post transfection to test effects of miRNA manipulation on GSIS (section 2.2.1).

A large number of repeats were performed for this assay to determine if over-expression of mir-410 had an effect on GSIS. Some assays showed large differences in GSIS fold change of controls. When the fold change of pm-410 transfected cells is within this range it is difficult to determine the effect of pm-410 transfection or if an effect is being disguised by the large range in GSIS of controls. Therefore, three replicate experiments where the effect of pm-410 was obvious and did not lie within the large range in GSIS of controls, were taken as representative experiments (appendix A, figures 17, 19 and 21). Over-expression of mir-410 in GSIS-competent MIN6 cells led to an increase in GSIS response in these cells, from 1.6 fold GSIS in pm-neg treated cells to 3.8 fold GSIS in pm-410 treated cells. The *t*-test of these replicates indicated that the increase in GSIS in pm-410 transfected cells relative to pm-neg transfected cells is statistically significant (figure 3.1.6).

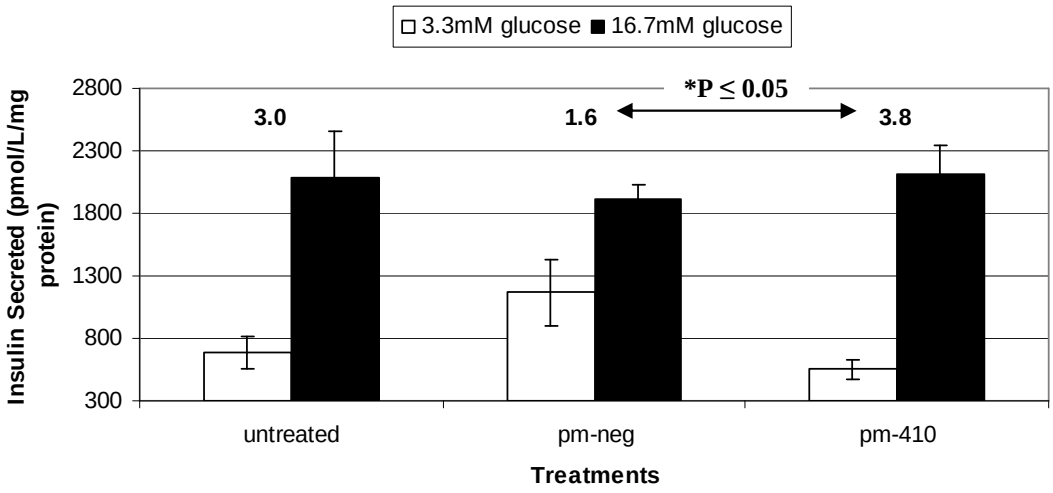

Figure 3.1.6 Over-expression of mir-410 in GSIS-competent MIN6 cells (error bars indicate standard error of biological triplicates) (* indicates statistical significance p-value ≤ 0.05).

3.1.4.2 Mir-200a

Mir-200a expression was reduced in non-GSIS MIN6 cells (table 3.1.2), therefore, knockdown of this target with anti-mir-200a (am-200a) was expected to reduce GSIS function of MIN6 cells, while mir-200a over-expression (pm-200a) was expected to improve GSIS function.

(a) Knockdown of mir-200a

Three assays (appendix A, figures 25, 26 and 27) were picked as representatives of the effect of mir-200a over-expression. Knockdown of mir-200a in GSIS-competent MIN6 cells led to a reduction in GSIS response in these cells, from 1.6 fold GSIS in am-neg treated cells to 0.9 fold GSIS in am-200a treated cells. The Student's *t*-test of these replicates (figure 3.1.7) indicated a statistically significant decrease in GSIS of am-200a transfected cells relative to am-neg transfected cells.

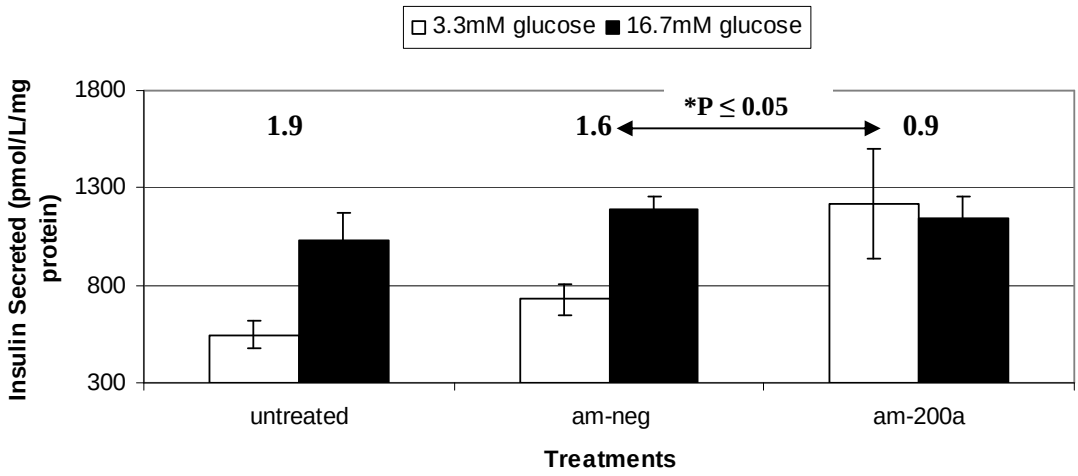

Figure 3.1.7 Knockdown of mir-200a levels in GSIS-competent MIN6 cells (error bars indicate standard error of biological triplicates) (* indicates statistical significance p-value ≤ 0.05).

(b) Over-expression of mir-200a

Three replicates for mir-200a over-expression were tested; however, no clear trend for mir-200a functional effect on GSIS was seen.

3.1.4.3 Mir-130a

Mir-130a expression was reduced in non-GSIS MIN6 cells (table 3.1.2), therefore knockdown of this target with mir-130a inhibitors was expected to reduce GSIS function of MIN6 cells, while mir-130a mimics were expected to improve GSIS function.

(a) Knockdown of mir-130a

Appendix A, figure 34, 36 and 37, were chosen as representative assays for the effect of mir-130a knockdown. Knockdown of mir-130a in GSIS-competent cells led to a decrease in GSIS in these cells, from 1.8 fold GSIS in am-neg treated cells to 1.1 fold GSIS in am-130a treated cells. The Student's *t*-test determined that the decrease in GSIS of am-130a cells relative to am-neg transfected cells was statistically significant (figure 3.1.8).

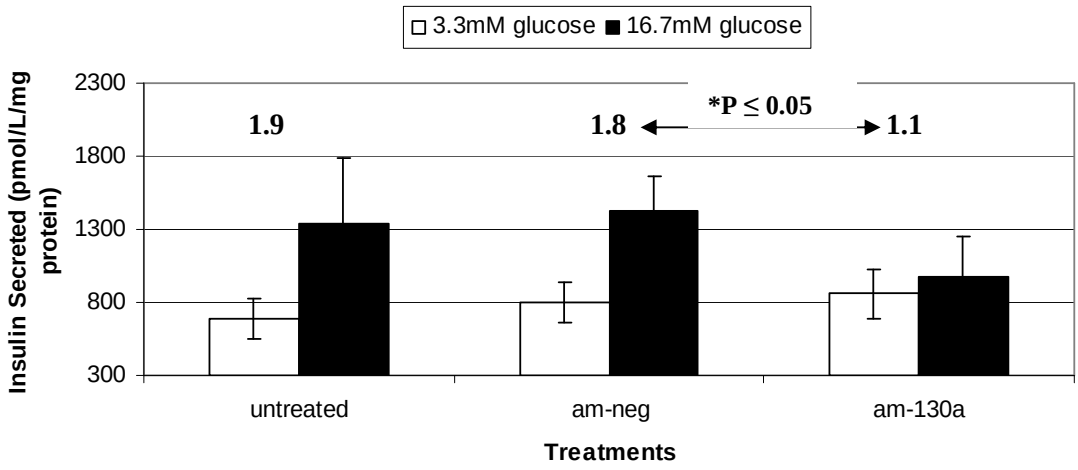

Figure 3.1.8 Knockdown of mir-130a levels in GSIS-competent MIN6 cells (error bars indicate standard error of biological triplicates) (* indicates statistical significance p-value ≤ 0.05).

(b) Over expression of mir-130a

Over-expression of mir-130a showed reduced GSIS relative to control cells in three of five replicates performed (appendix A, figures 41, 42 and 44). These replicates were taken as representatives of the effect of over-expression of mir-130a. Over-expression of mir-130a in GSIS-competent cells led to a slight, but not statistically significant reduction in GSIS response in these cells from 2.2 fold GSIS in pm-neg treated cells to 1.3 fold GSIS in pm-130a treated cells (figure 3.1.9).

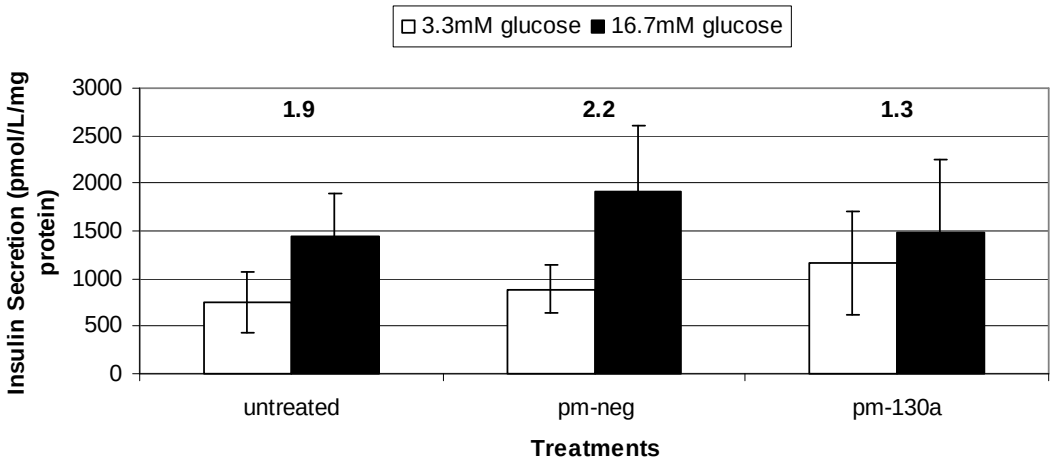

Figure 3.1.9 Over-expression of mir-130a in MIN6 cells (error bars indicate standard error of biological replicates).

3.1.4.4 Mir-376a

Mir-376a expression was reduced in non-GSIS MIN6 cells (table 3.1.2), therefore knockdown of this target with mir-376a inhibitors was expected to reduce GSIS function of MIN6 cells, while mir-376a mimics were expected to improve GSIS function.

(a) Knockdown of mir-376a

Knockdown of mir-376a levels was performed in five replicates, with two replicates showing no effect on GSIS, two replicates showing slightly reduced GSIS relative to control cells, while the last replicate had unreliable controls. Therefore there were no clear trends of an effect on GSIS following knockdown of mir-376a levels.

(b) Over-expression of mir-376a

Over-expression of mir-376a was assessed in five replicates, two replicates showing increased GSIS relative to control cells, two replicates showed decreased GSIS, while one replicate showed unreliable controls, therefore no clear trends of an effect were observed in GSIS for over-expression of mir-376a.

3.1.4.5 Mir-369-5p

(a) Large-scale assays for over-expression and knockdown of mir-369-5p expression

Performing transfection GSIS assays in bulk (appendix A, figures 55 and 56) led to diminished GSIS response compared to cells at the previous passage when a single GSIS assay was performed. Therefore, the numbers of transfection controls were reduced. Also, knockdown transfections were performed separate to over-expression transfections, to try to maintain a good GSIS response of cells.

(b) Knockdown of mir-369-5p

Knockdown of mir-369-5p transfections were performed a number of times, three replicates showed no change in GSIS of am-369-5p transfected cells, two replicates showed unreliable controls, while five replicates showed a decrease in GSIS following knockdown of mir-369-5p levels relative to controls cells. Three of these replicates were taken as representatives of the effect of am-369-5p (appendix A, figure 60, 61 and 64). An average of 1.3 fold GSIS was seen for am-neg treated cells compared to 0.8 fold GSIS for am-369-5p treated cells. The Student's t-test was applied to these replicates; however, the decrease in GSIS was not statistically significant (figure 3.1.10).

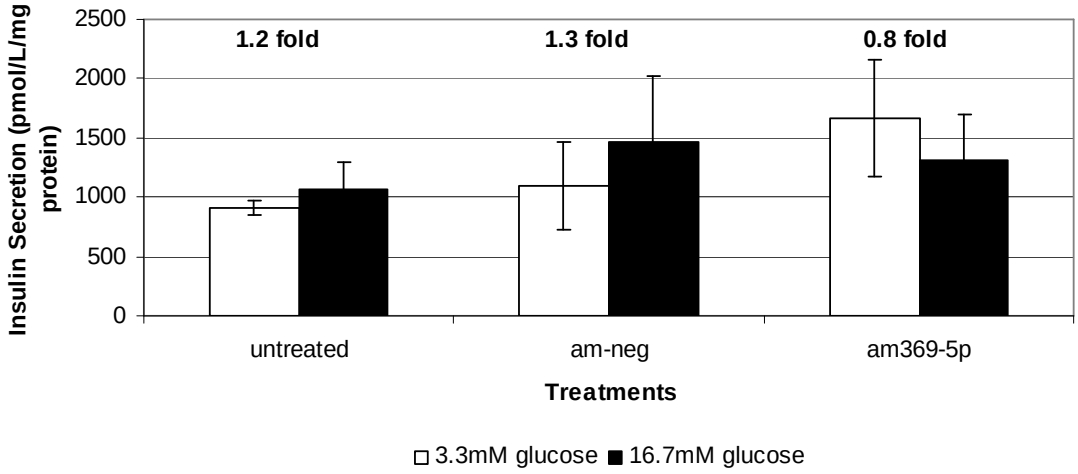

Figure 3.1.10 Knockdown of mir-369-5p levels in MIN6 cells (error bars indicate standard error of biological triplicates).

(c) Over-expression of mir-369-5p

Seven replicates of mir-369-5p over-expression were performed; four replicates showed no effect of mir-369-5p over-expression on GSIS, one replicate showed improved GSIS, while two replicate showed unreliable controls. Therefore, the trend showed that over-expression of mir-369-5p did not affect GSIS.

3.1.4.6 Mir-27a

(a) Large-scale assays for over-expression and knockdown of mir-369-5p expression

Performing transfection GSIS assays in bulk (appendix A, figure 70 and 71) led to diminished GSIS response compared to cells at the previous passage when a single GSIS assay was performed. Therefore the numbers of transfection controls were reduced; also knockdown transfections were performed separate to over-expression transfections, to try to maintain a good GSIS response of cells.

(b) Knockdown of mir-27a

Five replicates of mir-27a knockdown were performed, three of which indicated that knockdown of mir-27a did not effect GSIS relative to control cells (appendix A, figure 71, 72 and 74).

(c) Over-expression of mir-27a

Six replicates of mir-27a over-expression were performed, three indicated that over-expression of mir-27a did not have any effect on GSIS relative to control cells (appendix A, figures 71, 75 and 76), two replicates showed decreased GSIS (appendix A, figures 77 and 78) and one replicate had inconsistent controls (appendix A, figure 70). Therefore, the general trend of mir-27a over-expression is no effect on GSIS.

3.1.4.7 Mir-124a

Mir-124a expression was reduced in non-GSIS MIN6 cells (table 3.1.2), therefore, increasing and decreasing mir-124a expression should increase and decrease GSIS response of these cells, respectively.

(a) Knockdown of mir-124a

Mir-124a knockdown assay was performed a number of times to determine the effect on GSIS, the general trend to the assays indicates that knockdown of mir-124a does not affect GSIS relative to control cells.

(b) Over-expression of mir-124a

Seven replicates of mir-124a over-expression were performed, two of which showed no effect on GSIS (appendix A, figures 91 and 92), two showed in increase in GSIS (appendix A, figure 87 and 88), and a further two showed a decrease in GSIS (appendix A, figures 86 and 89), therefore no clear trend was observed for effect of mir-124a over-expression on GSIS.

3.1.4.8 Mir-337

Mir-337 expression was manipulated in MIN6 cells to determine if changes in the expression levels of this miRNA could affect GSIS phenotype of the cells.

(a) Knockdown of mir-337

The general trend for mir-337 knockdown, showed that knockdown of mir-337 levels did not affect GSIS compared to control cells.

(b) Over-expression of mir-337

No clear trends are observed for the effect of over-expression of mir-337 on GSIS response of MIN6 cells.

3.1.4.9 Mir-532

Mir-532 expression was reduced in non-GSIS MIN6 cells according to TLDA analysis (table 3.1.2), therefore manipulation of miRNA expression to increase and decrease mir-532 levels would be expected to increase and decrease GSIS responsiveness of the cells respectively.

(a) Knockdown of mir-532

Duplicate assays for knockdown of mir-532 showed no effect on GSIS relative to control cells; therefore no triplicates were performed as the trend was clear from duplicate assays.

(b) Over-expression of mir-532

Of three replicate performed, two experiments show no effect on GSIS for pm-532 transfected cells, therefore, the general trend indicates that over-expression of mir-532 does not affect the GSIS capability of MIN6 cells.

3.1.4.10 Mir-320

Mir-320 levels were manipulated in MIN6 to determine if this miRNA played a functional role in GSIS of these cells.

(a) Knockdown of mir-320

Six replicates were performed for knockdown of mir-320; five replicates were in agreement that no effect on GSIS was observed for am-320 treated cells. Therefore, the trend indicates that knockdown of mir-320 does not effect the GSIS capability of MIN6 cells.

(b) Over-expression of mir-320

Appendix A, figure 111 indicates that over-expression of mir-320 may lead to a decrease in GSIS; however, this transfection would have to be repeated to determine if this is a true effect of mir-320 over-expression.

3.1.4.11 Mir-192

Mir-192 levels were reduced in non-GSIS MIN6 cells, therefore, manipulation to increase and decrease levels of this miRNA would be expected to increase and decrease GSIS responsiveness, respectively.

(a) Knockdown of mir-192

Three of four replicates for knockdown of mir-192 showed no effect on GSIS, therefore, the trend indicates that knockdown of mir-192 did not affect the GSIS capability of MIN6 cells.

(b) Over-expression of mir-192

Two of three replicates for over-expression of mir-192 showed a decrease in GSIS; therefore, the general trend indicates that over-expression led to a decrease in GSIS capability of MIN6 cells.

3.1.4.12 Mir-379

Mir-379 levels were manipulated in MIN6 cells to determine if this miRNA played a role in the GSIS phenotype of these cells.

(a) Knockdown of mir-379

Duplicate assays for knockdown of mir-379 showed no effect on GSIS relative to control cells; therefore, no triplicates were performed as the trend was clear from duplicate assays.

(b) Over-expression of mir-379

Two of three replicates showed a decrease in GSIS of pm-379 transfected cells, therefore, the general trend indicates that over-expression of mir-379 led to a decrease in the GSIS capability of MIN6 cells.

3.1.4.13 Summary of Functional Validation Studies

Table 3.1.6 summarises results of functional validation of miRNA targets. Mir-410, mir-200a and mir-130a exhibited significant effects on GSIS following manipulation with miRNA inhibitors and mimics.

MicroRNA	Anti-Mir knockdown of miRNA	Pre-Mir over-expression of miRNA
mir-376a	No effect	No effect
mir-369-5p	Reduced GSIS minimally	No effect
mir-130a	Reduced GSIS *	Reduced GSIS minimally
mir-27a	No effect	No effect
mir-410	Reduced GSIS *	Improved GSIS *
mir-124a	No effect	No effect
mir-200a	Reduced GSIS *	No effect
mir-337	No effect	No effect
mir-532	No effect	No effect
mir-320	No effect	Reduced GSIS minimally
mir-192	No effect	Reduced GSIS minimally
mir-379	No effect	Reduced GSIS minimally

Table 3.1.6 Functional validation of miRNA targets in MIN6 cells. (* denotes statistical significance).

3.1.5 Summary of miRNAs involved in GSIS in MIN6 cells

Using TLDA technology, this study identified 12 miRNAs differentially expressed between glucose responsive and glucose non-responsive MIN6 cells (table 3.1.2), as well as 12 novel murine miRNAs (table 3.1.1). Over-expression and knockdown studies were performed on these miRNA targets in MIN6 cells to determine if these miRNAs played a functional role in the regulation of GSIS. Knockdown of mir-410, mir-200a and mir-130a in GSIS competent MIN6 cells led to a significant decrease in GSIS response compared to anti-mir negative transfected control cells. These three miRNAs may function in supporting the capability of MIN6 cells to secrete insulin in response to stimulatory levels of glucose. Experiments with over-expression of mir-410 supported the rational that it may enhance levels of glucose stimulated insulin secretion.

The MIN6 cell line as a model for study GSIS can be undependable due to considerable day-to-day variations in GSIS response between control cells. This varying GSIS response of control cells makes it difficult to decipher the effect of treatment on GSIS. Therefore, as iPS technology became available it represented a potential technique for generation of a human pancreatic beta cell model for studying the regulation of GSIS, without the ethical and moral concerns associated with embryonic stem cell research.

3.2 Attempts to generate iPS cells and differentiation of an established iPS cell line towards pancreatic phenotypes

Induced pluripotent stem cells (iPS cells) can be generated from fully differentiated adult somatic cells by forced expression of a defined set of transcription factors (Takahashi, Tanabe et al. 2007). iPS cells represent a potential route for the generation of human pancreatic beta cell models. However the technology is currently technically challenging with very low efficiency rates for the reprogramming of somatic cells back to a pluripotent, embryonic stem cell-like phenotype. These low efficiency rates differ among different cell types and this issue was considered in the selection of starting cell populations chosen for reprogramming.

Three different cell types were selected for generation of iPS cells in this study, MiaPaCa2 pancreatic adenocarcinoma cell line, normal primary epidermal keratinocytes and limbal epithelial cells. MiaPaCa2 cells were selected due to their pancreatic origin as MiaPaCa2 generated iPS cells may maintain some pancreatic epigenetic memory and be more easily pushed towards pancreatic lineages in subsequent directed differentiation experiments. Keratinocytes were used as the reported reprogramming efficiencies were 100 fold higher than fibroblasts (Aasen, Raya et al. 2008), which were the standard cell type used for reprogramming at the time this work was undertaken. Limbal epithelial cells are the stem cell population for the cornea epithelia. These cells were used for reprogramming as reports suggest that reprogramming occurs with increased efficiency in such cultures of stem cell populations.(Kim, Zaehres et al. 2008)

3.2.1 Generation of Virus Particles

iPS cell generation by forced expression of transcription factors- oct4, sox2, c-myc and klf4 was attempted using a lenti-viral expression system.

Lentiviral particles were generated by co-transfecting the lentiviral ORF expression clone (containing oct4, sox2, c-myc or klf4 gene) together with the lentiviral packaging plasmids (protocol outlined in section 2.3.1). The lentiviral ORF plasmid contains the elements required for packaging, transduction and stable integration on the viral construct into the host genomic DNA, however, it lacks the elements required for transcription and packaging of an RNA copy of the ORF construct into active viral particles. These elements are provided by the lentiviral packaging plasmids. The packaging plasmids are two plasmids which contain all the structural, regulatory and replication genes required to produce lentivirus.

3.2.2 Validation of correct insert in lenti-viral ORF expression clones

The lentiviral ORF expression clones containing oct4, sox2, c-myc and klf4 were used to transform competent *E.coli* cells (protocol outlined in section 2.3.1.1). The lentiviral ORF plasmids also contain the ampicillin resistance gene (figure 3.2.1), thereby allowing selection of the *E.coli* cells which have taken up the plasmid. Transformed cells were seeded into small scale 5mL cultures. After overnight incubation, plasmid DNA was isolated. Plasmid DNA was then analysed to verify that the correct insert was contained in the lentiviral plasmid backbone. To verify this, the lentiviral plasmids was digested with Nhe1 and Xba1 restriction enzymes to release the ORF insert, the resultant mixes were then run on an agarose gel, and based on the size of the excised ORF it was deduced that a sequence of the correct size has been inserted into the plasmids.

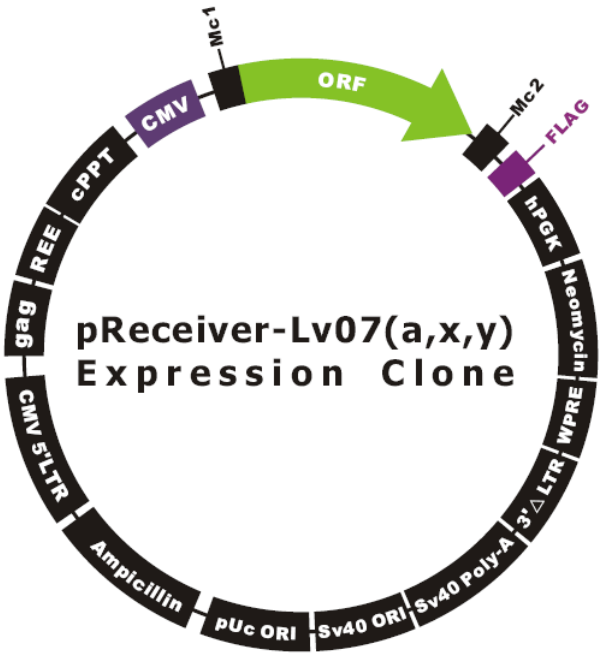

Figure 3.2.1 Lentiviral ORF expression clone plasmid map. Oct4, sox2, c-myc or klf4 genes were inserted into the region labelled ORF. Plasmid also contains ampicillin resistance gene to allow for selection of cells which have taken up the plasmid.

The klf4 insert was expected to be 1413 base pairs, c-myc was 1365 base pairs, sox2 was 954 base pairs and oct4 was 495 base pairs (figure 3.2.2). Bands at the expected sizes were seen on the agarose gel, indicating that sequences of the correct size were inserted in the expression plasmids.

Once confirmed that correct size insert was present in the expression plasmids, large 250mL cultures were initiated in order to generate large stocks of each of the expression plasmids and also to create glycerol stocks of transformed cells for storage.

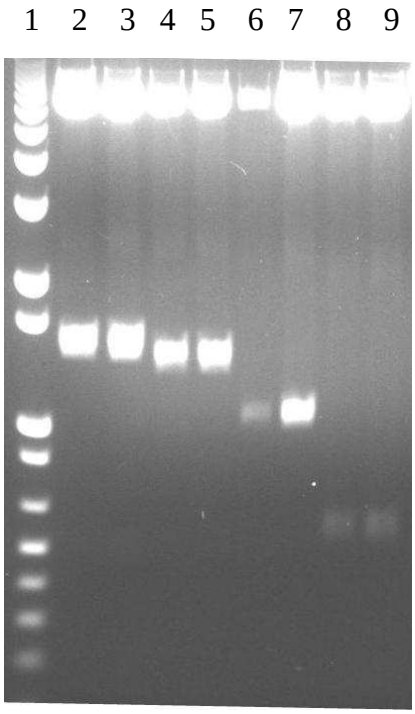

Figure 3.2.2 Agarose gel of digested plasmid DNA
Lane 1- DNA marker
Lane 2&3 – Klf4 (1413 bp)
Lane 4&5 – c-myc (1365 bp)
Lane 6&7 – sox2 (954 bp)
Lane 8&9 – oct4 (495 bp)

3.2.3 Optimisation of plasmid transfection conditions

A lentiviral ORF expression plasmid containing the GFP (green fluorescent protein) reporter gene was used for optimisation of transfection conditions. This plasmid was co-transfected with the lentiviral packaging plasmids into 293 cells and transfection efficiency was determined based on transient expression of the GFP reporter gene (section 2.3.1). Different transfection reagents, volume of transfection reagent and plasmid concentration were analysed for transfection efficiency (figure 3.2.3).

The lowest volume of fugene transfection reagent showed the greatest transfection efficiency (figure 3.2.3). Lipofectamine transfection reagent also showed good transfection efficiency. Supernatant containing active viral particles was harvested from the fugene 18μL 4:2:2 plasmid concentration, and lipofectamine 10μL 4:2:2 plasmid concentration wells for optimisation of viral infection.

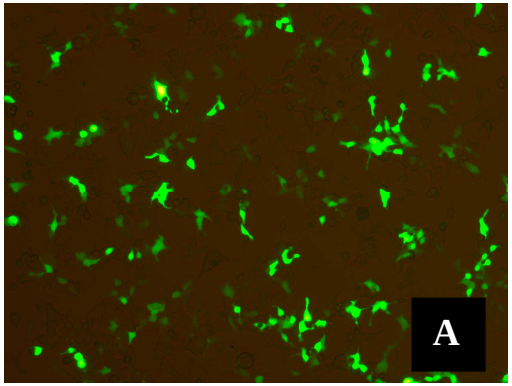

A: Fugene 18µL, 2:1:1 µg/plasmid

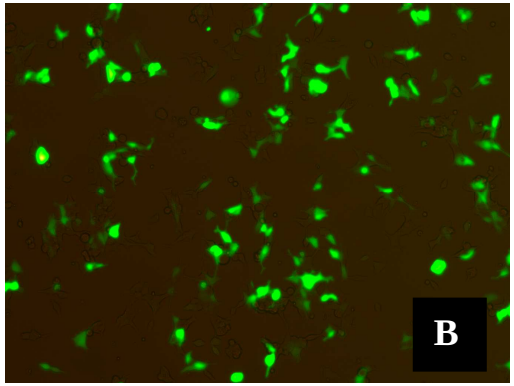

B: Fugene 18µL, 4:2:2 µg/plasmid

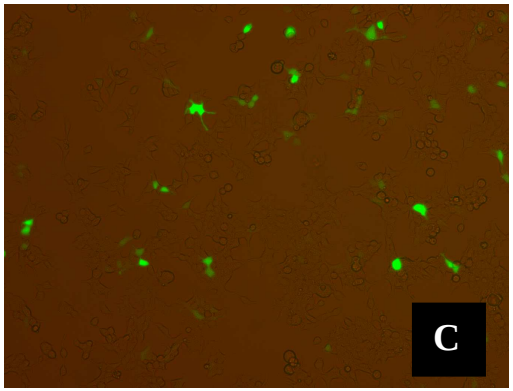

C: Fugene 18µL, 8:4:4 µg/plasmid

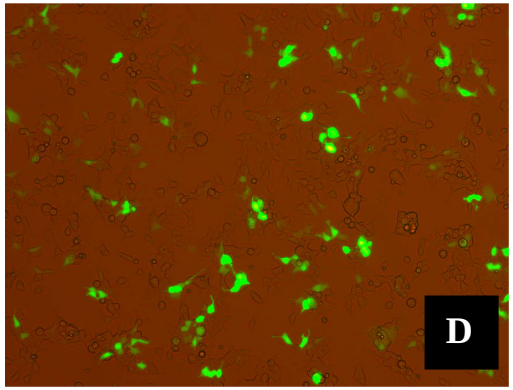

D: Fugene 36µL, 2:1:1 µg/plasmid

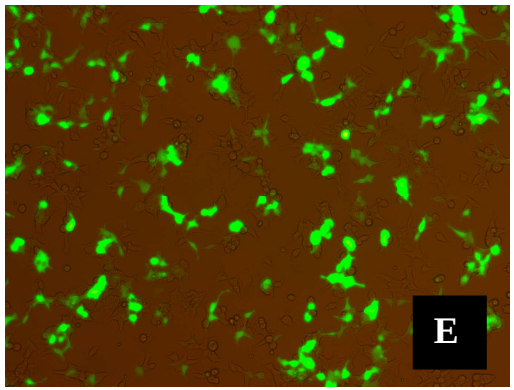

E: Fugene 36µL, 4:2:2 µg/plasmid

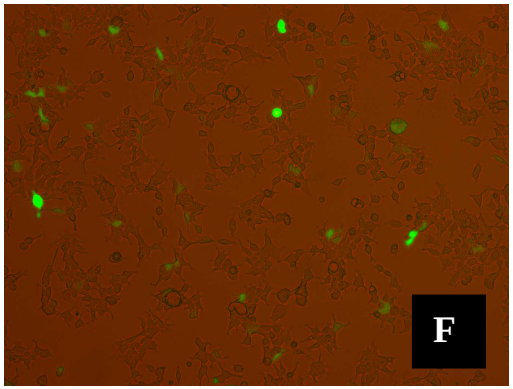

F: Fugene 36µL, 8:4:4 µg/plasmid

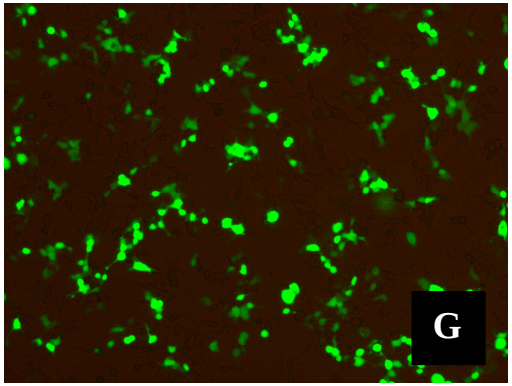

G: Lipofect 10µL, 2:1:1 µg/plasmid

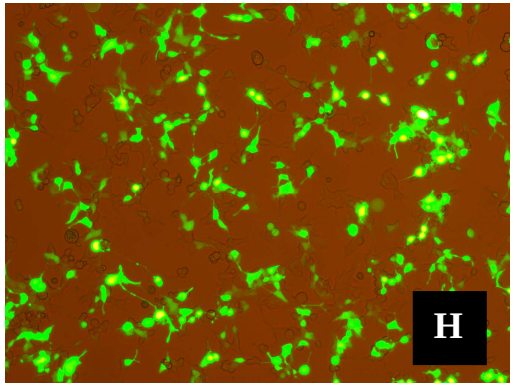

H: Lipofect 10µL, 4:2:2 µg/plasmid

Transfection Reagent	**Transfection Efficiency 2:1:1 plasmid conc**	**Transfection Efficiency 4:2:2 plasmid conc**	**Transfection Efficiency 8:4:4 plasmid conc**
Fugene 18µl	60%	90%	<5%
Fugene 36µl	30%	70%	<5%
Lipofectamine 10µl	70%	80%	

I: Summary table of percentage of cells expressing GFP for each transfection condition

Figure 3.2.3 GFP reporter gene expression in transfected cells. Images A-H are fluorescent microscope images of GFP expression in transfected cells. Cells were transfected with either Fugene or Lipofectamine transfection reagents, and with differing volumes of transfection reagents. Differing concentration of plasmids were also transfected. Ratios of plasmid concentrations represent concentration of expression clone to each of the packaging plasmids, with the expression clone being transfected at double the concentration of each packaging plasmid for each treatment. Table I shows a summary of percentage GFP positive cells achieved for each transfection condition.

3.2.4 Optimisation of viral transduction

MiaPaCa2 pancreatic adenocarcinoma cells were used for optimisation of viral transduction, as these cells would subsequently be used for transduction with the four factor viruses for iPS cell generation. Cells were treated with either lipofectamine (10µL 4:2:2) or fugene (18µL 4:2:2) generated virus, for either a single dose, or double dose (with the second dose being administered 24hrs after first virus treatment). Virus treated cells were then analysed for transduction efficiency by monitoring GFP expression using a fluorescent microscope (figure 3.2.4).

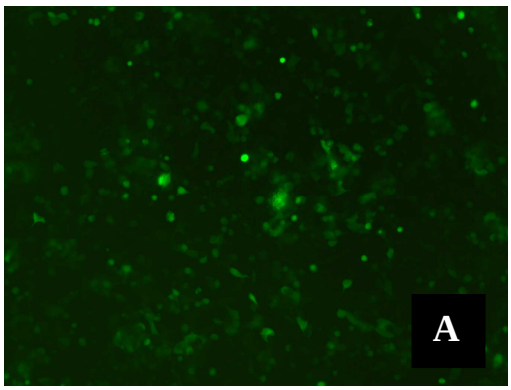

A: MiaPaca, 1 dose of Fugene (18µL, 4:2:2 µg/plasmid) virus

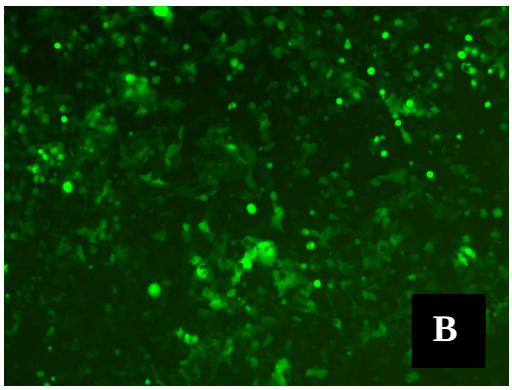

B: MiaPaca, 2 doses of Fugene (18µL, 4:2:2 µg/plasmid) virus

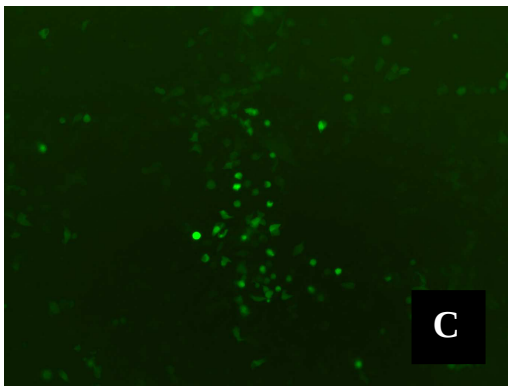

C: MiaPaca, 1 dose of lipofectamine (10µL, 4:2:2 µg/plasmid) virus

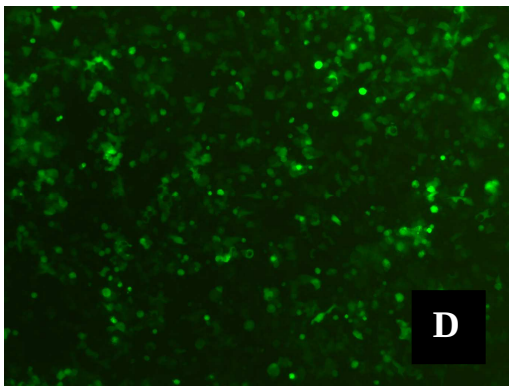

D: MiaPaca, 2 doses of lipofectamine (10µL, 4:2:2 µg/plasmid) virus

Figure 3.2.4 GFP reporter gene expression in cells treated with GFP virus. Images A-D are fluorescent microscope images of GFP expression in infected MiaPaCa2 cells. Cells were infected with either Fugene or Lipofectamine generated virus, with either a single dose, or two doses of virus. Images were taken 7 days post first virus treatment.

Treating MiaPaCa2 cells with a second dose of virus greatly improved the percentage of GFP positive cells compared to single dosed cells, for both fugene and lipofectamine generated virus (figure 3.2.4). Cells treated with a second dose of fugene or lipofectamine generated virus showed approximately 90% GFP positive cells, as assessed by eye using a fluorescent microscope, indicating the high efficiency of viral infection. As the infection efficiencies were very similar for virus generation with fugene and lipofectamine, fugene was used for all subsequent viral experiments.

3.2.4.1 Calculation of multiplicity of infection (MOI)

The viral titre was quantified to allow calculation of multiplicity of infection (MOI). Guava flow cytometer was used to determine the percentage of cells expressing GFP after viral infection, as a more accurate calculation was required than estimating infection efficiency from fluorescent microscope images. MiaPaCa2 cells were infected using the optimised transduction conditions, for either one or two doses of virus. Cells were analysed by the Guava flow cytometer for GFP expression at 3 time-points, 24, 48 and 72 hours after the second dose of virus was administered (table 3.2.1).

Cell counts were performed on wells to be analysed by the guava flow cytometer (table 3.2.1). A multiplicity of infection (MOI) of 5 is recommended for generation of iPS cells (Park and Daley 2009), i.e. 5 viral particles per cell. As described in section 2.3.2, $5x10^4$ cells were seeded per well of a 6-well plate for iPS cell generation, therefore, to allow for an MOI of 5, $2.5x10^5$ viral particles would be required to achieve this MOI. Table 3.2.1 shows that per 1mL of viral suspension $3.3x10^5$ were infected, indicating there were at least $3.3x10^5$ active viral particles per mL of viral suspension. As this is above the threshold of $2.5x10^5$ viral particles required for an MOI of 5, this indicates that the viral suspension is sufficiently concentrated and does not require any additional concentrating procedures. This technique represents a relatively crude method for determining MOI, as the infected cells may have been infected by more than one active viral particle. Therefore, this technique was utilised to ensure that cells were being treated with the minimum number of active viral particles required.

Treatment	24 hours	48 hours	72 hours
Single Dose	41%	66%	60%
Twice Dosed	75%	83%	80%
Total Cell Count	$8x10^5$	$1.6x10^6$	$2.5x10^6$
Number of infected cells for single virus treatment	$3.3x10^5$	$1.1x10^6$	$1.5x10^6$

Table 3.2.1 Percentage of GFP positive cells as measured by Guava cytometer, at three different time points following treatment with virus. Cell counts were performed on cell suspensions before guava flow cytometer analysis.

3.2.5 Development of protocol to generate iPS cells

MiaPaCa2 pancreatic adenocarcinoma cell line, epidermal keratinocytes and limbal epithelial cells were subjected to the iPS protocol (section 2.3.2), using the conditions optimised in section 3.2.4.

3.2.5.1 Attempt to generate iPS cells from MiaPaCa2 cell line

Cells were either treated with the four factor cocktail- oct4, sox2, c-myc and klf4, or the three factor cocktail- oct4, sox2 and klf4. c-myc was excluded from the 3 factor cocktail as c-myc is thought to lead to the generation of an increased number of false positive colonies (Eggan 2009). Cells were treated with 2 doses of virus. After four days cells were trypsinised onto a mitomycin C treated MEF feeder layer, and cultured in embryonic stem cell (ES) media. By day 8 following the second viral treatment, cells with distinctly different cell morphology to untreated parent MiaPaCa2 had emerged (figure 3.2.5).

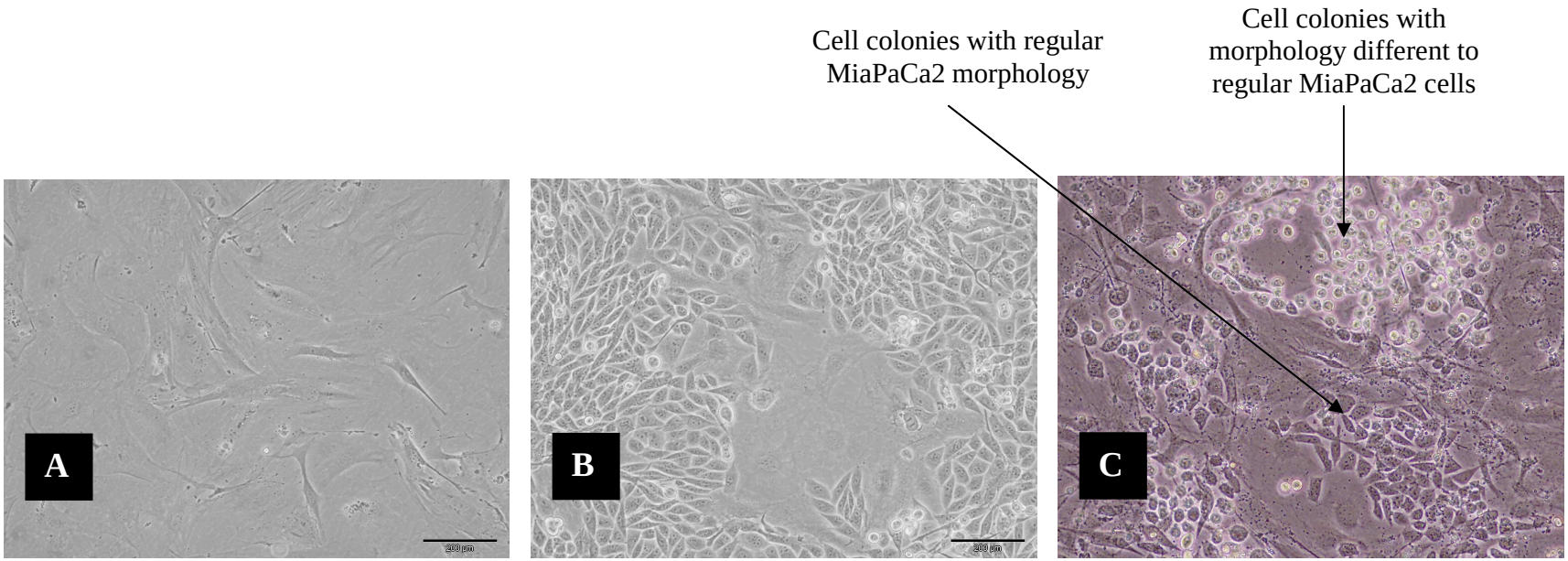

Figure 3.2.5 iPS virus treatment of MiaPaCa2 cells. **A**- mitomycin C treated MEF cells. **B**- untreated MiaPaCa2 parental cells growing on a mitomycin C treated MEF feeder layer. **C**- MiaPaCa2 cells at 8 days post second viral treatment, grown on MEF feeder layer with ES media.

Cultures treated with either 3-factors or 4-factors showed the same mixture of cell morphologies at 8 days post second viral treatment. Cultures were a mixture of colonies of typical MiaPaCa2 morphology and colonies of more rounded, less-stretched out cells (figure 3.2.5, image C).

By day 24 the colonies of rounded, less-stretched cells grew to form large clusters with a tightly packed core of cells with rounded morphology, while cells at the periphery of these clusters displayed ‘typical’ MiaPaCa2 morphology (figure 3.2.6). Cultures treated with either 3 factors (oct4, sox2 and klf4) or 4 factors (oct4, sox2, klf4 and c-myc) showed similar cell morphology trends.

Colonies were grown until they were visible by eye (figure 3.2.7). Single colonies with the best ‘ES-like’ morphology i.e. tightly packed core and clear defined colony edges, were then picked and trypsinised into single cell suspensions. Cell suspensions were then seeded into wells with mitomycin C treated MEF feeder layer. 4 wells were seeded for each colony trypsinised, 2 wells for RNA isolation, and 2 wells to continue the culture.

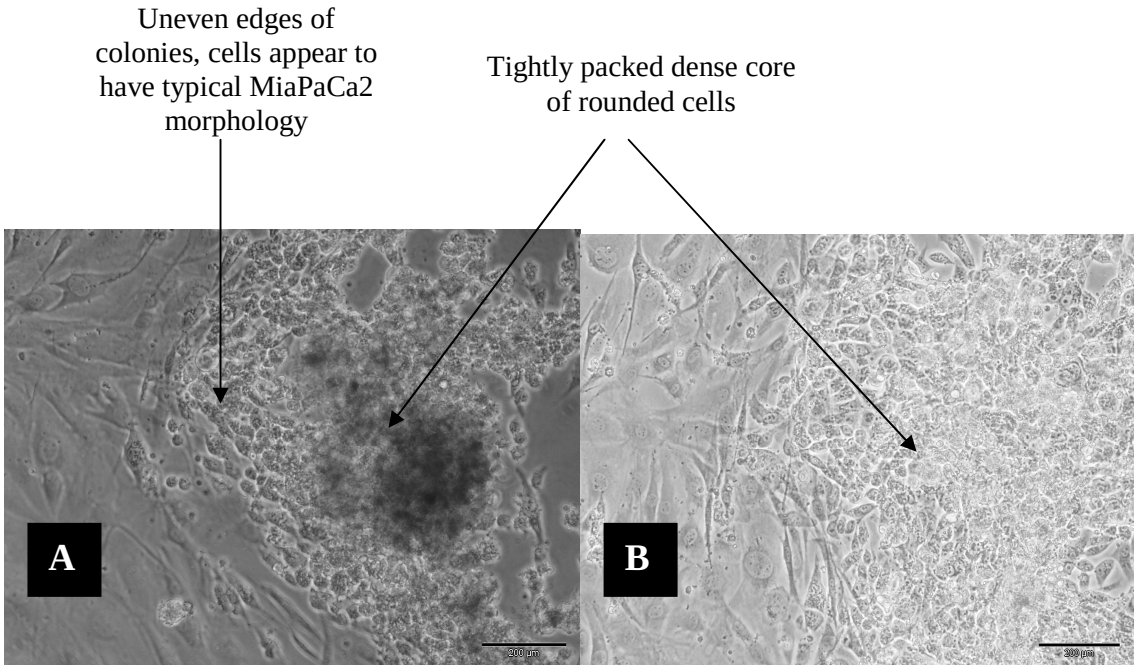

Figure 3.2.6 Virus treated MiaPaCa2 cells 24 days post infection. **A**- MiaPaCa2 cells treated with 3-factor cocktail. **B**- MiaPaCa2 cells treated with 4-factor cocktail. Both treatments resulted in colonies of similar morphologies.

Colonies displayed some morphological properties somewhat similar to ES cells, such as the tightly packed core; however, all colonies formed had uneven edges, with cells of typical MiaPaCa2 morphology, unlike the defined edges of ES colonies.

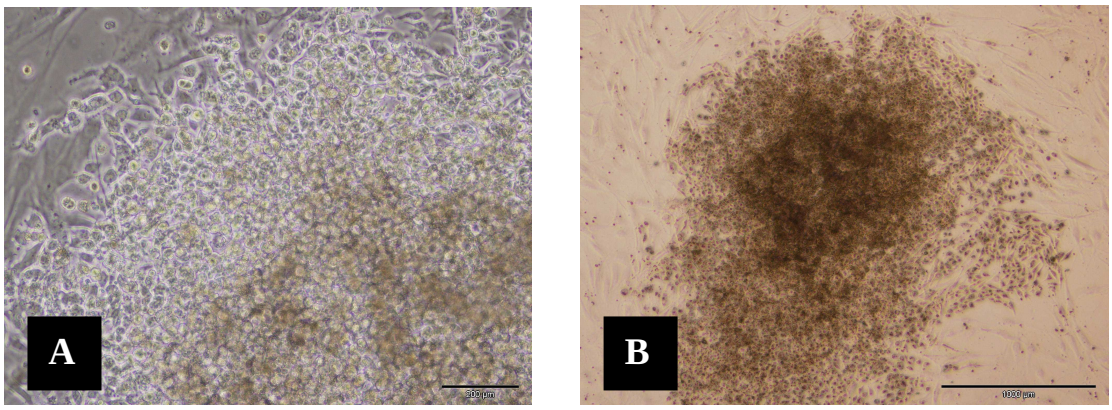

Figure 3.2.7 MiaPaCa2 cells 31 days post virus treatment. A- 10X magnification of colonies formed. B- 4X magnification of colonies formed.

3.2.5.2 Validation of MiaPaCa2 reprogramming

Two wells of each clone were harvested for RNA (section 2.4.1), while the remaining two wells were maintained in culture to freeze stocks of each clone. Five clones of 3-factor treated cells and five clones of 4-factor treated cells were analysed for expression of oct4, sox2, c-myc and klf4 (figure 3.2.8). After treatment with virus, cells which are reprogrammed should reactivate endogenous expression of these factors, to maintain cells in a pluripotent state. Clones were analysed to determine expression levels of these factors (protocol outlined in section 2.4.6).

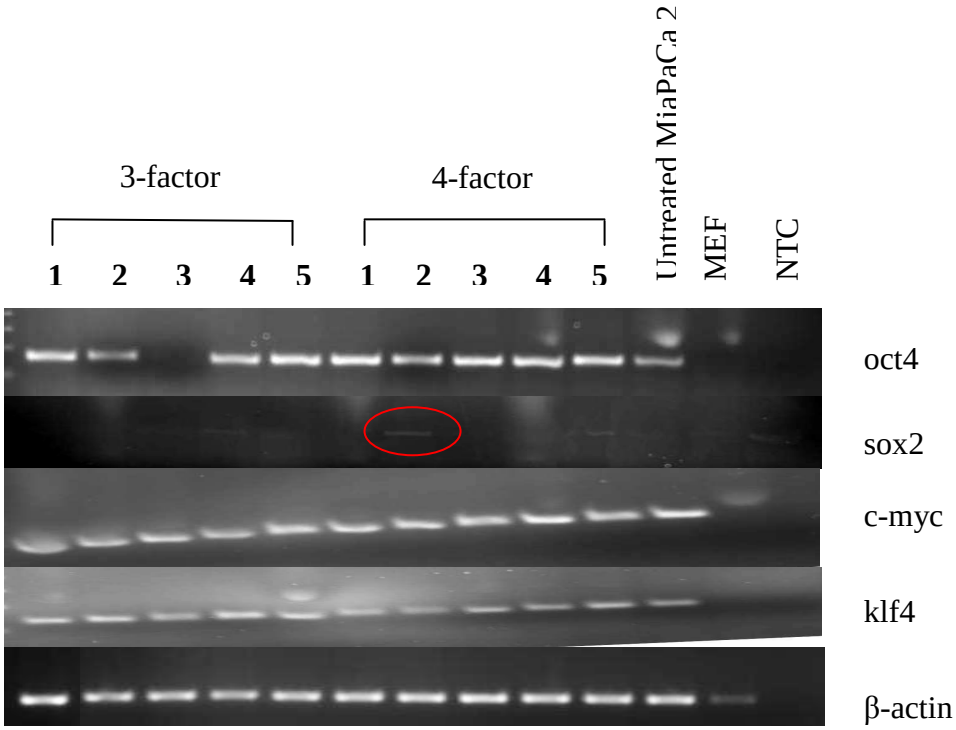

Figure 3.2.8 Agarose gel electrophoresis of PCR products generated from MiaPaCa2 virus treated colony clones. 5 three-factor clones, and 5 four-factor clones were analysed for expression of oct4, sox2, c-myc, klf4 and endogenous control β-actin. Untreated MiaPaCa2 cells, MEF murine feeder cells and NTC (no template control) control were also analysed.

C-myc and klf4 expression was detected in all clones; untreated MiaPaCa2 cells also expressed these factors (figure 3.2.7). Very low level sox2 expression was seen in some clones. Levels of Oct4 expression are seen to increase in the virus treated cells compared to untreated parental MiaPaCa2 cells, except for MiaPaCa2 3-factor treated clone 3 cells, which has lost expression of the oct4 gene. β-actin expression was also analysed in these cells as an endogenous control to demonstrate equal concentrations of RNA used in reverse transcription reactions.

MiaPaCa2 virus treated cells were growing on a MEF feeder layer when the cells were trypsinised to harvest cells for RNA, there may have been some contaminating MEF cells. Hence, MEF cells were included in analysis to determine if PCR primers also amplified murine cDNA and if so, was expression of factors in MEF cells leading to false positive results in virus treated MiaPaCa2 clones.

Amylase expression which is characteristic of pancreatic MiaPaCa2 cells was analysed to determine if virus treated cells still expressed this pancreatic marker (figure 3.2.9).

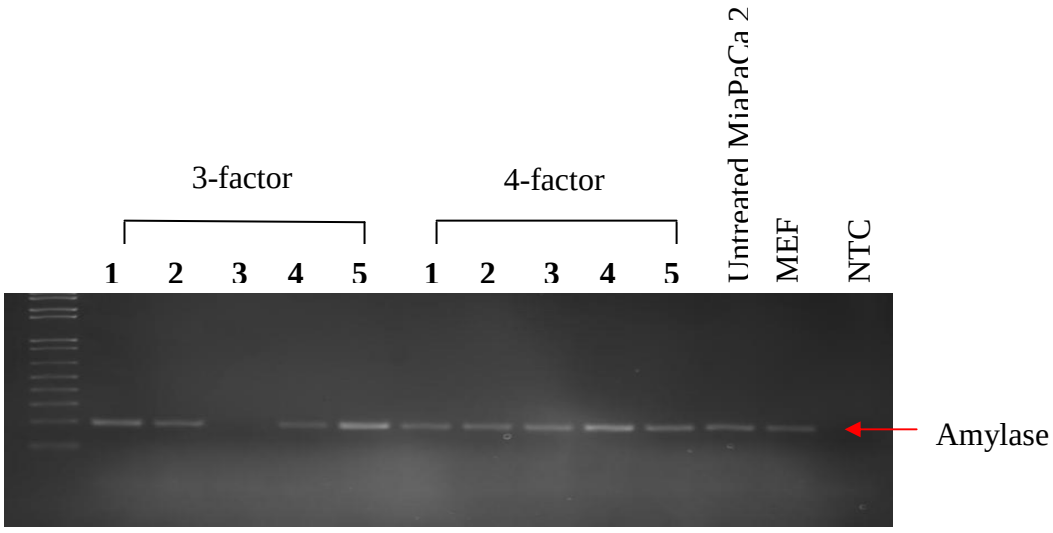

Figure 3.2.9 Agarose gel electrophoresis of amylase PCR products. Amylase expression was analysed in MiaPaCa2 3-factor treated cells, clones 1 to 5 and MiaPaCa2 4-factor treated cells, clones 1 to 5. Parent untreated MiaPaCa2 cells, MEF murine feeder cells and NTC (no template control) were also analysed.

Three-factor clone 3 MiaPaCa2 cells differ from untreated parental MiaPaCa2 cells by lack of amylase expression (figure 3.2.9). However, these cells have not become reprogrammed into iPS cells, as they lack expression of the pluripotency marker Oct4 (figure 3.2.8).

Although virus-treated cells display altered morphology (figure 3.2.5, 3.2.6 and 3.2.7) these cells have not been reprogrammed to iPS cells as they have maintained expression of the mature differentiation marker amylase (figure 3.2.9).

3.2.5.3 Attempt to generate iPS cells from keratinocytes

Normal human epidermal keratinocytes were initially treated with GFP virus using the conditions optimised using MiaPaCa2 cells (outlined in section 2.3.2), to ensure that this treatment led to efficient transduction efficiency in these cells. High levels of GFP expression was seen after treatment with GFP virus using the conditions optimised.

Keratinocytes were treated with the four factor cocktail- oct4, sox2, c-myc and klf4, or the three factor cocktail- oct4, sox2 and klf4. Cells were treated with 2 doses of virus, after four days cells were trypsinised onto a mitomycin C treated MEF feeder layer, and cultured in embryonic stem cell (ES) media (figure 3.2.10).

The morphology of keratinocytes changed considerably once plated onto MEF feeder layer cells, this change in morphology was also observed for control keratinocytes not treated with virus. Keratinocytes on MEF feeder layer formed dense colonies of cells, while cells not on MEF feeder layer formed a monolayer of cells. Control cells not treated with virus, cells treated with 4-factor virus cocktails and cells treated with 3-factor virus cocktail all showed the same morphology. However, once attached to the MEF feeder layer, these cells did not proliferate and subsequently died off.

Reprogrammed iPS cells were not generated from keratinocyte cultures, as iPS cells maintain unlimited proliferative potential in the undifferentiated state unlike the cells generated by virus-treatment in this study which failed to proliferate and eventually died (figure 3.2.10).

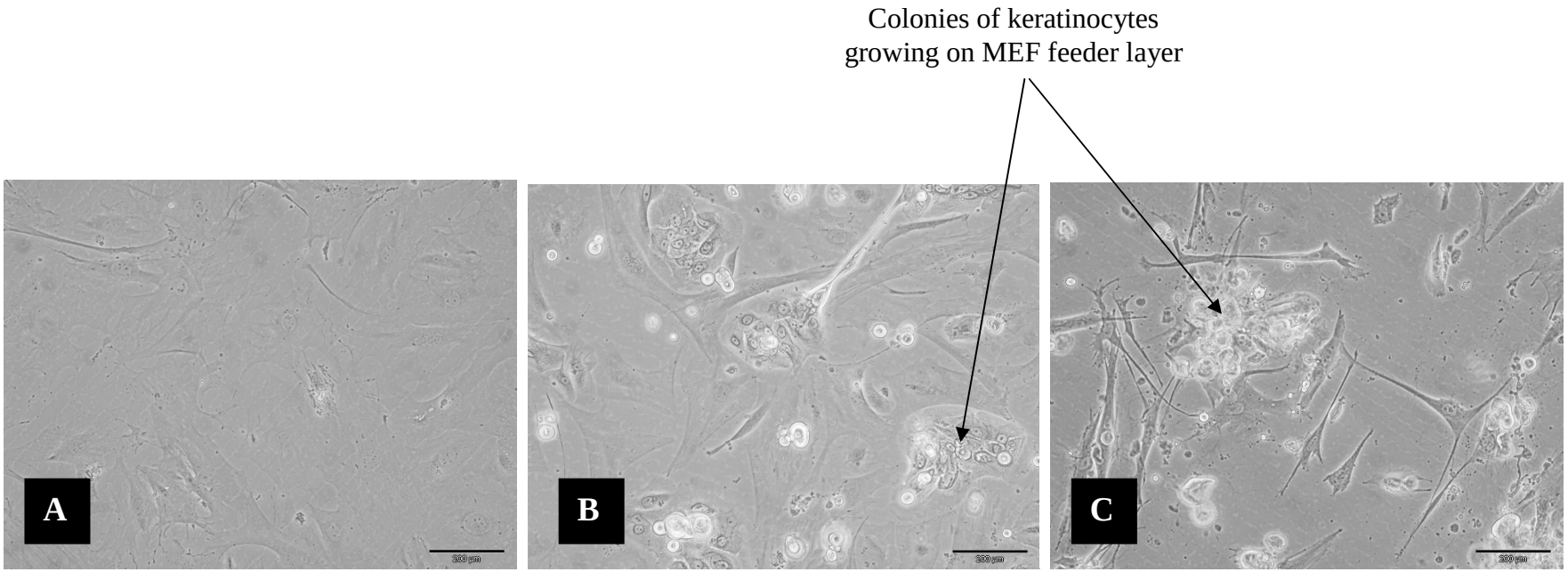

Figure 3.2.10 Viral reprogramming of keratinocytes. **A**- Mitomycin C treated MEF feeder layer. **B**- Untreated keratinocytes growing on MEF feeder layer. **C**- Virus treated keratinocytes growing on MEF feeder layer, 14 days after virus treatment.

3.2.5.4 Attempt to generate iPS cells from limbal epithelial cells using 4-factor virus cocktail

The limbal epithelial ring was dissected from donor cornea and then cut into small pieces and cultured using the explant technique to allow proliferation of the limbal epithelial cells. Once sufficient outgrowth from explant was achieved, these cells were then trypsinised and prepared for virus treatment. Cells were initially treated with GFP virus using the optimised conditions (outlined in section 2.3.2), to ensure that these conditions led to efficient transduction efficiency in these cells. High levels of GFP expression was seen after treatment with GFP virus using the optimised conditions (figure 3.2.11).

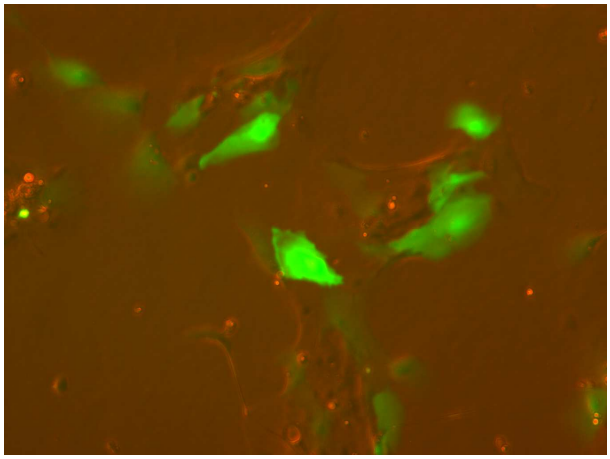

Figure 3.2.11 Fluorescent microscope images of GFP expression in limbal epithelial cells 48 hours post transduction with GFP virus.

To generate iPS cells, limbal epithelial cells were treated with the 4-factor virus cocktail (as per section 2.3.2). Following 72 hours the second virus treatment some morphology changes were seen in virus treated cells compared to controls (figure 3.2.12).

Untreated limbal epithelial cells show the typical cuboidal epithelial morphology, figure 3.2.12 A. While cells treated with virus begin to show cell processes and cell clusters (figure 3.2.12 B & C), however, some cells in virus treated cultures did maintain the typical cuboidal morphology. These cells (shown in figure 3.2.12 B & C) were then trypsinised and seeded into plates with mitomycin C treated MEFs and cultured in ES media. However, following trypsinisation and seeding onto MEFs, these virus-treated cells failed to proliferate any further. These cells did not represent fully reprogrammed cells, as genuine iPS cells exhibit unlimited proliferative potential in the undifferentiated state.

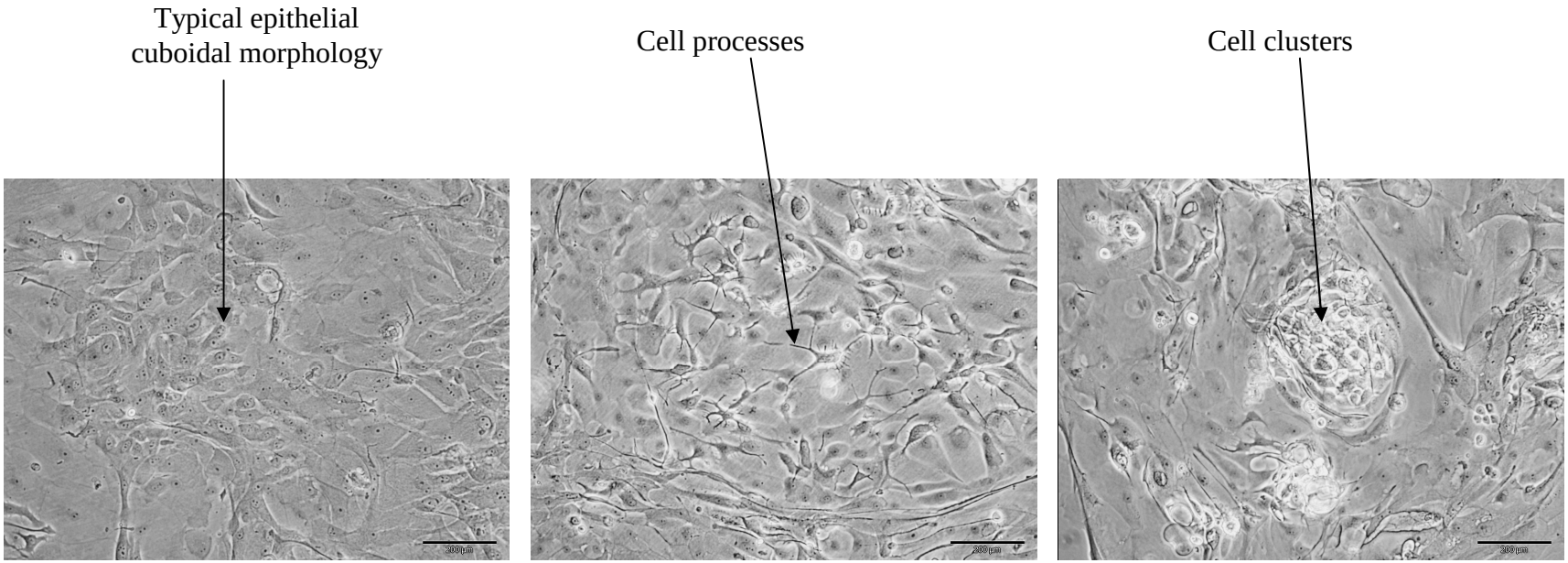

A. Untreated cells **B**. Cells treated with virus **C**. Cells treated with virus

Figure 3.2.12 Limbal epithelial cells 72 hours post virus treatment. **A**: Limbal epithelial control cells, not treated with virus. **B & C**: Limbal epithelial cells treated with 4-factor cocktail of viruses.

3.2.5.5 Attempt to generate of iPS cells from limbal epithelial cells using conditioned media

In this study retroviral based induction of iPS cells did not generate fully reprogrammed iPS cells (section 3.2.5.1 to 3.2.2.4). Therefore an alternative method was utilised for generating iPS cells from limbal epithelial cells using a conditioned media based reprogramming technique identified by Balasubramanian *et al.,* (Balasubramanian, Babai et al. 2009). Generation of iPS cells using the ESD3 conditioned media technique involved a 2-stage protocol (figure 3.2.13) (outlined in section 2.3.3).

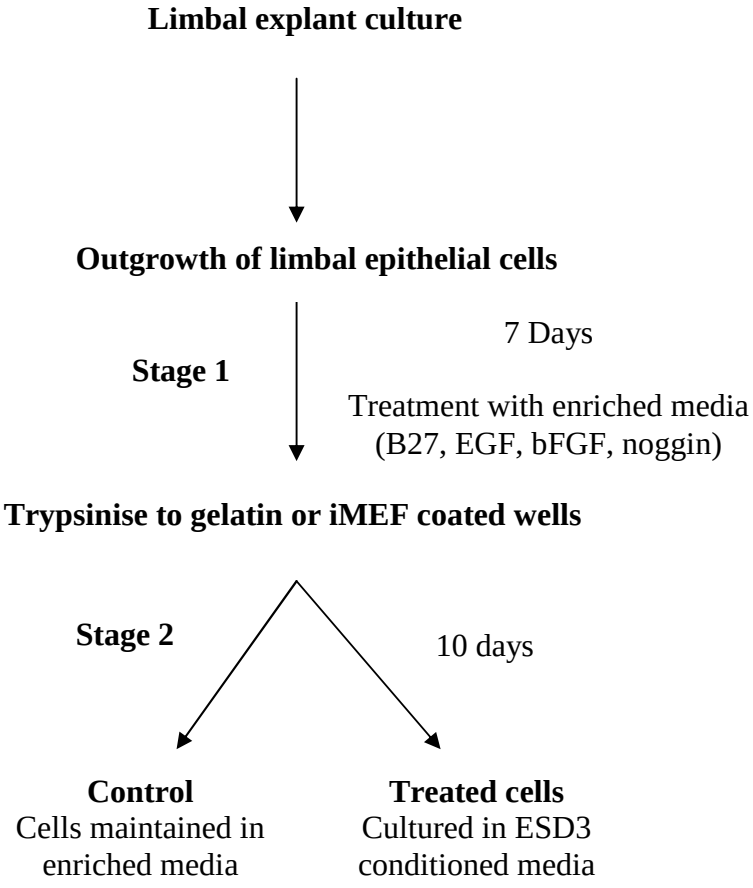

Figure 3.2.13 Flowchart of limbal epithelial cell treatment. Stage 1 involves treatment of cells with enriched media, followed by stage 2 treatment with ESD3 conditioned media. Control cells are maintained in enriched media for the duration of the experiment.

Stage one of the treatment with enriched media led to a distinct change in cell morphology. In contrast to the typical epithelial cuboidal morphology of the control cells maintained in normal culture media (figure 3.2.14 A), cells treated with enriched media exhibited a stretched spindle type morphology with cell processes (figure 3.2.14 B and C). No neurospheres were observed, in contrast to the observations reported by Balasubramanian *et al* (Balasubramanian, Babai et al. 2009).

Stage two involved trypsinisation of enriched media treated cells onto gelatin coated or irradiated MEF (iMEF) coated wells. Cells were treated with ESD3 conditioned media (ESD3 CM) (section 2.3.3.1) for 10 days, and control cells were maintained in stage 1 enriched media for the entire duration of the protocol.

At the halfway point of stage 2, control cells maintained in enriched media resumed the standard limbal epithelial cell morphology (figure 3.2.15 A and D). Cells treated with ESD3 CM displayed altered morphology (figure 3.2.15 B, C, E and F). Cell clusters were observed in ESD3 CM treated cultures on iMEF feeder layer (figure 3.2.15 E and F). Similar clusters were observed at a slightly later time point in ESD3 CM treated cultures grown on gelatin.

At day 14, the end of stage 2 treatment, the cell clusters observed in ESD3 CM treated cells on iMEF at day 7 of stage 2, did not show any obvious increase in size (figure 3.2.16 E), nor was there any obvious outgrowth from the cluster. A single cluster of a different morphology was also seen in ESD3 CM treated cells grown on iMEFs (indicated with red arrow, figure 3.2.16 E), this cluster contained tightly packed cells which appeared to be more adherent to the culture dish, rather than the smaller clusters observed in both treatment conditions.

At the end of stage 2, control cells maintained in the stage 1 enriched media maintained the typical cuboidal epithelial morphology (figure 3.2.16 A and D).

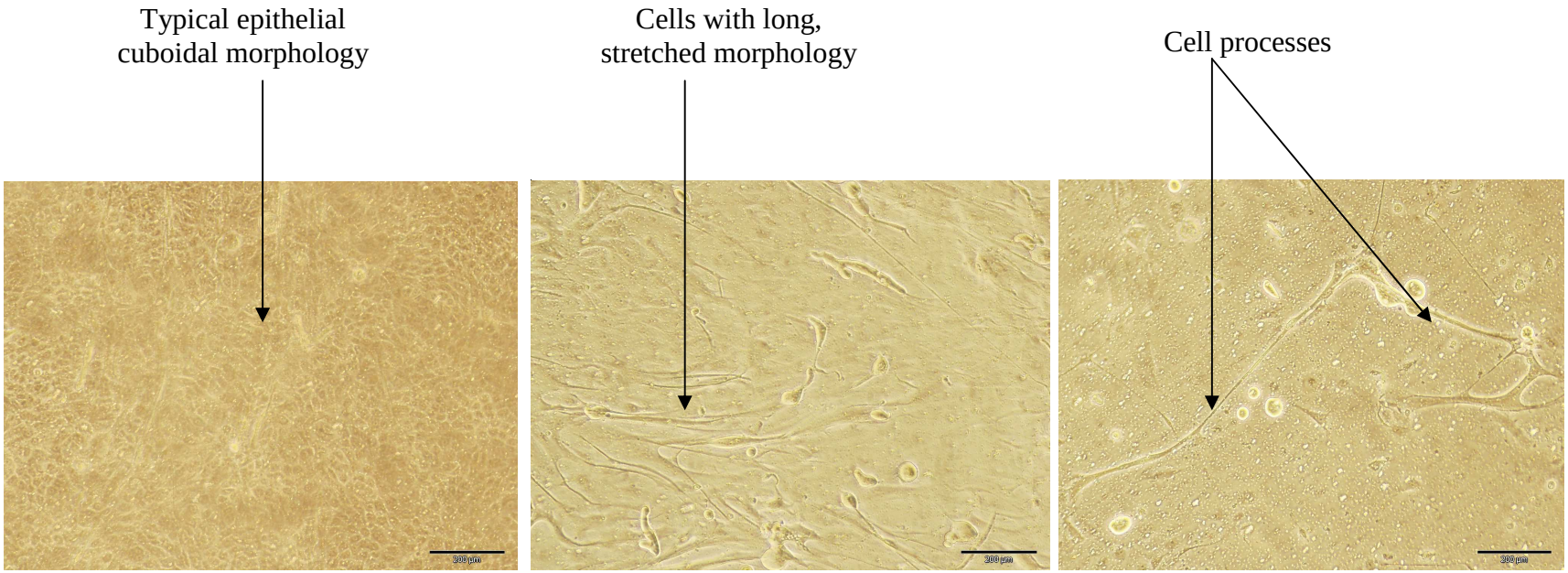

A: untreated cells grown eye media **B**: cells grown in enriched media **C**: cells grown in enriched media

Figure 3.2.14 Limbal epithelial cells after stage 1 treatment with enriched media for 7 days. Limbal epithelial cells grown in 6-well plate inserts, with 3T3 feeder cells in bottom layer of well. Control cells (A) were maintained in the standard eye media and exhibit typical epithelial cuboidal morphology. Cells treated with enriched media (B & C) show a different morphology with long stretched cells with protrusions.

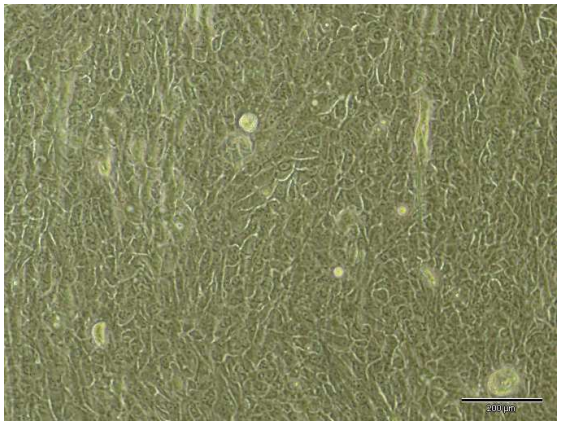

A: control cells on gelatin

B: treated cells on gelatin

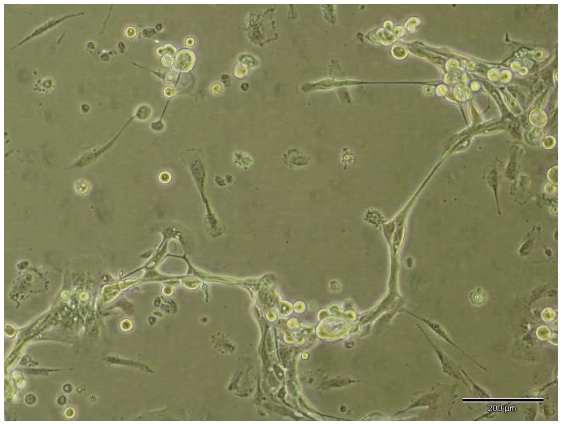

C: treated cells on gelatin

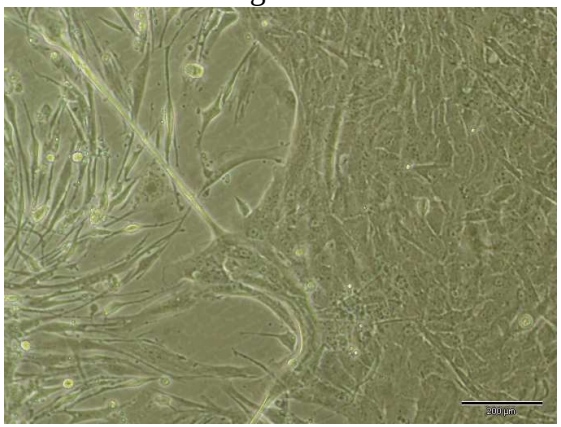

D: control cells on iMEFs

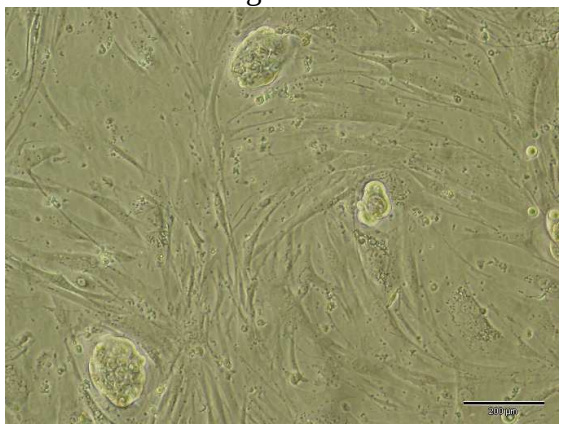

E: treated cells on iMEFs

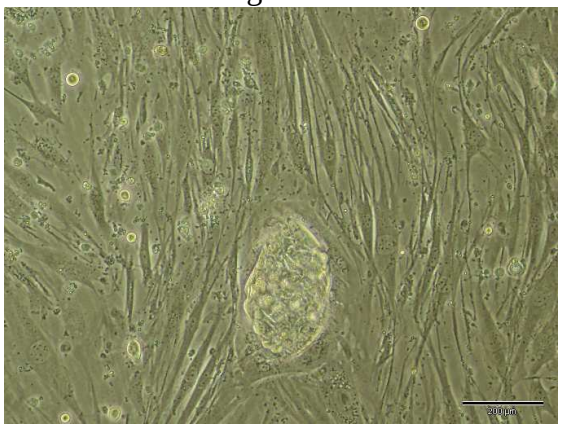

F: treated cells on iMEFs

Figure 3.2.15 Limbal epithelial cells during stage 2 at 7 days of ESD3 CM treatment. Cells were grown on plates coated with gelatin alone (A, B & C) or gelatin and iMEFs (D, E & F). Control cells (A & D) were maintained in enriched media and did not receive ESD3 CM. Cells in B, C, E & F were treated with enriched media for 7 days followed by ESD3 CM for 7 days.

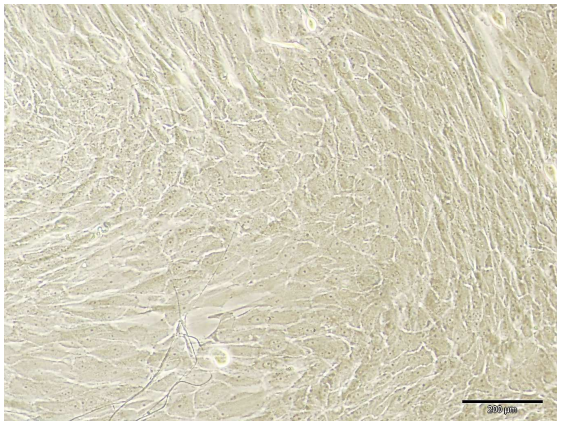

A: Control cells on gelatine (10X)

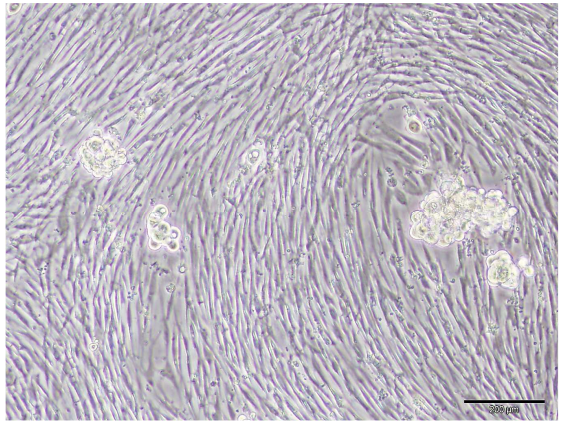

B: Treated cells on gelatine (10X)

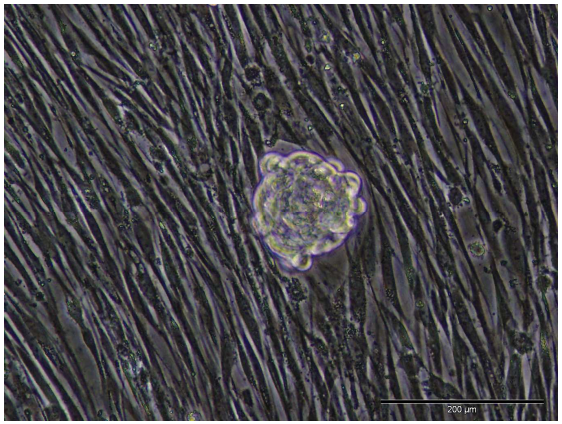

C: Treated cells on gelatine (20X)

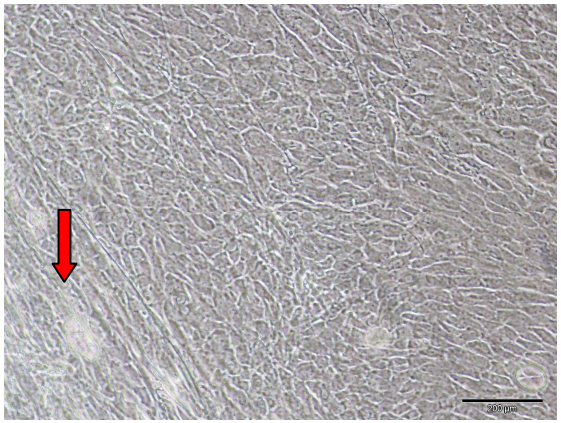

D: Control on iMEF (10X)

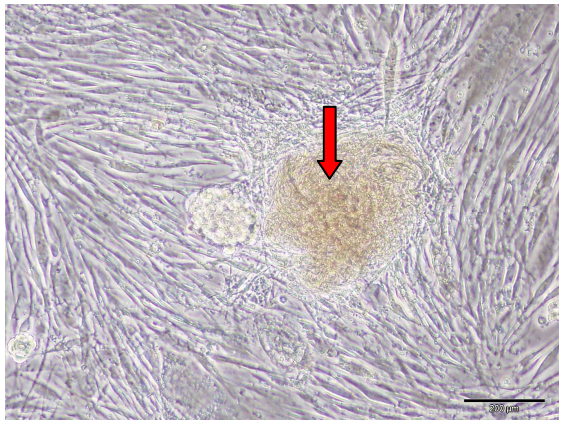

E: Treated cells on iMEF (10X)

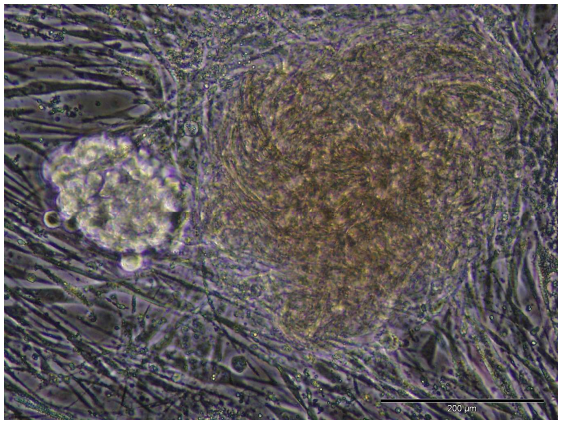

F: Treated cells on iMEF (20X)

Figure 3.2.16 Limbal epithelial cells at the end of stage 2, after 14 days of ESD3 CM treatment. Cells were grown on plates coated with gelatin and iMEFs (D, E & F) or gelatin alone (A, B & C). Control cells (A & D) were maintained in enriched media and did not receive ESD3 CM. Cells treated with enriched media for 7 days followed by ESD3 CM for 14 days were plated on gelatin or gelatin and iMEF coated plates (B, C, E & F). (10X and 20X indicate the magnification at which these images were taken).

3.2.5.6 Validation of limbal epithelial cell reprogramming

Cells from these wells were harvested for RNA analysis (section 2.4.1) to check if different marker expression was seen between the control cells exhibiting cuboidal morphology and treated cells on gelatin and iMEFs with fibroblast morphology (figure 3.2.17 and 3.2.18). Limbal epithelial cells from the same donor, maintained in standard limbal epithelial cell culture were also analysed for marker expression, as a control, to determine if conditioned media treatment induced changes in marker expression. Limbal stromal cells were also analysed for marker expression to determine if fibroblast-like cell types emerging at the end of stage 2 treatment were a result of stromal cell contamination. RNA from an established iPS cell line was also analysed to determine if ESD3 CM treatment induced full reprogramming of limbal epithelial cells, and hence marker expression similar to established iPS cells.

C-myc, oct4 and klf4 expression was detected in all cell types and for all conditions analysed (figure 3.2.17), however, iPS cells had much higher expression levels of oct4 compared to other cell types. Sox2 pluripotency marker was only detected in iPS cells, untreated limbal epithelial cells maintained in eye media, and ESD3 CM treated cells. Limbal epithelial cells maintained in the enriched media, or ESD3 CM treated cells on gelatin had lost expression of this marker (figure 3.2.17). Control limbal epithelial cells maintained in enriched media express terminal differentiation markers CK-3 and CK-12 (figure 3.2.18). N-cadherin is associated with adult stem cells. Levels of this marker are reduced in control cells maintained in enriched media, while high levels are maintained in ESD3 CM treated cells. Control cells maintained in enriched media showed similar expression of ΔNp63 as untreated limbal epithelial cells. ABCG2 levels were only detected at very low levels in limbal epithelial, stromal and iPS cells. Pluripotency marker, nanog, was only detected in iPS cells.

It is clear that ESD3 CM treatment has induced specific cell morphology (figure 3.2.16) and marker expression changes (figure 3.2.17 and 3.2.18) compared to untreated limbal epithelial cells, and control cells maintained in enriched media for the entire duration of the experiment. However, as these cells do not express the pluripotency marker nanog (figure 3.2.18), therefore, they do not represent fully reprogrammed cells.

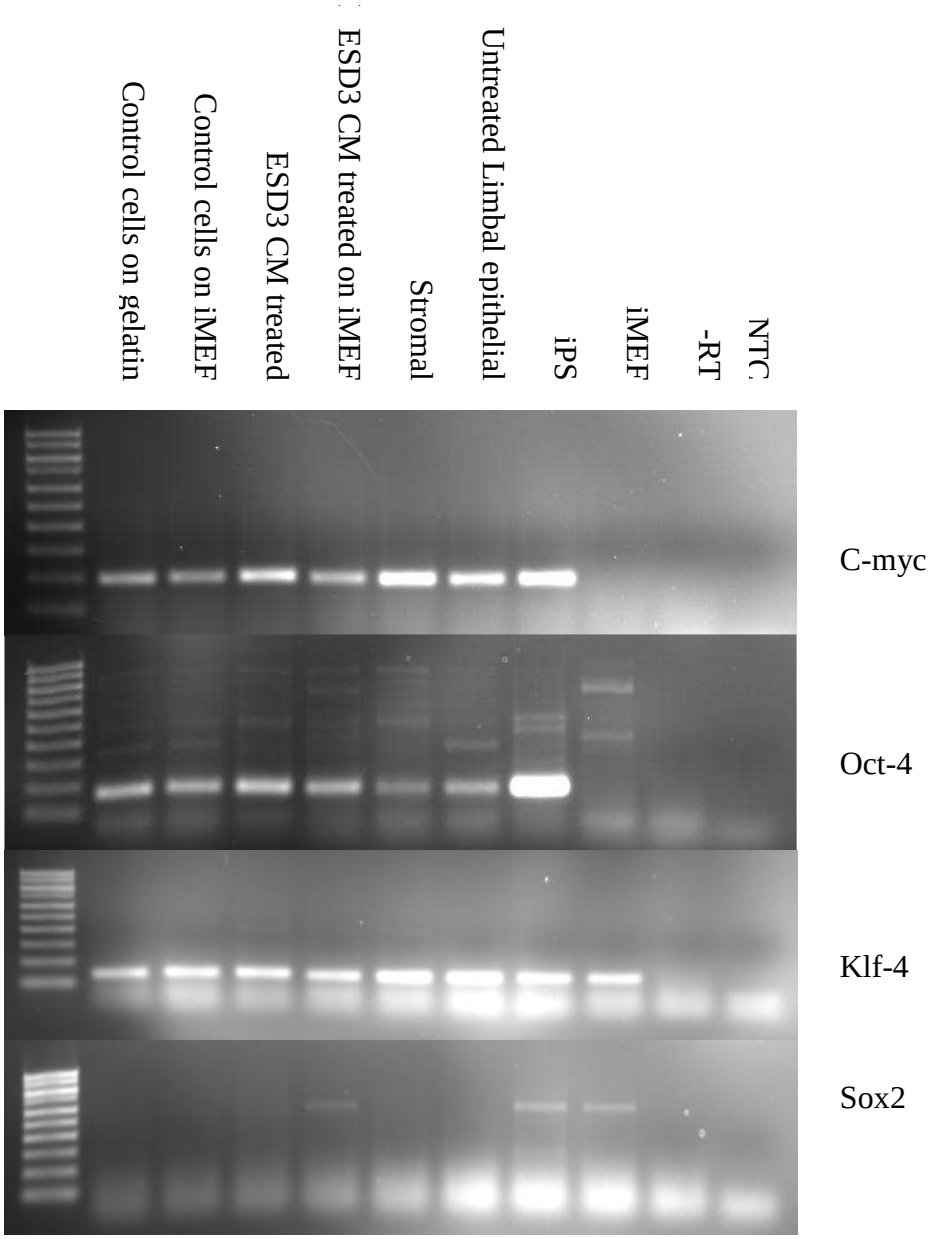

Figure 3.2.17 Expression levels of oct4, sox2, c-myc and klf4 in limbal epithelial cells treated with ESD3 CM for 14 days, as well as control cells which were maintained in enriched media. Stromal cells, limbal epithelial cells (untreated, in eye media), iPS cells and iMEFs were also included for comparison.

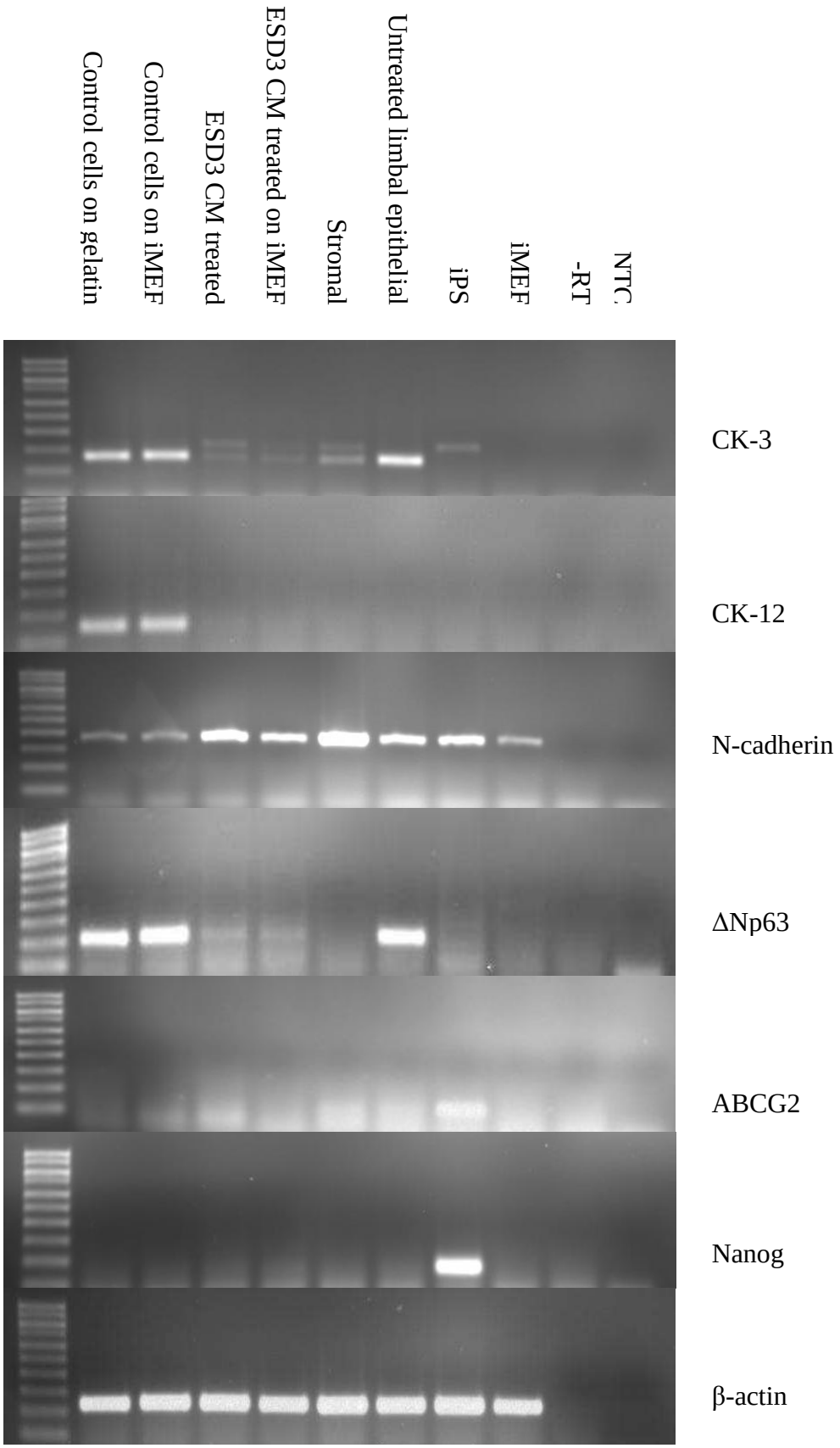

Figure 3.2.18 Expression levels of CK-3, CK-12, N-cadherin, ΔNp63, ABCG2, nanog and endogenous control β-actin, in limbal epithelial cells treated with ESD3 CM for 14 days, as well as control cells which were maintained in enriched media. Stromal cells, limbal epithelial cells (untreated), iPS cells and iMEFs were also included to allow comparison.

3.2.5.7 Summary of attempts to generate iPS cells

Attempts at using retro-viral and conditioned media based reprogramming technology were unsuccessful in generating fully reprogrammed iPS cells. Cells displaying altered morphology and marker expression may represent cells stuck in a semi-reprogrammed state. At this time, commercially available iPS cell lines were beginning to come on stream. In order to continue the aim of establishing a human pancreatic beta cell model, one such iPS line- hFib2-iPS4 was purchased from George Daley's lab, Children's Hospital Boston. Additionally, a transdifferentiation approach was also undertaken using human limbal stromal cells available in our lab. Recent studies have suggested that these cells resemble bone marrow derived mesenchymal stem cells and possess similar differentiation potential towards ectoderm, mesoderm and endoderm lineages (Dravida, Pal et al. 2005; Polisetty, Fatima et al. 2008). Directed differentiation protocols were applied to both iPS and stromal cells to establish the potential of these cells to differentiate towards pancreatic lineages.

3.2.6 Differentiation of an established iPS cell line towards pancreatic phenotypes

A directed differentiation protocol established by Jiang J. *et al.*, was used to differentiate iPS cell line- hFib2-iPS4 towards pancreatic lineages (protocol described in section 2.2.5.1) (Jiang, Au et al. 2007). Treated cells were then analysed for expression of pancreatic markers. Differentiation protocols were performed on iPS cells in 2D culture- grown on a thin matrigel layer, and cells in 3D culture- suspended within a thick matrigel/collagen gel (described in section 2.2.5). Marker expression was then compared to assess which culture method led to the highest efficiency of pancreatic differentiation.

iPS cells grown in 2D culture spread out from the tightly packed core of the iPS cluster (figure 3.2.19 A). iPS cells grown in 3D culture were suspended within the matrigel/collagen gel. These cells maintained tight, densely packed colonies with even edges and minimal outgrowth (figure 3.2.19 B). Cells in 2D and 3D cultures were maintained in iMEF conditioned iPS media for 2 days following seeding of cultures.

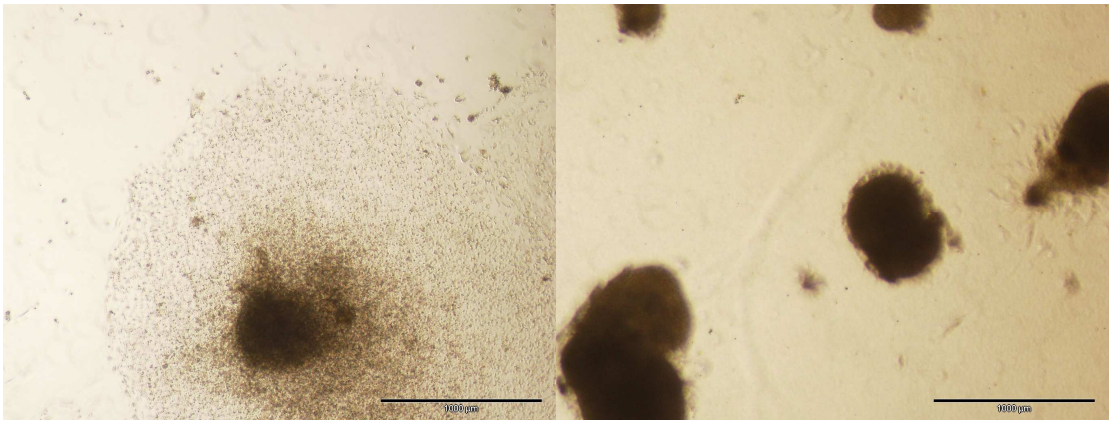

A: iPS cells in 2D culture **B**: iPS cells in 3D culture

Figure 3.2.19 iPS cells grown in 2D and 3D culture. A-iPS cells grown on matrigel coated dishes. B-iPS cells embedded in a thick matrigel/collagen gel. 4X magnification for both images.

After allowing cells to settle and grow in the 2D and 3D culture conditions for 2 days, differentiation media was then added to initiate differentiation of iPS cells towards pancreatic phenotypes. While control cells were maintained in iMEF conditioned ES media. Following 8 days of treatment, cells were monitored for changes in cell morphology (figure 3.2.20) and mRNA expression (figure 3.2.21). 2D control cells exhibited small compact cell morphology, while 2D cultures treated with differentiation media exhibited larger cell morphology, with more distinguished cell-cell boundaries (figure 3.2.20 A & B). In 3D control cultures, cells maintained tight, densely packed colonies, while cultures treated with differentiation media displayed slightly different morphology, with less densely packed colonies and outgrowth of cells from colonies (figure 3.2.20 C & D).

Cxcr4 definitive endoderm marker expression was detected in untreated iPS cells, with increased expression in 2D and 3D differentiation media treated cells. Similar trends in marker expression were seen for Foxa2 and Hnf4α, low expression in untreated iPS and higher expression in 2D and 3D differentiation media treated cells (figure 3.2.21). No change in nanog pluripotency marker expression level was seen in control or treated cells.

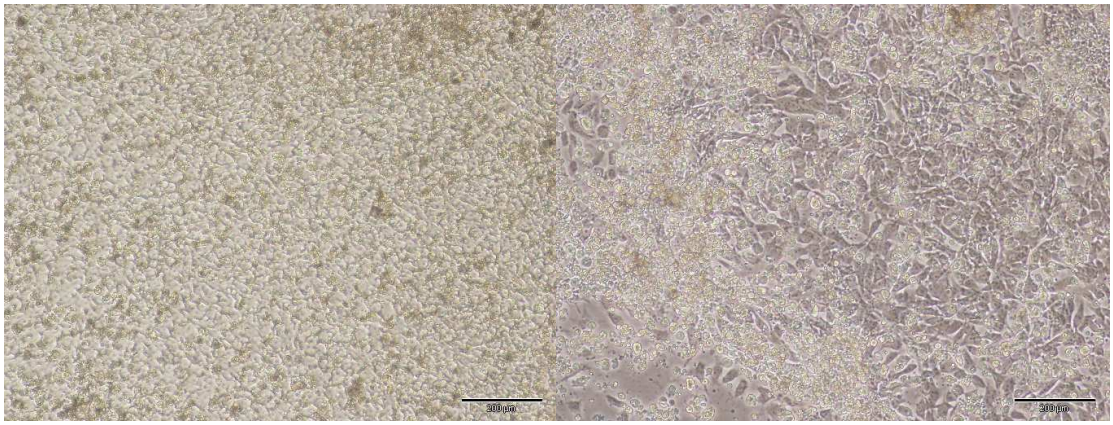

A: 2D control cells **B**: 2D differentiated cells

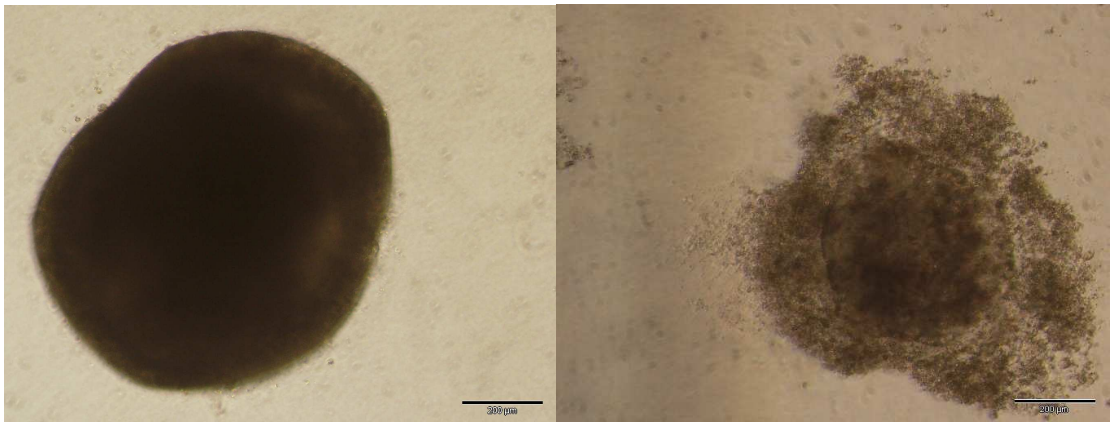

C: 3D control cells **D**: 3D differentiated cells

Figure 3.2.20 Day 8 iPS cells in 2D and 3D culture. A and C represent iPS control cells maintained in iMEF conditioned iPS media, while B and D cultures were treated with differentiation media.

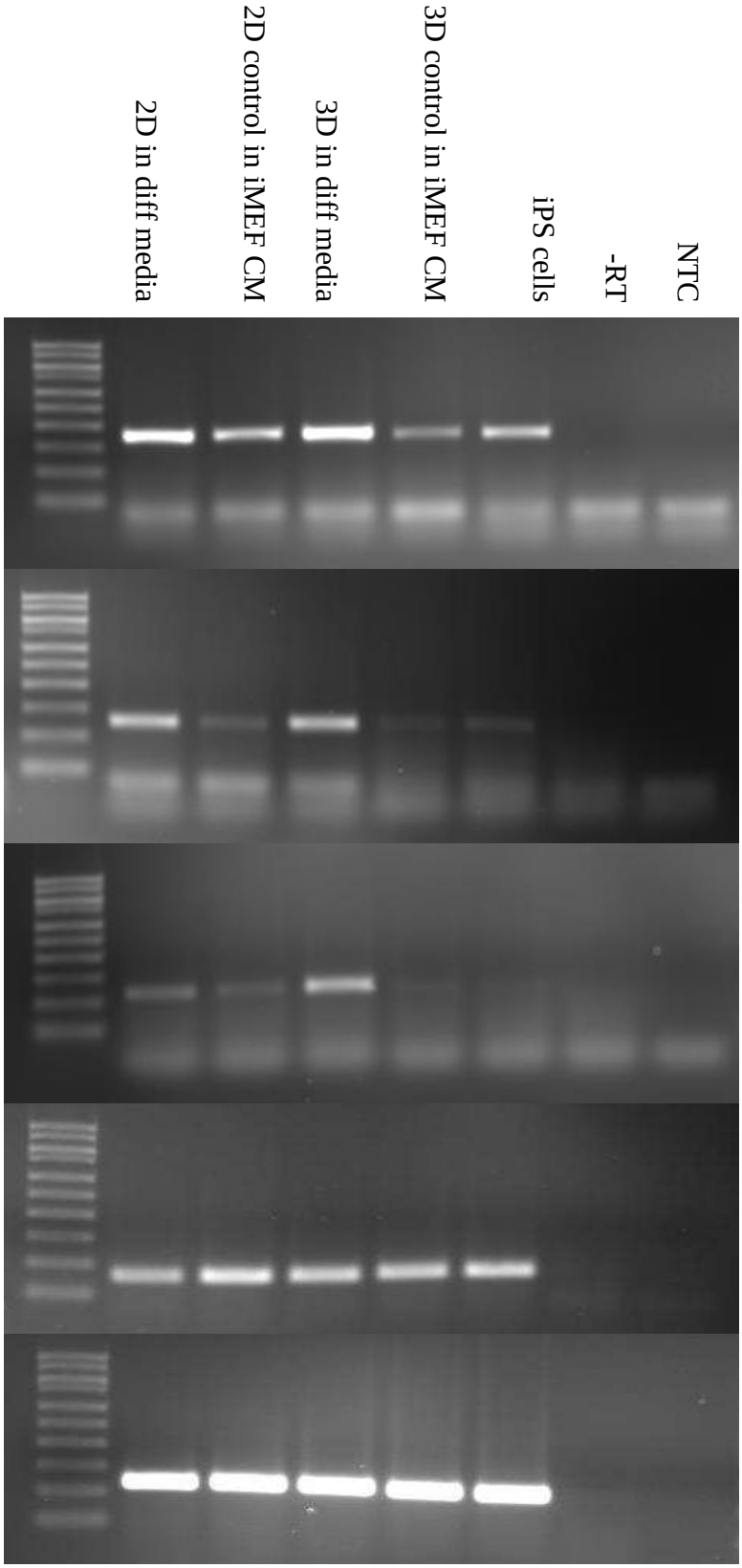

Figure 3.2.21 PCR of day 8 differentiation and control cultures. Expression levels of definitive endoderm markers- cxcr4, foxa2 and hnf4a were examined, as well as pluripotency marker- nanog, and endogenous control B-actin.

At day 8, once cells had reached the definitive endoderm stage of the protocol, 2D cell cultures were treated with 200units/mL of collagenase IV and transferred to low-attachment 6-well plates to allow spheroid formation. 2D cultures did not respond well to collagenase treatment and culture on low-attachment plates, a large proportion of cells died. The remaining cells failed to proliferate, some small irregular shaped clumps were observed (see red arrow, figure 3.2.22 A and B) in control and differentiated cultures, with the majority of cells remaining in a single cell suspension.

The 3D cultures were maintained in the same matrigel/collagen gel. The 3D differentiated clusters exhibited a large degree of dense outgrowth from the original cluster by day 21. The outgrowth in 3D control conditions was minimal in comparison to differentiated wells (figure 3.2.22 C and D). Cells from both 2D and 3D cultures were harvested for RNA on day 21 to check expression of pancreatic endoderm markers (figure 3.2.23). However, insufficient cell number remained in the 2D conditions to perform mRNA expression analysis.

PDX-1 is used as a marker of pancreatic endoderm. Very low expression of this marker was detected in the 3D control condition, while it was absent from 3D differentiated cells (figure 3.2.23). Nanog, a marker of pluripotency, showed very slightly reduced expression in 3D differentiated cells relative to 3D control and iPS cells. β-actin expression was also analysed as an endogenous control (figure 3.2.23). Hlxb9, ngn3, nkx6.1 and ptf1a pancreatic endoderm marker expression was also examined in 3D control and differentiated cultures, but expression was undetected.

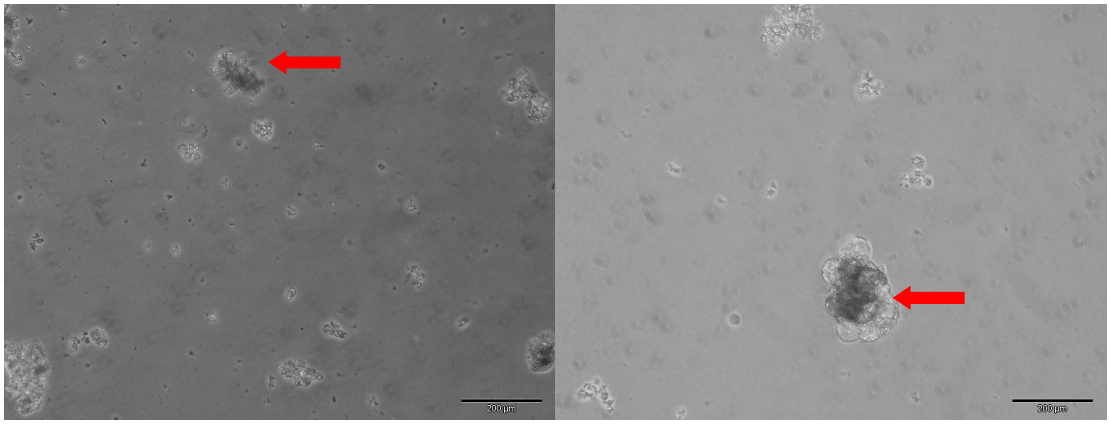

A: 2D control cells B: 2D differentiated cells

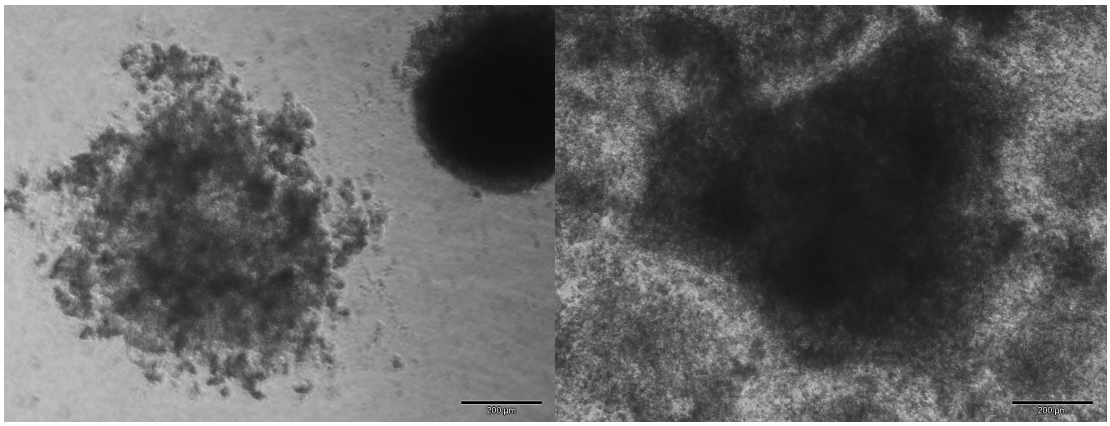

C: 3D control cells D: 3D differentiated cells

Figure 3.2.22 Morphology of cells in 2D and 3D cultures on day 21, treated with iMEF conditioned iPS media or differentiation media.

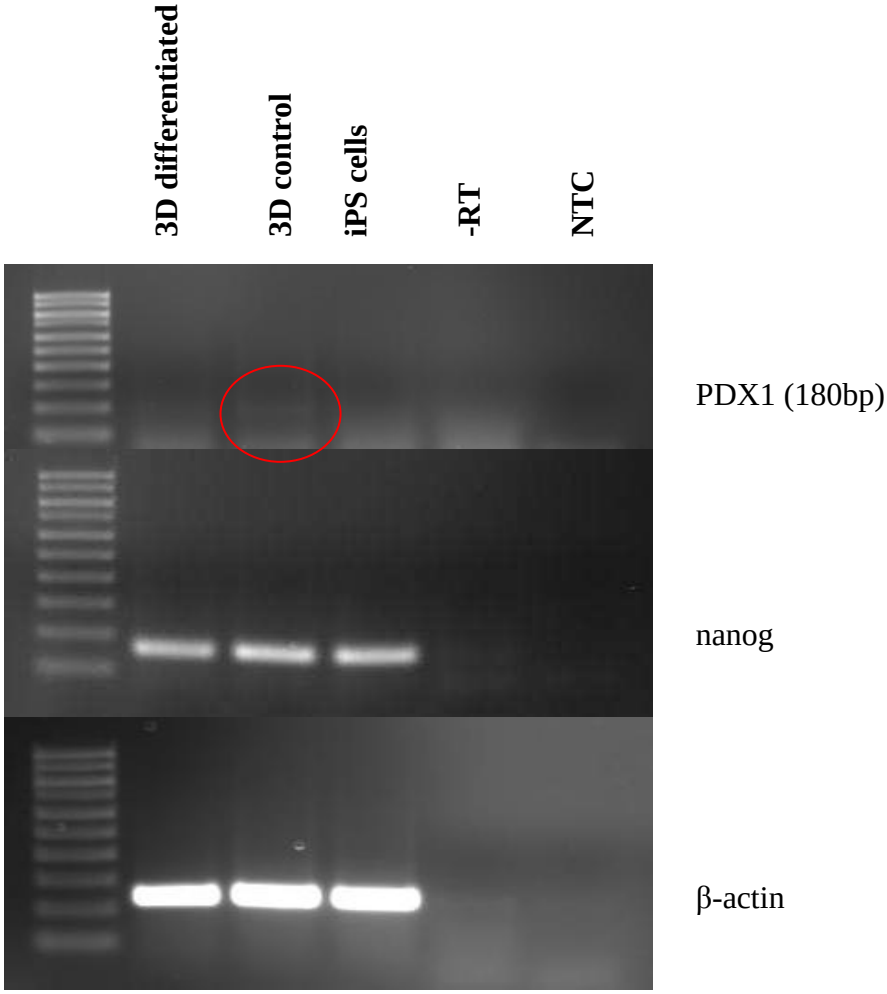

Figure 3.2.23 mRNA expression of 3D differentiated and control cultures after 21 days of treatment. B-actin is used as an endogenous control to show equal cDNA levels

At day 29, pancreatic endocrine/exocrine stage of differentiation protocol, cells had similar morphology to day 21. The 2D control and differentiated cultures still remained sparse (figure 3.2.24 A and B). The 3D control cells showed some outgrowth from clusters, while 3D differentiated cultures showed very dense outgrowth of very small cells (figure 3.2.24 C and D, respectively). 3D control and differentiated cultures were harvested for RNA. Nkx6.1, nkx2.2, ngn3 and pax4 expression levels were analysed to determine if cells had differentiated to the pancreatic endocrine/exocrine stage. Expression levels for these markers were undetected in both control and differentiated 3D cultures.

At day 36, mature islet stage of the differentiation protocol, cell morphology was observed (figure 3.2.25). The 2D control and differentiation cultures maintained the same morphology from day 21 and 29, very few live cells remained and a lot of cell debris could be seen in the media. The 3D control and differentiated cells displayed outgrowth of cells from the original cluster, with a larger area of outgrowth for the differentiated cultures (figure 3.2.25).

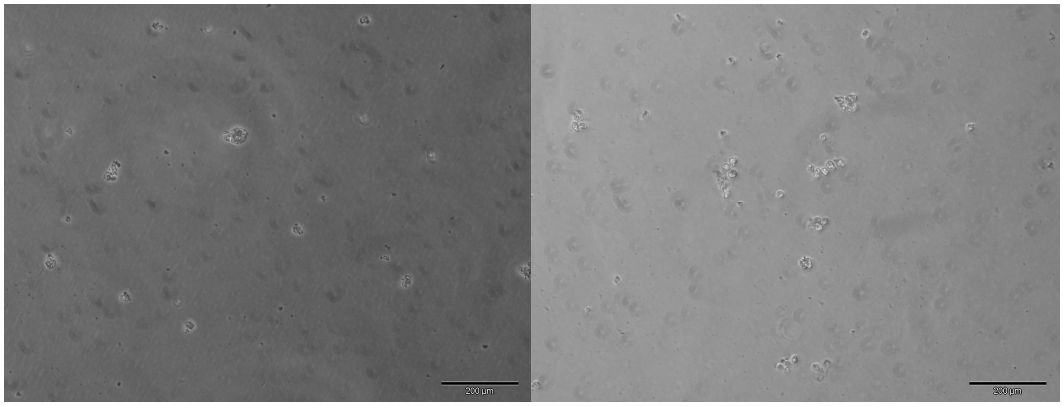

A: 2D control culture B: 2D differentiated culture

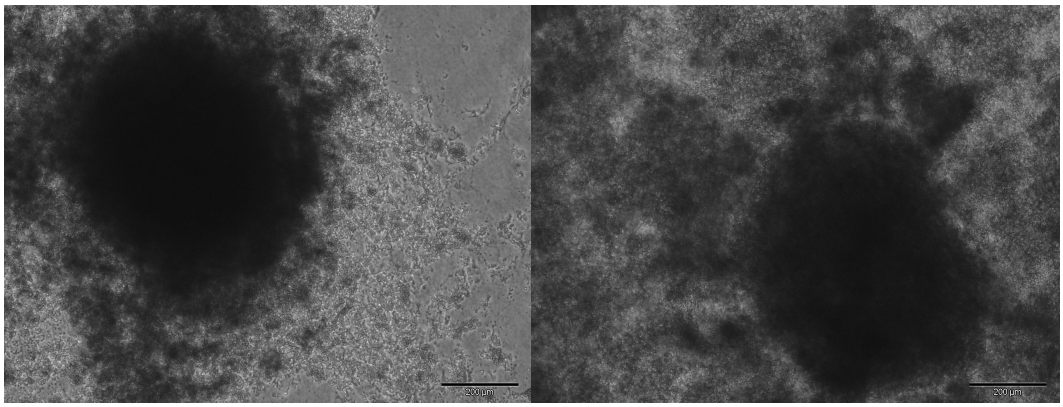

C: 3D control culture D: 3D differentiated culture

Figure 3.2.24 Morphology of 2D and 3D cultures on day 29, treated with iMEF conditioned iPS media as control or differentiation media.

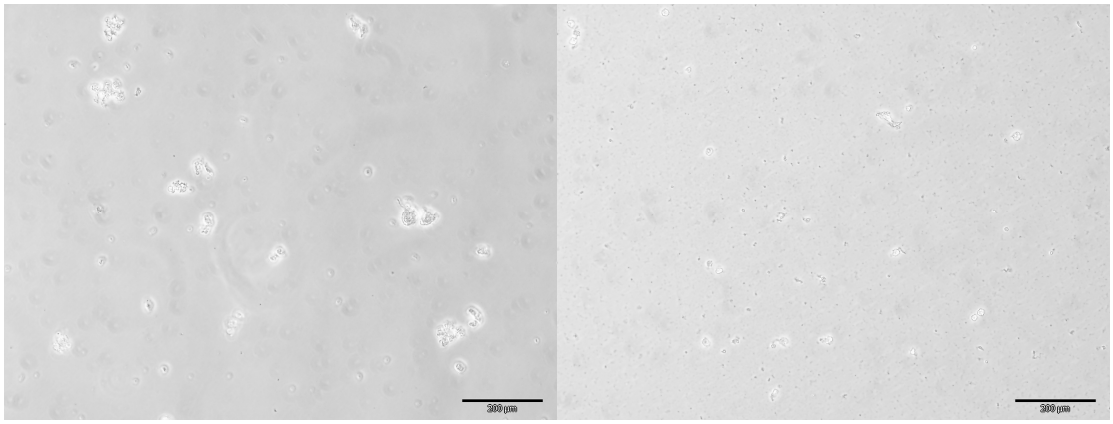

A: 2D control culture B: 2D differentiated culture

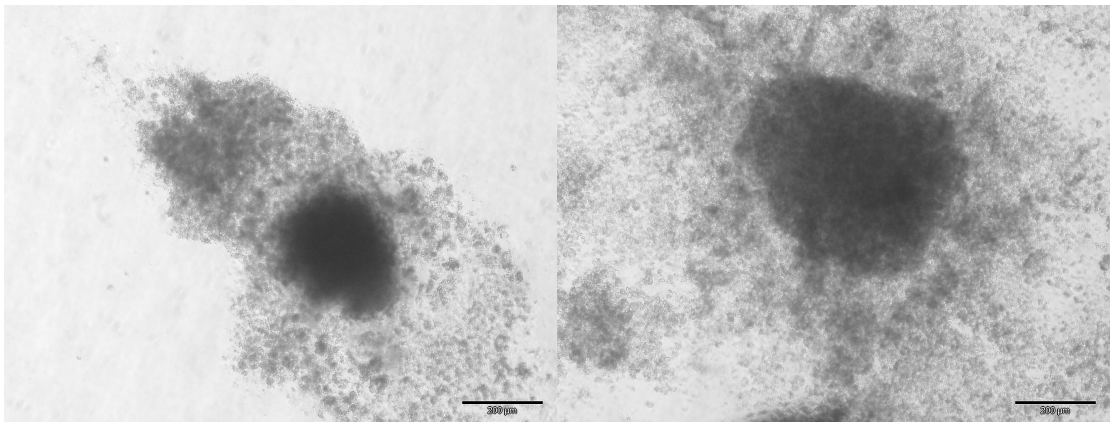

C: 3D control culture D: 3D differentiated culture

Figure 3.2.25 Morphology of 2D and 3D cultures on day 36, treated with iMEF conditioned iPS media as control or differentiation media.

RNA was isolated from day 36 3D differentiation and 3D control cultures. The expression of mature islet markers was examined in day 36 cultures in addition to the intermediate time points of the experiment (figure 3.2.26). Insulin, a marker of pancreatic beta cells, was detected in day 36 control cultures, and absent in all other time points and conditions examined. Somatostatin and amylase, which are markers of pancreatic delta cells and acinar cells respectively, was detected in untreated iPS cells and in the early stages of the experiment on day 8 and 21 in both control and differentiated cultures. Somatostatin and amylase levels became undetectable in day 29 cultures and day 36 differentiation culture, with increased levels observed in day 36 control cultures. Ghrelin, a marker of pancreatic epsilon cells, detected only in day 36 control cultures. Glut2, another marker of mature pancreatic beta cells was detected at low levels in day 8 and 21 control and differentiation cultures, and day 36 control cultures. Glut2 expression was undetectable in day 29 control and differentiation cultures and day 36 differentiation culture.

Nanog expression was used as a marker of pluripotency. Nanog levels were high in untreated iPS cells and day 8 control and differentiation cultures. Nanog levels were lower in day 21 differentiation and control cultures, lower again in day 29 control and differentiation cultures, and undetectable in day 36 differentiation cultures. Nanog expression appeared to rise again in day 36 control cultures. B-actin expression was used as an endogenous control; however, levels of this were lower in day 29 control and differentiation cultures and day 36 differentiation cultures (figure 3.2.26).

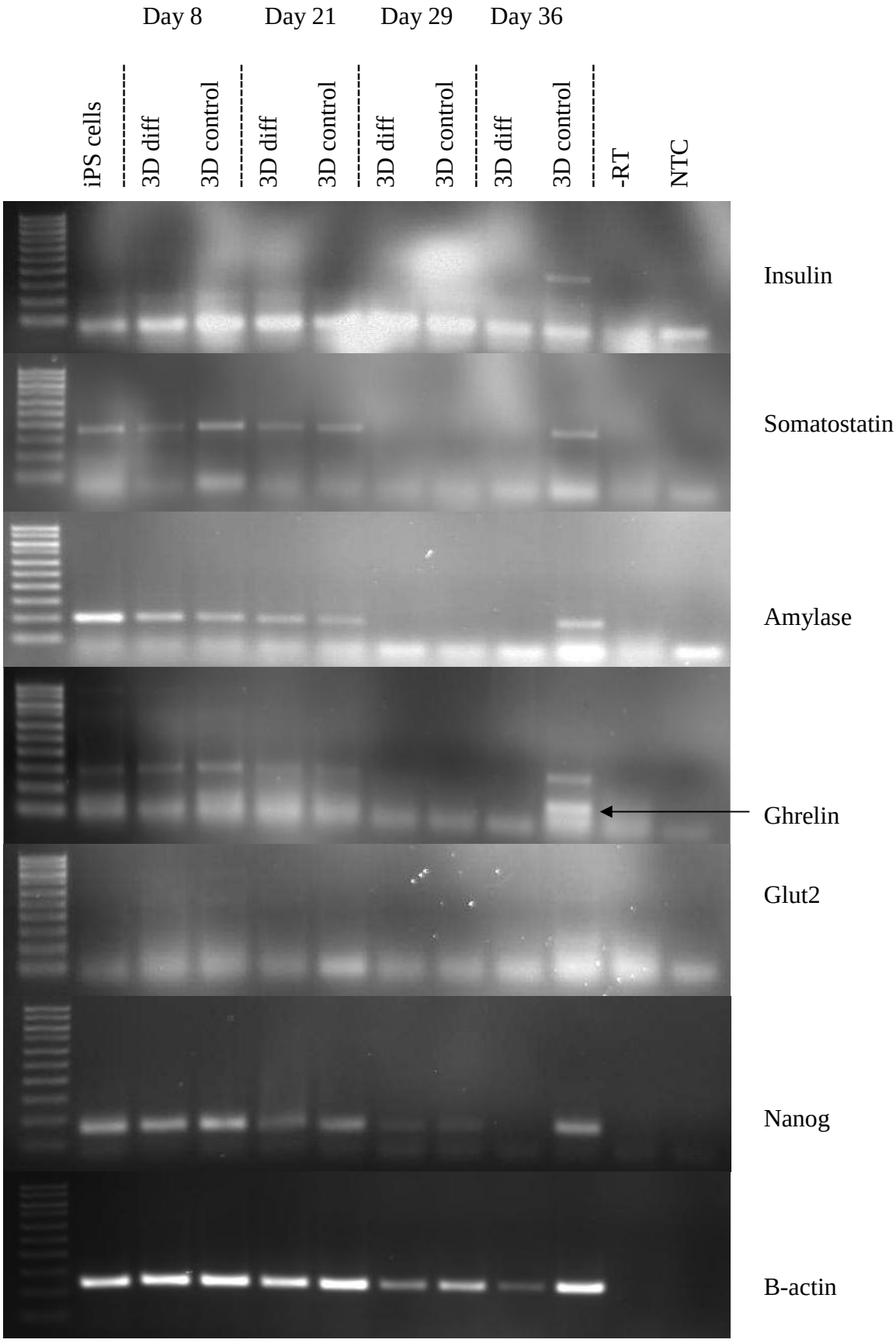

Figure 3.2.26 mRNA expression of 3D differentiated and control cultures after each stage of the pancreatic differentiation protocol. B-actin is used as an endogenous control for normalisation of mRNA expression levels.

A second biological replicate of the 3D iPS cell differentiation to pancreatic phenotype was performed. At day 8, cultures were harvested for RNA to check for expression of definitive endoderm markers. Cxcr4, hnf4a and foxa2 expression was detected at higher levels in 3D differentiated cells compared to 3D control cells (figure 3.2.27). Sox17 expression was undetected in all samples analysed. Expression of nanog pluripotency marker remains the same in untreated iPS cells and day 8 control and differentiated cells (figure 3.2.27).

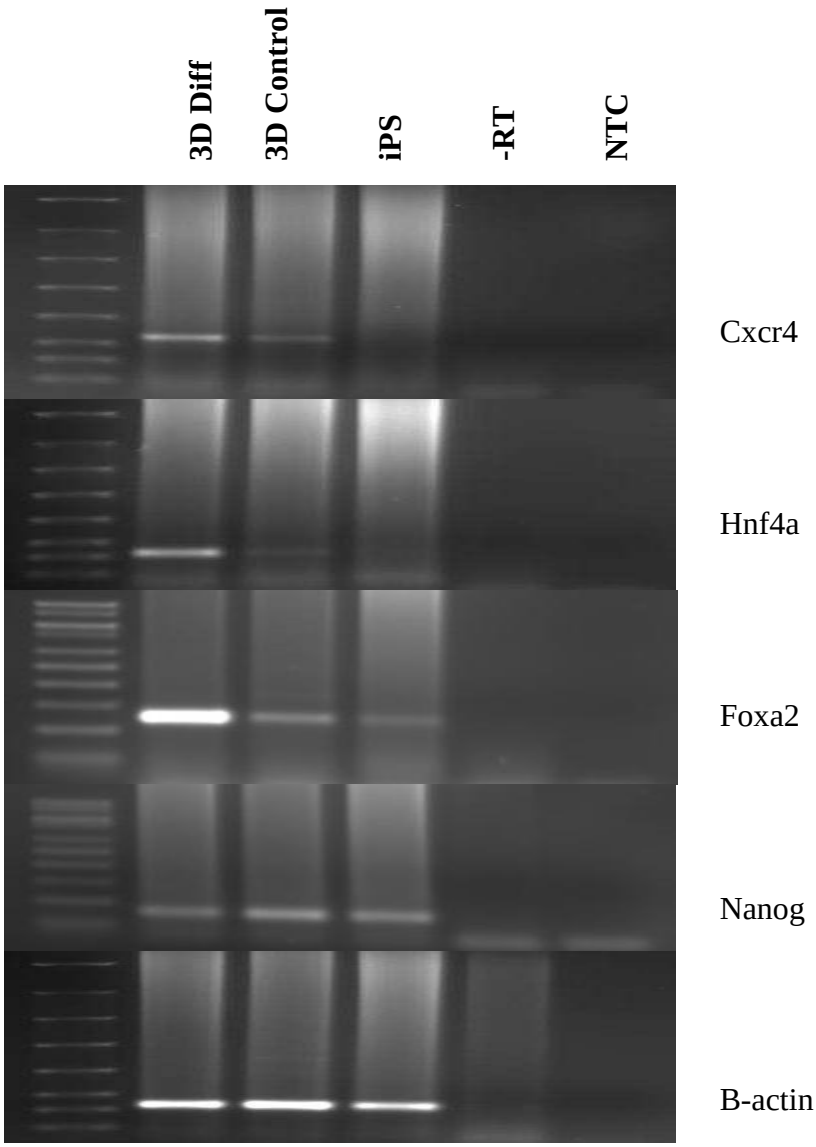

Figure 3.2.27 PCR of day 8 differentiation and control cultures. Expression levels of definitive endoderm markers- cxcr4, foxa2 and hnf4a were examined, as well as pluripotency marker- nanog, and endogenous control B-actin.

At day 21 control and differentiated cells were harvested for RNA to monitor expression of pancreatic endoderm markers. Pancreatic endoderm markers ngn2, nkx6.1, hlxb9 and ptf1a were undetected in all samples. PDX1 expression was detected in both 3D differentiated and control cells, with higher levels seen in 3D control cells (figure 3.2.28). Nanog pluripotency marker was also detected in all samples analysed.

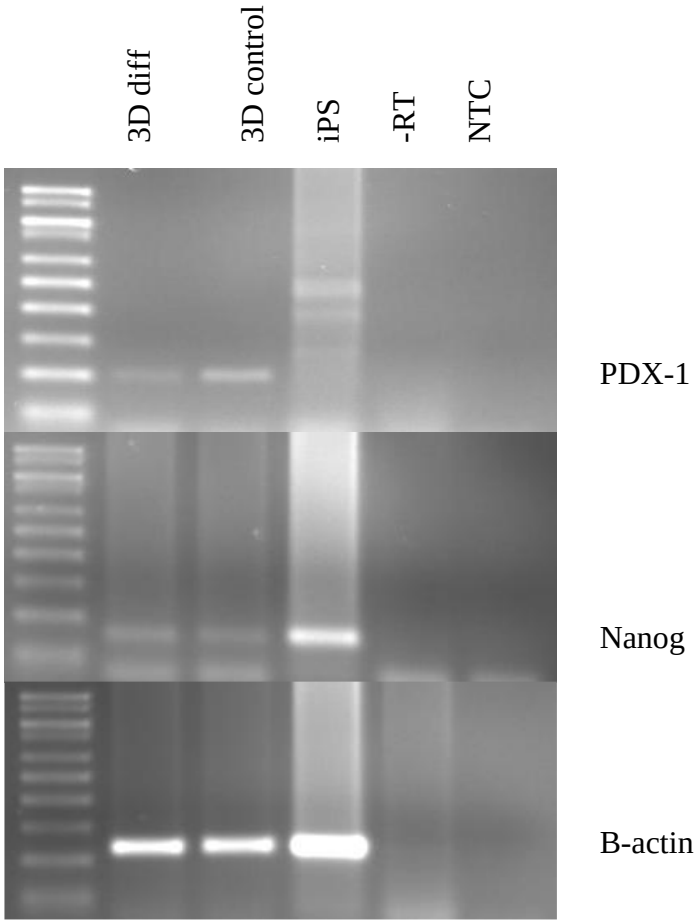

Figure 3.2.28 PCR of day 21 3D differentiation and control cultures. Expression levels of pancreatic endoderm marker PDX-1 is shown, as well as pluripotency marker nanog, and b-actin endogenous control.

Cultures were also harvested at day 29 and day 36. RNA from day 8, 21, 29 and 36 was analysed for expression of mature islet markers (figure 3.2.29). Somatostatin, amylase and ghrelin showed a similar expression pattern. Expression of these three markers was detected in untreated iPS cells, day 8 control and differentiated cells, and day 29 control cells. Low amylase expression is also seen in day 36 control cells. Mature islet markers insulin and glut2 were undetected in all samples analysed. Pluripotency marker nanog shows higher expression in untreated iPS cells, day 8 control and differentiated cells and day 29 cells, compared to low expression in day 21 control and differentiated cells, day 29 differentiated cells and day 36 control and differentiated cells. B-actin endogenous control expression shows varying expression levels between samples.

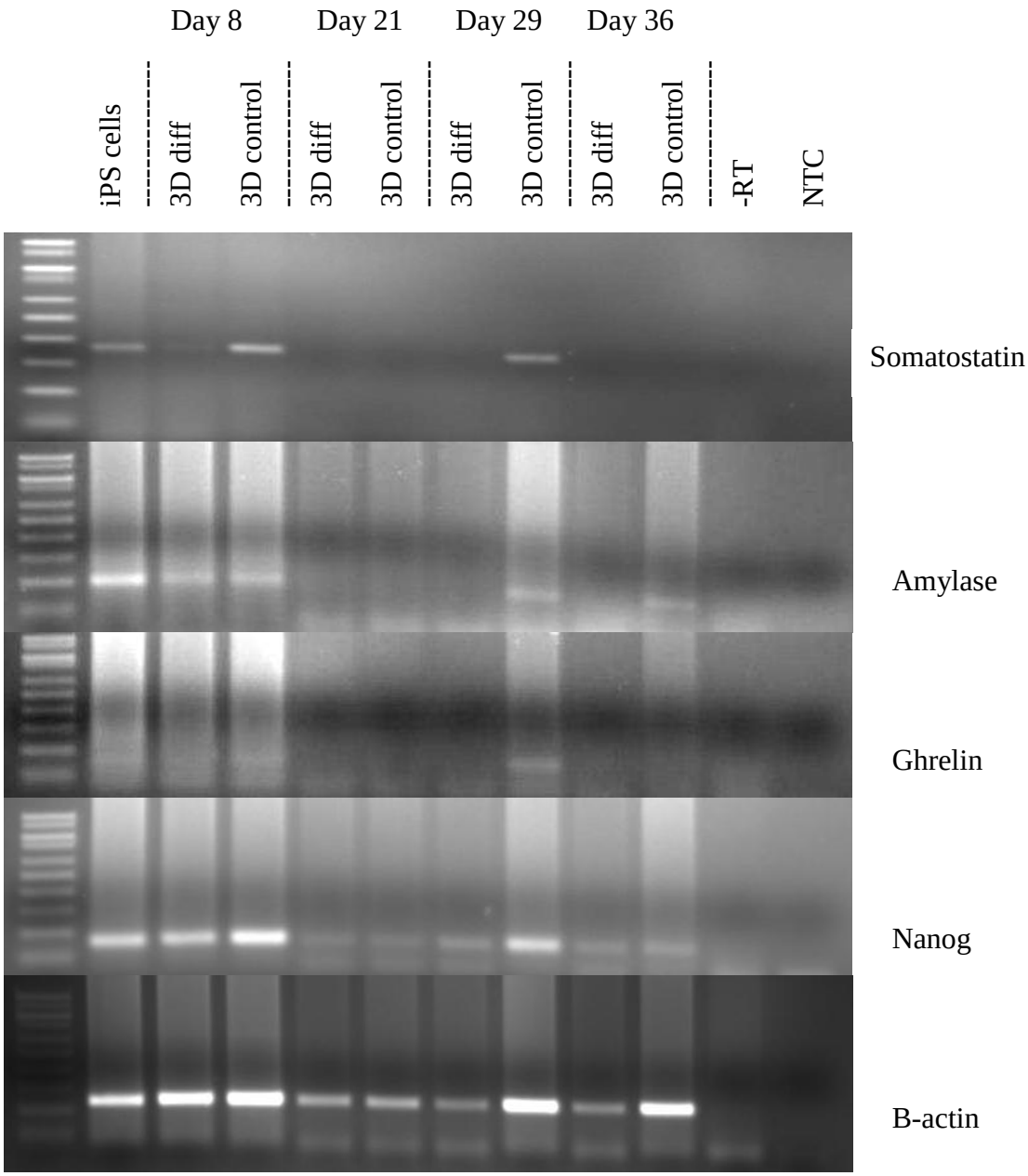

Figure 3.2.29 PCR of 3D differentiated and control cultures after each stage of the pancreatic differentiation protocol.

3.2.6.1 Summary of directed differentiation of iPS cell line hFib2-iPS4

iPS cells differentiated in 3D culture showed improved efficiency for definitive endoderm formation compared to 2D culture, based on expression of definitive endoderm markers cxcr4, foxa2 and hnf4α (figure 3.3.21). Further differentiation towards more mature pancreatic lineages showed less conclusive results, as untreated iPS cells expressed a number of mature pancreatic markers (figure 3.2.26 and 3.2.29), indicating that these cells may have already undergone some spontaneous differentiation prior to beginning the directed differentiation protocol.

3.2.7 Trans-differentiation of limbal stromal cells towards pancreatic phenotypes

Stromal cells isolated from donor cornea-sclera ring were differentiated towards definitive endoderm (protocol outlined in section 2.2.5.1 stage 1). These cells grow in monolayer culture, therefore monolayer cells were treated with differentiation media while control cells were maintained in standard stomal media (DMEM, 10% FCS). Following 8 days treatment with differentiation or control media cells were harvested to monitor expression of definitive endoderm associated genes such as cxcr4, foxa2, hnf4α and sox17. However, under these conditions, stromal cells in control or differentiation media did not express detectable levels of definitive endoderm associated genes.

Cell clusters of stromal cells were generated using the hanging drop technique (figure 3.2.30 B) (section 2.2.6). Clusters were then either cultured in 3D in a thick matrigel/collagen gel, 2D on a thin matrigel layer, or clusters were trypsinised to a single cell suspension and grown in monolayer. Cells were allowed to settle and proliferate in their 3D, 2D or monolayer conditions for 2 days before initiation of differentiation (figure 3.2.30) (section 2.2.5).

Differentiation media was added to cells for 8 days to allow definitive endoderm formation (as outlined in section 2.2.5.1 stage 1). Control cells were also prepared in 3D, 2D and monolayer cultures, and maintained in the standard stromal cell media (DMEM, 10% FCS). No obvious cell morphology changes were observed by day 8 in control or differentiation media treated cells (figure 3.2.31). At day 8, control and differentiation media treated cells were harvested to monitor expression of definitive endoderm associated genes (figure 3.2.32).

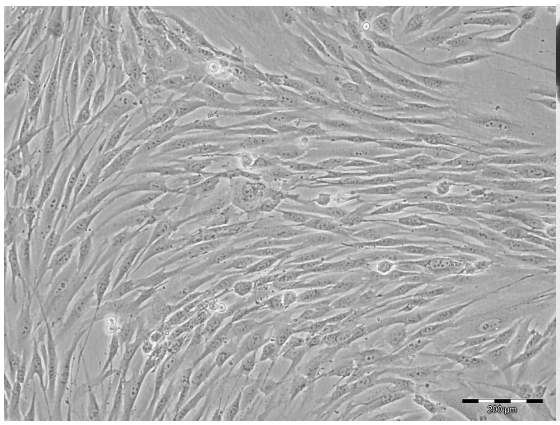

A: untreated stromal cells (10X)

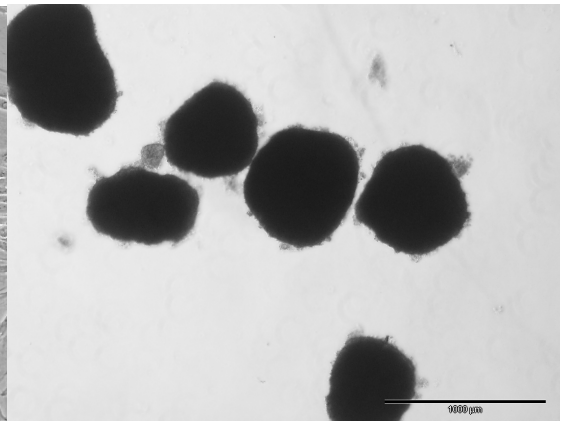

B: stromal aggregates in suspension (4X)

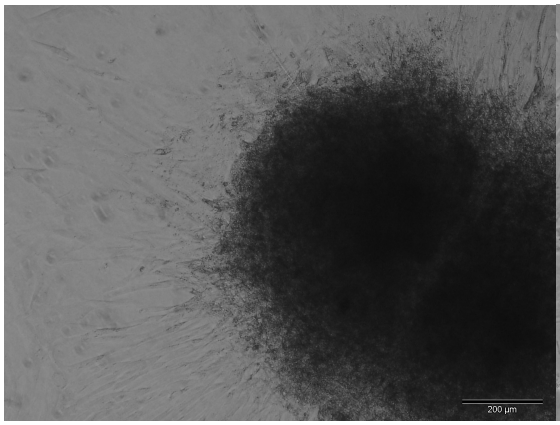

C:stromal aggregates in 3D culture (10X)

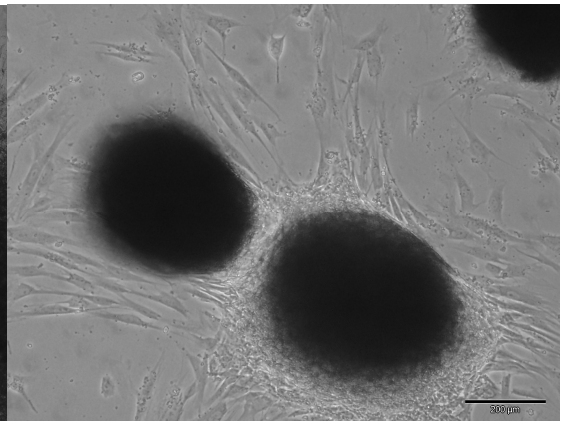

D: stromal aggregates in 2D culture (10X)

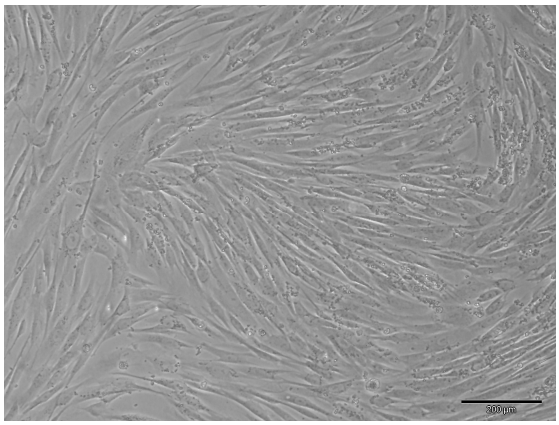

E: stromal aggregates trypsinised (10X)

Figure 3.2.30 Stromal cell culture treatments. Stromal cell aggregates were prepared using hanging drop technique (B), these aggregates were then cultured in 3D in a thick matrigel/collagen gel (C), in 2D on a thin matrigel layer (D), or were subject to trysinisation and subsequent single cells suspension cells formed a monolayer (E). Untreated cells before aggregate formation (A). 10X and 4X indicate magnification at which images were taken.

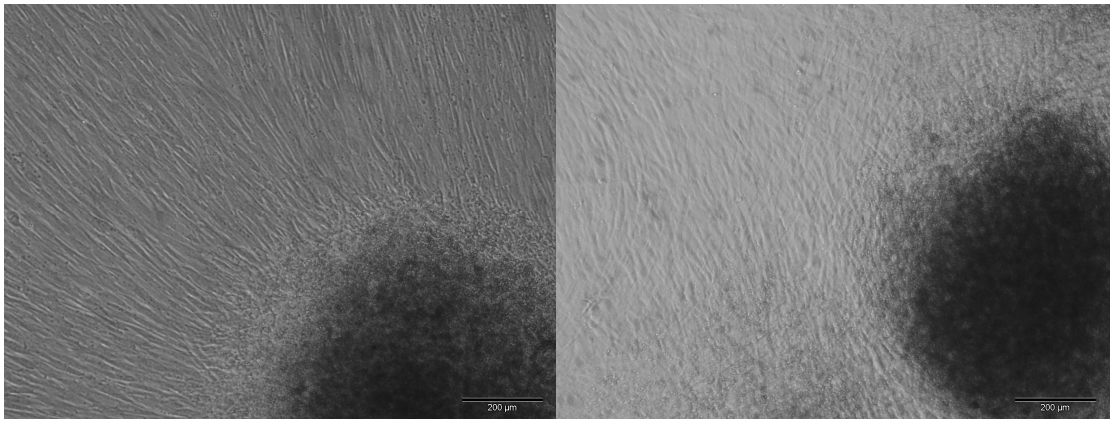

A: 3D control stromal cells **B**: 3D differentiated stromal cells

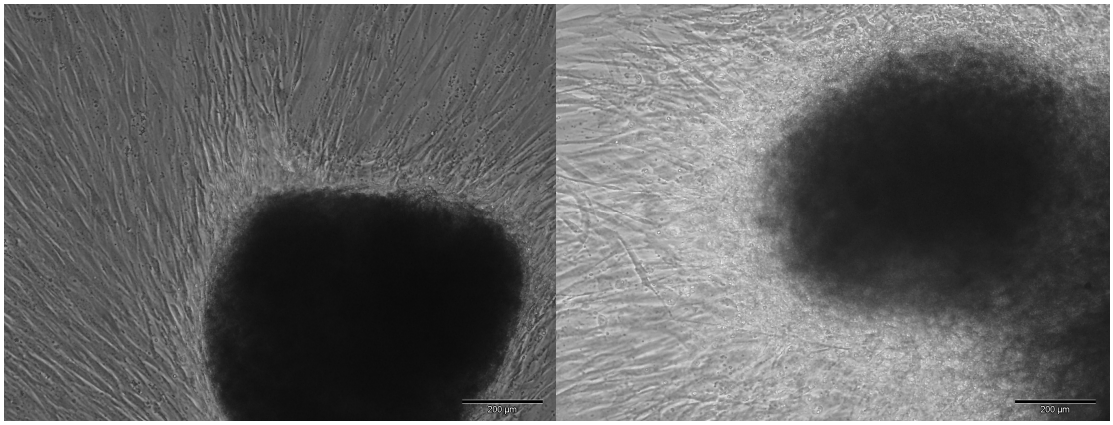

C: 2D control stromal cells **D**: 2D differentiated stromal cells

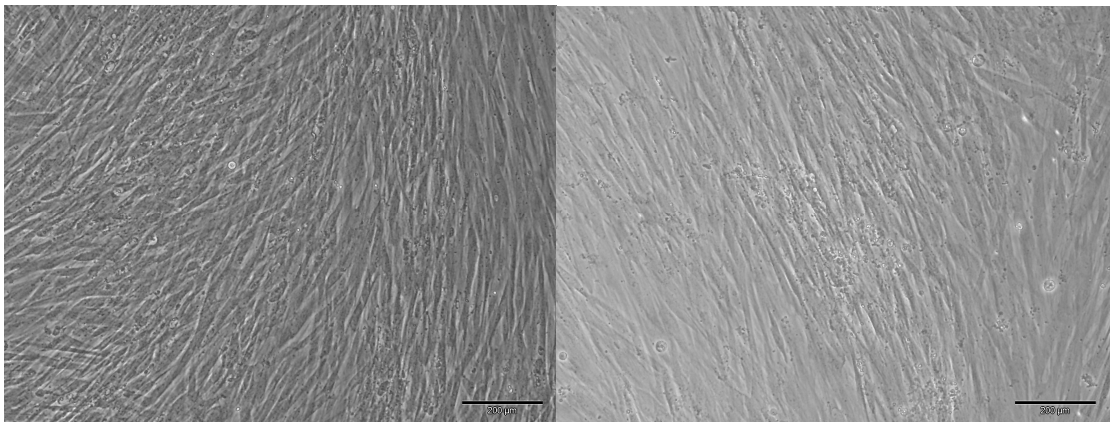

E: Control trypsinised aggregates **F**: Differentiated trypsinised aggregates

Figure 3.2.31 Day 8 of stromal cell differentiation protocol. Stromal cell aggregates were cultured in 3D (A & B), 2D (C & D) or aggregates were trypsinised and grown in monolayer format (E & F). Cells were treated with differentiation media to induce definitive endoderm formation (A, C & E), or standard stromal media (B, D & F) as a control.

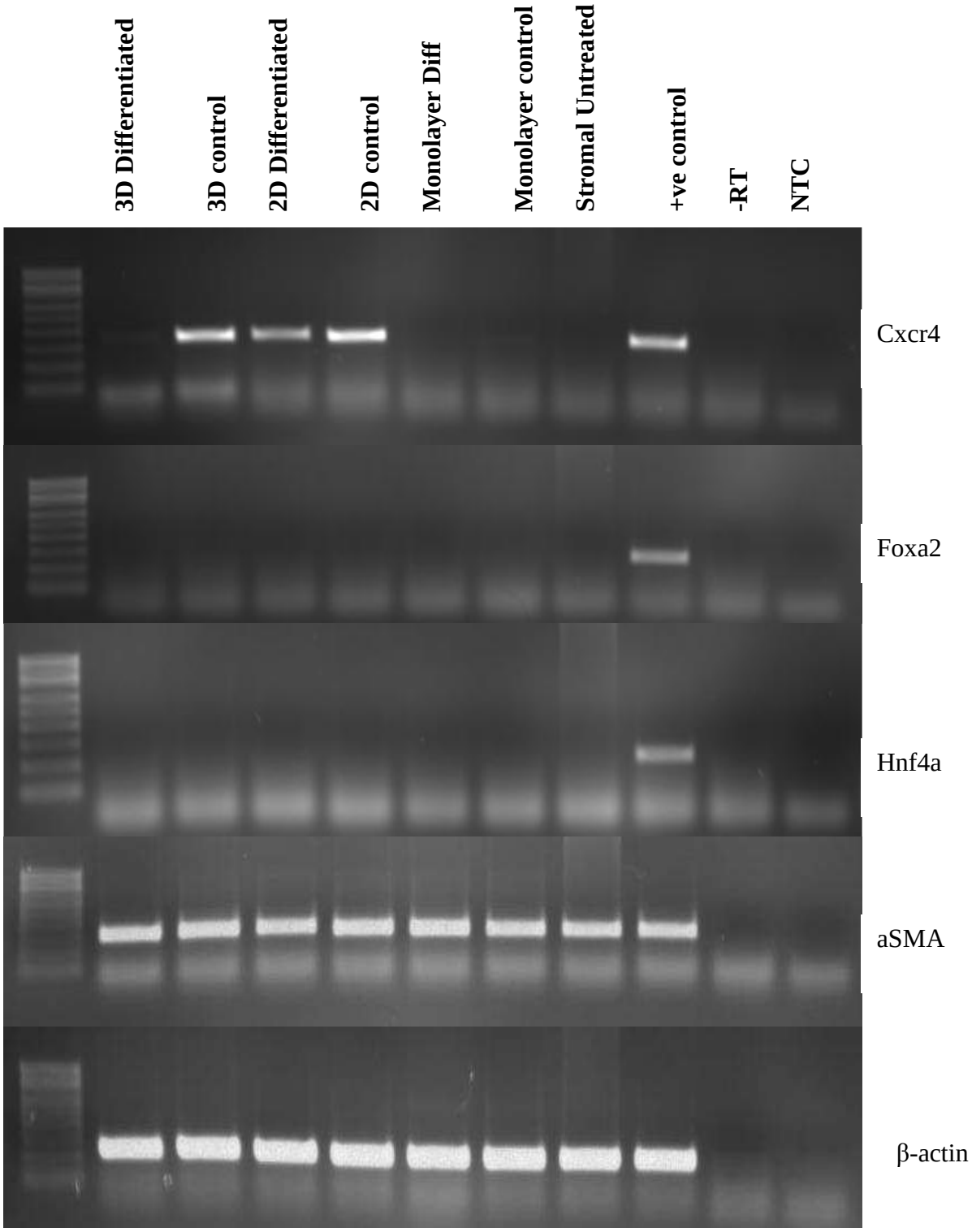

Figure 3.2.32 Gene expression in differentiated stromal cells. Definitive endoderm markers cxcr4, foxa2 and Hnf4α and mesenchymal marker αSMA in differentiated and control stromal cells. β-actin is used as an endogenous control.

Definitive endoderm marker expression was examined in stromal cells in 3D, 2D and monolayer cultures treated with differentiation media and standard stromal media (figure 3.2.32). Cxcr4, Foxa2 and Hnf4α are markers of definitive endoderm. Foxa2 and Hnf4α expression was not detected in differentiated or control cells. 2D cultured stromal cells showed the highest expression of cxcr4 compared to 3D or monolayer cultured cells (figure 3.2.32). Higher cxcr4 expression was seen in control cells maintained in standard stromal cell media (DMEM 10% FCS) compared to cells cultured in differentiation media (RPMI with 1X B27, 4nM activin A, 1mM sodium butyrate) (section 2.2.5.1). This trend was seen in both 3D and 2D cultures. Very low levels of cxcr4 expression were seen in monolayer cultures. Expression of cxcr4 was absent from untreated stromal cells without hanging drop treatment. αSMA is a mesenchymal marker which is expressed in stromal cells, expression levels of this marker remained similar in control cells and cells treated with differentiation media.

As 2D stromal cultures showed the highest cxcr4 expression (figure 3.2.32), 2D cultures were extended to the next step of the differentiation protocol- the pancreatic endoderm stage. 2D stromal cells were treated with pancreatic endoderm differentiation media from day 8 to day 21, while control cells were maintained in standard stromal cell media. At day 21 no obvious cell morphology changes were observed in control and differentiation media treated cells (figure 3.2.33), RNA was harvested from cells at this time point to monitor pancreatic endoderm marker expression (figure 3.2.34).

Pancreatic endoderm markers pdx-1, hlxb9, ptf1a and nkx6.1 were undetected in all samples analysed. Ngn3 expression was detected at low levels in untreated stromal cells, but was undetected in control and differentiated cells in 2D culture (figure 3.2.34).

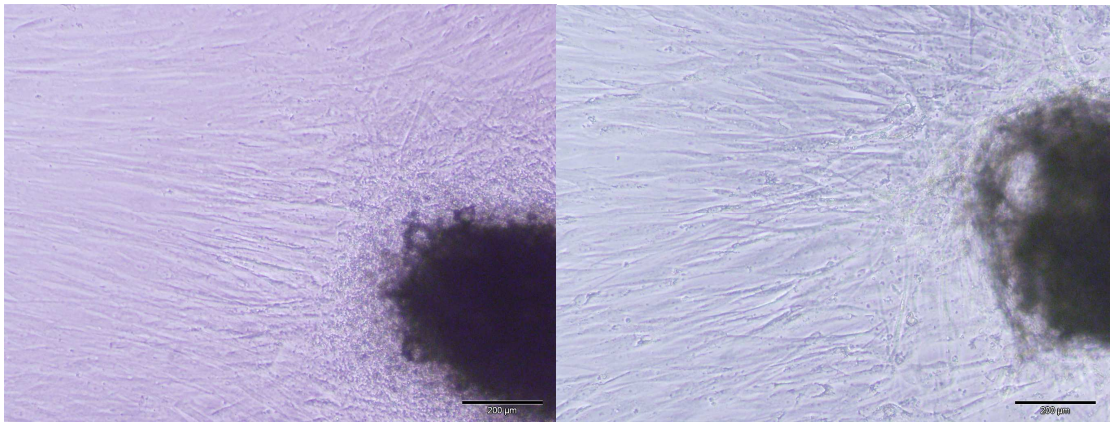

A: 2D control stromal cells **B**: 2D differentiated stromal cells

Figure 3.2.33 Day 21 of stromal cell differentiation protocol. Stromal cell aggregates were seeded into matrigel coated plates, control cells were maintained in stromal media (**A**), and differentiated cells were treated with differentiation media to induce pancreatic endoderm formation (**B**).

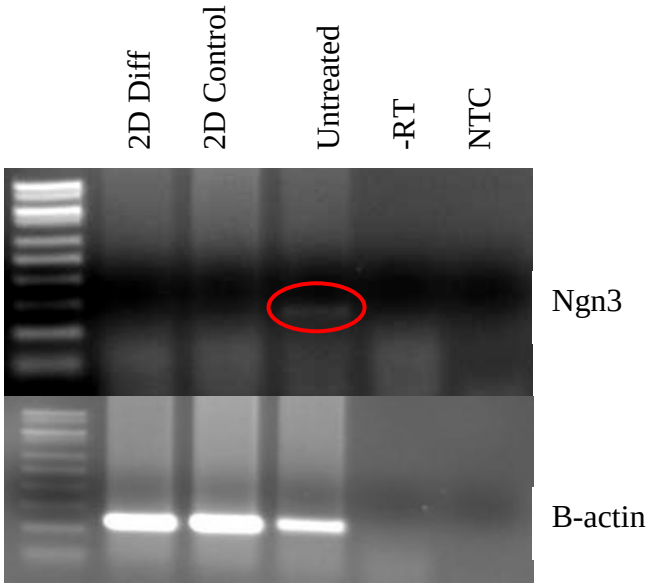

Figure 3.2.34 Day 21 PCR of stromal differentiation and control cells in 2D culture.

3.2.7.1 Summary of directed differentiation of stromal cells

Directed differentiation of stromal cells in standard monolayer culture showed no potential for pancreatic differentiation. However, when hanging drops were generated with these cells, subsequent directed differentiation induced expression of definitive endoderm marker cxcr4 (figure 3.2.32). Cell-cell interactions and signalling which occur while cells are in hanging drop and cluster formation may influence the propensity of stromal cells to differentiation towards pancreatic lineages. Further directed differentiation towards more mature pancreatic lineages did not yield any positive marker expression.

3.2.8 Stromal cell treatment with iMEF conditioned media

Irradiated MEF conditioned media seemed to induce expression of some mature pancreatic markers in iPS cells (figure 3.2.26 and 3.2.29). Therefore stromal cells were treated with iMEF CM to determine if this treatment could induce pancreatic differentiation in these cells.

Stromal cell aggregates were prepared using the hanging drop technique (section 2.2.6), aggregates were then embedded in a 3D thick matrigel/collagen gel (as described in section 2.2.5), and fed with either standard stromal media – DMEM with 10% FCS, or irradiated MEF conditioned ES media (iMEF CM). Cells were maintained under these conditions for 36 days before harvesting cells for RNA (as described in section 2.4.2) for analysis of mature pancreatic islet marker expression. Cells morphology differences were seen between stromal cells treated with standard media and iMEF CM. In the control condition cell aggregate outline is unclear with outgrowth of cells from the aggregate (figure 3.2.35 A), while iMEF CM treated aggregates still have a very clear aggregate border (figure 3.2.35 C). iMEF CM treated cells which have grown out from the aggregate also have a more stretched morphology, with more defined cell junctions compared to control cells in DMEM with 10% FCS (figure 3.2.35 B and D).

Mature pancreatic islet marker expression was also analysed in control and iMEF CM treated 3D stromal cultures, untreated stromal cells in standard monolayer culture were also analysed as a comparison. Amylase expression was detected in 3D control and 3D iMEF CM treated cells, with higher expression in iMEF CM treated cells (figure 3.2.36). Amylase expression was undetected in untreated stromal cells in standard monolayer culture. Insulin, somatostatin, glut2 and ghrelin expression were undetected in all samples analysed.

This experiment was repeated to confirm the observed results. While similar cell morphology changes were seen as figure 3.2.36, the amylase expression in these cells was different. Equal amylase expression was seen in untreated 2D stromal cells, 3D stromal cells in standard stromal media, and 3D stromal cells in iMEF CM. Increased amylase expression was seen in stromal cell hanging drops (figure 3.2.37).

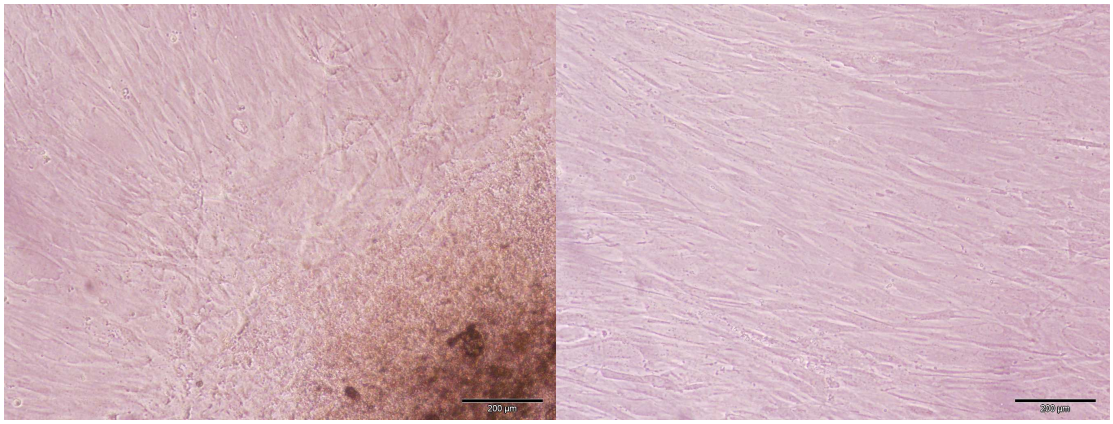

A: Stomal cells in DMEM 10% FCS **B**: Stromal cells in DMEM 10% FCS

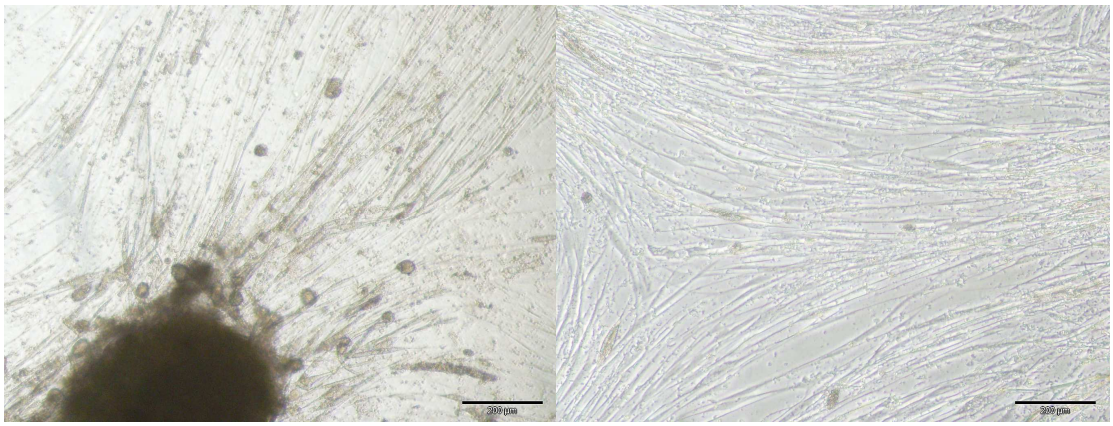

C: Stomal cells in iMEF CM **D**: Stromal cells in iMEF CM

Figure 3.2.35 Day 36 stromal cells. Stromal cell aggregates were cultured in 3D format in a thick matrigel/collagen gel. Cells were then treated with the standard stromal media DMEM and 10% FCS (A & B), or iMEF conditioned media with 8ng/mL bFGF (C & D).

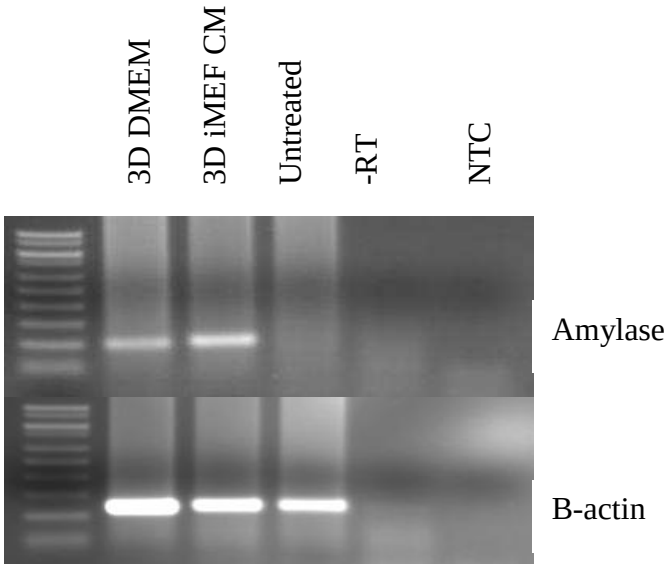

Figure 3.2.36 Day 36 PCR of stomal cells in 3D treated with iMEF CM or standard stromal media, DMEM 10% FCS. Untreated stromal cells in standard monolayer culture were also analysed.

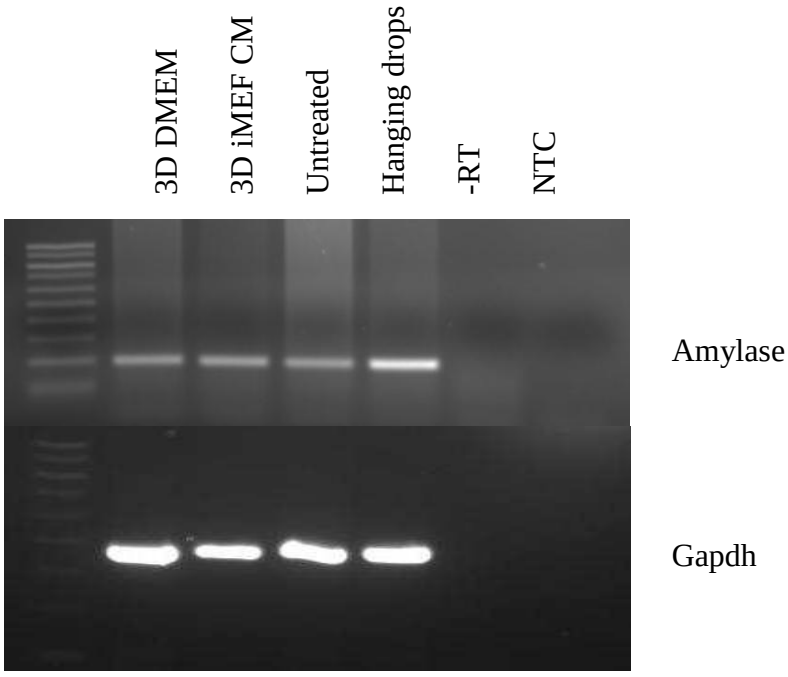

Figure 3.2.37 Day 36 PCR of stomal cells in 3D treated with iMEF CM or standard stromal media, DMEM 10% FCS. Untreated stromal cells in standard monolayer culture, and hanging drop culture were also analysed.

3.2.8.1 Summary of iMEF CM treatment of stromal cells

Stromal cell hanging drops in 3D culture were treated with iMEF CM for 36 days to induce pancreatic differentiation. Mature pancreatic exocrine marker- amylase, was detected in untreated and iMEF CM treated stromal cells (figure 3.2.37). Higher amylase levels were detected in stromal cells in hanging drop suspension culture. This highlights the influence of the poorly understood cell-cell signalling interactions which take place when cells are altered from monolayer cultures to cell clusters.

3.3 Biomarker discovery in diabetes serum specimens

A clinical study of diabetes serum was performed in parallel to the cell culture based studies in section 3.1 and 3.2. A number of techniques were used in this study to identify serum biomarkers of potential use for the diagnosis, treatment and management of diabetes patients. MicroRNAs (miRNAs) identified in section 3.1 as being potentially involved in glucose stimulated insulin secretion in MIN-6 cells, were analysed in diabetes serum to determine if these miRNAs were dysregulated in type 1 and type 2 diabetes patients. MiRNA profiling was also performed to identify additional miRNAs which may play a role in the pathogenesis of diabetes.

New proteomic profiling technologies in the form of label-free LC-MS became available through the core facilities in the NICB during the course of this study. Therefore, the opportunity was taken to perform proteomic profiling of diabetes serum specimens using this new technology. Proteomic profiling was performed on serum specimens from newly diagnosed and established type 1 diabetes patients, to identify proteins which may be involved in the establishment and progression of disease state.

Metabolomic profiling, which is now available as a commercial service provided by Metabolon Inc., was also performed on newly diagnosed type 1 diabetes serum samples, in addition to potentially identifying disease biomarkers, metabolomic profiling also allows insight into the metabolic dysregulation characteristic of diabetes patients.

3.3.1 Analysis of serum for miRNA biomarkers

In the study of miRNAs involved in glucose stimulated insulin secretion in MIN-6 cells (section 3.1) a set of 12 miRNAs were identified as potentially involved in this process. Advancing on these findings, we hypothesised that these miRNAs may also be differentially expressed in the serum of people with and without diabetes.

3.3.1.1 Evaluation of target miRNA levels in serum from type 1 diabetes patients and control serum

Initial experiments were performed on serum from three type one diabetes mellitus (T1DM) patients with established disease, compared to three non-diabetic control serum specimens. Levels of 14 different miRNAs were tested in these specimens (figure 3.3.1). Two of which had been identified from the literature (mir-9 and mir-375) (Poy, Eliasson et al. 2004; Plaisance, Abderrahmani et al. 2006), and 12 of which were identified from miRNA arrays of the pancreatic beta cell line MIN6 (table 3.1.2). MiRNA levels were tested using TaqMan real-time PCR chemistries, ct values are shown in appendix B, table 2.1. Mir-337, mir-200a and mir-410 expression was undetected in these samples.

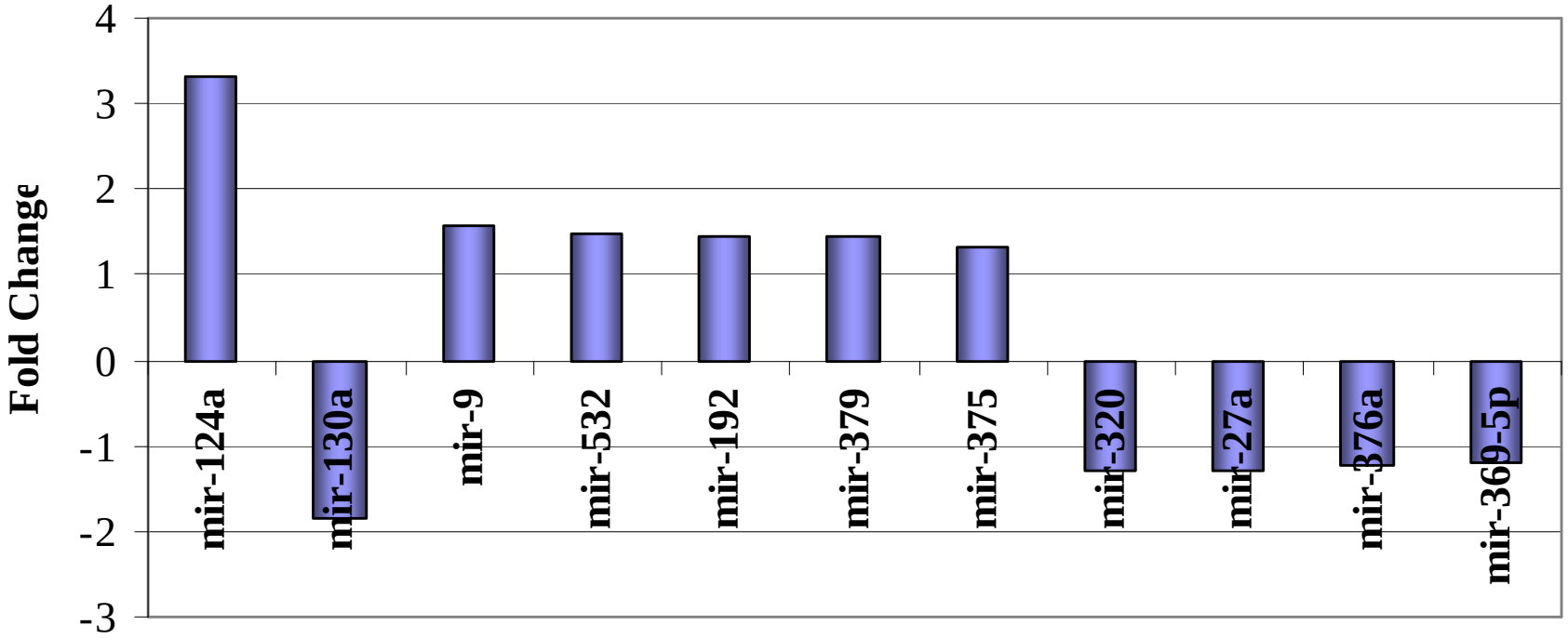

Figure 3.3.1. Fold change of miRNA levels in T1DM sera (n=3) compared to non-diabetic sera controls (n=3). T1DM and control samples were not matched for this initial analysis. Fold changes were calculated from group average ct values by $2^{-(ct(T1DM)-ct(Control)}$, as no suitable endogenous control identified for this work. As fold changes were calculated from averaged ct values, therefore no standard deviations are shown.

Mir-124a, mir-130a, mir-9, mir-532, mir-192 and mir-379 were identified from this initial study as being present at differing levels in T1DM serum compared to control sera (> 1.4 fold differential expression). Analysis of these six miRNAs was expanded to an additional 5 T1DM serum specimens compared to 5 non-diabetic control sera, which were age, gender and BMI matched (figure 3.3.2 – 3.3.6). Ct values are plotted rather than fold change, as no suitable endogenous control was identified for these serum specimens.

Mir-124a :

Mir-124a levels were significantly higher in T1DM sera compared to non-diabetic sera by 5.33 fold, in all five matched pairs (reflecting an average increase in C_t value of 2.17) (figure 3.3.2). Lower Ct value indicates increased target expression. Individual ct values for each matched pair shown in appendix B, table 2.2.

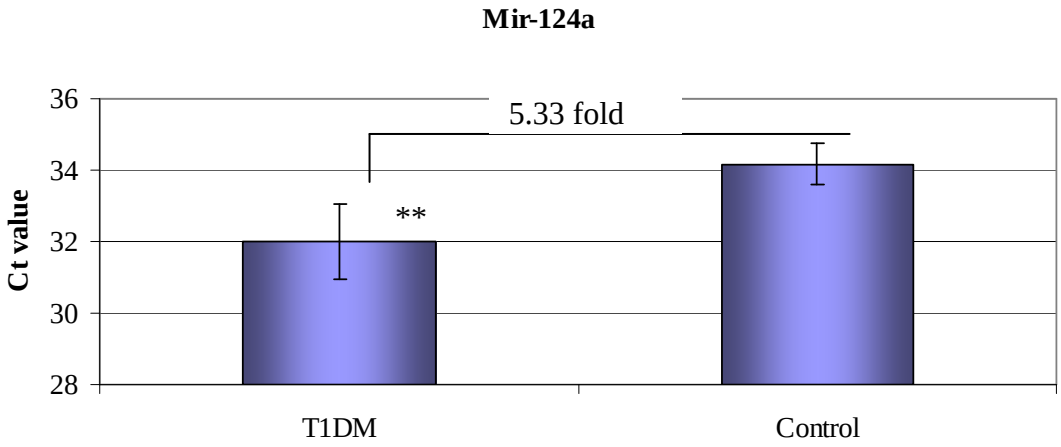

Figure 3.3.2 Ct values of mir-124a in T1DM sera (n=5) compared to non-diabetic sera (n=5). Significance indicated by * ≤ 0.05, ** ≤ 0.01, *** ≤ 0.005. Fold changes calculated from $2^{-(ct(T1DM)-ct(Control)}$, as no suitable endogenous control identified for this serum specimens. Error bars indicate standard deviation.

Mir-130a :

In the initial analysis of 3 T1DM samples and 3 controls, mir-130a was down-regulated in T1DM samples (figure 3.3.1). In this expanded study mir-130a is present at higher levels in T1DM sera relative to matched non-diabetic control sera in three sets of matched pairs. While in the remaining two pairs higher levels of mir-192 are detected in the control non-diabetic sera. There is no consistent trend seen in this miRNA in these samples (figure 3.3.3). Individual ct values for each matched pair is shown in appendix B, table 2.3.

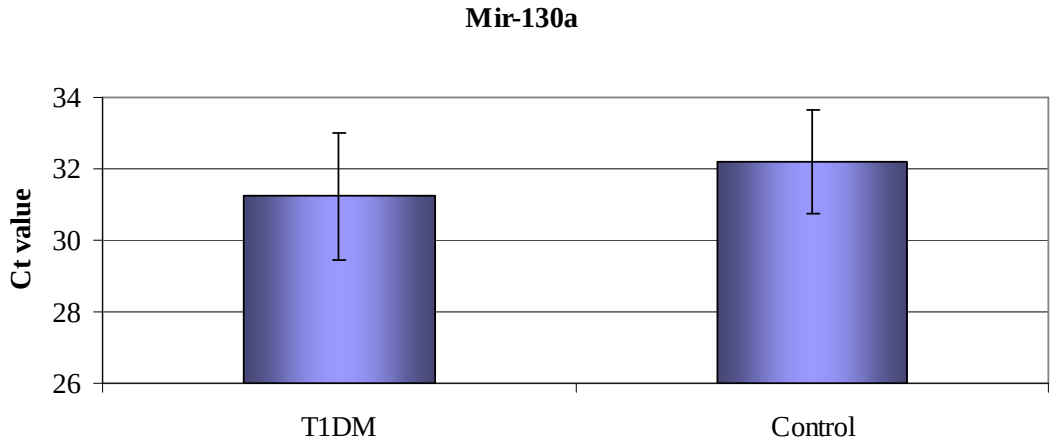

Figure 3.3.3 Ct value of mir-130a in T1DM sera (n=5) compared to non-diabetic sera (n=5). Error bars indicate standard deviation.

Mir-9 :

Mir-9 levels were present at higher levels in T1DM serum compared to non-diabetic serum in one set of matched pairs. In a further two sets of matched pairs mir-9 levels went from present in T1DM sera to undetected in non-diabetic sera, and in the remaining two sets of matched patients, mir-9 was undetected in both non-diabetic and T1DM sera (appendix B, table 2.4).

Mir-532 :

Mir-532 is present at higher levels in T1DM sera relative to matched non-diabetic control sera in three sets of matched pairs. In the remaining two pairs higher levels of mir-532 are detected in the control sera. There is no consistent trend seen in mir-532 levels in these serum specimens (figure 3.3.4). Individual ct values for each matched pair are shown in appendix B, table 2.5.

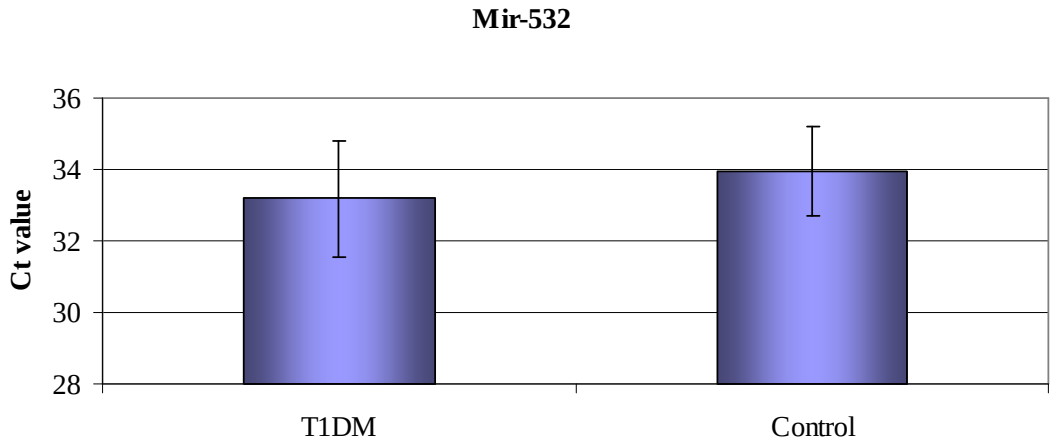

Figure 3.3.4 Ct value of mir-9 in T1DM sera (n=5) compared to non-diabetic sera (n=5). Error bars indicate standard deviation.

Mir-192:

Mir-192 is present at higher levels in T1DM sera compared to matched non-diabetic sera controls, in four of the five matched pairs (figure 3.3.5), although not significantly so. In the additional matched pair, mir-192 expression is detected in T1DM sample- DS-35, while it is undetected in its matched control- DS-33. Ct values for each matched pair are shown in appendix B, table 2.6.

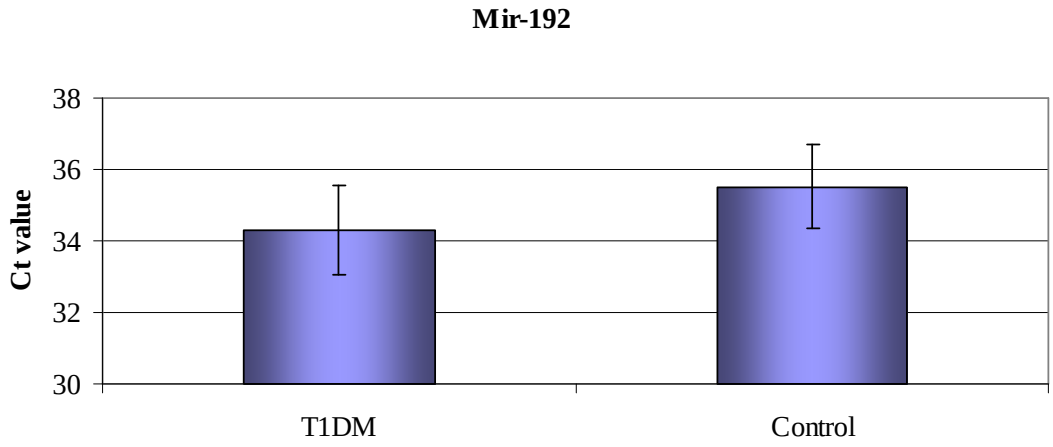

Table 3.3.5 Ct values of mir-9 levels in T1DM sera (n=4) compared to non-diabetic sera (n=4). The additional matched pair is not included on this graph as mir-192 levels were undetected in the matched control specimen. Error bars indicate standard deviation.

Mir-379 :

Mir-379 levels were on average higher in T1DM sera compared to non-diabetic sera (figure 3.3.6). Four of the five matched pairs showed higher mir-379 levels in T1DM sera, however, one matched pair T1DM sample- DS-13 and control sample- DS-18 showed the opposite trend, therefore this change in mir-379 level was not significant. Individual ct values for each sample are shown in appendix B, table 2.7.

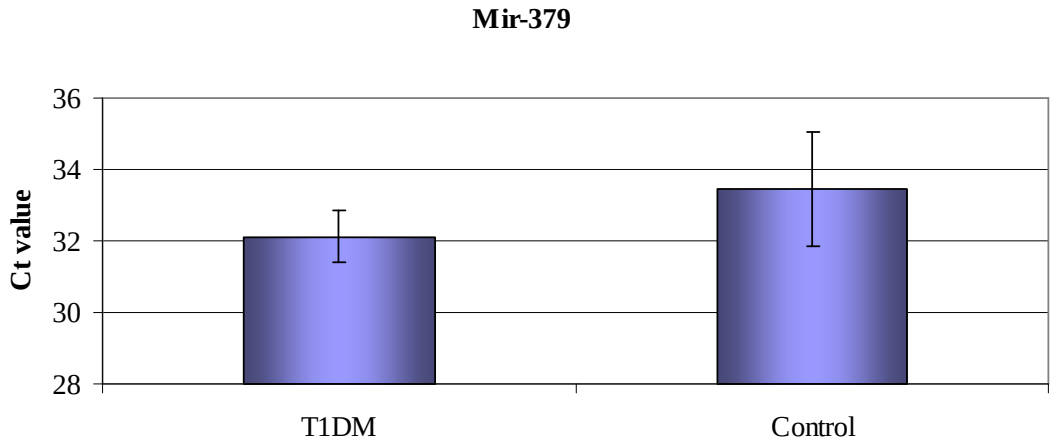

Table 3.3.6 Ct values of mir-379 in T1DM sera (n=5) compared to non-diabetic control sera (n=5). Error bars indicate standard deviation.

Mir-124a expanded study :

Figure 3.3.2 showed a promising trend in the levels of mir-124a present in T1DM sera relative to non-diabetic control sera. On average, in T1DM sera, mir-124a levels were significantly increased by 5.33 fold. An additional 10 T1DM samples and matched controls were analysed to assess if the mir-124a trend remained in a larger cohort of patients (figure 3.3.7)

Of the additional 10 sets of T1DM matched pairs analysed, 6 pairs showed the same trend of increased levels of mir-124a in T1DM as observed previously (figure 3.9). While 4 matched pairs showed reduced levels of mir-124a in T1DM sera. Ct values of individual samples are shown in appendix B, table 2.8.

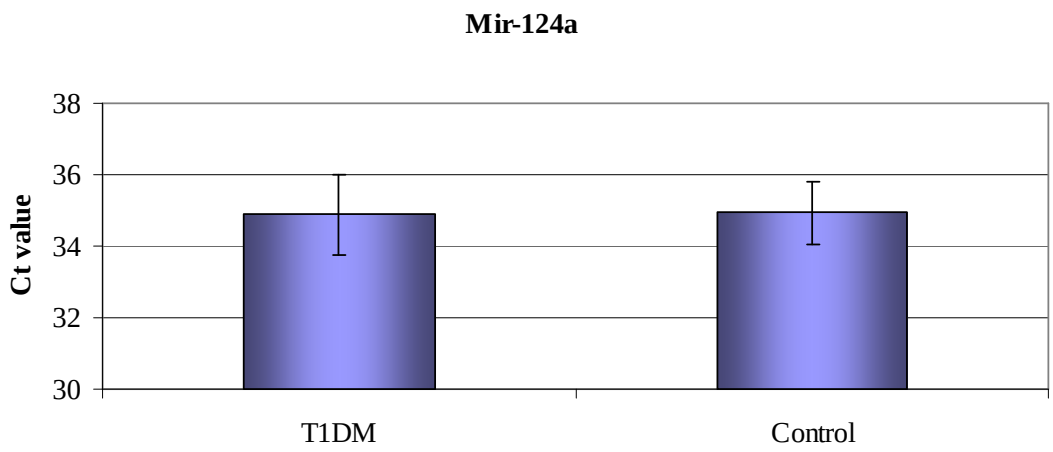

Figure 3.3.7 Ct values of mir-124a in T1DM sera (n=10) compared to non-diabetic sera (n=10). Error bars indicate standard deviation.

3.3.1.2 TaqMan Low Density miRNA array profiling of T1DM serum

TaqMan low density miRNA arrays were performed on three T1DM sera and three matched non-diabetic control sera. These miRNA arrays profile 365 target miRNAs plus three endogenous controls – RNU44, RNU48 and RNU6B. These endogenous controls were undetected in all sera samples analysed, therefore, all target miRNA results were analysed to identify a suitable miRNA to act as endogenous control.

Mir-28 and mir-326 were identified as potential endogenous controls for this diabetic sera study, due to their low ct (cycle threshold), standard deviation and insignificant p-values (i.e. these miRNAs not present at significantly different levels in T1DM sera compared to control sera) (table 3.3.1).

TLDA results were normalised against mir-28 and separately against mir-326 as endogenous controls. MiRNAs with significant p-values and fold changes according to both endogenous controls were identified for follow-up analysis (table 3.3.2).

Following normalisation against both endogenous controls seven miRNAs were identified as present at significantly higher levels in T1DM sera compared to non-diabetic control sera (table 3.3.2).

Endogenous Control	Average Ct	P-value	Standard Deviation
mir-28	25.81	0.147	0.484
mir-326	31.59	0.47	0.831

Table 3.3.1 Potential sera miRNA endogenous controls

	Mir-28 control		Mir-326 control	
MicroRNA	Fold Change	P-value	Fold Change	P-value
miR-140	6.851	0.038	6.506	0.012
miR-21	6.931	0.048	6.583	0.011
miR-24	5.723	0.042	5.436	0.008
miR-29a	6.326	0.022	6.008	0.002
miR-29c	8.388	0.025	7.967	0.016
miR-30d	5.64	0.044	5.357	0.018
miR-345	7.624	0.036	7.242	0.001

Table 3.3.2 MiRNA targets from TLDA analysis. Fold changes indicated miRNA levels in T1DM sera (n=3) relative to non-diabetic control sera (n=3).

3.3.1.3 Validation of TLDA miRNA targets in T1DM serum

Levels of endogenous control mir-28 were analysed in 5 T1DM samples and their matched controls using single-plex PCR, however mir-28 was undetected in one T1DM sample and one control sample. In the remaining samples mir-28 was present at significantly different levels in T1DM sera relative to control sera indicating that this miRNA is not a suitable endogenous control for normalisation of PCR data, therefore for further validation of TLDA targets no endogenous control was used.

Seven miRNAs- mir-140, mir-21, mir-24, mir-29a, mir-29c, mir-30d and mir-345 were identified from TLDA analysis as present at significantly higher levels in T1DM sera relative to control sera (table 3.3.2). However in the expansion of this study to a further 10 sets of matched pairs, none of the miRNAs tested showed a consistent trend in all matched pairs (table 3.3.3). Though the trends were not consistent throughout all specimens, it was noted that subgroups of matched pairs showed the same trends of miRNA expression. T1DM pairs DS-68, DS-74, DS-82, DS-84 and DS-95 pairs all showed reduced levels of miRNA targets relative to their matched controls, while DS-88, DS-93 and DS-98 pairs were in agreement with the samples used for TLDA analysis, and showed increased levels of target miRNAs relative to their matched controls.

Matched Pairs		MiRNA fold change						
T1DMs	**Controls**	**Mir-140**	**Mir-21**	**Mir-24**	**Mir-29a**	**Mir-29c**	**Mir-30d**	**Mir-345**
DS-68	DS-56	-7.91	-7.17	-7.08	-5.41	-4.47	-3.8	-3.72
DS-74	DS-36	-4.51	-5.3	-3.67	-3.67	-2.63	-3.34	-2.4
DS-82	DS-7	-4.55	-3.81	-3.37	-2.97	-5.23	-4.78	-4.6
DS-84	DS-27	-2.81	-1.65	-2.78	-1.93	-1.35	-2.13	-1.4
DS-95	DS-51	-1.34	-2.57	-2.04	-1.08	-1.52	-2.15	-1.28
DS-88	DS-39	40.79	26.8	19.93	10.46	19.83	4.85	4.54
DS-90	DS-53	1.27	-1.26	-1.06	1.09	-1.05	-1.74	1.17
DS-93	DS-33	120.34	103.54	44.38	26.23	61.65	19.6	9.03
DS-98	DS-50	4.45	2.18	3.17	4.64	3.58	1.87	4.75
DS-99	DS-53	1.02	-1.19	1.03	1.02	1.15	-1.29	1.09

Table 3.3.3 Single-plex validation of miRNA array targets in T1DM (n=10) and matched control (n=10) sera. Fold change indicates change in expression level in T1DM serum compared to control serum for each matched pair. Fold changes calculated from $2^{-(ct(T1DM)-ct(Control)}$, as no suitable endogenous control identified for this work. Red indicates reduced level of miRNA target in T1DM serum relative to control. Yellow indicates increased level of miRNA target in T1DM serum relative to control serum.

3.3.1.4 Evaluation of GSIS related miRNAs in serum from type 2 diabetes patients relative to control serum

Expression levels of the 12 miRNAs which were identified from miRNA arrays of the pancreatic beta cell line MIN6 (table 3.1.2) were tested in six type 2 diabetes mellitus (T2DM) sera and matched non-diabetic controls.

Mir-369-5p :

Mir-369-5p expression was down-regulated in glucose non-responsive cells compared to glucose responsive cells (table 3.1.2). In accordance with this result, mir-369-5p levels are decreased in T2DM sera compared to control non-diabetic sera for four of the matched pairs analysed. For the additional two pairs mir-369-5p is detected in the control samples, but is beyond the level of detection in the T2DM samples (figure 3.3.8) (appendix B, table 2.9).

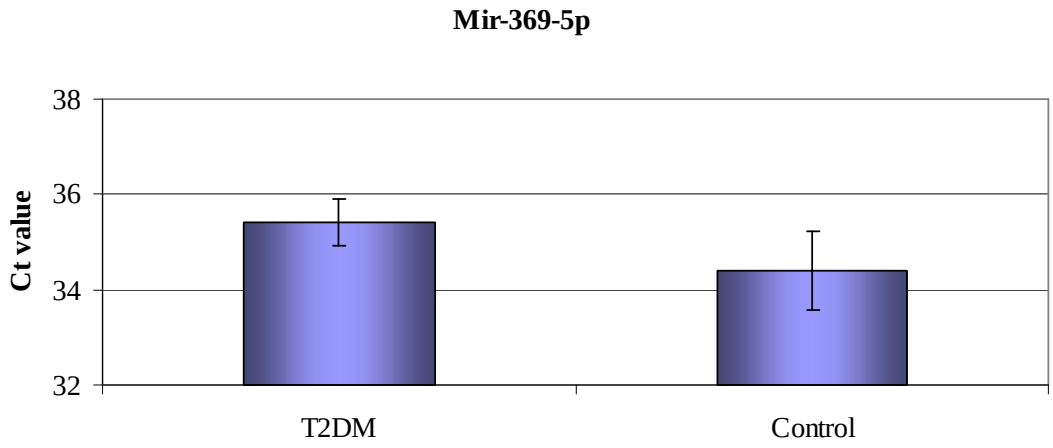

Figure 3.3.8 Average Ct value of mir-369-5p levels in T2DM sera (n=4) compared to non-diabetic sera (n=4). The two additional matched pairs were not included in this graph as mir-369-5p levels were undetected in the T2DM specimens. Error bars indicate standard deviation.

Mir-130a :

Mir-130a expression was down-regulated in glucose non-responsive cells compared to glucose responsive cells. In accordance with this result, mir-130a levels are decreased in T2DM sera compared to control non-diabetic sera, for three sets of matched pairs. For the remaining three sets of matched pairs, mir-130a levels are increased in T2DM sera relative to control sera. Therefore no consistent change was seen in mir-130a expression in these samples (figure 3.3.9) (appendix B, table 2.10).

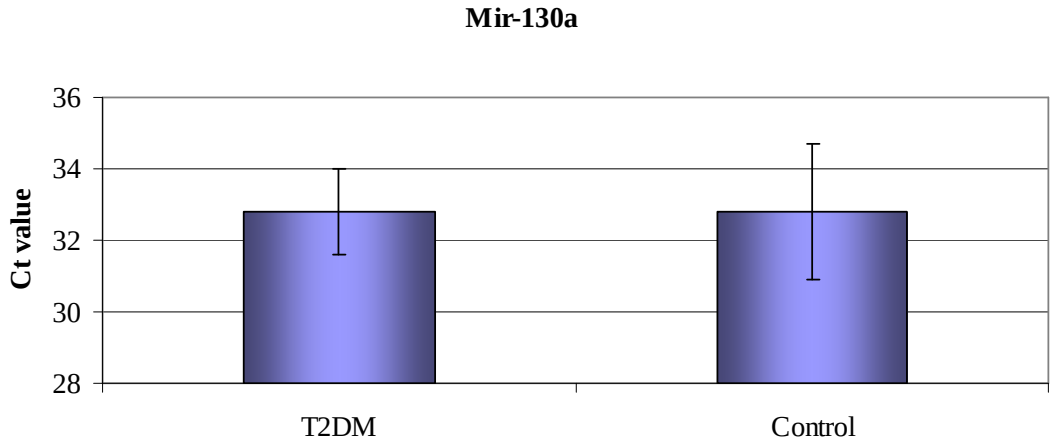

Figure 3.3.9 Average Ct value of mir-130a in T2DM sera (n=6) compared to non-diabetic sera (n=6). Error bars indicate standard deviation.

Mir-27a :

Mir-27a expression was down-regulated in glucose non-responsive cells compared to glucose responsive cells. In accordance with this result, mir-27a levels are decreased in T2DM serum for 5 of the 6 matched pairs, but increased in the remaining T2DM sample, this change is not significant (figure 3.3.10) (appendix B, table 2.11).

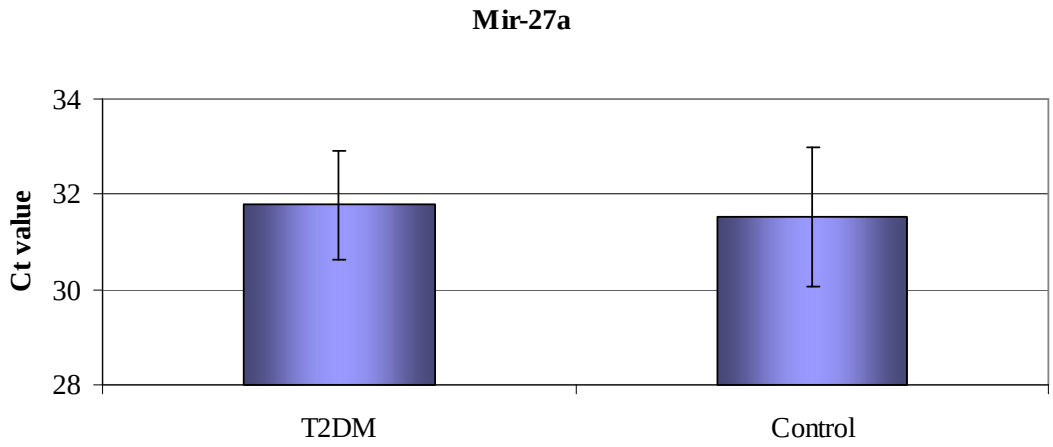

Figure 3.3.10 Average Ct value of mir-27a levels in T2DM sera (n=6) compared to control sera (n=6). Error bars indicate standard deviation.

Mir-124a

Mir-124a expression was down-regulated in glucose non-responsive cells compared to glucose responsive cells. In accordance with this result, mir-124a levels were decreased in T2DM sera compared to control non-diabetic sera, for three sets of matched pairs. For the remaining three sets of matched pairs, mir-124a levels were increased in T2DM sera relative to control sera in 2 sets of matched pairs, but levels remained unchanged in the last set (figure 3.3.11) (appendix B, table 2.12).

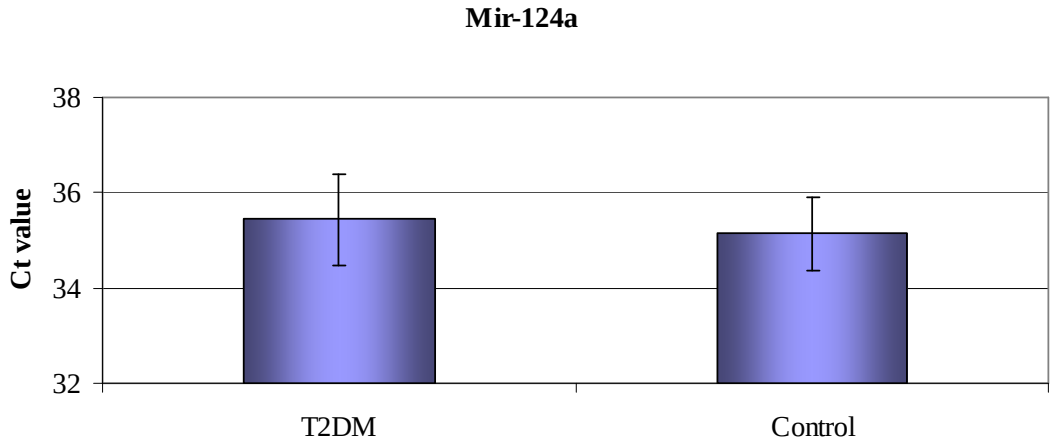

Figure 3.3.11 Ct value for mir-124a in T2DM sera (n=6) compared to non-diabetic sera (n=6). Error bars indicate standard deviation.

Mir-410 :

Mir-410 expression was down-regulated in glucose non-responsive cells compared to glucose responsive cells. In accordance with this result, mir-410 levels were decreased in T2DM sera compared to control non-diabetic sera, for three sets of matched pairs. For the remaining three sets of matched pairs, mir-410 levels are unchanged in T2DM sera relative to control sera (figure 3.3.12) (appendix B, table 2.13).

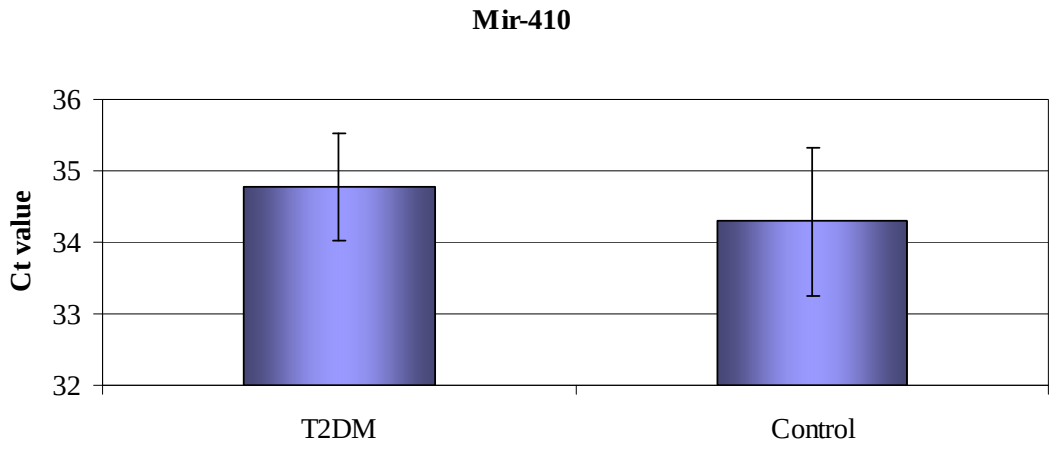

Figure 3.3.12 Ct value for mir-410 levels in T2DM sera (n=6) compared to non-diabetic sera (n=6). Error bars indicate standard deviation.

Mir-200a :

Mir-200a expression was down-regulated in glucose non-responsive cells compared to glucose responsive cells. In accordance with this result, mir-200a levels are decreased in T2DM sera compared to control non-diabetic sera, for two sets of matched pairs. For the remaining three sets of matched pairs, mir-200a levels are increased in T2DM sera relative to control sera, and the remaining matched pair mir-200a is undetected in both specimens and control sera (figure 3.3.13) (appendix B, table 2.14).

.

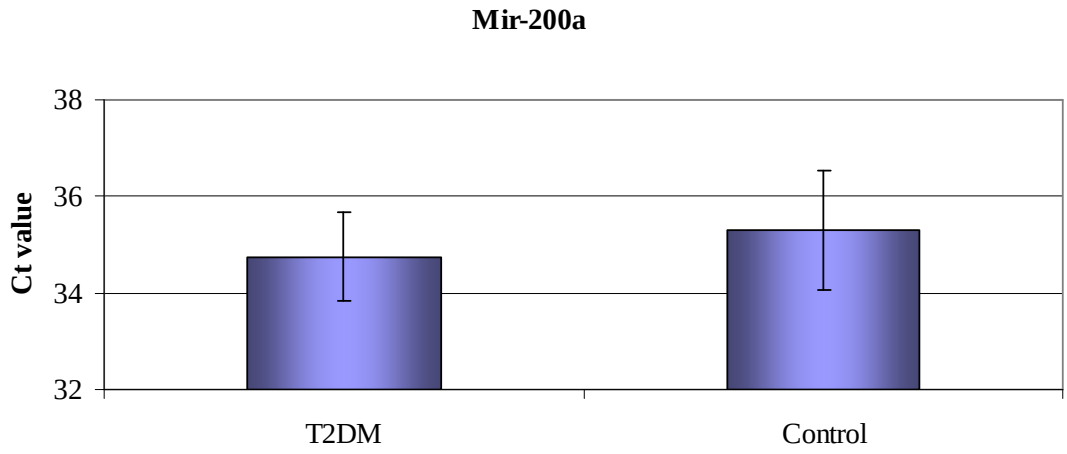

Figure 3.3.13 Ct value for mir-200a levels in T2DM sera (n=4) compared to non-diabetic sera (n=4). The two additional matched pairs were not plotted on this graph as mir-200a levels were undetected in the control specimens and one of the T2DM, while low level mir-200a were detected in the additional T2DM sample. Error bars indicate standard deviation.

Mir-532 :

Mir-532 expression was down-regulated in glucose non-responsive cells compared to glucose responsive cells. In accordance with this result, mir-532 levels are decreased in T2DM sera compared to control non-diabetic sera, for two sets of matched pairs. Mir-532 levels are increased in T2DM sera relative to control sera for two sets of matched pairs, and the remaining two sets of matched pairs mir-200a levels are unchanged in sample and control sera (figure 3.3.14) (appendix B, table 2.15).

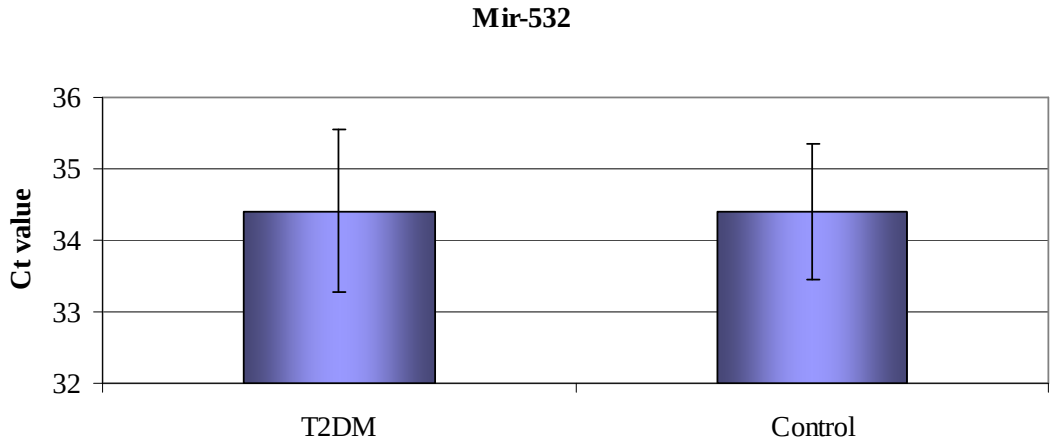

Figure 3.3.14 Ct value for mir-532 levels in T2DM sera (n=6) compared to non-diabetic sera (n=6). Error bars indicate standard deviation.

Mir-376a, mir-337, mir-320, mir-192 and mir-379 :

Mir-376a, mir-337, mir-320, mir-192 and mir-379 expression levels were reduced in non-glucose responsive cells relative to glucose responsive MIN6 cells, however, in this study of T2DM and control sera, levels of these miRNAs were undetected.

A summary of target miRNA expression in T2DM sera is shown in figure 3.3.15. Some slight changes were seen in expression of these miRNAs, however these changes were not statistically significant.

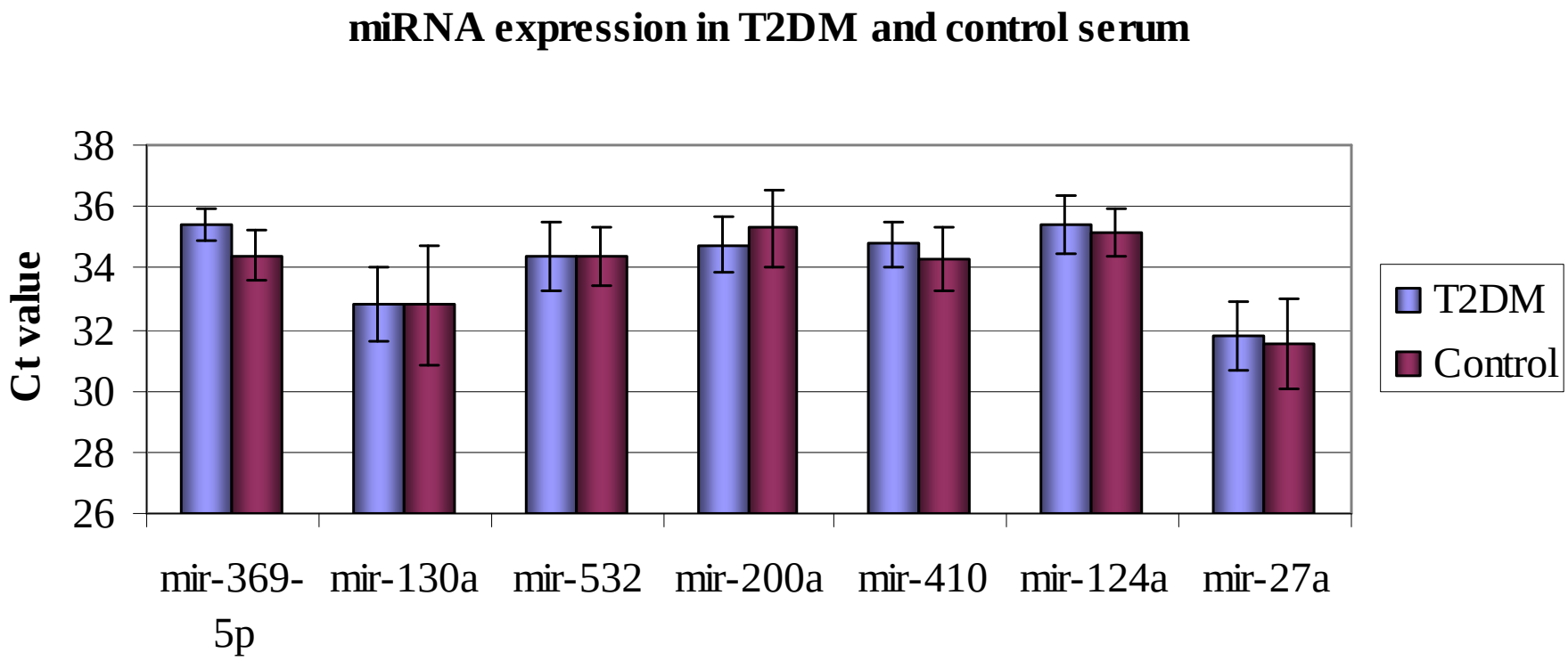

Figure 3.3.15 MiRNA expression levels in T2DM (n=6) and control (n=6) serum specimens. Expression levels are represented by Ct values. Error bars indicate standard deviation.

3.3.1.5 Summary of miRNA biomarker study

- Levels of GSIS related miRNAs were examined in T1DM old and control old samples
    - Mir-124a, mir-130a, mir-9, mir-532, mir-192 and mir-379 were differentially expressed (n=3)
    - Study was expanded to n=5 (n=15 for mir-124a), however miRNA expression trends were not consistent
- TLDA miRNA profiling of T1DM old and control old (n=3) identified 7 differentially expressed miRNAs
    - mir-140, mir-21, mir-24, mir-29a, mir-29c, mir-30d and mir-345
    - TLDA miRNA targets validated in 6 T1DM and control samples
    - miRNA expression trends were not consistent
- Levels of GSIS related miRNAs were examined in T2DM and control samples
    - No statistically significant changes were seen in these miRNA levels in T2DM and control samples (n=6)

3.3.2 Proteomic profiling of type 1 diabetes serum

3.3.2.1 Patient characteristics

Serum from newly diagnosed type 1 diabetes (3.14 ± 2.66 months mean duration since diagnosis) and type 1 diabetics with established disease (minimum 18 months), as well as age/BMI/gender matched healthy controls for each group (n=8) were used for the analysis. Table 3.3.4 shows the general characteristics of newly diagnosed type 1 diabetes (T1DM new) patients and healthy controls (control new) used in the study. Table 3.3.5 shows the general characteristics of type 1 diabetes patients with established disease (T1DM old) and their matched controls (control old) which were used in this study.

An additional group of serum samples from patients with a range of autoimmune and inflammatory diseases such as rheumatoid arthritis, ulcerative colitis, asthma, eczema, systemic lupus erythematosus, hashimoto's thyroiditis, psoriatic arthritis and pernicious anemia were also analysed in this experiment. The mean age of these patients was 31.4 ± 4.9 years. The autoimmune group was included in this experiment to allow identification of markers directly related to type 1 diabetes rather than markers of general autoimmune/inflammatory conditions.

	T1DM new (n=8)	Control new (n=8)	P-value
Age (years)	26 ± 5	27 ± 2	0.50
BMI (Kg/m^2)	24.64 ± 4.2	24.94 ± 2.6	0.87
Fasting glucose (mmol/L)	6.49 ± 3.06	4.49 ± 0.37	0.11
HbA1c (%)	7.69 ± 1.96	5.15 ± 0.30	0.008
Cholesterol (mmol/L)	4.29 ± 0.55	5.05 ± 0.44	0.013
HDL-cholesterol (mmol/L)	1.25 ± 0.42	1.35 ± 0.39	0.63
LDL-cholesterol (mmol/L)	2.53 ± 0.41	3.19 ± 0.55	0.02
Triglyceride (mmol/L)	1.09 ± 0.38	1.37 ± 1.07	0.50

Table 3.3.4 General characteristics of the newly diagnosed type 1 diabetes patients and their matched controls. Mean values shown for 8 patients per group.

	T1DM old (n=8)	Control old (n=8)	P-value
Age (years)	44.75 ± 12.84	42.25 ± 4.80	0.62
BMI (Kg/m^2)	28.46 ± 4.36	28.37 ± 4.88	0.97
Fasting glucose (mmol/L)	11.06 ± 5.69	4.79 ± 0.38	0.017
HbA1c (%)	7.99 ± 1.29	5.37 ± 0.24	0.00016
Cholesterol (mmol/L)	3.95 ± 0.66	5.19 ± 0.54	0.0011
HDL-cholesterol (mmol/L)	1.56 ± 0.39	1.45 ± 0.17	0.49
LDL-cholesterol (mmol/L)	1.91 ± 0.29	2.74 ± 1.09	0.071
Triglyceride (mmol/L)	1.02 ± 0.87	1.35 ± 0.89	0.47

Table 3.3.5 General characteristics of the type 1 diabetes patients with established disease and their matched controls. Mean values shown for 8 patients per group.

3.3.2.2 Serum pre-treatment with ProteoMiner™

Identification of protein biomarkers in serum can be difficult due to the large dynamic range of proteins present in this biological fluid. Serum proteins span a concentration range of 11 orders of magnitude, with the 20 most abundant proteins representing 97-99% of the total protein mass (Anderson and Anderson 2002). The presence of high abundance proteins interferes with detection of low abundance proteins, which may be of importance to the biological dysfunction being studied. Therefore a new sample preparation tool- ProteoMiner™, was used for the preparation of serum samples in this study.

ProteoMiner™ facilitates compression of the dynamic range of protein concentrations by decreasing the concentration of a number of well know high abundance proteins such as albumin and IgG, hence enriching for medium and low abundance proteins. ProteoMiner™ is a column based procedure, whereby serum samples are passed through a column containing a highly diverse bead-based library of combinatorial peptide ligands, with each unique peptide ligand binding a unique protein. High abundance proteins saturate their ligands and excess protein is washed through, while low abundance proteins are concentrated on their specific ligands (figure 4.3.1). ProteoMiner™ has many advantages over standard immunodepletion techniques for removal of the high abundance serum proteins. ProteoMiner™ facilitates protein elution in small volumes, combining low abundance protein concentration and compressing of the dynamic range in one step. While standard immunodepletion techniques remove a number of high abundance proteins but may still leave low abundance proteins relatively dilute, requiring a separate concentrating step. Immunodepletion may also lead to co-depletion of low abundance proteins of interest (Shen, Kim et al. 2005), whereas ProteoMiner™ prevents co-depletion of proteins bound to high abundance proteins.

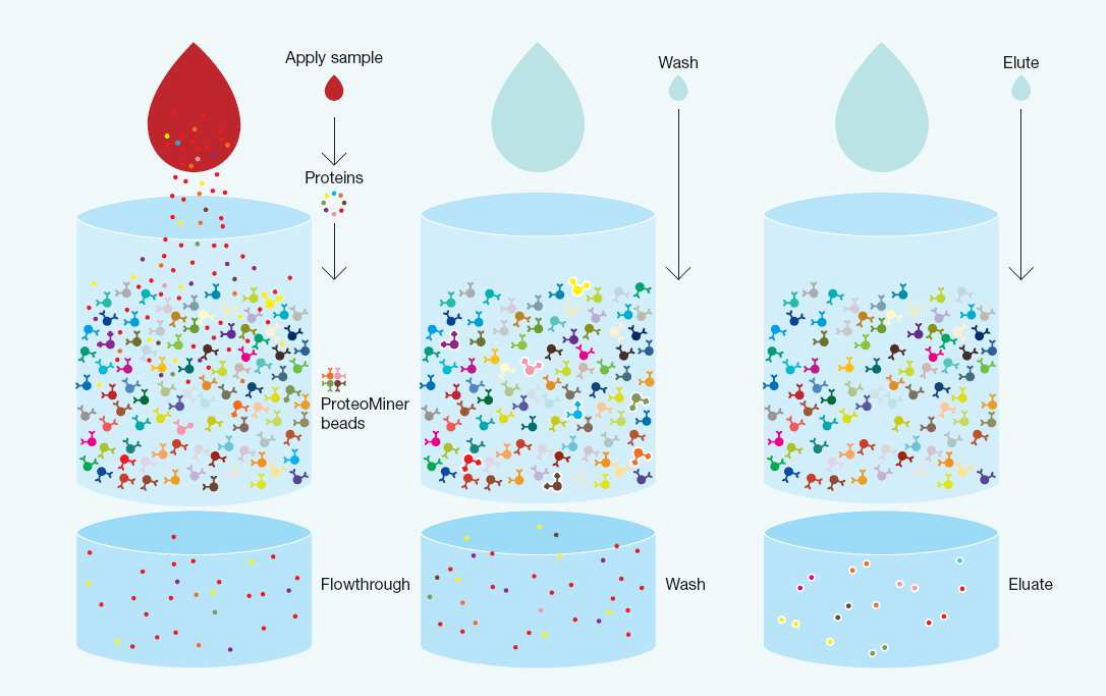

Figure 4.3.1 Representation of ProteoMiner™ protocol. Image taken from Proteominer™ Protein Enrichment Technology sample preparation guide (http://wolfson.huji.ac.il/purification/PDF/AlbuminRemoval/BIORAD_ProteoMiner.pdf)

3.3.2.3 Label-free LC-MS data analysis

Following the preparation of serum samples by ProteoMiner^{TM}, label-free liquid chromatography coupled to tandem mass spectrometry (LC-MS/MS) was performed for analysis of peptide composition in these samples. LC-MS/MS measures the peptide constituents rather than intact proteins as peptides are more suitable for LC analysis and have better ionization properties. Trypsin was used for protein digestion as it cleaves at well-defined sequence locations, resulting in non-overlapping peptide mixtures (Christin, Bischoff et al. 2011).

Label-free LC-MS/MS does not utilise isotopic labelling of proteins, instead, signal intensities are directly compared between LC-MS/MS runs. Label-free LC-MS/MS is now being used more frequently where previously 2D DIGE gels were used as standard for biomarker discovery. 2D DIGE gels have several limitations including insufficient resolving power to fully separate peptides in the gel, difficulty in analysing hydrophobic proteins, restricted sample throughput, complex sample preparation, incomplete labelling, as well as high costs (Ong and Pandey 2001; Tuli and Ressom 2009; Sandin, Krogh et al. 2011). Label-free LC-MS overcomes these issues while allowing increased proteome coverage compared to gel based techniques.

LC is the most commonly used method for separating peptides before downstream mass spectrometry analysis (Tuli and Ressom 2009). A nano LC system was used for this proteomic profiling application, where the stationary phase consisted of silica based C18 reverse phase column. The mobile phase used consisted of a 10-35% gradient of solvent B (98% acetonitrile, 0.04% FA) with solvent A (2% acetonitrile, 0.05% trifluroroacetic acid) over a 150 minute period. Reverse phase LC columns are most suited for analysis of complex peptide mixtures (Tuli and Ressom 2009) with the most polar or hydrophilic peptides eluting first and most non-polar hydrophobic peptides eluting towards the end of the 150 minute period.

The mass spectrometer consists of three main components: the ionisation source which converts the eluting peptides into the gas phase, the mass analyser which separates the ions based on the mass to charge ratio (m/z), and the detector which registers relative

abundance of ions (Tuli and Ressom 2009). In this study, tandem mass spectrometry was employed. This incorporates several mass analysers in series, which enables ions from the first analyser (parent ions) to undergo collision induced dissociation (CID) to generate product ions which are then separated based on m/z in the subsequent mass analysers. Detection of parent and daughter ions allows extra confidence in peptide identification. MS/MS spectral files from the mass spectrometer containing m/z information of parent and product ions of each peptide can be compared to identify differentially abundant ions or peptides which can be directly searched against a database of proteins which have been digested in silico.

Data analysis was performed using Progenesis LC-MS software available from Non-Linear Dynamics. Raw MS data files were imported to Progenesis LC-MS software package. A reference run is selected as the sample which is most representative of the data, all additional sample runs are then aligned to the reference sample run. Alignment of sample runs allows correction of variable peptide retention times during chromatographic separation and hence allows comparison of different sample runs. Once sample runs have been aligned, the software is then able to detect features in each run. Detected features are then filtered based on an anova p-value of less than 0.2; this cut-off value was chosen so as not to exclude too many peptides from the analysis, as subsequent identified proteins would be filtered with more stringent criteria at a later stage. From this list of filtered features a principal component analysis (PCA) plot is generated. The MS/MS data from this list of filtered features is then exported into the external search engine MASCOT to match these identified features to known peptides, using the following search criteria: database-Swissprot/UniProt, enzyme-trypsin, allow up to 2 missed cleavages, taxonomy-homo sapiens, fixed modifications-carbamidomethyl (C), variable modifications-oxidation (M), peptide tolerance-10ppm, MS/MS tolerance-0.8Da, and peptide charge-2+, 3+ and 4+. Once identifications have been assigned, this information is then imported to progenesis. Various statistical criteria can then be applied to identified peptides to generate a list of proteins. For this experiment a statistical criteria of anova p-value less than 0.05, and peptide number greater than 1 was applied to generate lists of differentially expressed proteins.

3.3.2.4 All groups analysis

8 serum samples per group were included in this experiment. One control sample (DS-171) was incompatible for alignment with any reference sample selected, this may be due to sub-optimal sample handling or a problem associated with the LC-MS run, therefore this sample could not be used in the data analysis. All other sample runs aligned with reference run without any problems. LC-MS data for all samples from each group were imported to the progenesis software (excluding control sample DS-171), following successful alignment and filtering of detected features (anova p-value ≤ 0.2), a PCA plot is generated. Figure 3.3.16 shows the PCA plot for all sample groups. The pink spots represent the T1DM new samples while the purple spots represent the control new samples, which are the matched controls for the T1DM new samples. While they didn't form distinctly separate clusters, the control new sample spots were clustered quite closely on the bottom right part of the PCA plot. The T1DM new sample spots, while not as closely clustered, were mainly located in the top left corner of the plot. The autoimmune/inflammatory disease serum specimens were represented by the cyan spots, these showed a very similar clustering pattern to the T1DM new samples. The T1DM old samples were represented by the blue spots while the control old samples, which are the matched controls for the T1DM old samples were represented by the orange spots. The T1DM old spots were mainly located in the right portion of the plot while the control old spots were located in the left of the plot. While each sample group did not result in the formation of distinctly separate clusters, each sample group clustered in a separate area of the plot. The loose filter criteria for peptide identification (anova p-value 0.2) would also contribute to the samples not clustering as tight as we would like, however, we did not want to apply too stringent criteria at this stage to exclude peptides from the analysis, as identified proteins would be filtered using more stringent criteria at a later stage.

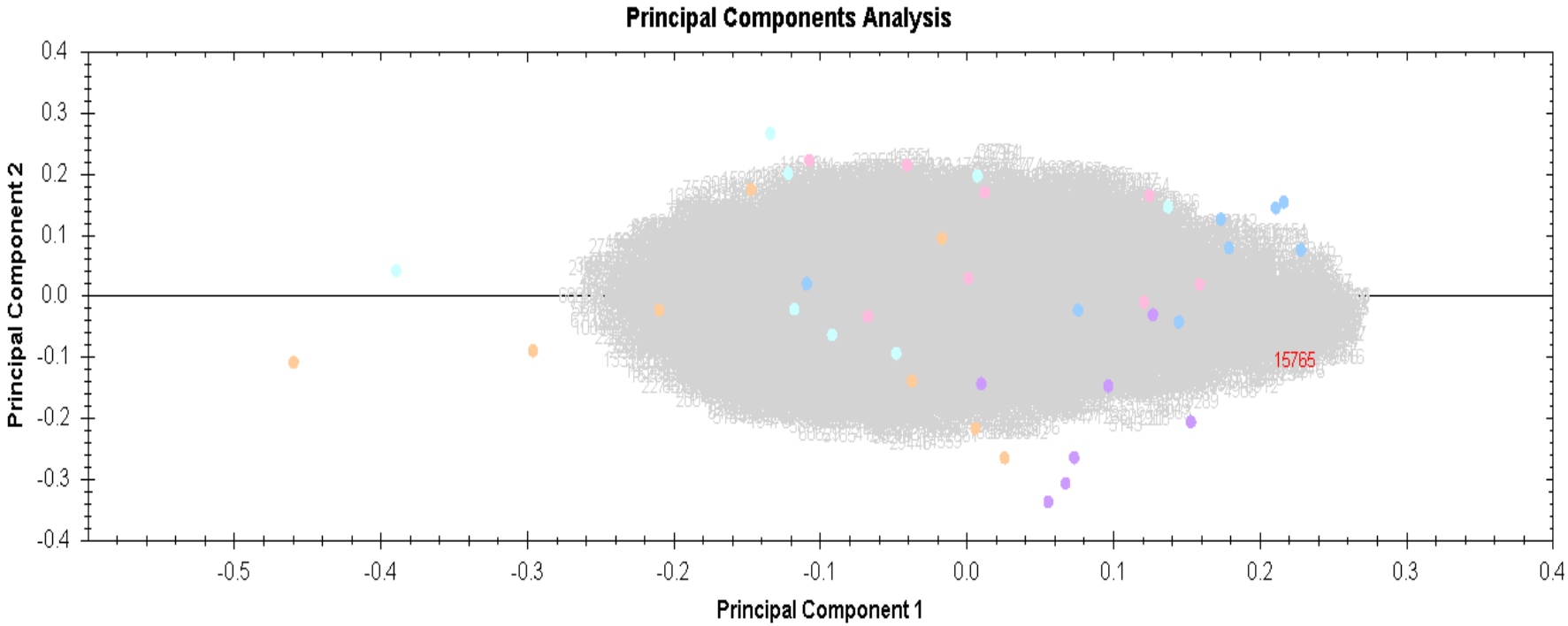

Figure 3.3.16 PCA plot for all sample groups. Pink spots represent T1DM new samples, blue spots represent T1DM old samples, purple spots represent control new samples, orange spots represent control old sample and the cyan spots represent the autoimmune samples.

3.3.2.5 Type 1 newly diagnosed (T1DM new) versus matched controls (control new)

Progenesis analysis was performed in triplicate for all comparisons analysed, using a different reference sample for each replicate. Samples with the highest number of detected features were chosen as reference samples. Therefore, 3 lists of differentially expressed proteins were generated for each comparison analysed (these lists are shown in appendix C). Proteins common to all three lists were then identified, and reported in the results section.

For the T1DM new versus control new comparison, the first replicate was performed with a T1DM new sample (DS-169) as reference sample, the second replicate with a control new sample (DS- 175) and the third replicate with another control new sample (DS-178). A PCA plot was generated for each analysis performed. The PCA plot is used to determine if the data clusters according to the experimental conditions. Figures 3.3.17 shows a very clear distinction between the T1DM new and control new sample clusters, T1DM new samples are shown in pink, while the control new samples are shown in blue. DS sample codes used in this study are identifier codes given to serum specimens as the volunteers are recruited, to avoid using patient names to identify individual specimens.

A list of differentially expressed proteins was also generated for each replicate analysis performed (see appendix C, table 1, 2 and 3). Proteins that were common to all three lists are identified in table 3.3.6, these included the proteins complement C5, clusterin, inter-alpha-trypsin inhibitor heavy chain H3, c-reactive protein, POTE ankyrin domain family member E and beta-actin-like protein 3.

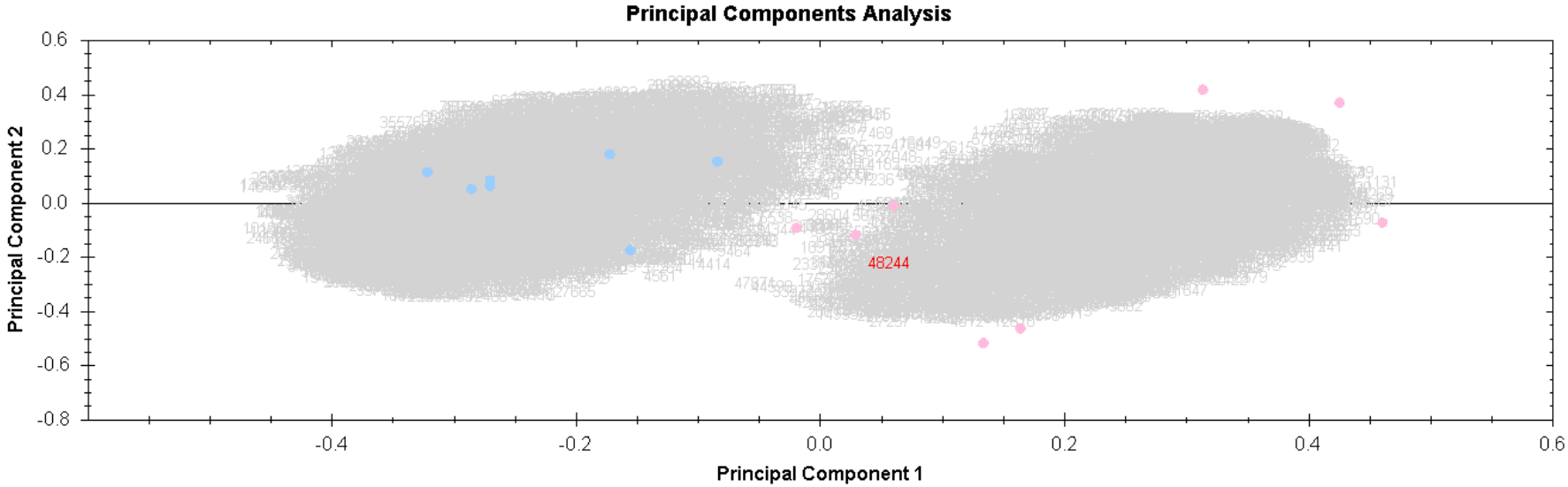

Figure 3.3.17 PCA plot for T1DM new and control new samples. DS-175 control new sample was used as reference run. Pink spots indicate the T1DM new samples while the blue spots indicate the control new samples.

						Average Normalised Abundances	
Accession	**Description**	**Reference run used**	**Fold**	**Anova (p)**	**peptides**	**T1DM new**	**Control New**
P01031	**Complement C5**	DS-169	+1.65	0.03	20	1.88E+006	1.14E+006
		DS-175	+1.74	0.004	20	2.24E+006	1.28E+006
		DS-178	+1.63	0.04	9	4.70E+005	2.88E+005
P10909	**Clusterin**	DS-169	+1.72	0.04	13	1.78E+007	1.03E+007
		DS-175	+1.68	0.01	12	2.68E+007	1.59E+007
		DS-178	+1.57	0.02	4	8.49E+005	5.41E+005
Q06033	**Inter-alpha-trypsin inhibitor heavy chain H3**	DS-169	+2.43	0.01	3	9.40E+004	3.88E+004
		DS-175	+2.7	0.007	5	1.53E+005	5.66E+004
		DS-178	+2.5	0.02	2	8.37E+004	3.34E+004
P02741	**C-reactive protein**	DS-169	+6.09	0.02	6	1.22E+006	2.00E+005
		DS-175	+6.22	0.01	4	1.24E+006	1.99E+005
		DS-178	+8.05	0.02	4	4.21E+005	5.23E+004
Q6S8J3	**POTE ankyrin domain family member E**	DS-169	-1.97	0.02	3	5.39E+004	1.06E+005
		DS-175	-1.92	0.03	2	6.34E+004	1.22E+005
		DS-178	-2.02	0.03	3	6.91E+004	1.40E+005
Q9BYX7	**Beta-actin-like protein 3**	DS-169	-1.98	0.02	2	4.86E+004	9.63E+004
		DS-175	-1.92	0.03	2	6.34E+004	1.22E+005
		DS-178	-2.03	0.03	2	6.31E+004	1.28E+005

Table 3.3.6 Proteins differentially expressed in T1DM new compared to control new samples.

3.3.2.6 Type 1 diabetes with established disease (T1DM old) versus matched controls (control old)

The analysis of these groups was performed in triplicate using a different reference sample for each replicate. The first replicate was performed with a T1DM old sample (DS-84) as reference sample, the second replicate with a control old sample (DS- 162) and the third replicate with another control old sample (DS-39) as reference sample. A PCA plot was generated (figure 3.3.18), showing two distinct clusters, however one of the T1DM old samples (pink) clustered with the control old samples (blue), rather than with the other T1DM old samples.

A list of differentially expressed proteins was also generated for each replicate analysis performed (see appendix C, table 4, 5 and 6). Proteins that were common to all three lists were identified in table 3.3.7, these included the proteins antithrombin III, apolipoprotein E, apolipoprotein C-II, vitronectin, ficolin-2, ceruloplasmin, vitamin K-dependent protein S, apolipoprotein A-1, transthyretin, C4b binding protein alpha chain, serum amyloid A-4 protein, mannan-binding lectin serine protease 1, apolipoprotein L1, platelet factor 4, apolipoprotein C-IV, von willebrand factor, complement component C8 beta chain, actin- cytoplasmic 2, complement factor H related protein 1, POTE ankyrin domain family member E and beta-actin-like protein 3.

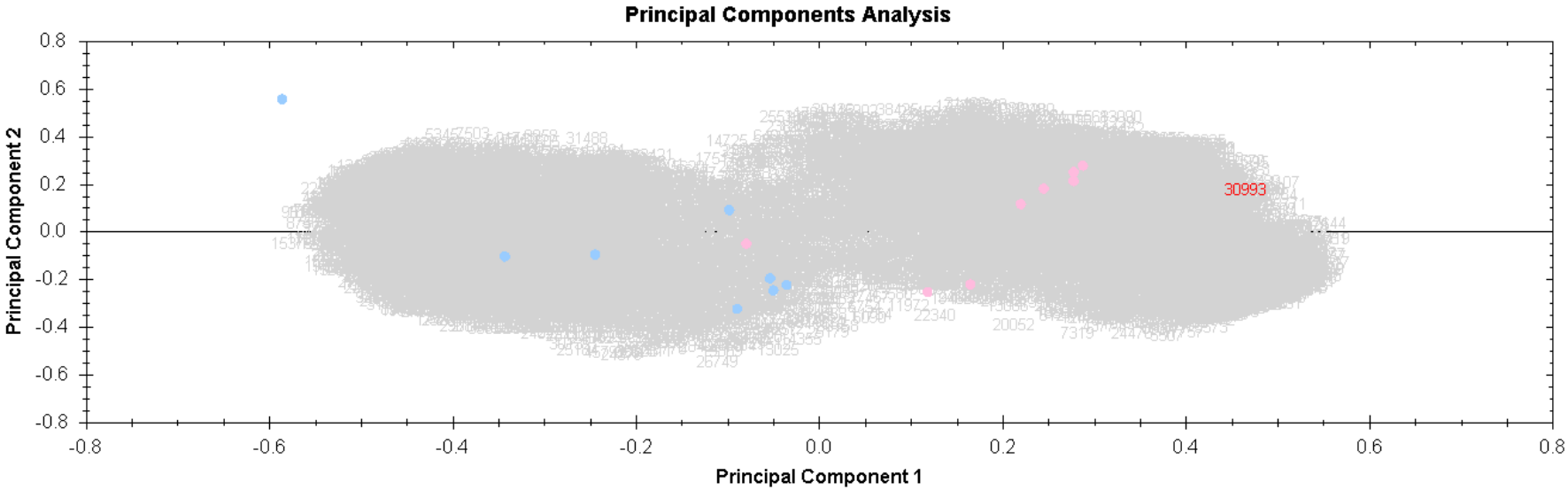

Figure 3.3.18 PCA plot for T1DM old and control old samples. DS-84 T1DM old sample was used as reference run. Pink spots indicate the T1DM old samples while the blue spots indicate the control old samples.

						Average Normalised Abundances	
Accession	**Description**	**Reference run used**	**Fold**	**Anova (p)**	**peptides**	**T1DM old**	**Control old**
P01008	**Antithrombin-III**	DS-84	-2.55	0.05	18	6.43E+007	1.64E+008
		DS-162	-2.31	0.03	17	3.15E+007	7.27E+007
		DS-39	-2.37	0.03	16	2.79E+007	6.63E+007
P02649	**Apolipoprotein E**	DS-84	-2.19	0.02	12	1.46E+007	3.20E+007
		DS-162	-2.05	0.02	15	1.07E+007	2.19E+007
		DS-39	-2.05	0.02	15	1.05E+007	2.16E+007
P02655	**Apolipoprotein C-II**	DS-84	-2.41	0.01	4	4.06E+006	9.79E+006
		DS-162	-2.25	0.01	5	3.13E+006	7.05E+006
		DS-39	-2.5	0.007	5	2.76E+006	6.88E+006
P04004	**Vitronectin**	DS-84	-1.72	0.03	5	2.55E+007	4.39E+007
		DS-162	-1.62	0.03	5	1.71E+007	2.77E+007
		DS-39	-1.57	0.03	6	1.76E+007	2.77E+007
Q15485	**Ficolin-2**	DS-84	-3	0.02	5	5.81E+005	1.75E+006
		DS-162	-2.81	0.02	7	4.37E+005	1.23E+006
		DS-39	-2.88	0.02	6	4.10E+005	1.18E+006
P00450	**Ceruloplasmin**	DS-84	+1.7	0.03	6	5.53E+005	3.25E+005
		DS-162	+1.44	0.04	8	4.51E+005	3.13E+005

		DS-39	+1.6	0.03	7	5.17E+005	3.23E+005
P07225	**Vitamin K-dependent protein S**	DS-84	-2.47	0.05	7	1.52E+006	3.75E+006
		DS-162	-2.13	0.006	4	4.03E+005	8.59E+005
		DS-39	-2.24	0.005	6	4.03E+005	9.04E+005
P02647	**Apolipoprotein A-I**	DS-84	-1.9	0.05	5	2.66E+007	5.06E+007
		DS-162	-1.76	0.04	4	1.99E+007	3.50E+007
		DS-39	-1.75	0.05	5	1.96E+007	3.44E+007
P02766	**Transthyretin**	DS-84	-2.69	0.04	4	2.14E+006	5.74E+006
		DS-162	-2.39	0.03	3	1.63E+006	3.91E+006
		DS-39	-2.46	0.04	3	1.51E+006	3.71E+006
P04003	**C4b-binding protein alpha chain**	DS-84	-2.62	0.04	3	5.67E+006	1.49E+007
		DS-162	-2.39	0.03	3	4.23E+006	1.01E+007
		DS-39	-2.4	0.03	4	4.16E+006	9.97E+006
P35542	**Serum amyloid A-4 protein**	DS-84	-2.34	0.02	2	8.40E+005	1.97E+006
		DS-162	-2.25	0.02	2	5.16E+005	1.16E+006
		DS-39	-2.37	0.01	3	5.00E+005	1.19E+006
P48740	**Mannan-binding lectin serine protease 1**	DS-84	-1.97	0.005	4	4.04E+005	7.95E+005
		DS-162	-1.95	0.002	4	2.82E+005	5.49E+005
		DS-39	-1.91	0.002	4	2.79E+005	5.35E+005

O14791	**Apolipoprotein L1**	DS-84	-4.07	0.003	2	7.27E+004	2.96E+005
		DS-162	-2.44	0.03	3	7.75E+004	1.89E+005
		DS-39	-2	0.02	3	1.25E+005	2.49E+005
P02776	**Platelet factor 4**	DS-84	-2.1	0.05	2	7.12E+005	1.49E+006
		DS-162	-1.98	0.05	2	5.30E+005	1.05E+006
		DS-39	-1.97	0.05	2	5.22E+005	1.03E+006
P63261	**Actin, cytoplasmic 2**	DS-84	-3.42	0.03	4	1.28E+005	4.38E+005
		DS-162	-3.14	0.02	4	1.45E+005	4.56E+005
		DS-39	-3.09	0.03	4	1.52E+005	4.71E+005
Q9BYX7	**Beta-actin-like protein 3**	DS-84	-3.99	0.01	3	6.77E+004	2.70E+005
		DS-162	-3.72	0.009	3	4.79E+004	1.78E+005
		DS-39	-3.63	0.02	3	5.17E+004	1.88E+005
Q6S8J3	**POTE ankyrin domain family member E**	DS-84	-3.99	0.01	3	6.77E+004	2.70E+005
		DS-162	-3.72	0.009	3	4.79E+004	1.78E+005
		DS-39	-3.63	0.02	3	5.17E+004	1.88E+005
P55056	**Apolipoprotein C-IV**	DS-84	-2.9	0.02	2	5.04E+004	1.46E+005
		DS-162	-3.53	0.003	2	2.86E+004	1.01E+005
		DS-39	-3.03	0.004	2	3.58E+004	1.08E+005
P04275	**von Willebrand factor**	DS-84	-4.42	0.02	2	1.76E+004	7.80E+004
		DS-162	-3.51	0.01	2	1.67E+004	5.87E+004
		DS-39	-3.9	0.01	2	1.41E+004	5.50E+004

Q03591	**Complement factor H-related protein 1**	DS-84	-1.88	0.006	3	2.30E+006	4.34E+006
		DS-162	-1.74	0.02	3	1.42E+006	2.47E+006
		DS-39	-1.74	0.03	2	1.34E+006	2.33E+006
P07358	**Complement component C8 beta chain**	DS-84	+1.46	0.01	3	8.24E+004	5.64E+004
		DS-162	+1.86	0.001	2	6.35E+004	3.41E+004
		DS-39	+1.91	0.00005	2	6.34E+004	3.31E+004

Table 3.3.7 Proteins differentially expressed in T1DM old compared to control old samples.

3.3.2.7 Type 1 newly diagnosed (T1DM new) versus type 1 diabetes with established disease (T1DM old)

The analysis of this comparison was performed in triplicate using a different reference sample for each replicate. The first replicate was performed with a T1DM new sample (DS-169) as reference sample, the second replicate with a T1DM old sample (DS-74) and the third replicate with another T1DM old sample (DS-90). A PCA plot was generated for this comparison (figure 3.3.19), showing two distinct clusters, however one of the T1DM old sample- DS-29 (blue) clustered slightly closer to the T1DM new (pink), rather than with the other T1DM old samples.

A list of differentially expressed proteins was also generated for each replicate analysis performed (see appendix C, table 7, 8 and 9). Proteins that were common to all three lists were identified in table 3.3.8, these included the proteins complement C4-B, prothrombin, clusterin, Ig mu chain C region, antithrombin III, Ig kappa chain C region, vitronectin, vitamin K-dependent protein and apolipoprotein C-1.

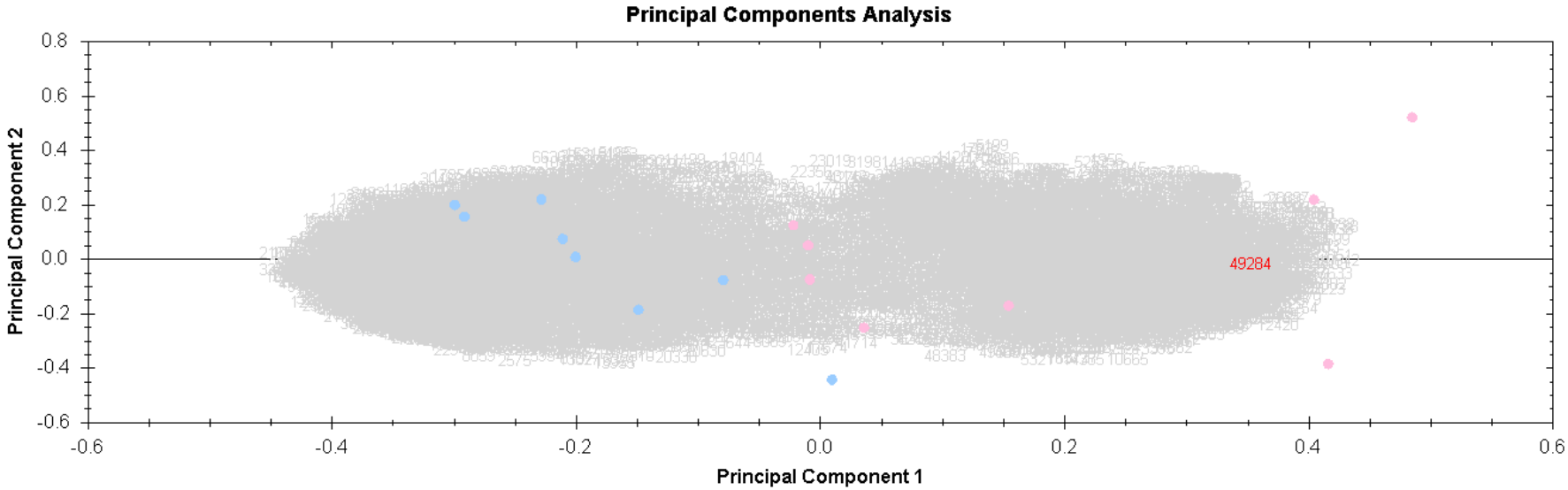

Figure 3.3.19 PCA plot for T1DM new and T1DM old. DS-169 control sample was used as reference run. Pink spots indicate the T1DM new samples while the blue spots indicate the T1DM old samples.

						Average Normalised Abundances	
Accession	**Description**	**Reference run used**	**Fold**	**Anova (p)**	**Peptides**	**T1DM new**	**T1DM old**
P0C0L5	**Complement C4-B**	DS-169	+1.35	0.02	47	1.11E+08	8.23E+07
		DS-74	+1.45	0.01	46	1.56E+08	1.08E+08
		DS-90	+1.48	0.01	44	1.62E+08	1.09E+08
P00734	**Prothrombin**	DS-169	+1.39	0.05	19	3.08E+07	2.22E+07
		DS-74	+1.4	0.05	15	4.57E+07	3.27E+07
		DS-90	+1.42	0.03	17	4.69E+07	3.31E+07
P10909	**Clusterin**	DS-169	+1.43	0.005	7	2.10E+07	1.47E+07
		DS-74	+1.42	0.003	9	3.31E+07	2.34E+07
		DS-90	+1.45	0.003	10	3.35E+07	2.31E+07
P01871	**Ig mu chain C region**	DS-169	+1.57	0.04	4	6.61E+06	4.21E+06
		DS-74	+1.57	0.04	5	1.26E+07	8.04E+06
		DS-90	+1.55	0.03	6	1.43E+07	9.25E+06
P01008	**Antithrombin-III**	DS-169	+1.44	0.006	10	2.35E+07	1.63E+07
		DS-74	+1.43	0.01	13	3.12E+07	2.18E+07
		DS-90	+1.46	0.007	13	4.18E+07	2.87E+07
P01834	**Ig kappa chain C region**	DS-169	+1.54	0.03	4	6.15E+06	4.00E+06
		DS-74	+1.55	0.02	5	9.42E+06	6.07E+06
		DS-90	+1.58	0.02	4	9.56E+06	6.06E+06

P04004	**Vitronectin**	DS-169	+1.45	0.03	4	1.72E+07	1.18E+07
		DS-74	+1.46	0.03	5	2.57E+07	1.76E+07
		DS-90	+1.42	0.03	4	3.39E+07	2.38E+07
P07225	**Vitamin K-dependent protein S**	DS-169	+1.71	0.007	4	6.27E+05	3.67E+05
		DS-74	+1.49	0.0009	5	6.24E+05	4.18E+05
		DS-90	+2.2	0.003	2	6.16E+05	2.80E+05
P02654	**Apolipoprotein C-I**	DS-169	+1.55	0.004	4	2.59E+06	1.67E+06
		DS-74	+1.56	0.002	2	3.78E+06	2.42E+06
		DS-90	+1.59	0.002	3	3.88E+06	2.45E+06

Table 3.3.8 Proteins differentially expressed in T1DM new compared to T1DM old.

3.3.2.8 Target protein selection for follow up

Proteins for follow up were selected based on their potential interest in both the T1DM new and T1DM old studies. Clusterin was identified as being up-regulated in T1DM new samples relative to T1DM old (table 3.3.8) and control new samples (table 3.3.6). Vitronectin was down-regulated in T1DM old samples relative to T1DM new (table 3.3.8) and control old (table 3.3.7). Vitronectin was also up-regulated in two of the three replicates for T1DM new versus control new comparison (appendix C, table 1 and 2). Vitamin K-dependent protein S levels showed the same pattern as vitronectin. This protein was down regulated in T1DM old samples relative to T1DM new (table 3.3.8) and control old samples (table 3.3.7), it was also up-regulated in two of the three replicate comparisons of T1DM new versus control new samples (appendix C, table 1 and 2). Apolipoprotein L1 was down-regulated in T1DM old relative to control old samples (table 3.3.6), while it was also down-regulated in one of the replicates for T1DM old versus T1DM new comparisons (appendix C, table 9).

These proteins were also selected on the basis that they had no conflicting identified peptides. Conflicting peptides are peptides that are not unique to the named protein, and may be present in a number of other different proteins. Performing each comparison in triplicate with different reference samples, as well as assigning filter criteria of anova p-value less than 0.05 and proteins with no conflicting peptides allowed identification of the most robustly changed proteins in the samples analysed. Using these criteria, clusterin, vitronectin, apolipoprotein L1 and vitamin K-dependent protein S were selected for follow up validation in a larger cohort of patient samples.

Control new and control old samples were compared to determine if protein changes seen in disease versus control samples were related to disease phenotype or were related to control samples used. A PCA plot of control new and control old samples was generated (appendix C, figure 1), this indicated that DS-7 was a slight outlier for the control old group. Differentially expressed protein lists were generated with and without the DS-7 outlier sample (appendix C, table 10, 11 and 12). Apolipoprotein L1 and vitronectin were unchanged in the control old versus the control new comparison, with and without outlier DS-7 sample included in analysis. This indicates that changing

levels of these proteins are due to the disease phenotype. Clusterin and vitamin K-dependent protein S were seen to be up-regulated in the control old samples relative to the control new samples in comparisons with and without outlier sample DS-7 (appendix C, table 10, 11 and 12). However, as these proteins were also identified as being differentially expressed in the T1DM new versus T1DM old comparison (table 3.3.8), therefore their differential expression is not alone due to the control samples being used.

Protein changes between autoimmune (n=8) and control samples (n=16) were also analysed, to determine if protein targets identified in the T1DM study were specifically type 1 diabetes related, or if they were general autoimmune or inflammation related proteins. Three lists of differentially expressed proteins were generated for autoimmune versus control sample comparison, using control samples DS-175, DS-178 and DS-39 as reference run, complete lists shown in appendix C, table 13, 14 and 15. No changes in vitronectin, clusterin or vitamin K-dependent protein S were seen in any of the autoimmune versus control comparisons, indicating that changes in these protein levels in the T1DM study were specifically diabetes related. One of the three comparisons (appendix C, table 14) showed decreased levels of apolipoprotein L1 in autoimmune samples. Therefore, it is possible that decreased levels of apolipoprotein L1 in T1DM old samples could be related to a general autoimmune or inflammatory response. However, as apolipoprotein L1 were increased in T1DM new samples, this protein for selected for validation studies.

3.3.2.9 ELISA validation of target proteins

Protein targets identified in label-free LC-MS study were validated using ELISA technology. Validation was performed on the same 8 T1DM new, T1DM old and control samples which were used in the label-free study, as well as an additional 22 T1DM old and control old samples.

3.3.2.9.1 Vitronectin

Vitronectin: T1DM new vs. control new

Label free proteomics analysis showed vitronectin levels to be significantly increased in T1DM new samples compared to controls by approximately 1.44 fold. An ELISA kit was sourced from American Diagnostica GmbH (catalogue number 803) for validation of this target protein (protocol outlined in section 2.6.1.1). ELISA detection of vitronectin in these same T1DM new and matched controls showed no change in vitronectin levels, with a fold change of 1.02 (figure 3.3.20). Looking at each individual matched pair separately (figure 3.3.21), vitronectin levels were higher in the T1DM new specimens in four of the eight matched pairs.

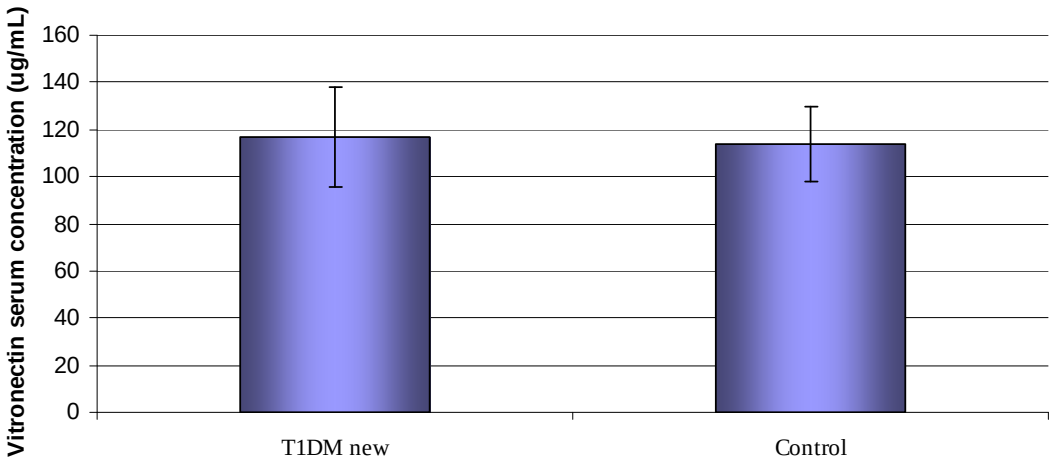

Figure 3.3.20 Average vitronectin serum concentration in T1DM new and control new specimens. Error bars indicate standard deviation.

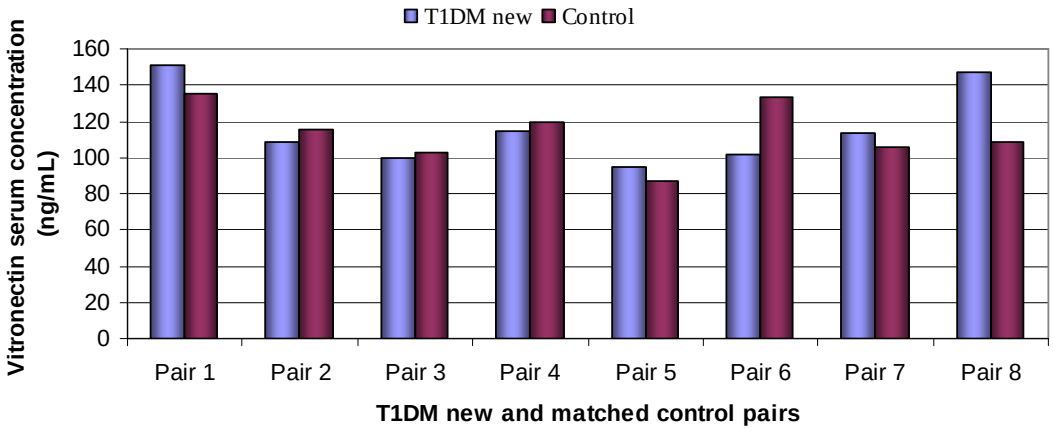

Figure 3.3.21 Vitronectin serum concentrations in 8 T1DM new and control new serum specimens.

Vitronectin: T1DM old vs. control old

In T1DM old compared to control old serum specimens, vitronectin was shown to be significantly reduced in the label free proteomic experiment by approximately 1.64 fold. Validation of this target was performed in a larger cohort of 30 T1DM old samples, including the samples used for the label free proteomics experiment. ELISA validation also showed reduced vitronectin levels (1.14 fold) in T1DM old samples compared to matched controls (figure 3.3.22). The student's t-test indicated that this reduction in vitronectin was significant with a p-value less than 0.05.

Looking at each individual matched pair, reduced vitronectin levels in T1DM old serum is seen in 23 of the 30 matched pairs (figure 3.3.23).

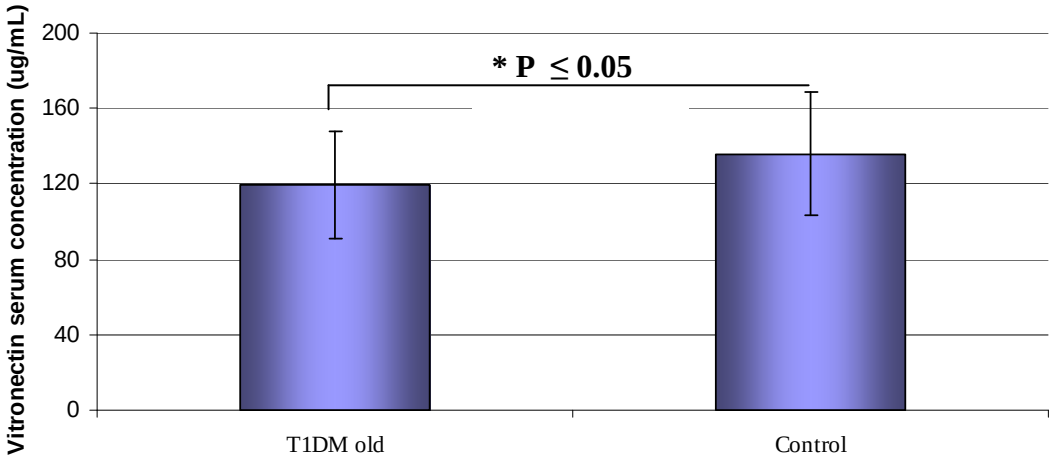

Figure 3.3.22 Average vitronectin serum concentrations in 30 T1DM old and 30 control old serum specimens. Error bars indicate standard deviation.

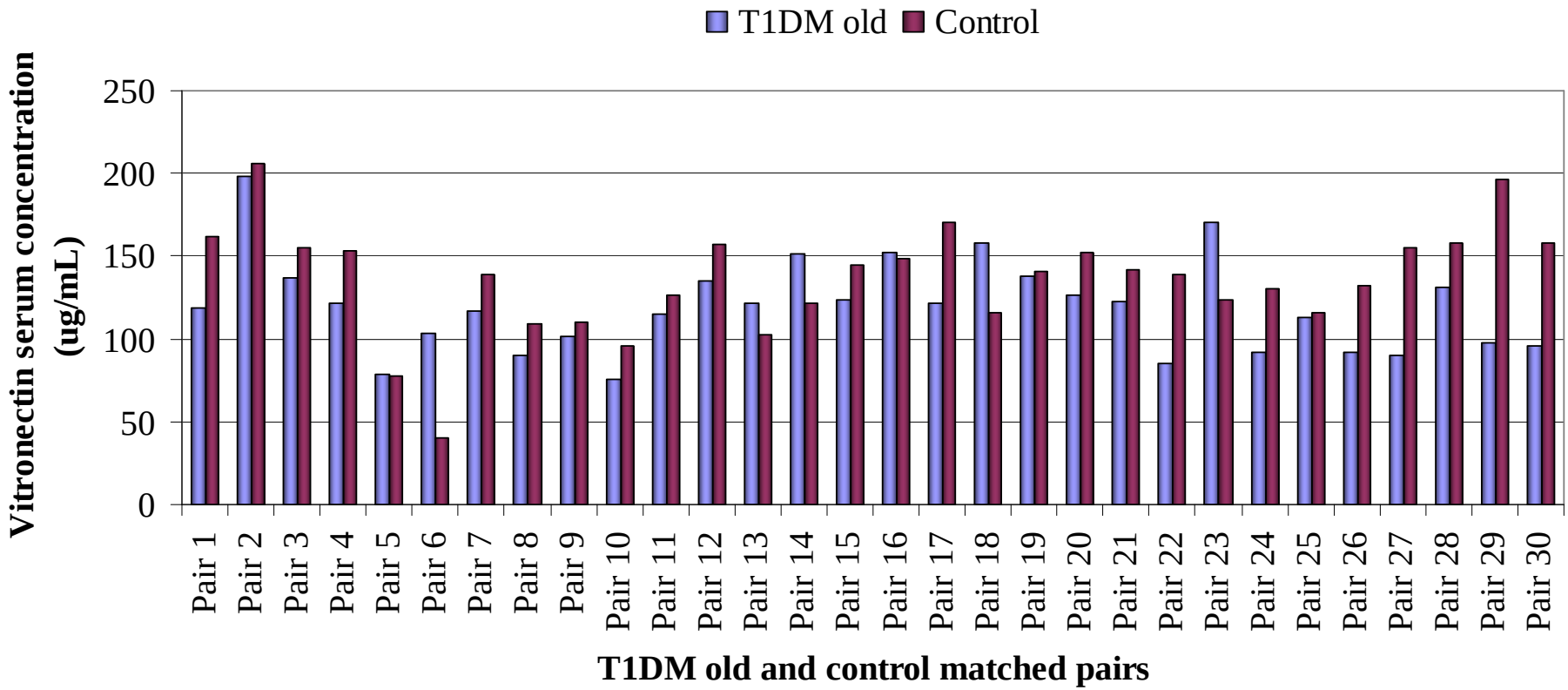

Figure 3.3.23 Vitronectin serum concentrations in 30 T1DM old and 30 matched control old serum specimens.

Vitronectin: T1DM new vs. T1DM old

In the label free proteomics experiment vitronectin levels were significantly decreased in T1DM old serum specimens compared to T1DM new specimens by approximately 1.44 fold. On expansion of the T1DM old sample cohort to 30 specimens vitronectin levels were unchanged (1.02 fold) in T1DM new and T1DM old serum specimens, according to ELISA quantification (figure 3.3.24).

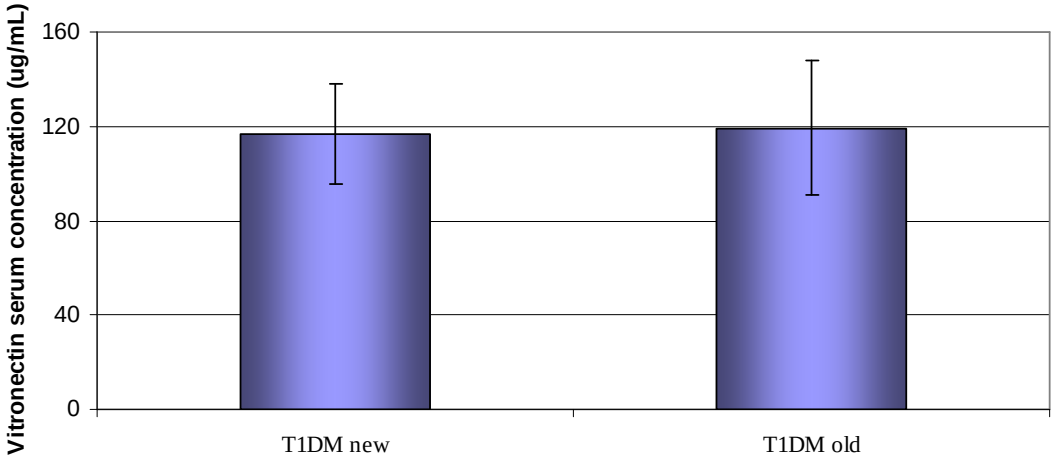

Figure 3.3.24 Average vitronectin serum concentration of T1DM new (n=8) and T1DM old (n=30) serum specimens. Error bars indicate standard deviation.

3.3.2.9.2 Clusterin

Clusterin: T1DM new vs. control new

Clusterin protein levels were found to be significantly up-regulated (1.66 fold) in T1DM new (n=8) versus control new samples (n=8) from the label free proteomics experiment. This target was validated using a clusterin ELISA sourced from phoenix pharmaceuticals (catalogue number EK-018-35) in the same T1DM new and control new serum specimens (protocol outlined in section 2.6.1.2); however, the same trend was not seen (figure 3.3.25). Looking at the ELISA results of each matched pair individually (figure 3.3.26), 6 of the 8 sets of matched pairs show reduced clusterin levels in T1DM new sample compared to control. The increased clusterin expression detected in the label-free experiment may have been skewed by the outlier T1DM new sample in pair 1 (figure 3.3.26), which shows almost double the level of clusterin compared to the other T1DM new samples analysed.

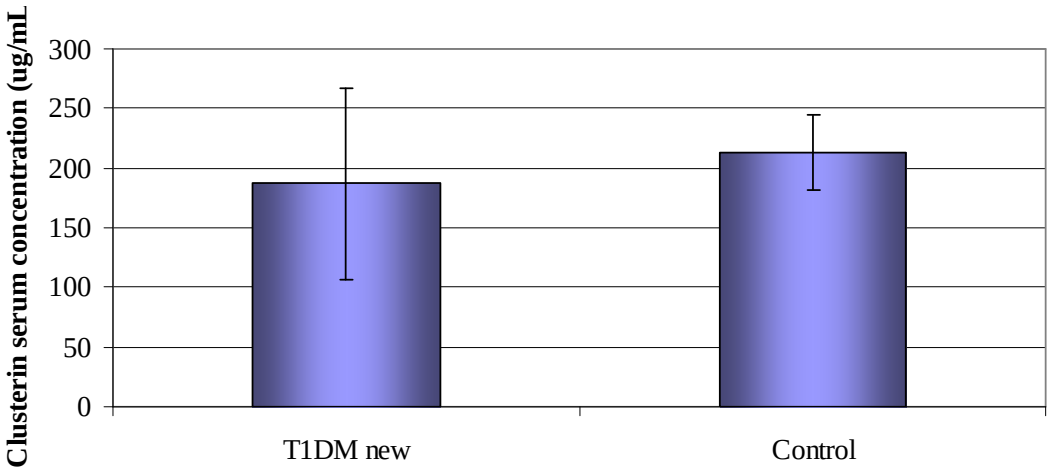

Figure 3.3.25 Average clusterin serum concentration of T1DM new (n=8) and control (n=8) serum specimens. Error bars indicate standard deviation.

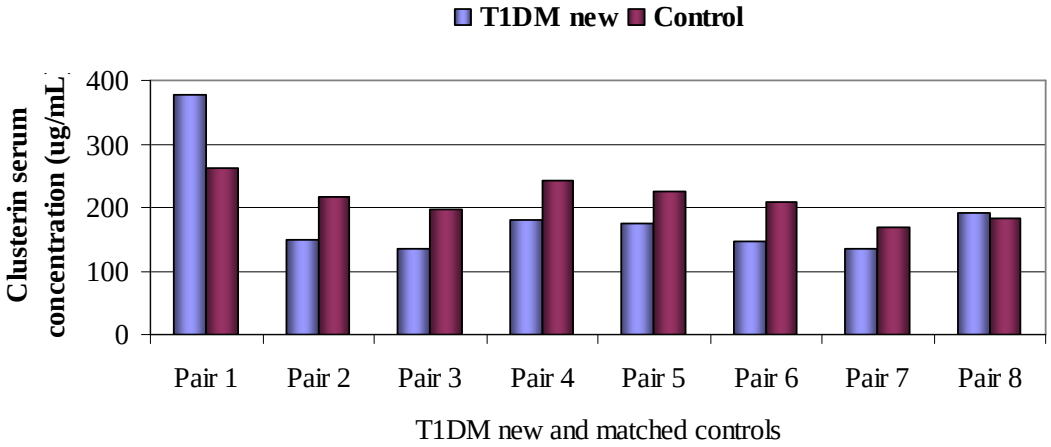

Figure 3.3.26 Clusterin serum concentrations of 8 T1DM new and matched control new serum specimens.

Clusterin: T1DM old vs control old

Clusterin levels were unchanged in T1DM old and control old samples from the label-free proteomics results. No change in expression level of this protein was seen when 30 T1DM old and 30 control samples were analysed (figure 3.3.27). Looking at the matched pairs individually (figure 3.3.28), large fluctuations in clusterin expression was seen in both control and T1DM old serum specimens. 16 of 30 matched pairs showed lower clusterin levels in T1DM old samples relative to control; with the remaining 14 pairs showing higher clusterin levels in the T1DM old samples (figure 3.3.28).

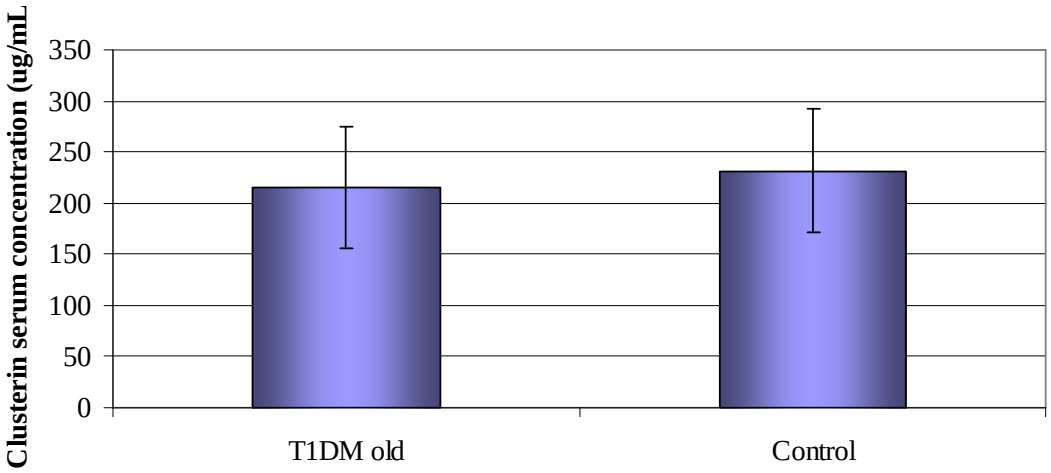

Figure 3.3.27 Average clusterin serum concentration of T1DM old (n=30) and control old (n=30) serum specimens. Error bars indicate standard deviation.

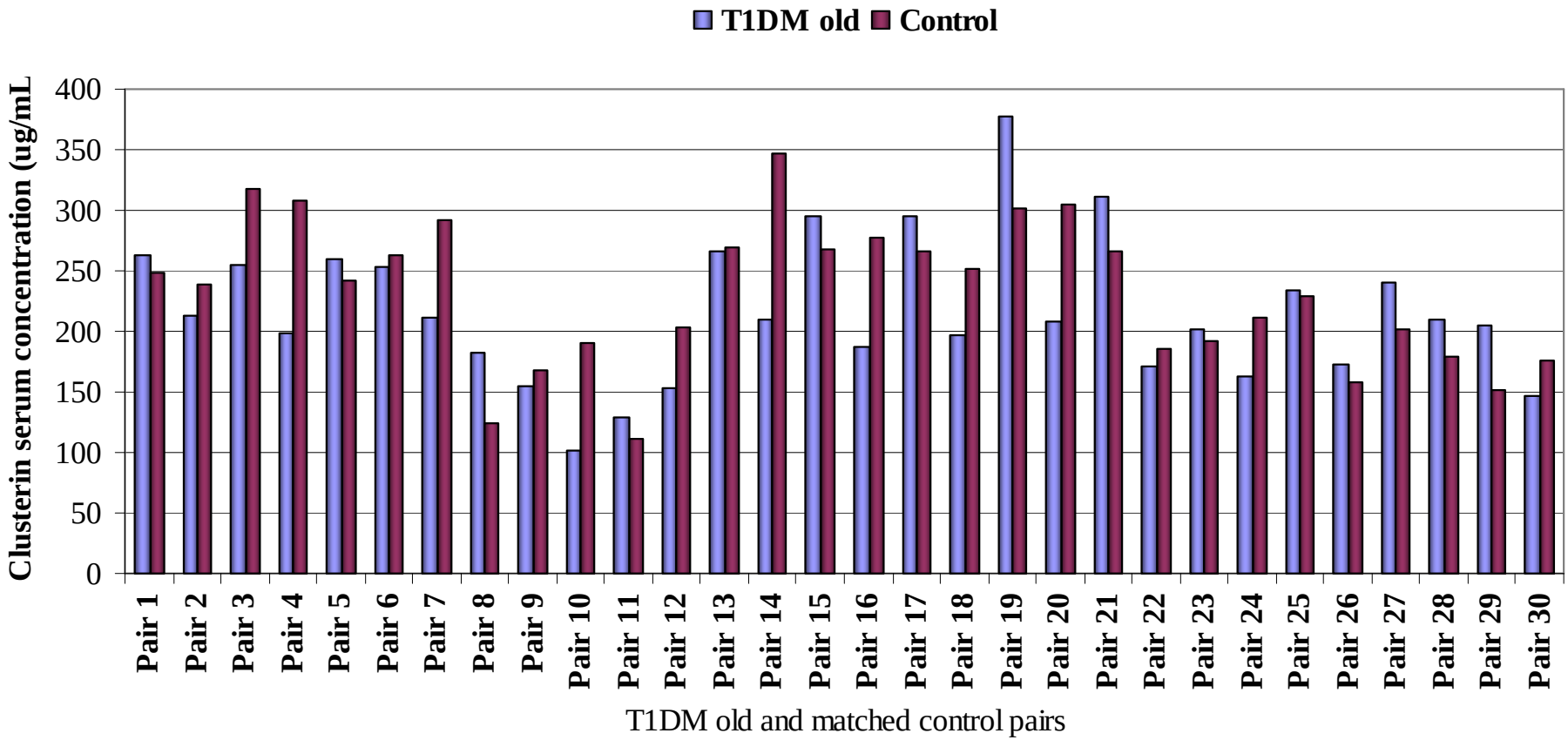

Figure 3.3.28 Clusterin serum concentrations in 30 T1DM old and 30 matched control old serum specimens.

Clusterin: T1DM old vs. T1DM new

Clusterin expression was significantly up-regulated by 1.43 fold in T1DM new samples relative to T1DM old samples according to the label-free proteomics analysis. However, validation of clusterin expression by ELISA in 30 T1DM old samples and the same 8 T1DM new samples used in the initial analysis showed no significant change in clusterin expression (figure 3.3.29).

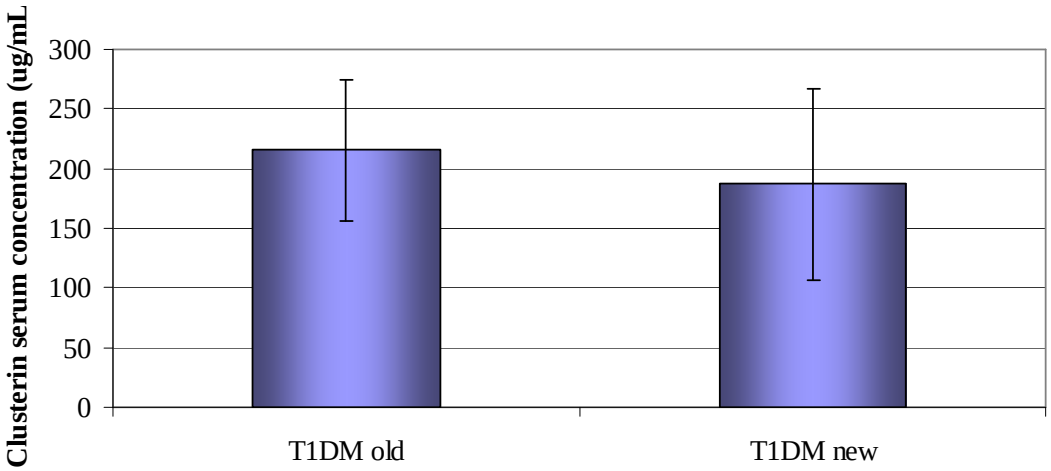

Figure 3.3.29 Average clusterin serum concentration of T1DM old (n=30) and T1DM new (n=8) serum specimens. Error bars indicate standard deviation.

3.3.2.9.3 Vitamin K-dependent protein S

Vitamin K-dependent protein S: T1DM new vs. control new

Vitamin K-dependent protein S was found to be significantly up-regulated in T1DM new serum compared to control new serum, by approximately 1.42 fold, from the label free proteomics experiment. An ELISA kit was sourced from USCN Life Science Inc. (catalogue number E1971h) for validation of this target protein (protocol outlined in section 2.6.1.3). On validation of this target protein using ELISA with the same T1DM new and control new samples, vitamin K-dependent protein S was seen to be significantly down-regulated in T1DM new samples by 1.24 fold (figure 3.3.30). Figure 3.3.31 shows the individual levels of vitamin K-dependent protein S in each of the matched pairs. Lower levels of vitamin K-dependent protein S are seen in T1DM new samples for 6 of the 8 matched pairs. One matched pair shows no change, while one pair shows higher vitamin K-dependent protein S levels in the T1DM new specimen.

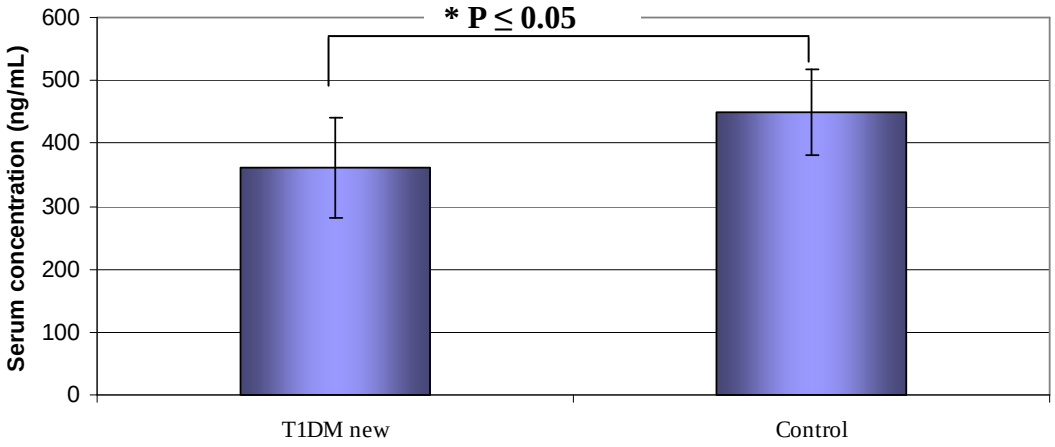

Figure 3.3.30 Average vitamin K-dependent protein S serum concentration in T1DM new (n=8) and control new (n=8) serum specimens. Error bars indicate standard deviation.

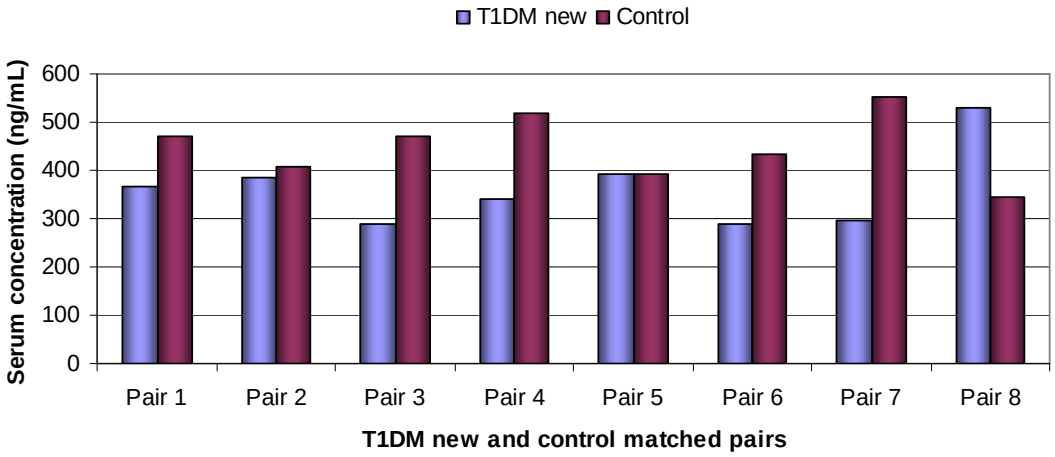

Figure 3.3.31 Vitamin K-dependent protein S serum concentration in T1DM new and matched control serum pairs.

Vitamin K-dependent protein S: T1DM old vs. control old

In T1DM old compared to control old label free proteomic analysis, vitamin K-dependent protein S was significantly down-regulated in T1DM old serum specimens by approximately 2.28 fold. ELISA validation of this target was performed using an expanded cohort of 30 T1DM old and 30 control old samples; however no significant change in vitamin K-dependent protein S levels were seen in these samples (figure 3.3.32). Looking at each matched pair individually (figure 3.3.33) no consistent change was seen in vitamin K-dependent protein S expression, this target was present at lower levels in T1DM old serum in 15 of the 30 matched pairs, higher levels in 14 of 30 matched pairs, and no change in one pair.

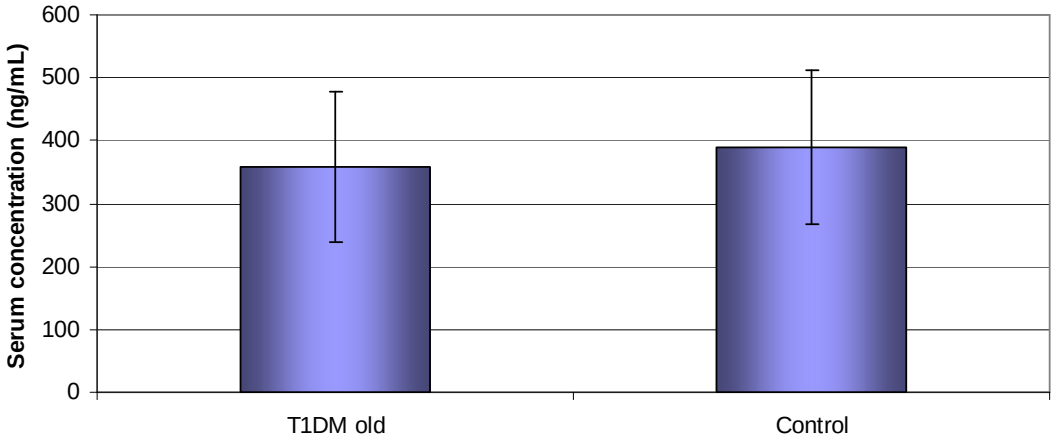

Figure 3.3.32 Average vitamin K-dependent protein S serum concentration of T1DM old (n=30) and control old (n=30) serum specimens. Error bars indicate standard deviation.

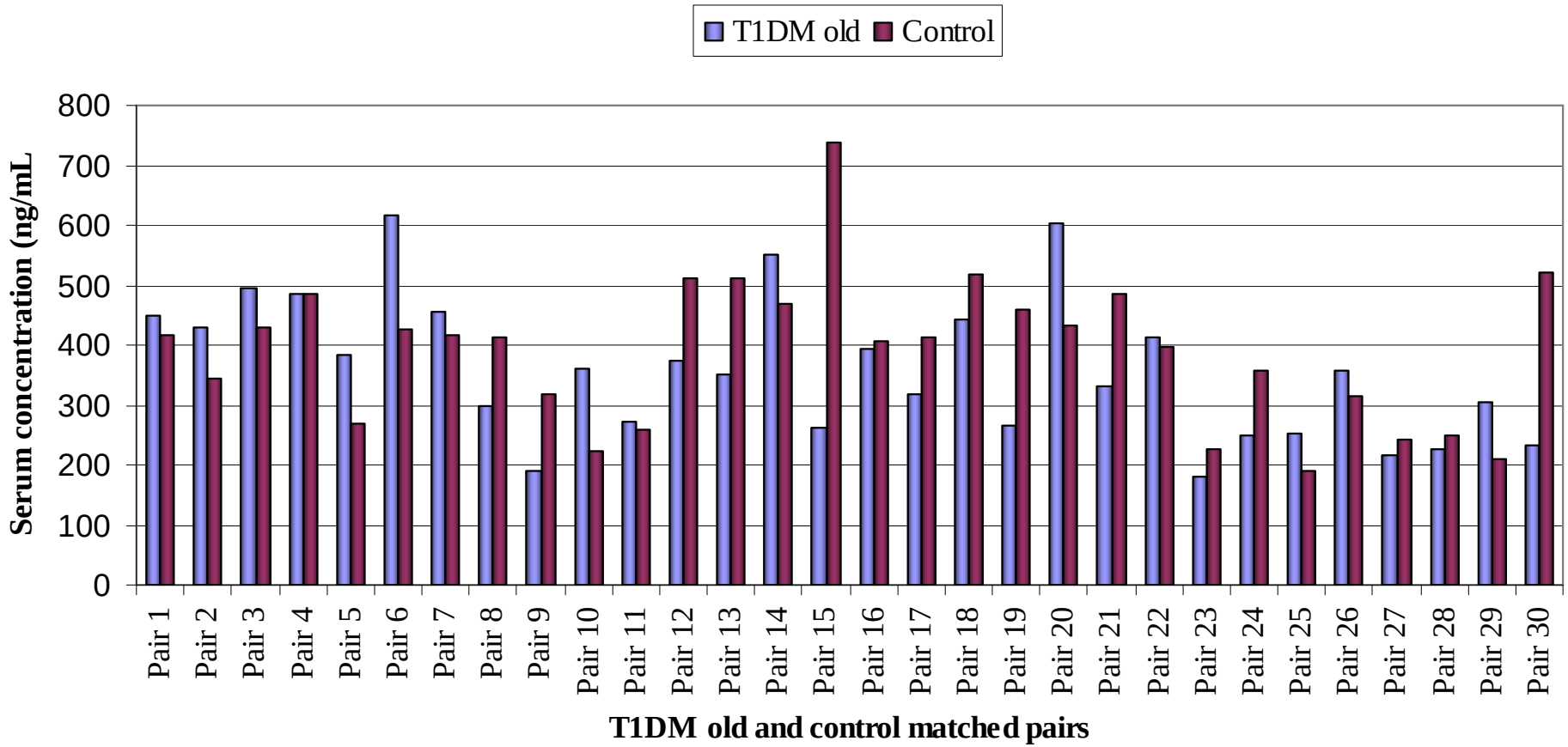

Figure 3.3.33 Vitamin K-dependent protein S serum concentration in individual matched pairs of T1DM old (n=30) and control old (n=30) serum specimens.

Vitamin K-dependent protein S: T1DM old vs. T1DM new

Label free proteomics analysis identified vitamin K-dependent protein S as being significantly up-regulated in T1DM new serum specimens compared to T1DM old. However, on expansion of the T1DM old cohort, ELISA quantification of vitamin K-dependent protein S found no significant change in levels of this target in T1DM new and old serum (figure 3.3.34).

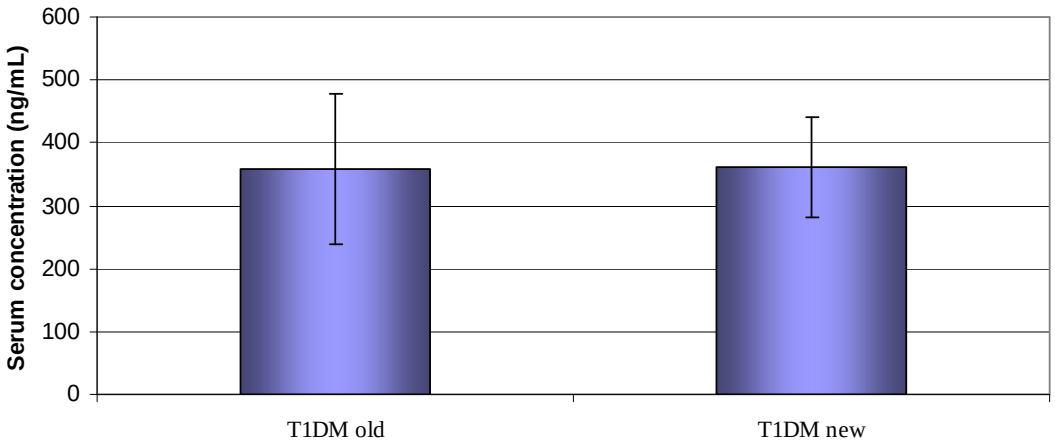

Figure 3.3.34 Average vitamin K-dependent protein S serum concentration in T1DM old (n=30) and T1DM new (n=8) serum specimens. Error bars indicate standard deviation.

3.3.2.9.4 Apolipoprotein L1

Label free proteomics analysis showed a significant 2.84 fold decrease in apolipoprotein L1 in T1DM old serum relative to control old serum, in addition to a 1.88 fold decrease when T1DM old specimens were compared to T1DM new specimens.

The human apolipoprotein L1 ELISA used for this validation study was sourced from USCN Life Science Inc. (catalogue number E9374Hu), however no suggested serum dilutions were included in this kit. Therefore, an apolipoprotein L1 concentration estimation was performed using two serum samples (T1DM old sample DS-100 and T1DM new sample DS-170), and three dilutions of each sample, at 1:10, 1:500 and 1:5,000, as well as the lowest and highest points of the standard curve. The apolipoprotein L1 ELISA used for this experiment is based on a sandwich ELISA technique (protocol outlined in section 2.6.1.4), therefore higher concentrations of apolipoprotein L1 should lead to high absorbance readings at 450nm. For each sample analysed, the 1:10 dilution showed the highest absorbance, with a lower absorbance reading for the 1:500 dilutions, as expected. However, absorbance readings for 1:5,000 dilutions showed higher absorbance reading than the 1:500 dilutions for both samples tested (table 3.3.9). As the lowest dilution (1:10) absorbance readings were only marginally above the lowest standard curve reading, therefore a 1:5 dilution was chosen to perform ELISA on all remaining samples.

Sample	Absorbance
1.25ng/mL standard	0.21
80ng/mL standard	Too high
DS-100 1:10 dilution	0.349
DS-100 1:500 dilution	0.120
DS-100 1:5000 dilution	0.262
DS-170 1:10 dilution	0.297
DS-170 1:500 dilution	0.138
DS-170 1:5000 dilution	0.251

Table 3.3.9 Apolipoprotein L1 serum concentration estimation. Absorbance values measured at 450nm for two serum samples (DS-100 and DS-170), serially diluted to 1:10, 1:500 and 1:5000.

8 T1DM new and controls, as well as 30 T1DM old and matched control samples were diluted 1:5 before performing the apolipoprotein L1 ELISA. All sample absorbances were below the lowest point on the standard curve, therefore apolipoprotein L1 concentrations could not be deduced. DS-100 and DS-170 samples which were used for the concentration estimation were also diluted 1:5 and assayed again with all other samples. However, the absorbance reading was lower than the lowest point on the standard curve for DS-170, and the DS-100 absorbance reading was lower than the blank absorbance reading of the standard diluent solution.

The low absorbance readings of serum samples may indicate that apolipoprotein L1 levels were beyond the level of detection, however, as more dilute samples showed higher absorbance readings during the concentration estimate, this may indicate that these pre-coated ELISA plates may not have been uniformly coated with the anti-apolipoprotein L1 capture antibody.

3.3.2.10 Summary of proteomic biomarker study

Label-free proteomics and ELISA validation results for each target analysed are shown in table 3.3.10. Only two comparisons reached statistical significance when validated using ELISA technology, 1) vitamin K-dependent protein S, in the T1DM new versus control comparison, and 2) vitronectin, in the T1DM old versus control comparison.

	T1DM new vs control new		T1DM old vs control old		T1DM new vs T1DM old	
	Proteomics (n=8)	**ELISA (n=8)**	**Proteomics (n=8)**	**ELISA (n=30)**	**Proteomics (n=8)**	**ELISA (T1DM new=8, T1DM old=30)**
Vitronectin	1.45 fold up in T1DM new (2/3)	No change	1.64 fold down in T1DM old	**1.14 fold down in T1DM old (significant)**	1.44 fold up in T1DM new	No change
Clusterin	1.66 fold up in T1DM new	No change	No change	No change	1.43 fold up in T1DM new	No change
Vitamin K-dependent protein S	1.42 fold up in T1DM new (2/3)	**1.24 fold down in T1DM new (significant)**	2.28 fold down in T1DM old	No change	1.80 fold up in T1DM new	No change
Apolipoprotein L1	No change	Un-measurable	2.84 fold down in T1DM old	Un-measurable	1.88 fold up in T1DM new (1/3)	Un-measurable

Table 3.3.10 Changes in target protein levels according to label-free proteomic analysis and ELISA validation

3.3.3 Metabolomic profiling of type 1 diabetes serum

Metabolomics is the study of all metabolites in an organism and how they change in relation to a biological perturbation. In comparison to other 'omics' technologies metabolomics provides the added advantage of not only taking into account genetics, but also the effects of lifestyle, diet and environment of the individual being analysed. The Human Metabolome Database (HMDB) is an electronic database containing information on all known small molecule metabolites in the human body (Wishart, Knox et al. 2009). Currently, HMDB contains information on over 7,900 metabolites.

Metabolites can vary greatly in their physical properties, as of yet no single technique is capable of detecting and quantifying such a diverse range of compounds. The diagnostic company Metabolon incorporate three independent analysis platforms in their procedure for metabolite profiling, in order to get maximum separation of the different types of biochemicals present in the samples. Two separate ultra-high performance liquid chromatography / tandem mass spectrometry (UHPLC/MS/MS) injections and one GC/MS injection are performed per sample. One UHPLC/MS/MS injection was optimised for detection of positive ions while the second injection was optimised for negative ion detection. While the GC/MS platform allows for better separation of carbohydrates which are difficult to detect with LC methods.

Two types of metabolomic analysis exist, targeted and non-targeted. Targeted approaches allow for highly sensitive metabolite detection, over a wide dynamic range. However, only metabolites which are targeted for detection will be profiled; hence, unknown biochemicals of potential biological relevance may be missed. The non-targeted approach employed by Metabolon allows detection of all small molecules present in the sample being analysed, compound characteristics are then compared against Metabolon's proprietary library of chemical standards. This platform also allows for detection of new metabolites not yet documented in the reference library. Therefore, non-targeted metabolomic profiling allows the greatest biochemical coverage for analysis of the human metabolome (Evans, DeHaven et al. 2009).

This study aimed to identify small molecule biomarkers in newly diagnosed type 1 diabetes serum specimens, to potentially aid in early diagnosis of type 1 diabetes. It is generally believed that by the time of diagnosis of type 1 diabetes, up to 90% of pancreatic beta cells exhibit either impaired beta cell function or have undergone apoptosis as a result of autoimmune mediated attack (Matveyenko and Butler 2008). Once such a significant portion of beta cell mass is lost, patients will require insulin therapy for the remainder of their life. For this reason, it is of great interest to identify biomarkers for early detection of type 1 diabetes to allow treatment of autoimmune disease before substantial pancreatic damage has been done.

3.3.3.1 Patient characteristics

Metabolomic profiling of diabetes serum samples was performed by Metabolon Inc. USA. Serum from newly diagnosed type 1 diabetes patients (3.14 ± 2.66 months mean duration since diagnosis) and age/BMI/gender matched healthy controls (n=8) were used for the analysis. Table 3.3.11 shows the general characteristics of patients involved in the study.

	Type 1 Diabetes Patients (n=8)	Healthy Controls (n=8)	P-value
Age (years)	26 ± 5	27 ± 2	0.50
BMI (Kg/m^2)	24.64 ± 4.2	24.94 ± 2.6	0.87
Fasting glucose (mmol/L)	6.49 ± 3.06	4.49 ± 0.37	0.11
HbA1c (%)	7.69 ± 1.96	5.15 ± 0.30	0.008
Cholesterol (mmol/L)	4.29 ± 0.55	5.05 ± 0.44	0.013
HDL-cholesterol (mmol/L)	1.25 ± 0.42	1.35 ± 0.39	0.63
LDL-cholesterol (mmol/L)	2.53 ± 0.41	3.19 ± 0.55	0.02
Triglyceride (mmol/L)	1.09 ± 0.38	1.37 ± 1.07	0.50

Table 3.3.11 General characteristics of the study population. Mean values shown for 8 patients per group.

3.3.3.2 Identification of metabolite targets

An internal standard was added to each sample before injection onto the mass spectrometers. Instrument variability was determined by calculating the median relative standard deviation (RSD) for the internal standard (table 3.3.12). A small amount of each study sample was also used to create a homogenous pool called the – client matrix. Technical replicates of this client matrix were used to determine overall process variability by calculating the median relative standard deviation of all endogenous metabolites (table 3.3.12). Process variability as measured by median RSD passed Metabolon's quality control criteria (table 3.3.12). Metabolon recommend an RSD cut off value of 13% to ensure minimum process variability.

Overall, 302 biochemicals were detected in the serum samples. Biochemical data was analysed using two different methods- Welch's two-sample t-test was used to compare disease group versus control group as a whole, while matched pairs t-test was used to analyse the individual matched pairs. A p-value of less than or equal to 0.05 was used as a cut-off for identification of significantly different biochemicals.

Comparing disease group to control group- 19 biochemicals reached statistical significance, with 5 biochemicals at higher levels and 14 biochemicals at lower levels in disease group relative to control. A further 13 biochemicals were just beyond the level of significance and were termed 'approaching significance', with p-value greater than 0.05 but less than 0.1. Of the 13 biochemicals approaching significance 4 were present at higher levels and 9 at lower levels in disease versus control specimens (table 3.3.13).

The matched pairs analysis showed very similar results to the group analysis. 21 biochemicals were significantly different, 5 of which were at higher levels and 16 at lower levels in disease versus control. 11 biochemicals were in the approaching significance group, 6 of which were at higher levels and 5 at lower levels in disease group (table 3.3.13).

QC sample	Measurement	Median RSD
Internal standards	Instrument variability	4%
Endogenous Metabolites	Overall process variability	11%

Table 3.3.12 QC measurements of instrument and process variability

	Welch's Two-Sample t-Test	Matched Pairs t-Test
Biochemical with $p \leq 0.05$	19	21
Biochemicals (↑↓)	5|14	5|16
Biochemicals approaching significance 0.05<p>0.10	13	11
Biochemicals (↑↓)	4|9	6|5

Table 3.3.13 Biochemicals detected at significantly altered levels in type 1 newly diagnosed diabetes versus control serum specimens.

Table 3.3.14 lists all biochemicals which were identified as significantly different either by Welch's two-sample analysis or by matched pair analysis. The fold change for the matched pair analysis is reported as the average fold changes for each of the individual matched pairs. Direction of fold change for all biochemicals in table 3.3.14 is consistent whether analysed with Welch's two sample analysis or matched pair analysis, although in a limited number of cases the biochemical only reaches statistical significance with one of analysis methods. Box and whisker plots of all significantly different biochemicals are shown in appendix D, figure 1.

Metabolite	Group Analysis		Matched Pairs Analysis	
	Fold Change	P-value	Average Fold Change	P-value
1,5-anhydroglucitol	2.85	0.0036	2.7	0.0063
fibrinogen cleavage peptide	2.67	0.0085	5.01	0.012
caffeine	2.5	0.0439	1.96	0.0156
isovalerylcarnitine	1.92	0.0081	1.69	0.0138
Theophylline	1.89	0.059	1.61	0.0316
1-pentadecanoylglycerophosphocholine	1.82	0.0038	1.67	0.0053
Paraxanthine	1.78	0.0962	1.51	0.0358
malate	1.72	0.0036	1.61	0.0022
3-carboxy-4-methyl-5-propyl-2-furanpropanoate	1.72	0.0847	1.67	0.0176
1,7-dimethylurate	1.67	0.0424	1.43	0.0474
2-methylbutyroylcarnitine	1.64	0.0214	1.41	0.0469
glucose	1.58	0.0162	1.59	0.0175
arginine	1.56	< 0.001	1.59	< 0.001
N-acetyl threonine	1.54	0.0337	1.35	0.0659
hexanoylcarnitine	1.49	0.0256	1.33	0.0746
catechol sulfate	1.49	0.0099	1.59	0.0027
sebacate	1.47	0.0081	1.41	0.0239

propionylcarnitine	1.39	0.0335	1.33	0.0209
succinylcarnitine	1.37	0.0445	1.33	0.0441
1,3-dimethylurate	1.37	0.0345	1.28	0.0223
urate	1.23	0.0758	1.22	0.0281
5-oxyproline	1.16	0.0225	1.16	0.0082
Glutamine	1.14	0.0339	1.14	0.0361

Table 3.3.14 Significantly altered biochemicals in newly diagnosed type 1 diabetes specimens compared to healthy controls. Red boxes indicate biochemicals which are present at significantly higher levels in newly diagnosed type 1 diabetes serum specimens compared to control specimens. Green boxes indicate biochemicals which are present at lower levels in type 1 diabetes serum specimens compared to control specimens.

.

3.3.3.3 Validation of metabolomics targets

Fibrinopeptide A – T1DM new Vs. Control new

Fibrinopeptide A (FPA) levels were increased in T1DM new samples according to the metabolomics analysis by 2.67 and 5.01 fold in the groups and matched pairs analysis respectively. Levels of this peptide were assessed in the same T1DM new and control samples using an ELISA (Hyphen BioMed catalogue number RK016A) (protocol outlined in section 2.7.1). ELISA confirmed a significant increase (1.8 fold) in FPA levels in T1DM new samples (figure 3.3.35).

Figure 3.3.36 shows ELISA quantification of FPA in individual matched pairs. Fold change for pair 2 and pair 3 was 10 and 14 fold respectively according to metabolomics analysis, however, according to ELISA quantification, fold changes for these pairs was 1.37 and 1.49 respectively.

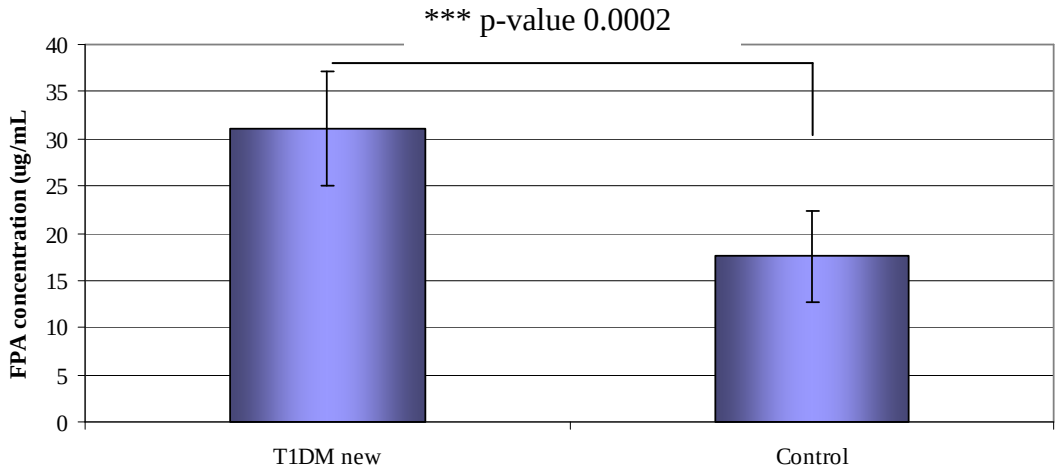

Figure 3.3.35 Average FPA concentration in T1DM new (n=8) and control (n=8) serum specimens. Error bars indicate standard deviation.

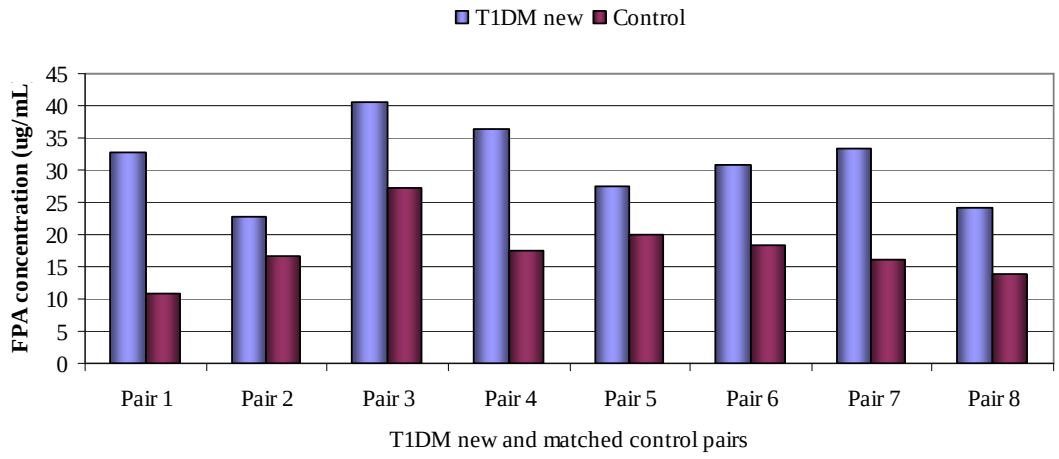

Figure 3.3.36 FPA concentration in each T1DM new and matched control specimen.

Fibrinopeptide A- Type 1 old versus control old

To test whether increased FPA levels was specifically seen in newly diagnosed T1DM patients, or a more general diabetes related event, FPA levels were assessed in T1DM patients with established disease (T1DM old). No change in FPA levels was seen in T1DM old (n=30) compared to matched controls (n=30) (figure 3.3.37).

Figure 3.3.38 shows FPA levels in individual T1DM old matched pairs. FPA was down-regulated in T1DM old in 11 of 30 matched pairs, while it was up-regulated in 17 of 30 matched pairs.

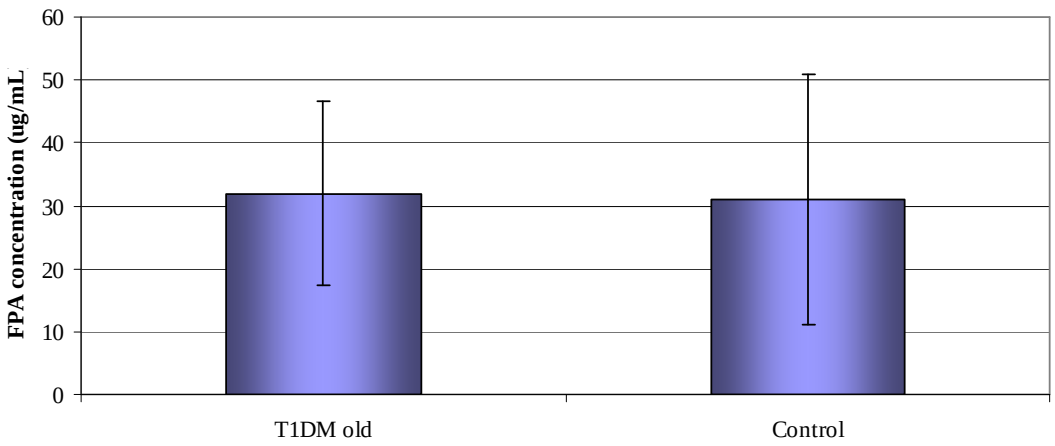

Figure 3.3.37 Average FPA concentration in T1DM old (n=30) compared to controls (n=30). Error bars indicate standard deviation.

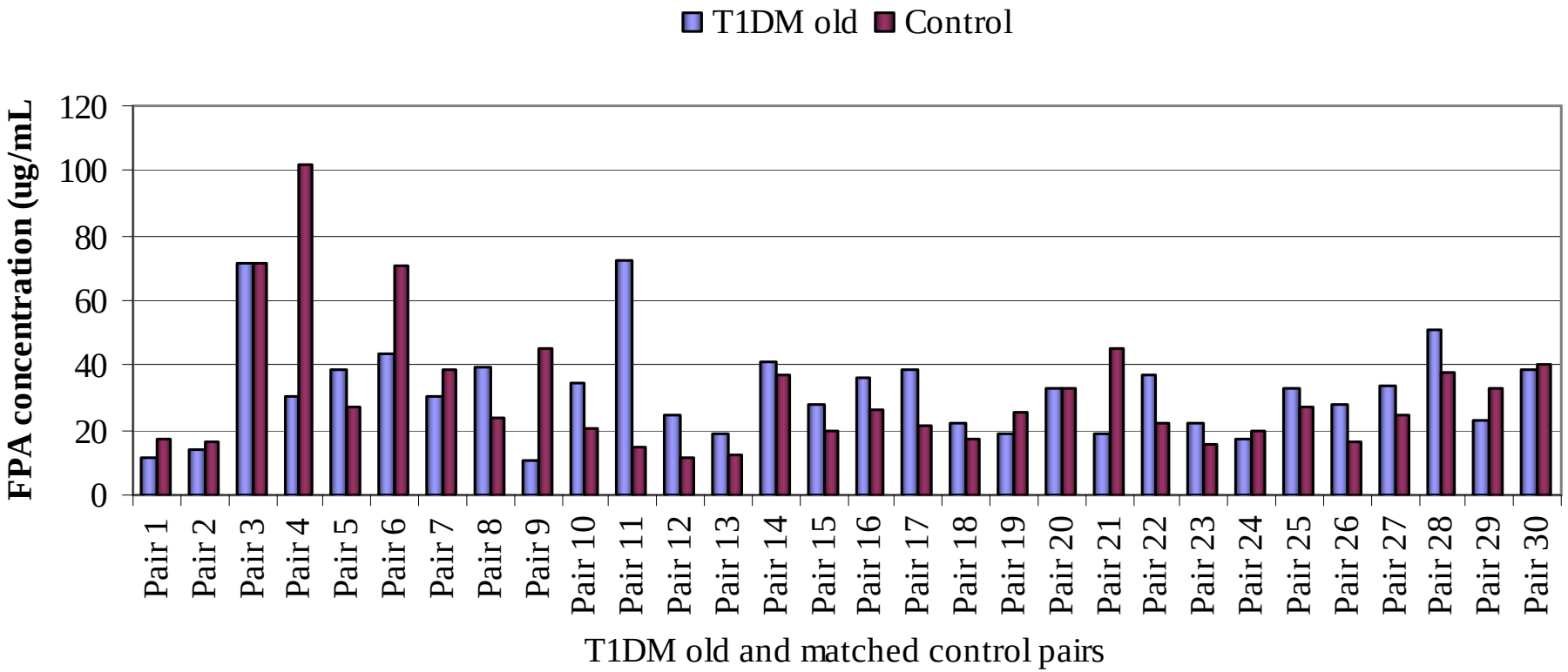

Figure 3.3.38 FPA concentration in T1DM old (n=30) and matched control (n=30) pairs.

Fibrinopeptide A- Type 1 old versus control old

FPA levels were assessed in T1DM new (n=8) compared to T1DM old (n=30) serum specimens, however, no significant change in expression levels was seen in these groups (figure 3.3.39).

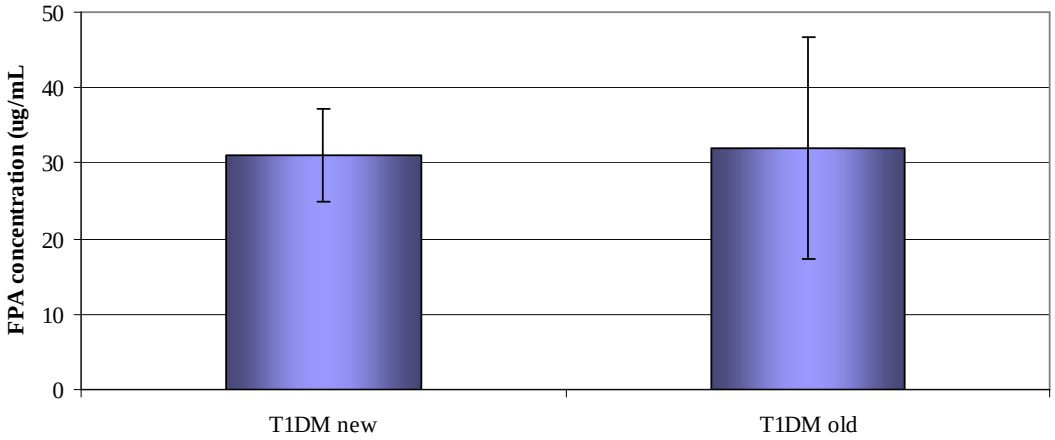

Figure 3.3.39 Average FPA concentration in T1DM new (n=8) and T1DM old (n=30) serum specimens. Error bars indicate standard deviation.

FPA levels were decreased significantly in control new samples relative to T1DM new and control old samples (figure 3.3.40). Therefore differential expression seen in figure 3.3.35 seems to be related to the control samples used rather than a disease specific change.

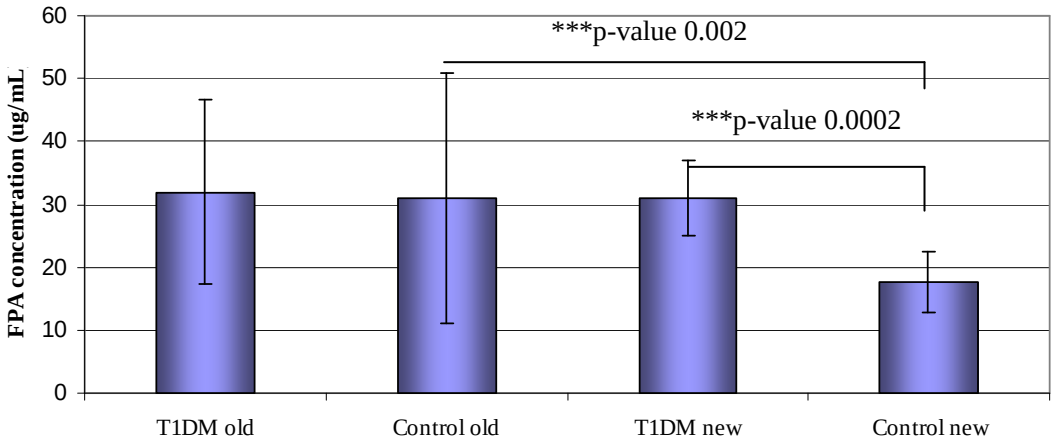

Figure 3.3.40 Average FPA concentration in T1DM old (n=30), control old (n=30) T1DM new (n=8) and control new (n=8) serum specimens. Significance indicated by * ≤ 0.05, ** ≤ 0.01, *** ≤ 0.005. Error bars indicate standard deviation.

3.3.3.4 Summary of metabolomic biomarker study

- Metabolomic profiling of T1DM new and control new samples (n=8)
- 23 differentially expressed metabolites
    - Mostly relating to carbohydrate, energy and lipid metabolism
    - Caffeine metabolites related the increase coffee consumption of controls
- Fibrinogen cleavage peptide- fibrinopeptide A selected for validation
    - T1DM new and control new (n=8)
    - T1DM old and control old (n=30)
    - Fibrinopeptide A levels decreased in young control group, unrelated to disease phenotype.

4.0 Discussion

4.1 MicroRNAs with a role in glucose stimulated insulin secretion

The aim of this study was to gain insight into molecular mechanisms governing regulated insulin secretion, in particular the role that miRNAs play in this process. To begin to identify miRNAs related to the pancreatic beta-cell phenotype, a study of miRNAs involved in regulated insulin secretion was performed, using the rodent insulinoma cell line MIN6. Two independent populations of MIN6 cells were analysed i.e. glucose responsive compared to glucose non-responsive cells. In order to identify miRNAs involved in GSIS, it was necessary to screen all possible miRNAs to check for differential expression between these two MIN6 variants.

TLDA systems have been developed for this purpose; they enable relative quantification of expression of 365 different miRNAs using TaqMan real-time PCR chemistries. The TLDAs used here were designed for analysis of human miRNA expression; however, the GSIS cell line model used in this study was of murine origin (as there are no human GSIS cell lines available for analysis). In order to overcome this problem, human and murine homology comparisons were performed using the miRNA database, miRBase, to determine the quantity of miRNAs conserved between the two species. 67% of the 365 miRNAs were found to be conserved between human and mouse. Due to this high level of conservation, the human TLDAs were deemed suitable for profiling murine miRNA expression.

Of the remaining 33% of the human miRNAs represented on the TLDA card, which were thought not to have a murine homolog according to miRBase (release 18; as of November 2011), during the course of this study, 21 of these miRNAs were discovered to be reproducibly detected in all murine RNA samples evaluated. Prior to this analysis, 1283 miRNAs were known to be present in the murine species (miRBase, release 18; as of November 2011). The result from the study reported here potentially increases this to 1304 murine miRNAs, indicating the high level of complexity of post-transcriptional regulation in this species.

As indicated in figure 3.1.1, MIN6 cells secrete insulin in a glucose regulated manner; however, with increasing time in culture they lose this GSIS phenotype. Using TLDAs

to identify miRNAs involved in the GSIS mechanism, a panel of 12 miRNAs (i.e. mir-376a, -369-5p, -130a, -27a, -410, -124a, -200a, -337, -532, -320, -192 and -379) were identified as down-regulated in glucose non-responsive cells compared to glucose responsive cells (table 3.1.2).

Previous microarray and proteomic profiling studies in our laboratory identified mRNAs (Gammell 2002; O'Driscoll, Gammell et al. 2006; Rani 2008) and proteins (Dowling, O'Driscoll et al. 2006) differentially expressed in GSIS responsive compared to non-responsive MIN6 and MIN6 B1 cells. The miRanda algorithm was applied to determine if any of these mRNAs and proteins contained potential binding sites for regulation by the miRNAs identified in this study as potentially being involved in regulating GSIS (table 3.1.4). A number of mRNAs considered to be important for beta cell function such as neuroD1 and Isl1, contained potential binding sites for miRNA regulation. Thioredoxin-interacting protein (Txnip), identified as up-regulated in glucose non-responsive compared to GSIS responsive MIN6 B1 cells (Rani 2008), is an inhibitor of thioredoxin which plays a role in reducing oxidative stress. It is thought that, through this mechanism, Txnip reduces the glucose responsiveness of MIN6 cells. Conversely, down-regulation of Txnip (and hence removal of the repressive effects on thioredoxin) led to improved glucose responsiveness of MIN6 cells (figure 4.1) (Rani 2008).

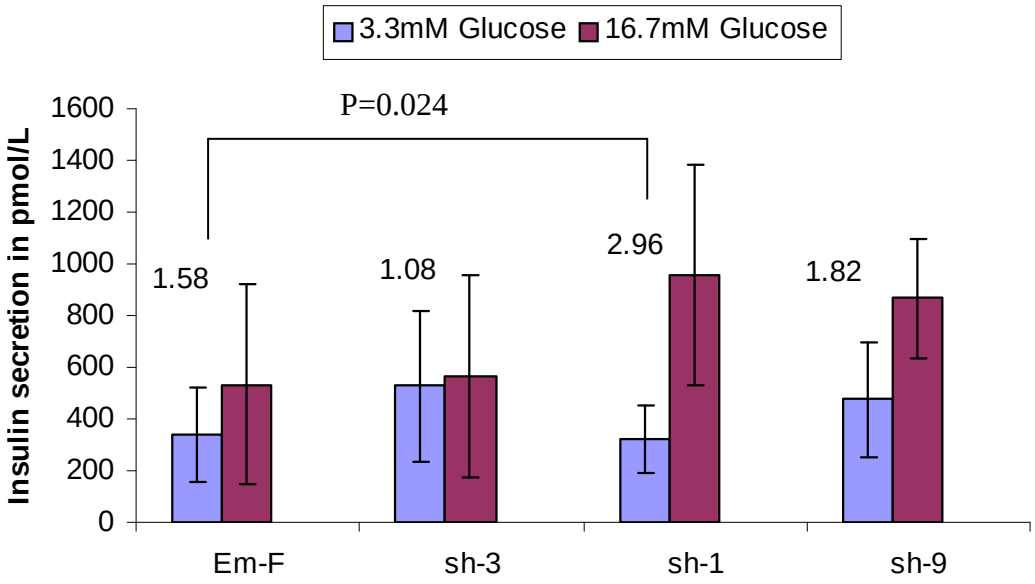

Figure 4.1 shRNA-mediated knock-down of Txnip led to a significant increase in GSIS in sh-1 clone (Txnip shRNA-transfected cells clone #1). Changes in sh-3 and sh-9 clones were not statistically significant. Performed by Dr. Sweta Rani (Rani 2008).

Here we report that Txnip contains a potential binding site for mir-130a and mir-200a regulation. Furthermore, knockdown of mir-200a and mir-130a expression led to reduction of GSIS in MIN6 cells (figure 3.1.7 and figure 3.1.8), although it has yet to be established if the effects of mir-130a and mir-200a on GSIS are directly mediated through Txnip. A previous study has also identified mir-130a as being regulated by hyperglycaemia in a comparison of islets from the Goto-Katizaki rat model of type 2 diabetes compared to control rats (Esguerra, Bolmeson et al. 2011).

In this study, anti-mir transfections suggest that knockdown of mir-410 (figure 3.1.5), mir-200a (figure 3.1.7) and mir-130a (figure 3.1.8) may decrease the magnitude of GSIS in MIN6 cells, while pre-mir transfections suggest over-expression of mir-410 (figure 3.1.6) may increase the GSIS response of MIN6 cells. However, the likely involvement of multiple miRNAs in GSIS and fluctuations in the GSIS assay makes it difficult to arrive at definitive functional assignments for individual miRNAs. Little is known of mir-410 in general, and its role in pancreatic beta cells has not been previously identified. This study suggests mir-410 may be involved in the regulation of insulin secretion, as manipulation of this miRNA in MIN6 cells led to changes in the

GSIS of these cells, although the mechanisms through which it functions still remain to be deciphered.

Previous studies have reported mir-375, mir-9 and mir-96 to play a role in regulation of insulin secretion in rodent cell models (Poy, Eliasson et al. 2004; Plaisance, Abderrahmani et al. 2006; Lovis, Gattesco et al. 2008; Ramachandran, Roy et al. 2011). However, in this study, mir-375, mir-9 and mir-96 were not differentially expressed between the two populations, indicating that the loss of GSIS in these cells may potentially be *via* a myotrophin- and granuphilin- independent mechanism. In relation to mir-124a, over-expression in MIN6 B1 cells can contribute to increased insulin secretion at basal glucose levels and decreased insulin secretion in response to stimulatory glucose levels (Lovis, Gattesco et al. 2008). Conversely, in MIN6 and INS-1E cells mir-124a was found to affect intracellular free calcium levels (*via* Foxa2 and its downstream targets i.e. potassium channel subunits SUR1 and Kir6.2), no effects on insulin secretion were observed (Baroukh, Ravier et al. 2007). In agreement with this latter study, we did not observe any effect on GSIS of MIN6 cells following over-expression or knockdown of mir-124a (section 3.1.4.7), suggesting that this effect may be somewhat specific to the MIN6 B1 clonal population.

While we identified potential functional relevance in GSIS for some of the 12 differentially expressed miRNAs identified in this study, a number of those identified here did not exhibit any functional effect on GSIS when their levels were manipulated in MIN6 cells. These miRNAs may require combined action of more than one miRNA, as miRNAs were only tested individually. Alternatively, these miRNAs may be involved in other changes the cells are undergoing as they lose their GSIS.

The GSIS response of MIN6 cells displays considerable day-to-day variation, while being the best cell-line model available for the study of regulated insulin secretion; it is not robust or routinely dependable. Pluripotent stem cells represent a potential route for the generation of a human pancreatic beta cell model for studying GSIS.

4.2 Generation and differentiation of iPS cells

Generation of the first induced pluripotent stem (iPS) cells in 2006 (Takahashi and Yamanaka 2006) revolutionised the area of stem cell research. This discovery represents the most significant development in stem cell research since the isolation of the first human embryonic stem (ES) cell lines in 1998 (Thomson, Itskovitz-Eldor et al. 1998). iPS cells hold several advantages over ES cells. Human iPS cells can be used for autologous tissue repair or replacement, without the ethical and immunological issues associated with ES cells. An additional advantage of iPS cells lies in their potential for modelling human diseases, for analysis of disease mechanisms and for screening of potential drug candidates (Yamanaka and Blau 2010).

4.2.1 Generation of iPS cells using retroviral transduction

iPS cells were first generated by Yamanaka and colleagues in 2006. They used retroviral transduction to over-express four transcription factors- oct4, sox2, c-myc and klf4 (Takahashi and Yamanaka 2006; Takahashi, Tanabe et al. 2007). In this study we used lentivirus transduction for over-expression of these four factors. Lentiviruses are a subclass of the retrovirus family, but hold several transduction related advantages over retroviruses such as MMLV. Lentiviruses can infect and stably integrate into the host genome in both dividing and non-dividing cells, whereas retroviruses are limited to dividing cells (Naldini, Blomer et al. 1996), therefore increasing the range of cell types which can be used for iPS cell generation. Lentiviruses also elicit a lower immune response in target cells, relative to retroviruses (Naldini, Blomer et al. 1996). Generation of iPS cells using lentiviral transduction has previously been shown in human and mouse somatic cells, but with similarly low efficiency levels as retroviral generated iPS cells (Blelloch, Venere et al. 2007; Yu, Vodyanik et al. 2007).

4.2.1.1 Attempt to generate iPS cell from MiaPaCa2 cell line

MiaPaCa2 pancreatic adenocarcinoma cells were treated with a virus cocktail of 3 (oct4, sox2 and klf4) or 4 (oct4, sox2, klf4 and c-myc) transcription factors. C-myc was excluded from the 3 transcription factor cocktail, as c-myc has been suggested to increase the incidence of false positive colonies (Eggan 2009). Changes in cell morphology were seen in virus treated MiaPaCa2 cultures. Untreated MiaPaCa2 cells grow in monolayer formation, even when cultured on MEF feeder layer (figure 3.2.5 B). However, 3 and 4 factor virus treated cells formed clusters, with densely packed cores of small rounded cells, while the periphery of clusters were cells with the standard MiaPaCa2 morphology (figure 3.2.6 and 3.2.7). Colonies were picked and levels of the four factors examined by RT-PCR. Untreated MiaPaCa2 cells already express three of the four factors, oct4, c-myc and klf4. Virus treated cells express similar levels of c-myc and klf4 to untreated MiaPaCa2 cells, while slight increase in expression of oct4 is seen in virus treated cells relative to control (figure 3.2.8). Very low levels of sox2 were seen in some of the virus treated clones; however, these bands were barely visible (figure 3.2.8). RT-PCR of the pancreatic marker amylase (figure 3.2.9) showed that this very low expression of sox2 was not sufficient to induce full reprogramming. Clone 3 of 3-transcription factor virus treated cells displayed altered expression of oct4 and amylase compared to other virus treated clones (figute 3.2.8 and figure 3.2.9), this may be caused by insertational mutagenesis at the oct4 and amylase locus, since lentiviruses insert into the host genome in a non-targeted manner. Virus treated MiaPaCa2 cells did not display the standard ES cell morphology (densely packed colonies with clearly defined borders), however, the morphology of these virus treated cells was distinctly different from untreated cells. These colonies may represent partially reprogrammed cells.

4.2.1.2 Attempt to generate iPS cells from keratinocytes

Normal keratinocyte cultures were also treated with 3 factor and 4 factor virus cocktails. Following transfer of the lentivirus treated cells to MEF feeder layer cultures, cell clusters were observed (figure 3.2.10). However, similar clusters were observed in both untreated control and virus treated cultures. These clusters did not proliferate further and subsequently died off. Growth arrest and cell death were unexpected in these cultures, as growth of keratinocytes on feeder cells is known to enhance cell morphology and growth characteristics (Masson-Gadais, Fugere et al. 2006). MEF feeder layer cells used in this experiment were treated with mitomycin C to arrest growth. Any contaminating mitomycin C remaining could have caused the growth arrest and subsequent cell death observed with keratinocyte clusters. It could also have been the use of ES media which caused the growth arrest of keratinocyte cultures, as keratinocytes require a very specific culture medium with growth factors (bovine pituitary extract, epidermal growth factor, insulin, hydrocortisone, epinephrine and transferrin) to maintain viability of cells. Increased calcium concentrations in ES media may also have caused terminal differentiation and growth arrest of keratinocytes (Huang, Wang et al. 2006).

4.2.1.3 Attempt to generate iPS cells from limbal epithelial cells using 4-factor virus cocktail

Limbal epithelial cells were also used for the generation of iPS cells; these cells were treated with 3 factor and 4 factor virus cocktails. Morphology changes such as cell clusters and cell processes were seen in 3 factor and 4 factor treated cells after 72 hours (figure 3.2.12). However, similarly to keratinocyte cultures, once cells were transferred to MEF feeder layer cultures with ES media, no subsequent proliferation was observed.

4.2.1.4 Summary of attempts to generate iPS cells using lenti-viral over-expression of transcription factor cocktail

While distinct cell morphology changes were seen in each of the different cell types transduced with lenti-virus containing 4 factors (oct4, sox2, klf4 and c-myc) or 3 factors (oct4, sox2 and klf4), no true iPS cells were generated. However, these morphology changes may indicate partially reprogrammed cells. iPS cell generation using 3 or 4 factor virus cocktails remains a very inefficient procedure, with approximately 0.01% successful reprogramming rate reported from human dermal fibroblast and 0.8% for epidermal keratinocyte cultures (Aasen, Raya et al. 2008). Reprogramming depends on the transduction of each of the 3 or 4 individual viruses into each individual cell. However, even cells which have been successfully transduced with all four viruses and express all four transgenes are not guaranteed to become fully reprogrammed (Chan, Ratanasirintrawoot et al. 2009). In addition to expression of the four transgenes, it is also likely that the relative ratio of expression of these genes is also an important factor for true reprogramming. Even though cells are treated with equal MOI for each virus, this may not result in equal number of integration sites in the target cell genome, and hence varying expression levels for each factor. Reprogramming of somatic cells also requires heterochromatin reorganisation, with partially reprogrammed cells exhibiting densely packed chromatin fibres compared to the poorly defined chromcentre boundaries of fully reprogrammed iPS and ES cells (Fussner, Djuric et al. 2011).

The lentivirus used in this study stably integrates into the host genome, although not in a targeted manner. Therefore, viral gene integration may occur in housekeeping gene sequences, or in genes necessary for reprogramming to occur, consequently adding to the low efficiency of iPS generation observed in this study and in the published literature (Yamanaka 2009). A recent study has shown that integration of the viral genome alone, without the use of exogenous factors is sufficient to transform somatic cells to a semi reprogrammed state, these cells were termed- lentivirus induced pluripotent-like (ViP) cells (Kane, Nowrouzi et al. 2010). In these cells a number of viral integration sites were observed in iPS signature genes. It is thought that the mutagenic effect of viral integration results from dysregulation of host genes in the vicinity of viral integration sites (Kane, Nowrouzi et al. 2010).

As induction of iPS cells is still a relatively new technology, the mechanisms of transcription factor-induced reprogramming of somatic cells have not been fully elucidated. The lack of truly reprogrammed iPS in this study could be a result of the reasons discussed above, or possibly from reasons not yet fully understood. Using currently available protocols, iPS cell generation is a very inefficient process, indicating that we still have a long way to go to fully understanding the mechanisms behind reprogramming, so these low efficiencies can be improved.

4.2.2 Attempt to generate iPS cells using ESD3 conditioned media

Balasubramanian et al. 2009, have recently succeeded in the generation of iPS cells using conditioned media from rat corneal limbal epithelial cells (Balasubramanian, Babai et al. 2009). To our knowledge, this procedure has not yet been applied to human limbal epithelial cells.

Limbal epithelial cells cultured in 6-well plate inserts with 3T3 feeder cells in the bottom layer led to improved yield of limbal progenitor cells, compared to standard culture protocols (Reddy et al., unpublished data). It was thought that using this newly established culture protocol with higher yield of limbal progenitor cells would lead to improved efficiency of iPS generation.

Limbal epithelial cells were treated with enriched media containing B-27 supplement, noggin, bFGF and EGF for 7 days (figure 3.2.13). Noggin is thought to induce the generation of neural progenitors from limbal epithelial cells (Zhao, Das et al. 2008). After 7 days in enriched media Balasubramanian et al. 2009 observed the formation of neurospheres. In our own cultures we did not observe any neurosphere formation; however, a change in cell morphology was observed (figure 3.2.14). Untreated limbal epithelial cells (figure 3.2.14 A) displayed standard epithelial cuboidal morphology, while cultures treated with enriched media (figure 3.2.14 B and C) displayed long stretched cells with processes, reminiscent of neuronal cells.

Cells were trypsinised and seeded onto plates coated with either gelatin alone, or gelatin and irradiated MEF (iMEF) feeder layer, and media was changed to 50% ESD3 conditioned media (ESD3 CM) and 50% ES media. Control limbal epithelial cells were maintained in enriched media, to determine if iPS cells could be formed from enriched media treatment alone. After a total of 14 days in enriched media cells with the standard epithelial morphology became confluent and the long stretched cells with processes were no longer seen (figure 3.2.15 A and D). Cells which were switched to ESD3 CM and plated on an iMEF feeder layer displayed colony formation after 7 days (figure 3.2.15 E and F). However, after a further 7 days, total 14 days ESD3 CM treatment, these colonies did not appear to be proliferating and no outgrowth was observed (figure

3.2.16). A single colony with a slightly different morphology, indicated by a red arrow in figure 3.2.16 D, was observed. This colony contained tightly packed cells and appeared more adherent to the culture dish, however the edges were less clearly defined compared to rat limbal iPS cells developed by Balasubramanian et al. 2009, (figure 4.2).

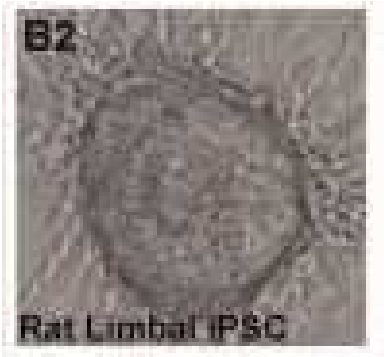

Figure 4.2 Rat limbal iPS cells generated by Balasubramanian *et al*., (Balasubramanian, Babai et al. 2009). Colonies exhibit tightly packed cells with well defined colony edges.

In cultures grown with iMEF feeder cells or on gelatin for 14 days ESD3 CM, a confluent monolayer of fibroblast/mesenchymal-like cells was observed (figure 3.2.16 B, C, E and F). PCR analysis of marker expression was performed to investigate if the cells observed represented contamination or a semi-reprogrammed population. Stromal cell contamination of epithelial cultures is possible during dissection of the limbal ring and outgrowing from the explant. As stromal cells share similar morphology to the ESD3 CM treated limbal epithelial cells (figure 4.3), RNA from these cells was also included in the PCR analysis of marker expression, as a control (figure 3.2.17 and figure 3.2.18).

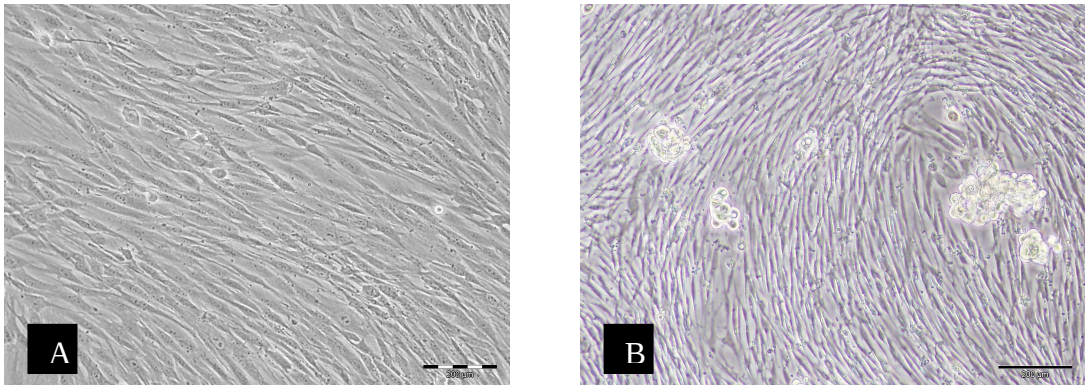

Figure 4.3 Comparison of stromal cells and ESD3 CM treated limbal epithelial cells. Image **A** represents stromal cells isolated from donor cornea-sclera ring. Image **B** represents limbal epithelial cells after 7 days of treatment with enriched media and 14 days treatment with ESD3 conditioned media. Same scale bar used in both images.

Oct-4, Klf-4 and c-myc expression was detected in control and ESD3 CM treated cells at similar levels to that of parental limbal epithelial cells. Sox2 however, was only expressed only in ESD3 CM treated cells on iMEFs, at a similar level to that of control iPS cells. iMEF cells could potentially contribute to marker expression, hence iMEF cells were also included in the PCR as a control for contamination. Sox2 primers, which also detected murine sox2, detected sox2 in the iMEF control cells. However, these were freshly thawed healthy iMEF cells, while iMEF feeder layer in ESD3 CM treated cultures was 15 days old at the time of harvesting cultures for RNA by which stage the iMEF cells would mostly have been apoptotic and unlikely to contribute to the positive sox2 expression seen in ESD3 CM treated cells. The same density of iMEF cells would also have been present in cultures of controls cells on iMEFs, but these cultures remained negative for sox2, indicating that the sox2 present in the ESD3 CM treated cells on iMEFs was due to the ESD3 CM treated cells, and not the iMEFs. This result indicates that an iMEF feeder layer is required to induce sox2 expression, as sox2 was not detected in ESD3 CM treated cells on gelatin. It is unknown if the induction is due to secreted factors or cell to cell contact with the iMEF feeder layer. Additionally, as sox2 expression is negative in stromal cells, this would indicate that ESD3 CM treated cells on iMEFs are different from stromal cells, and did not arise from stromal cell contamination.

In various types of epithelia, cytokeratin expression can be linked to the differentiation status. In the stratified epithelia each stratified layer represents a more differentiated state. These differentiation states can be characterised by the expression of unique keratin pairs (Daly, Meleady et al. 1998). In the cornea the expression of keratin-3 (CK3) and keratin-12 (CK12) are markers of terminal differentiation (Schermer, Galvin et al. 1986; Kasper, Moll et al. 1988). In our experiment, parental limbal epithelial cells do not express CK-12, due to high population of progenitor/trans-amplifying cells (Dua and Azuara-Blanco 2000) and the short time of *in-vitro* culture. The limbal epithelial control cells maintained in enriched media for 21 days express CK-12, representing the more differentiated or mature state of these cells (figure 3.2.18). This is possibly due to the longer *in-vitro* culture time relative to parental limbal epithelial cells. In confluent limbal epithelial cell cultures, stretched elongated cells can sometimes appear on top of the cuboidal cells (figure 3.2.16 D, indicated by the red arrow); however, the elongated fibroblast/mesenchymal-like cells shown in figure 3.2.16 B and E are not the result of confluent limbal epithelial cells, as verified by the lack of CK-12 expression. Lack of CK-12 expression in ESD3 CM treated cells indicates that these cells are less differentiated than control cells maintained in enriched media. This less-differentiated phenotype is due to the ESD3 conditioned media treatment, as ESD3 CM treated and control cells were cultured *in vitro* for the same period of time.

CK-3 is also a marker for terminally differentiated epithelial cells (Schermer, Galvin et al. 1986). Control cells in enriched media were positive for CK-3 expression, as expected, due to their more differentiated state. However, parental limbal epithelial cells are also positive for CK-3, which could suggest a sub-population of differentiated cells in the limbal epithelium, or alternatively could indicate CK-3 to be less specific marker for terminal differentiation. Low levels of CK-3 expression was seen in stromal cells, ESD3 CM treated cells and iPS cells, representing a less differentiated phenotype. Analysis of marker expression using RT-PCR may not always give a true reflection of protein expression, as these mRNAs may potentially be regulated by post-translational control. Double bands are seen in some cases of CK-3 expression, this second band possibly represents a splice variant of CK-3. The second band is not a result of genomic DNA contamination as primer amplification of genomic DNA would result in a 924bp product, which is approximately the size of the highest band on the DNA gel (figure 3.2.18), while the CK-3 mRNA amplification resulted in a band at 261 base pairs.

N-cadherin is a marker associated with adult stem cells, especially neuronal stem cells, it is also critical for the maintenance of the progenitor phenotype of limbal epithelial cells (Higa, Shimmura et al. 2009). Therefore, it was not surprising to find high levels of expression of this marker in iPS cells, parental limbal epithelial cells which have an abundant population of progenitor/trans-amplifying cells, and stromal cells which are thought to possess properties similar to mesenchymal stem cells (Reddy unpublished data). Reflecting the lack of neurosphere development following noggin treatment, N-cadherin expression levels in enriched media treated cells were low relative to parental limbal epithelial cells (figure 3.2.18). This also indicates that these control cells represent a more differentiated corneal epithelial phenotype. ESD3 CM treated cells however, have maintained a high level of N-cadherin expression, indicating that these cells still possess some 'stem-like' properties.

ΔNp63 and ABCG2 are putative limbal stem cell markers (Parsa, Yang et al. 1999; Di Iorio, Barbaro et al. 2005; Kolli, Lako et al. 2008). In contrast to high CK-3/12 expression and low N-cadherin expression indicating terminal differentiation in control cells, potential stem cell marker ΔNp63 is expressed at a level comparable to that of parental limbal epithelial cells (figure 3.2.18). ABCG2 expression is very low in parental limbal epithelial and stromal cells, and undetected in ESD3 CM treated cells, indicating that while ESD3 CM treated cells may lack expression of differentiation markers, the expression level of stem cell markers in these cells in still quite low relative to limbal epithelial cells and iPS cells.

ESD3 CM treated limbal cells on iMEFs show increased expression of stem cell-associated N-cadherin and reduced expression of terminal differentiation markers CK-12 and CK-3. These cells also express the 4-factor cocktail thought to induce reprogramming of somatic cells to an iPS phenotype. However, these cells have not achieved full reprogramming, as they remain negative for pluripotency marker nanog (figure 3.2.18). It is possible that a partial reprogramming has occurred in these cells, as an altered cell morphology and mRNA expression pattern is observed in these cells. Partial reprogramming is frequently reported in the literature, however, it is not know what the distinguishes cells which will become fully reprogrammed from cells which remain partially reprogrammed, or if these partially reprogrammed cells have properties similar to lineage committed progenitors (Nagy and Nagy 2010).

This experiment was performed on limbal epithelial cells from a single donor cornea-sclera ring; it is possible that subtle difference between donated tissues may impact the efficiency of iPS generation. Repeating this experiment with a number of donor cornea-sclera rings should determine if it is possible to reprogram human limbal epithelial cells to iPS cells using non-cell autonomous techniques, or if this is a murine specific phenomena.

In addition to retroviral and conditioned media induction of reprogramming attempted in this study, a number of other techniques for generation of iPS cells have recently been reported, including using mRNA transfection (Warren, Manos et al. 2010; Yakubov, Rechavi et al. 2010) and recombinant protein transduction (Kim, Kim et al. 2009) for over-expression of the four factor cocktail. A number of pluripotency associated miRNAs have also recently been identified, over-expression of which is sufficient to induce reprogramming (Anokye-Danso, Trivedi et al. 2011; Miyoshi, Ishii et al. 2011). As the molecular mechanisms of cellular reprogramming become more apparent, developments in iPS generation techniques have significantly increased reprogramming efficiencies since the first reprogramming papers in 2006 and 2007, which reported efficiencies of approximately 0.001% (Takahashi and Yamanaka 2006; Takahashi, Tanabe et al. 2007). Reprogramming kits available today from Stemgent using mRNA reprogramming technology quote efficiencies in the range of 5%, while (if verified) would make iPS technologies more amenable to labs less established in the reprogramming field.

4.2.3 Differentiation of iPS cells

The iPS cell line hFib2-iPS4 generated from human fibroblasts in the George Daley lab, Children's University Hospital, Boston, was used for differentiation studies presented in this thesis (Park, Zhao et al. 2008). A differentiation protocol by Jiang J. *et al.*, designed to recapitulate the important *in vivo* signals that drive pluripotent stem cells towards pancreatic phenotypes was selected for differentiation of these iPS cells (Jiang, Au et al. 2007). Using this protocol Jiang J. et al., have achieved 2-8% insulin positive cells from human ES cells, which secrete insulin in a glucose regulated manner, however, the glucose stimulated insulin secretion (GSIS) profile of these cells more closely resembles that of fetal islets, rather than mature adult islets (Jiang, Au et al. 2007). As of yet, no group has been able to fully differentiate pluripotent stem cells to mature adult islet cells *in vitro*. Differentiation studies with the murine cell line ESD3 in 3D culture have achieved up to 60% insulin positive cells, in comparison to fewer than 10% in standard 2D cultures, using a slight different differentiation factor cocktail (Wang and Ye 2009). 3D culture more closely reflects *in vivo* development and tissue organisation compared to 2D differentiation, the combination of 3D culture and growth factors present in the 3D matrix led to a significant improvement in *in vitro* pancreatic differentiation protocols. A combination of the Jiang J. et al. 2007, directed differentiation protocol and 3D culture was used to determine if the iPS cells used in this study could be differentiated towards pancreatic cells *in vitro*, and if an improvement in pancreatic differentiation was achieved with 3D culture compared to 2D culture.

The effectiveness of differentiation was monitored by measuring expression levels of known markers for each stage of pancreatic differentiation. Definitive endoderm is the first stage of pancreatic development; definitive endoderm formation was assessed using markers- cxcr4, foxa2 and hnf4a. Cxcr4, foxa2 and hnf4a were up-regulated in both the 2D and 3D differentiation cultures compared to the original iPS cells (figure 3.2.20). Improved definitive endoderm formation was seen in 3D cultures compared to 2D cultures, based on increased expression of hnf4a (figure 3.2.21). Definitive endoderm differentiated 2D cultures were then transferred to suspension culture, however, cells did not respond well to suspension culture and entered growth arrest and eventually cell death (figure 3.2.22). 3D cultures were maintained in the same 3D

matrigel/collagen cultures for the complete duration of differentiation protocol (36 days).

3D cultures were further differentiated to pancreatic endoderm, the formation of which was assessed by pdx1, hlxb9, ngn3, nkx6.1 and ptf1a expression. Hlxb9, ngn3, nkx6.1 and ptf1a levels were undetected, while very low levels of pdx1 were seen in differentiated cultures (figure 3.2.23). Differentiated cells also maintained similar levels of the pluripotency marker nanog as untreated iPS cells. In the replicate differentiation experiment, increased levels of pdx1 were seen in 3D control cells (figure 3.2.28), maintained in irradiated MEF conditioned ES media, indicating that growth factors present in the 3D matrigel matrix may have played a role in induction of pdx1 expression in these control cells.

A number of markers were also tested for presence of pancreatic exocrine and endocrine precursors – nkx6.1, nkx2.2, ngn3 and pax4; however, levels of these markers were undetected.

Pancreatic hormone and mature pancreatic marker expression was examined in each differentiation stage (figure 3.2.26). β-actin endogenous control shows unequal expression levels in day 29 and day 36 cultures, in spite of equal RNA and cDNA concentrations being using for reverse transcription and PCR reactions. RNA quality and purity, as assessed by nanodrop 260/280nm absorbance readings, was also comparable between different time-points and treatments. As unequal β-actin endogenous control levels are seen, direct comparison cannot be taken from day 36 control and differentiated cultures, however, equal β-actin levels are seen for day 36 control cells and untreated iPS cells. Mature pancreatic markers- insulin, somatostatin and amylase were detected in day 36 control cells treated with iMEF conditioned ES media; however, these markers were also present in untreated iPS cells (figure 3.2.26). The expression of these markers in untreated iPS cells possibly indicates that these cells had undergone some spontaneous differentiation in culture before initiation of this differentiation experiment. Additional markers of mature pancreatic cells- insulin, ghrelin and glut2 were detected in day 36 control cells. Appearance of mature pancreatic markers- insulin, ghrelin and glut2 in day 36 3D control cultures and absence of these markers in untreated iPS cells indicated that the use of the 3D culture system

itself or the growth factors contained in the matrigel induced expression of these markers.

Similar issues were seen in the repeat of the 36 day differentiation experiment. Levels on β-actin endogenous control were unequal between different time points and treatments (figure 3.2.29). Somatostatin and amylase were also detected in untreated iPS cells and 3D controls cells at day 29, however, unlike the previous experiment insulin and glut2 expression was not detected. Ghrelin levels were increased in day 29 control cells compared to untreated iPS cells. By day 36 the pluripotency marker nanog has significantly decreased expression levels compared to untreated iPS cells. These results also suggest that untreated iPS cells may be partially differentiated prior to beginning the directed differentiation protocol. Also, the 3D culture system also seems to be having an effect on expression of differentiation markers in control cells.

Matrigel is one of the most commonly used matrices for 3D culture systems (Kraehenbuehl, Langer et al. 2011); however, as matrigel is an animal product, batch to batch variations of growth factor concentrations occur. As different batches of matrigel were used for each replicate experiment, this may explain some of the difference between experiments.

Due to the presence of the 3D matrix, it is technically difficult to remove the cells from this matrix for immunofluoresence or flow cytometry analysis. Therefore percentage efficiencies of pancreatic differentiation cannot be determined to allow direct comparison with efficiencies reported in the literature. However, assessment was possible using RT-PCR analysis for expression of differentiation markers. This assessment showed that the 3D differentiation system was superior to the 2D differentiation system used by Jiang J. et al.

The expression of differentiation markers in untreated iPS cells potentially indicates that these cells may have undergone some spontaneous differentiation in culture, prior to initiation of the directed differentiation experiment; however cells did not display a differentiated morphology, but maintained colonies with ES-like characteristics. Alternatively, this may also indicate that these cells may not have been fully reprogrammed. The iPS cell line hFib2-iPS4 purchased from George Daley's group

which was used for all experiments in this thesis did not have pluripotency tests such as teratoma formation and bisulphite sequencing of promoters of pluripotency genes oct4 and nanog performed (Park, Zhao et al. 2008). Without pluripotency tests such as these, cell lines cannot be conclusively determined to be fully reprogrammed iPS cells (Daley, Lensch et al. 2009). In mouse iPS studies, germ line chimera formation is the definitive assay of choice for proving full reprogramming and true pluripotency. Currently, it is difficult to prove full reprogramming in human cells (Yamanaka 2009). Aberrant reprogramming may subsequently result in an impaired ability to differentiate using directed differentiation protocols (figure 4.3) (Yamanaka 2009).

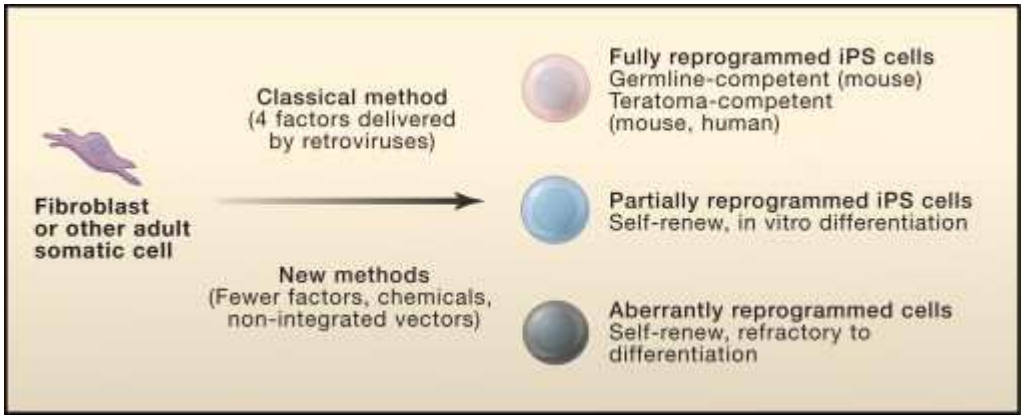

Figure 4.3 Types of reprogrammed cells. Reprogramming on somatic cells could result in fully reprogrammed iPS cells that are comparable to ES cells, partially reprogrammed iPS cells that can self-renew and differentiate into certain cell lineages, or aberrantly reprogrammed cells that self-renew but are refractory to differentiation (Yamanaka 2009).

Viral transgenes are usually silenced in established iPS cell lines. Leaky expression of transgenes may also inhibit complete iPS cell differentiation and maturation (Okita, Ichisaka et al. 2007). Transgene expression was not monitored in iPS untreated cells in this study, however, on establishing this cell line, it was shown that viral c-myc expression was not completely silenced (Park, Zhao et al. 2008).

Another issue which may be of importance for directed differentiation of iPS cells is the tissue of origin of the somatic cells. iPS cells generated from some cell types may have an inherent inability to re-differentiate to different lineages (Yamanaka 2009). A recent

study of pancreatic beta cell derived iPS cells (BiPS cells), showed that these BiPS cells retained epigenetic memory of their original cell type and maintained an open chromatin structure in key beta cell genes (Bar-Nur, Russ et al. 2011). BiPS cells were shown to have an increased propensity to differentiate towards pancreatic lineages in both spontaneous and directed differentiation experiments, compared to ES cells and iPS cells originating from non-beta cell types (Bar-Nur, Russ et al. 2011). The iPS cells used in this study were originally derived from adult dermal fibroblasts (Park, Zhao et al. 2008), therefore mature pancreatic genes may be epigenetically silenced in these cells, leading to reduced efficiencies of pancreatic differentiation.

Similarly to ES cell lines, iPS cell lines also show considerable differences in differentiation potential (Tateishi, He et al. 2008). Directed differentiation protocols may need to be optimised for individual ES and iPS cell lines, a universal directed differentiation protocol is unlikely to achieve equal levels of pancreatic differentiation in a range of cell lines. D'Amour et al., a well established group in the pancreatic differentiation field, have reported promising results both *in vitro* and *in vivo* (D'Amour, Bang et al. 2006; Kroon, Martinson et al. 2008), however, this success is limited to a single ES cell line, attempts at replicating these results in iPS cell lines has also come up short. Ideally for differentiation experiments, a range of ES or iPS cell lines should be used as they will invariable differ in their differentiation potential.

This study has shown that iPS cells generated from adult dermal fibroblasts can be differentiated to definitive endoderm-like cells through directed differentiation protocols. Further differentiation of these cells towards mature pancreatic cell types showed more varied results and is extremely inefficient. Ideally, for directed differentiation experiments, a range of iPS cell lines, generated from a number of different types of somatic cells should be used, specifically iPS cell lines from closely related cell lineages as the target tissue of interest. iPS cell lines should also be conclusively determined to be truly pluripotent, as variability in epigenetic remodelling, the extent of methylation, and the persistence of expression of integrated viral transgenes can alter the differentiation potential of iPS cell lines (Daley, Lensch et al. 2009).

4.2.4 Differentiation of limbal stromal cells

Limbal stromal cells have been shown to resemble bone marrow derived mesenchymal stem cells and possess differentiation potential into ectoderm, mesoderm and endoderm lineages (Dravida, Pal et al. 2005; Polisetty, Fatima et al. 2008). The differentiation potential of these cells was assessed in this study to determine if these cells could be differentiated towards pancreatic lineages.

Stromal cells were treated with differentiation factors to induce formation of definitive endoderm in standard monolayer culture; however, no expression of definitive endoderm markers was detected using this technique. Previous studies with this cell type have shown that initial embryoid body formation of these cells can improve their differentiation potential in subsequent directed differentiation experiments (Reddy unpublished data). Following embryoid body formation, these cells were seeded into 3D, 2D or monolayer cultures, and potential for definitive endoderm differentiation examined. Cxcr4 was the only definitive endoderm marker detected in these cells; cxcr4 was detected in 2D and 3D cultures, with higher expression in control compared to differentiation cultures (figure 3.2.32). This result is reminiscent of iPS cell differentiation in 3D culture (figure 3.2.29). It would seem that the effect of matrigel and the growth factors contained within the matrigel improve the ability of limbal stromal cells to differentiate towards pancreatic endoderm compared to the directed differentiation media (containing activin A, sodium butyrate and B27). Further differentiation of these cells towards pancreatic endoderm did not achieve expression of pancreatic endoderm markers (figure 3.2.34).

In light of the iPS differentiation experiments discussed above (section 4.2.3), which yielded superior differentiation marker expression in control cultures compared to directed differentiation cultures, the same 3D culture conditions with iMEF conditioned media, were applied to stromal cells for 36 days. After 36 days in 3D culture with either iMEF conditioned ES media or standard stromal media (DMEM, 10% FCS), mature exocrine marker- amylase expression was detected (figure 3.2.36). Amylase expression was also detected in the repeat experiment after 36 days; however, untreated and hanging drop cells were also positive for amylase expression (figure 3.2.37).

Limbal stromal cells have been suggested to possess a differentiation capacity similar to bone marrow-derived mesenchymal stem cells, with potential towards osteogenic, chrondrogenic and adipogenic lineages (Sosnova, Bradl et al. 2005; Polisetty, Fatima et al. 2008). Bone marrow-derived mesenchymal stem cells have previously shown differentiation potential towards pancreatic lineages (Zhang, Shen et al. 2010). However, the protocol used in this study did not achieve any substantial pancreatic differentiation. Since this study has been performed, an article has been published based on directed differentiation of limbal stromal cells towards functioning pancreatic beta cells (Criscimanna, Zito et al. 2011), however a different cocktails of growth factors was used in this study compared to the directed differentiation protocol used here. The lack of pancreatic endocrine differentiation in the limbal stromal cells used in this study may be a result of the specific directed differentiation protocol used, as this was designed for use with ES cells (Jiang, Au et al. 2007), and may be incompatible with adult stem cells, and may not support transdifferentiation of a more committed stem/progenitor cell type. Additionally, stromal cells isolated from the corneal-scleral ring may also exhibit subtle differences in differentiation potential between donors. In this thesis, all stromal experiments were performed with cells from a single donor. Using a range of stromal cell lines from different donors may give a more accurate view of the effectiveness of this directed differentiation protocol for stromal cell differentiation towards pancreatic cell types.

4.2.5 Summary of differentiation studies

Two different approaches were used in this study to generate iPS cells; lentiviral transduction of the transcription factor cocktail and conditioned media induced reprogramming. However, cells have not progressed beyond the semi-reprogrammed state. Despite challenges with directed differentiation of iPS cells towards pancreatic phenotypes, our 3D culture system improved differentiation marker expression compared to 2D systems, using established directed differentiation protocols.

Recent studies have identified miRNA families associated with regulation of pluripotency. Over-expression of these pluripotency related miRNAs induces reprogramming of somatic cells to iPS cells (Lin, Chang et al. 2008; Anokye-Danso, Trivedi et al. 2011; Miyoshi, Ishii et al. 2011). If miRNAs can be used to induce reprogramming, then maybe pancreatic beta cell related miRNAs could potentially direction differentiation of pluripotent stem cells towards pancreatic cell types.

4.3 Biomarker discovery in diabetes serum

4.3.1 Serum miRNA biomarkers

Serum miRNAs have been shown to be differentially expressed in a range of pathological conditions such as ovarian cancer (Resnick, Alder et al. 2009), lung cancer (Chen, Ba et al. 2008), large B-cell lymphoma (Lawrie, Gal et al. 2008), breast cancer (Zhu, Qin et al. 2009), colorectal cancer (Huang, Huang et al. 2009) and liver damage (Wang, Zhang et al. 2009), as well as physiological conditions such as pregnancy (Chim, Shing et al. 2008). Recent studies have also identified differential miRNA expression in serum from T2DM (Chen, Ba et al. 2008; Zampetaki, Kiechl et al. 2010; Kong, Zhu et al. 2011) and gestational diabetes (Zhao, Dong et al.) patients. Serum miRNAs are particularly resistant to digestion by serum RNases, in comparison to large mRNA fragments which are more sensitive to RNaseA action (Chen, Ba et al. 2008). This quality of serum miRNAs makes them particularly suitable for use as RNA biomarkers, and could represent a non-invasive method for diagnosis or monitoring of diseased state.

As indicated in section 3.2.3.4, 12 miRNAs were identified as being differentially expressed in glucose responsive compared to glucose non-responsive MIN-6 cells. Expression levels of these miRNAs were subsequently tested in serum specimens from T1DM and T2DM patients in comparison to levels in serum from non-diabetic controls.

4.3.1.1 Serum miRNA analysis in T1DM serum specimens

From the initial analysis of T1DM serum specimens, only mir-124a was found to be consistently differentially expressed in T1DM serum specimens tested (figure 3.3.2). Therefore, analysis of this miRNA was extended to examine a total of 15 T1DM serum specimens and BMI/age/gender matched controls. Of these 15 specimens, mir-124a was up-regulated in 11 of 15 T1DM specimens by approximately 1.9 fold; however, this increase was not statistically significant.

As the majority of pancreatic beta cells in T1DM patients are dysfunctional or have been destroyed by autoimmune attack (Matveyenko and Butler 2008), it was hypothesised that reduced expression of these GSIS related miRNAs would be seen in T1DM sera. However, this was not the case, 11 of the 12 GSIS-related miRNAs tested showed no consistent change in expression levels in serum, while mir-124a was up-regulated in 11 of 15 T1DM samples compared to the control specimens tested. The up-regulation of mir-124a in T1DM serum specimens is unlikely to be related to its function in GSIS in pancreatic beta cells, as the majority of these cells have been destroyed. Mir-124 has previously been shown to be involved in neuronal differentiation, with increased expression leading to increased differentiation towards neuronal cell types, while knockdown of expression maintained cells in a stem cell state (Cheng, Pastrana et al. 2009). Increased levels of mir-124a in serum from T1DM patients could potentially reflect the body's stem cell population attempting to differentiate towards beta cell types to compensate for the beta cells lost by autoimmune attack.

Large scale miRNA profiling of T1DM serum specimens was performed in order to identify other potential miRNA biomarkers for this disease using TaqMan low density miRNA arrays (TLDAs). The endogenous controls incorporated in the TLDA cards were undetected in all serum specimens tested; therefore, the TLDA data was assessed to determine if any of the target miRNAs analysed could represent potential endogenous control miRNAs. Mir-28 and mir-326 levels were unchanged in T1DM samples compared to controls and also showed a low standard deviation across all samples analysed. Therefore, these two miRNAs were selected as endogenous controls for use in

this experiment. All TLDA data was normalised to these 'endogenous control' miRNAs individually to generate two lists of differentially expressed miRNAs. Only miRNAs common to both lists were chosen as targets for further investigation. Using this criterion a list of seven miRNAs (i.e. mir-140, -21, -24, -29a, 29c, -30d and -345) were identified as differentially expressed in T1DM sera relative to control sera, all of which were up-regulated in T1DM sera.

Expression of these seven miRNA targets were examined in a total of 13 T1DM serum specimens and matched controls. Expression levels were not consistent among all samples analysed. However, the expression patterns of these miRNAs seemed to split the specimens into two distinct groups – T1DM specimens where all target miRNAs were over-expressed (n=6), and T1DM specimens where all target miRNAs showed reduced expression (n=5) (table 3.3.3). A further 2 T1DM specimens showed varying trends of miRNA expression and, hence, did not fit into either category (table 3.3.3). A comparison of the patient history and medical information was performed on the patients in these two categories, to determine any possible difference that may help explain why they grouped in separate categories and why patients with similar miRNA expression grouped together. Specimens with increased levels of the miRNA targets showed statistically significant higher alcohol and cigarette consumption (p-values 0.036 and 0.044, respectively). These patients also showed increased exercise minutes per week; however, this increase was not significant (p-value 0.064).

Control serum specimens used in this study were matched to patient sera based on age, gender and BMI; but not on smoking or alcohol intake. The trend of high expression of miRNA targets being associated with high smoking and alcohol intake is not mirrored in the control serum specimens. However, ignoring the normalisation of PCR data against these matched control serum specimens, the trends remain the same for T1DM specimens, i.e. T1DM specimens with higher smoking and alcohol consumption had higher expression of these miRNA targets, while the T1DM specimens, from low/non-smoking and low alcohol consumption patients showed lower expression of these target miRNAs.

In a study reported by Chen et al., (Chen, Ba et al. 2008), mir-140, mir-21, mir-24, mir-29a and mir-30d were shown to be up-regulated in serum specimens from lung cancer

patients, while mir-29c was down-regulated in these specimens (Chen, Ba et al. 2008). These miRNAs showed dysregulation in our study of T1DM serum specimens compared to healthy control serum specimens. This overlap of miRNA targets in lung cancer and T1DM may reflect the body's immune response or general inflammatory response to diseased state, rather than being disease-specific miRNAs. Alternatively, these miRNAs may reflect an effect of smoking, as these miRNAs were up-regulated in the T1DM serum specimens from our study with high cigarette consumption. There was no information on patient smoking habits or diabetes status published in the lung cancer serum study by Chen et al. However, as 90% of lung cancer cases can be attributed to smoking (Peto, Lopez et al. 1992), it is possible that the increased levels of these miRNAs in serum from lung cancer patients could also be related to smoking.

As there is no available data on the direct effects of smoking or alcohol on miRNA levels in serum, we can only suggest that these changes in miRNA expression levels in T1DM serum specimens may be smoking-related. As the trend is not observed in smoking and non-smoking control serum specimens, it may be that this expression trend represents a 'diabetic-smoking specific' phenomenon. To further test this possibility, a large cohort of serum specimens would need to be examined, in smokers and non-smokers, with and without lung cancer or type 1 diabetes, as well as non-diabetic and non-cancer controls.

Mir-345 was the only miRNA identified from the TLDA experiment which did not overlap with the lung cancer study; therefore, this miRNA may more likely be diabetes-related. However, much work on this target still needs to be carried out to determine its applicability as a biomarker of this disease, as this target also shows differential expression in T1DM serum specimens of high smoking and alcohol intake relative to low/non-smoking and low alcohol consumption T1DM patients.

Mir-21, mir-24, mir-29a and mir-30d were identified in this study in the TLDA experiment with T1DM serum, however, expansion of the study to an additional ten T1DM and control samples did not show a consistent trend in expression levels. These miRNAs have since been shown to also be differentially expressed in serum from T2DM patients (Zampetaki, Kiechl et al. 2010; Kong, Zhu et al. 2011), indicating a potential commonality between serum markers in T1DM and T2DM.

4.3.1.2 Serum miRNA analysis in T2DM serum specimens

Levels of GSIS related miRNAs (identified from section 3.2.3.2) were also analysed in serum from type 2 diabetic patients (T2DM). It was hypothesised that as these miRNAs were down-regulated in non-GSIS MIN6 cells, that this trend may be reflected in T2DM sera, as an indication of beta cell dysfunction associated with this disease. Mir-369-5p was the only miRNA of the 12 analysed which showed a consistent change in all serum samples tested (6 T2DM specimens and 6 BMI/age/gender matched controls). Mir-369-5p was reduced approximately 2.1 fold in T2DM serum specimens; in two T2DM specimens mir-369-5p was reduced to the extent that it was undetectable by real-time PCR, however, this change was not statistically significant. This consistent reduction of mir-369-5p in T2DM serum specimens could potentially represent beta cell dysfunction in these patients.

In a study by Kong *et al.* 2011, mir-124a levels were significantly up-regulated in T2DM serum compared to patients with pre-diabetes or control patients with normal glucose tolerance (Kong, Zhu et al. 2011). However, in our study no significant change was seen in mir-124a levels in T2DM patients (figure 3.3.11). These conflicting results could be related to the ethnicity of patients used in the study, as the patients used in the Kong *et al*. 2011 study were from a Chinese population, while the samples used in our study were from Caucasian patients.

This pilot study demonstrated the feasibility of using miRNAs as serum biomarkers for T1DM and T2DM patients. We have shown that the miRNA profile of T1DM serum is distinct from the miRNA profile in healthy control serum. We have also shown the differential expression of miRNAs in serum from T2DM specimens. This proof-of-principle work has established that differences in miRNA expression profiles in diabetes versus healthy control sera could be potentially exploited for development of biomarkers for monitoring and diagnosis of T1DM and T2DM.

4.3.2 Serum protein biomarkers

Serum specimens from diabetes patients were analysed using the latest proteomics technologies to identifiy biomarkers of potential use for diagnosis, prognosis and monitoring of disease progression. Label-free LC-MS techniques were employed for the analysis of these serum specimens.

With the dawn of label-free LC-MS/MS technologies new software packages were developed to allow analysis of the resulting data from such experiments. Progenesis label-free LC-MS software (NonLinear Dynamics) is one such software package. Progenesis displays the MS/MS data as a 2D image, where one axis represents m/z and the other retention time. A reference sample which is most representative of the data is chosen. The 2D image of the reference sample is aligned against the 2D images of each of the other samples in the study to allow identification of matching peak clusters called features, which correspond to peptides. The software can identify all the common features or peptides between the reference sample and remaining samples. Identification of features and aligning of samples allows clean up of data, by the removal of signals resulting from white noise, background ions or chemical noise (Christin, Bischoff et al. 2011). Data analysis was performed separately for each comparison to be analysed. Samples were designated into groups for comparison, while features/peptides were then filtered based on an ANOVA value of less than or equal to 0.2, to identify features/peptides which were present at different levels in the sample groups. The MS/MS data for each peptide which fulfilled the filter criteria was exported to an external database search engine called MASCOT. MASCOT software correlates the uninterpreted MS/MS data with sequences in a database to identify the proteins from which these peptides originated. Each identified peptide is then given a score based on the probability that the observed match between the experimental data and the database sequence is a random event. Resulting peptides are then filtered based on MASCOT score of greater than 40, and hits greater than 1. Subsequent identified proteins are then filtered based on the criteria of ANOVA value less than or equal to 0.05 and identification of at least two unique peptides.

One of the issues associated with label-free LC-MS/MS and Progenesis analysis is the requirement for alignment of sample 2D images against a reference sample (Tuli and

Ressom 2009). Alignment allows correction of experimental variation in the LC dimension between LC-MS/MS runs, which subsequently allows the detection of corresponding peptides in each run (Sandin, Krogh et al. 2011). The reference sample should be chosen as the sample which is most representative of the data; choosing a reference sample which differs greatly from the rest of the data severely affects the quality of the alignment (Sandin, Krogh et al. 2011). In this study we found that choosing the sample with the highest number of detected features as the reference sample gave the most reproducible results. To identify the most robustly changed proteins each comparison was performed three times, using different reference samples with highest number of identified features, for each analysis. Three protein lists were generated for each comparison to be analysed. Only proteins which were present on all three lists were reported in the results section, individual lists are reported in appendix C. Performing the data analysis three times with different reference samples allowed us to identify proteins with increased confidence that these protein changes were the result of a real differential expression rather than a false positive result.

4.3.2.1 All groups analysis

Control sample DS-171 could not be aligned to any reference sample selected; therefore this sample was not included in the analysis. A number of issues could have contributed this problem, such as variability in sample preparation process or variability due to analytical equipment performance (Tuli and Ressom 2009).

Principal component analysis (PCA) plots are a statistical technique commonly used for the identification of patterns in data of high dimensions. PCA plots can be useful when interpreting relationships between different experimental groups. Outliers can also be easily identified from PCA plots. A PCA plot was generated using all sample groups (figure 3.3.16). While distinct cloud clusters were not seen for each individual sample group, the diabetes samples T1DM new (pink spots), T1DM old (blue spots), and control samples (orange and purple spots), were loosely localised in separate quadrants of the cloud cluster. While the autoimmune/inflammatory samples clustered in a similar pattern to the T1DM new samples, indicating that these samples have a similar protein expression pattern. Type 1 diabetes patients have previously been reported to have T cells responsive to a number of islet proteins for up to 1 year post-diagnosis (Brooks-Worrell, Starkebaum et al. 1996; Brooks-Worrell, Greenbaum et al. 2004), therefore the T1DM new samples used in this study which are approximately 3.14 months post diagnosis are likely to still express autoimmune related proteins.

4.3.2.2 Selection of target proteins

Each comparison to be analysed was performed in triplicate using a different reference sample for each replicate. Long lists of proteins were identified as being significantly differentially expressed for each comparison performed. However, only proteins which were consistently changed in each replicate analysis using a different reference sample were reported in the results section, leaving a long list of proteins which were not consistently changed. Therefore, we believe it is a good idea to do repeat analysis of sample data using different reference samples to get a reliable list of differentially expressed proteins.

Proteins for follow-up were selected based on their potential interest in both T1DM newly diagnosed (T1DM new) and established disease (T1DM old) studies. Comparison of control groups used for T1DM new and T1DM old stuies (i.e. control new and control old samples) was also performed to ensure that the proteins of interest were not related to the control samples used, but were indeed patient related. Additionally, comparison of autoimmune versus control samples was performed, to ensure that target proteins, while patient related, were not due to general autoimmune or inflammatory related causes, but rather a diabetes specific effect. Vitronectin, clusterin, vitamin K-dependent protein S and apolipoprotein L1 satisfied the selection criteria and were chosen for further analysis.

Levels of these proteins were quantified using ELISA technology in the same 8 T1DM new, T1DM old and control samples as well as an additional 22 T1DM old samples and matched controls.

4.3.2.3 Vitronectin

Vitronectin belongs to a family of adhesive glycoproteins which play a role in attachment of cells to their surrounding matrix and may be involved in regulation of cell differentiation, proliferation, migration and morphogenesis (Preissner and Jenne 1991; Tomasini and Mosher 1991). Vitronectin is also involved in regulation of complement activation and blood coagulation (Preissner and Jenne 1991). In conjunction with

plasminogen activator inhibitor-1 (PAI-1) levels, vitronectin has been shown to be a marker of metabolic syndrome incidence (Alessi, Nicaud et al. 2011), possibly through its regulatory role in insulin signalling (Lebrun, Baron et al. 2000). Vitronectin depositions have been suggested to be a marker of tissue injury and necrosis, playing a possible role as a protective factor against tissue destruction (Preissner and Seiffert 1998). In our study, increased levels of vitronectin were seen in T1DM new samples (n=8) according to the label-free proteomics analysis; however this finding was not supported by the ELISA data. Higher levels of vitronectin in T1DM new samples could potentially be indicative of recent β-cell destruction in these samples. Conversely, in the T1DM old samples, vitronectin levels were significantly down-regulated (1.14 fold) compared to old controls (n=30).

4.3.2.4 Clusterin

Clusterin, also know as apolipoprotein J, has been proposed to be involved in a number of biological functions including complement activity, lipid transport and apoptosis (Aronis, Kim et al. 2011). A number of studies have evaluated clusterin levels in diabetes patients. Clusterin levels can be measured as circulating clusterin or lipoprotein associated clusterin. In T2DM patients, high circulating clusterin (Trougakos, Poulakou et al. 2002; Kujiraoka, Hattori et al. 2006) and LDL-associated clusterin (Pettersson, Karlsson et al. 2011) have been detected, while low levels of HDL-associated clusterin is seen in patients with metabolic syndrome (Hoofnagle, Wu et al. 2010). Polymorphisms of the clusterin gene have also been associated with prevalence of T2DM (Daimon, Oizumi et al. 2011). Oxidation of lipoproptein lipids is raised in T2DM patients (Dimitriadis, Griffin et al. 1996), therefore altered levels of circulating clusterin and lipoprotein associated clusterin may be related to altered lipid metabolism in these patients (Kujiraoka, Hattori et al. 2006).

Clusterin levels in T1DM are less well studied, as lipid metabolism dysfunction is less extreme in these patients. One previous study identified decreased circulating clusterin levels in T1DM samples compared to controls (Metz, Qian et al. 2008). In our initial biomarker discovery experiment, increased clusterin levels were detected in T1DM new samples compared to controls; however, follow up validation of this target using ELISA

technology did not show any significant change in clusterin levels in these patients. The increased clusterin expression detected in the label-free experiment may have been skewed by the outlier T1DM new sample in pair 1 (figure 3.2.26), which shows almost double the level of clusterin compared to the other T1DM new samples. As the label-free proteomics approach analyses sample groups rather than individual samples, therefore outlier samples could potentially skew the results. Increased clusterin levels in the label-free proteomics could also be as a result of increased LDL- or HDL-associated clusterin. Proteins associated with complexes in serum may be quantified using label-free LC-MS, as long as a protein on the surface of the complex associates with the ProteoMiner^{TM} beads, so the complex is retained. Subsequent sample preparation and digestion steps release all proteins from complexes allowing them to be quantified. However, in an ELISA setup, if the protein is not at the surface of the complex, with the specific epitope exposed for capture antibody recognition, then this protein will not be bound and quantified. Therefore, conflicting results in the label-free proteomics and ELISA data may indicate the involvement of protein complexes, hindering quantification by ELISA.

Increased total clusterin levels in T1DM new samples (according to label-free proteomic analysis) negatively correlated with HDL levels, as T1DM new group had the lowest HDL measurement of the sample groups (table 3.3.4). As with the T2DM and metabolic syndrome studies mentioned previously (Trougakos, Poulakou et al. 2002; Kujiraoka, Hattori et al. 2006; Hoofnagle, Wu et al. 2010; Pettersson, Karlsson et al. 2011), it may be interesting to determine clusterin levels in isolated HDL and LDL complexes in T1DM samples.

4.3.2.5 Vitamin K-dependent protein S

Vitamin K-dependent protein S functions as an anticoagulant, it may also be involved in regulation of complement activation through binding of C4b-binding protein (Dahlback 2007). Protein S can also bind cells undergoing apoptosis and stimulate phagocytosis of these cells (Anderson, Maylock et al. 2003). Label-free proteomic analysis found this protein to be increased in T1DM new samples and decreased in T1DM old samples (n=8). Higher levels of vitamin K-dependent protein S in T1DM new samples may be indicative of increased β-cell apoptosis in these samples, as β-cell apoptosis has been

suggested to be the initiating factor in T-cell mediated autoimmunity associated with type 1 diabetes (Mathis, Vence et al. 2001). Conversely, ELISA validation of this target in the same T1DM new samples showed that Vitamin K-dependent protein S was significantly down-regulated in these patients. As diabetes patients have increased incidence of coagulation abnormalities (Ceriello 1993), a reduced level of the anticoagulant vitamin K-dependent protein S may be a contributory factor to this effect. However, as vitamin K-dependent protein S levels in T1DM new patients are conflicting according to proteomic profiling and ELISA results, the potential of this protein as a biomarker in T1DM patients needs to be further studied.

4.3.2.6 Apolipoprotein L1

Apolipoprotein L1 is a HDL-associated protein (Duchateau, Pullinger et al. 1997). Levels of apolipoprotein L1 were decreased in T1DM old samples compared to controls. Apolipoprotein L1 levels were also shown to be increased in the T1DM new versus T1DM old comparison. However, as no change is seen in T1DM new versus control comparison, therefore the increased level in T1DM new is most likely due to the reduced levels in T1DM old samples rather than an increase in T1DM new apolipoprotein L1 levels. A negative correlation with HDL measurements is also seen with apolipoprotein L1, T1DM old samples with decreased levels of apolipoprotein L1 display the highest HDL measurement of each of the sample groups (table 3.3.5). A number of studies have linked apolipoprotein L1 with non-diabetic renal disease (Tzur, Rosset et al. 2010; Freedman, Langefeld et al. 2011), but in the context of diabetes, this protein is relatively unstudied. The ELISA kit employed in this study was unable to measure apolipoprotein L1 levels in our serum samples; therefore an alternative method for measurement of this protein is required to validate apolipoprotein L1 as a potential biomarker of T1DM.

4.3.2.7 Summary of proteomics target validation

A number of proteomic profiling studies have previously been performed in the attempt to identify biomarkers for early diagnosis, treatment and management of diabetes (Matsumura, Suzuki et al. 2006; Kruger, Yang et al. 2010; Zhang, Sun et al. 2010), as well as biomarkers to detect the onset of secondary complications in these patients (Otu, Can et al. 2007; Madan, Gupt et al. 2010). Of the potential biomarker proteins identified in this study, only clusterin has been previously linked to T1DM (Metz, Qian et al. 2008).

In this study, differentially expressed proteins of interest initially detected by proteomic profiling studies, were further validated by an additional technique, ELISA, to ensure protein changes observed were consistent. In the T1DM new study, the same eight samples used in the profiling experiment were used in the ELISA validation. However, no change was seen in vitronectin and clusterin levels, but decreased levels of vitamin K-dependent protein S were detected, directly opposing the initial result of the proteomic profiling experiment. Four and five unique peptides of vitamin K-dependent protein S were identified for protein ID confirmation; therefore, the opposing results from label-free LC-MS and ELISA technologies on the same samples may potentially indicate the presence of multiple isoforms/variants of vitamin K-dependent protein S in serum. If the capture antibody used in the ELISA is specific for one isoform, this may explain the discrepancies seen between the label-free proteomics and ELISA analysis. As sample numbers are quite small, additional samples would be required to assess the validity of vitamin K-dependent protein S as a potential T1DM new biomarker. In the T1DM old versus control study, additional samples were available for validation of target proteins. Protein levels were assessed in 22 T1DM old samples and controls, in addition to the 8 T1DM old and control samples that were also used for the profiling experiment. In this larger cohort of patients, clusterin and vitamin K-dependent protein S levels were not significantly different. However, vitronectin was significantly decreased in the larger sample group, in agreement with the profiling data. While, in the T1DM new versus T1DM old comparison, no significant change was detected in levels of vitronectin, clusterin and vitamin K-dependent protein S. Lack of correlation between label-free LC-MS and ELISA findings could also be attributed to the sample pre-treatment – ProteoMiner^{TM} if target proteins are associated with high abundance

proteins. As high abundance proteins quickly saturate their ligands, therefore quantitative information on these high abundance proteins and interacting proteins may be effected.

Pancreatic beta-cell specific markers would make ideal biomarkers for T1DM, with decreasing levels leading up to diagnosis of diabetes reflecting the gradual beta-cell destruction seen in these patients in the months prior to diagnosis. However, as serum is such a complex mixture, containing factors secreted from all tissues in the body, it is difficult to detect changes in beta-cell specific proteins, as beta-cells make up a very small percentage of the total cell mass in humans. Biomarkers identified in this study, although seemingly not directly related to pathogenesis of diabetes could potentially be reflective of the effect of beta cell destruction on other cells and tissues in the body, as insulin has many target tissues in the body, a lack of insulin signalling may affect a number of different organs and signalling mechanisms.

4.3.3 Serum metabolite biomarkers

In this study 8 newly diagnosed type 1 diabetes (T1N) serum samples were analysed in comparison to 8 non-diabetic healthy controls. Samples were matched according to age, BMI and gender. Table 3.3.11 shows mean values for general characteristics of control and T1N groups. Fasting plasma glucose and HbA1c tests are used routinely for monitoring glycemic control in diabetes patients. T1N samples show increased fasting glucose and HbA1c values compared to control samples. T1N fasting plasma glucose levels fall within the impaired/pre-diabetes glucose range (table 4.3.1) (Genuth, Alberti et al. 2003). Mean HbA1c level of T1N group is also above the American Diabetes Associations (ADA) recommended level of 7% . T1N serum samples used in this study were taken approximately 3 months following diagnosis, although these patients are receiving insulin therapy, their fasting glucose and HbA1c levels signify the need for optimisation of insulin therapy and glucose monitoring for maintenance of glycemic control.

Condition	Fasting Plasma Glucose
Normal	< 5.6 mmol/L (< 100 mg/dL)
Impaired (Pre-diabetes)	5.6 – 6.9 mmol/L (100 – 125 mg/dL)
Diabetes	> 7.0 mmol/L (> 126 mg/dL)

Table 4.3.1 Diagnostic threshold for diabetes and impaired fasting glucose (Genuth, Alberti et al. 2003).

4.3.3.1 Carbohydrate Metabolism

This study identified 23 metabolites which were present at significantly different levels in our T1N population relative to control. The metabolite with the greatest fold change was 1,5-anhydroglucitol (1,5-AG). 1,5-AG is a naturally occurring unmetabolisable dietary monosaccharide (Yamanouchi, Tachibana et al. 1992). After filtering of the blood by the kidney, 1,5-AG competes with glucose for re-absorption (Akanuma, Morita et al. 1988). When glucose levels rise above the renal threshold for glucose, increased glucose levels prevent re-absorption of 1,5-AG in the kidney, therefore as a direct result of hyperglycaemia, 1,5-AG levels in blood are reduced, while levels in urine are increased (figure 4.3.2) (Yamanouchi, Moromizato et al. 1992; Yamanouchi, Ogata et al. 1996). In this study 1,5-AG levels were decreased by 2.8 fold in T1N patients, in agreement with published effects of glucose on 1,5-AG (Yamanouchi, Moromizato et al. 1992; Yamanouchi, Ogata et al. 1996), these T1N patients also exhibit higher fasting glucose levels of approximately 1.5 fold, as measured by metabolic profiling by Metabolon, as well as part of routine blood work performed at Connolly Hospital, Blanchardstown following sample collection. 1,5-AG has also been identified in recent metabolomic profiling studies of type 2 diabetes in humans (Suhre, Meisinger et al. 2010) and a rodent model of hepatic insulin resistance (Li, Hu et al. 2010). In agreement with our observations and previously published data (Yamanouchi, Moromizato et al. 1992; Yamanouchi, Ogata et al. 1996), decreased 1,5-AG levels in type 2 diabetes serum was accompanied by higher levels of glucose relative to control non-diabetes serum (Suhre, Meisinger et al. 2010). While in the rodent model of hepatic insulin resistance, 1,5-AG levels were shown to be decreased in both liver and plasma samples (Li, Hu et al. 2010).

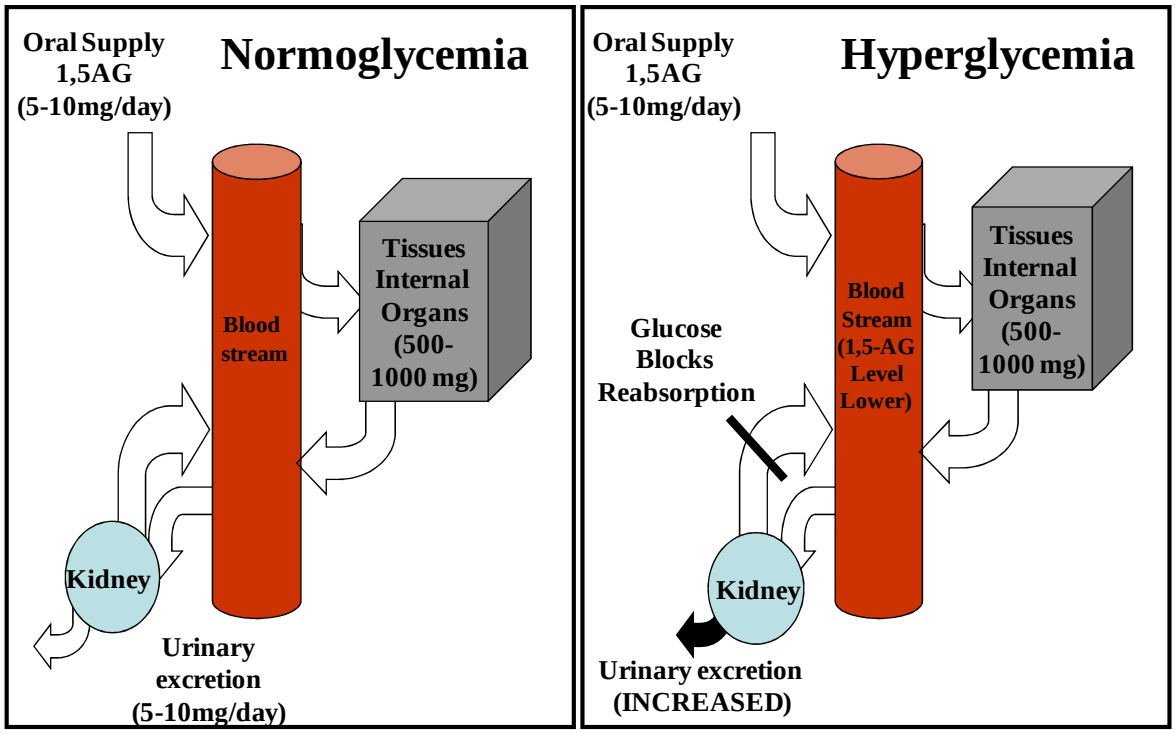

Figure 4.3.2 1,5-anhydroglucitol in normoglycemic and hyperglycaemic conditions. During normoglycemia 1,5-AG is filtered in the kidneys and reabsorbed into the blood stream, maintaining constant levels in the blood. Under hyperglycaemic conditions glucose competes with 1,5-AG for reabsorption in the kidneys, thereby causing reduced levels of 1,5-AG in blood and increased levels in urine.

Routinely used markers for glycemic control such as HbA1c and fructosamine give an average value for glycemic control; this average value may mask glycemic instability as hyperglycaemic events may be balanced by hypoglycaemic events (Dungan, Buse et al. 2006). Patients with seemingly well controlled diabetes, HbA1c values between 6.5 – 8%, may experience significant postprandial hyperglycaemia (Erlinger and Brancati 2001). 1,5-AG levels correlate more robustly with post-prandial glucose compared to HbA1c (Yamanouchi, Inoue et al. 2001; Dungan, Buse et al. 2006). 1,5-AG levels also respond more rapidly to fluctuations in glucose levels (Yamanouchi, Moromizato et al. 1992; Yamanouchi, Ogata et al. 1996). Therefore 1,5-AG may be of use as a marker of short-term post-prandial glucose control in patients at or near target HbA1c levels (Kishimoto, Yamasaki et al. 1995; McGill, Cole et al. 2004; Dungan, Buse et al. 2006). A reduction of 1,5-AG levels in serum from patients with pre-diabetes conditions-impaired glucose tolerance and impaired fasting glucose, indicates the possible use of 1,5-AG screening for determining patients at risk of developing diabetes (Tsukui, Fukumura et al. 1996; Won, Park et al. 2009).

Other metabolites involved in glucose metabolism such as pyruvate and lactate also showed slightly decreased levels in T1N patients (1.6 and 1.2 fold respectively), however, this reduction was not statistically significant (figure 4.3.3). Low levels of lactate have previously been observed in studies of Type 1 diabetes, Type 2 diabetes and hepatic insulin resistance (Bao, Zhao et al. 2009; Lanza, Zhang et al. 2010; Li, Hu et al. 2010). High serum levels of glucose, in conjunction with low levels of 1,5-AG and glycolysis end products- pyruvate and lactate could possibly indicate a reduction of glucose utilisation, or glucose transportation into cells in T1N patients. Transport of glucose across the cell membrane is the rate limiting step in glucose utilisation pathways in mammals (Pickup and Williams 1997), inefficient insulin levels may hinder transport of glucose into target cells, leading to lower levels of glycolysis intermediates.

Other glycolysis intermediates were not detected in this serum study, as all nine glycolysis intermediates are phosphorylated, which prevents these high energy sugar molecules from leaving the cell as cell membranes generally lack transporter molecules for phosphorylated sugars (Nelson and Cox 2005).

Pyruvate, the end-product of glycolysis, is the starting material in the TCA cycle. Possibly due to the reduced pyruvate, lower levels of some TCA cycle intermediates and by-products- malate and succinylcarnitine were seen in T1N samples (1.72 and 1.37 fold respectively) (figure 4.3.3). Succinylcarnitine is likely formed from TCA cycle component succinyl CoA (Carrozzo, Dionisi-Vici et al. 2007). High glucose levels in addition to low levels of TCA cycle intermediates have also been reported in studies of type 2 diabetes and impaired glucose regulation (Zhang, Wang et al. 2009).

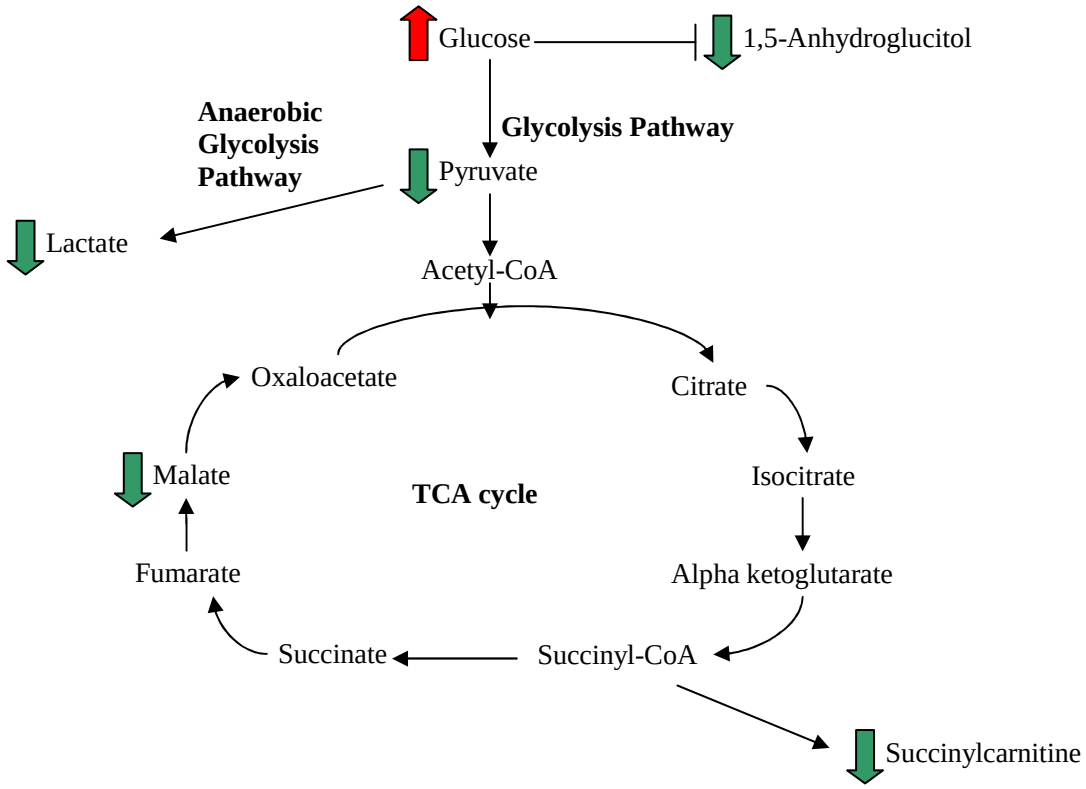

Figure 4.3.3 Glycolysis and Citric Acid Cycle. Molecules marked with red arrow were present at higher levels and molecules marked with green arrow were present at lower levels in serum from newly diagnosed Type 1 diabetes patients.

Lactate levels generated in muscle tissue through anaerobic glycolysis are transported to the liver to undergo gluconeogenesis. This transport of lactate from muscle to liver is known as the Cori cycle (figure 4.3.4). Reduced levels of lactate may indicate reduced Cori cycle activity in T1N patients.

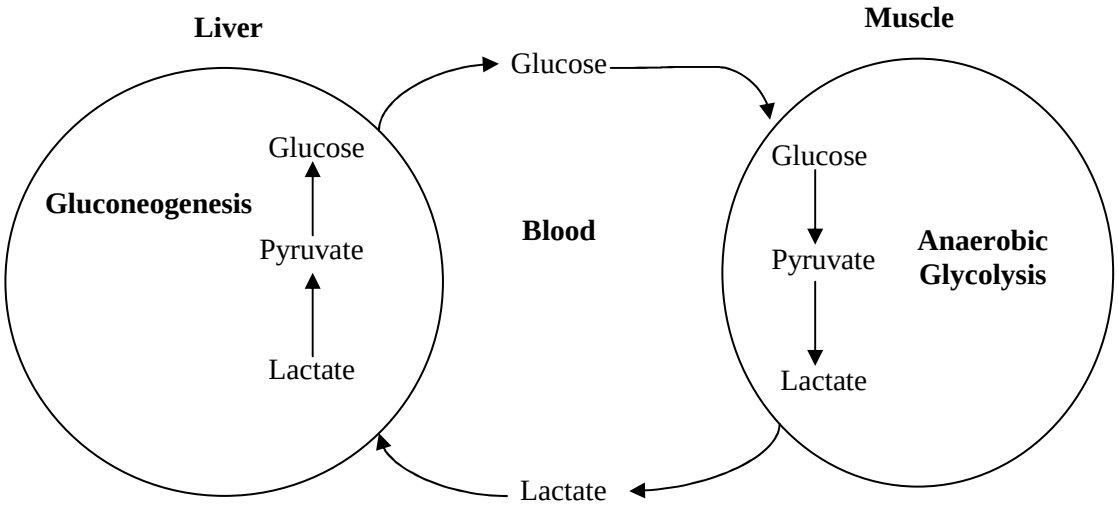

Figure 4.3.4 Cori Cycle. Lactate produced in muscle under anaerobic glycolysis is transported to the liver to undergo gluconeogenesis where glucose supplies are replenished and then transported back to the muscle for energy.

4.3.3.2 Fat Metabolism

The lipid profile of serum samples was measured along with the routine blood work at Connolly Hospital, Blanchardtown. Total triglycerides, cholesterol, HDL-cholesterol and LDL-cholesterol were lower in T1N serum compared to control serum. Metabolomic analysis also showed that cholesterol was slightly lower in T1N patients (1.09 fold), but not significantly so. Poorly controlled type 1 diabetes patients can exhibit raised cholesterol, triglyceride and LDL-cholesterol levels, in addition to low HDL-cholesterol levels (Pickup and Williams 1997), however, the within-normal range lipid profile (table 4.3.2) of T1N patients used in this study indicates that they are relatively well controlled. Total cholesterol and LDL-cholesterol values for control samples were beyond the Irish Heart Foundations (http://www.irishheart.ie/iopen24/) recommended healthy values (table 4.3.2). Lower cholesterol and triglyceride levels in T1N serum specimens could be indicative of a healthier diet and lifestyle. High cholesterol levels in control serum could also be indicative of genetic predisposition to high cholesterol; however, none of the control specimens included in this study has reported familial hypercholesterolemia.

Lipid Profile	Recommended Level (mmol/L)
Total cholesterol	< 5
LDL cholesterol	< 3
HDL cholesterol	> 1
Triglycerides	< 2

Table 4.3.2 Healthy cholesterol and triglyceride levels, as recommended by the Irish Heart Foundation.

Fatty acid dicarboxylates- sebacate and 3-carboxy-4-methyl-5-propy-2-furanpropanoate (CMPF) were present at significantly lower levels in serum from T1N patients compared to control serum, at 1.47 and 1.72 fold respectively. Serum fatty acids may originate from 3 different sources, 1- fatty acids consumed in the diet, 2- stored in adipocytes as triglycerides, or 3- be biosynthesized in the body from excess glucose (Nelson and Cox 2005).

Decreased levels of fatty acid dicarboxylates seen in T1N patients could potentially be indicative of decreased levels of lipolysis in the adipose tissue, or reduction of fatty acid biosynthesis. Fatty acid biosynthesis requires acetyl-CoA, most of which is obtained from pyruvate oxidation (Nelson and Cox 2005), as pyruvate levels are decreased in T1N samples (1.6 fold), this may lead to reduced fatty acid biosynthesis.

Reduced lipolysis could also be the cause of decreased serum fatty acid dicarboxylate levels in T1N serum. High levels of lipolysis are characteristically seen in untreated or poorly controlled type 1 diabetes patients, therefore lower levels of fatty acid dicarboxylates and reduced lipolysis indicates that these patients are well-controlled.

Lipolysis involves the hydrolyzation of adipose tissue stored triglycerides into free fatty acids when hormones signal the need for metabolic energy. FFAs can then pass into the blood stream and travel to sites of energy requirements. β-oxidation is the breakdown of FFAs to acetyl coenzyme-A (CoA), which can enter the TCA cycle to generate energy. β-oxidation of FFAs occurs in the mitochondrial matrix and in order for FFAs to access the mitochondrial matrix they must be transported via a carnitine shuttle (figure 4.3.5). Firstly FFAs undergo conjugation to CoA generating fatty acyl-CoA. Fatty acyl-CoA is then transiently attached to carnitine via a transesterification reaction to form fatty acyl-carnitine, which can then be translocated into the mitochondrial matrix via the acyl-carnitine transporter. Once inside the mitochondrial matrix the fatty acyl-CoA is regenerated while the carnitine molecule is released and transported back into the intermembrane space ready to transport the next fatty acyl-CoA molecule (Nelson and Cox 2005). In this study, a number of these fatty acyl-carnitine compounds were present at lower levels in the T1N group compared to controls.

Propionylcarnitine and hexanoylcarnitine levels were significantly lower in T1N versus control group by 1.39 and 1.47 fold respectively. While butyrylcarnitine (1.72 fold), deoxycarnitine (1.15 fold), carnitine (1.15 fold), acetylcarnitine (1.18 fold), octanoylcarnitine (1.54 fold) and decanoylcarnitine (1.32 fold) were also present at slightly lower levels in diabetes patients, but these changes were not significant. A number of acyl-carnitines including propionylcarnitine and hexanoylcarnitine have previously been reported to correlate with insulin resistance (Gall, Beebe et al. 2010; Li, Hu et al. 2010).

Decreased levels of fatty acyl-carnitine compounds in T1N group could indicate a reduced level of β-oxidation in these patients. Lower levels of carnitine were also seen in diabetes serum relative to control. As carnitine-shuttle mediated transportation of fatty acyl-CoA molecules into the mitochondrial matrix is the rate limiting step of fatty acid β-oxidation, therefore lower levels of free carnitine would lead to lower levels of fatty acid β-oxidation, and subsequently lower levels of fatty acid dicarboxylates.

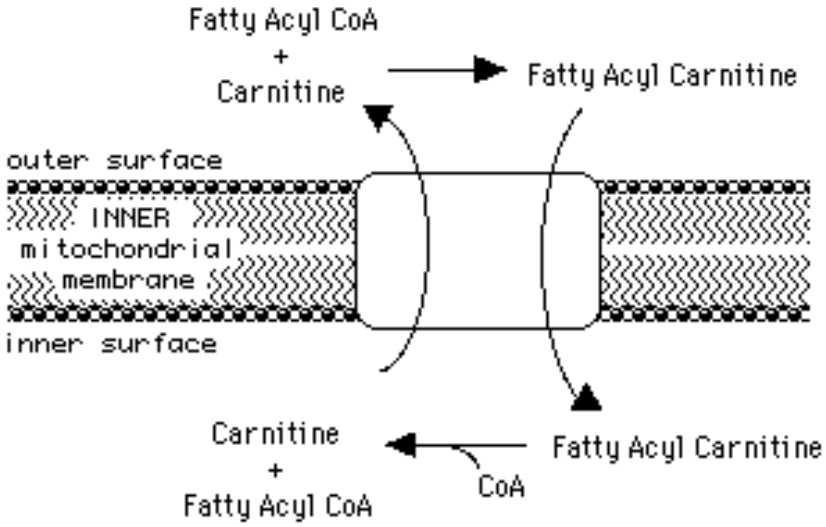

Figure 4.3.5 Transport of fatty acyl-CoA into mitochondria by the carnitine shuttle. Image taken from Mountain West Digital Library, Utah Academic Library Consortium (http://mwdl.org/index.php/home).

During low glucose conditions such as fasting, the brain cannot utilise fatty acids for energy, therefore acetyl-CoA from fatty acid β-oxidation is converted to ketone bodies. The ketone body- 3-hydroxybutyrate, is the main energy source for the brain under fasting conditions (Owen, Morgan et al. 1967). Raised levels of 3-hydroxybutyrate were seen in serum from T1N patients relative to controls. Raised levels of 3-hydroxybutyrate have also been seen in serum from type 2 diabetes patients (Suhre, Meisinger et al. 2010). Ketone bodies are known to be raised in the insulin deficient state (Balasse and Fery 1989). Insulin inhibits ketogenesis, while insulin deficiency stimulates it (Johnston and Alberti 1982; McGarry, Woeltje et al. 1989). Ketogenesis is necessary in small amounts; however, excess ketogenesis as a result of insulin deficiency can lead to diabetic ketoacidosis.

The lysolipid- 1-pentadecanoylglyerophosphocholine was also present at significantly lower levels (1.82 fold) in diabetes serum relative to control serum. Lysolipids are involved in the formation of lipid bilayers of cell membranes. Of the 16 lysolipids detected in this study 1-pentadecanoylglycerophosphocholine is the only lysolipid which is significantly changed in diabetes serum. No obvious trend was seen in the other lysolipids analysed.

Previous studies have shown altered levels of free fatty acids (Li, Xu et al. 2009; Gall, Beebe et al. 2010; Lucio, Fekete et al. 2010), long chain fatty acids (Bao, Zhao et al. 2009), essential fatty acids (Li, Xu et al. 2009; Lucio, Fekete et al. 2010), acyl-carnitines (Gall, Beebe et al. 2010) and ketone bodies (Huo, Cai et al. 2009; Gall, Beebe et al. 2010; Suhre, Meisinger et al. 2010) in type 2 diabetes and insulin resistant patients. Although lipid abnormities occur more frequently in type 2 diabetes patients (Pickup and Williams 1997), we have identified changes in lipid metabolites in serum from type 1 diabetes patients compared to control samples. Altered lipid metabolism is also seen in children who later develop type 1 diabetes, these lipid changes are evident before the patients exhibit autoantibody positivity (Oresic, Simell et al. 2008), therefore lipid metabolites may represent a good target for screening patients at risk of developing type 1 diabetes.

Lipid metabolite changes identified in this study cannot be conclusively determined to be related to the T1DM disease state. As control samples used in this study displayed

high cholesterol, this may have a knock on effect on lipid metabolism; therefore metabolite changes may be more characteristic of high cholesterol rather than the presence of diabetes.

4.3.3.3 Amino Acid Metabolism

A number of amino acid metabolites were also significantly changed in diabetes patients relative to control. Of the 247 amino acid metabolites detected in these serum samples, 7 were significantly different in T1N versus control, indicating that no vast differences were present in amino acid metabolism of diabetes and control patients. Altered amino acid metabolism has also previously been reported in metabolomic profiling studies of type 1 diabetes (Oresic, Simell et al. 2008; Zhang, Nagana Gowda et al. 2008; Lanza, Zhang et al. 2010; Godzien, Ciborowski et al. 2011), type 2 diabetes (van Doorn, Vogels et al. 2007; Bao, Zhao et al. 2009; Cai, Huo et al. 2009; Huo, Cai et al. 2009; Zhang, Yan et al. 2009; Connor, Hansen et al. 2010; Suhre, Meisinger et al. 2010) and impaired glucose tolerance / insulin resistance (Atherton, Bailey et al. 2006; Zhang, Wang et al. 2009; Gall, Beebe et al. 2010; Lankinen, Schwab et al. 2010; Li, Hu et al. 2010; Tsutsui, Maeda et al. 2010; Zhao, Fritsche et al. 2010) studies.

The amino acids arginine and glutamine were present at significantly increased levels in T1N samples relative to control, 1.56 and 1.14 fold respectively (table 3.3.14). Increased levels of amino acids could be an indication of increased proteolysis or increased amino acid synthesis. However, increased levels of protein metabolites in overnight fasting serum samples generally indicate increased proteolysis in the fasting state, to allow the release of amino acids for oxidation and energy production (Pickup and Williams 1997). Arginine and glutamine are glucogenic amino acids, therefore, on amino acid degradation the carbon skeleton of these amino acids are diverted to gluconeognesis (figure 4.3.6) (Nelson and Cox 2005). Arginine is also a urea cycle intermediate (figure 4.3.6), further indicating an increase in proteolysis, as the urea cycle functions to convert ammonia from amino acid oxidation to urea for excretion. Glutamine is also a major component of amino acid oxidation (figure 4.3.6). Ammonia generated from amino acid oxidation is toxic to tissues, therefore, it is combined with glutamate to yield glutamine, which can then be transported safely to the liver or kidneys for excretion (Nelson and Cox 2005). Therefore, increased levels of glutamine

also suggest increased activity of the amino acid degradation pathway. Increased levels of glutamine were also identified in a study of type 2 diabetes serum (van Doorn, Vogels et al. 2007). Newly presenting patients with type 1 diabetes and patients with poorly controlled established diabetes typically exhibit increased protein catabolism and muscle wasting (Pickup and Williams 1997). However, as arginine and glutamine were the only amino acids to show increased levels in T1N patients and the fold change of these metabolites was relatively small, below 1.6 fold, this may indicate that these patients were in relatively good metabolic control at the time the samples were taken, as also indicated by HbA1c levels of approximately 7.69. Enhanced urea cycle activity has previously been suggested to be a feature of hepatic insulin resistance (Li, Hu et al. 2010), therefore this could indicate that these patients are beginning to display effects of insulin resistance.

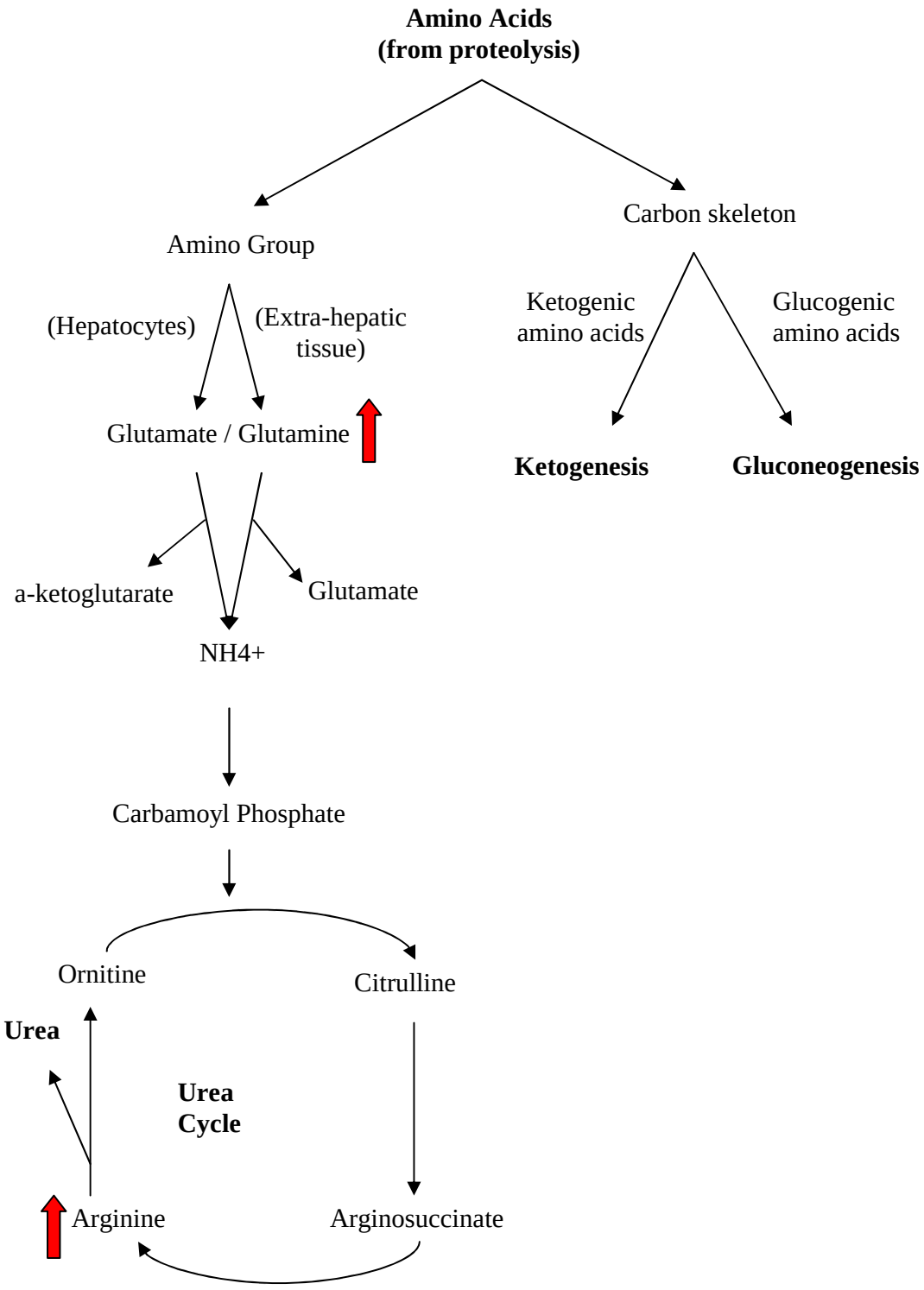

Figure 4.3.6 Overview of amino acid catabolism. Glutamine and arginine shown with red arrows were increased in serum from T1N patients relative to control serum.

Other proteolysis and amino acid oxidation related metabolites which were significantly different include isovalerylcarnitine, 2-methylbutyroylcarnitine and propionylcarnitine involved in valine, leucine and isoleucine metabolism were down regulated by 1.92, 1.64 and 1.39 fold respectively, in T1N serum compared to control. Isovalerylcarnitine, 2-methylbutyroylcarnitine and propionylcarnitine have also been shown to correlate with impaired glucose tolerance and impaired fasting glucose (Gall, Beebe et al. 2010). As valine, leucine and isoleucine are essential amino acids, and cannot by synthesized in the body, therefore metabolites of these amino acids are an indication of amino acid oxidation rather than amino acid synthesis. Valine, leucine and isoleucine amino acids contain aliphatic side chains and are therefore known as the branched chain amino acids (BCAA). BCAAs have previously been reported to be of significance in diabetes, with raised BCAA levels presenting prior to autoantibody positivity in children which later develop type 1 diabetes (Oresic, Simell et al. 2008). Increased levels of BCAAs are also seen in poorly controlled type 1 and type 2 diabetes patients (Vannini, Marchesini et al. 1982; Tessari, Biolo et al. 1990; Lanza, Zhang et al. 2010). As BCAA metabolites in this study were decreased this may indicate that the patients used in this study were under good metabolic control. BCAAs and BCAA metabolites may be useful for detection of people who will develop type 1 diabetes later in life, and also for monitoring of metabolic control in patients with established diabetes.

N-acetyl threonine involved in threonine metabolism, another essential amino acid, was also down regulated by 1.54 fold in T1N samples. 5-oxyproline, involved in glutathione metabolism was also down regulated 1.16 fold in T1N patient serum.

Essential amino acid metabolites were seen to be present at lower levels in T1N patients compared to control. These amino acids cannot be synthesized in the body and need to be taken up in the diet, therefore lower levels of essential amino acid metabolites could indicate a lower level of essential amino acid intake in the diet or reduced essential amino acid oxidation in the body. Conversely, non-essential or conditionally essential amino acid metabolites are present at higher levels, indicating increased levels of non-essential amino acid oxidation. If low levels of essential amino acids are taken up in the diet these amino acids are required for protein synthesis, while surplus non-essential amino acids may be oxidised for energy production.

4.3.3.4 Nucleotide Metabolism

Urate levels were significantly decreased in T1N samples relative to control, by 1.23 fold. Urate is formed from the degradation of purine containing nucleotides (adenine and guanine), and is excreted in the urine. Altered urate levels have previously been linked to development of insulin resistance (Gall, Beebe et al. 2010), type 2 diabetes (Lin, Tsai et al. 2004; Bao, Zhao et al. 2009; Gall, Beebe et al. 2010), and kidney dysfunction in diabetes (Fukui, Tanaka et al. 2008; Xia, Liang et al. 2009). Low levels of urate could indicate reduced activity of nucleotide catabolism, due to either reduced purine intake in the diet, or reduced proteolysis, or could indicate altered excretion of urate by the kidneys. Altered urate levels may also be indicative of kidney dysfunction, however, kidney function markers creatinine and 3-indoxyl sulphate were unchanged in the T1N serum samples used in this study, relative to control serum.

11 nucleotide related metabolites were detected in the samples used in this study. However, as urate was the only significantly altered nucleotide-related metabolite in T1N versus control samples, and the fold change was quite low, therefore the alterations in nucleotide metabolism in T1N serum were relatively minor.

4.3.3.5 Benzoate Metabolism

Benzoates are frequently used as preservatives for acidic foods such as fruit juices and soft drinks (Warth 1991). Increased levels of catechol sulphate, a benzoate metabolite could indicate that T1N patients consume more benzoate containing food items than the control group.

4.3.3.6 Caffeine Metabolism

Caffeine metabolism was the most obviously altered pathway in T1N compared to control samples. Of the 7 caffeine related metabolites detected in these samples, all 7 metabolites were down-regulated in T1N samples. Caffeine (2.5 fold), paraxanthine (1.78 fold), theophylline (1.89 fold), 1,3-dimethylurate (1.37 fold) and 1,7-dimethylurate (1.67 fold) were all significantly down-regulated. While theobromine and

1,3,7-trimethylurate were not significantly down-regulated they still followed the same trend.

An obvious explanation for this trend would be that the T1N patients consumed lower levels of caffeine containing products. The control samples used in this study were taken from healthy medical interns. The intern year of medical training is well known to be very demanding and stressful. It is generally accepted that people in high stress jobs tend to drink more coffee than those in less stressful jobs (Conway, Vickers et al. 1981), therefore it is likely that the reduced levels of caffeine and caffeine related metabolites in T1N samples are due to the higher than normal caffeine consumption of the control group.

Caffeine is also known to have a negative effect on insulin sensitivity (Keijzers, De Galan et al. 2002). While patients in this study were not specifically advised against caffeine consumption, some may have become aware of the effect of caffeine on their disease through their own research, and are limiting caffeine intake accordingly.

4.3.3.7 Peptides

A number of peptides were also detected by the metabolon platform. The fibrinogen cleavage peptide – fibrinopeptide A (FPA) was significantly increased in T1N samples. FPA is produced during the clotting process, when thrombin cleaves fibrinogen to produce fibrin and fibrinopeptide. Up-regulation of FPA has previously been reported in type 1 (Gianazza, Mainini et al. 2010) and type 2 diabetes (Meigs, D'Agostino et al. 1997), and may be associated with diabetic nephropathy (Gianazza, Mainini et al. 2010).

FPA levels were validated in the same 8 T1N and control samples used in the metabolomic profiling study using an ELISA. The ELISA showed a significant up-regulation of FPA levels in T1N samples compared to controls (figure 3.3.36). Additionally, FPA levels were quantified in 30 T1DM old and control samples, to determine if this change in FPA levels was specifically related to newly diagnosed diabetes, or a more general diabetes marker. When looking at the additional T1DM old and control old sample groups, it appears than FPA levels are reduced in control new samples, rather than increased in the T1N samples, as originally thought (figure 3.3.41). Altered levels of FPA have previously been linked with alcohol consumption (Nomura, Tomonaga et al. 2004). T1N patients in this study, on average consume 5.8 units of alcohol per week, while this number is raised to 14.3 for the control new subjects. While this difference in alcohol consumption is not statistically significant, it may play a role in the altered levels of FPA in these samples. These results may also indicate potential dysregulation of FPA in the control old samples, possibly due to clotting related issue in these patients, however, no clotting or coagulation related conditions had been diagnosed in these patients at the time of sample collection.

4.3.3.8 Metabolites as biomarkers

Twenty-three metabolites were significantly different between T1N and control serum, incorporating metabolites from varying pathways of carbohydrate, lipid and amino acid metabolism. Untreated diabetes is characterised by increased carbohydrate anabolism via gluconeogenesis, in addition to increased lipid and amino acid catabolism. Diabetes patients used in this study have been on insulin treatment for approximately 3 months, the metabolomic profiling of these patients shows that while some differences in these metabolic pathways still remain, these patients are in relatively good metabolic control.

The usefulness of multiple markers for diagnosis, prognosis and for predicting the risk of developing diseases or their complications is now widely recognised (Landers, Burger et al. 2005; Zethelius, Berglund et al. 2008). Metabolite biomarkers have been used extensively over the years for monitoring disease, e.g. glucose for diabetes, cholesterol for heart disease. Individual metabolites can also be very easily and rapidly quantified using biochemical assays or ELISAs, once a select panel has been identified for a particular disease. Biomarkers for early diagnosis of type 1 diabetes, could potentially allow treatment of the autoimmune disease before extensive beta cell death has occurred, thereby potentially avoiding the need for insulin therapy and the long term secondary complications of diabetes, such as diabetic nephropathy, retinopathy and microvascular disease.

However, to conclusively determine if the metabolites identified in this study are of use as biomarkers for early diagnosis, these metabolites would need to be analysed in a larger cohort of patients at various stages of development of the disease.

5.0 Summary and Conclusions

5.1 MIN6 as a model for studying GSIS

- MIN6 cells exhibit glucose stimulated insulin secretion (GSIS) when exposed to 3.3mM to 16.7mM glucose concentrations. With increasing time in culture the GSIS response of these cells diminishes.
- Some assays performed during the course of this study needed to be repeated a large number of times to determine if the treatment effects on GSIS were significant, as we observed considerable interplate variations in GSIS and basal insulin secretion. Also, the same pre/anti-mirs and controls sometimes stimulated or decreased insulin secretion.
- However, in spite of these problems, as there is no human pancreatic beta cell line available, in order to study the mechanisms of GSIS we had no alternative but to continue this study with MIN6 cells; being mindful of its limitations.

5.2 MicroRNAs involved in glucose stimulated insulin secretion

- MIN6 cells at passage 37 showed a glucose concentration-dependent increase in insulin secretion producing a 3.3 fold increased insulin secretion when glucose stimulation was increased from 3.3 mmol/L to 16.7 mmol/L for 1 hr and so these cells were subsequently termed glucose-responsive MIN6 cells. In contrast, the same increase in glucose concentration when added to MIN6 cells at passage 40 resulted in 1.3-fold increase in insulin secretion only i.e. non-glucose responsive MIN6 cells (figure 3.1.1).
- Gradual loss of GSIS was observed in continuously cultured MIN6 cells from passage 37 to 40 (figure 3.1.1).
- TaqMan low density miRNA arrays were performed on passage 37 glucose responsive and passage 40 glucose non-responsive MIN6 cells. 12 miRNAs were identified as differentially expressed in these two cell populations (table 3.1.2). All 12 were down-regulated in glucose non-responsive cells. This data was presented at RNAi 2008, Oxford, UK (see poster appendix E).

- 21 novel murine miRNAs were also detected in MIN6 cells in this study, these 21 miRNAs have not been previously reported to be present in mouse cells (table 3.1.1).
- Validation of the TLDA miRNA targets showed that 5 of the 12 targets were not significantly differentially expressed using single-plex PCR (table 3.1.3).
- Bioinformatic analysis using MiRanda software identified putative targets of differentially expressed miRNAs from microarray and proteomics profiling data on glucose responsive and glucose non-responsive MIN6 cells (table 3.1.4). Among these miRNA targets were a number of genes considered important for beta cell function, such as *neuroD1*, *Isl1 and txnip*. Txnip knockdown has previously been shown to increase GSIS responsiveness in MIN6 cells. Mir-200a and mir-130a may potentially mediate their effect on GSIS by regulation of Txnip.
- Functional validation of miRNA targets was performed using pre-mirs and anti-mirs for over- and under-expression of miRNAs. All miRNA targets were under-expressed in non-glucose responsive cells in TLDA analysis; therefore, over-expression using pre-mirs would be expected to improve GSIS in MIN6 cells, while under-expression using anti-mirs would be expected to reduce GSIS in MIN6 cells.
- Due to large variations in GSIS response of control cells, pre-mir and anti-mir transfections were performed a number of times to achieve consistent GSIS response in the control untreated and negative control (am-neg and pm-neg) cells, to allow effect of over-expression and knockdown of target miRNA on GSIS response to be assessed.
- Knockdown of mir-410 in GSIS-competent cells using anti-mir-410 led to a significantly reduced GSIS response in these cells compared to untreated and negative control cells (figure 3.1.5). Over-expression of mir-410 in GSIS-competent cells using pre-mir-410 led to a significant increase in GSIS responsiveness (figure 3.1.6).
- Knockdown of mir-200a in GSIS-competent cells using anti-mir-200a led to a significant decrease in GSIS response (figure 3.1.7). No consistent effect was seen on GSIS for over-expression of mir-200a.

- Knockdown of mir-130a in GSIS-competent cells using anti-mir-130a led to a significant decrease in GSIS (figure 3.1.8). No significant difference was seen in GSIS-competent cells treated with pm-130a for over-expression of mir-130a.
- No significant changes were seen in GSIS response in cells treated with pre-mirs and anti-mirs for mir-376a, mir-369-5p, mir-27a, mir-124a, mir-337, mir-532, mir-320, mir-192 and mir-379.
- MiRNAs identified in this study as exhibiting functional effects on GSIS could potentially represent therapeutic targets for manipulation to maintain/restore GSIS in insulin-producing cells. However, the mechanism by which these miRNAs are involved in insulin secretion still remains to be elucidated.
- Study of miRNAs involved in GSIS in MIN6 cells was published as: Hennessy E., Clynes M., Jeppesen P.B. and O'Driscoll L. 2010 Identification of microRNAs with a role in glucose stimulated insulin secretion by expression profiling of MIN6 cells. BBRC 396(2):457-62 (appendix E).
- The MIN6 cell line as a model for studying GSIS can be undependable due to considerable day to day variations in GSIS response between control cells. This varying GSIS response of control cells makes it difficult to decipher effect of treatment on GSIS i.e. the assay, while being the best available is not robust or routinely dependable.
- During the course of this study, somatic cell reprogramming and induced pluripotent stem cell generation was beginning to be widely reported in the literature, following the landmark paper by Yamanaka et al in 2006 (Takahashi and Yamanaka 2006; Takahashi, Tanabe et al. 2007). This new technology represented a route to developing human pancreatic beta cells *in vitro* from iPS cells for the study of GSIS.

MicroRNA	Anti-Mir knockdown of miRNA	Pre-Mir over-expression of miRNA
mir-376a	No effect	No effect
mir-369-5p	Reduced GSIS minimally	No effect
mir-130a	Reduced GSIS *	Reduced GSIS minimally
mir-27a	No effect	No effect
mir-410	Reduced GSIS *	Improved GSIS *
mir-124a	No effect	No effect
mir-200a	Reduced GSIS *	No effect
mir-337	No effect	No effect
mir-532	No effect	No effect
mir-320	No effect	Reduced GSIS minimally
mir-192	No effect	Reduced GSIS minimally
mir-379	No effect	Reduced GSIS minimally

Table 5.1 Functional validation of miRNA targets in MIN6 cells. (* denotes statistical significance).

5.3 Attempt to generate iPS cells and differentiation of an established iPS cell line towards pancreatic phenotypes

5.3.1 Attempt to generate iPS cells

- Four retro-viruses were generated to over-express oct4, sox2, c-myc and klf4 in transduced target cells. Optimised transduction conditions were identified to achieve up to 80% transduction efficiency after 72 hours, measured using GFP (figure 3.2.3)
- Attempts were made to generate iPS cells from a number of different cell types
    - MiaPaCa2 pancreatic adenocarcinoma cell line
    - Normal human epidermal keratinocytes
    - Limbal epithelial cells
- Virus-treated MiaPaCa2 cells displayed morphological changes, cell colonies with a tightly packed dense core but uneven colony edges were seen (figure 3.2.7). PCR analysis of these colonies indicated that they expressed oct4, c-myc and klf4, but at similar levels to parental untreated MiaPaCa2 cells. Very low sox2 expression was seen in one virus treated clone, however, this low sox2 expression was evidently not sufficient to drive full reprogramming (figure 3.2.8).
- Virus-treated keratinocytes also displayed morphological changes, but similar morphology changes were also seen for control keratinocytes not treated with virus; therefore, the morphology changes observed were probably a result of growth on MEF feeder layer rather than viral transduction (figure 3.2.10). Virus treated and control keratinocytes did not proliferate once transferred to MEF feeder layer culture, therefore, PCR analysis could not be performed to check if they expressed the four factors (oct4, sox2, c-myc and klf4).
- Morphological changes were also seen in virus-treated limbal epithelial cells. Virus-treated cultures displayed cell processes and cell clusters, while untreated cultures displayed typical cuboidal morphology (figure 3.2.12). Unfortunately, virus-treated cells did not proliferate further, therefore oct4, sox2, c-myc and klf4 expression could not be examined.

5.3.2 Attempts to generate iPS cells using conditioned media

- Attempts were also made to reprogram limbal epithelial cells using conditioned media from the murine embryonic stem cell line ESD3 (Balasubramanian, Babai et al. 2009). Cells were firstly treated with enriched media for 7 days (stage 1), followed by treatment with ESD3 conditioned media (ESD3 CM) for 14 days (stage 2).
- Cell morphology changes were seen in ESD3 conditioned media treated cells; cell clusters formed initially, but did not proliferate much further, while a fibroblast-like cell type proliferated rapidly until confluence (figure 3.2.16). Control cells maintained in enriched media (extended stage 1) displayed similar morphology to untreated limbal epithelial cells (figure 3.2.16).
- PCR analysis showed that parental cells expressed c-myc, oct4 and klf4, expression of these factors was maintained in control and ESD3 CM treated cells, however, treatment did not induce expression of the stem cell marker sox2 (figure 3.2.17).
- ESD3 CM treated cells lack expression of the differentiation markers CK-3 and CK-12 and have high expression of the stem cell associated marker N-cadherin. These cells lack expression of stem cell markers ABCG2 and nanog, indicating that these cells are not fully reprogrammed (figure 3.2.18). These cells may represent a semi-reprogrammed state.

.

5.3.3 Differentiation of an established iPS cell line towards pancreatic phenotypes

- During the course of this study iPS cell lines became commercially available from the George Daley lab, Children's Hospital, Boston. The hFib-iPS2 cell line was purchased for pancreatic differentiation experiments, as we had not achieved fully reprogrammed iPS cells from our own attempts.
- Directed differentiation was performed in 2D and 3D cultures. 2D cultures consisted of cells grown on top of a thin matrigel layer, while in 3D culture cell clusters were suspended within a thick matrigel/collagen layer. Differentiation growth factor cocktail was used as described by Jiang J. et al., (Jiang, Au et al. 2007).

- iPS cells differentiated in 3D culture showed improved efficiency for definitive endoderm formation compared to 2D culture, based on expression of definitive endoderm markers cxcr4, foxa2 and hnf4α (figure 3.2.21). This work was presented at 'Stem Cells in Development and Disease 2011' in Berlin, Germany (see poster appendix E).
- Further differentiation of 2D cultures towards pancreatic endoderm and pancreatic endocrine cells failed, as cell died off after the definitive endoderm stage.
- Untreated iPS cells expressed mature pancreatic markers- somatostatin and amylase, indicating that iPS cells may have undergone some spontaneous differentiation before initiation of differentiation experiment.
- 3D control cells maintained in iMEF conditioned media at 36 days displayed induced expression of insulin, ghrelin and glut2 (figure 3.2.26). Therefore the use of 3D culture, or growth factors present in the matrigel may be responsible for induction of mature pancreatic markers in these control cells. Similar results were observed in the repeat experiment (figure 3.2.29), while somatostatin and amylase were present in untreated iPS cells, ghrelin expression was induced in 3D control cultures in iMEF conditioned media.
- The differentiation protocol used in this study from Jiang J. et al. (Jiang, Au et al. 2007), is a 36 day procedure, the long duration of this procedure allows for increased variability between replicate experiments. Different batches of matrigel used for replicate experiments may also lead to subtle differences between repeat experiments.

5.3.4 Transdifferentiation of limbal stromal cells to pancreatic phenotypes

- Limbal stromal cells isolated from donor cornea-sclera ring possess differentiation properties similar to mesenchymal stem cells (Dravida, Pal et al. 2005; Polisetty, Fatima et al. 2008).
- Embryoid bodies were initially formed with these limbal stromal cells followed by subsequent differentiation to definitive endoderm in 3D, 2D and monolayer cultures. 3D cultures involved embedding stromal embryoid bodies in a thick matrigel/collagen gel, for 2D cultures embryoid bodies were cultured on top of a thin matrigel layer, while in monolayer cultures embryoid bodies were disaggregated using trypsin and single cell suspension was cultured on standard tissue culture plastic.
- Stromal embryoid body cells in 2D culture showed an increased propensity to differentiate towards definitive endoderm compared to 3D and monolayer cultures, based on expression of definitive endoderm marker- cxcr4 (figure 3.2.32). Further differentiation towards pancreatic endoderm did not induce expression of pancreatic endoderm markers.
- High cxcr4 expression was also observed in 3D control cells in iMEF CM. Cultures were maintained in these conditions for 36 days and levels of mature pancreatic markers assessed. Mature pancreatic exocrine marker – amylase was detected in 3D cultures maintained in iMEF CM or standard stromal media (DMEM, 10% FCS), indicating that it was the use of the 3D culture system rather than CM which induced expression of this marker. However, repeats of this experiment showed slightly different results, amylase expression was present in untreated stromal cells as well as 3D cultures, but increased amylase was observed in hanging drop generated embryoid bodies.
- All limbal stromal cell experiments conducted in this study were performed using limbal stromal cells from a single donor. Differences may exist between tissue from different donors. Using tissue from a range of donors may give a more accurate determination of pancreatic differentiation efficiency using this directed differentiation protocol.

5.4 Biomarker discovery in diabetes serum specimens

All in all the results were disappointing in that leads from profiling of small numbers of patients did not, in general, validate using specific assays for the candidate markers in larger patient numbers.

5.4.1 Analysis of serum for miRNA biomarkers

- Levels of GSIS-related miRNAs (table 3.1.2) were examined in T1DM old and control old serum specimens
    - Mir-124a, mir-130a, mir-9, mir-532, mir-192 and mir-379 were differentially expressed (n=3)
    - The study was expanded to n=5 (n=15 for mir-124a), however miRNA expression trends were not consistent
- TLDA miRNA profiling of T1DM old and control old (n=3) identified 7 differentially expressed miRNAs
    - mir-140, mir-21, mir-24, mir-29a, mir-29c, mir-30d and mir-345
    - TLDA miRNA targets validated in 6 T1DM and control samples
    - miRNA expression trends were not consistent
- Levels of GSIS related miRNAs were examined in T2DM and control samples
    - No statistically significant changes were seen in these miRNA levels in T2DM and control samples (n=6)
    - Although mir-369-5p levels did not reach statistical significant ($p \leq 0.05$), it did show a consistent trend in expression levels in T2DM and control serum.
    - Mir-369-5p was down-regulated approximately 2.1 fold in 6 T2DM serum specimens relative to matched controls; in two specimens mir-369-5p was down-regulated to the extent that it was undetectable by real-time PCR. This down-regulation of mir-369-5p in T2DM serum specimens could potentially reflect beta cell dysfunction in these patients.

5.4.2 Analysis of serum for proteomic biomarkers

- Proteomic profiling was performed on newly diagnosed type 1 diabetes (T1DM new) and established type 1 diabetes (T1DM old). Age/BMI/gender matched controls were also included in the analysis control new samples matched to the T1DM new group and control old samples matched to the T1DM old group.
- Principal component analysis (PCA) plots showed clear distinctions between control and disease groups (figure 3.3.17, 3.3.18 and 3.3.19).
- Data analysis was performed in triplicate using a different reference sample for each repeat. Only proteins which were common to all three lists were reported in the results section (table 3.3.6, 3.3.7 and 3.3.8), to improve confidence in identification of differentially expressed proteins in the respective studies.
- Targets for follow-up validation were chosen based on their potential interest in multiple comparisons, i.e. T1DM new versus control new, T1DM old versus control old, or T1DM new versus T1DM old.
- Vitronectin, clusterin, vitamin K-dependent protein S and apolipoprotein L1 were selected for follow-up validation using ELISAs to measure levels of these proteins in serum samples.
- Follow-up validation was performed on the same 8 T1DM new and control new samples, while in addition to the 8 T1DM old and control old samples used in the initial profiling experiment, a further 22 T1DM old and control old samples were analysed.
- Vitronectin levels were up-regulated in T1DM new versus control new, T1DM old versus control old, and T1DM new versus T1DM old comparisons according to label-free LC-MS experiment. However, ELISA validation showed a significant down-regulation of vitronectin in T1DM old versus control old comparison, but no significant change in expression levels was seen in the other comparisons (table 3.3.10).
- Clusterin levels were up-regulated in T1DM new versus control new and T1DM new versus T1DM old comparisons, according to label-free LC-MS experiment. However, ELISA showed no significant change in clusterin levels in any comparison analysed (table 3.3.10).

- Vitamin K-dependent protein S levels were up-regulated in T1DM new versus control new and T1DM new versus T1DM old comparison, and down-regulated in the T1DM old versus control old comparison according to label-free LC-MS experiment. However, according to the ELISA data, vitamin K-dependent protein S levels were significantly down-regulated in T1DM new versus control new comparison, while no significant change was seen in other comparisons analysed. In this instance, ELISA shows directly opposite result to label-free LC-MS data.
- Apolipoprotein L1 was down-regulated in T1DM old versus control old comparison and up-regulated in T1DM new versus T1DM old. Expression levels of this protein could not be validated using ELISA, due to technical issues with the assay.

5.4.3 Analysis of serum for metabolite biomarkers

- Metabolomic analysis was performed on 8 T1DM new and control new serum specimens by Metabolon, a commercial metabolomic profiling company.
- 23 metabolites were differentially expressed between the T1DM new and control new serum specimens (table 3.3.14). 18 of which were down-regulated in T1DM new serum relative to controls. The remaining 5 metabolites were up-regulated in T1DM new serum.
- The most consistently altered metabolic pathway in these samples was the caffeine metabolism, with 5 caffeine metabolites being significantly down-regulated in T1DM new serum.
- Control new samples used in this study were from medical interns. Therefore reduced levels of caffeine metabolites in the T1DM new versus control new comparison most likely reflects a higher intake of caffeine by the medical intern controls.
- Other pathways significantly altered in T1DM new and control new samples were carbohydrate and lipid metabolism. 1,5-AG a known marker of glycemic control was significantly down-regulated in T1DM new samples, in conjunction with significantly raised glucose levels in these patients.
- Lipid metabolites were reduced in T1DM new versus control new samples.

- Control new samples used in this study displayed high cholesterol and LDL-cholesterol (table 3.3.11), above the Irish Heart Foundation recommended healthy guidelines (table 4.3.2). Therefore it is unknown if changes in lipid metabolites are reflective of T1DM or due to the high cholesterol in control samples.
- Fibrinopeptide A (FPA) was identified as 2.7 fold increased in T1DM new samples compared to control.
- Follow-up validation of FPA was performed on the 8 T1DM new and control samples used for the profiling experiment, in addition to 30 T1DM old and control samples.
- Similar levels of FPA were detected in T1DM new, T1DM old and control old samples. While FPA levels were significantly decreased in control new samples (figure 3.3.40).
- This study highlighted the importance of using adequately matched control samples for biomarker discovery experiments. Suitable controls allow the identification of biomarkers related to disease phenotype, rather than an effect of the control samples.

6.0 Future Work

6.1 MicroRNAs involved in glucose stimulated insulin secretion

- If a more consistent GSIS responsive pancreatic beta cell line became available, stable knockdown and over-expression of mir-410 expression could be performed using shRNA technology, to investigate if effect of mir-410 on GSIS could be maintained in long term culture. Followed by proteomic analysis of shRNA-treated cells to identify proteins which are responsible for the effector functions of mir-410.
- Over-expression of mir-410 in mouse models with impaired insulin secretion. Conditional over-expression of mir-410 by inserting mir-410 sequence under the control of beta cell specific promoter, thereby allowing over-expression specifically in pancreatic beta cells. Effects of mir-410 on insulin secretion could be monitored by testing blood insulin and glucose levels.
- Expression patterns of mir-410, mir-200a and mir-130a could be examined in isolated human islets to determine if these miRNAs can also play a role in human beta cells. Purified beta cells could be isolated using laser-capture micro dissection and miRNA levels could be manipulated using pre/anti-mir technology, to check if these miRNAs play a functional role in GSIS in humans. If miRNAs were found to enhance GSIS of human beta cells, they could be manipulated in islet cultures and transplanted into mice to determine if these miRNA manipulations led to improved control of blood glucose levels, achieved longer period of insulin independence and extended graft survival following transplantation.
- Determine if mir-200a and mir-130a effect on GSIS is mediated by Txnip. Functional validation of mir-200a and mir-130a regulation of Txnip by cloning 3’UTR of Txnip into a mammalian expression vector containing the luciferase reporter gene. If Txnip is regulated by mir-200a and mir-130a, manipulation of these miRNAs will lead to altered levels of luciferase, measured with a luminometer.

6.2 Attempt to generate iPS cells and differentiation of an established iPS cell line towards pancreatic phenotypes

- Generation of iPS cells using new mRNA transient transfection technique, which promises improved reprogramming efficiency and in a shorter duration (Warren, Manos et al. 2010).
- Initial cell types for reprogramming could be selected from tissues of endodermal lineage, as recent evidence shows that reprogramming cells retain epigenetic memory, and differentiate more efficiently towards cell types of a related lineage to the starting cell population (Bar-Nur, Russ et al. 2011).
- Screening of a number of different iPS cells line for pancreatic differentiation potential, as iPS and ES cell lines are known for the variability of differentiation potential between cell lines.
- iPS cell differentiation shows successful definitive endoderm formation in 3D culture, if definitive endoderm marker expressing cells (cxcr4, foxa2, hnf4α) were sorted using FACS, this sub-population may differentiate further towards pancreatic endoderm and pancreatic endocrine cells, more efficiently than when in a mixed population with undifferentiated cells.
- MicroRNAs have recently been show to have the potential to reprogram somatic cells to iPS cells (Lin, Chang et al. 2008; Anokye-Danso, Trivedi et al. 2011; Miyoshi, Ishii et al. 2011), therefore miRNAs involved in functions of mature pancreatic beta cells, such as those identified in table 3.1.2 may have the potential to direct re-differentiation towards pancreatic phenotypes.
- ES cell conditioned media has the ability to reprogram cells to an iPS phenotype (Balasubramanian, Babai et al. 2009), therefore, conditioned media from islet cell preparations may have potential to direct differentiation towards islet cell phenotypes.

6.3 Biomarker discovery in diabetes serum specimens

6.3.1 miRNA biomarkers

- Mir-369-5p showed a consistent trend in this study in T2DM serum. Larger cohorts of patients should be examined to determine if the expression trend remains consistent.
- To determine if mir-369-5p plays a role in the pathogenesis of T2DM, levels of this miRNA could be determined in muscle, liver and adipose tissue of T2DM and control patients to assess if this miRNA plays a role in insulin resistance. If mir-369-5p was suspected of being directly involved in insulin resistance, mouse models of insulin resistance could also be used for manipulation of mir-369-5p for elucidation of biological function.

6.3.2 Proteomic biomarkers

- Vitronectin levels in T1DM old versus control comparison, and vitamin K-dependent protein S in T1DM new versus control new comparison were the only targets which achieved statistical significance when validated using ELISA. Levels of these proteins should be assessed in a larger cohort of patients to determine if the expression trend of these proteins in maintained.
- Additionally, a large number of proteins identified from the label-free LC-MS remain to be validated in larger cohorts of patients, to evaluate their potential use as biomarkers.
- Serum samples could be collected periodically, from patients with T1DM and T2DM from date of diagnosis. Once secondary complications of diabetes occur, large scale profiling of miRNA, mRNA and protein expression could be performed to identify miRNA, mRNA and proteins differentially expressed in association with the secondary complications. Such targets could then be tested in pre-secondary complications serum specimens to determine if these targets could be used as early biomarkers for prediction of development of secondary complications.

6.3.3 Metabolite biomarkers

- 23 metabolites were identified as differentially expressed in T1DM new compared to control new serum samples. Considering that caffeine and lipid metabolite changes are likely to be related to control samples used. Therefore there are 10 remaining metabolites which could represent potential biomarkers for T1DM.
- Validation of these 10 metabolites could be performed in a larger cohort of patient, with adequately matched control samples.

7.0 Bibliography

"Standards of medical care in diabetes--2011." Diabetes Care **34 Suppl 1**: S11-61.

(1993). "The effect of intensive treatment of diabetes on the development and progression of long-term complications in insulin-dependent diabetes mellitus. The Diabetes Control and Complications Trial Research Group." N Engl J Med **329**(14): 977-86.

(2008). "Screening for gestational diabetes mellitus: U.S. Preventive Services Task Force recommendation statement." Ann Intern Med **148**(10): 759-65.

Aasen, T., A. Raya, et al. (2008). "Efficient and rapid generation of induced pluripotent stem cells from human keratinocytes." Nat Biotechnol **26**(11): 1276-84.

Abderrahmani, A., V. Plaisance, et al. (2006). "Mechanisms controlling the expression of the components of the exocytotic apparatus under physiological and pathological conditions." Biochem Soc Trans **34**(Pt 5): 696-700.

Adrian, T. E., H. S. Besterman, et al. (1977). "Mechanism of pancreatic polypeptide release in man." Lancet **1**(8004): 161-3.

Afelik, S., Y. Chen, et al. (2006). "Combined ectopic expression of Pdx1 and Ptf1a/p48 results in the stable conversion of posterior endoderm into endocrine and exocrine pancreatic tissue." Genes Dev **20**(11): 1441-6.

Ahlgren, U., J. Jonsson, et al. (1996). "The morphogenesis of the pancreatic mesenchyme is uncoupled from that of the pancreatic epithelium in IPF1/PDX1-deficient mice." Development **122**(5): 1409-16.

Ahlgren, U., J. Jonsson, et al. (1998). "beta-cell-specific inactivation of the mouse Ipf1/Pdx1 gene results in loss of the beta-cell phenotype and maturity onset diabetes." Genes Dev **12**(12): 1763-8.

Akanuma, Y., M. Morita, et al. (1988). "Urinary excretion of 1,5-anhydro-D-glucitol accompanying glucose excretion in diabetic patients." Diabetologia **31**(11): 831-5.

Alberti, K. G., N. J. Christensen, et al. (1973). "Inhibition of insulin secretion by somatostatin." Lancet **2**(7841): 1299-301.

Alderdice, J. T., W. W. Dinsmore, et al. (1985). "Gastrointestinal hormones in anorexia nervosa." J Psychiatr Res **19**(2-3): 207-13.

Alessi, M. C., V. Nicaud, et al. (2011). "Association of vitronectin and plasminogen activator inhibitor-1 levels with the risk of metabolic syndrome and type 2 diabetes mellitus. Results from the D.E.S.I.R. prospective cohort." Thromb Haemost **106**(3): 416-22.

Anderson, H. A., C. A. Maylock, et al. (2003). "Serum-derived protein S binds to phosphatidylserine and stimulates the phagocytosis of apoptotic cells." Nat Immunol **4**(1): 87-91.

Anderson, N. L. and N. G. Anderson (2002). "The human plasma proteome: history, character, and diagnostic prospects." Mol Cell Proteomics **1**(11): 845-67.

Anokye-Danso, F., C. M. Trivedi, et al. (2011). "Highly efficient miRNA-mediated reprogramming of mouse and human somatic cells to pluripotency." Cell Stem Cell **8**(4): 376-88.

Apelqvist, A., H. Li, et al. (1999). "Notch signalling controls pancreatic cell differentiation." Nature **400**(6747): 877-81.

Ariyasu, H., K. Takaya, et al. (2001). "Stomach is a major source of circulating ghrelin, and feeding state determines plasma ghrelin-like immunoreactivity levels in humans." J Clin Endocrinol Metab **86**(10): 4753-8.

Aronis, K. N., Y. B. Kim, et al. (2011). "Clusterin (apolipoprotein J): wither link with diabetes and cardiometabolic risk?" Metabolism **60**(6): 747-8.

Asfari, M., D. Janjic, et al. (1992). "Establishment of 2-mercaptoethanol-dependent differentiated insulin-secreting cell lines." Endocrinology **130**(1): 167-78.

Atherton, H. J., N. J. Bailey, et al. (2006). "A combined 1H-NMR spectroscopy- and mass spectrometry-based metabolomic study of the PPAR-alpha null mutant mouse defines profound systemic changes in metabolism linked to the metabolic syndrome." Physiol Genomics **27**(2): 178-86.

Atkinson, M. A. and N. K. Maclaren (1994). "The pathogenesis of insulin-dependent diabetes mellitus." N Engl J Med **331**(21): 1428-36.

Balasse, E. O. and F. Fery (1989). "Ketone body production and disposal: effects of fasting, diabetes, and exercise." Diabetes Metab Rev **5**(3): 247-70.

Balasubramanian, S., N. Babai, et al. (2009). "Non cell-autonomous reprogramming of adult ocular progenitors: generation of pluripotent stem cells without exogenous transcription factors." Stem Cells **27**(12): 3053-62.

Bao, Y., T. Zhao, et al. (2009). "Metabonomic variations in the drug-treated type 2 diabetes mellitus patients and healthy volunteers." J Proteome Res **8**(4): 1623-30.

Barg, S., L. Eliasson, et al. (2002). "A subset of 50 secretory granules in close contact with L-type Ca2+ channels accounts for first-phase insulin secretion in mouse beta-cells." Diabetes **51 Suppl 1**: S74-82.

Barg, S., X. Ma, et al. (2001). "Fast exocytosis with few Ca(2+) channels in insulin-secreting mouse pancreatic B cells." Biophys J **81**(6): 3308-23.

Bar-Nur, O., H. A. Russ, et al. (2011). "Epigenetic memory and preferential lineage-specific differentiation in induced pluripotent stem cells derived from human pancreatic islet Beta cells." Cell Stem Cell **9**(1): 17-23.

Baroukh, N., M. A. Ravier, et al. (2007). "MicroRNA-124a regulates Foxa2 expression and intracellular signaling in pancreatic beta-cell lines." J Biol Chem **282**(27): 19575-88.

Bartel, D. P. (2004). "MicroRNAs: genomics, biogenesis, mechanism, and function." Cell **116**(2): 281-97.

Bhushan, A., N. Itoh, et al. (2001). "Fgf10 is essential for maintaining the proliferative capacity of epithelial progenitor cells during early pancreatic organogenesis." Development **128**(24): 5109-17.

Blelloch, R., M. Venere, et al. (2007). "Generation of induced pluripotent stem cells in the absence of drug selection." Cell Stem Cell **1**(3): 245-7.

Blyszczuk, P., J. Czyz, et al. (2003). "Expression of Pax4 in embryonic stem cells promotes differentiation of nestin-positive progenitor and insulin-producing cells." Proc Natl Acad Sci U S A **100**(3): 998-1003.

Bonal, C. and P. L. Herrera (2008). "Genes controlling pancreas ontogeny." Int J Dev Biol **52**(7): 823-35.

Bratanova-Tochkova, T. K., H. Cheng, et al. (2002). "Triggering and augmentation mechanisms, granule pools, and biphasic insulin secretion." Diabetes **51 Suppl 1**: S83-90.

Brennan, J., C. C. Lu, et al. (2001). "Nodal signalling in the epiblast patterns the early mouse embryo." Nature **411**(6840): 965-9.

Brink, C., K. Chowdhury, et al. (2001). "Pax4 regulatory elements mediate beta cell specific expression in the pancreas." Mech Dev **100**(1): 37-43.

Brooks-Worrell, B. M., C. J. Greenbaum, et al. (2004). "Autoimmunity to islet proteins in children diagnosed with new-onset diabetes." J Clin Endocrinol Metab **89**(5): 2222-7.

Brooks-Worrell, B. M., G. A. Starkebaum, et al. (1996). "Peripheral blood mononuclear cells of insulin-dependent diabetic patients respond to multiple islet cell proteins." J Immunol **157**(12): 5668-74.

Burlison, J. S., Q. Long, et al. (2008). "Pdx-1 and Ptf1a concurrently determine fate specification of pancreatic multipotent progenitor cells." Dev Biol **316**(1): 74-86.

Cai, S., T. Huo, et al. (2009). "Effect of mitiglinide on Streptozotocin-induced experimental type 2 diabetic rats: a urinary metabonomics study based on ultra-

performance liquid chromatography-tandem mass spectrometry." J Chromatogr B Analyt Technol Biomed Life Sci **877**(29): 3619-24.

Carrozzo, R., C. Dionisi-Vici, et al. (2007). "SUCLA2 mutations are associated with mild methylmalonic aciduria, Leigh-like encephalomyopathy, dystonia and deafness." Brain **130**(Pt 3): 862-74.

Cerasi, E. and R. Luft (1963). "Plasma-Insulin Response to Sustained Hyperglycemia Induced by Glucose Infusion in Human Subjects." Lancet **2**(7322): 1359-61.

Ceriello, A. (1993). "Coagulation activation in diabetes mellitus: the role of hyperglycaemia and therapeutic prospects." Diabetologia **36**(11): 1119-25.

Chan, E. M., S. Ratanasirintrawoot, et al. (2009). "Live cell imaging distinguishes bona fide human iPS cells from partially reprogrammed cells." Nat Biotechnol **27**(11): 1033-7.

Chen, X., Y. Ba, et al. (2008). "Characterization of microRNAs in serum: a novel class of biomarkers for diagnosis of cancer and other diseases." Cell Res **18**(10): 997-1006.

Cheng, L. C., E. Pastrana, et al. (2009). "miR-124 regulates adult neurogenesis in the subventricular zone stem cell niche." Nat Neurosci **12**(4): 399-408.

Chiang, M. K. and D. A. Melton (2003). "Single-cell transcript analysis of pancreas development." Dev Cell **4**(3): 383-93.

Chim, S. S., T. K. Shing, et al. (2008). "Detection and characterization of placental microRNAs in maternal plasma." Clin Chem **54**(3): 482-90.

Christin, C., R. Bischoff, et al. (2011). "Data processing pipelines for comprehensive profiling of proteomics samples by label-free LC-MS for biomarker discovery." Talanta **83**(4): 1209-24.

Cissell, M. A., L. Zhao, et al. (2003). "Transcription factor occupancy of the insulin gene in vivo. Evidence for direct regulation by Nkx2.2." J Biol Chem **278**(2): 751-6.

Cockell, M., B. J. Stevenson, et al. (1989). "Identification of a cell-specific DNA-binding activity that interacts with a transcriptional activator of genes expressed in the acinar pancreas." Mol Cell Biol **9**(6): 2464-76.

Collombat, P., J. Hecksher-Sorensen, et al. (2005). "The simultaneous loss of Arx and Pax4 genes promotes a somatostatin-producing cell fate specification at the expense of the alpha- and beta-cell lineages in the mouse endocrine pancreas." Development **132**(13): 2969-80.

Collombat, P., J. Hecksher-Sorensen, et al. (2007). "Embryonic endocrine pancreas and mature beta cells acquire alpha and PP cell phenotypes upon Arx misexpression." J Clin Invest **117**(4): 961-70.

Collombat, P., A. Mansouri, et al. (2003). "Opposing actions of Arx and Pax4 in endocrine pancreas development." Genes Dev **17**(20): 2591-603.

Conlon, F. L., K. M. Lyons, et al. (1994). "A primary requirement for nodal in the formation and maintenance of the primitive streak in the mouse." Development **120**(7): 1919-28.

Connor, S. C., M. K. Hansen, et al. (2010). "Integration of metabolomics and transcriptomics data to aid biomarker discovery in type 2 diabetes." Mol Biosyst **6**(5): 909-21.

Conway, T. L., R. R. Vickers, Jr., et al. (1981). "Occupational stress and variation in cigarette, coffee, and alcohol consumption." J Health Soc Behav **22**(2): 155-65.

Correa-Medina, M., V. Bravo-Egana, et al. (2009). "MicroRNA miR-7 is preferentially expressed in endocrine cells of the developing and adult human pancreas." Gene Expr Patterns **9**(4): 193-9.

Cowan, C. A., J. Atienza, et al. (2005). "Nuclear reprogramming of somatic cells after fusion with human embryonic stem cells." Science **309**(5739): 1369-73.

Criscimanna, A., G. Zito, et al. (2011). "In Vitro Generation of Pancreatic Endocrine Cells from Human Adult Fibroblast-Like Limbal Stem Cells." Cell Transplant.

Dahlback, B. (2007). "The tale of protein S and C4b-binding protein, a story of affection." Thromb Haemost **98**(1): 90-6.

Daimon, M., T. Oizumi, et al. (2011). "Association of the clusterin gene polymorphisms with type 2 diabetes mellitus." Metabolism **60**(6): 815-22.

D'Alessio, D. (2011). "The role of dysregulated glucagon secretion in type 2 diabetes." Diabetes Obes Metab **13 Suppl 1**: 126-32.

Daley, G. Q., M. W. Lensch, et al. (2009). "Broader implications of defining standards for the pluripotency of iPSCs." Cell Stem Cell **4**(3): 200-1; author reply 202.

Daly, N., P. Meleady, et al. (1998). "Regulation of keratin and integrin gene expression in cancer and drug resistance." Cytotechnology **27**(1-3): 321-44.

D'Amour, K. A., A. D. Agulnick, et al. (2005). "Efficient differentiation of human embryonic stem cells to definitive endoderm." Nat Biotechnol **23**(12): 1534-41.

D'Amour, K. A., A. G. Bang, et al. (2006). "Production of pancreatic hormone-expressing endocrine cells from human embryonic stem cells." Nat Biotechnol **24**(11): 1392-401.

Date, Y., M. Kojima, et al. (2000). "Ghrelin, a novel growth hormone-releasing acylated peptide, is synthesized in a distinct endocrine cell type in the gastrointestinal tracts of rats and humans." Endocrinology **141**(11): 4255-61.

de Caestecker, M. (2004). "The transforming growth factor-beta superfamily of receptors." Cytokine Growth Factor Rev **15**(1): 1-11.

de la Tour, D., T. Halvorsen, et al. (2001). "Beta-cell differentiation from a human pancreatic cell line in vitro and in vivo." Mol Endocrinol **15**(3): 476-83.

Demeterco, C., G. M. Beattie, et al. (2000). "A role for activin A and betacellulin in human fetal pancreatic cell differentiation and growth." J Clin Endocrinol Metab **85**(10): 3892-7.

Di Iorio, E., V. Barbaro, et al. (2005). "Isoforms of DeltaNp63 and the migration of ocular limbal cells in human corneal regeneration." Proc Natl Acad Sci U S A **102**(27): 9523-8.

Dichmann, D. S., H. Yassin, et al. (2006). "Analysis of pancreatic endocrine development in GDF11-deficient mice." Dev Dyn **235**(11): 3016-25.

Dimitriadis, E., M. Griffin, et al. (1996). "Lipoprotein composition in NIDDM: effects of dietary oleic acid on the composition, oxidisability and function of low and high density lipoproteins." Diabetologia **39**(6): 667-76.

Dowling, P., L. O'Driscoll, et al. (2006). "Proteomic screening of glucose-responsive and glucose non-responsive MIN-6 beta cells reveals differential expression of proteins involved in protein folding, secretion and oxidative stress." Proteomics **6**(24): 6578-87.

Dravida, S., R. Pal, et al. (2005). "The transdifferentiation potential of limbal fibroblast-like cells." Brain Res Dev Brain Res **160**(2): 239-51.

Dua, H. S. and A. Azuara-Blanco (2000). "Limbal stem cells of the corneal epithelium." Surv Ophthalmol **44**(5): 415-25.

Duchateau, P. N., C. R. Pullinger, et al. (1997). "Apolipoprotein L, a new human high density lipoprotein apolipoprotein expressed by the pancreas. Identification, cloning, characterization, and plasma distribution of apolipoprotein L." J Biol Chem **272**(41): 25576-82.

Dungan, K. M., J. B. Buse, et al. (2006). "1,5-anhydroglucitol and postprandial hyperglycemia as measured by continuous glucose monitoring system in moderately controlled patients with diabetes." Diabetes Care **29**(6): 1214-9.

Dunning, B. E. and J. E. Gerich (2007). "The role of alpha-cell dysregulation in fasting and postprandial hyperglycemia in type 2 diabetes and therapeutic implications." Endocr Rev **28**(3): 253-83.

Duvillie, B., M. Attali, et al. (2006). "The mesenchyme controls the timing of pancreatic beta-cell differentiation." Diabetes **55**(3): 582-9.

Edlund, H. (2002). "Pancreatic organogenesis--developmental mechanisms and implications for therapy." Nat Rev Genet **3**(7): 524-32.

Eggan, K. (2009). Patient-derived iPS cell lines and their applications. iPS cells - Breaking down the barriers to therapeutics. C. Press, Cell Press.

El Ouaamari, A., N. Baroukh, et al. (2008). "miR-375 targets 3'-phosphoinositide-dependent protein kinase-1 and regulates glucose-induced biological responses in pancreatic beta-cells." Diabetes **57**(10): 2708-17.

Elghazi, L., C. Cras-Meneur, et al. (2002). "Role for FGFR2IIIb-mediated signals in controlling pancreatic endocrine progenitor cell proliferation." Proc Natl Acad Sci U S A **99**(6): 3884-9.

Erlinger, T. P. and F. L. Brancati (2001). "Postchallenge hyperglycemia in a national sample of U.S. adults with type 2 diabetes." Diabetes Care **24**(10): 1734-8.

Esau, C. C. and B. P. Monia (2007). "Therapeutic potential for microRNAs." Adv Drug Deliv Rev **59**(2-3): 101-14.

Esguerra, J. L., C. Bolmeson, et al. (2011). "Differential glucose-regulation of microRNAs in pancreatic islets of non-obese type 2 diabetes model Goto-Kakizaki rat." PLoS One **6**(4): e18613.

Evans, A. M., C. D. DeHaven, et al. (2009). "Integrated, nontargeted ultrahigh performance liquid chromatography/electrospray ionization tandem mass spectrometry platform for the identification and relative quantification of the small-molecule complement of biological systems." Anal Chem **81**(16): 6656-67.

Evans, M. J. and M. H. Kaufman (1981). "Establishment in culture of pluripotential cells from mouse embryos." Nature **292**(5819): 154-6.

Florio, T. and G. Schettini (2001). "[Somatostatin and its receptors. Role in the control of cell proliferation]." Minerva Endocrinol **26**(3): 91-102.

Freedman, B. I., C. D. Langefeld, et al. (2011). "Apolipoprotein L1 nephropathy risk variants associate with HDL subfraction concentration in African Americans." Nephrol Dial Transplant. **26**(11): 3805-10

Fujimoto, S., A. Inui, et al. (1997). "Increased cholecystokinin and pancreatic polypeptide responses to a fat-rich meal in patients with restrictive but not bulimic anorexia nervosa." Biol Psychiatry **41**(10): 1068-70.

Fukui, M., M. Tanaka, et al. (2008). "Serum uric acid is associated with microalbuminuria and subclinical atherosclerosis in men with type 2 diabetes mellitus." Metabolism **57**(5): 625-9.

Furukawa, M., Y. Eto, et al. (1995). "Expression of immunoreactive activin A in fetal rat pancreas." Endocr J **42**(1): 63-8.

Fussner, E., U. Djuric, et al. (2011). "Constitutive heterochromatin reorganization during somatic cell reprogramming." Embo J **30**(9): 1778-89.

Gall, W. E., K. Beebe, et al. (2010). "alpha-hydroxybutyrate is an early biomarker of insulin resistance and glucose intolerance in a nondiabetic population." PLoS One **5**(5): e10883.

Gammell, P. (2002). The molecular and cellular biology of pancreatic beta cell differentiation in vitro. NCTCC. Dublin, DCU.

Gannon, M., E. T. Ables, et al. (2008). "pdx-1 function is specifically required in embryonic beta cells to generate appropriate numbers of endocrine cell types and maintain glucose homeostasis." Dev Biol **314**(2): 406-17.

Gazdar, A. F., W. L. Chick, et al. (1980). "Continuous, clonal, insulin- and somatostatin-secreting cell lines established from a transplantable rat islet cell tumor." Proc Natl Acad Sci U S A **77**(6): 3519-23.

Genuth, S., K. G. Alberti, et al. (2003). "Follow-up report on the diagnosis of diabetes mellitus." Diabetes Care **26**(11): 3160-7.

Gerich, J. E., M. A. Charles, et al. (1976). "Regulation of pancreatic insulin and glucagon secretion." Annu Rev Physiol **38**: 353-88.

Gianazza, E., V. Mainini, et al. (2010). "Different expression of fibrinopeptide A and related fragments in serum of type 1 diabetic patients with nephropathy." J Proteomics **73**(3): 593-601.

Gilad, S., E. Meiri, et al. (2008). "Serum microRNAs are promising novel biomarkers." PLoS ONE **3**(9): e3148.

Gittes, G. K. (2009). "Developmental biology of the pancreas: a comprehensive review." Dev Biol **326**(1): 4-35.

Godzien, J., M. Ciborowski, et al. (2011). "Metabolomic approach with LC-QTOF to study the effect of a nutraceutical treatment on urine of diabetic rats." J Proteome Res **10**(2): 837-44.

Greenwood, A. L., S. Li, et al. (2007). "Notch signaling reveals developmental plasticity of Pax4(+) pancreatic endocrine progenitors and shunts them to a duct fate." Mech Dev **124**(2): 97-107.

Griffiths-Jones, S. (2004). "The microRNA Registry." Nucleic Acids Res **32**(Database issue): D109-11.

Griffiths-Jones, S., R. J. Grocock, et al. (2006). "miRBase: microRNA sequences, targets and gene nomenclature." Nucleic Acids Res **34**(Database issue): D140-4.

Griffiths-Jones, S., H. K. Saini, et al. (2008). "miRBase: tools for microRNA genomics." Nucleic Acids Res **36**(Database issue): D154-8.

Grodsky, G. M. (1972). "A threshold distribution hypothesis for packet storage of insulin and its mathematical modeling." J Clin Invest **51**(8): 2047-59.

Grodsky, G. M. (1972). "A threshold distribution hypothesis for packet storage of insulin. II. Effect of calcium." Diabetes **21**(2 Suppl): 584-93.

Gromada, J., I. Franklin, et al. (2007). "Alpha-cells of the endocrine pancreas: 35 years of research but the enigma remains." Endocr Rev **28**(1): 84-116.

Gu, G., J. Dubauskaite, et al. (2002). "Direct evidence for the pancreatic lineage: NGN3+ cells are islet progenitors and are distinct from duct progenitors." Development **129**(10): 2447-57.

Guz, Y., M. R. Montminy, et al. (1995). "Expression of murine STF-1, a putative insulin gene transcription factor, in beta cells of pancreas, duodenal epithelium and pancreatic exocrine and endocrine progenitors during ontogeny." Development **121**(1): 11-8.

Hale, M. A., H. Kagami, et al. (2005). "The homeodomain protein PDX1 is required at mid-pancreatic development for the formation of the exocrine pancreas." Dev Biol **286**(1): 225-37.

Hart, A., S. Papadopoulou, et al. (2003). "Fgf10 maintains notch activation, stimulates proliferation, and blocks differentiation of pancreatic epithelial cells." Dev Dyn **228**(2): 185-93.

He, A., L. Zhu, et al. (2007). "Overexpression of micro ribonucleic acid 29, highly up-regulated in diabetic rats, leads to insulin resistance in 3T3-L1 adipocytes." Mol Endocrinol **21**(11): 2785-94.

Hebrok, M., S. K. Kim, et al. (1998). "Notochord repression of endodermal Sonic hedgehog permits pancreas development." Genes Dev **12**(11): 1705-13.

Heller, R. S., M. Jenny, et al. (2005). "Genetic determinants of pancreatic epsilon-cell development." Dev Biol **286**(1): 217-24.

Heller, R. S., D. A. Stoffers, et al. (2004). "The role of Brn4/Pou3f4 and Pax6 in forming the pancreatic glucagon cell identity." Dev Biol **268**(1): 123-34.

Hennessy, E. and L. O'Driscoll (2008). "Molecular medicine of microRNAs: structure, function and implications for diabetes." Expert Rev Mol Med **10**: e24.

Henseleit, K. D., S. B. Nelson, et al. (2005). "NKX6 transcription factor activity is required for alpha- and beta-cell development in the pancreas." Development **132**(13): 3139-49.

Higa, K., S. Shimmura, et al. (2009). "N-cadherin in the maintenance of human corneal limbal epithelial progenitor cells in vitro." Invest Ophthalmol Vis Sci **50**(10): 4640-5.

Holland, A. M., M. A. Hale, et al. (2002). "Experimental control of pancreatic development and maintenance." Proc Natl Acad Sci U S A **99**(19): 12236-41.

Hoofnagle, A. N., M. Wu, et al. (2010). "Low clusterin levels in high-density lipoprotein associate with insulin resistance, obesity, and dyslipoproteinemia." Arterioscler Thromb Vasc Biol **30**(12): 2528-34.

Hosokawa, Y. A., H. Hosokawa, et al. (1996). "Mechanism of impaired glucose-potentiated insulin secretion in diabetic 90% pancreatectomy rats. Study using glucagonlike peptide-1 (7-37)." J Clin Invest **97**(1): 180-6.

Huang, B., W. Qin, et al. (2009). "MicroRNA expression profiling in diabetic GK rat model." Acta Biochim Biophys Sin (Shanghai) **41**(6): 472-7.

Huang, H. P., M. Liu, et al. (2000). "Regulation of the pancreatic islet-specific gene BETA2 (neuroD) by neurogenin 3." Mol Cell Biol **20**(9): 3292-307.

Huang, Y. C., T. Z. Wang, et al. (2006). Effect of calcium ion concentration on keratinocyte behaviors in the defined media. Biomedical Engineering-Applications, Basis & Communications**:** 37-41.

Huang, Z., D. Huang, et al. (2009). "Plasma microRNAs are promising novel biomarkers for early detection of colorectal cancer." Int J Cancer. **127**(1): 118-26

Huo, T., S. Cai, et al. (2009). "Metabonomic study of biochemical changes in the serum of type 2 diabetes mellitus patients after the treatment of metformin hydrochloride." J Pharm Biomed Anal **49**(4): 976-82.

Hutton, J. C. (1994). "Insulin secretory granule biogenesis and the proinsulin-processing endopeptidases." Diabetologia **37 Suppl 2**: S48-56.

Ishihara, H., T. Asano, et al. (1993). "Pancreatic beta cell line MIN6 exhibits characteristics of glucose metabolism and glucose-stimulated insulin secretion similar to those of normal islets." Diabetologia **36**(11): 1139-45.

Jacquemin, P., S. M. Durviaux, et al. (2000). "Transcription factor hepatocyte nuclear factor 6 regulates pancreatic endocrine cell differentiation and controls expression of the proendocrine gene ngn3." Mol Cell Biol **20**(12): 4445-54.

Jacquemin, P., F. P. Lemaigre, et al. (2003). "The Onecut transcription factor HNF-6 (OC-1) is required for timely specification of the pancreas and acts upstream of Pdx-1 in the specification cascade." Dev Biol **258**(1): 105-16.

Jacquemin, P., H. Yoshitomi, et al. (2006). "An endothelial-mesenchymal relay pathway regulates early phases of pancreas development." Dev Biol **290**(1): 189-99.

Jensen, J., R. S. Heller, et al. (2000). "Independent development of pancreatic alpha- and beta-cells from neurogenin3-expressing precursors: a role for the notch pathway in repression of premature differentiation." Diabetes **49**(2): 163-76.

Jensen, J., E. E. Pedersen, et al. (2000). "Control of endodermal endocrine development by Hes-1." Nat Genet **24**(1): 36-44.

Jiang, J., M. Au, et al. (2007). "Generation of insulin-producing islet-like clusters from human embryonic stem cells." Stem Cells **25**(8): 1940-53.

Jiang, W., Y. Shi, et al. (2007). "In vitro derivation of functional insulin-producing cells from human embryonic stem cells." Cell Res **17**(4): 333-44.

Joglekar, M. V., V. M. Joglekar, et al. (2009). "Expression of islet-specific microRNAs during human pancreatic development." Gene Expr Patterns **9**(2): 109-13.

Joglekar, M. V., V. S. Parekh, et al. (2007). "New pancreas from old: microregulators of pancreas regeneration." Trends Endocrinol Metab **18**(10): 393-400.

Joglekar, M. V., V. S. Parekh, et al. (2007). "MicroRNA profiling of developing and regenerating pancreas reveal post-transcriptional regulation of neurogenin3." Dev Biol **311**(2): 603-12.

Johnston, D. G. and K. G. Alberti (1982). "Hormonal control of ketone body metabolism in the normal and diabetic state." Clin Endocrinol Metab **11**(2): 329-61.

Jonsson, J., U. Ahlgren, et al. (1995). "IPF1, a homeodomain protein with a dual function in pancreas development." Int J Dev Biol **39**(5): 789-98.

Kallman, F. and C. Grobstein (1964). "Fine Structure of Differentiating Mouse Pancreatic Exocrine Cells in Transfilter Culture." J Cell Biol **20**: 399-413.

Kane, N. M., A. Nowrouzi, et al. (2010). "Lentivirus-mediated reprogramming of somatic cells in the absence of transgenic transcription factors." Mol Ther **18**(12): 2139-45.

Kasper, M., R. Moll, et al. (1988). "Patterns of cytokeratin and vimentin expression in the human eye." Histochemistry **89**(4): 369-77.

Kato, M., J. Zhang, et al. (2007). "MicroRNA-192 in diabetic kidney glomeruli and its function in TGF-beta-induced collagen expression via inhibition of E-box repressors." Proc Natl Acad Sci U S A **104**(9): 3432-7.

Kawaguchi, Y., B. Cooper, et al. (2002). "The role of the transcriptional regulator Ptf1a in converting intestinal to pancreatic progenitors." Nat Genet **32**(1): 128-34.

Keijzers, G. B., B. E. De Galan, et al. (2002). "Caffeine can decrease insulin sensitivity in humans." Diabetes Care **25**(2): 364-9.

Kim, D., C. H. Kim, et al. (2009). "Generation of human induced pluripotent stem cells by direct delivery of reprogramming proteins." Cell Stem Cell **4**(6): 472-6.

Kim, J. B., H. Zaehres, et al. (2008). "Pluripotent stem cells induced from adult neural stem cells by reprogramming with two factors." Nature **454**(7204): 646-50.

Kim, S. K., M. Hebrok, et al. (1997). "Notochord to endoderm signaling is required for pancreas development." Development **124**(21): 4243-52.

Kim, S. K. and D. A. Melton (1998). "Pancreas development is promoted by cyclopamine, a hedgehog signaling inhibitor." Proc Natl Acad Sci U S A **95**(22): 13036-41.

Kishimoto, M., Y. Yamasaki, et al. (1995). "1,5-Anhydro-D-glucitol evaluates daily glycemic excursions in well-controlled NIDDM." Diabetes Care **18**(8): 1156-9.

Kloosterman, W. P., A. K. Lagendijk, et al. (2007). "Targeted inhibition of miRNA maturation with morpholinos reveals a role for miR-375 in pancreatic islet development." PLoS Biol **5**(8): e203.

Kloppel, G., M. Lohr, et al. (1985). "Islet pathology and the pathogenesis of type 1 and type 2 diabetes mellitus revisited." Surv Synth Pathol Res **4**(2): 110-25.

Kojima, M., H. Hosoda, et al. (2001). "Purification and distribution of ghrelin: the natural endogenous ligand for the growth hormone secretagogue receptor." Horm Res **56 Suppl 1**: 93-7.

Kolli, S., M. Lako, et al. (2008). "Loss of corneal epithelial stem cell properties in outgrowths from human limbal explants cultured on intact amniotic membrane." Regen Med **3**(3): 329-42.

Kong, L., J. Zhu, et al. (2011). "Significance of serum microRNAs in pre-diabetes and newly diagnosed type 2 diabetes: a clinical study." Acta Diabetol **48**(1): 61-9.

Kong, L., J. Zhu, et al. (2011). "Significance of serum microRNAs in pre-diabetes and newly diagnosed type 2 diabetes: a clinical study." Acta Diabetol **48**(1): 61-9.

Kraehenbuehl, T. P., R. Langer, et al. (2011). "Three-dimensional biomaterials for the study of human pluripotent stem cells." Nat Methods **8**(9): 731-6.

Krapp, A., M. Knofler, et al. (1998). "The bHLH protein PTF1-p48 is essential for the formation of the exocrine and the correct spatial organization of the endocrine pancreas." Genes Dev **12**(23): 3752-63.

Kroon, E., L. A. Martinson, et al. (2008). "Pancreatic endoderm derived from human embryonic stem cells generates glucose-responsive insulin-secreting cells in vivo." Nat Biotechnol **26**(4): 443-52.

Kruger, A. J., C. Yang, et al. (2010). "Haptoglobin as an early serum biomarker of virus-induced autoimmune type 1 diabetes in biobreeding diabetes resistant and LEW1.WR1 rats." Exp Biol Med (Maywood) **235**(11): 1328-37.

Krutzfeldt, J., N. Rajewsky, et al. (2005). "Silencing of microRNAs in vivo with 'antagomirs'." Nature **438**(7068): 685-9.

Kujiraoka, T., H. Hattori, et al. (2006). "Serum apolipoprotein j in health, coronary heart disease and type 2 diabetes mellitus." J Atheroscler Thromb **13**(6): 314-22.

Lammert, E., O. Cleaver, et al. (2001). "Induction of pancreatic differentiation by signals from blood vessels." Science **294**(5542): 564-7.

Landers, K. A., M. J. Burger, et al. (2005). "Use of multiple biomarkers for a molecular diagnosis of prostate cancer." Int J Cancer **114**(6): 950-6.

Lankinen, M., U. Schwab, et al. (2010). "Dietary carbohydrate modification alters serum metabolic profiles in individuals with the metabolic syndrome." Nutr Metab Cardiovasc Dis **20**(4): 249-57.

Lanza, I. R., S. Zhang, et al. (2010). "Quantitative metabolomics by H-NMR and LC-MS/MS confirms altered metabolic pathways in diabetes." PLoS One **5**(5): e10538.

Lau, J., H. Kawahira, et al. (2006). "Hedgehog signaling in pancreas development and disease." Cell Mol Life Sci **63**(6): 642-52.

Lawrie, C. H., S. Gal, et al. (2008). "Detection of elevated levels of tumour-associated microRNAs in serum of patients with diffuse large B-cell lymphoma." Br J Haematol **141**(5): 672-5.

Lebrun, P., V. Baron, et al. (2000). "Cell adhesion and focal adhesion kinase regulate insulin receptor substrate-1 expression." J Biol Chem **275**(49): 38371-7.

Levinson-Dushnik, M. and N. Benvenisty (1997). "Involvement of hepatocyte nuclear factor 3 in endoderm differentiation of embryonic stem cells." Mol Cell Biol **17**(7): 3817-22.

Li, L. O., Y. F. Hu, et al. (2010). "Early hepatic insulin resistance in mice: a metabolomics analysis." Mol Endocrinol **24**(3): 657-66.

Li, X., Z. Xu, et al. (2009). "Comprehensive two-dimensional gas chromatography/time-of-flight mass spectrometry for metabonomics: Biomarker discovery for diabetes mellitus." Anal Chim Acta **633**(2): 257-62.

Li, Z., P. Manna, et al. (2004). "Multifaceted pancreatic mesenchymal control of epithelial lineage selection." Dev Biol **269**(1): 252-63.

Lieverse, R. J., A. A. Masclee, et al. (1994). "Plasma cholecystokinin and pancreatic polypeptide secretion in response to bombesin, meal ingestion and modified sham feeding in lean and obese persons." Int J Obes Relat Metab Disord **18**(2): 123-7.

Lin, J. W., A. V. Biankin, et al. (2004). "Differential requirement for ptf1a in endocrine and exocrine lineages of developing zebrafish pancreas." Dev Biol **274**(2): 491-503.

Lin, K. C., S. T. Tsai, et al. (2004). "Different progressions of hyperglycemia and diabetes among hyperuricemic men and women in the kinmen study." J Rheumatol **31**(6): 1159-65.

Lin, S. L., D. C. Chang, et al. (2008). "Mir-302 reprograms human skin cancer cells into a pluripotent ES-cell-like state." Rna **14**(10): 2115-24.

Ling, H. Y., H. S. Ou, et al. (2009). "Changes in microRNA profile and effects of miR-320 in insulin-resistant 3T3-L1 adipocytes." Clin Exp Pharmacol Physiol.

Liu, P., M. Wakamiya, et al. (1999). "Requirement for Wnt3 in vertebrate axis formation." Nat Genet **22**(4): 361-5.

Lottmann, H., J. Vanselow, et al. (2001). "The Tet-On system in transgenic mice: inhibition of the mouse pdx-1 gene activity by antisense RNA expression in pancreatic beta-cells." J Mol Med **79**(5-6): 321-8.

Lovis, P., S. Gattesco, et al. (2008). "Regulation of the expression of components of the exocytotic machinery of insulin-secreting cells by microRNAs." Biol Chem **389**(3): 305-12.

Lovis, P., E. Roggli, et al. (2008). "Alterations in microRNA expression contribute to fatty acid-induced pancreatic beta-cell dysfunction." Diabetes **57**(10): 2728-36.

Lucio, M., A. Fekete, et al. (2010). "Insulin sensitivity is reflected by characteristic metabolic fingerprints--a Fourier transform mass spectrometric non-targeted metabolomics approach." PLoS One **5**(10): e13317.

Lynn, F. C., P. Skewes-Cox, et al. (2007). "MicroRNA expression is required for pancreatic islet cell genesis in the mouse." Diabetes **56**(12): 2938-45.

Lynn, F. C., S. B. Smith, et al. (2007). "Sox9 coordinates a transcriptional network in pancreatic progenitor cells." Proc Natl Acad Sci U S A **104**(25): 10500-5.

MacFarlane, W. M., M. L. Read, et al. (1994). "Glucose modulates the binding activity of the beta-cell transcription factor IUF1 in a phosphorylation-dependent manner." Biochem J **303 (Pt 2)**: 625-31.

Madan, R., B. Gupt, et al. (2010). "Coagulation profile in diabetes and its association with diabetic microvascular complications." J Assoc Physicians India **58**: 481-4.

Maehr, R., S. Chen, et al. (2009). "Generation of pluripotent stem cells from patients with type 1 diabetes." Proc Natl Acad Sci U S A **106**(37): 15768-73.

Maestro, M. A., S. F. Boj, et al. (2003). "Hnf6 and Tcf2 (MODY5) are linked in a gene network operating in a precursor cell domain of the embryonic pancreas." Hum Mol Genet **12**(24): 3307-14.

Maherali, N., T. Ahfeldt, et al. (2008). "A high-efficiency system for the generation and study of human induced pluripotent stem cells." Cell Stem Cell **3**(3): 340-5.

Maherali, N. and K. Hochedlinger (2008). "Guidelines and techniques for the generation of induced pluripotent stem cells." Cell Stem Cell **3**(6): 595-605.

Maldonado, T. S., A. S. Kadison, et al. (2000). "Ontogeny of activin B and follistatin in developing embryonic mouse pancreas: implications for lineage selection." J Gastrointest Surg **4**(3): 269-75.

Mamin, A. and J. Philippe (2007). "Activin A decreases glucagon and arx gene expression in alpha-cell lines." Mol Endocrinol **21**(1): 259-73.

Marshak, S., H. Totary, et al. (1996). "Purification of the beta-cell glucose-sensitive factor that transactivates the insulin gene differentially in normal and transformed islet cells." Proc Natl Acad Sci U S A **93**(26): 15057-62.

Marsich, E., A. Vetere, et al. (2003). "The PAX6 gene is activated by the basic helix-loop-helix transcription factor NeuroD/BETA2." Biochem J **376**(Pt 3): 707-15.

Martin, G. R. (1981). "Isolation of a pluripotent cell line from early mouse embryos cultured in medium conditioned by teratocarcinoma stem cells." Proc Natl Acad Sci U S A **78**(12): 7634-8.

Masson-Gadais, B., C. Fugere, et al. (2006). "The feeder layer-mediated extended lifetime of cultured human skin keratinocytes is associated with altered levels of the transcription factors Sp1 and Sp3." J Cell Physiol **206**(3): 831-42.

Mathis, D., L. Vence, et al. (2001). "beta-Cell death during progression to diabetes." Nature **414**(6865): 792-8.

Matschinsky, F. M. (1990). "Glucokinase as glucose sensor and metabolic signal generator in pancreatic beta-cells and hepatocytes." Diabetes **39**(6): 647-52.

Matschinsky, F. M. (1996). "Banting Lecture 1995. A lesson in metabolic regulation inspired by the glucokinase glucose sensor paradigm." Diabetes **45**(2): 223-41.

Matsumura, T., T. Suzuki, et al. (2006). "Differential serum proteomic analysis in a model of metabolic disease." Biochem Biophys Res Commun **351**(4): 965-71.

Matveyenko, A. V. and P. C. Butler (2008). "Relationship between beta-cell mass and diabetes onset." Diabetes Obes Metab **10 Suppl 4**: 23-31.

McGarry, J. D., K. F. Woeltje, et al. (1989). "Regulation of ketogenesis and the renaissance of carnitine palmitoyltransferase." Diabetes Metab Rev **5**(3): 271-84.

McGill, J. B., T. G. Cole, et al. (2004). "Circulating 1,5-anhydroglucitol levels in adult patients with diabetes reflect longitudinal changes of glycemia: a U.S. trial of the GlycoMark assay." Diabetes Care **27**(8): 1859-65.

McKnight, K. D., P. Wang, et al. (2010). "Deconstructing pancreas development to reconstruct human islets from pluripotent stem cells." Cell Stem Cell **6**(4): 300-8.

Meigs, J. B., R. B. D'Agostino, Sr., et al. (1997). "Risk variable clustering in the insulin resistance syndrome. The Framingham Offspring Study." Diabetes **46**(10): 1594-600.

Melkman-Zehavi, T., R. Oren, et al. (2011). "miRNAs control insulin content in pancreatic beta-cells via downregulation of transcriptional repressors." Embo J **30**(5): 835-45.

Metz, T. O., W. J. Qian, et al. (2008). "Application of proteomics in the discovery of candidate protein biomarkers in a diabetes autoantibody standardization program sample subset." J Proteome Res **7**(2): 698-707.

Miettinen, P. J., M. Huotari, et al. (2000). "Impaired migration and delayed differentiation of pancreatic islet cells in mice lacking EGF-receptors." Development **127**(12): 2617-27.

Miralles, F., P. Czernichow, et al. (1998). "Follistatin regulates the relative proportions of endocrine versus exocrine tissue during pancreatic development." Development **125**(6): 1017-24.

Miralles, F., L. Lamotte, et al. (2006). "Interplay between FGF10 and Notch signalling is required for the self-renewal of pancreatic progenitors." Int J Dev Biol **50**(1): 17-26.

Mitchell, P. S., R. K. Parkin, et al. (2008). "Circulating microRNAs as stable blood-based markers for cancer detection." Proc Natl Acad Sci U S A **105**(30): 10513-8.

Miyoshi, N., H. Ishii, et al. (2011). "Reprogramming of mouse and human cells to pluripotency using mature microRNAs." Cell Stem Cell **8**(6): 633-8.

Mortimer, C. H., W. M. Tunbridge, et al. (1974). "Effects of growth-hormone release-inhibiting hormone on circulating glucagon, insulin, and growth hormone in normal, diabetic, acromegalic, and hypopituitary patients." Lancet **1**(7860): 697-701.

Muller, W. A., G. R. Faloona, et al. (1973). "Hyperglucagonemia in diabetic ketoacidosis. Its prevalence and significance." Am J Med **54**(1): 52-7.

Munger, B. L. (1958). "A light and electron microscopic study of cellular differentiation in the pancreatic islets of the mouse." Am J Anat **103**(2): 275-311.

Murtaugh, L. C. (2007). "Pancreas and beta-cell development: from the actual to the possible." Development **134**(3): 427-38.

Nagy, A. and K. Nagy (2010). "The mysteries of induced pluripotency: where will they lead?" Nat Methods **7**(1): 22-4.

Naldini, L., U. Blomer, et al. (1996). "In vivo gene delivery and stable transduction of nondividing cells by a lentiviral vector." Science **272**(5259): 263-7.

Nathan, D. M. (1993). "Long-term complications of diabetes mellitus." N Engl J Med **328**(23): 1676-85.

Navarro-Tableros, V., T. Fiordelisio, et al. (2007). "Nerve growth factor promotes development of glucose-induced insulin secretion in rat neonate pancreatic beta cells by modulating calcium channels." Channels (Austin) **1**(6): 408-16.

Naya, F. J., H. P. Huang, et al. (1997). "Diabetes, defective pancreatic morphogenesis, and abnormal enteroendocrine differentiation in BETA2/neuroD-deficient mice." Genes Dev **11**(18): 2323-34.

Nelson, D. L. and M. M. Cox (2005). Lehniger- Principles of Biochemistry, Freeman.

Nelson, S. B., A. E. Schaffer, et al. (2007). "The transcription factors Nkx6.1 and Nkx6.2 possess equivalent activities in promoting beta-cell fate specification in Pdx1+ pancreatic progenitor cells." Development **134**(13): 2491-500.

Nesher, R. and E. Cerasi (2002). "Modeling phasic insulin release: immediate and time-dependent effects of glucose." Diabetes **51 Suppl 1**: S53-9.

Newgard, C. B. (1994). "Cellular engineering and gene therapy strategies for insulin replacement in diabetes." Diabetes **43**(3): 341-50.

Nilsson, T., P. Arkhammar, et al. (1989). "Suppression of insulin release by galanin and somatostatin is mediated by a G-protein. An effect involving repolarization and reduction in cytoplasmic free Ca2+ concentration." J Biol Chem **264**(2): 973-80.

Nomura, F., T. Tomonaga, et al. (2004). "Identification of novel and downregulated biomarkers for alcoholism by surface enhanced laser desorption/ionization-mass spectrometry." Proteomics **4**(4): 1187-94.

Norgaard, G. A., J. N. Jensen, et al. (2003). "FGF10 signaling maintains the pancreatic progenitor cell state revealing a novel role of Notch in organ development." Dev Biol **264**(2): 323-38.

O'Driscoll, L., P. Gammell, et al. (2004). "Mechanisms associated with loss of glucose responsiveness in beta cells." Transplant Proc **36**(4): 1159-62.

O'Driscoll, L., P. Gammell, et al. (2006). "Phenotypic and global gene expression profile changes between low passage and high passage MIN-6 cells." J Endocrinol **191**(3): 665-76.

Okita, K., T. Ichisaka, et al. (2007). "Generation of germline-competent induced pluripotent stem cells." Nature **448**(7151): 313-7.

Okita, K., M. Nakagawa, et al. (2008). "Generation of mouse induced pluripotent stem cells without viral vectors." Science **322**(5903): 949-53.

Olofsson, C. S., S. O. Gopel, et al. (2002). "Fast insulin secretion reflects exocytosis of docked granules in mouse pancreatic B-cells." Pflugers Arch **444**(1-2): 43-51.

Ong, S. E. and A. Pandey (2001). "An evaluation of the use of two-dimensional gel electrophoresis in proteomics." Biomol Eng **18**(5): 195-205.

Orci, L. (1984). "Patterns of cellular and subcellular organization in the endocrine pancreas. The Sir Henry Dale lecture for 1983." J Endocrinol **102**(1): 3-11.

Oresic, M., S. Simell, et al. (2008). "Dysregulation of lipid and amino acid metabolism precedes islet autoimmunity in children who later progress to type 1 diabetes." J Exp Med **205**(13): 2975-84.

Organization, W. H. (2011). Diabetes Fact Sheet.

Otu, H. H., H. Can, et al. (2007). "Prediction of diabetic nephropathy using urine proteomic profiling 10 years prior to development of nephropathy." Diabetes Care **30**(3): 638-43.

Owen, O. E., A. P. Morgan, et al. (1967). "Brain metabolism during fasting." J Clin Invest **46**(10): 1589-95.

Park, I. H. and G. Q. Daley (2009). "Human iPS cell derivation/reprogramming." Curr Protoc Stem Cell Biol **Chapter 4**: Unit 4A 1.

Park, I. H., R. Zhao, et al. (2008). "Reprogramming of human somatic cells to pluripotency with defined factors." Nature **451**(7175): 141-6.

Parsa, R., A. Yang, et al. (1999). "Association of p63 with proliferative potential in normal and neoplastic human keratinocytes." J Invest Dermatol **113**(6): 1099-105.

Pedersen, J. K., S. B. Nelson, et al. (2005). "Endodermal expression of Nkx6 genes depends differentially on Pdx1." Dev Biol **288**(2): 487-501.

Peto, R., A. D. Lopez, et al. (1992). "Mortality from tobacco in developed countries: indirect estimation from national vital statistics." Lancet **339**(8804): 1268-78.

Pettersson, C., H. Karlsson, et al. (2011). "LDL-associated apolipoprotein J and lysozyme are associated with atherogenic properties of LDL found in type 2 diabetes and the metabolic syndrome." J Intern Med **269**(3): 306-21.

Phillips, B. W., H. Hentze, et al. (2007). "Directed differentiation of human embryonic stem cells into the pancreatic endocrine lineage." Stem Cells Dev **16**(4): 561-78.

Pickup, J. and G. Williams (1997). Textbook of Diabetes.

Pictet, R. L., W. R. Clark, et al. (1972). "An ultrastructural analysis of the developing embryonic pancreas." Dev Biol **29**(4): 436-67.

Pin, C. L., J. M. Rukstalis, et al. (2001). "The bHLH transcription factor Mist1 is required to maintain exocrine pancreas cell organization and acinar cell identity." J Cell Biol **155**(4): 519-30.

Pipeleers, D. (1987). "The biosociology of pancreatic B cells." Diabetologia **30**(5): 277-91.

Plaisance, V., A. Abderrahmani, et al. (2006). "MicroRNA-9 controls the expression of Granuphilin/Slp4 and the secretory response of insulin-producing cells." J Biol Chem **281**(37): 26932-42.

Polisetty, N., A. Fatima, et al. (2008). "Mesenchymal cells from limbal stroma of human eye." Mol Vis **14**: 431-42.

Poy, M. N., L. Eliasson, et al. (2004). "A pancreatic islet-specific microRNA regulates insulin secretion." Nature **432**(7014): 226-30.

Poy, M. N., J. Hausser, et al. (2009). "miR-375 maintains normal pancreatic alpha- and beta-cell mass." Proc Natl Acad Sci U S A **106**(14): 5813-8.

Prado, C. L., A. E. Pugh-Bernard, et al. (2004). "Ghrelin cells replace insulin-producing beta cells in two mouse models of pancreas development." Proc Natl Acad Sci U S A **101**(9): 2924-9.

Preissner, K. T. and D. Jenne (1991). "Structure of vitronectin and its biological role in haemostasis." Thromb Haemost **66**(1): 123-32.

Preissner, K. T. and D. Seiffert (1998). "Role of vitronectin and its receptors in haemostasis and vascular remodeling." Thromb Res **89**(1): 1-21.

Prentki, M. and C. J. Nolan (2006). "Islet beta cell failure in type 2 diabetes." J Clin Invest **116**(7): 1802-12.

Radvanyi, F., S. Christgau, et al. (1993). "Pancreatic beta cells cultured from individual preneoplastic foci in a multistage tumorigenesis pathway: a potentially general technique for isolating physiologically representative cell lines." Mol Cell Biol **13**(7): 4223-32.

Ramachandran, D., U. Roy, et al. (2011). "Sirt1 and mir-9 expression is regulated during glucose-stimulated insulin secretion in pancreatic beta-islets." Febs J **278**(7): 1167-74.

Rani, S. (2008). Investigation of molecular and cellular events associated with beta cell function and elucidation of extracellular RNAs as potential biomarkers for diabetes. NICB. Dublin, DCU.

Raum, J. C., K. Gerrish, et al. (2006). "FoxA2, Nkx2.2, and PDX-1 regulate islet beta-cell-specific mafA expression through conserved sequences located between base pairs -8118 and -7750 upstream from the transcription start site." Mol Cell Biol **26**(15): 5735-43.

Rausa, F., U. Samadani, et al. (1997). "The cut-homeodomain transcriptional activator HNF-6 is coexpressed with its target gene HNF-3 beta in the developing murine liver and pancreas." Dev Biol **192**(2): 228-46.

Resnick, K. E., H. Alder, et al. (2009). "The detection of differentially expressed microRNAs from the serum of ovarian cancer patients using a novel real-time PCR platform." Gynecol Oncol **112**(1): 55-9.

Richardson, K. C. and F. G. Young (1938). "Histology of diabetes induced in dogs by injection of anterior-pituitary extracts." Lancet **231**(5985): 1098-1100.

Ricordi, C. and T. B. Strom (2004). "Clinical islet transplantation: advances and immunological challenges." Nat Rev Immunol **4**(4): 259-68.

Ritvos, O., T. Tuuri, et al. (1995). "Activin disrupts epithelial branching morphogenesis in developing glandular organs of the mouse." Mech Dev **50**(2-3): 229-45.

Ryals, J., K. Lawton, et al. (2007). "Metabolon, Inc." Pharmacogenomics **8**(7): 863-6.

Sander, M., A. Neubuser, et al. (1997). "Genetic analysis reveals that PAX6 is required for normal transcription of pancreatic hormone genes and islet development." Genes Dev **11**(13): 1662-73.

Sander, M., L. Sussel, et al. (2000). "Homeobox gene Nkx6.1 lies downstream of Nkx2.2 in the major pathway of beta-cell formation in the pancreas." Development **127**(24): 5533-40.

Sandin, M., M. Krogh, et al. (2011). "Generic workflow for quality assessment of quantitative label-free LC-MS analysis." Proteomics **11**(6): 1114-24.

Santerre, R. F., R. A. Cook, et al. (1981). "Insulin synthesis in a clonal cell line of simian virus 40-transformed hamster pancreatic beta cells." Proc Natl Acad Sci U S A **78**(7): 4339-43.

Schermer, A., S. Galvin, et al. (1986). "Differentiation-related expression of a major 64K corneal keratin in vivo and in culture suggests limbal location of corneal epithelial stem cells." J Cell Biol **103**(1): 49-62.

Sellick, G. S., K. T. Barker, et al. (2004). "Mutations in PTF1A cause pancreatic and cerebellar agenesis." Nat Genet **36**(12): 1301-5.

Serup, P., H. V. Petersen, et al. (1995). "The homeodomain protein IPF-1/STF-1 is expressed in a subset of islet cells and promotes rat insulin 1 gene expression dependent on an intact E1 helix-loop-helix factor binding site." Biochem J **310 (Pt 3)**: 997-1003.

Seymour, P. A., K. K. Freude, et al. (2007). "SOX9 is required for maintenance of the pancreatic progenitor cell pool." Proc Natl Acad Sci U S A **104**(6): 1865-70.

Shen, Y., J. Kim, et al. (2005). "Characterization of the human blood plasma proteome." Proteomics **5**(15): 4034-45.

Shim, J. H., S. E. Kim, et al. (2007). "Directed differentiation of human embryonic stem cells towards a pancreatic cell fate." Diabetologia **50**(6): 1228-38.

Shiroi, A., M. Yoshikawa, et al. (2002). "Identification of insulin-producing cells derived from embryonic stem cells by zinc-chelating dithizone." Stem Cells **20**(4): 284-92.

Skelin, M., M. Rupnik, et al. (2010). "Pancreatic beta cell lines and their applications in diabetes mellitus research." Altex **27**(2): 105-13.

Slack, J. M. (1995). "Developmental biology of the pancreas." Development **121**(6): 1569-80.

Smith, S. B., H. C. Ee, et al. (1999). "Paired-homeodomain transcription factor PAX4 acts as a transcriptional repressor in early pancreatic development." Mol Cell Biol **19**(12): 8272-80.

Sosa-Pineda, B., K. Chowdhury, et al. (1997). "The Pax4 gene is essential for differentiation of insulin-producing beta cells in the mammalian pancreas." Nature **386**(6623): 399-402.

Sosnova, M., M. Bradl, et al. (2005). "CD34+ corneal stromal cells are bone marrow-derived and express hemopoietic stem cell markers." Stem Cells **23**(4): 507-15.

Spence, J. R. and J. M. Wells (2007). "Translational embryology: using embryonic principles to generate pancreatic endocrine cells from embryonic stem cells." Dev Dyn **236**(12): 3218-27.

Stanger, B. Z., A. J. Tanaka, et al. (2007). "Organ size is limited by the number of embryonic progenitor cells in the pancreas but not the liver." Nature **445**(7130): 886-91.

Stoffers, D. A., N. T. Zinkin, et al. (1997). "Pancreatic agenesis attributable to a single nucleotide deletion in the human IPF1 gene coding sequence." Nat Genet **15**(1): 106-10.

St-Onge, L., B. Sosa-Pineda, et al. (1997). "Pax6 is required for differentiation of glucagon-producing alpha-cells in mouse pancreas." Nature **387**(6631): 406-9.

Straub, S. G. and G. W. Sharp (2002). "Glucose-stimulated signaling pathways in biphasic insulin secretion." Diabetes Metab Res Rev **18**(6): 451-63.

Suhre, K., C. Meisinger, et al. (2010). "Metabolic footprint of diabetes: a multiplatform metabolomics study in an epidemiological setting." PLoS One **5**(11): e13953.

Sussel, L., J. Kalamaras, et al. (1998). "Mice lacking the homeodomain transcription factor Nkx2.2 have diabetes due to arrested differentiation of pancreatic beta cells." Development **125**(12): 2213-21.

Tada, M., Y. Takahama, et al. (2001). "Nuclear reprogramming of somatic cells by in vitro hybridization with ES cells." Curr Biol **11**(19): 1553-8.

Takahashi, K., K. Tanabe, et al. (2007). "Induction of pluripotent stem cells from adult human fibroblasts by defined factors." Cell **131**(5): 861-72.

Takahashi, K. and S. Yamanaka (2006). "Induction of pluripotent stem cells from mouse embryonic and adult fibroblast cultures by defined factors." Cell **126**(4): 663-76.

Tang, X., L. Muniappan, et al. (2009). "Identification of glucose-regulated miRNAs from pancreatic {beta} cells reveals a role for miR-30d in insulin transcription." Rna **15**(2): 287-93.

Tateishi, K., J. He, et al. (2008). "Generation of insulin-secreting islet-like clusters from human skin fibroblasts." J Biol Chem **283**(46): 31601-7.

Teleman, A. A., S. Maitra, et al. (2006). "Drosophila lacking microRNA miR-278 are defective in energy homeostasis." Genes Dev **20**(4): 417-22.

Tessari, P., G. Biolo, et al. (1990). "Effects of insulin on whole body and forearm leucine and KIC metabolism in type 1 diabetes." Am J Physiol **259**(1 Pt 1): E96-103.

Thomas, M. K., O. N. Devon, et al. (2001). "Development of diabetes mellitus in aging transgenic mice following suppression of pancreatic homeoprotein IDX-1." J Clin Invest **108**(2): 319-29.

Thomas, M. K., J. H. Lee, et al. (2001). "Hedgehog signaling regulation of homeodomain protein islet duodenum homeobox-1 expression in pancreatic beta-cells." Endocrinology **142**(3): 1033-40.

Thomas, M. K., N. Rastalsky, et al. (2000). "Hedgehog signaling regulation of insulin production by pancreatic beta-cells." Diabetes **49**(12): 2039-47.

Thomson, J. A., J. Itskovitz-Eldor, et al. (1998). "Embryonic stem cell lines derived from human blastocysts." Science **282**(5391): 1145-7.

Thorens, B., H. K. Sarkar, et al. (1988). "Cloning and functional expression in bacteria of a novel glucose transporter present in liver, intestine, kidney, and beta-pancreatic islet cells." Cell **55**(2): 281-90.

Tomasini, B. R. and D. F. Mosher (1991). "Vitronectin." Prog Hemost Thromb **10**: 269-305.

Trougakos, I. P., M. Poulakou, et al. (2002). "Serum levels of the senescence biomarker clusterin/apolipoprotein J increase significantly in diabetes type II and during development of coronary heart disease or at myocardial infarction." Exp Gerontol **37**(10-11): 1175-87.

Tsukui, S., Y. Fukumura, et al. (1996). "Decreased serum 1,5-anhydroglucitol in nondiabetic subjects with a family history of NIDDM." Diabetes Care **19**(9): 940-4.

Tsutsui, H., T. Maeda, et al. (2010). "Practical analytical approach for the identification of biomarker candidates in prediabetic state based upon metabonomic study by ultraperformance liquid chromatography coupled to electrospray ionization time-of-flight mass spectrometry." J Proteome Res **9**(8): 3912-22.

Tuli, L. and H. W. Ressom (2009). "LC-MS Based Detection of Differential Protein Expression." J Proteomics Bioinform **2**: 416-438.

Turque, N., S. Plaza, et al. (1994). "Pax-QNR/Pax-6, a paired box- and homeobox-containing gene expressed in neurons, is also expressed in pancreatic endocrine cells." Mol Endocrinol **8**(7): 929-38.

Tzur, S., S. Rosset, et al. (2010). "Missense mutations in the APOL1 gene are highly associated with end stage kidney disease risk previously attributed to the MYH9 gene." Hum Genet **128**(3): 345-50.

van Doorn, M., J. Vogels, et al. (2007). "Evaluation of metabolite profiles as biomarkers for the pharmacological effects of thiazolidinediones in Type 2 diabetes mellitus patients and healthy volunteers." Br J Clin Pharmacol **63**(5): 562-74.

Vannini, P., G. Marchesini, et al. (1982). "Branched-chain amino acids and alanine as indices of the metabolic control in type 1 (insulin-dependent) and type 2 (non-insulin-dependent) diabetic patients." Diabetologia **22**(3): 217-9.

Vincent, R., N. Treff, et al. (2006). "Generation and characterization of novel tetracycline-inducible pancreatic transcription factor-expressing murine embryonic stem cell lines." Stem Cells Dev **15**(6): 953-62.

Vincent, S. D., N. R. Dunn, et al. (2003). "Cell fate decisions within the mouse organizer are governed by graded Nodal signals." Genes Dev **17**(13): 1646-62.

Wakayama, T., A. C. Perry, et al. (1998). "Full-term development of mice from enucleated oocytes injected with cumulus cell nuclei." Nature **394**(6691): 369-74.

Wang, J., L. Elghazi, et al. (2004). "The concerted activities of Pax4 and Nkx2.2 are essential to initiate pancreatic beta-cell differentiation." Dev Biol **266**(1): 178-89.

Wang, K., S. Zhang, et al. (2009). "Circulating microRNAs, potential biomarkers for drug-induced liver injury." Proc Natl Acad Sci U S A **106**(11): 4402-7.

Wang, Q., Y. Wang, et al. (2008). "MicroRNA-377 is up-regulated and can lead to increased fibronectin production in diabetic nephropathy." Faseb J **22**(12): 4126-35.

Wang, X. and K. Ye (2009). "Three-dimensional differentiation of embryonic stem cells into islet-like insulin-producing clusters." Tissue Eng Part A **15**(8): 1941-52.

Wang, X. H., R. Z. Qian, et al. (2009). "MicroRNA-320 expression in myocardial microvascular endothelial cells and its relationship with insulin-like growth factor-1 in type 2 diabetic rats." Clin Exp Pharmacol Physiol **36**(2): 181-8.

Warren, L., P. D. Manos, et al. (2010). "Highly efficient reprogramming to pluripotency and directed differentiation of human cells with synthetic modified mRNA." Cell Stem Cell **7**(5): 618-30.

Warth, A. D. (1991). "Mechanism of action of benzoic acid on Zygosaccharomyces bailii: effects on glycolytic metabolite levels, energy production, and intracellular pH." Appl Environ Microbiol **57**(12): 3410-4.

Weyer, C., D. G. Maggs, et al. (2001). "Amylin replacement with pramlintide as an adjunct to insulin therapy in type 1 and type 2 diabetes mellitus: a physiological approach toward improved metabolic control." Curr Pharm Des **7**(14): 1353-73.

Wierup, N., H. Svensson, et al. (2002). "The ghrelin cell: a novel developmentally regulated islet cell in the human pancreas." Regul Pept **107**(1-3): 63-9.

Wishart, D. S., C. Knox, et al. (2009). "HMDB: a knowledgebase for the human metabolome." Nucleic Acids Res **37**(Database issue): D603-10.

Won, J. C., C. Y. Park, et al. (2009). "1,5-Anhydroglucitol reflects postprandial hyperglycemia and a decreased insulinogenic index, even in subjects with prediabetes and well-controlled type 2 diabetes." Diabetes Res Clin Pract **84**(1): 51-7.

Wu, K. L., M. Gannon, et al. (1997). "Hepatocyte nuclear factor 3beta is involved in pancreatic beta-cell-specific transcription of the pdx-1 gene." Mol Cell Biol **17**(10): 6002-13.

Xia, J. F., Q. L. Liang, et al. (2009). "Ultraviolet and tandem mass spectrometry for simultaneous quantification of 21 pivotal metabolites in plasma from patients with diabetic nephropathy." J Chromatogr B Analyt Technol Biomed Life Sci **877**(20-21): 1930-6.

Xiao, J., X. Luo, et al. (2007). "MicroRNA miR-133 represses HERG K+ channel expression contributing to QT prolongation in diabetic hearts." J Biol Chem **282**(17): 12363-7.

Yakubov, E., G. Rechavi, et al. (2010). "Reprogramming of human fibroblasts to pluripotent stem cells using mRNA of four transcription factors." Biochem Biophys Res Commun **394**(1): 189-93.

Yamanaka, S. (2009). "A fresh look at iPS cells." Cell **137**(1): 13-7.

Yamanaka, S. and H. M. Blau (2010). "Nuclear reprogramming to a pluripotent state by three approaches." Nature **465**(7299): 704-12.

Yamanouchi, T., T. Inoue, et al. (2001). "Post-load glucose measurements in oral glucose tolerance tests correlate well with 1,5-anhydroglucitol, an indicator of overall glycaemic state, in subjects with impaired glucose tolerance." Clin Sci (Lond) **101**(3): 227-33.

Yamanouchi, T., H. Moromizato, et al. (1992). "Estimation of plasma glucose fluctuation with a combination test of hemoglobin A1c and 1,5-anhydroglucitol." Metabolism **41**(8): 862-7.

Yamanouchi, T., N. Ogata, et al. (1996). "Clinical usefulness of serum 1,5-anhydroglucitol in monitoring glycaemic control." Lancet **347**(9014): 1514-8.

Yamanouchi, T., Y. Tachibana, et al. (1992). "Origin and disposal of 1,5-anhydroglucitol, a major polyol in the human body." Am J Physiol **263**(2 Pt 1): E268-73.

Ye, F., B. Duvillie, et al. (2005). "Fibroblast growth factors 7 and 10 are expressed in the human embryonic pancreatic mesenchyme and promote the proliferation of embryonic pancreatic epithelial cells." Diabetologia **48**(2): 277-81.

Yu, J., M. A. Vodyanik, et al. (2007). "Induced pluripotent stem cell lines derived from human somatic cells." Science **318**(5858): 1917-20.

Zampetaki, A., S. Kiechl, et al. (2010). "Plasma microRNA profiling reveals loss of endothelial miR-126 and other microRNAs in type 2 diabetes." Circ Res **107**(6): 810-7.

Zecchin, E., A. Filippi, et al. (2007). "Distinct delta and jagged genes control sequential segregation of pancreatic cell types from precursor pools in zebrafish." Dev Biol **301**(1): 192-204.

Zecchin, E., A. Mavropoulos, et al. (2004). "Evolutionary conserved role of ptf1a in the specification of exocrine pancreatic fates." Dev Biol **268**(1): 174-84.

Zethelius, B., L. Berglund, et al. (2008). "Use of multiple biomarkers to improve the prediction of death from cardiovascular causes." N Engl J Med **358**(20): 2107-16.

Zhang, C., T. Moriguchi, et al. (2005). "MafA is a key regulator of glucose-stimulated insulin secretion." Mol Cell Biol **25**(12): 4969-76.

Zhang, D., W. Jiang, et al. (2009). "Highly efficient differentiation of human ES cells and iPS cells into mature pancreatic insulin-producing cells." Cell Res **19**(4): 429-38.

Zhang, J., L. Yan, et al. (2009). "Metabonomics research of diabetic nephropathy and type 2 diabetes mellitus based on UPLC-oaTOF-MS system." Anal Chim Acta **650**(1): 16-22.

Zhang, S., G. A. Nagana Gowda, et al. (2008). "Correlative and quantitative 1H NMR-based metabolomics reveals specific metabolic pathway disturbances in diabetic rats." Anal Biochem **383**(1): 76-84.

Zhang, S. X., H. Sun, et al. (2010). "Proteomic study of serum proteins in a type 2 diabetes mellitus rat model by Chinese traditional medicine Tianqi Jiangtang Capsule administration." J Pharm Biomed Anal **53**(4): 1011-4.

Zhang, X., Y. Wang, et al. (2009). "Human serum metabonomic analysis reveals progression axes for glucose intolerance and insulin resistance statuses." J Proteome Res **8**(11): 5188-95.

Zhang, Y., W. Shen, et al. (2010). "Pancreatic islet-like clusters from bone marrow mesenchymal stem cells of human first-trimester abortus can cure streptozocin-induced mouse diabetes." Rejuvenation Res **13**(6): 695-706.

Zhang, Y. Q., H. Mashima, et al. (2001). "Changes in the expression of transcription factors in pancreatic AR42J cells during differentiation into insulin-producing cells." Diabetes **50 Suppl 1**: S10-4.

Zhang, Z. W., L. Q. Zhang, et al. (2011). "MicroRNA-19b downregulates insulin 1 through targeting transcription factor NeuroD1." FEBS Lett **585**(16): 2592-8.

Zhao, C., J. Dong, et al. (2011). "Early second-trimester serum miRNA profiling predicts gestational diabetes mellitus." PLoS One **6**(8): e23925.

Zhao, X., A. V. Das, et al. (2008). "Derivation of neurons with functional properties from adult limbal epithelium: implications in autologous cell therapy for photoreceptor degeneration." Stem Cells **26**(4): 939-49.

Zhao, X., J. Fritsche, et al. (2010). "Metabonomic fingerprints of fasting plasma and spot urine reveal human pre-diabetic metabolic traits." Metabolomics **6**(3): 362-374.

Zhou, H., S. Wu, et al. (2009). "Generation of induced pluripotent stem cells using recombinant proteins." Cell Stem Cell **4**(5): 381-4.

Zhou, Q., A. C. Law, et al. (2007). "A multipotent progenitor domain guides pancreatic organogenesis." Dev Cell **13**(1): 103-14.

Zhu, W., W. Qin, et al. (2009). "Circulating microRNAs in breast cancer and healthy subjects." BMC Res Notes **2**: 89.

Zipf, W. B., T. M. O'Dorisio, et al. (1981). "Blunted pancreatic polypeptide responses in children with obesity of Prader-Willi syndrome." J Clin Endocrinol Metab **52**(6): 1264-6.

Appendix A

MiRNA functional analysis – Raw Data

1.1 Functional Validation Mir-410

Functional validation of TLDA targets (table 3.2.2) was performed to investigate if manipulation of expression of these miRNAs in MIN6 cells led to a phenotypic effect on GSIS on the cells.

(a) Knockdown of mir-410

Figure 1 shows the GSIS assay following knockdown of mir-410 levels in MIN6 cells. This experiment shows instability of the 3.3mM glucose baseline in control samples, therefore no conclusions can be drawn from this experiment.

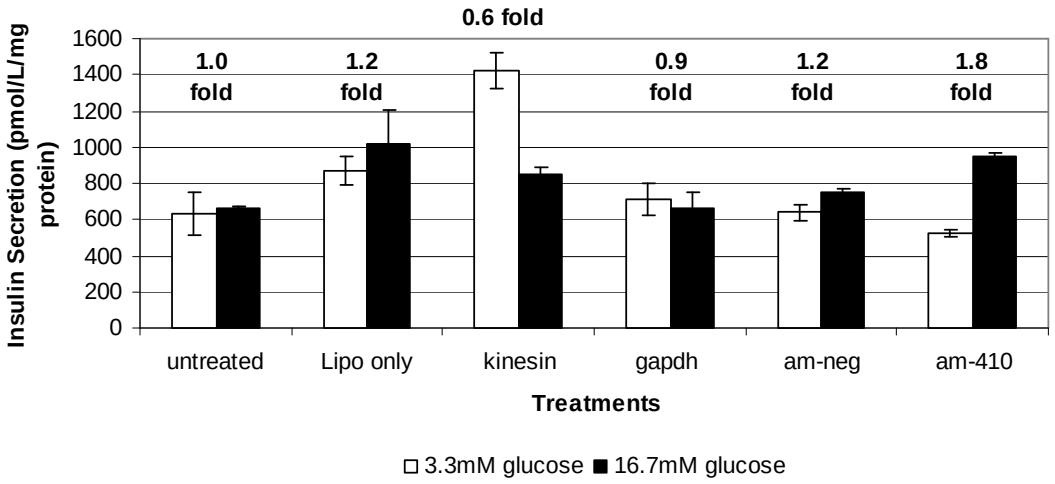

Figure 1. Knockdown of mir-410 levels in MIN6 cells (error bars indicate standard error of technical replicates).

Mir-410 knockdown, figure 2 was not taken as a representative of the effect of mir-410 on GSIS. Although am-410 showed knockdown of GSIS compared to controls, the 3.3mM baseline was very low compared to controls. Pm-410 showed slightly improved GSIS compared to pm-negative, however untreated cells showed very high GSIS compared to pm-negative control.

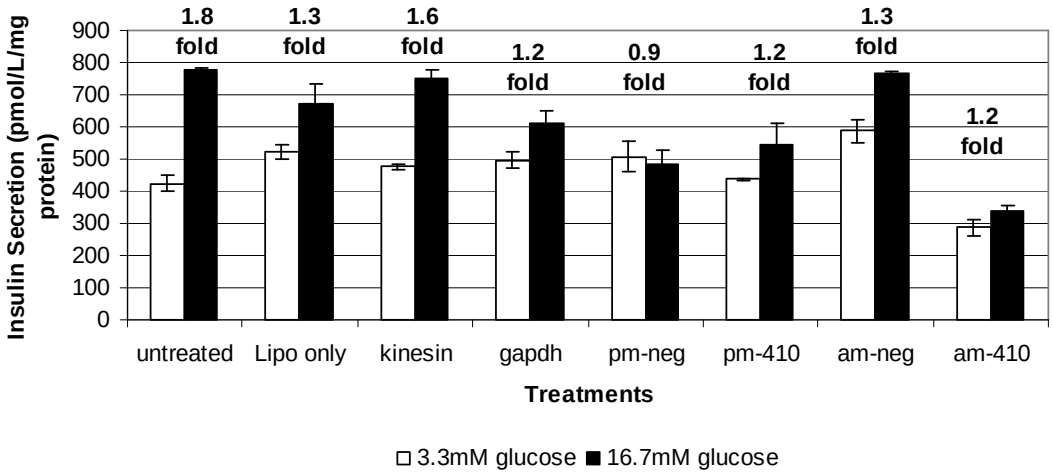

Figure 2. Knockdown of mir-410 levels in MIN6 cells (error bars indicate standard error of technical replicates).

Following analysis of bulk assays (figure 1 and figure 2) it was observed that performing assays in bulk led to a decrease in GSIS of all sample transfected cells as well as control cells, compared to the GSIS of cells at the previous passage where a single GSIS assay was performed. Therefore lipofectamine only and kinesin siRNA controls were not used in subsequent experiments in an attempt to reduce to length of assay setup and maintain high GSIS levels of MIN6 cells during transfection assays.

Knockdown of mir-410 (figure 3) shows a reduction of GSIS compared to untreated and am-negative treated cells.

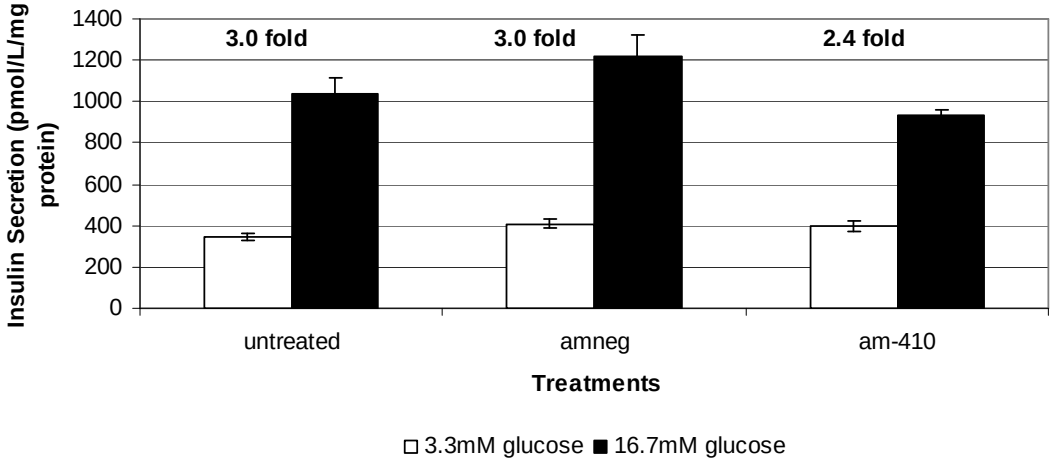

Figure 3. Knockdown of mir-410 levels in MIN6 cells (error bars indicate standard error of technical replicates).

Knockdown of mir-410 (figure 4) shows slightly increased GSIS compared to control cells. This is the opposite effect as expected, as mir-410 expression was reduced in glucose non-responsive cells therefore knockdown of mir-410 levels would be expected to reduce GSIS.

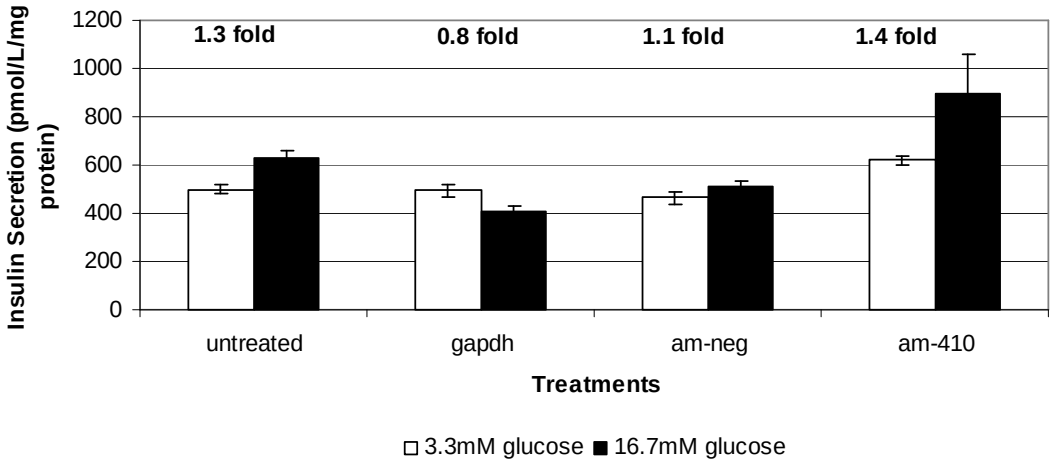

Figure 4. Knockdown of mir-410 levels in MIN6 cells (error bars indicate standard error of technical replicates).

Knockdown of mir-410 (figure 5) shows stable large decrease in GSIS of am-neg control transfected cells, however, in relation to untreated and gapdh siRNA treated cells, am-410 treated cells show a slight knockdown of GSIS.

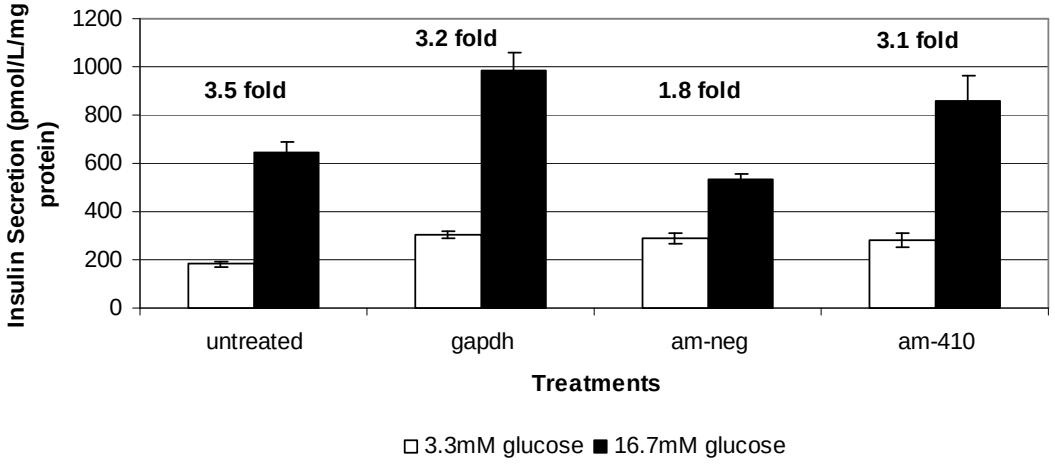

Figure 5. Knockdown of mir-410 levels in MIN6 cells (error bars indicate standard error of technical replicates).

Knockdown of mir-410 (figure 6) shows a reduction of GSIS compared to untreated and am-negative treated cells.

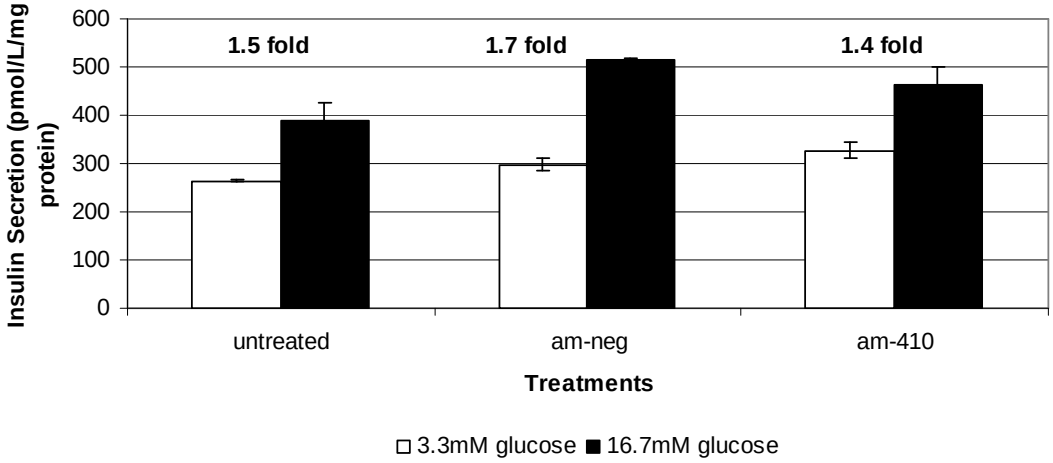

Figure 6. Knockdown of mir-410 levels in MIN6 cells (error bars indicate standard error of technical replicates).

Knockdown of mir-410 (figure 7) shows a reduction of GSIS compared to untreated and am-negative treated cells.

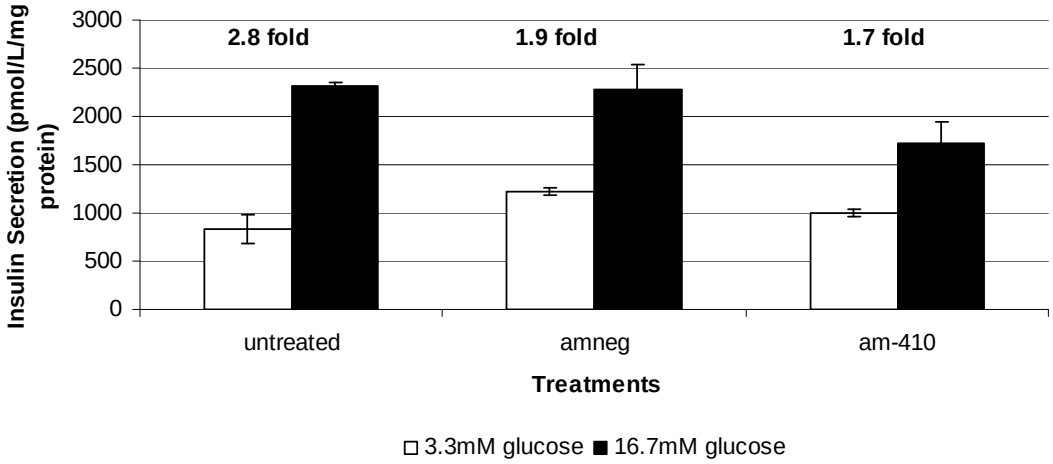

Figure 7. Knockdown of mir-410 levels in MIN6 cells (error bars indicate standard error of technical replicates).

Knockdown of mir-410 assay (figure 8) shows large decrease in GSIS of am-neg control and am-410 treated cells compared to untreated cells.

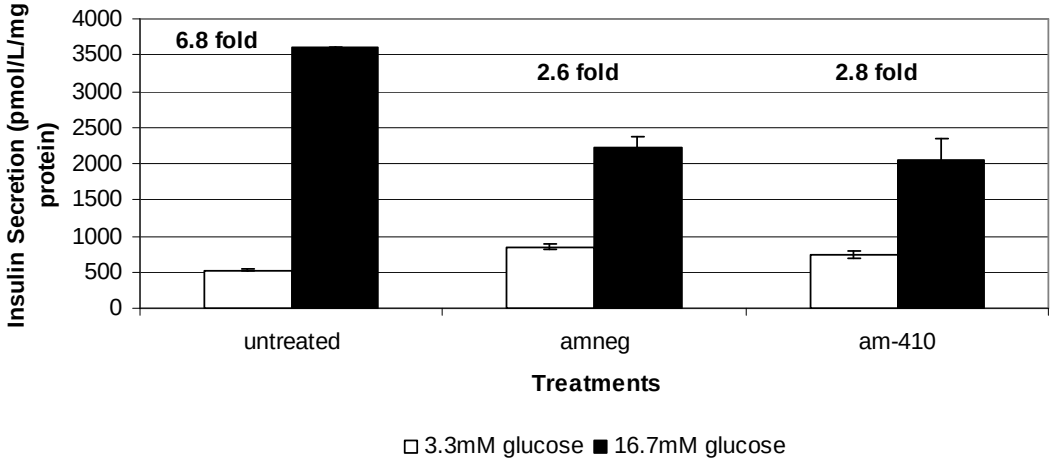

Figure 8. Knockdown of mir-410 levels in MIN6 cells (error bars indicate standard error of technical replicates).

Knockdown of mir-410 (figure 9) assay also shows a big difference in GSIS fold change between control samples.

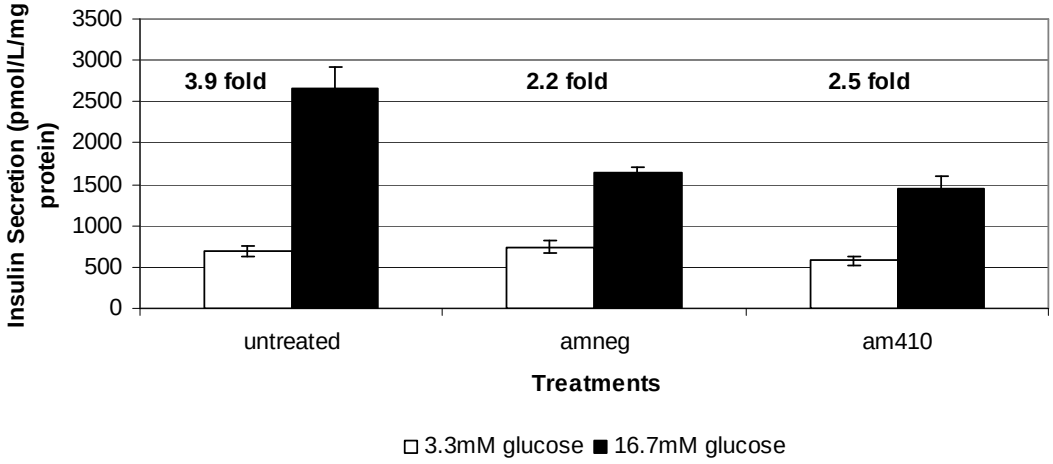

Figure 9. Knockdown of mir-410 levels in MIN6 cells (error bars indicate standard error of technical replicates).

Knockdown of mir-410 (figure 10) shows a reduction of GSIS for am-410 transfected cells compared to untreated and am-neg treated cells.

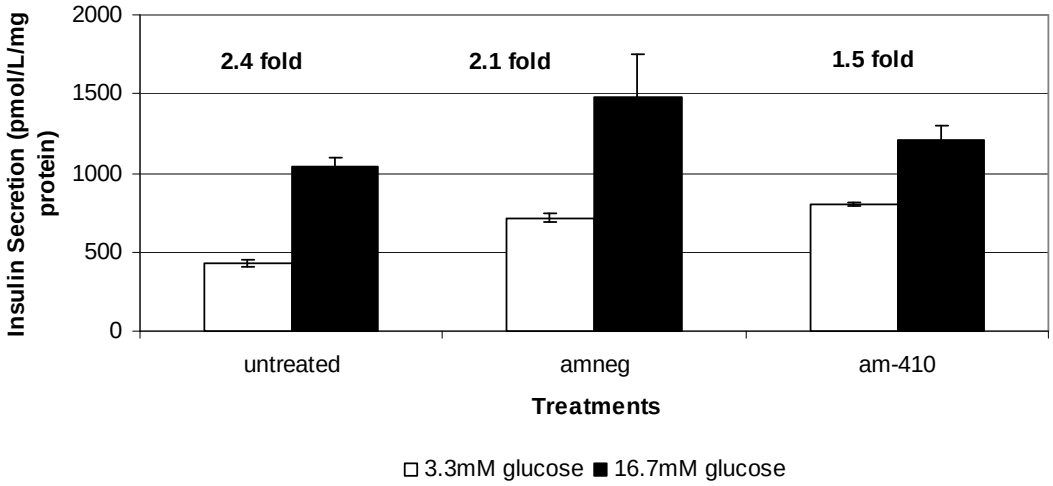

Figure 10. Knockdown of mir-410 levels in MIN6 cells (error bars indicate standard error of technical replicates).

Knockdown of mir-410 (figure 11) shows a reduction of GSIS for am-410 transfected cells compared to untreated and am-neg treated cells.

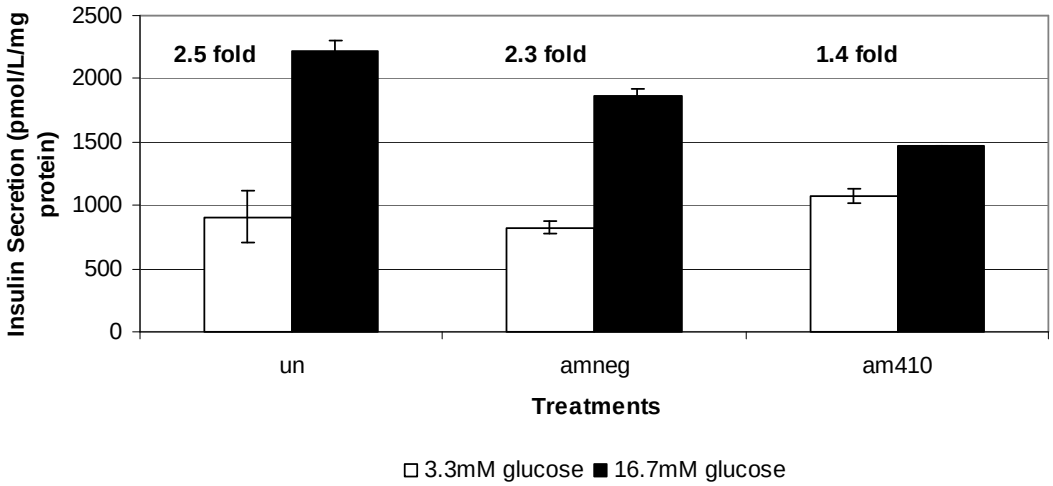

Figure 11. Knockdown of mir-410 levels in MIN6 cells (error bars indicate standard error of technical replicates).

(b) Over-expression of mir-410

Over-expression of mir-410 assay (figure 12) showed large differences in GSIS of control cells.

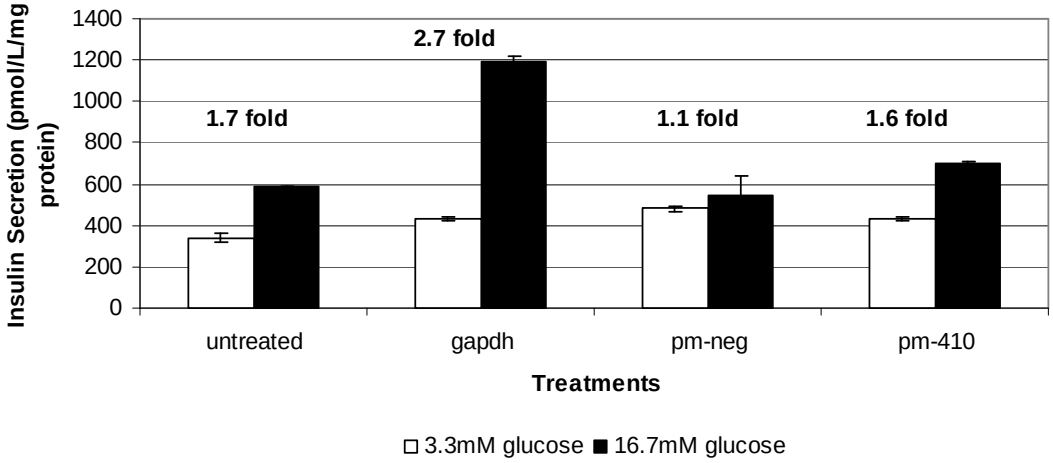

Figure 12. Over-expression of mir-410 levels in MIN6 cells (error bars indicate standard error of technical replicates).

Over-expression of mir-410 (figure 13) showed increased GSIS compared to untreated and pm-neg treated cells.

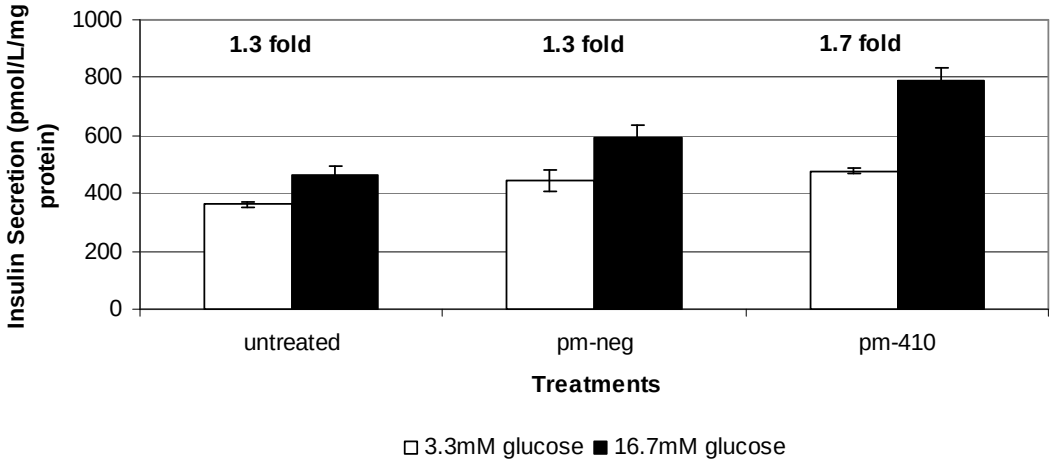

Figure 13. Over-expression of mir-410 levels in MIN6 cells (error bars indicate standard error of technical replicates).

Over-expression of mir-410 (figure 14) showed no change in GSIS compared to untreated and control transfected cells.

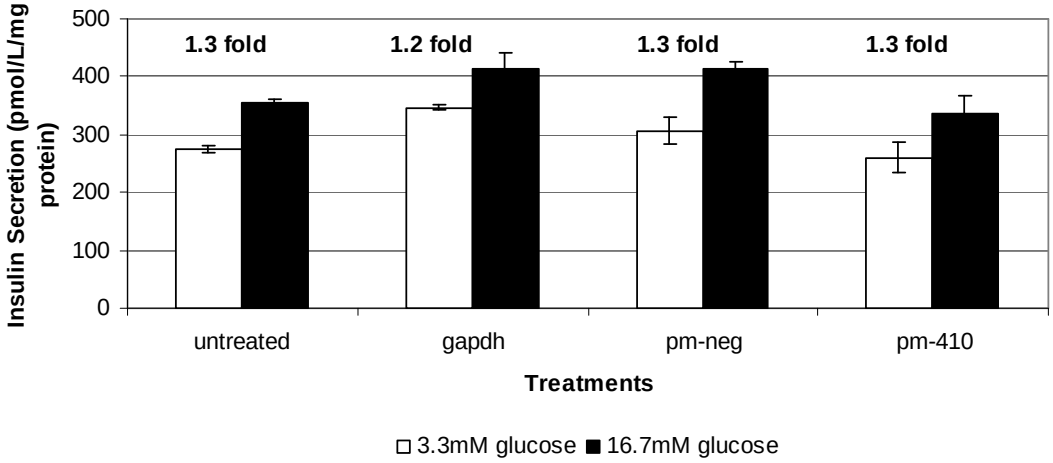

Figure 14. Over-expression of mir-410 levels in MIN6 cells (error bars indicate standard error of technical replicates).

Over-expression of mir-410 (figure 15) showed no change in GSIS compared to untreated and control transfected cells.

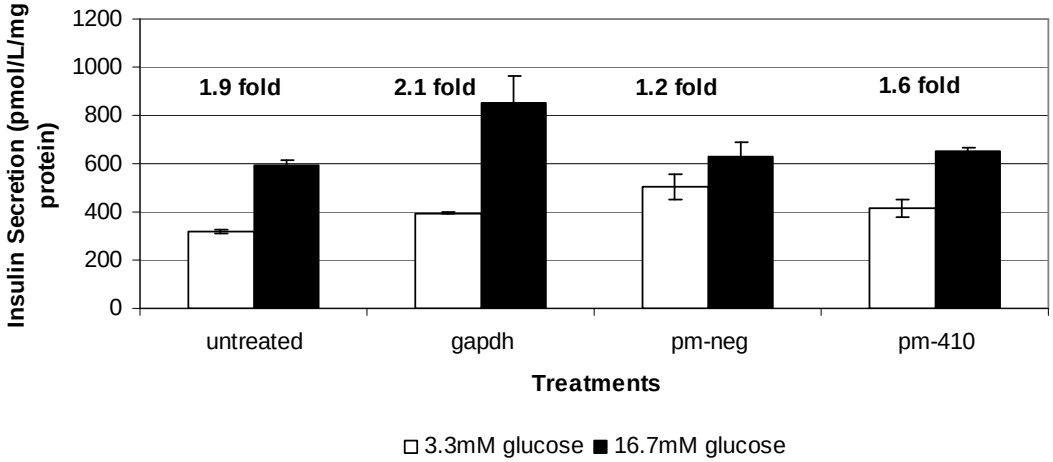

Figure 15. Over-expression of mir-410 levels in MIN6 cells (error bars indicate standard error of technical replicates).

Over-expression of mir-410 (figure 16) showed increased GSIS compared to untreated and pm-neg transfected cells.

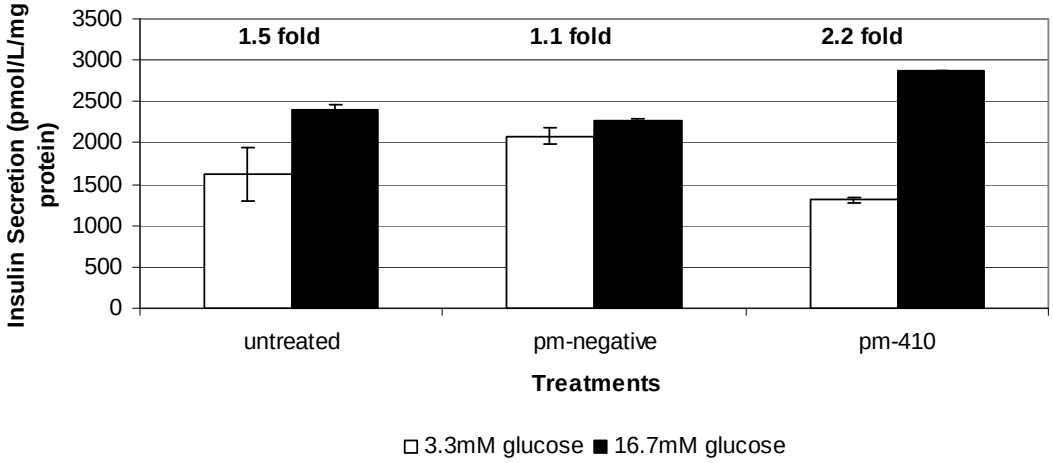

Figure 16. Over-expression of mir-410 levels in MIN6 cells (error bars indicate standard error of technical replicates).

Over-expression of mir-410 (figure 17) showed increased GSIS compared to untreated and pm-neg transfected cells.

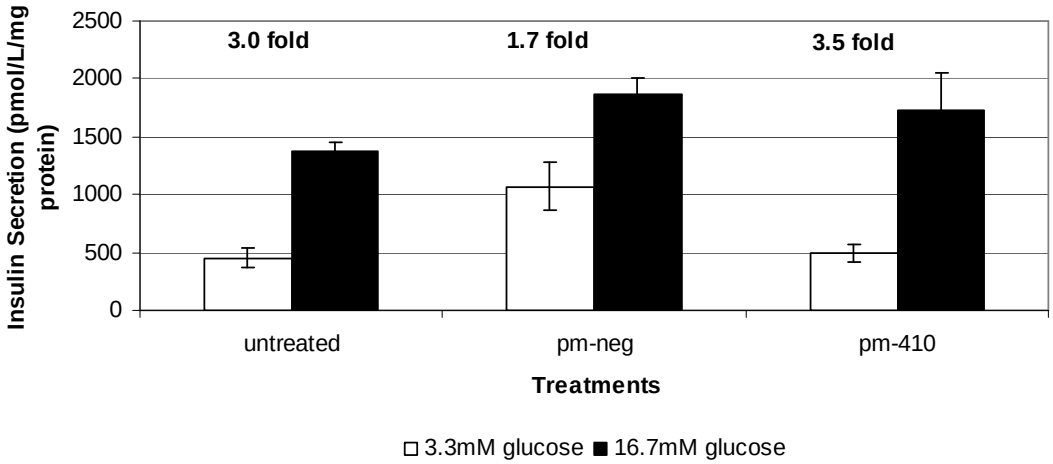

Figure 17. Over-expression of mir-410 levels in MIN6 cells (error bars indicate standard error of technical replicates).

Over-expression of mir-410 assay (figure 18) showed large differences in the GSIS fold change of control cells.

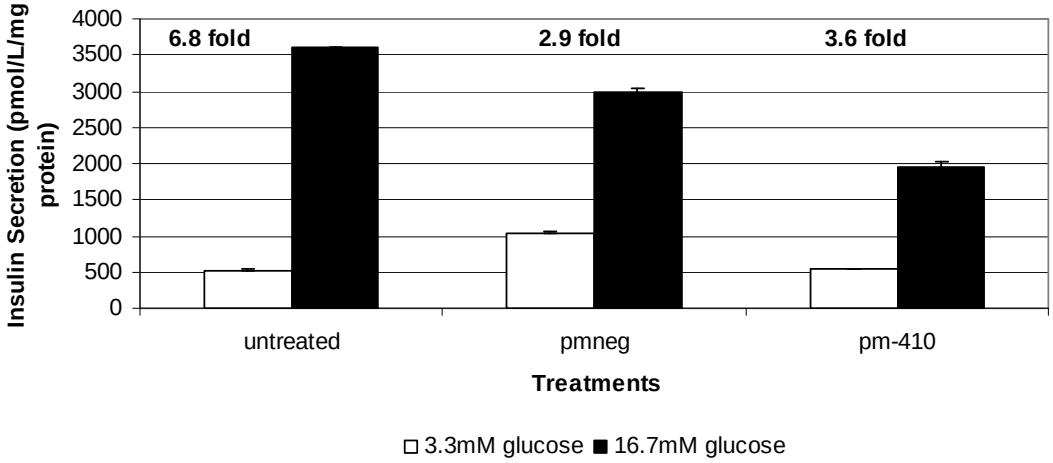

Figure 18. Over-expression of mir-410 levels in MIN6 cells (error bars indicate standard error of technical replicates).

Over-expression of mir-410 (figure 19) showed increased GSIS compared to untreated and pm-neg transfected cells.

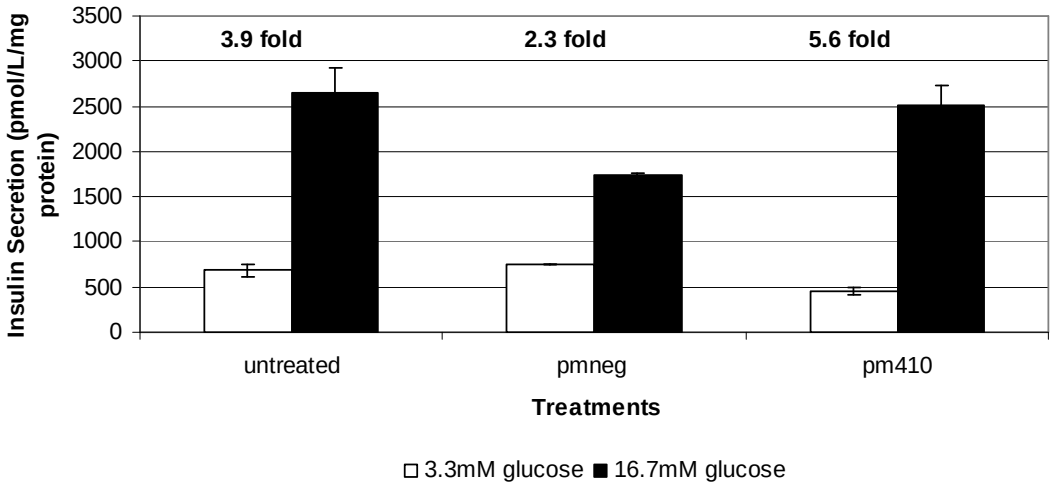

Figure 19. Over-expression of mir-410 levels in MIN6 cells (error bars indicate standard error of technical replicates).

Over-expression of mir-410 (figure 20) showed no change in GSIS compared to untreated and pm-neg transfected cells.

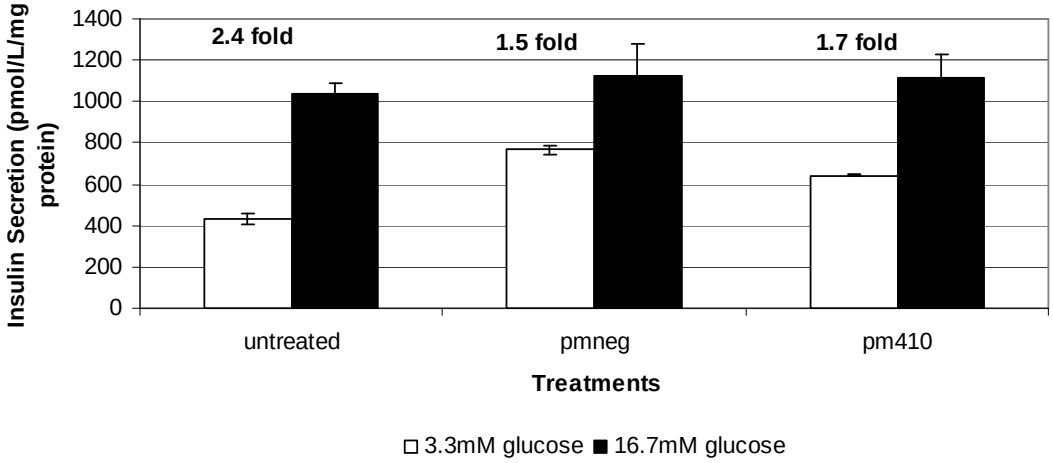

Figure 20. Over-expression of mir-410 levels in MIN6 cells (error bars indicate standard error of technical replicates).

Over-expression of mir-410 (figure 21) showed increased GSIS compared to untreated and pm-neg transfected cells.

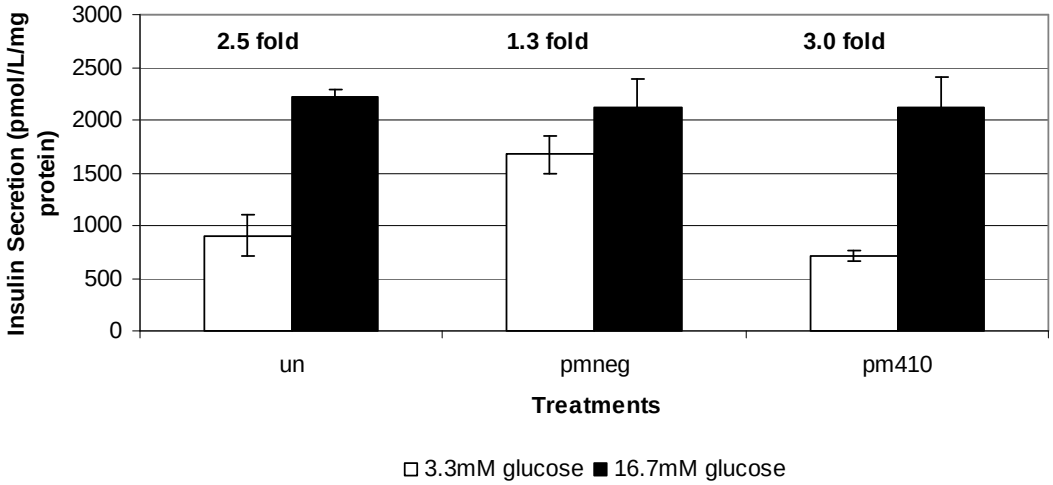

Figure 21. Over-expression of mir-410 levels in MIN6 cells (error bars indicate standard error of technical replicates).

1.2 Functional Validation of mir-200a

Mir-200a expression was reduced in non-GSIS MIN6 cells (table 3.2.2), therefore knockdown of this target with mir-410 inhibitors was expected to reduce GSIS function of MIN6 cells, while mir-410 over-expression was expected to improve GSIS function.

(a) Knockdown of mir-200a

Knockdown of mir-200a (figure 22) shows reduced GSIS relative to control cells.

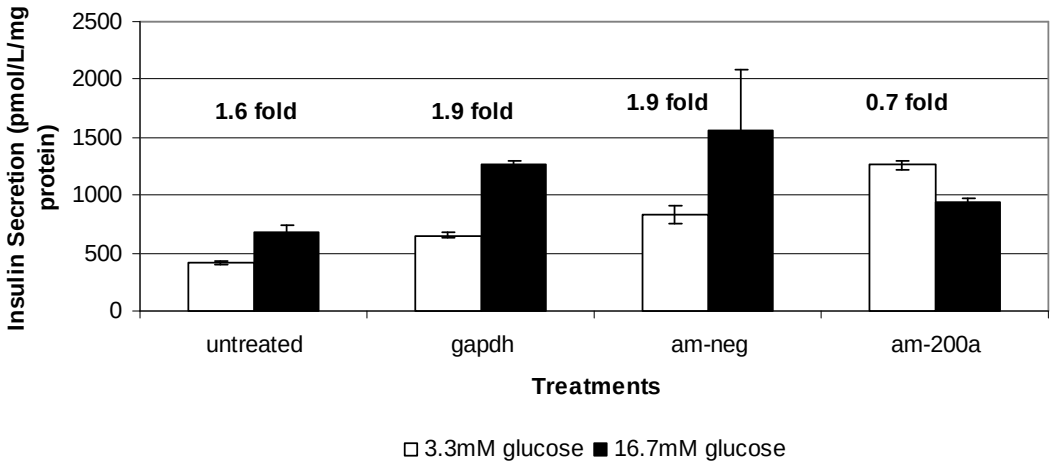

Figure 22. Knockdown of mir-200a levels in MIN6 cells (error bars indicate standard error of technical replicates).

Knockdown of mir-200a (figure 23) shows reduced GSIS compared to untreated and am-neg transfected cells.

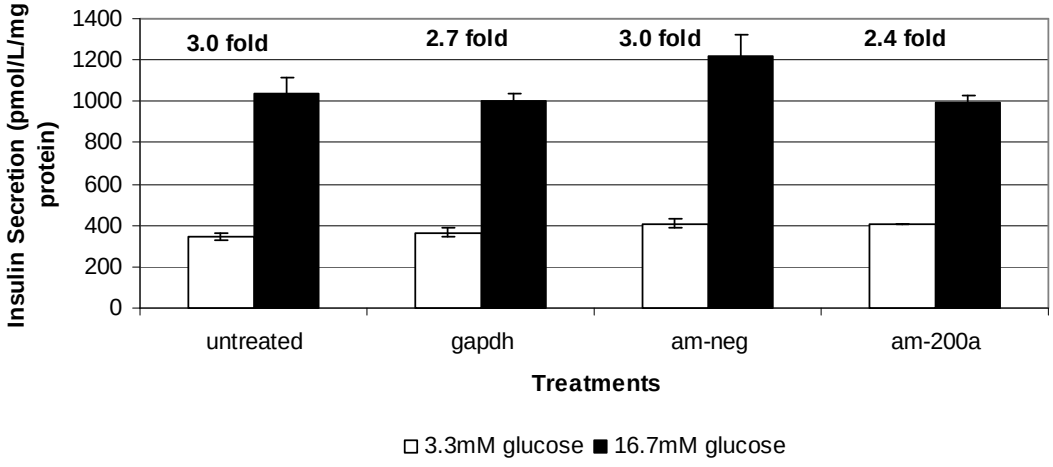

Figure 23. Knockdown of mir-200a levels in MIN6 cells (error bars indicate standard error of technical replicates).

Mir-200a knockdown assay (figure 24) shows large difference in GSIS response of control cells.

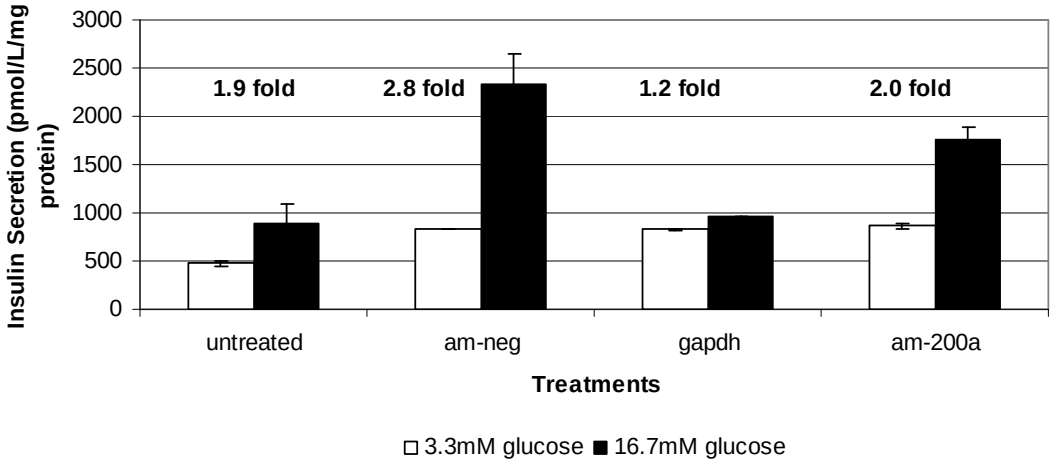

Figure 24. Knockdown of mir-200a levels in MIN6 cells (error bars indicate standard error of technical replicates).

Mir-200a knockdown (figure 25) shows reduced GSIS relative to untreated and am-neg transfected cells.

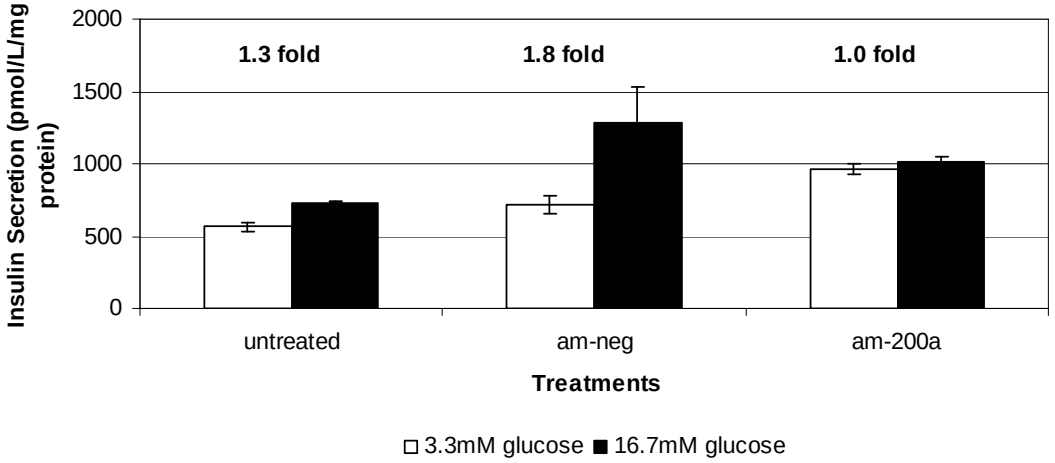

Figure 25. Knockdown of mir-200a levels in MIN6 cells (error bars indicate standard error of technical replicates).

Mir-200a knockdown (figure 26) shows reduced GSIS relative at untreated and am-neg transfected cells.

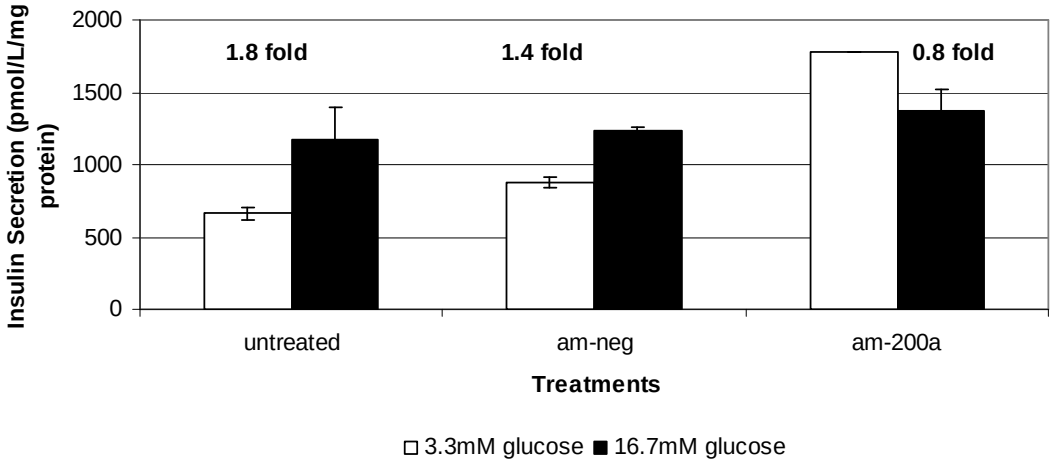

Figure 26. Knockdown of mir-200a levels in MIN6 cells (error bars indicate standard error of technical replicates).

Knockdown of mir-200a (figure 27) shows reduced GSIS relative to untreated and am-neg transfected cells.

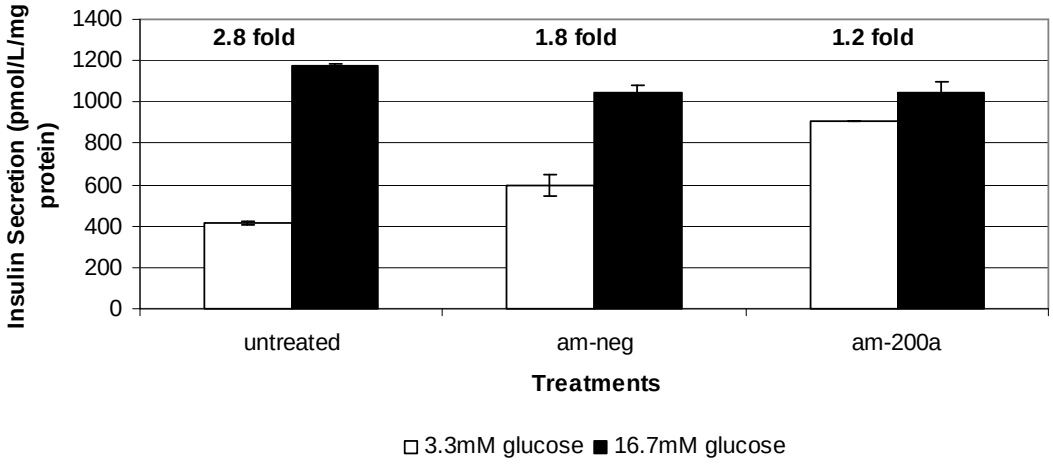

Figure 27. Knockdown of mir-200a levels in MIN6 cells (error bars indicate standard error of technical replicates).

Knockdown of mir-200a assay (figure 28) large differences in GSIS of controls are observed, making it difficult to draw any conclusion regarding an effect of mir-200a knockdown.

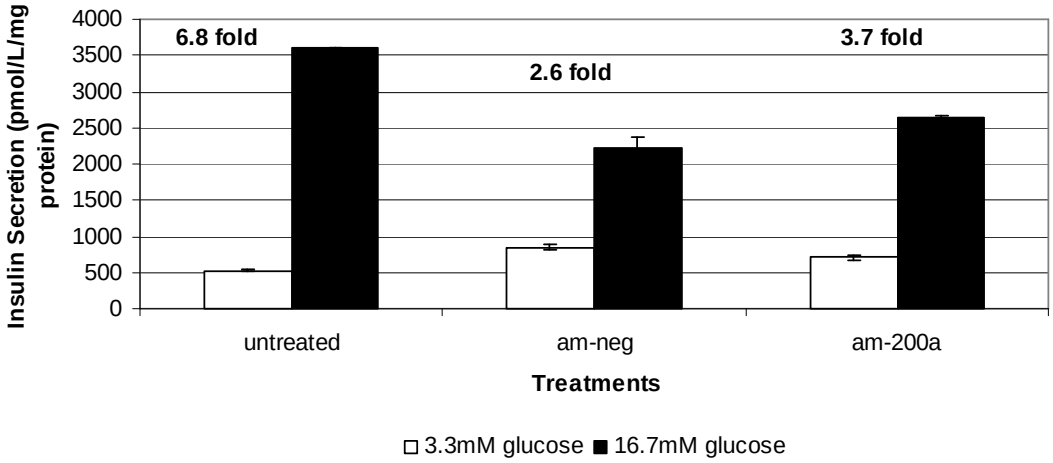

Figure 28. Knockdown of mir-200a levels in MIN6 cells (error bars indicate standard error of technical replicates).

Knockdown of mir-200a assay (figure 29), GSIS lies within the large GSIS range of controls therefore cannot draw any conclusions from this experiment.

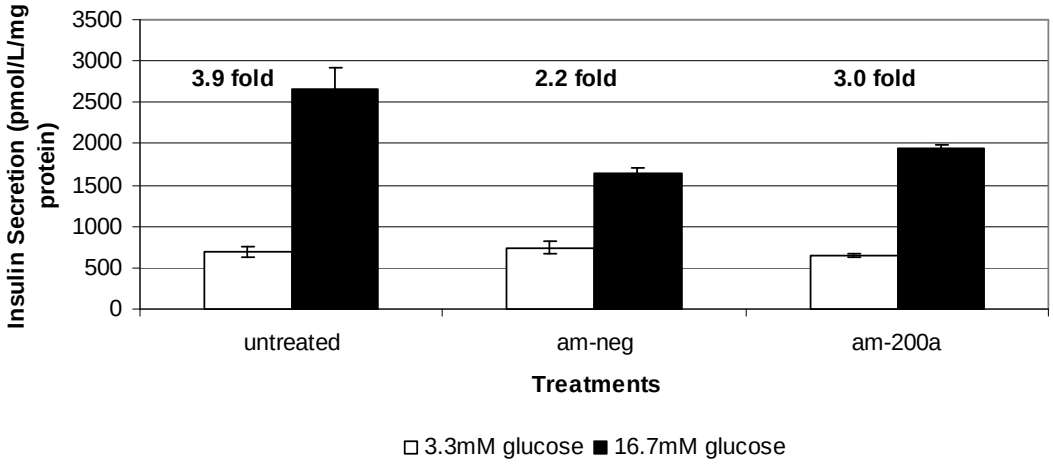

Figure 29. Knockdown of mir-200a levels in MIN6 cells (error bars indicate standard error of technical replicates).

Knockdown of mir-200a (figure 30) shows reduced GSIS relative to untreated and am-neg transfected cells.

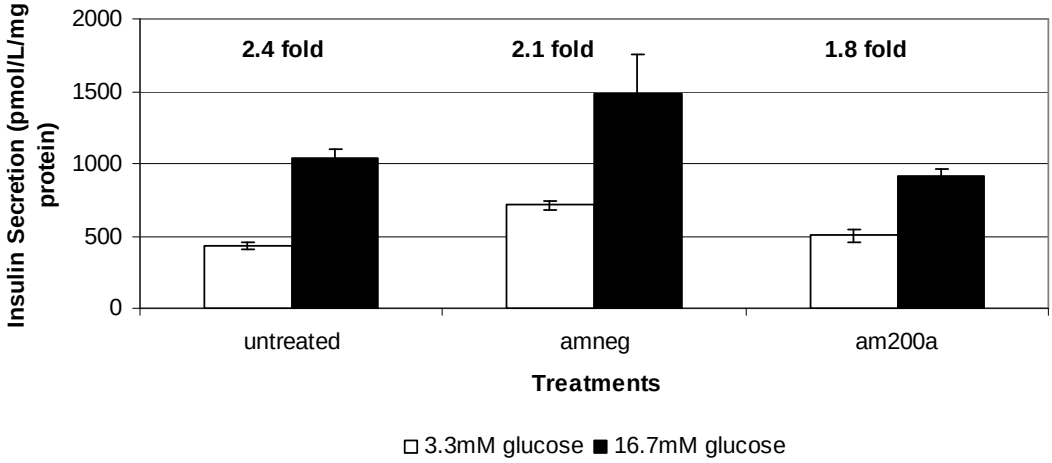

Figure 30. Knockdown of mir-200a levels in MIN6 cells (error bars indicate standard error of technical replicates).

(b) Over-expression of mir-200a

GAPDH siRNA treated cells show a high GSIS fold change in figure 31. However, relative to untreated and pm-neg transfected cells, over-expression of mir-200a showed no change in GSIS.

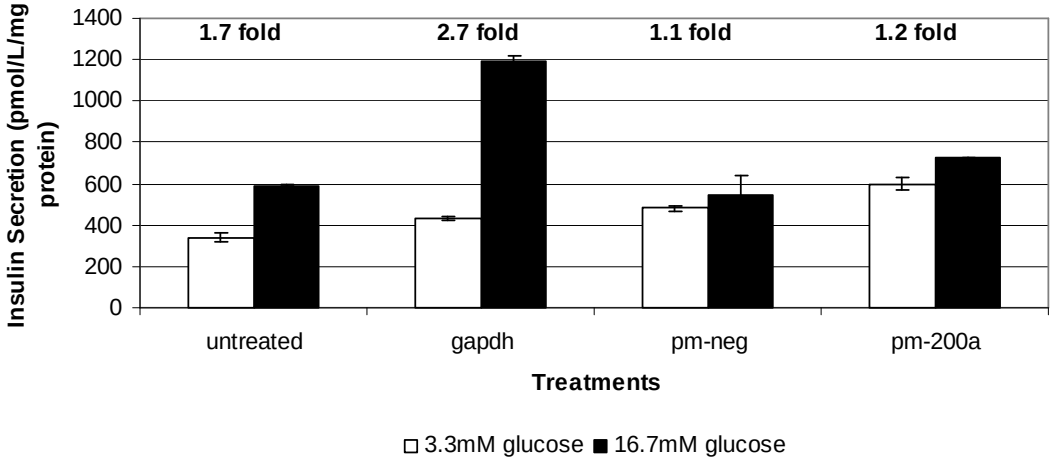

Figure 31. Over-expression of mir-200a in MIN6 cells (error bars indicate standard error of technical replicates).

Over-expression of mir-200a (figure 32) showed reduced GSIS relative to control cells.

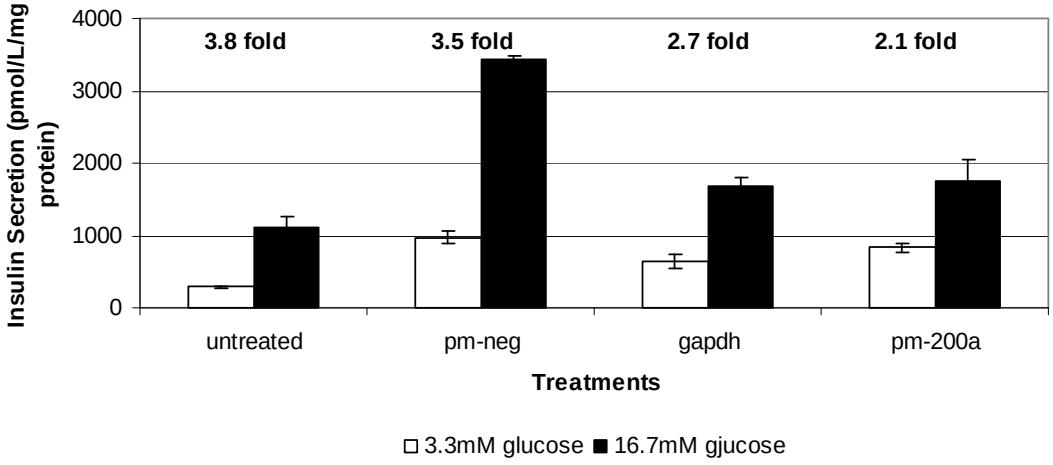

Figure 32. Over-expression of mir-200a in MIN6 cells (error bars indicate standard error of technical replicates).

Over-expression of mir-200a (figure 33) showed increased GSIS relative to untreated and pm-neg transfected cells.

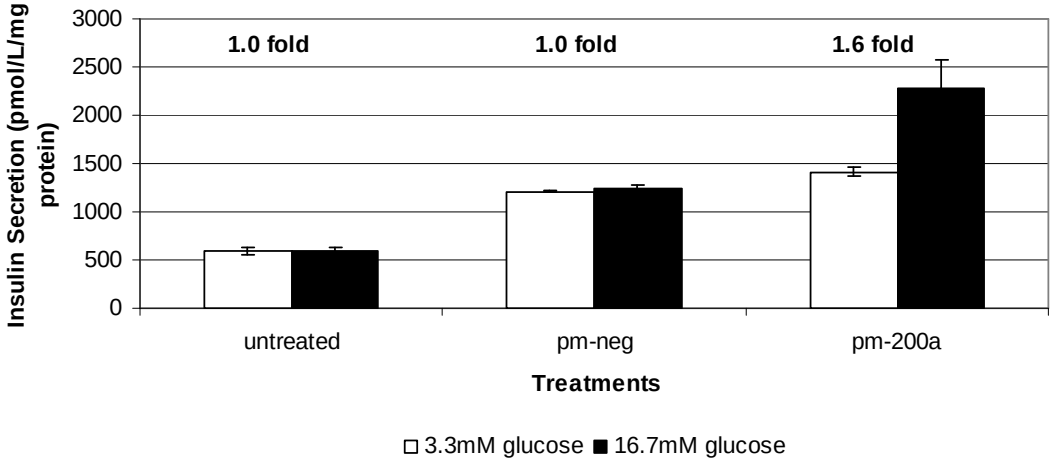

Figure 33. Over-expression of mir-200a in MIN6 cells (error bars indicate standard error of technical replicates).

1.3 Functional Validation of mir-130a

Mir-130a expression was manipulated using pre- and anti-mir miRNA mimics and inhibitors to increase and decrease mir-130a expression respectively. GSIS of transfected cells was examined to determine if manipulation of mir-130a effected GSIS phenotype.

(a) Knockdown of mir-130a

Knockdown of mir-130a (figure 34) reduced GSIS relative to control cells.

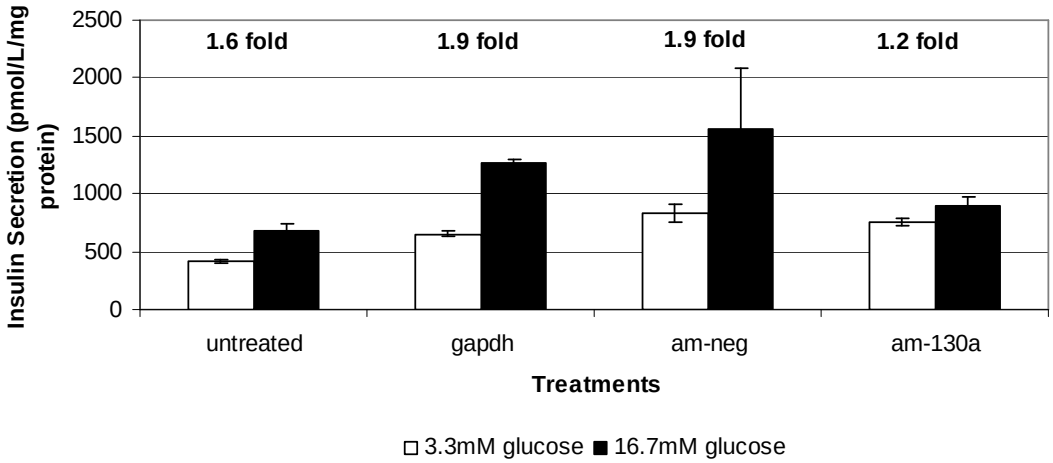

Figure 34. Knockdown of mir-130a levels in MIN6 cells (error bars indicate standard error of technical replicates).

Knockdown of mir-130a (figure 35) reduced GSIS relative to control cells.

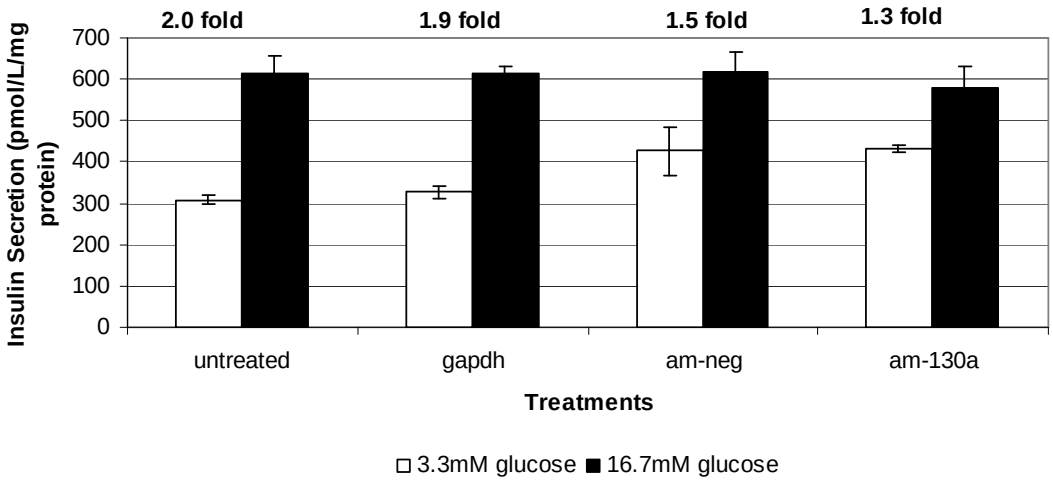

Figure 35. Knockdown of mir-130a levels in MIN6 cells (error bars indicate standard error of technical replicates).

Knockdown of mir-130a (figure 36) reduced GSIS relative to untreated and am-neg tranfected cells.

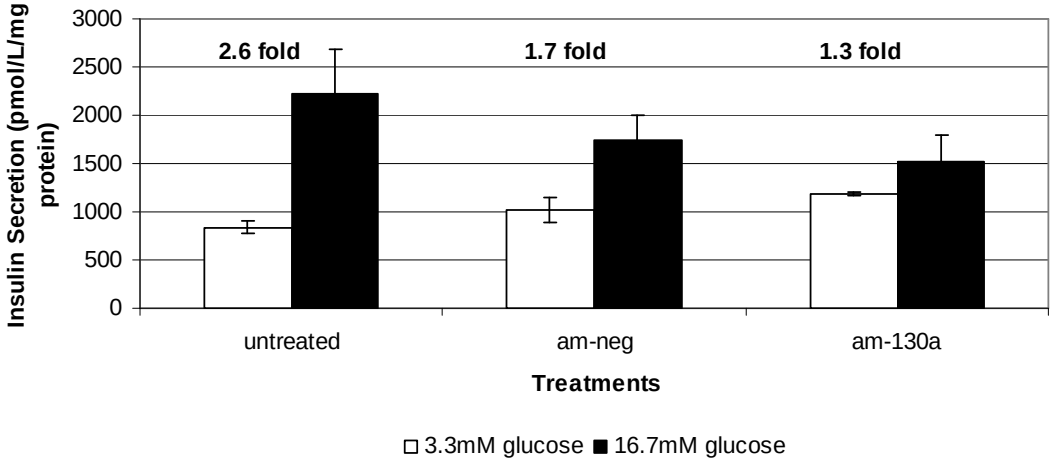

Figure 36. Knockdown of mir-130a levels in MIN6 cells (error bars indicate standard error of technical replicates).

Knockdown of mir-130a (figure 37) reduced GSIS relative to control cells.

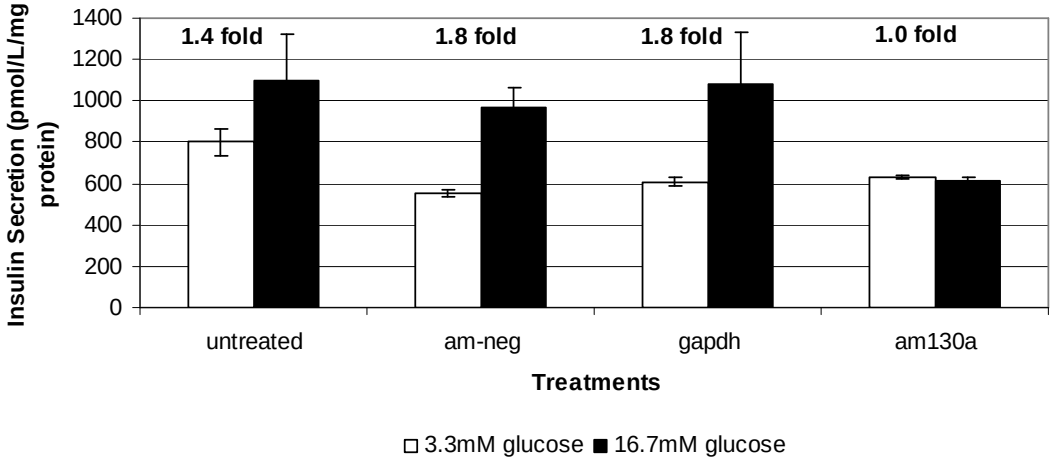

Figure 37. Knockdown of mir-130a levels in MIN6 cells (error bars indicate standard error of technical replicates).

Large differences are observed between GSIS of control cells (figure 38) making it difficult to draw conclusions regarding the effect of mir-130a knockdown.

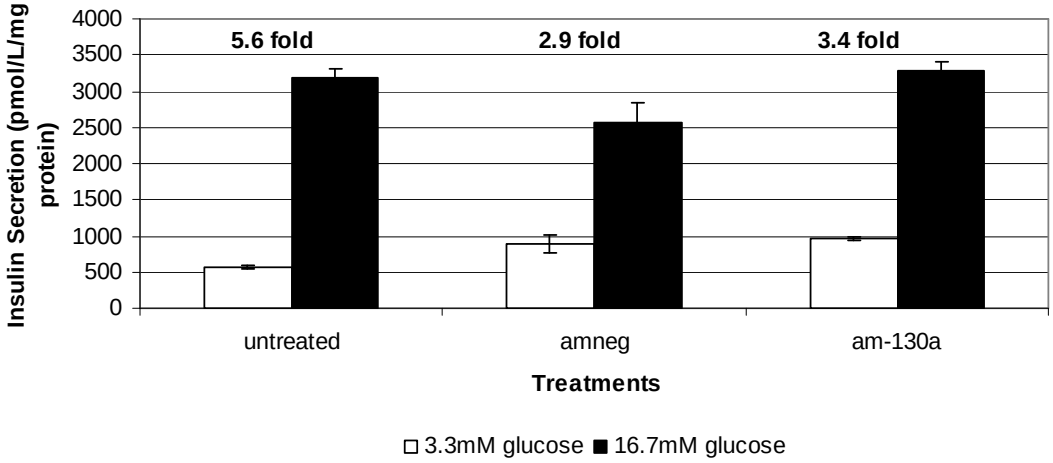

Figure 38. Knockdown of mir-130a levels in MIN6 cells (error bars indicate standard error of technical replicates).

Large differences are observed between the GSIS of control cells (figure 39) making it difficult to draw conclusions regarding the effect of mir-130a knockdown.

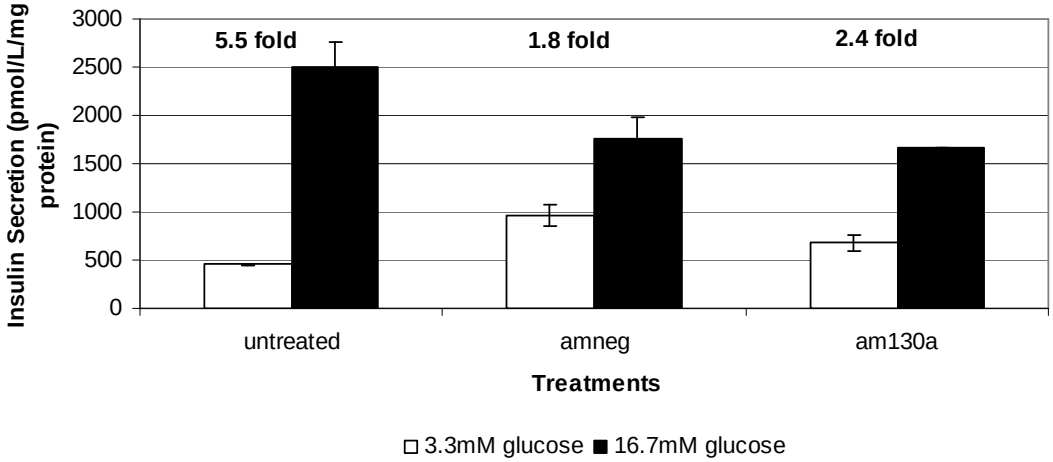

Figure 39. Knockdown of mir-130a levels in MIN6 cells (error bars indicate standard error of technical replicates).

(b) Over-expression of mir-130a

Over-expression of mir-130a (figure 40) showed no effect on GSIS relative to controls.

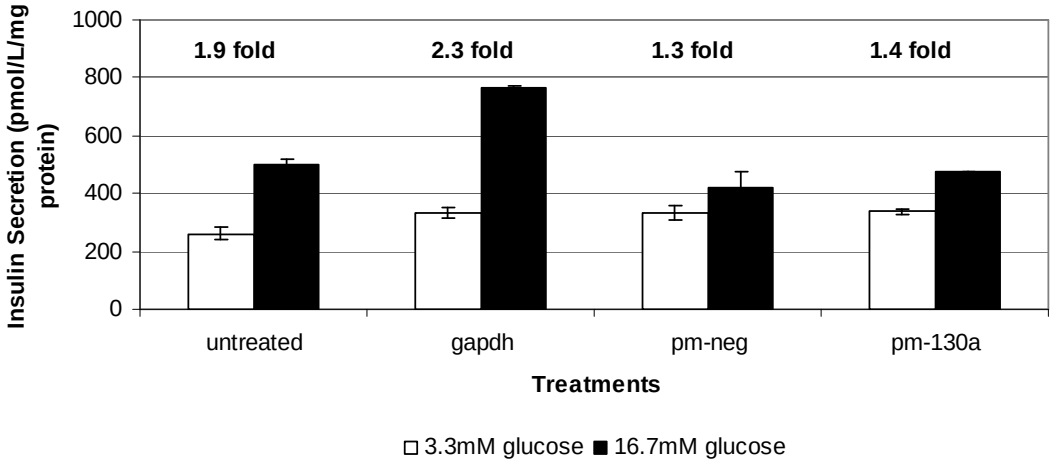

Figure 40. Over-expression of mir-130a in MIN6 cells (error bars indicated standard error of technical replicates).

Over-expression of mir-130a (figure 41) showed reduced GSIS relative to controls.

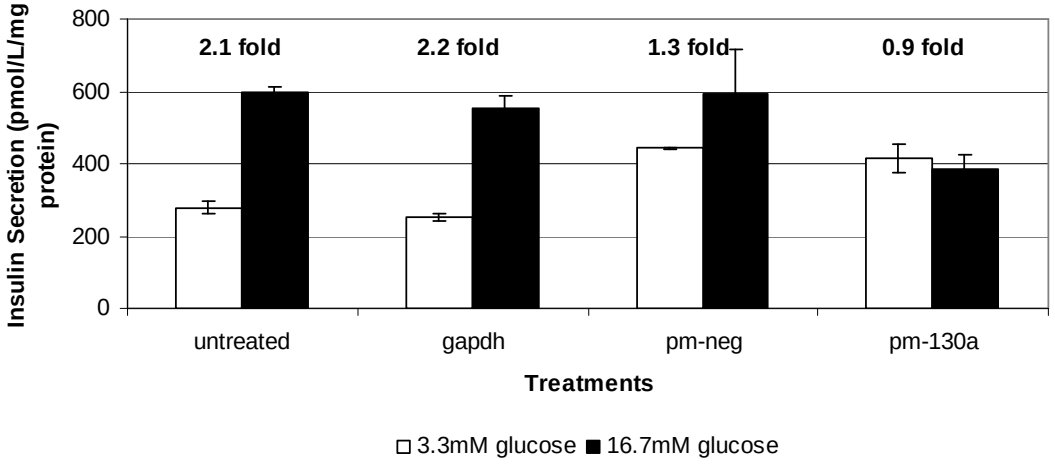

Figure 41. Over-expression of mir-130a in MIN6 cells (error bars indicated standard error of technical replicates).

Over-expression of mir-130a (figure 42) showed reduced GSIS relative to untreated and pm-neg transfected cells.

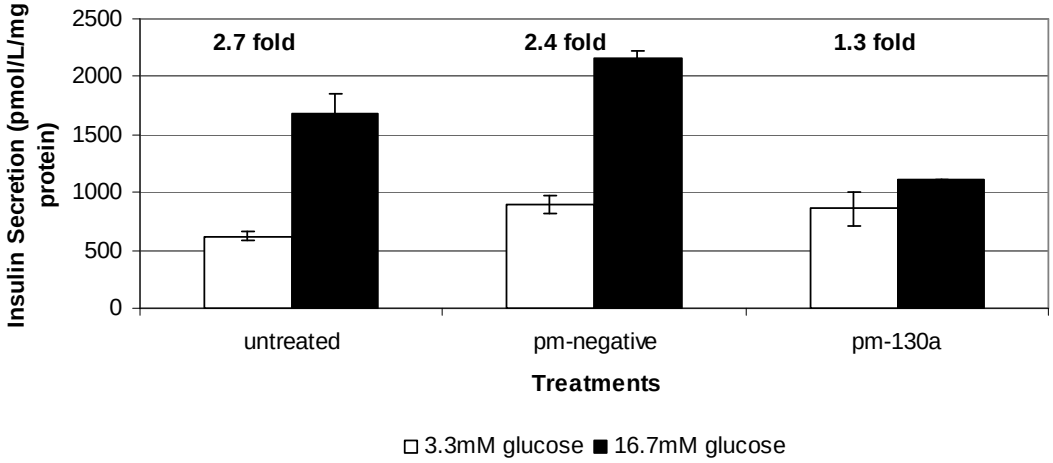

Figure 42. Over-expression of mir-130a in MIN6 cells (error bars indicated standard error of technical replicates).

Over-expression of mir-130a (figure 43) showed no effect on GSIS relative to controls.

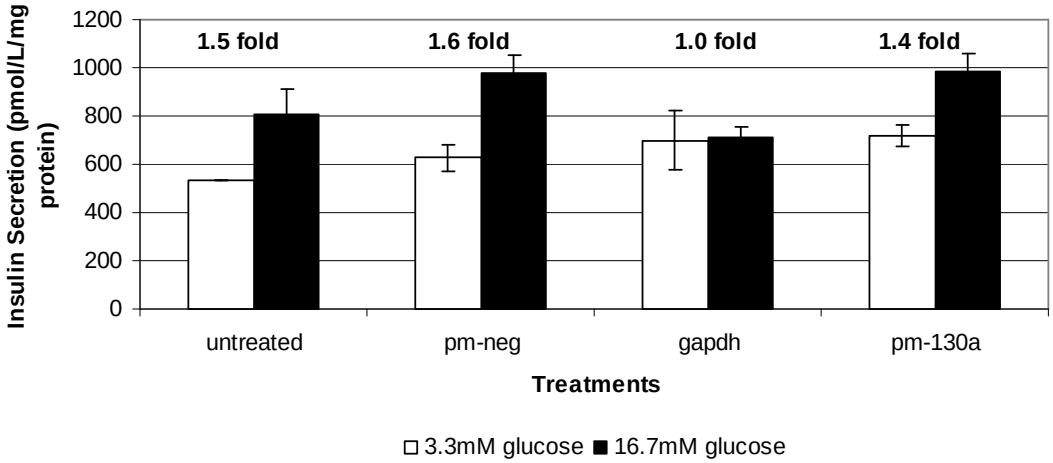

Figure 43. Over-expression of mir-130a in MIN6 cells (error bars indicated standard error of technical replicates).

Over-expression of mir-130a (figure 44) showed reduced GSIS relative to untreated and pm-neg transfected cells.

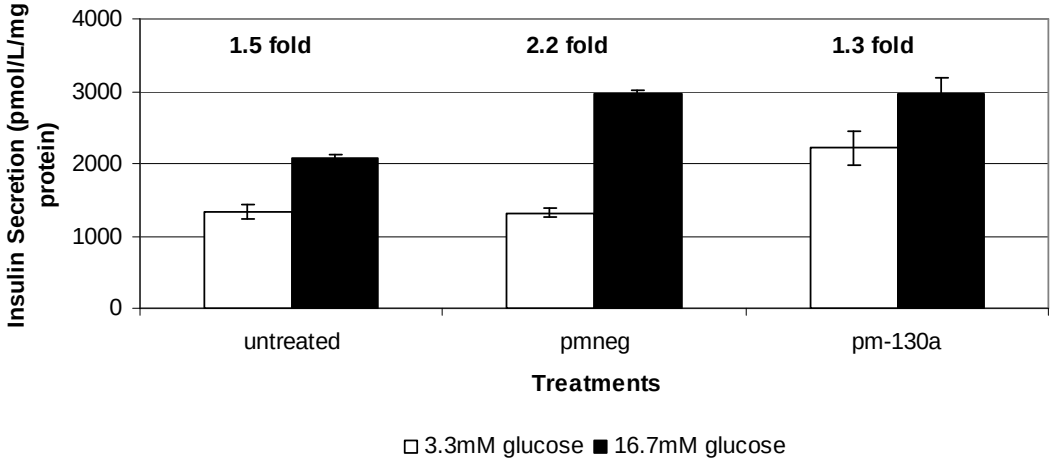

Figure 44. Over-expression of mir-130a in MIN6 cells (error bars indicated standard error of technical replicates).

1.4 Functional Validation of mir-376a

Functional validation of mir-376a was carried out in MIN6 cells to determine if manipulation of this miRNA led to changes in the GSIS phenotype of these cells.

(a) Knockdown of mir-376a

Knockdown of mir-376a (figure 45) showed reduced GSIS relative to control cells.

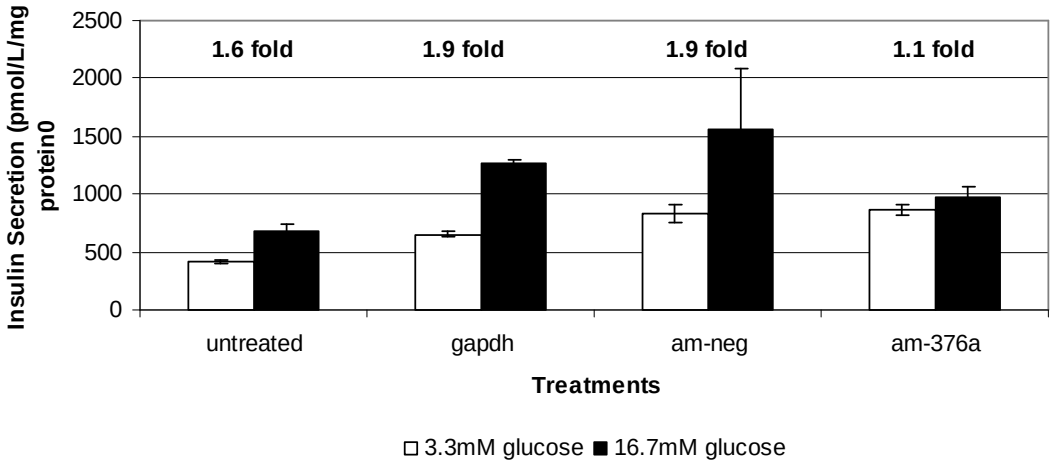

Figure 45. Knockdown of mir-376a levels in MIN6 cells (error bars indicate standard error of technical replicates).

Knockdown of mir-376a (figure 46) showed reduced GSIS relative to control cells.

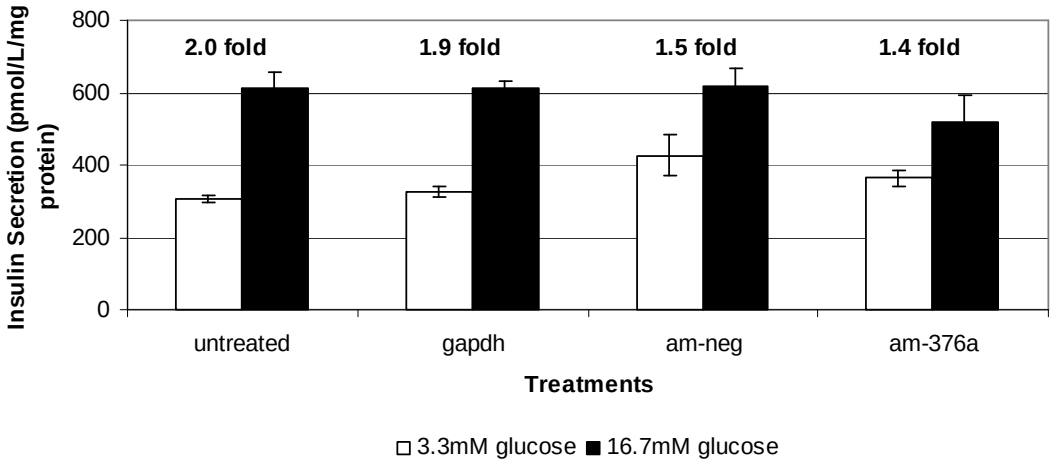

Figure 46. Knockdown of mir-376a levels in MIN6 cells (error bars indicate standard error of technical replicates).

Large differences in GSIS of control cells was observed (figure 47), making it difficult to draw conclusions on the effect of mir-376a knockdown.

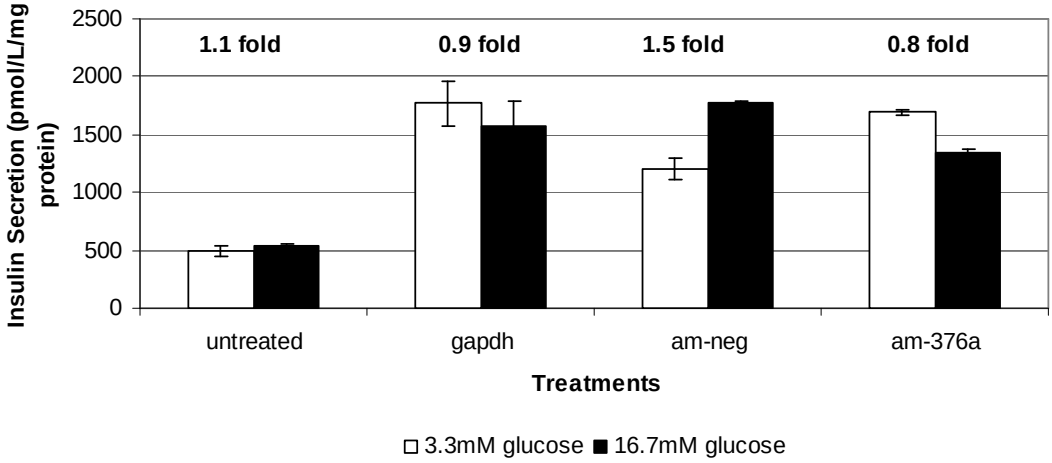

Figure 47. Knockdown of mir-376a levels in MIN6 cells (error bars indicate standard error of technical replicates).

No effects on GSIS were observed for mir-376a knockdown (figure 48).

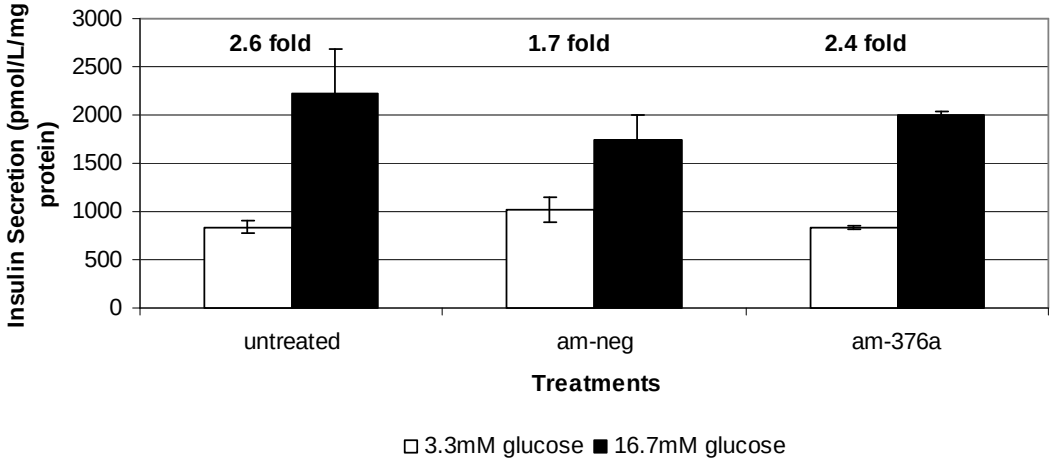

Figure 48. Knockdown of mir-376a levels in MIN6 cells (error bars indicate standard error of technical replicates).

No effects on GSIS were observed for mir-376a knockdown (figure 49).

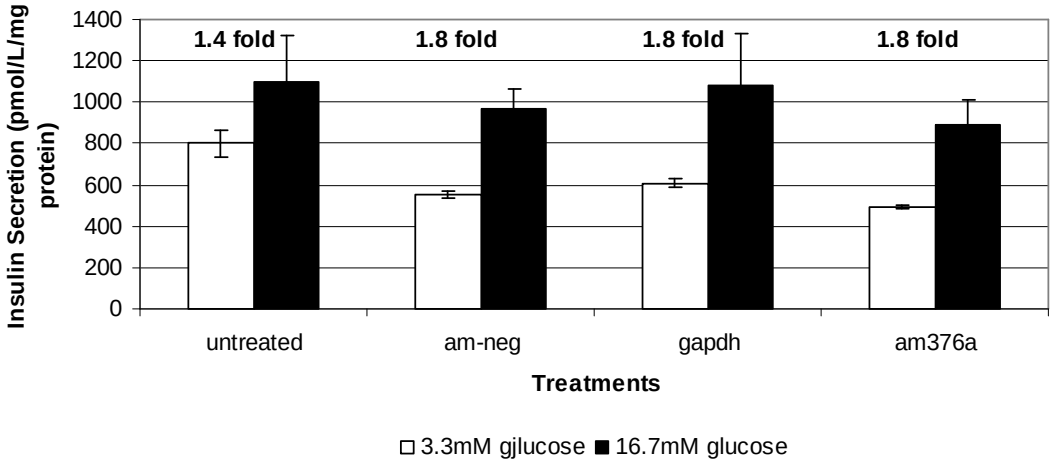

Figure 49. Knockdown of mir-376a levels in MIN6 cells (error bars indicate standard error of technical replicates).

(b) Over-expression of mir-376a

Over-expression of mir-376a (figure 50) showed reduced GSIS relative to control cells.

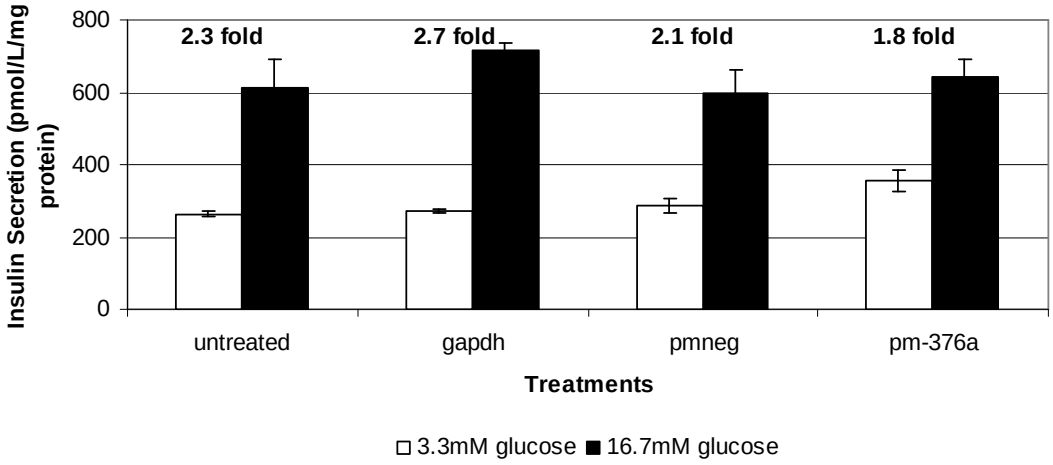

Figure 50. Over-expression of mir-376a in MIN6 cells (error bars indicate standard error of technical replicates).

Large differences in GSIS were observed between untreated and am-neg transfected cells (figure 51), therefore no conclusions could be drawn from this experiment.

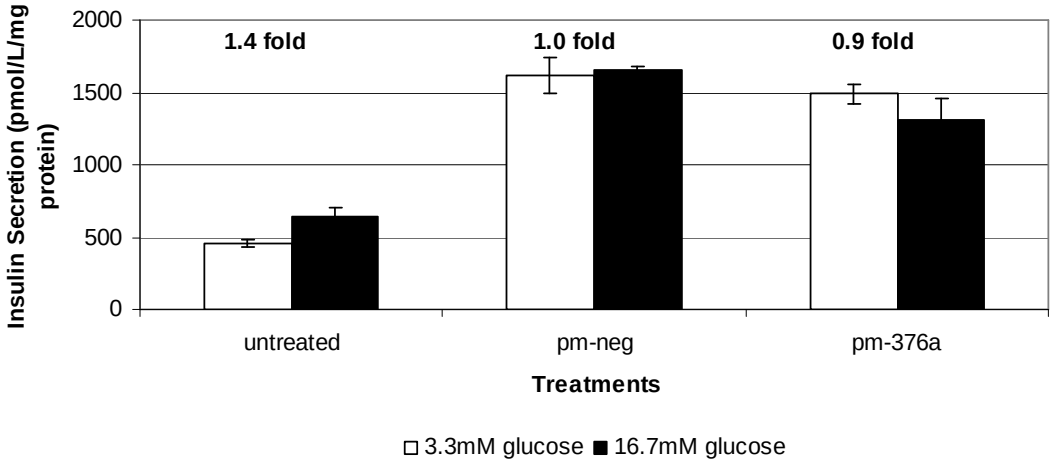

Figure 51. Over-expression of mir-376a in MIN6 cells (error bars indicate standard error of technical replicates).

Over-expression of mir-376a (figure 52) showed improved GSIS relative to untreated and pm-neg transfected cells.

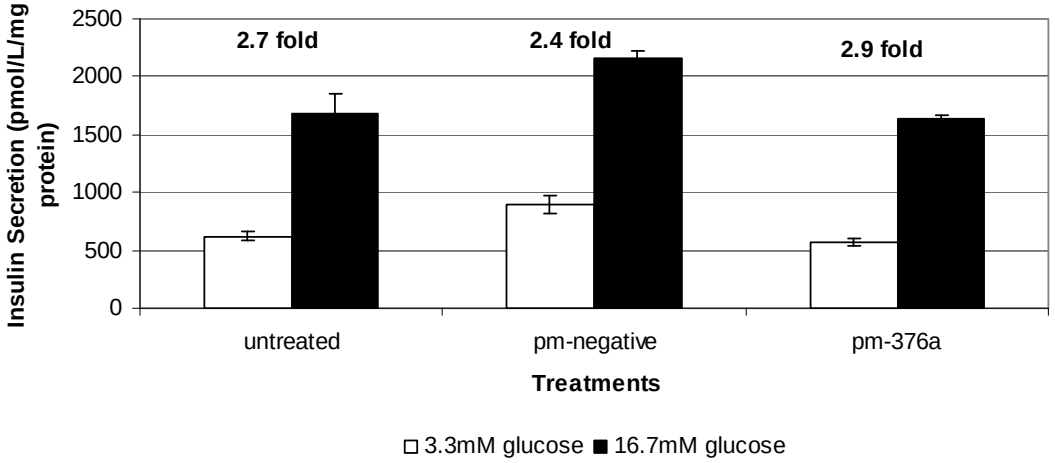

Figure 52. Over-expression of mir-376a in MIN6 cells (error bars indicate standard error of technical replicates).

Over-expression of mir-376a (figure 53) showed increased GSIS relative to control cells).

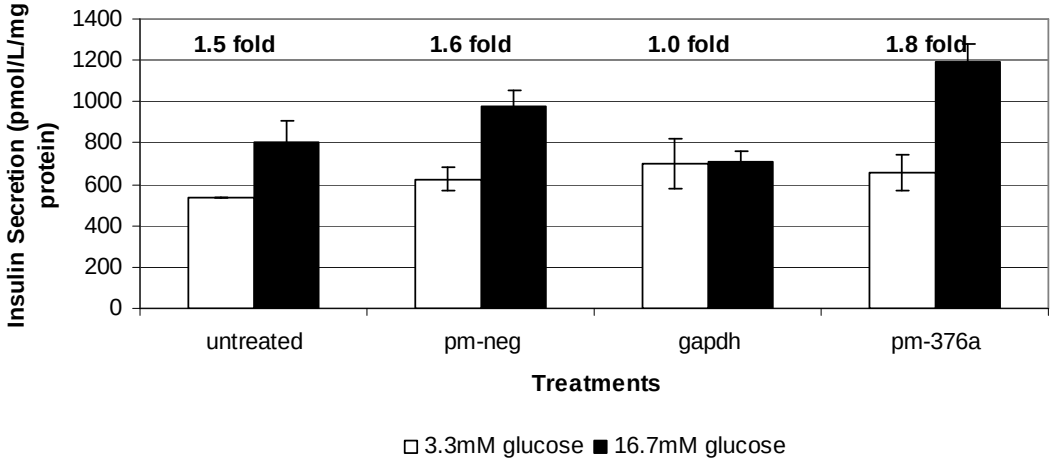

Figure 53. Over-expression of mir-376a in MIN6 cells (error bars indicate standard error of technical replicates).

Over-expression of mir-376a (figure 54) showed decreased GSIS relative to untreated and pm-neg transfected cells.

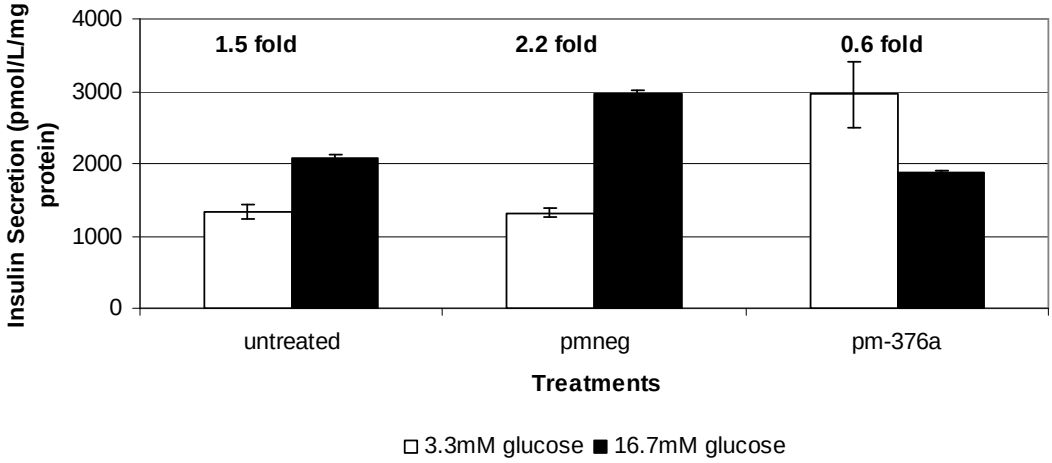

Figure 54. Over-expression of mir-376a in MIN6 cells (error bars indicate standard error of technical replicates).

1.5 Functional Validation of mir-369-5p

Mir-369-5p expression was manipulated to determine if this miRNA could affect the GSIS function of MIN6 cells.

(a) Large-scale assays for over-expression and knockdown of mir-369-5p expression

Large fluctuations were observed in baseline insulin secretion in response to 3.3mM glucose of control cells (figure 55), therefore no conclusions could be drawn on the effects of mir-369-5p over-expression and knockdown.

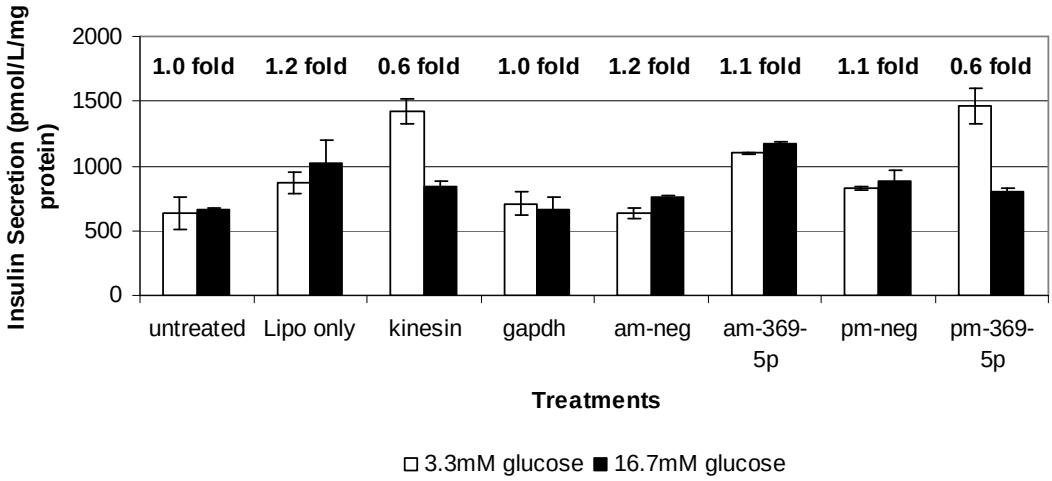

Figure 55. Over-expression and knockdown of mir-369-5p levels in MIN6 cells (error bars indicate standard error of technical replicates).

No effect on GSIS is observed for knockdown or over-expression of mir-369-5p relative to control cells (figure 56).

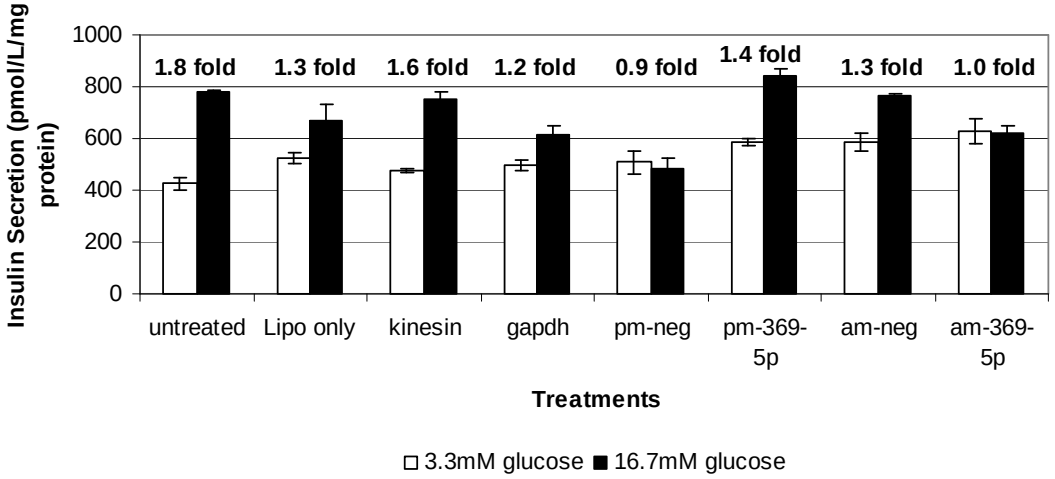

Figure 56. Over-expression and knockdown of mir-369-5p levels in MIN6 cells (error bars indicate standard error of technical replicates).

(b) Knockdown of mir-369-5p

Large differences observed in baseline insulin secretion in response to 3.3mM glucose on control cells (figure 57), therefore cannot draw any conclusions on effects of mir-369-5p knockdown.

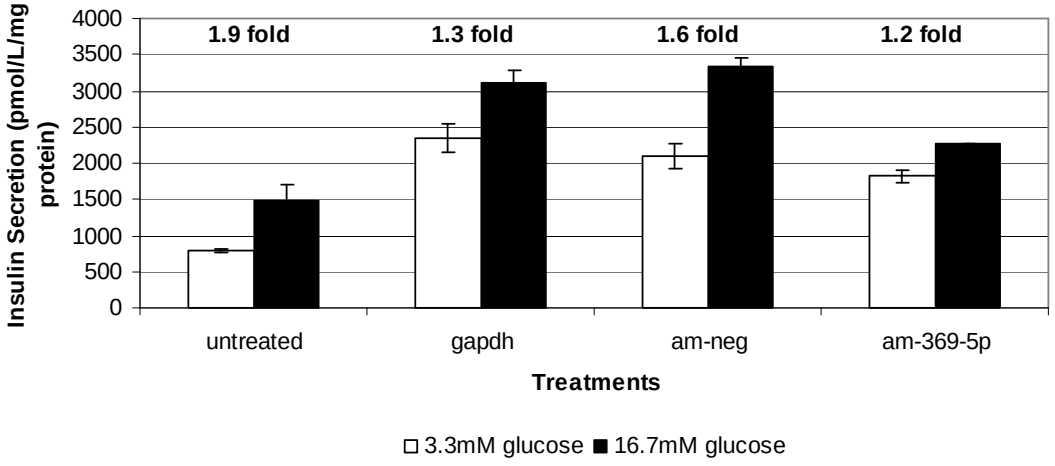

Figure 57. Knockdown of mir-369-5p levels in MIN6 cells (error bars indicated standard error of technical replicates).

No change in GSIS observed for knockdown of mir-369-5p levels (figure 58) relative to control cells.

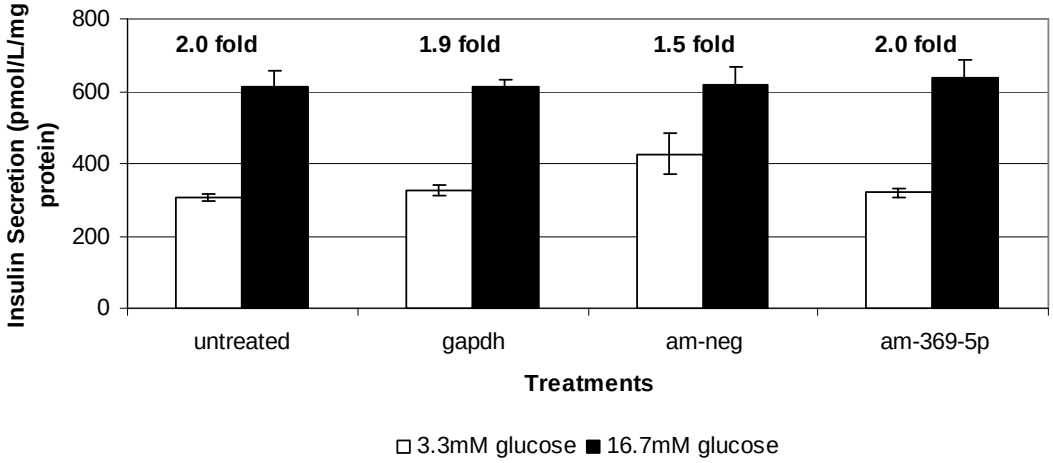

Figure 58. Knockdown of mir-369-5p levels in MIN6 cells (error bars indicated standard error of technical replicates).

Large differences in baseline insulin secretion in response to 3.3mM glucose observed for control cells (figure 59) therefore cannot draw any conclusions on effects on mir-369-5p knockdown.

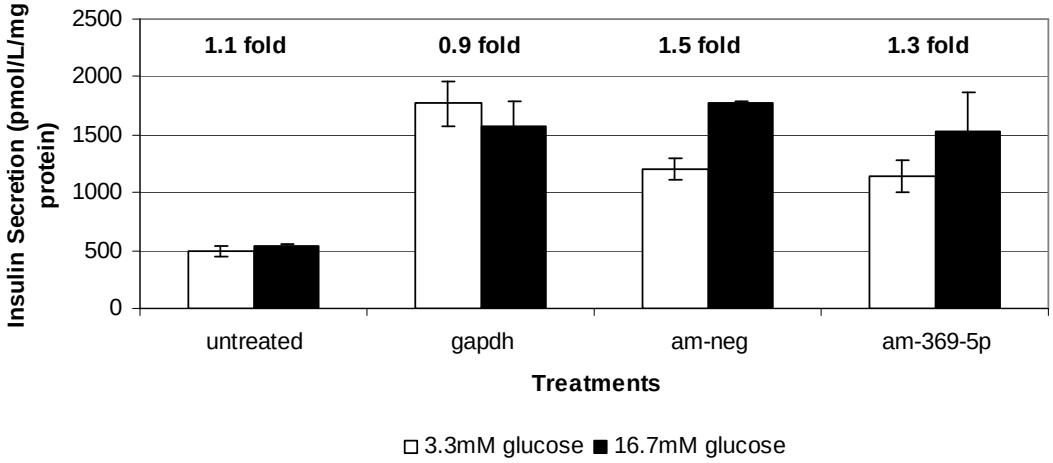

Figure 59. Knockdown of mir-369-5p levels in MIN6 cells (error bars indicated standard error of technical replicates).

Knockdown of mir-369-5p (figure 60) shows decreased GSIS and a large increase in basal insulin secretion relative to untreated and am-neg transfected cells

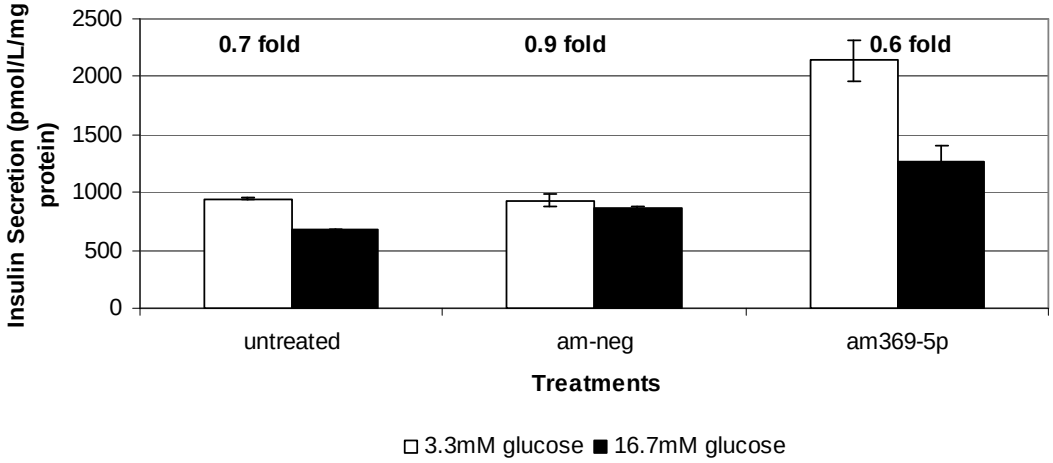

Figure 60. Knockdown of mir-369-5p levels in MIN6 cells (error bars indicated standard error of technical replicates).

Knockdown of mir-369-5p (figure 61) shows decreased GSIS relative to untreated and am-neg transfected cells.

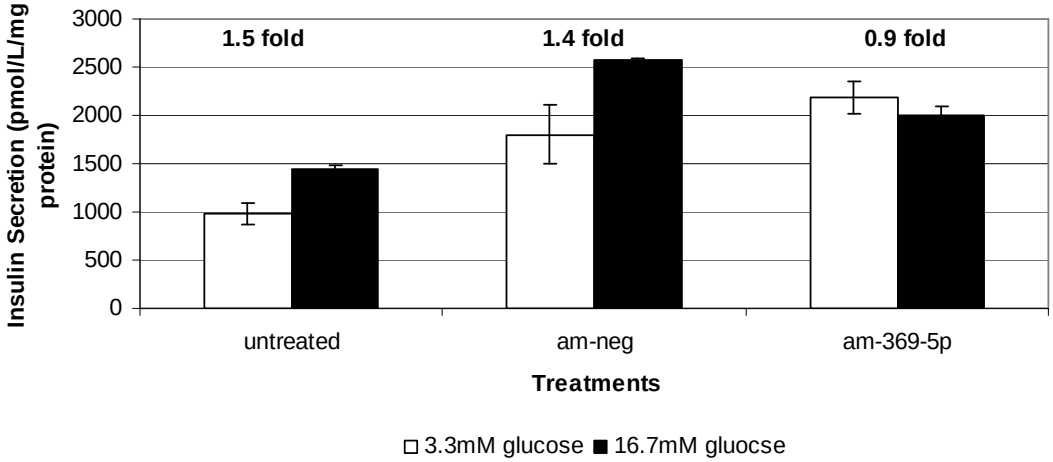

Figure 61. Knockdown of mir-369-5p levels in MIN6 cells (error bars indicated standard error of technical replicates).

Knockdown of mir-369-5p (figure 62) shows decreased GSIS relative to untreated and am-neg transfected cells.

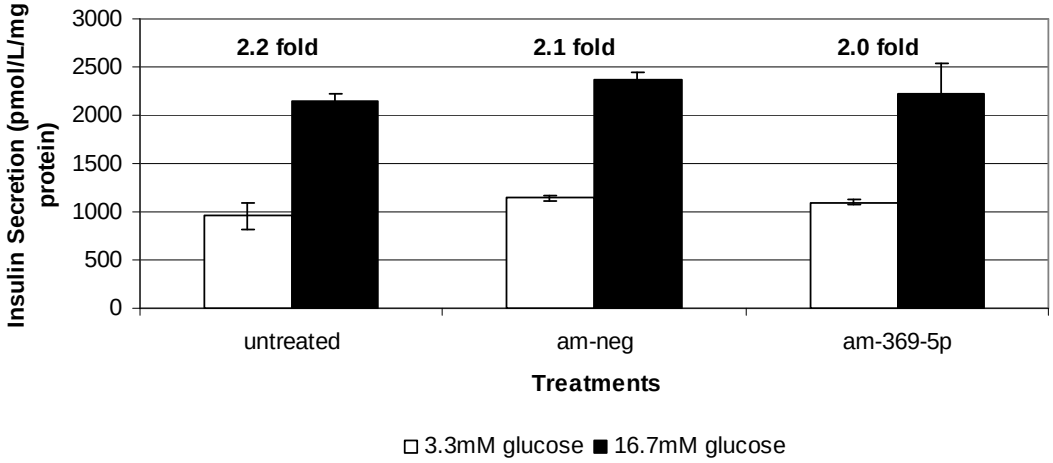

Figure 62. Knockdown of mir-369-5p levels in MIN6 cells (error bars indicated standard error of technical replicates).

Knockdown of mir-369-5p (figure 63) shows no effect on GSIS relative to control cells.

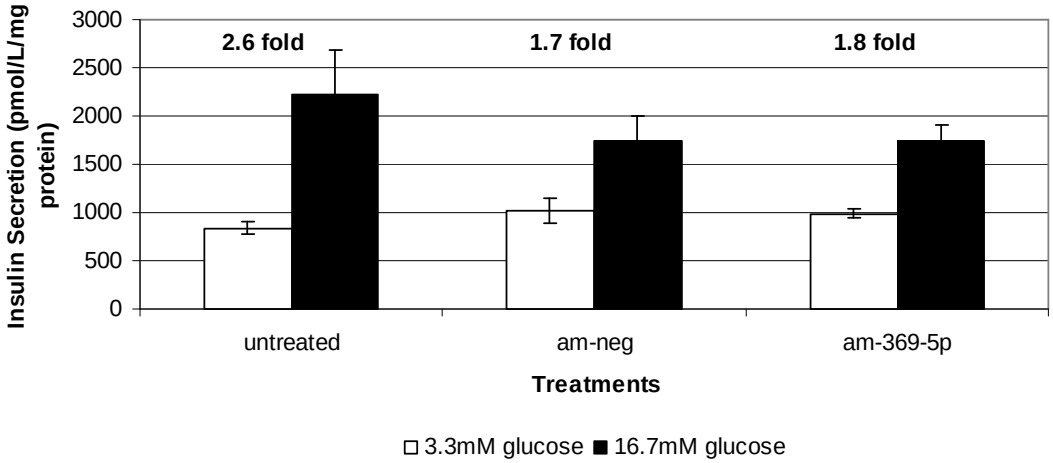

Figure 63. Knockdown of mir-369-5p levels in MIN6 cells (error bars indicated standard error of technical replicates).

Knockdown of mir-369-5p (figure 64) shows decreased GSIS relative to control cells.

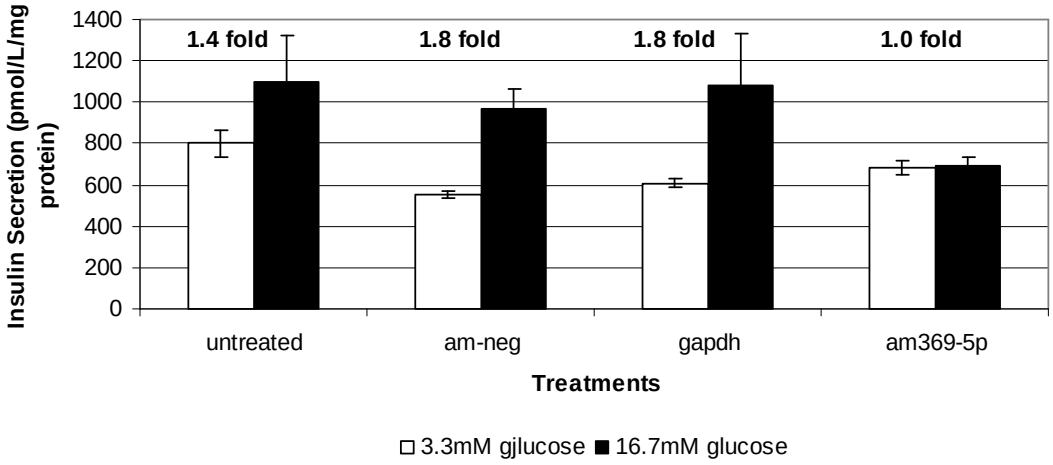

Figure 64. Knockdown of mir-369-5p levels in MIN6 cells (error bars indicated standard error of technical replicates).

(c) Over-expression of mir-369-5p

Over-expression of mir-369-5p (figure 65) showed no effect on GSIS relative to control cells.

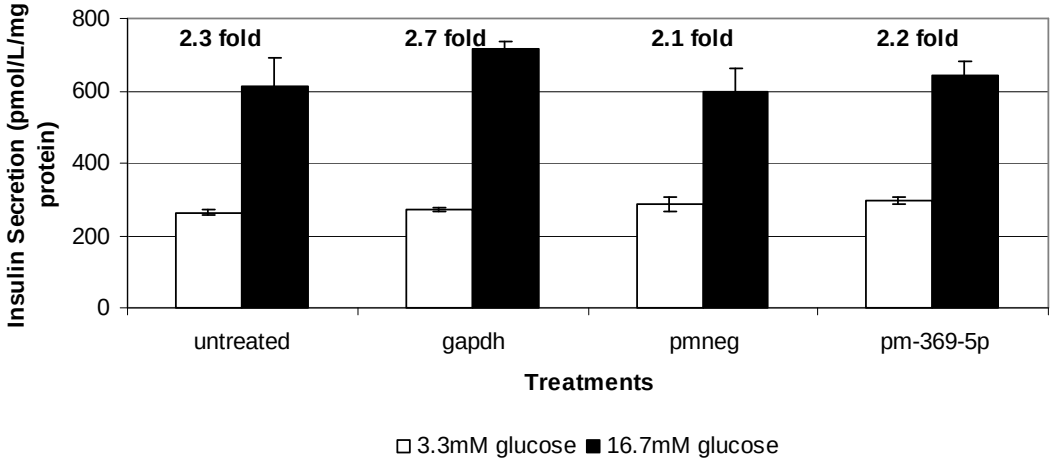

Figure 65. Over-expression of mir-369-5p in MIN6 cells (error bars indicate standard error of technical replicates).

Large differences in baseline insulin secretion in response to 3.3mM glucose were observed for control cells (figure 66) therefore cannot draw any conclusions on effects on mir-369-5p over-expression.

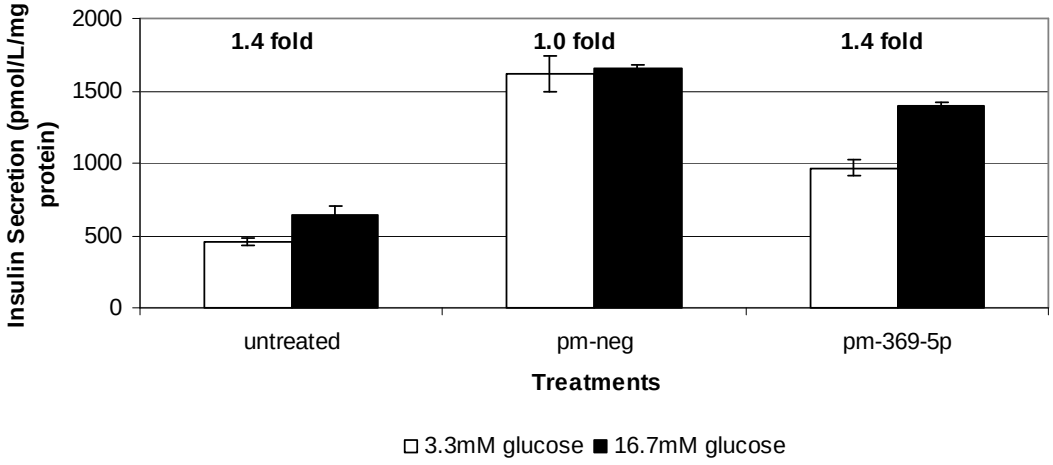

Figure 66. Over-expression of mir-369-5p in MIN6 cells (error bars indicate standard error of technical replicates).

Over-expression of mir-369-5p (figure 67) shows increased GSIS relative to untreated and pm-neg transfected cells).

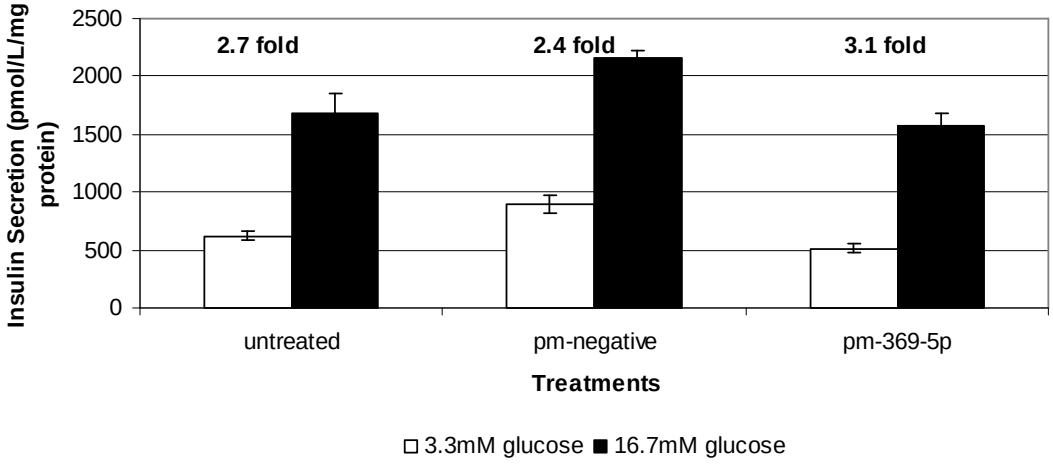

Figure 67. Over-expression of mir-369-5p in MIN6 cells (error bars indicate standard error of technical replicates).

Over-expression of mir-369-5p (figure 68) shows no effect on GSIS relative to control cells.

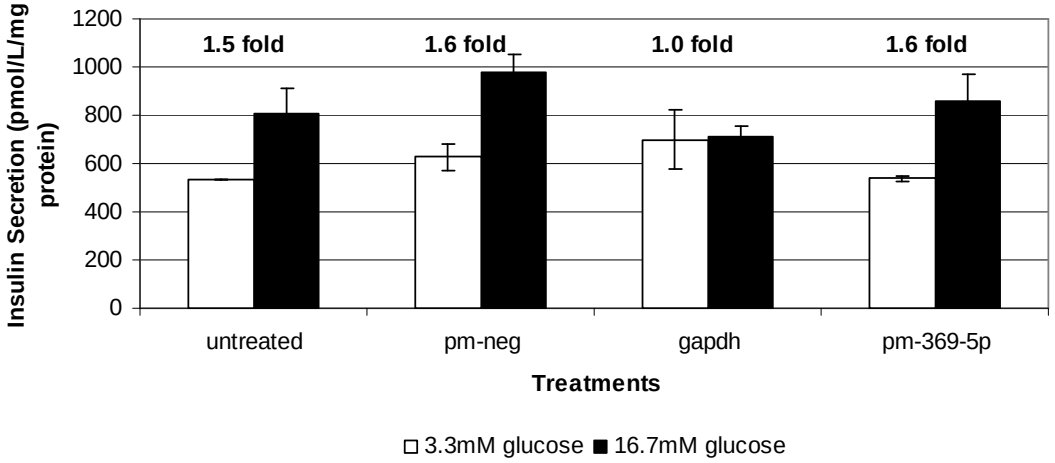

Figure 68. Over-expression of mir-369-5p in MIN6 cells (error bars indicate standard error of technical replicates).

Over-expression of mir-369-5p (figure 69) shows no effect on GSIS fold change, however a large is observed in basal insulin secretion at 3.3mM glucose, relative to untreated and pm-neg transfected cells.

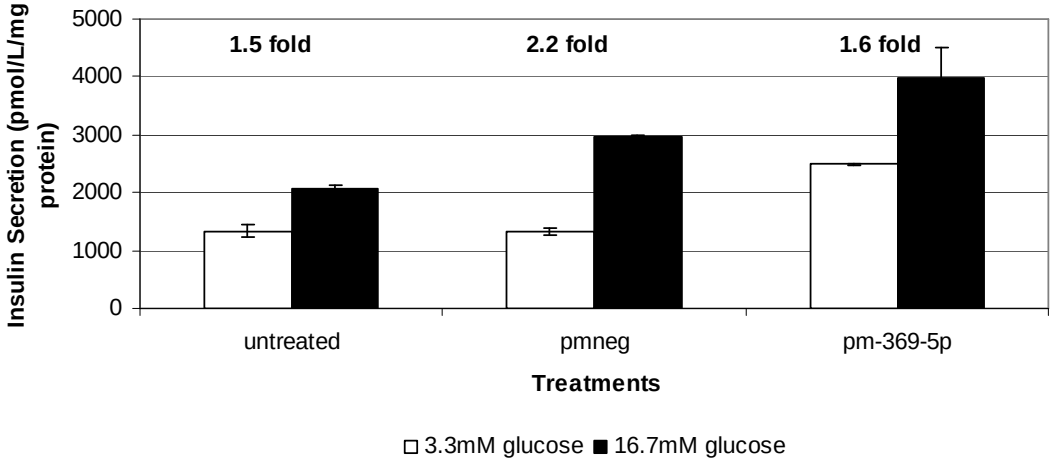

Figure 69. Over-expression of mir-369-5p in MIN6 cells (error bars indicate standard error of technical replicates).

1.6 Functional Validation of mir-27a

Over-expression and knockdown experiments were performed on MIN6 cells with miRNA targets identified from TLDA analysis (table 3.1.2), to determine if manipulation of these miRNAs led to changes in GSIS phenotype of the cells.

(a) Large-scale assays for over-expression and knockdown of mir-27a

Large fluctuations were observed in baseline insulin secretion in response to 3.3mM glucose of control cells (figure 70) therefore no conclusions could be drawn on the effects of mir-27a over-expression and knockdown.

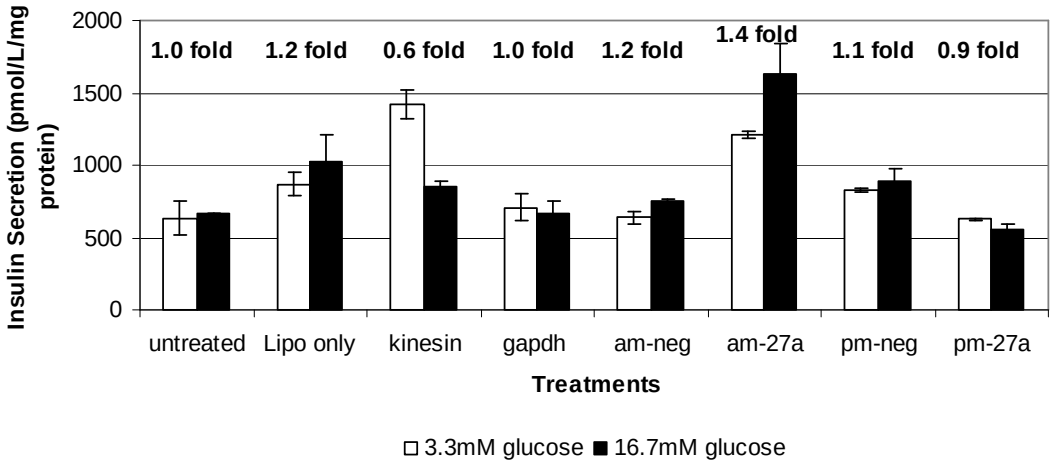

Figure 70. Knockdown of mir-27a levels in MIN6 cells (error bars indicate standard error of technical replicates).

No effect on GSIS was observed for mir-27a over-expression or knockdown relative to control cells (figure 71).

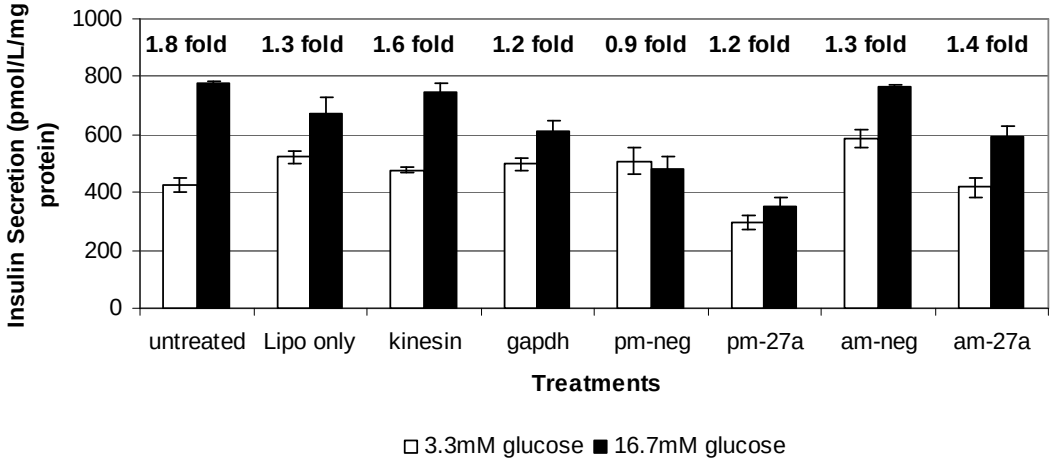

Figure 71. Knockdown of mir-27a levels in MIN6 cells (error bars indicate standard error of technical replicates).

(b) Knockdown of mir-27a

No effect on GSIS was observed for knockdown of mir-27a relative to control cells (figure 72)

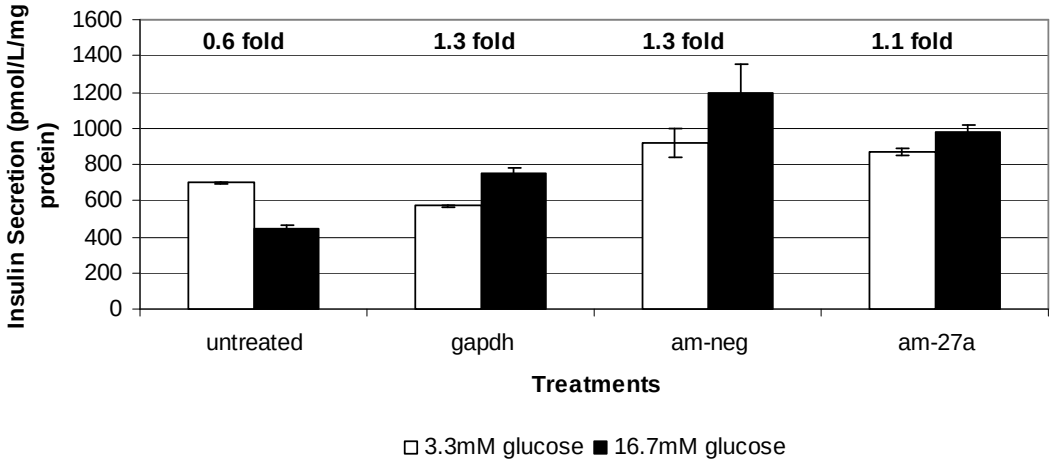

Figure 72. Knockdown of mir-27a levels in MIN6 cells (error bars indicate standard error of technical replicates).

Knockdown of mir-27a (figure 73) showed a reduction in GSIS relative to control cells.

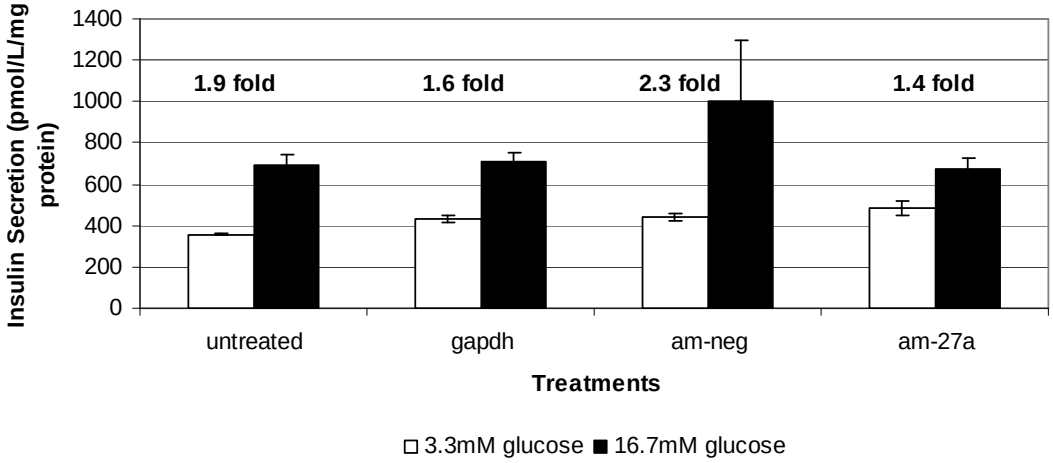

Figure 73. Knockdown of mir-27a levels in MIN6 cells (error bars indicate standard error of technical replicates).

No effect on GSIS is observed for mir-27a knockdown relative to untreated and am-neg transfected cells (figure 74).

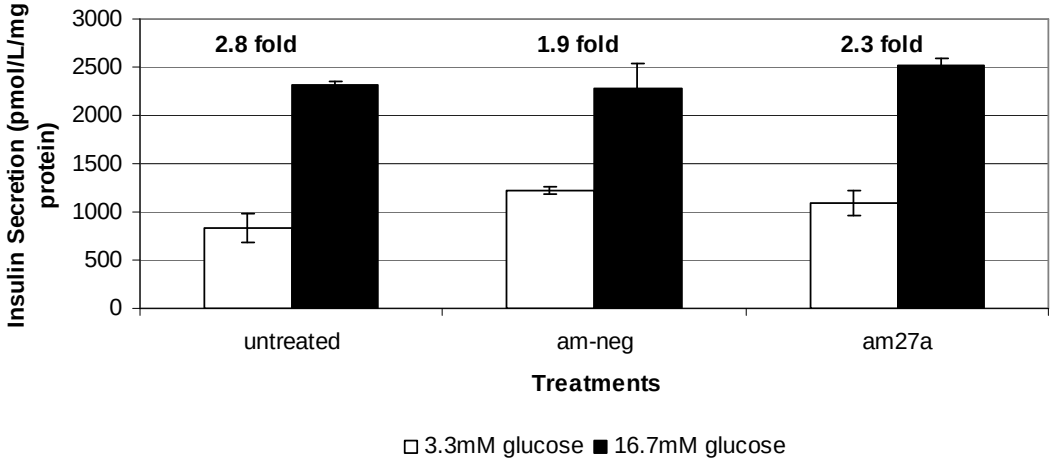

Figure 74. Knockdown of mir-27a levels in MIN6 cells (error bars indicate standard error of technical replicates).

(c) Over-expression of mir-27a

No effect on GSIS was observed for mir-27a over-expression relative to control cells (figure 75).

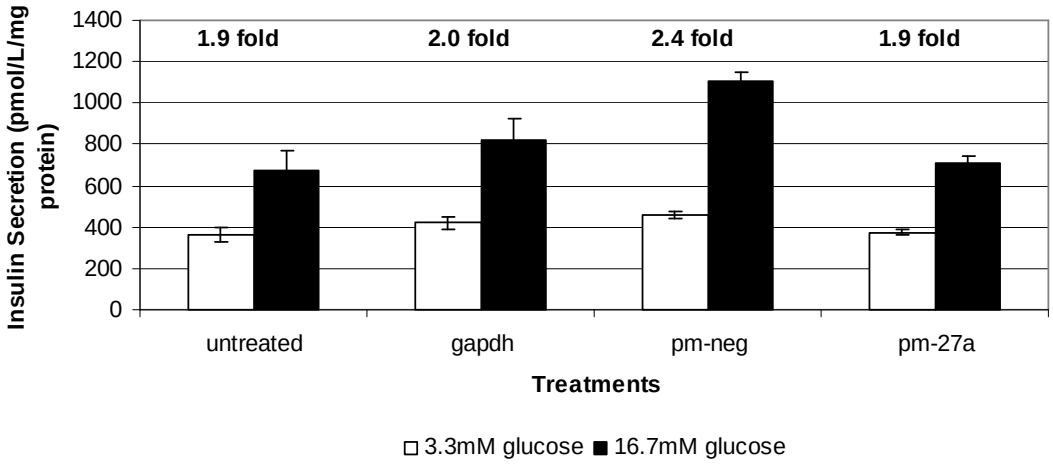

Figure 75. Over-expression of mir-27a in MIN6 cells (error bars indicate standard error of technical replicates).

No effect on GSIS was observed for mir-27a over-expression relative to control cells (figure 76).

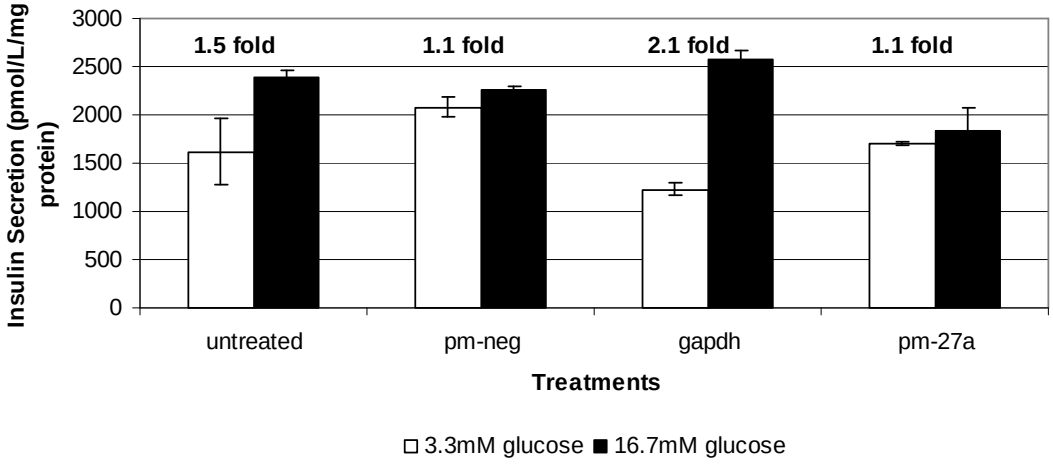

Figure 76. Over-expression of mir-27a in MIN6 cells (error bars indicate standard error of technical replicates).

Over-expression of mir-27a (figure 77) showed a decrease in GSIS relative to untreated and pm-neg transfected cells.

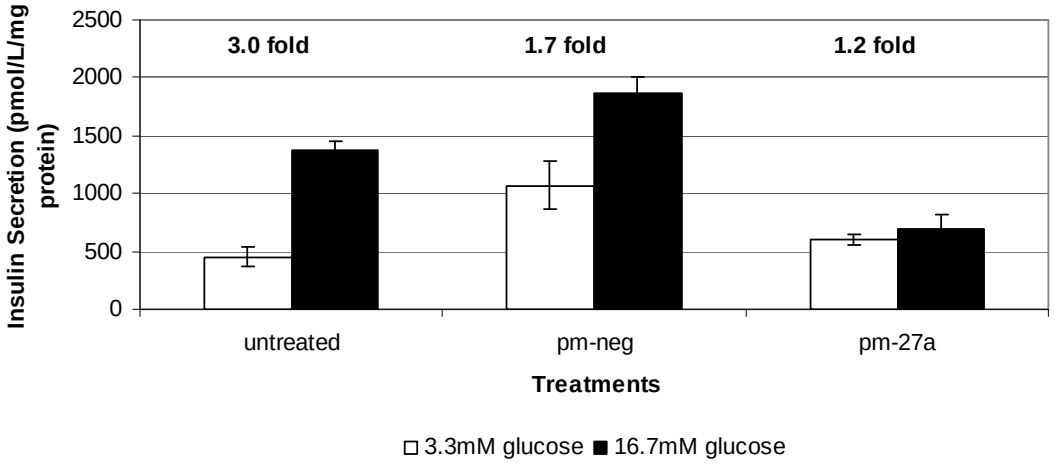

Figure 77. Over-expression of mir-27a in MIN6 cells (error bars indicate standard error of technical replicates).

Over-expression of mir-27a (figure 78) showed a decrease in GSIS relative to untreated and pm-neg transfected cells.

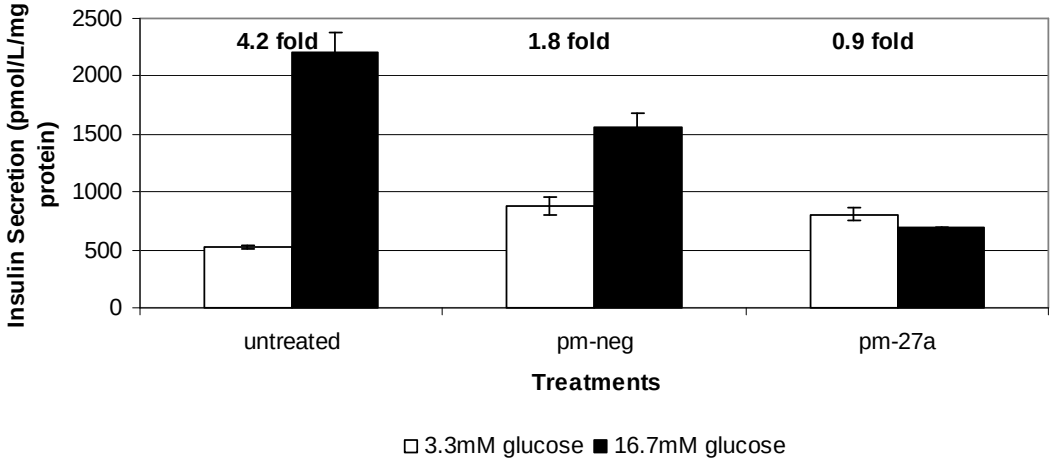

Figure 78. Over-expression of mir-27a in MIN6 cells (error bars indicate standard error of technical replicates).

1.7 Functional Validation of mir-124a

Mir-124a expression was increased and decreased using miRNA inhibitors and mimics to determine if manipulation of this miRNA could affect the GSIS phenotype of MIN6 cells.

(a) Knockdown of mir-124a

Knockdown of mir-124a (figure 79) showed a decrease in GSIS relative to control cells.

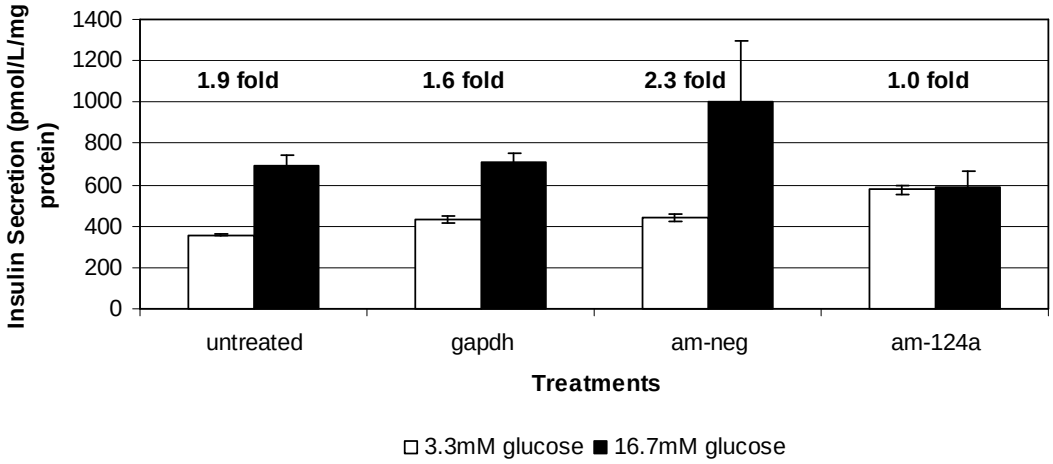

Figure 79. Knockdown of mir-124a levels in MIN6 cells (error bars indicate standard error of technical replicates).

Knockdown of mir-124a (figure 80) showed an increase in GSIS relative to control cells.

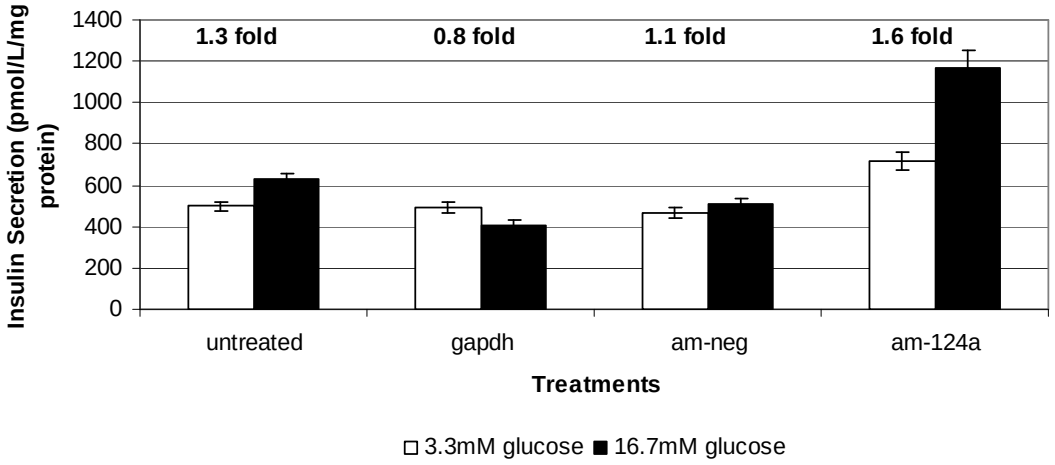

Figure 80. Knockdown of mir-124a levels in MIN6 cells (error bars indicate standard error of technical replicates).

No effect on GSIS of am-124a transfected cells was observed relative to control cells (figure 81).

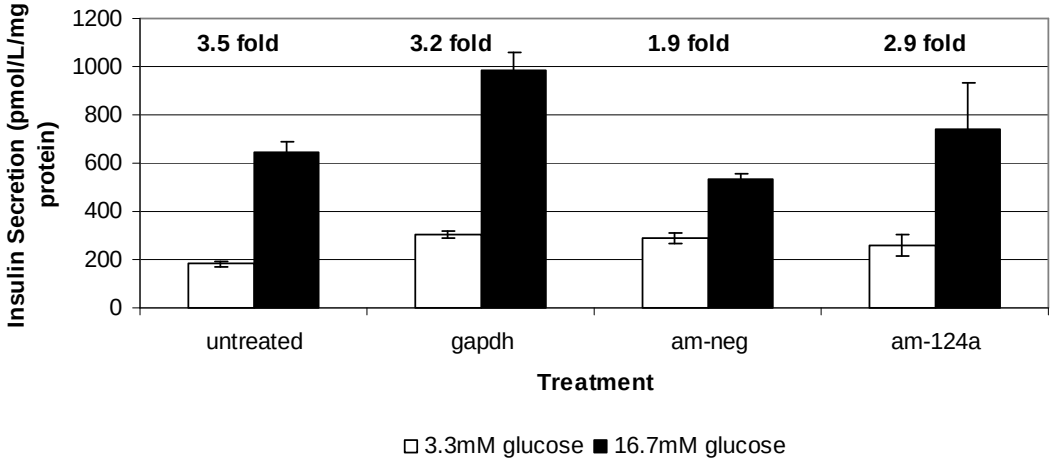

Figure 81. Knockdown of mir-124a levels in MIN6 cells (error bars indicate standard error of technical replicates).

No effect on GSIS of am-124a transfected cells was observed relative to control cells (figure 82).

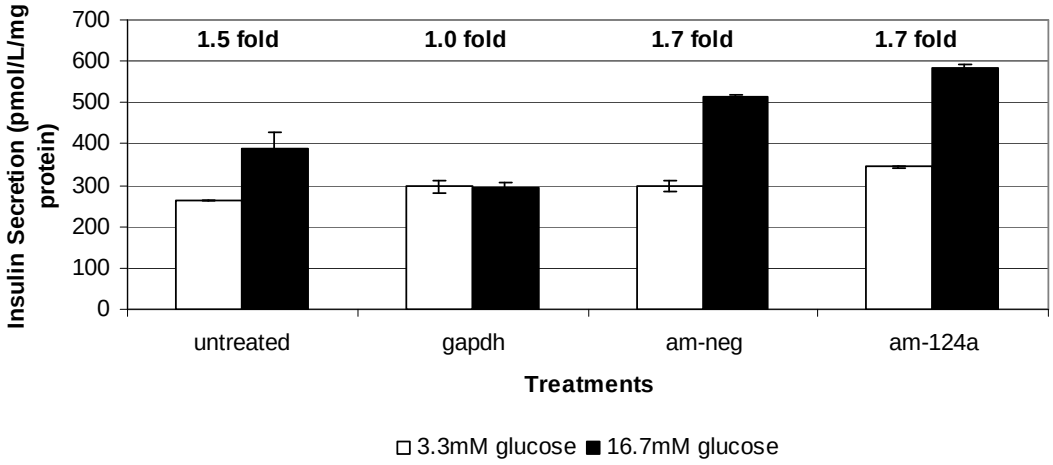

Figure 82. Knockdown of mir-124a levels in MIN6 cells (error bars indicate standard error of technical replicates).

Large differences in baseline insulin secretion in response to 3.3mM glucose were observed for control cells (figure 83) therefore cannot draw any conclusions on effects on mir-124a knockdown.

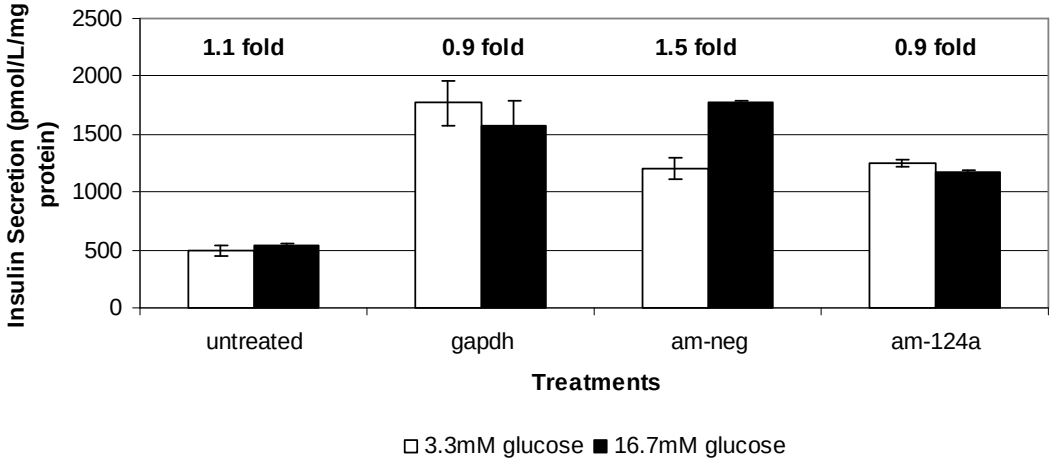

Figure 83. Knockdown of mir-124a levels in MIN6 cells (error bars indicate standard error of technical replicates).

No effect on GSIS of am-124a transfected cells was observed relative to control cells (figure 84).

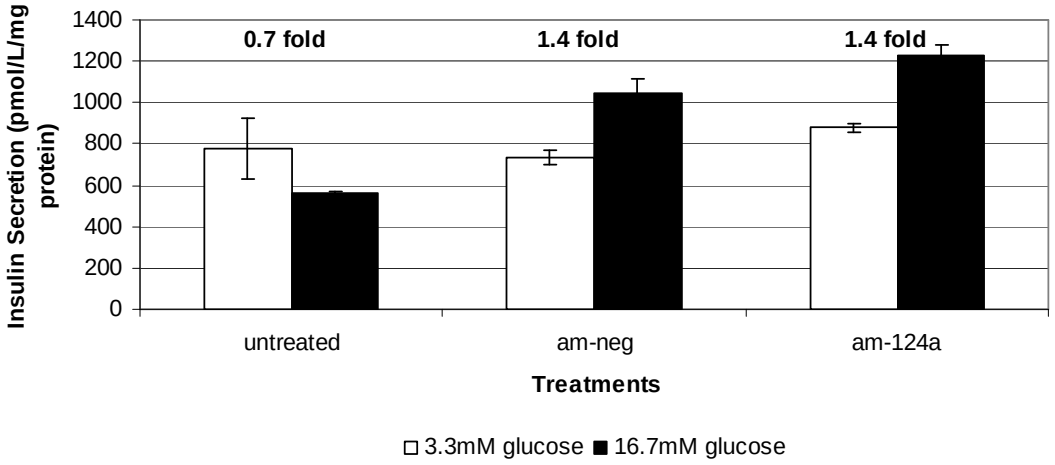

Figure 84. Knockdown of mir-124a levels in MIN6 cells (error bars indicate standard error of technical replicates).

Knockdown of mir-124a (figure 85) showed a decrease in GSIS relative to untreated and am-neg transfected cells.

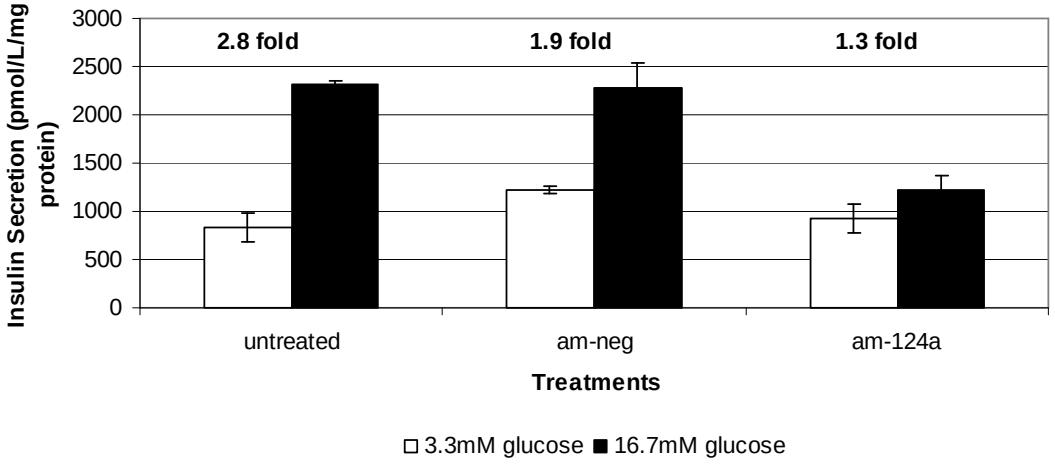

Figure 85. Knockdown of mir-124a levels in MIN6 cells (error bars indicate standard error of technical replicates).

(b) Over-expression of mir-124a

Over-expression of mir-124a (figure 86) shows a decrease in GSIS relative to control cells.

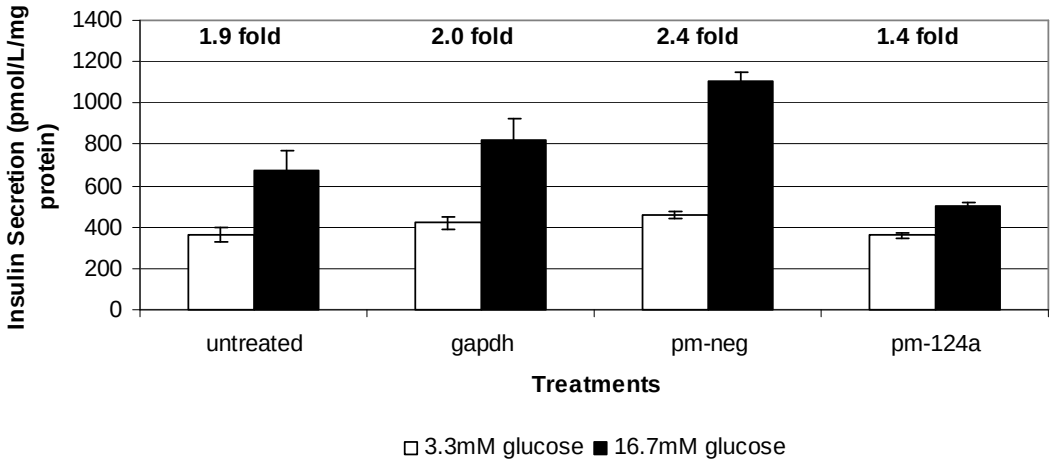

Figure 86. Over-expression of mir-124a in MIN6 cells (error bars indicate standard error of technical replicates).

Over-expression of mir-124a (figure 87) shows an increase in GSIS relative to untreated and pm-neg transfected cells.

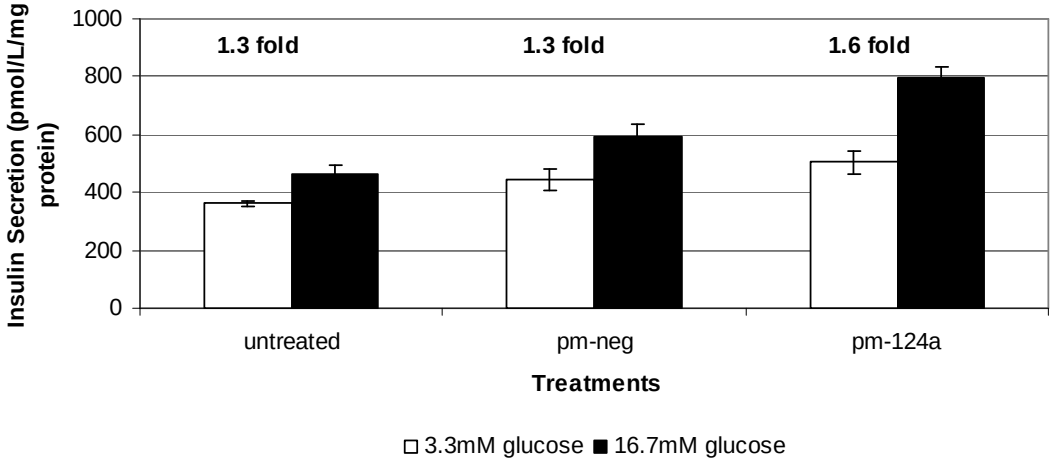

Figure 87. Over-expression of mir-124a in MIN6 cells (error bars indicate standard error of technical replicates).

Over-expression of mir-124a (figure 88) shows a slight increase in GSIS relative to control cells.

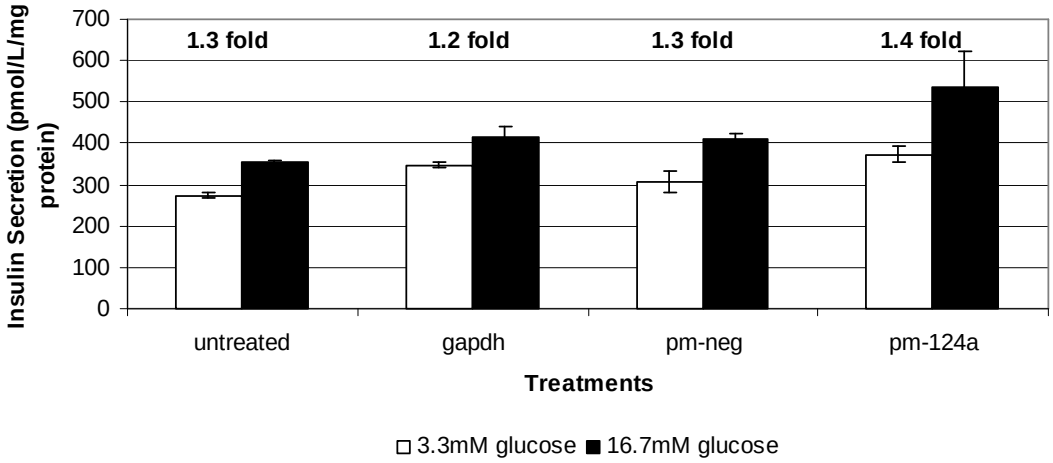

Figure 88. Over-expression of mir-124a in MIN6 cells (error bars indicate standard error of technical replicates).

Over-expression of mir-124a (figure 89) shows a decrease in GSIS relative to control cells.

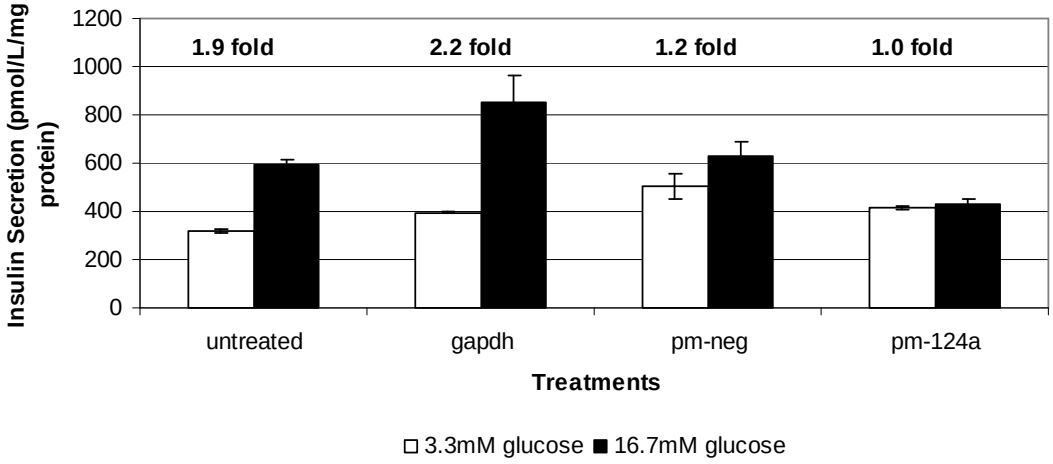

Figure 89. Over-expression of mir-124a in MIN6 cells (error bars indicate standard error of technical replicates).

Large differences in baseline insulin secretion in response to 3.3mM glucose were observed for control cells (figure 90) therefore cannot draw any conclusions on effects on mir-124a over-expression.

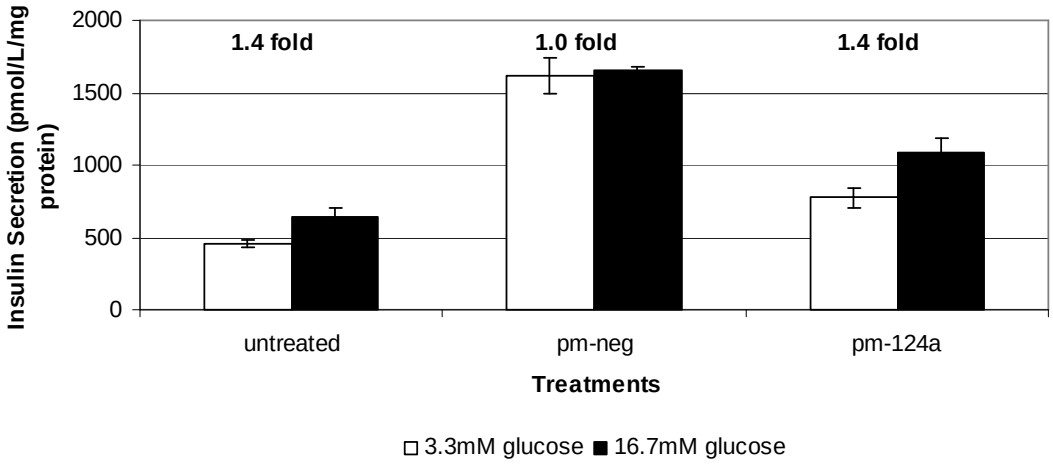

Figure 90. Over-expression of mir-124a in MIN6 cells (error bars indicate standard error of technical replicates).

No effect on GSIS is observed for over-expression of mir-124a relative to control cells (figure 91).

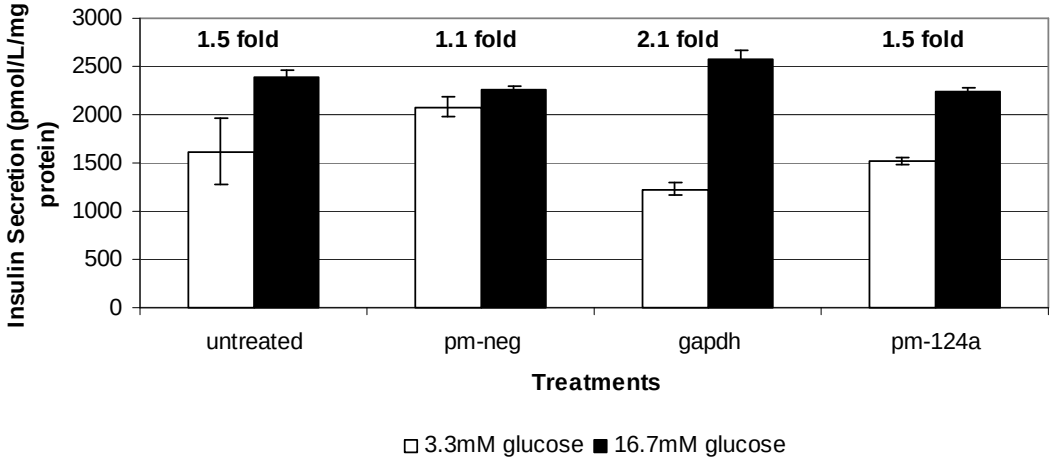

Figure 91. Over-expression of mir-124a in MIN6 cells (error bars indicate standard error of technical replicates).

No effect on GSIS is observed for mir-124a over-expression relative to control cells (figure 92).

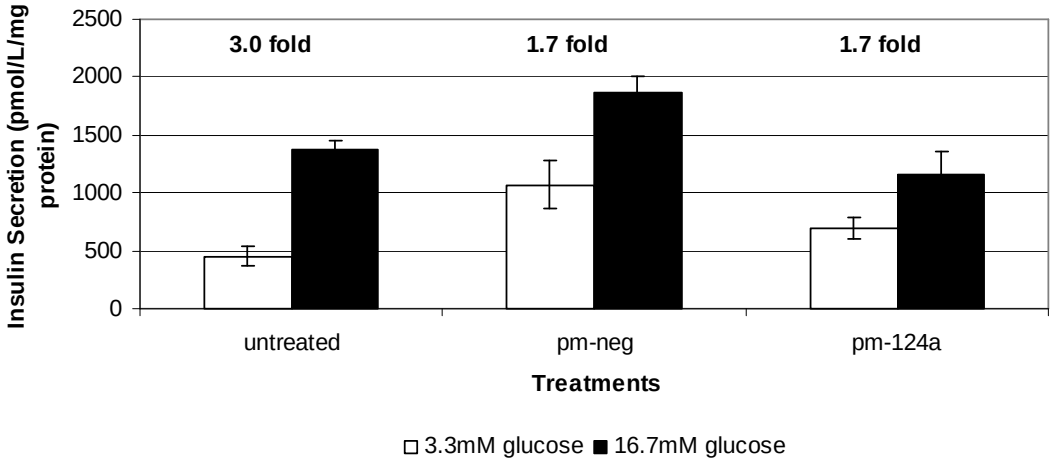

Figure 92. Over-expression of mir-124a in MIN6 cells (error bars indicate standard error of technical replicates).

1.8 Functional Validation of mir-337

Mir-337 expression was reduced in non-GSIS MIN6 cells, therefore it was expected that manipulation to increase and decrease expression levels of this miRNA in MIN6 cells could lead to increased and decreased GSIS response in these cells.

(a) Knockdown of mir-337

No effect on GSIS was observed for knockdown of mir-337 compared to control cells (figure 93).

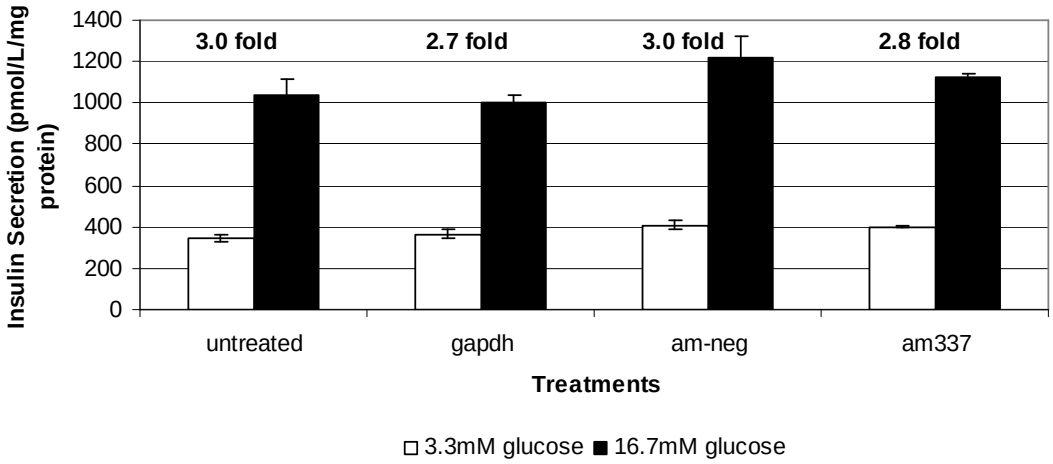

Figure 93. Knockdown of mir-337 levels in MIN6 cells (error bars indicate standard error of technical replicates).

No effect on GSIS was observed for knockdown of mir-337 relative to control cells (figure 94).

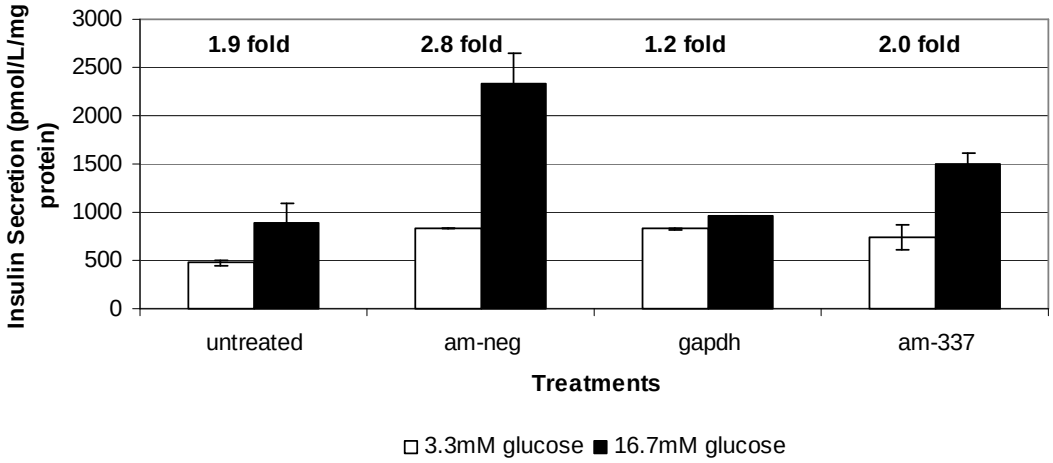

Figure 94. Knockdown of mir-337 levels in MIN6 cells (error bars indicate standard error of technical replicates).

Knockdown of mir-337 (figure 95) showed an increase in GSIS relative to untreated and am-neg transfected cells.

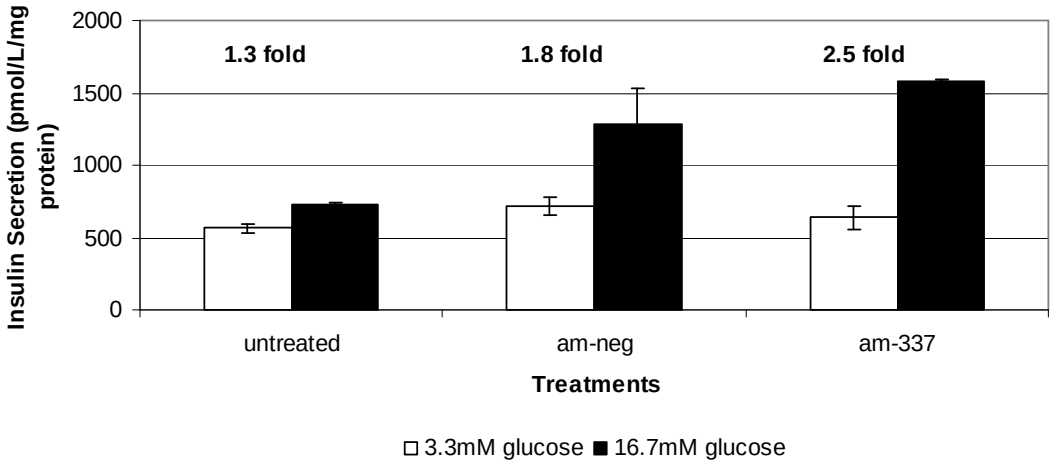

Figure 95. Knockdown of mir-337 levels in MIN6 cells (error bars indicate standard error of technical replicates).

No effect on GSIS was observed for knockdown of mir-337 levels relative to untreated and am-neg transfected cells (figure 96).

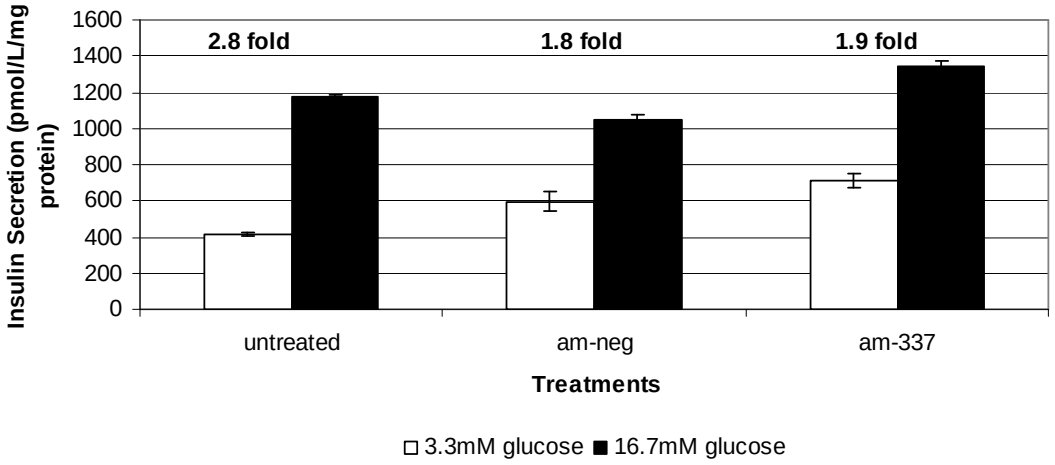

Figure 96. Knockdown of mir-337 levels in MIN6 cells (error bars indicate standard error of technical replicates).

A slight decrease in GSIS was observed for knockdown of mir-337 relative to untreated and am-neg transfected cells (figure 97).

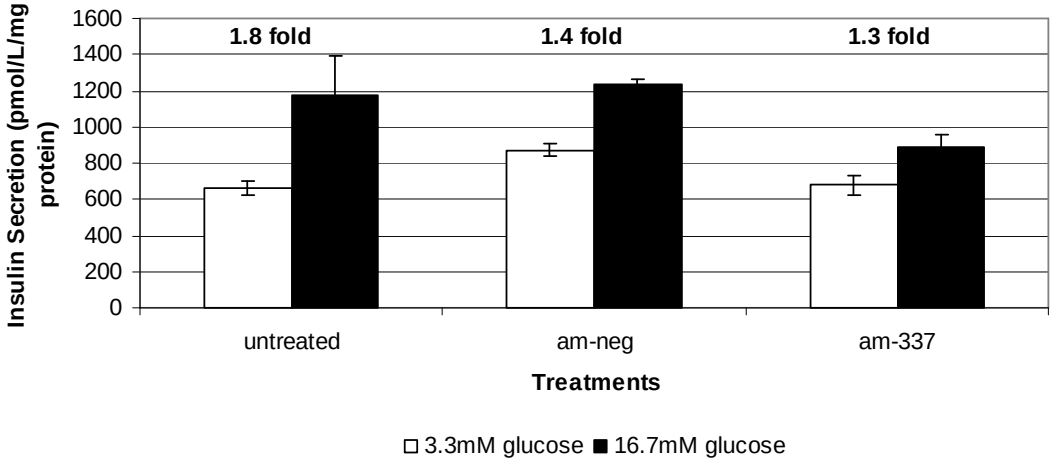

Figure 97. Knockdown of mir-337 levels in MIN6 cells (error bars indicate standard error of technical replicates).

(b) Over-expression of mir-337

No effect on GSIS is observed for over-expression of mir-337 relative to control cells (figure 98).

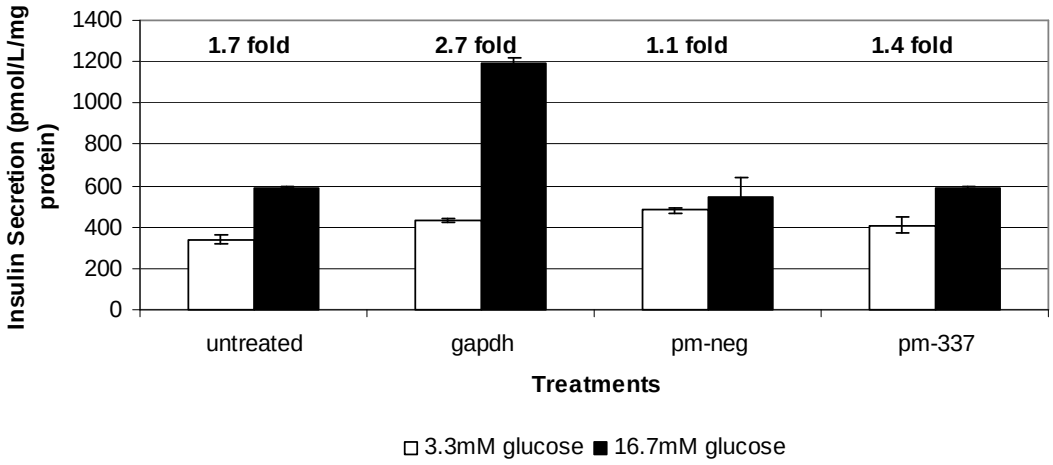

Figure 98. Over-expression of mir-337 in MIN6 cells (error bars indicate standard error of technical replicates).

Over-expression of mir-337 (figure 99) shows an increase in GSIS relative to control cells.

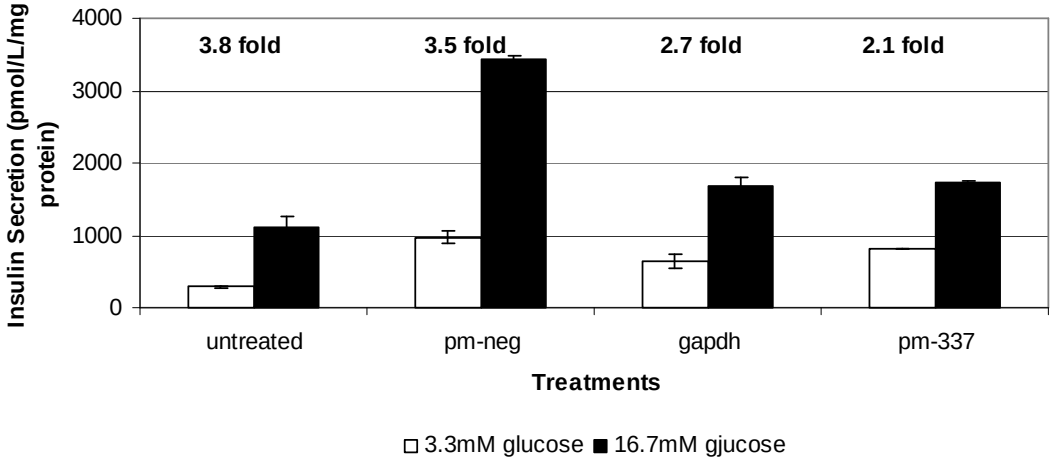

Figure 99. Over-expression of mir-337 in MIN6 cells (error bars indicate standard error of technical replicates).

Large differences in baseline insulin secretion in response to 3.3mM glucose were observed for control cells (figure 100) therefore cannot draw any conclusions on effects on mir-337 over-expression.

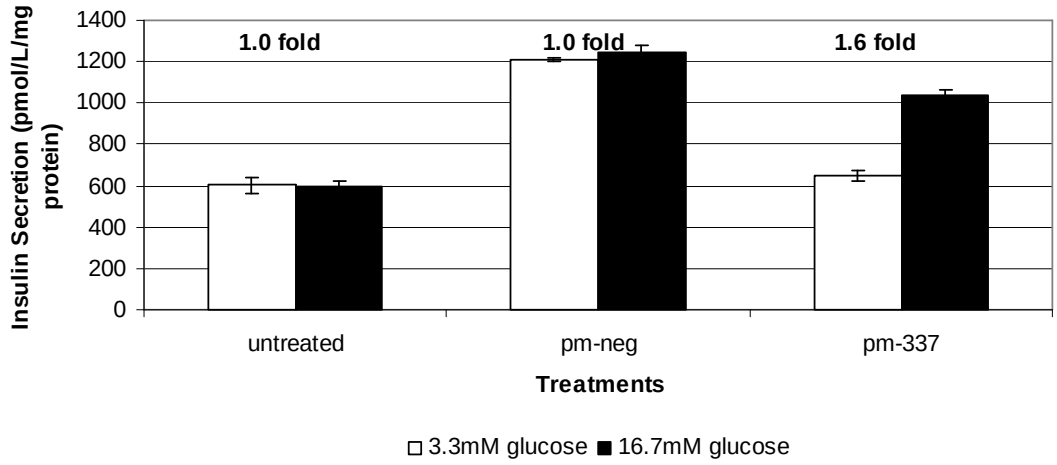

Figure 100. Over-expression of mir-337 in MIN6 cells (error bars indicate standard error of technical replicates).

1.9 Functional Validation of mir-532

Expression levels of mir-532 were manipulated using miRNA inhibitors and mimics to determine if differential expression of this miRNA could affect GSIS phenotype of MIN6 cells.

(a) Knockdown of mir-532

No effect on GSIS is observed for knockdown of mir-532 relative to control cells (figure 101).

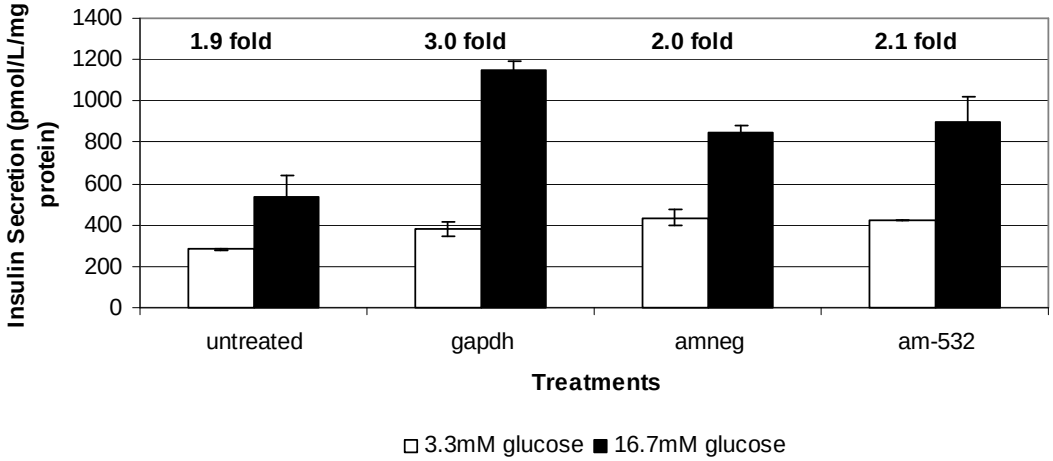

Figure 101. Knockdown of mir-532 levels in MIN6 cells (error bars indicate standard error of technical replicates).

No effect on GSIS is observed for knockdown of mir-532 levels relative to control cells (figure 102).

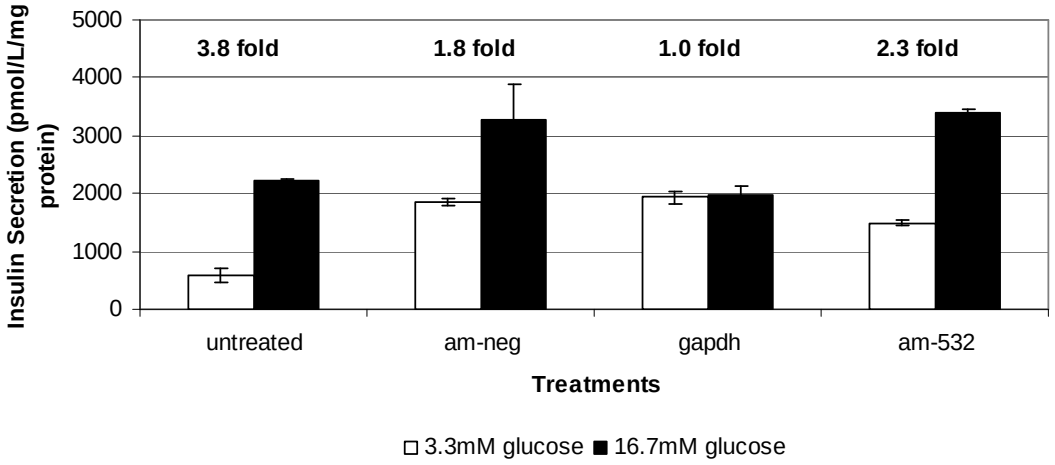

Figure 102. Knockdown of mir-532 levels in MIN6 cells (error bars indicate standard error of technical replicates).

(b) Over-expression of mir-532

No effect on GSIS was observed for over-expression of mir-532 relative to control cells (figure 103).

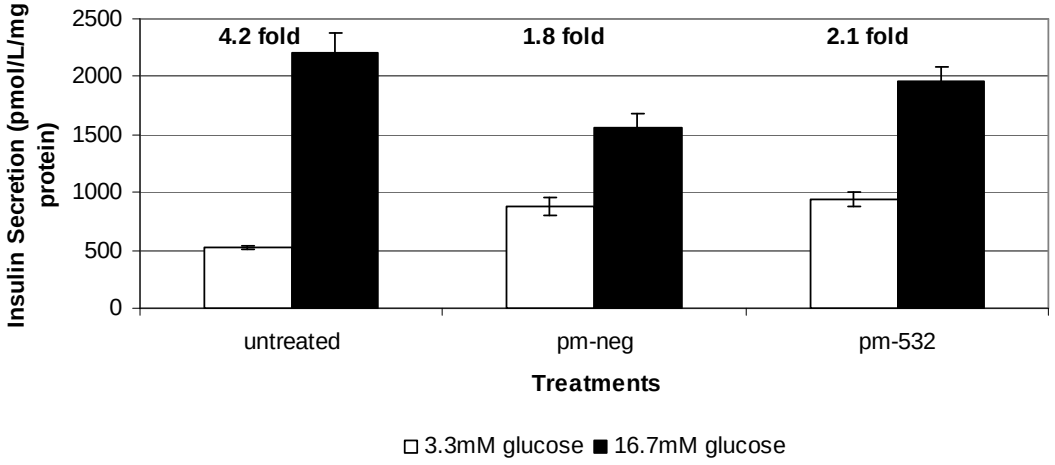

Figure 103. Over-expression of mir-532 in MIN6 cells (error bars indicate standard error of technical replicates).

A slight decrease in GSIS was observed for cells treated with pm-532 relative to untreated and pm-neg transfected cells (figure 104).

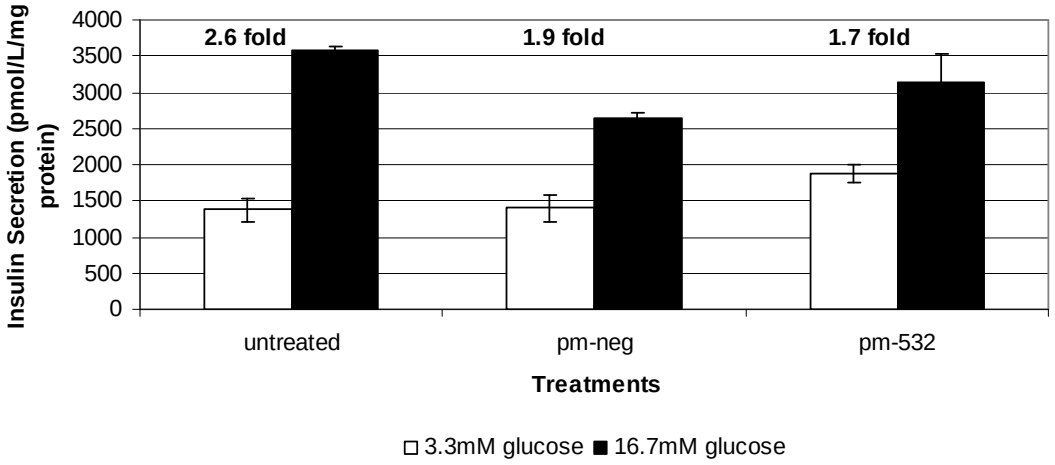

Figure 104. Over-expression of mir-532 in MIN6 cells (error bars indicate standard error of technical replicates).

No effect on GSIS was observed for pm-532 treated cells relative to untreated and pm-neg transfected cells (figure 105).

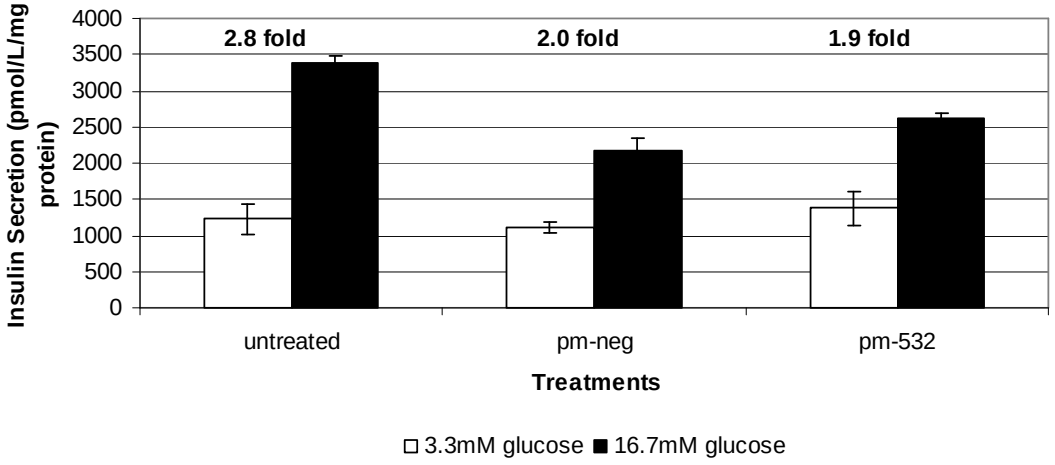

Figure 105. Over-expression of mir-532 in MIN6 cells (error bars indicate standard error of technical replicates).

1.10 Functional Validation of mir-320

Mir-320 expression was manipulated using anti- and pre-mirs as miRNA inhibitors and mimics for altering miRNA levels *in vitro*.

(a) Knockdown of mir-320

No effect on GSIS is observed for knockdown of mir-320 relative to control cells (figure 106).

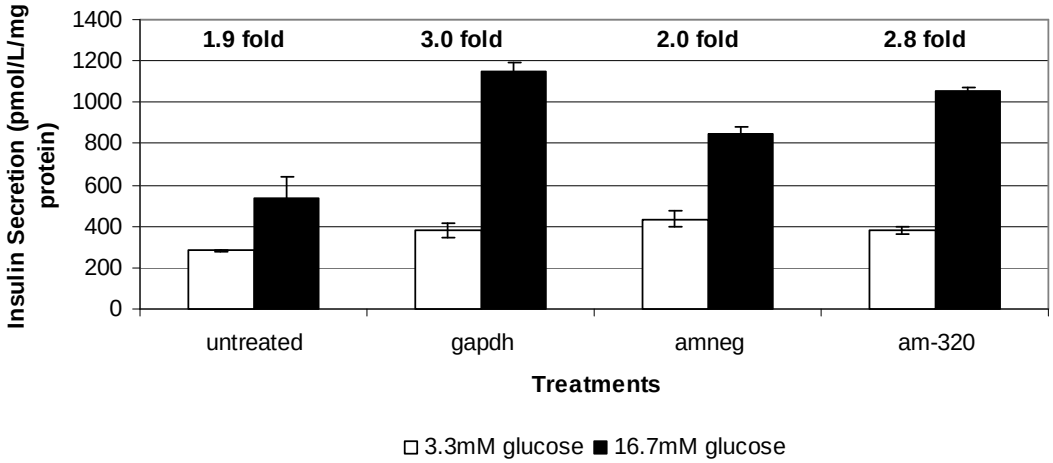

Figure 106. Knockdown of mir-320 levels in MIN6 cells (error bars indicate standard error of technical replicates).

No effect on GSIS is observed for mir-320 knockdown relative to control cells (figure 107).

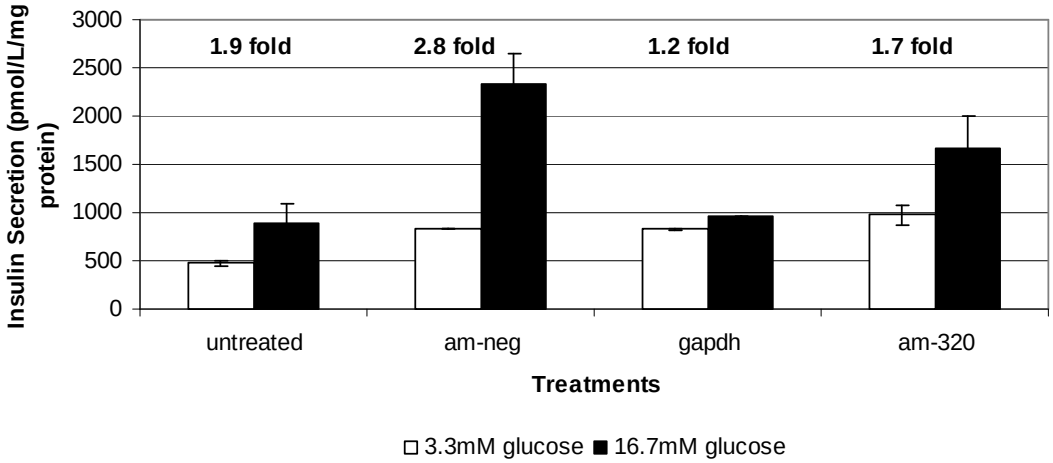

Figure 107. Knockdown of mir-320 levels in MIN6 cells (error bars indicate standard error of technical replicates).

No effect on GSIS is observed for knockdown of mir-320 relative to control cells (figure 108).

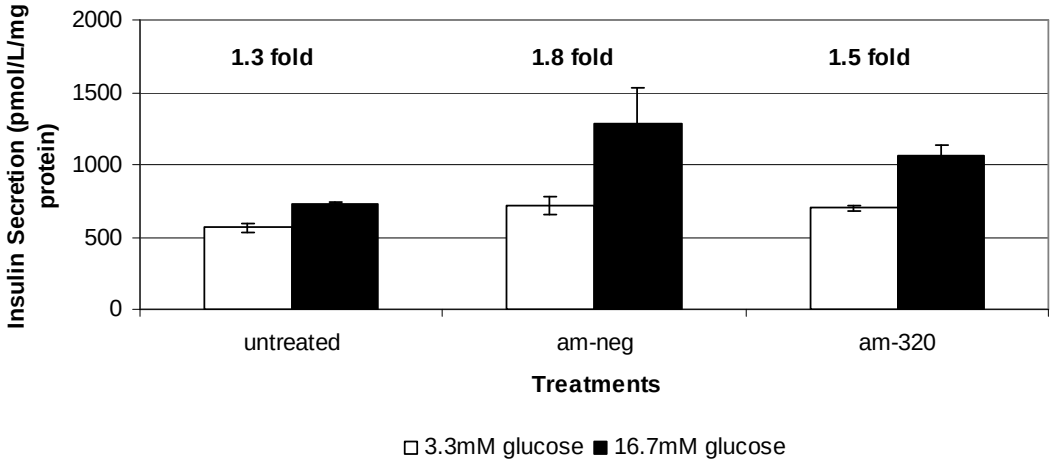

Figure 108. Knockdown of mir-320 levels in MIN6 cells (error bars indicate standard error of technical replicates).

No effect on GSIS is observed for knockdown of mir-320 relative to control cells (figure 109).

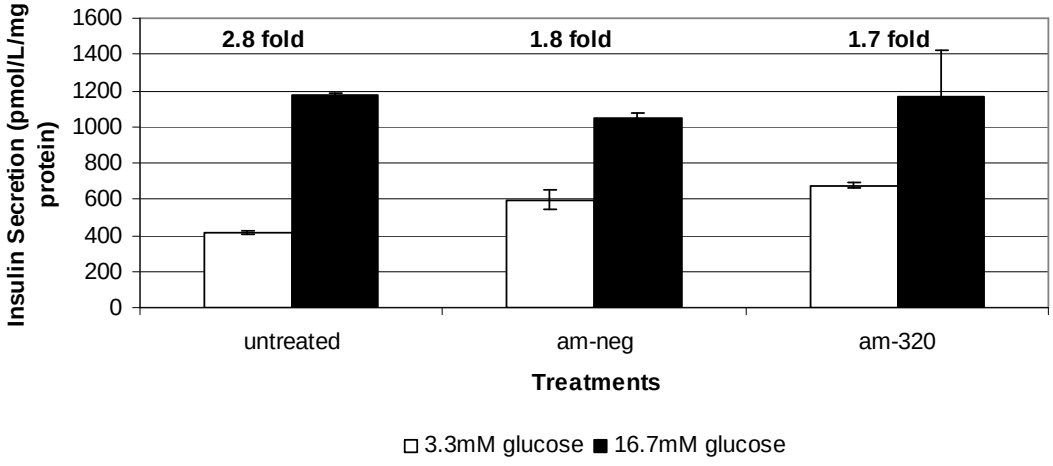

Figure 109. Knockdown of mir-320 levels in MIN6 cells (error bars indicate standard error of technical replicates).

Knockdown of mir-320 (figure 110) shows a decrease in GSIS relative to untreated and am-neg transfected cells.

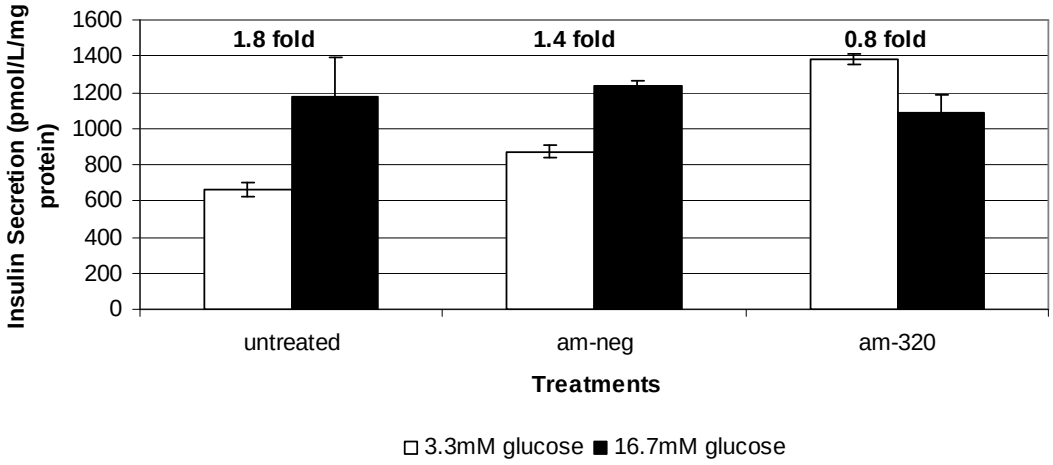

Figure 110. Knockdown of mir-320 levels in MIN6 cells (error bars indicate standard error of technical replicates).

(b) Over-expression of mir-320

Over-expression of mir-320 (figure 111) shows a decrease in GSIS relative to control cells.

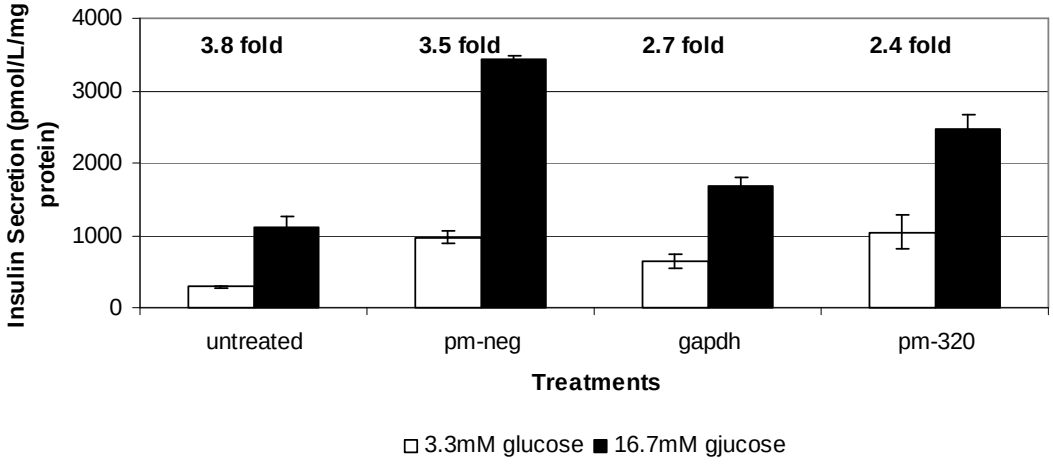

Figure 111. Over-expression of mir-320 in MIN6 cells (error bars indicate standard error of technical replicates).

Large differences in baseline insulin secretion in response to 3.3mM glucose were observed for control cells (figure 112) therefore cannot draw any conclusions on effects on mir-320 over-expression.

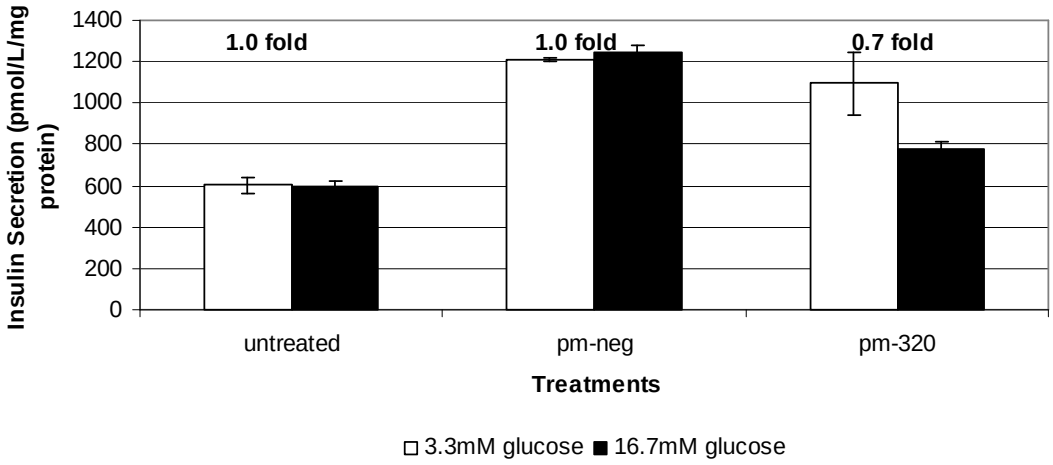

Figure 112. Over-expression of mir-320 in MIN6 cells (error bars indicate standard error of technical replicates).

1.11 Functional Validation of mir-192

Expression levels of mir-192 were manipulated in MIN6 cells to determine if this miRNA plays a role in GSIS in these cells.

(a) Knockdown of mir-192

No effect on GSIS is observed for knockdown of mir-192 relative to control cells (figure 113).

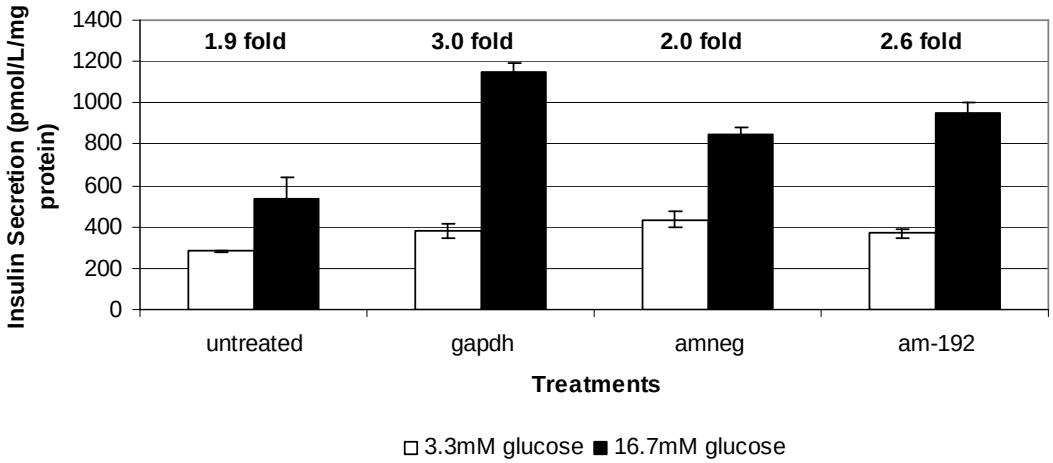

Figure 113. Knockdown of mir-192 levels in MIN6 cells (error bars indicate standard error of technical replicates).

No effect on GSIS is observed for knockdown of mir-192 relative to untreated and am-neg transfected cells (figure 114).

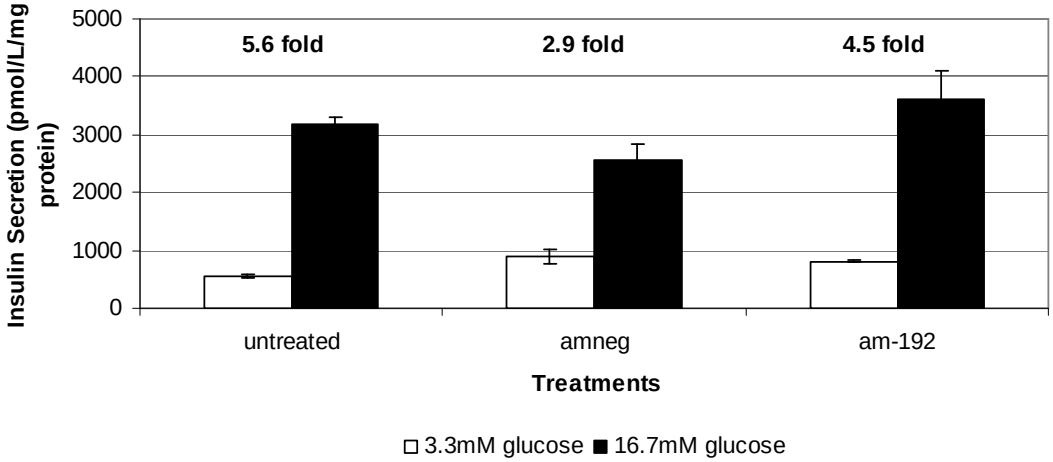

Figure 114. Knockdown of mir-192 levels in MIN6 cells (error bars indicate standard error of technical replicates).

Knockdown of mir-192 (figure 115) shows a decrease in GSIS relative to untreated and am-neg transfected cells.

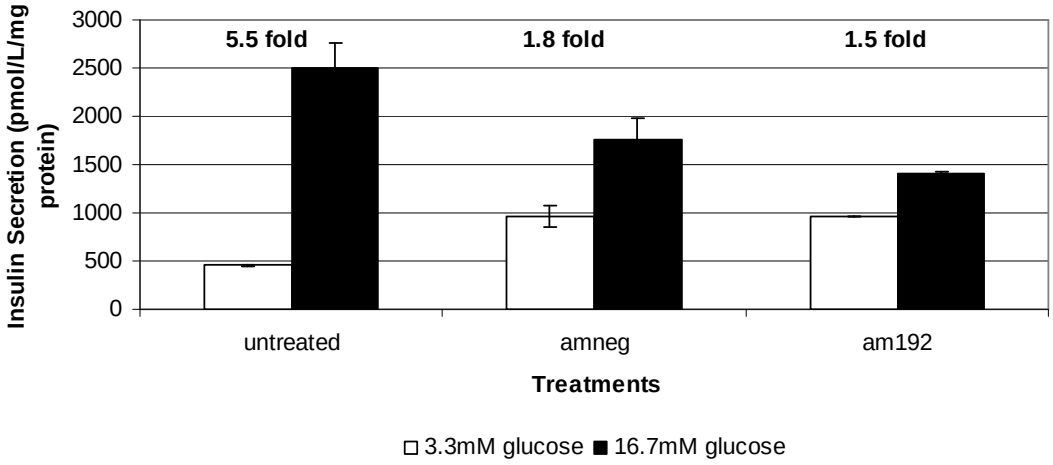

Figure 115. Knockdown of mir-192 levels in MIN6 cells (error bars indicate standard error of technical replicates).

No effect on GSIS is observed for knockdown of mir-192 relative to control cells (figure 116).

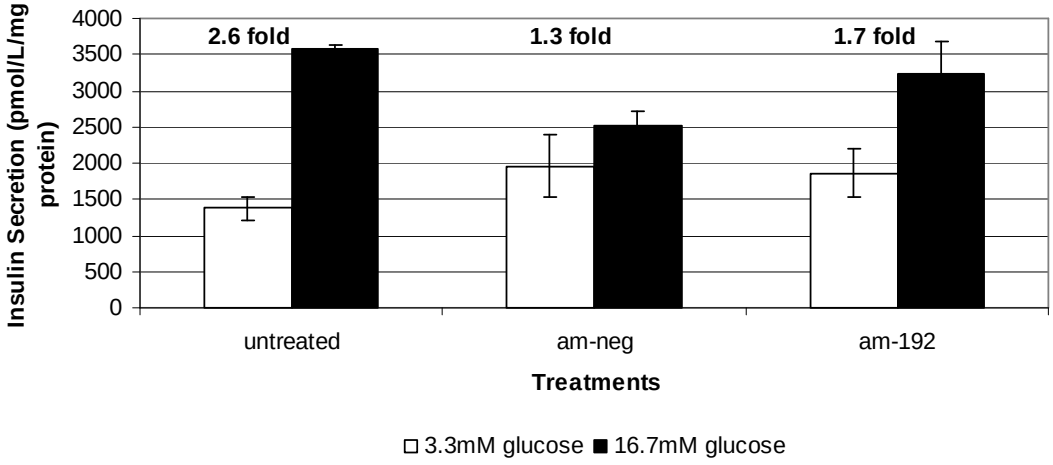

Figure 116. Knockdown of mir-192 levels in MIN6 cells (error bars indicate standard error of technical replicates).

(b) Over-expression of mir-192

Over-expression of mir-192 (figure 117) shows a decrease in GSIS relative to untreated and pm-neg transfected cells.

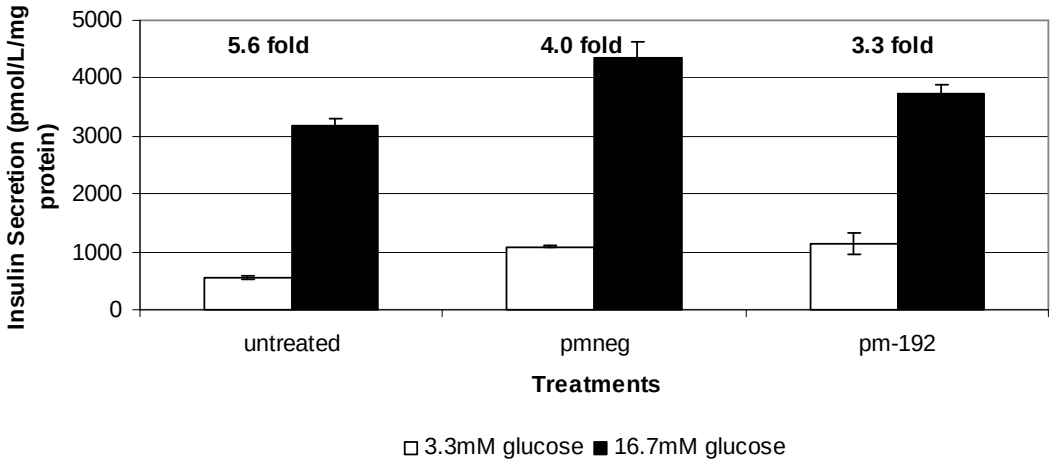

Figure 117. Over-expression of mir-192 in MIN6 cells (error bars indicate standard error of technical replicates).

Over-expression of mir-192 (figure 118) shows a decrease in GSIS relative to untreated and pm-neg transfected cells.

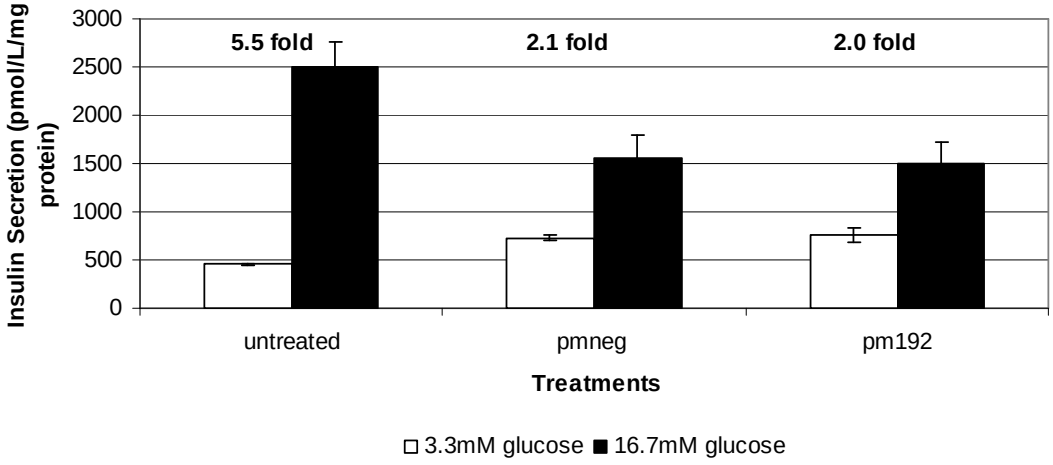

Figure 118. Over-expression of mir-192 in MIN6 cells (error bars indicate standard error of technical replicates).

Over-expression of mir-192 (figure 119) shows no effect on GSIS fold change, however a large increase in basal insulin secretion and stimulated insulin secretion is observed.

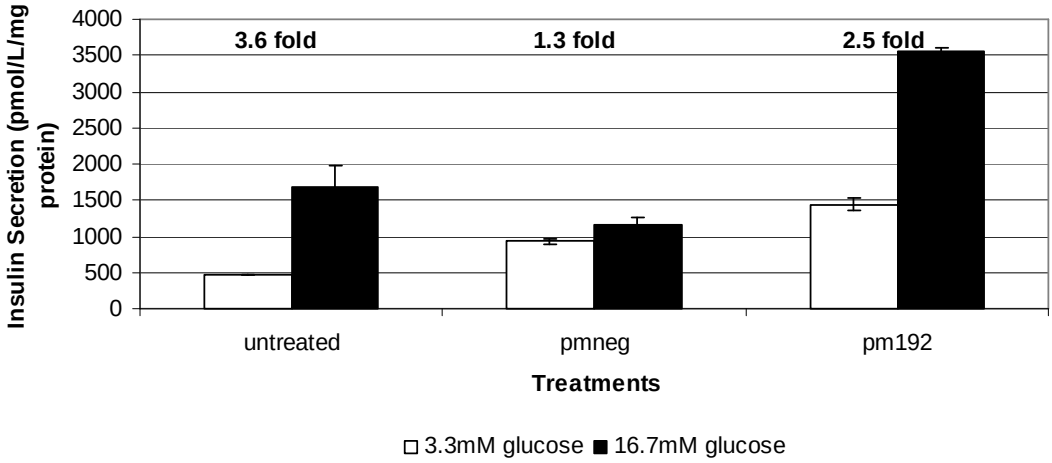

Figure 119. Over-expression of mir-192 in MIN6 cells (error bars indicate standard error of technical replicates).

1.12 Functional Validation of mir-379

Mir-379 expression levels were reduced in non-GSIS MIN6 cells, therefore increasing and decreasing levels of this miRNA would be expected to increase and decrease the GSIS responsiveness to these cells, respectively.

(a) Knockdown of mir-379

No effect on GSIS is observed for knockdown of mir-379 relative to control cells (figure 120).

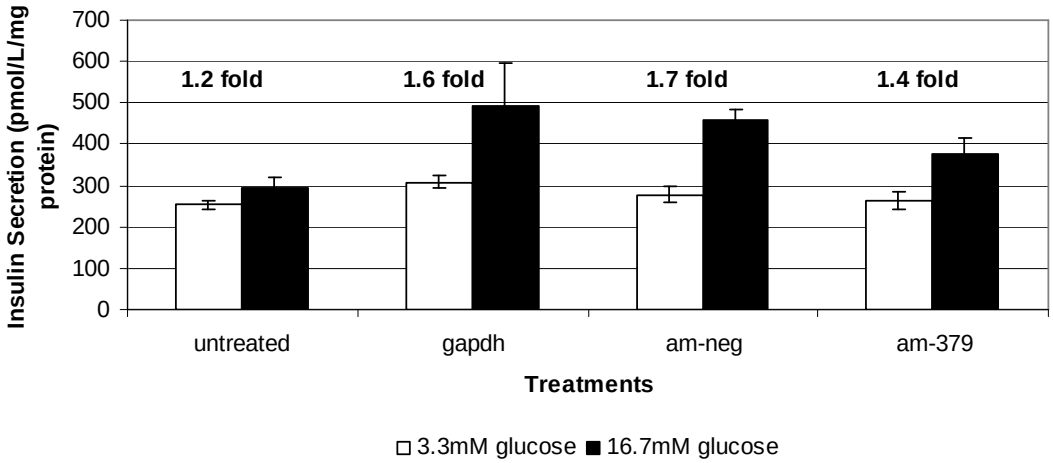

Figure 120. Knockdown of mir-379 levels in MIN6 cells (error bars indicate standard error of technical replicates).

No effect on GSIS is observed for knockdown of mir-379 relative to control cells (figure 121).

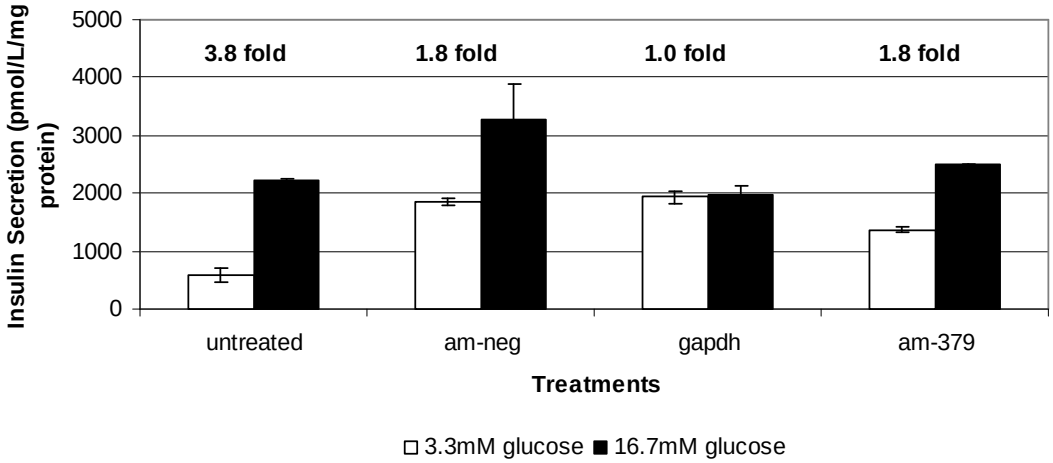

Figure 121. Knockdown of mir-379 levels in MIN6 cells (error bars indicate standard error of technical replicates).

(b) Over-expression of mir-379

Over-expression of mir-379 (figure 122) showed a decrease in GSIS relative to untreated and pm-neg transfected cells.

Figure 122. Over-expression of mir-379 in MIN6 cells (error bars indicate standard error of technical replicates).

No effect on GSIS was observed for over-expression of mir-379 relative to control cells (figure 123).

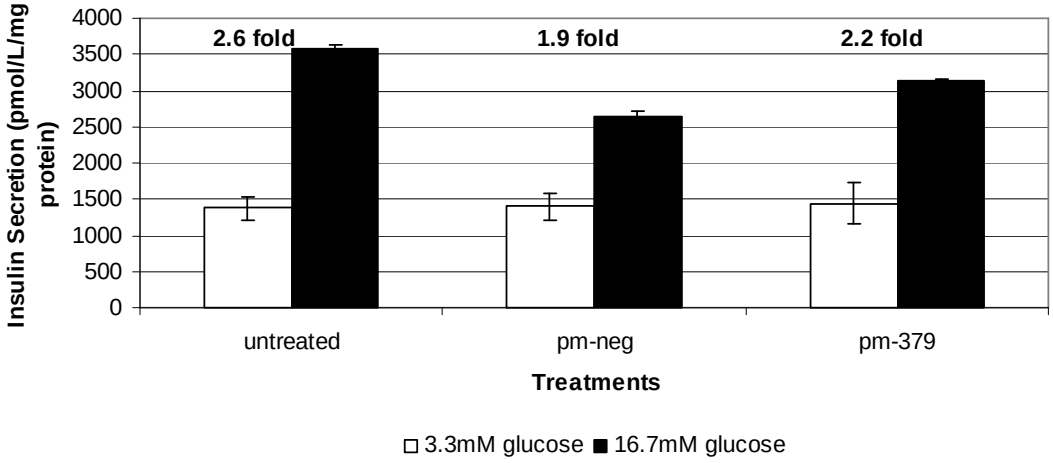

Figure 123. Over-expression of mir-379 in MIN6 cells (error bars indicate standard error of technical replicates).

Over-expression of mir-379 (figure 124) showed a decrease in GSIS relative to untreated and pm-neg transfected cells.

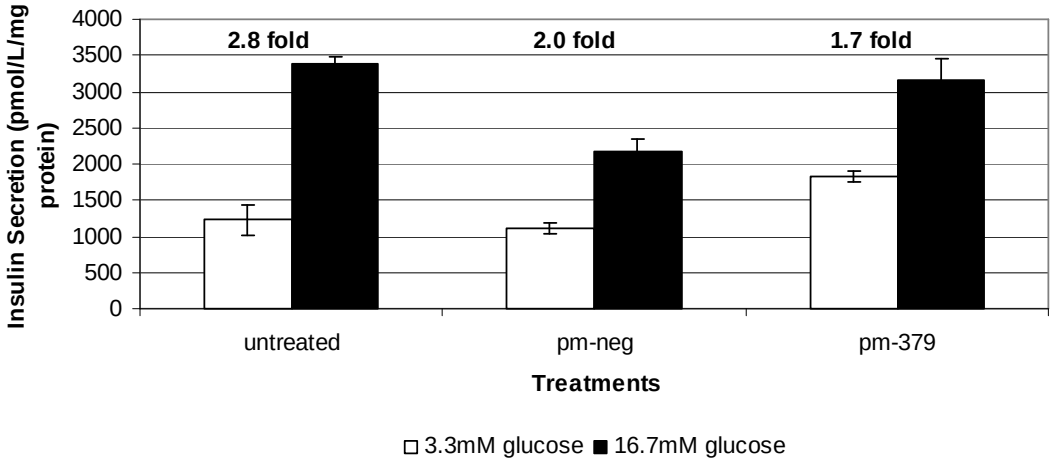

Figure 124. Over-expression of mir-379 in MIN6 cells (error bars indicate standard error of technical replicates).

Appendix B

miRNA biomarker study – raw data

Evaluation of target miRNA levels in serum from type 1 diabetes patients and control serum :

Target	C_t		ΔC_t	Fold Change
	Control	T1DM		
mir-9*	33.914	33.271	-0.643	1.56
mir-376a	35.046	35.348	0.302	-1.23
mir-192	32.496	31.945	-0.551	1.46
mir-375*	32.588	32.173	-0.415	1.33
mir-532	31.735	31.175	-0.56	1.47
mir-320	28.073	28.442	0.369	-1.29
mir-130a	28.944	29.846	0.902	-1.86
mir-369-5p	34.185	34.461	0.276	-1.21
mir-27a	28.11	28.477	0.367	-1.28
mir-124a	34.152	32.424	1.728	3.31
mir-379	33.506	32.979	0.527	1.44
mir-337	Not detected			
mir-200a	Not detected			
mir-410	Not detected			

Table 2.1 Fold changes of miRNA levels in T1DM sera compared to non-diabetic sera controls. Fold changes calculated from $2^{-(ct(T1DM)-ct(Control)}$ (as no suitable endogenous control identified for this work) (* miRNAs identified from the literature).

Mir-124a					
T1DM	**C_t**	**Control**	**C_t**	**ΔC_t**	**Fold change**
DS-29	33.615	DS-39	34.85	1.235	2.35
DS-35	30.847	DS-33	34.147	3.3	9.85
DS-11	32.144	DS-49	34.467	2.323	5
DS-13	32.159	DS-18	33.271	1.112	2.16
DS-25	31.253	DS-19	34.119	2.866	7.29
				average	
				fold change	**5.33**
				Stdev	**+/-3.29**
				P-value	**0.004**

Table 2.2 Fold changes in mir-124a levels in T1DM sera compared to non-diabetic sera. Fold changes calculated from $2^{-(ct(T1DM)-ct(Control)}$ (as no suitable endogenous control identified for this work).

Mir-130a					
T1DM	**C_t**	**Control**	**C_t**	**ΔC_t**	**Fold Change**
DS-11	34.055	DS-49	32.414	-1.641	-3.11
DS-13	30.856	DS-18	30.251	-0.605	-1.52
DS-25	30.966	DS-72	33.947	2.981	7.89
DS-29	31.095	DS-37	31.258	0.163	1.11
DS-35	29.1899	DS-33	33.091	3.901	14.94

Table 2.3 Fold changes in mir-9 levels in T1DM sera compared to non-diabetic sera. Fold changes calculated from $2^{-(ct(T1DM)-ct(Control)}$ (as no suitable endogenous control identified for this work).

Mir-9					
T1DM	**C_t**	**Control**	**C_t**	**ΔCt**	**Fold change**
DS-11	undet	DS-49	undet		
DS-13	31.828	DS-18	33.8995	-2.07	4.2
DS-25	33.861	DS-72	undet		
DS-29	undet	DS-37	undet		
DS-35	34.7	DS-33	undet		

Table 2.4 Fold changes in mir-9 levels in T1DM sera compared to non-diabetic sera. Fold changes calculated from $2^{-(ct(T1DM)-ct(Control)}$ (as no suitable endogenous control identified for this work).

Mir-532					
T1DM	**C_t**	**Control**	**C_t**	**ΔC_t**	**Fold Change**
DS-11	35.732	DS-49	33.963	1.769	-3.41
DS-13	32.944	DS-18	32.115	0.829	-1.78
DS-25	32.725	DS-72	35.545	-2.82	7.06
DS-29	33.328	DS-37	33.765	-0.44	1.35
DS-35	31.235	DS-33	34.432	-3.19	9.17

Table 2.5 Fold changes in mir-9 levels in T1DM sera compared to non-diabetic sera. Fold changes calculated from $2^{-(ct(T1DM)-ct(Control)}$ (as no suitable endogenous control identified for this work).

Mir-192					
T1DM	**C_t**	**Control**	**C_t**	**ΔC_t**	**Fold Change**
DS-11	36.087	DS-49	36.255	-0.168	1.12
DS-13	34.252	DS-18	34.261	-0.009	1.006
DS-25	33.26	DS-72	36.749	-3.489	11.23
DS-29	33.664	DS-37	34.827	-1.163	2.23
DS-35	32.01	DS-33	undet		

Table 2.6 Fold changes in mir-9 levels in T1DM sera compared to non-diabetic sera. Fold changes calculated from $2^{-(ct(T1DM)-ct(Control)}$ (as no suitable endogenous control identified for this work).

Mir-379					
T1DM	**C_t**	**Control**	**C_t**	**ΔC_t**	**Fold change**
DS-29	33.061	DS-39	34.9	1.839	3.58
DS-35	31.01	DS-33	33.23	2.22	4.66
DS-11	32.387	DS-49	33.457	1.07	2.1
DS-13	**32.103**	**DS-18**	**30.881**	**-1.222**	**-2.33**
DS-25	32.043	DS-19	34.7	2.657	6.31
				average	
				fold change	**4.16**
				Stdev	**1.77**
				P-value	**0.017**

Table 2.7 Fold changes in mir-379 levels in T1DM sera compared to non-diabetic sera. Fold changes calculated from $2^{-(ct(T1DM)-ct(Control)}$ (as no suitable endogenous control identified for this work). DS-13 / DS-18 pair were removed from average fold change calculations as they were outliers.

Mir-124a expanded study :

Mir-124a						
T1DMs	**C_t**	**Controls**	**C_t**	**ΔC_t**	**RQ**	**Fold**
DS-68	33.286	DS-56	33.834	-0.548	1.46206	1.46
DS-74	33.993	DS-36	34.898	-0.905	1.87254	1.87
DS-82	35.938	DS-7	34.032	1.906	0.26683	-3.75
DS-84	36.061	DS-27	35.588	0.473	0.72047	-1.39
DS-88	33.459	DS-39	35.044	-1.585	3.00008	3.00
DS-90	35.02	DS-53	34.175	0.845	0.55671	-1.80
DS-93	34.389	DS-33	35.629	-1.24	2.36199	2.36
DS-98	34.543	DS-50	35.431	-0.888	1.85061	1.85
DS-95	36.427	DS-51	36.449	-0.022	1.01537	1.02
DS-99	35.717	DS-53	34.175	1.542	0.34341	-2.91

Table 2.8 Fold change of mir-124a levels in T1DM sera compared to non-diabetic sera. Fold changes calculated from $2^{-(ct(T1DM)-ct(Control)}$ (as no suitable endogenous control identified for this work).

Evaluation of GSIS related miRNAs in serum from type 2 diabetes patients relative to control serum :

Mir-369-5p					
T2DM	**C_t**	**Control**	**C_t**	**ΔC_t**	**Fold Change**
DS-9	35.884	**DS-52**	35.494	0.39	-1.31
DS-10	undet	**DS-3**	35.516		
DS-14	undet	**DS-2**	36.162		
DS-15	35.7335	**DS-54**	34.517	1.2165	-2.33
DS-21	35.108	**DS-16**	33.828	1.28002	-2.43
DS-23	34.8782	**DS-18**	33.699	1.17921	-2.26
				Average	
				Fold	**-2.08**

Table 2.9 Fold change of mir-369-5p levels in T2DM sera compared to non-diabetic sera. Fold changes calculated from $2^{-(ct(T1DM)-ct(Control)}$ (as no suitable endogenous control identified for this work).

Mir-130a					
T2DM	**C_t**	**Control**	**C_t**	**ΔC_t**	**Fold Change**
DS-9	31.499	**DS-52**	32.018	-0.519	1.433
DS-10	35.012	**DS-3**	36.321	-1.309	2.478
DS-14	32.825	**DS-2**	33.345	-0.52	1.434
DS-15	32.826	**DS-54**	32.147	0.679	-1.601
DS-21	32.061	**DS-16**	30.876	1.185	-2.27
DS-23	32.531	**DS-18**	31.967	0.564	-1.478

Table 2.10 Fold change of mir-130a levels in T2DM sera compared to non-diabetic sera. Fold changes calculated from $2^{-(ct(T1DM)-ct(Control)}$ (as no suitable endogenous control identified for this work).

Mir-27a					
T2DM	**C_t**	**Control**	**C_t**	**ΔC_t**	**Fold Change**
DS-9	31.192	**DS-52**	30.975	0.217	-1.62
DS-10	34.07	**DS-3**	33.776	0.294	-1.22
DS-14	31.559	**DS-2**	32.853	-1.294	2.45
DS-15	31.291	**DS-54**	30.853	0.438	-1.35
DS-21	30.947	**DS-16**	29.986	0.961	-1.95
DS-23	31.611	**DS-18**	30.715	0.896	-1.86

Table 2.11 Fold change of mir-27a levels in T2DM sera compared to non-diabetic sera. Fold changes calculated from $2^{-(ct(T1DM)-ct(Control)}$ (as no suitable endogenous control identified for this work).

Mir-124a					
T2DM	**C_t**	**Control**	**C_t**	**ΔC_t**	**Fold Change**
DS-9	33.899	**DS-52**	34.828	-0.929	1.9
DS-10	34.879	**DS-3**	35.573	-0.694	1.62
DS-14	36.598	**DS-2**	35.403	1.195	-2.29
DS-15	35.969	**DS-54**	36.085	-0.116	1.08
DS-21	35.912	**DS-16**	35.062	0.85	-1.8
DS-23	35.396	**DS-18**	33.854	1.542	-2.91

Table 2.12 Fold change of mir-124a levels in T2DM sera compared to non-diabetic sera. Fold changes calculated from $2^{-(ct(T1DM)-ct(Control)}$ (as no suitable endogenous control identified for this work).

Mir-410					
T2DM	**C_t**	**Control**	**C_t**	**ΔC_t**	**Fold Change**
DS-9	35.344	**DS-52**	35.135	0.209	-1.16
DS-10	35.65	**DS-3**	35.523	0.127	-1.09
DS-14	34.711	**DS-2**	34.795	-0.084	1.06
DS-15	35.172	**DS-54**	34.012	1.16	-2.23
DS-21	34.026	**DS-16**	33.482	0.544	-1.46
DS-23	33.772	**DS-18**	32.799	0.973	-1.96

Table 2.13 Fold change of mir-410 levels in T2DM sera compared to non-diabetic sera. Fold changes calculated from $2^{-(ct(T1DM)-ct(Control)}$ (as no suitable endogenous control identified for this work).

Mir-200a					
T2DM	**C_t**	**Control**	**C_t**	**ΔC_t**	**Fold change**
DS-9	33.634	**DS-52**	36.617	-2.983	7.91
DS-10	undeter	**DS-3**	undeter		
DS-14	36.03	**DS-2**	undeter		
DS-15	34.867	**DS-54**	35.687	-0.82	1.76
DS-21	35.859	**DS-16**	35.28	0.579	-1.49
DS-23	34.615	**DS-18**	33.649	0.966	-1.95

Table 2.14 Fold change of mir-200a levels in T2DM sera compared to non-diabetic sera. Fold changes calculated from $2^{-(ct(T1DM)-ct(Control)}$ (as no suitable endogenous control identified for this work).

Mir-532					
T2DM	**Ct**	**Control**	**Ct**	**ΔCt**	**Fold change**
DS-9	32.535	**DS-52**	34.605	-2.07	4.2
DS-10	35.5208	**DS-3**	36.103	-0.5822	1.5
DS-14	34.463	**DS-2**	34.29	0.173	-1.13
DS-15	34.3358	**DS-54**	34.195	0.1408	-1.1
DS-21	34.0148	**DS-16**	33.314	0.7008	-1.62
DS-23	35.6051	**DS-18**	33.876	1.7291	-3.31

Table 2.15 Fold change of mir-532 levels in T2DM sera compared to non-diabetic sera. Fold changes calculated from $2^{-(ct(T1DM)-ct(Control)}$ (as no suitable endogenous control identified for this work).

Appendix C

Label-free LC-MS serum study raw data

T1DM new versus control new- Analysis 1

Accession	Peptides	Score	Anova (p)*	Fold	Description	Average Normalised Abundances	
						T1DM new	Control new
P0C0L4	43	4138	0.02	1.58	Complement C4-A	1.56E+008	9.88E+007
P01024	35	3123	0.05	1.55	Complement C3	4.95E+007	3.19E+007
P01031	20	1427	0.03	1.65	Complement C5	1.88E+006	1.14E+006
P02647	16	1126	0.03	1.53	Apolipoprotein A-I	7.57E+007	4.94E+007
P10909	13	988	0.04	1.72	Clusterin	1.78E+007	1.03E+007
P02748	10	950	0.008	1.79	Complement component C9	4.28E+006	2.39E+006
P04004	8	689	0.05	1.43	Vitronectin	4.72E+007	3.30E+007
P06727	9	652	0.01	1.58	Apolipoprotein A-IV	9.07E+006	5.74E+006
P23142	7	640	0.03	1.61	Fibulin-1	5.67E+006	3.53E+006
P02768	8	628	0.04	1.64	Serum albumin	9.07E+006	5.54E+006
Q08380	8	581	0.05	1.58	Galectin-3-binding protein	1.77E+006	1.12E+006
Q14624	6	520	0.04	7.81	Inter-alpha-trypsin inhibitor heavy chain H4	1.23E+006	1.58E+005
P01009	6	490	0.02	1.78	Alpha-1-antitrypsin	8.31E+005	4.66E+005
P18428	4	392	0.02	2.29	Lipopolysaccharide-binding protein	5.66E+005	2.47E+005
P07996	6	368	0.008	1.65	Thrombospondin-1	3.03E+005	5.00E+005
P02741	6	334	0.02	6.09	C-reactive protein	1.22E+006	2.00E+005
P02746	3	279	0.03	1.59	Complement C1q subcomponent subunit B	2.60E+006	1.63E+006
P10643	4	272	0.003	2.24	Complement component C7	4.26E+005	1.90E+005
P04003	3	270	0.03	1.51	C4b-binding protein alpha chain	3.63E+006	2.40E+006

P00450	4	258	0.01	2.41	Ceruloplasmin	2.70E+005	1.12E+005
P68032	4	232	0.02	1.95	Actin, alpha cardiac muscle 1	9.88E+004	1.93E+005
P07225	4	218	0.03	1.51	Vitamin K-dependent protein S	3.45E+005	2.29E+005
P02788	3	205	0.04	1.74	Lactotransferrin	3.86E+004	6.70E+004
Q06033	3	180	0.01	2.43	Inter-alpha-trypsin inhibitor heavy chain H3	9.40E+004	3.88E+004
Q6S8J3	3	178	0.02	1.97	POTE ankyrin domain family member E	5.39E+004	1.06E+005
P07358	3	171	0.05	1.86	Complement component C8 beta chain	5.52E+005	2.97E+005
P04070	2	164	0.03	1.81	Vitamin K-dependent protein C	2.12E+005	1.17E+005
Q9UK55	2	153	0.02	2.69	Protein Z-dependent protease inhibitor	1.97E+005	7.33E+004
Q12805	2	136	0.05	1.94	EGF-containing fibulin-like extracellular matrix protein 1	1.78E+005	9.16E+004
P09871	3	135	0.03	1.5	Complement C1s subcomponent	4.01E+004	2.67E+004
Q562R1	2	117	0.02	1.91	Beta-actin-like protein 2	5.31E+004	1.02E+005
Q9BYX7	2	113	0.02	1.98	Beta-actin-like protein 3	4.86E+004	9.63E+004

Table 1. Differentially expressed proteins in T1DM new verus control new comparison.T1DM new sample DS-169 was used as reference run.

T1DM new versus control new- Analysis 2

Accession	Peptides	Score	Anova (p)*	Fold	Description	Average Normalised Abundances	
						T1DM new	Control new
P0C0L5	40	3836	0.005	1.65	Complement C4-B	1.95E+008	1.18E+008
P01024	42	3693	0.03	1.56	Complement C3	6.88E+007	4.41E+007
P01031	20	1420	0.004	1.74	Complement C5	2.24E+006	1.28E+006
P02647	17	1233	0.02	1.57	Apolipoprotein A-I	8.52E+007	5.43E+007
P10909	12	1010	0.01	1.68	Clusterin	2.68E+007	1.59E+007
P02748	11	1000	0.003	1.86	Complement component C9	4.93E+006	2.66E+006
P06727	14	972	0.005	1.64	Apolipoprotein A-IV	1.15E+007	7.06E+006
P02768	10	777	0.03	1.58	Serum albumin	1.29E+007	8.20E+006
P04004	7	644	0.04	1.46	Vitronectin	5.38E+007	3.70E+007
P23142	7	631	0.02	1.64	Fibulin-1	6.42E+006	3.93E+006
P18428	5	541	0.02	2.29	Lipopolysaccharide-binding protein	1.30E+006	5.68E+005
P02743	7	530	0.04	1.48	Serum amyloid P-component	7.41E+006	5.02E+006
P08603	8	521	0.02	1.41	Complement factor H	2.70E+006	1.92E+006
P01008	9	512	0.05	1.47	Antithrombin-III	2.75E+007	1.87E+007
P01871	7	500	0.05	1.42	Ig mu chain C region	1.44E+007	1.02E+007
P07996	7	425	0.01	1.53	Thrombospondin-1	5.18E+005	7.94E+005
P01009	5	412	0.004	2.19	Alpha-1-antitrypsin	9.02E+005	4.11E+005
P04003	3	346	0.01	1.61	C4b-binding protein alpha chain	4.45E+006	2.77E+006
P07225	5	297	0.02	1.33	Vitamin K-dependent protein S	1.22E+006	9.16E+005
Q06033	5	278	0.007	2.7	Inter-alpha-trypsin inhibitor heavy chain H3	1.53E+005	5.66E+004

P10643	3	267	0.001	2.35	Complement component C7	5.43E+005	2.31E+005
P68133	5	246	0.01	2.19	Actin, alpha skeletal muscle	1.11E+005	2.43E+005
P02745	2	241	0.02	1.47	Complement C1q subcomponent subunit A	2.71E+006	1.84E+006
P02741	4	236	0.01	6.22	C-reactive protein	1.24E+006	1.99E+005
Q9UK55	3	228	0.03	2.51	Protein Z-dependent protease inhibitor	3.81E+005	1.52E+005
P02788	3	218	0.02	2.26	Lactotransferrin	4.63E+004	1.05E+005
P01834	2	210	0.05	1.5	Ig kappa chain C region	1.23E+007	8.18E+006
P12259	3	200	0.04	1.63	Coagulation factor V	2.57E+005	1.57E+005
P02746	2	195	0.02	1.55	Complement C1q subcomponent subunit B	1.68E+006	1.09E+006
P13671	3	185	0.04	1.58	Complement component C6	4.21E+005	2.66E+005
P09871	2	124	0.03	1.7	Complement C1s subcomponent	2.47E+005	1.46E+005
Q9BYX7	2	113	0.03	1.92	Beta-actin-like protein 3	6.34E+004	1.22E+005
Q6S8J3	2	113	0.03	1.92	POTE ankyrin domain family member E	6.34E+004	1.22E+005
A5A3E0	2	113	0.03	1.92	POTE ankyrin domain family member F	6.34E+004	1.22E+005
P04196	2	95	0.05	2.61	Histidine-rich glycoprotein	1.13E+004	2.94E+004

Table 2. Differentially expressed proteins in T1DM new versus control new comparison. Control sample DS-175 was used as reference run.

T1DM new versus control new- Analysis 3

Accession	Peptides	Score	Anova (p)*	Fold	Description	Average Normalised Abundances	
						T1DM new	Control new
P0C0L5	26	2000	0.05	3.01	Complement C4-B	4.46e+007	1.48e+007
P01031	9	586	0.04	1.63	Complement C5	4.70e+005	2.88e+005
P00734	7	555	0.04	35.59	Prothrombin	1.05e+007	2.96e+005
P60709	8	446	0.04	1.66	Actin, cytoplasmic 1	3.25e+005	5.40e+005
P68032	7	357	0.009	2.30	Actin, alpha cardiac muscle 1	1.24e+005	2.84e+005
P63267	6	314	0.009	2.23	Actin, gamma-enteric smooth muscle	1.16e+005	2.60e+005
P10909	4	246	0.02	1.57	Clusterin	8.49e+005	5.41e+005
P02741	4	196	0.02	8.05	C-reactive protein	4.21e+005	5.23e+004
A5A3E0	3	178	0.03	2.02	POTE ankyrin domain family member F	6.91e+004	1.40e+005
Q6S8J3	3	178	0.03	2.02	POTE ankyrin domain family member E	6.91e+004	1.40e+005
P05154	3	167	0.02	2.08	Plasma serine protease inhibitor	2.81e+004	5.83e+004
Q08380	2	121	0.04	1.54	Galectin-3-binding protein	4.31e+005	2.79e+005
Q06033	2	117	0.02	2.50	Inter-alpha-trypsin inhibitor heavy chain H3	8.37e+004	3.34e+004
Q562R1	2	117	0.03	1.87	Beta-actin-like protein 2	6.40e+004	1.20e+005
Q9BYX7	2	113	0.03	2.03	Beta-actin-like protein 3	6.31e+004	1.28e+005
P08697	2	111	0.03	1.58	Alpha-2-antiplasmin	7.70e+004	1.22e+005

Table 3. Differentially expressed proteins in T1DM new and control new comparison. Control samples DS-178 was used as reference run.

T1DM old versus control old- Analysis 1

Accession	Peptides	Score	Anova (p)*	Fold	Description	Average Normalised Abundances	
						T1DM old	Control old
P04114	56	4308	0.05	2.5	Apolipoprotein B-100	7.65E+006	1.91E+007
P01008	18	1712	0.05	2.55	Antithrombin-III	6.43E+007	1.64E+008
P02649	12	1248	0.02	2.19	Apolipoprotein E	1.46E+007	3.20E+007
P07225	7	545	0.05	2.47	Vitamin K-dependent protein S	1.52E+006	3.75E+006
P04004	5	491	0.03	1.72	Vitronectin	2.55E+007	4.39E+007
P02655	4	456	0.01	2.41	Apolipoprotein C-II	4.06E+006	9.79E+006
P02647	5	429	0.05	1.9	Apolipoprotein A-I	2.66E+007	5.06E+007
P00450	6	412	0.03	1.7	Ceruloplasmin	5.53E+005	3.25E+005
Q15485	5	406	0.02	3	Ficolin-2	5.81E+005	1.75E+006
P02766	4	377	0.04	2.69	Transthyretin	2.14E+006	5.74E+006
P35542	2	245	0.02	2.34	Serum amyloid A-4 protein	8.40E+005	1.97E+006
P48740	4	243	0.005	1.97	Mannan-binding lectin serine protease 1	4.04E+005	7.95E+005
P04003	3	243	0.04	2.62	C4b-binding protein alpha chain	5.67E+006	1.49E+007
Q03591	3	227	0.006	1.88	Complement factor H-related protein 1	2.30E+006	4.34E+006
P01776	1	211	0.04	2.78	Ig heavy chain V-III region WAS	4.24E+005	1.18E+006
P01774	1	211	0.04	2.78	Ig heavy chain V-III region POM	4.24E+005	1.18E+006
P02776	2	211	0.05	2.1	Platelet factor 4	7.12E+005	1.49E+006
P63261	4	201	0.03	3.42	Actin, cytoplasmic 2	1.28E+005	4.38E+005
P05546	3	189	0.04	1.98	Heparin cofactor 2	2.49E+004	4.94E+004
O14791	2	189	3.71E-003	4.07	Apolipoprotein L1	7.27E+004	2.96E+005

P36980	2	168	0.02	1.88	Complement factor H-related protein 2	7.12E+005	1.34E+006
P07358	3	158	0.01	1.46	Complement component C8 beta chain	8.24E+004	5.64E+004
Q9BYX7	3	154	0.01	3.99	Beta-actin-like protein 3	6.77E+004	2.70E+005
Q6S8J3	3	154	0.01	3.99	POTE ankyrin domain family member E	6.77E+004	2.70E+005
P55056	2	135	0.02	2.9	Apolipoprotein C-IV	5.04E+004	1.46E+005
P04275	2	117	0.02	4.42	von Willebrand factor	1.76E+004	7.80E+004
P07357	2	98	0.03	1.73	Complement component C8 alpha chain	5.12E+004	2.96E+004
P01023	2	96	0.02	2.27	Alpha-2-macroglobulin	8.06E+004	3.55E+004

Table 4. Differentially expressed proteins in T1DM old and control old comparison. T1DM old sample DS-84 was used as reference run.

T1DM old versus control old- Analysis 2

Accession	Peptides	Score	Anova (p)*	Fold	Description	Average Normalised Abundances	
						T1DM old	Control old
P01008	17	1510	0.03	2.31	Antithrombin-III	3.15E+007	7.27E+007
P02649	15	1226	0.02	2.05	Apolipoprotein E	1.07E+007	2.19E+007
Q15485	7	544	0.02	2.81	Ficolin-2	4.37E+005	1.23E+006
P02655	5	518	0.01	2.25	Apolipoprotein C-II	3.13E+006	7.05E+006
P04004	5	446	0.03	1.62	Vitronectin	1.71E+007	2.77E+007
P00450	8	445	0.04	1.44	Ceruloplasmin	4.51E+005	3.13E+005
P02647	4	347	0.04	1.76	Apolipoprotein A-I	1.99E+007	3.50E+007
P07225	4	337	0.006	2.13	Vitamin K-dependent protein S	4.03E+005	8.59E+005
P02766	3	335	0.03	2.39	Transthyretin	1.63E+006	3.91E+006
P19827	4	298	0.01	2.14	Inter-alpha-trypsin inhibitor heavy chain H1	2.66E+005	5.69E+005
P48740	4	243	0.002	1.95	Mannan-binding lectin serine protease 1	2.82E+005	5.49E+005
P04003	3	243	0.03	2.39	C4b-binding protein alpha chain	4.23E+006	1.01E+007
P01765	1	211	0.05	2.5	Ig heavy chain V-III region TIL	3.20E+005	8.00E+005
P02776	2	211	0.05	1.98	Platelet factor 4	5.30E+005	1.05E+006
P35542	2	202	0.02	2.25	Serum amyloid A-4 protein	5.16E+005	1.16E+006
P63261	4	201	0.02	3.14	Actin, cytoplasmic 2	1.45E+005	4.56E+005
O14791	3	186	0.03	2.44	Apolipoprotein L1	7.75E+004	1.89E+005
P05154	2	184	0.05	2.01	Plasma serine protease inhibitor	5.14E+004	1.03E+005
Q03591	3	160	0.02	1.74	Complement factor H-related protein 1	1.42E+006	2.47E+006
P08697	3	159	0.03	3.54	Alpha-2-antiplasmin	2.47E+004	8.74E+004

Q6S8J3	3	154	0.009	3.72	POTE ankyrin domain family member E	4.79E+004	1.78E+005
A5A3E0	3	154	0.009	3.72	POTE ankyrin domain family member F	4.79E+004	1.78E+005
Q9BYX7	3	154	0.009	3.72	Beta-actin-like protein 3	4.79E+004	1.78E+005
P07357	3	139	0.02	1.67	Complement component C8 alpha chain	4.30E+004	2.58E+004
P55056	2	135	0.003	3.53	Apolipoprotein C-IV	2.86E+004	1.01E+005
P01023	2	133	0.03	2.08	Alpha-2-macroglobulin	8.89E+004	4.28E+004
P02654	2	117	0.02	2.32	Apolipoprotein C-I	1.37E+006	3.18E+006
P04275	2	117	0.01	3.51	von Willebrand factor	1.67E+004	5.87E+004
P68032	2	108	0.01	3.64	Actin, alpha cardiac muscle 1	4.64E+004	1.69E+005
P68133	2	108	0.01	3.64	Actin, alpha skeletal muscle	4.64E+004	1.69E+005
P02774	2	106	0.05	3.04	Vitamin D-binding protein	2.71E+004	8.23E+004
P36980	2	101	0.02	1.71	Complement factor H-related protein 2	2.27E+005	3.89E+005
P07358	2	92	0.001	1.86	Complement component C8 beta chain	6.35E+004	3.41E+004

Table 5. Differentially expressed proteins in T1DM old and control old comparison. Control old sample DS-162 was used as reference run.

T1DM old versus control old- Analysis 3

Accession	Peptides	Score	Anova (p)*	Fold	Description	Average Normalised Abundances	
						T1DM old	Control old
P01008	16	1381	0.03	2.37	Antithrombin-III	2.79E+007	6.63E+007
P02649	15	1269	0.02	2.05	Apolipoprotein E	1.05E+007	2.16E+007
P02655	5	518	0.007	2.5	Apolipoprotein C-II	2.76E+006	6.88E+006
P04004	6	501	0.03	1.57	Vitronectin	1.76E+007	2.77E+007
Q15485	6	494	0.02	2.88	Ficolin-2	4.10E+005	1.18E+006
P00450	7	477	0.03	1.6	Ceruloplasmin	5.17E+005	3.23E+005
P07225	6	446	0.005	2.24	Vitamin K-dependent protein S	4.03E+005	9.04E+005
P02647	5	429	0.05	1.75	Apolipoprotein A-I	1.96E+007	3.44E+007
P02766	3	335	0.04	2.46	Transthyretin	1.51E+006	3.71E+006
P04003	4	316	0.03	2.4	C4b-binding protein alpha chain	4.16E+006	9.97E+006
P35542	3	287	0.01	2.37	Serum amyloid A-4 protein	5.00E+005	1.19E+006
P05154	3	245	0.05	2.13	Plasma serine protease inhibitor	5.80E+004	1.24E+005
P48740	4	243	0.002	1.91	Mannan-binding lectin serine protease 1	2.79E+005	5.35E+005
O14791	3	233	0.02	2	Apolipoprotein L1	1.25E+005	2.49E+005
P19827	3	224	0.007	2.26	Inter-alpha-trypsin inhibitor heavy chain H1	2.13E+005	4.81E+005
P01774	1	211	0.05	2.51	Ig heavy chain V-III region POM	3.13E+005	7.87E+005
P01776	1	211	0.05	2.51	Ig heavy chain V-III region WAS	3.13E+005	7.87E+005
P02776	2	211	0.05	1.97	Platelet factor 4	5.22E+005	1.03E+006
P63261	4	201	0.03	3.09	Actin, cytoplasmic 2	1.52E+005	4.71E+005
A5A3E0	3	154	0.02	3.63	POTE ankyrin domain family member F	5.17E+004	1.88E+005
Q9BYX7	3	154	0.02	3.63	Beta-actin-like protein 3	5.17E+004	1.88E+005
Q6S8J3	3	154	0.02	3.63	POTE ankyrin domain family member E	5.17E+004	1.88E+005
P55056	2	135	0.004	3.03	Apolipoprotein C-IV	3.58E+004	1.08E+005
P05546	2	125	0.02	2.81	Heparin cofactor 2	1.05E+004	2.95E+004

P04275	2	117	0.01	3.9	von Willebrand factor	1.41E+004	5.50E+004
Q9UK55	2	112	0.02	1.98	Protein Z-dependent protease inhibitor	3.47E+004	1.75E+004
P00742	2	111	0.04	2.96	Coagulation factor X	3.78E+004	1.12E+005
P68032	2	108	0.02	3.59	Actin, alpha cardiac muscle 1	4.97E+004	1.79E+005
Q03591	2	106	0.03	1.74	Complement factor H-related protein 1	1.34E+006	2.33E+006
P02774	2	106	0.05	3.2	Vitamin D-binding protein	2.52E+004	8.07E+004
P07358	2	92	5.89E-004	1.91	Complement component C8 beta chain	6.34E+004	3.31E+004

Table 6. Differentially expressed proteins in T1DM old and control old comparison. Control old sample DS-39 was used as reference run.

T1DM new versus T1DM old- Analysis 1

Accession	Peptides	Score	Anova (p)*	Fold	Description	Average Normalised Abundances	
						T1DM new	T1DM old
P0C0L5	47	4330	0.02	1.35	Complement C4-B	1.11E+08	8.23E+07
P00734	19	1580	0.05	1.39	Prothrombin	3.08E+07	2.22E+07
P00450	12	841	0.03	1.55	Ceruloplasmin	8.18E+05	1.27E+06
P10909	7	766	0.005	1.43	Clusterin	2.10E+07	1.47E+07
P01871	4	763	0.04	1.57	Ig mu chain C region	6.61E+06	4.21E+06
P01031	13	749	0.03	1.59	Complement C5	6.09E+05	3.83E+05
P01008	10	724	0.006	1.44	Antithrombin-III	2.35E+07	1.63E+07
P19823	9	697	0.02	1.47	Inter-alpha-trypsin inhibitor heavy chain H2	2.58E+06	1.76E+06
P01009	8	586	0.05	1.49	Alpha-1-antitrypsin	5.32E+05	3.57E+05
P01834	4	483	0.03	1.54	Ig kappa chain C region	6.15E+06	4.00E+06
P04004	4	375	0.03	1.45	Vitronectin	1.72E+07	1.18E+07
P07225	4	316	0.007	1.71	Vitamin K-dependent protein S	6.27E+05	3.67E+05
P02768	4	255	0.007	1.69	Serum albumin	4.50E+05	2.66E+05
P00747	3	255	0.05	1.29	Plasminogen	3.79E+05	4.91E+05
P02654	4	213	0.004	1.55	Apolipoprotein C-I	2.59E+06	1.67E+06
Q06033	4	213	0.05	1.81	Inter-alpha-trypsin inhibitor heavy chain H3	1.03E+05	5.70E+04
P04180	3	183	0.05	1.24	Phosphatidylcholine-sterol acyltransferase	5.96E+05	4.80E+05
P07996	3	171	0.05	1.48	Thrombospondin-1	1.52E+05	2.24E+05
Q03591	2	153	0.02	1.77	Complement factor H-related protein 1	6.05E+04	3.42E+04
P01617	2	121	0.05	1.48	Ig kappa chain V-II region TEW	2.07E+05	1.40E+05
P04264	2	96	0.04	4.01	Keratin, type II cytoskeletal 1	1.49E+04	3.72E+03

Table 7. Differentially expressed proteins in T1DM new and T1DM old comparison. T1DM new sample DS-169 was used as reference run.

T1DM new versus T1DM old- Analysis 2

Accession	Peptides	Score	Anova (p)*	Fold	Description	Average Normalised Abundances	
						T1DM new	T1DM old
P0C0L5	46	4003	0.01	1.45	Complement C4-B	1.56E+08	1.08E+08
P00734	15	1402	0.05	1.4	Prothrombin	4.57E+07	3.27E+07
P01871	5	1006	0.04	1.57	Ig mu chain C region	1.26E+07	8.04E+06
P10909	9	889	0.003	1.42	Clusterin	3.31E+07	2.34E+07
P01008	13	886	0.01	1.43	Antithrombin-III	3.12E+07	2.18E+07
P19827	9	781	0.04	1.46	Inter-alpha-trypsin inhibitor heavy chain H1	2.25E+06	1.55E+06
P01834	5	524	0.02	1.55	Ig kappa chain C region	9.42E+06	6.07E+06
P04004	5	437	0.03	1.46	Vitronectin	2.57E+07	1.76E+07
P02748	5	355	0.05	1.53	Complement component C9	2.39E+06	1.56E+06
P08603	4	287	0.04	1.57	Complement factor H	7.80E+05	4.96E+05
P07225	5	259	9.13E-04	1.49	Vitamin K-dependent protein S	6.24E+05	4.18E+05
P02654	2	123	0.002	1.56	Apolipoprotein C-I	3.78E+06	2.42E+06

Table 8. Differentially expressed proteins in T1DM new and T1DM old comparison. T1DM old samples DS-74 was used as reference run.

T1DM new versus T1DM old- Analysis 3

Accession	Peptides	Score	Anova (p)*	Fold	Description	Average Normalised Abundances	
						T1DM new	T1DM old
P0C0L5	44	3766	0.01	1.48	Complement C4-B	1.62E+08	1.09E+08
P00734	17	1532	0.03	1.42	Prothrombin	4.69E+07	3.31E+07
P01871	6	963	0.02	1.55	Ig mu chain C region	1.43E+07	9.25E+06
P10909	10	962	0.003	1.45	Clusterin	3.35E+07	2.31E+07
P19827	10	959	0.04	1.48	Inter-alpha-trypsin inhibitor heavy chain H1	2.56E+06	1.73E+06
P01008	13	912	0.007	1.46	Antithrombin-III	4.18E+07	2.87E+07
P19823	10	766	0.009	1.46	Inter-alpha-trypsin inhibitor heavy chain H2	4.43E+06	3.04E+06
P04004	4	447	0.03	1.42	Vitronectin	3.39E+07	2.38E+07
P01834	4	418	0.02	1.58	Ig kappa chain C region	9.56E+06	6.06E+06
P07225	2	190	0.003	2.2	Vitamin K-dependent protein S	6.16E+05	2.80E+05
P04180	3	183	0.03	1.26	Phosphatidylcholine-sterol acyltransferase	8.95E+05	7.09E+05
P02654	3	171	0.002	1.59	Apolipoprotein C-I	3.88E+06	2.45E+06
O14791	3	147	0.02	1.88	Apolipoprotein L1	1.43E+05	7.61E+04

Table 9. Differentially expressed proteins in T1DM new and T1DM old comparison. T1DM old sample DS-90 was used as reference run.

Comparison of control groups for newly diagnosed and controls for established diabetes

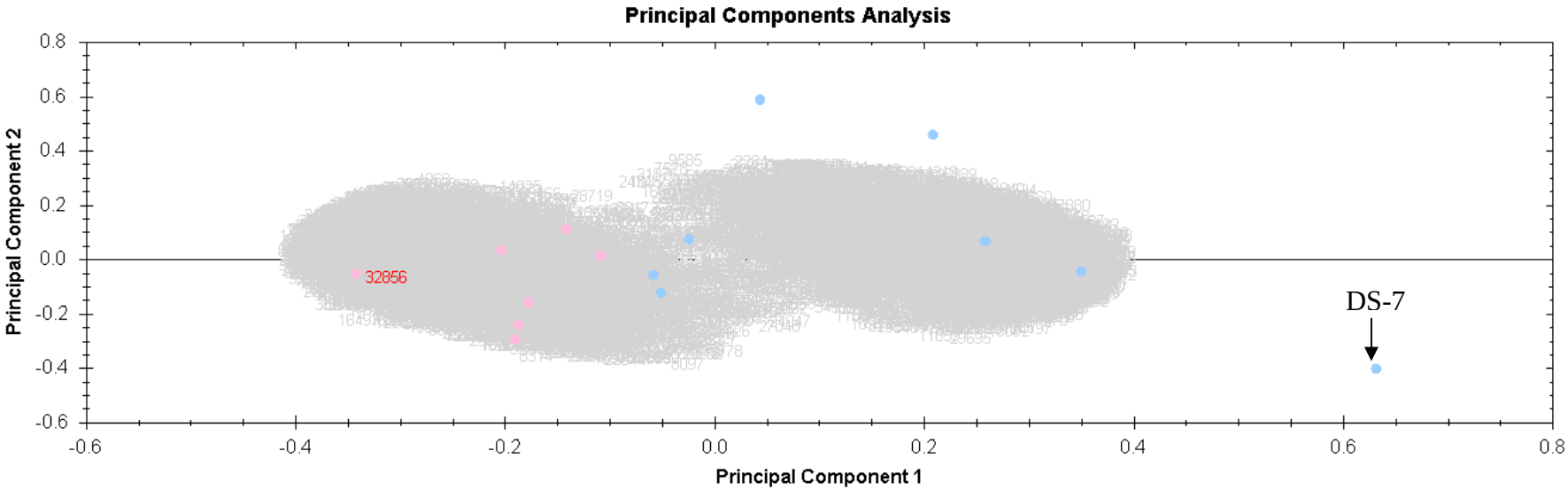

Figure 1. PCA plot for control new and control old samples. Sample DS-178 as reference run. Blue spots indicate the control old, while pink spots indicate control new samples. Old control sample DS-7 is a slight outlier relative to the rest of the control old group.

Control new versus control old- Analysis 1

Accession	Peptides	Score	Anova (p)*	Fold	Description	Average Normalised Abundances	
						control new	control old
P02649	9	844	0.02	2.35	Apolipoprotein E	8.81E+06	2.07E+07
Q08380	8	786	0.02	2.55	Galectin-3-binding protein	1.65E+06	4.22E+06
P01871	8	557	0.04	1.6	Ig mu chain C region	5.71E+06	3.57E+06
P10909	6	516	0.05	2.33	Clusterin	7.93E+06	1.85E+07
P07225	6	429	0.05	2.69	Vitamin K-dependent protein S	8.16E+05	2.19E+06
P02655	3	422	0.004	2.61	Apolipoprotein C-II	2.76E+06	7.18E+06
P02741	5	353	0.01	10.84	C-reactive protein	2.18E+05	2.36E+06
P04003	3	251	0.03	2.61	C4b-binding protein alpha chain	4.22E+06	1.10E+07
Q12805	2	212	0.04	2.35	EGF-containing fibulin-like extracellular matrix protein 1	1.62E+05	3.82E+05
P18428	2	210	0.04	2.01	Lipopolysaccharide-binding protein	2.92E+05	5.88E+05
P48740	3	191	0.02	1.77	Mannan-binding lectin serine protease 1	2.71E+05	4.79E+05
Q06033	3	178	0.01	2.21	Inter-alpha-trypsin inhibitor heavy chain H3	4.41E+04	9.75E+04
P08603	2	176	0.003	1.52	Complement factor H	1.12E+06	7.35E+05
P35542	2	173	0.03	2.34	Serum amyloid A-4 protein	5.48E+05	1.28E+06

Table 10. Differentially expressed proteins in control old versus control new comparison. DS-162 control old sample was used as reference run.

Control new versus control old- Analysis 2

Accession	Peptides	Score	Anova (p)*	Fold	Description	Average Normalised Abundances	
						control new	control old
P00734	12	1100	0.05	2.31	Prothrombin	2.30E+07	5.31E+07
P02649	9	844	0.02	2.33	Apolipoprotein E	8.78E+06	2.05E+07
Q08380	6	676	0.005	2.94	Galectin-3-binding protein	1.40E+06	4.10E+06
P01871	9	612	0.04	1.57	Ig mu chain C region	7.37E+06	4.68E+06
P10909	6	516	0.05	2.25	Clusterin	8.14E+06	1.83E+07
P19823	7	512	0.04	1.39	Inter-alpha-trypsin inhibitor heavy chain H2	8.33E+05	5.98E+05
P02671	6	507	0.01	2.34	Fibrinogen alpha chain	4.72E+05	1.10E+06
P02655	3	422	0.008	2.83	Apolipoprotein C-II	2.52E+06	7.13E+06
P08603	6	357	0.005	1.5	Complement factor H	1.54E+06	1.02E+06
P02741	5	353	0.01	10.73	C-reactive protein	2.20E+05	2.37E+06
P12259	3	263	0.02	2.58	Coagulation factor V	1.80E+05	4.64E+05
P35542	3	260	0.01	2.21	Serum amyloid A-4 protein	6.65E+05	1.47E+06
Q06033	4	259	0.01	2.32	Inter-alpha-trypsin inhibitor heavy chain H3	4.72E+04	1.09E+05
P04003	3	251	0.03	2.51	C4b-binding protein alpha chain	4.33E+06	1.09E+07
P04070	3	240	0.05	2.24	Vitamin K-dependent protein C	1.66E+05	3.72E+05
P48740	3	191	0.02	1.72	Mannan-binding lectin serine protease 1	2.80E+05	4.81E+05
P02765	2	112	0.03	1.4	Alpha-2-HS-glycoprotein	3.06E+05	2.19E+05
P01834	2	106	0.03	1.79	Ig kappa chain C region	4.31E+05	2.40E+05
P07996	2	105	0.05	1.72	Thrombospondin-1	7.02E+04	4.07E+04
P02788	2	100	0.02	3.19	Lactotransferrin	1.88E+04	5.89E+03

Table 11. Differentially expressed proteins in control old versus control new comparison. DS-178 control new sample was used as reference run.

Control new versus control old- Analysis 3

Accession	Peptides	Score	Anova (p)*	Fold	Description	Average Normalised Abundances	
						control new	control old
P0C0L5	53	4906	0.05	1.53	Complement C4-B	1.21E+08	1.85E+08
P02649	15	1315	0.02	1.71	Apolipoprotein E	1.13E+07	1.92E+07
P00734	16	1221	0.05	1.34	Prothrombin	2.48E+07	3.33E+07
Q08380	12	964	0.02	1.73	Galectin-3-binding protein	1.78E+06	3.08E+06
P10909	12	927	0.01	1.64	Clusterin	1.47E+07	2.41E+07
P07225	8	566	0.05	1.55	Vitamin K-dependent protein S	9.76E+05	1.52E+06
P04003	7	503	0.005	1.55	C4b-binding protein alpha chain	5.05E+06	7.83E+06
P02655	4	469	0.003	1.99	Apolipoprotein C-II	2.91E+06	5.80E+06
P08603	5	446	0.001	1.6	Complement factor H	1.90E+06	1.19E+06
P00450	5	441	0.05	1.5	Ceruloplasmin	1.99E+05	3.00E+05
P02741	5	353	0.03	10.3	C-reactive protein	2.19E+05	2.25E+06
P02671	4	308	0.03	2.24	Fibrinogen alpha chain	1.26E+05	2.81E+05
P35542	4	295	0.008	1.66	Serum amyloid A-4 protein	7.99E+05	1.32E+06
P01620	3	226	0.04	1.5	Ig kappa chain V-III region SIE	6.89E+05	4.60E+05
P48740	3	191	0.03	1.38	Mannan-binding lectin serine protease 1	2.80E+05	3.85E+05
Q06033	3	178	0.03	1.93	Inter-alpha-trypsin inhibitor heavy chain H3	4.42E+04	8.54E+04
P04070	2	169	0.05	1.58	Vitamin K-dependent protein C	1.36E+05	2.15E+05
P02656	2	168	0.008	1.58	Apolipoprotein C-III	4.03E+06	6.38E+06
P04180	3	161	0.04	1.41	Phosphatidylcholine-sterol acyltransferase	1.72E+05	2.43E+05
P55056	2	120	7.18E-06	3.07	Apolipoprotein C-IV	2.65E+04	8.13E+04
P03950	2	118	0.01	1.69	Angiogenin	6.20E+04	1.05E+05

Table 12. Differentially expressed proteins in control old versus control new comparison. DS-39 control old sample was used as reference run. DS-7 was excluded from this analysis as protein expression pattern for this sample differed from other samples in the same group.

Autoimmune versus control- Analysis 1

Accession	Peptides	Score	Anova (p)*	Fold	Description	Average Normalised Abundances	
						Autoimmune	All controls
P02751	32	2998	0.02	1.52	Fibronectin	3.23E+07	4.91E+07
P02768	24	2101	0.009	1.86	Serum albumin	2.72E+07	1.46E+07
P20742	17	1420	0.01	5.03	Pregnancy zone protein	2.40E+06	4.78E+05
P06727	10	990	0.02	1.53	Apolipoprotein A-IV	2.12E+07	1.39E+07
P02748	10	968	0.02	1.6	Complement component C9	5.83E+06	3.64E+06
P00450	6	736	0.05	1.42	Ceruloplasmin	1.20E+06	8.48E+05
P01009	10	626	0.02	1.53	Alpha-1-antitrypsin	1.07E+06	7.00E+05
P04264	5	546	0.05	2.95	Keratin, type II cytoskeletal 1	3.49E+05	1.18E+05
P13645	7	509	0.04	3.27	Keratin, type I cytoskeletal 10	2.57E+05	7.84E+04
P18428	6	457	0.05	1.77	Lipopolysaccharide-binding protein	1.60E+06	9.04E+05
P00734	5	404	0.03	1.79	Prothrombin	2.71E+06	1.51E+06
P10643	5	396	0.02	2	Complement component C7	1.07E+06	5.38E+05
P01008	5	396	0.05	1.94	Antithrombin-III	3.50E+06	1.80E+06
P51884	6	395	0.03	1.9	Lumican	4.56E+05	2.40E+05
Q06033	6	364	0.01	1.77	Inter-alpha-trypsin inhibitor heavy chain H3	2.21E+05	1.25E+05
P35527	2	177	0.04	2.37	Keratin, type I cytoskeletal 9	4.22E+04	1.78E+04
Q15848	2	174	0.02	1.83	Adiponectin	1.98E+06	1.08E+06
P07357	3	170	0.003	1.44	Complement component C8 alpha chain	9.45E+04	6.56E+04
P00488	2	146	0.03	2.47	Coagulation factor XIII A chain	1.45E+04	3.58E+04
P55056	2	121	0.04	2.12	Apolipoprotein C-IV	3.88E+04	8.23E+04
P07360	2	108	0.05	1.47	Complement component C8 gamma chain	7.82E+04	5.31E+04
P02746	2	96	0.02	1.48	Complement C1q subcomponent subunit B	8.02E+04	5.43E+04

Table 13. Differentially expressed proteins in autoimmune versus control samples. Control sample DS-175 was used as reference run.

Autoimmune versus control- Analysis 2

Accession	Peptides	Score	Anova (p)*	Fold	Description	Average Normalised Abundances	
						Autoimmune	All controls
P02751	36	2983.27	0.005	1.53	Fibronectin	2.59E+07	3.97E+07
P04114	36	2388.22	0.03	1.52	Apolipoprotein B-100	1.72E+06	2.60E+06
P02768	24	1979.44	0.01	1.93	Serum albumin	2.41E+07	1.25E+07
P20742	18	1452.68	0.009	5.19	Pregnancy zone protein	2.43E+06	4.69E+05
P06727	12	1049.54	0.02	1.53	Apolipoprotein A-IV	1.87E+07	1.22E+07
P02748	12	973.92	0.02	1.65	Complement component C9	4.92E+06	2.97E+06
P00450	7	787.88	0.05	1.44	Ceruloplasmin	1.16E+06	8.06E+05
P13645	9	661.8	0.04	3.78	Keratin, type I cytoskeletal 10	2.87E+05	7.58E+04
P01009	10	625.66	0.03	1.55	Alpha-1-antitrypsin	9.69E+05	6.24E+05
P10643	4	347.48	0.01	2.5	Complement component C7	6.79E+05	2.71E+05
P18428	5	312.49	0.03	1.7	Lipopolysaccharide-binding protein	9.40E+05	5.53E+05
P51884	5	307.51	0.04	1.88	Lumican	4.02E+05	2.14E+05
Q06033	5	305.6	0.02	1.65	Inter-alpha-trypsin inhibitor heavy chain H3	1.94E+05	1.17E+05
P13671	4	286.31	0.03	1.53	Complement component C6	4.13E+05	2.69E+05
Q15848	3	251.12	0.02	1.86	Adiponectin	2.00E+06	1.08E+06
P00734	3	219.48	0.03	1.78	Prothrombin	2.39E+06	1.34E+06
O14791	3	185.39	0.03	1.35	Apolipoprotein L1	1.13E+05	1.53E+05
P07360	3	162.9	0.05	1.44	Complement component C8 gamma chain	9.52E+04	6.63E+04
P07357	2	121.76	0.03	1.38	Complement component C8 alpha chain	5.57E+04	4.03E+04
P01700	2	113.45	0.02	1.6	Ig lambda chain V-I region HA	7.18E+04	4.47E+04

Table 14. Differentially expressed proteins in autoimmune versus control samples. Control sample DS-178 was used as reference run.

Autoimmune versus control- Analysis 3

Accession	Peptides	Score	Anova (p)*	Fold	Description	Average Normalised Abundances	
						Autoimmune	All Controls
P02751	35	3096.62	0.03	1.53	Fibronectin	3.14E+07	4.80E+07
P0C0L4	27	2157.02	0.05	1.39	Complement C4-A	5.43E+07	3.92E+07
P02768	25	2054.78	0.02	1.86	Serum albumin	2.53E+07	1.36E+07
P20742	22	1472.88	0.009	4.39	Pregnancy zone protein	3.21E+06	7.32E+05
P06727	13	1084.59	0.02	1.52	Apolipoprotein A-IV	1.98E+07	1.31E+07
P02748	13	997.78	0.03	1.59	Complement component C9	5.33E+06	3.35E+06
P04264	10	906.06	0.05	2.67	Keratin, type II cytoskeletal 1	4.86E+05	1.82E+05
P13645	10	685.93	0.04	3.24	Keratin, type I cytoskeletal 10	3.06E+05	9.45E+04
P35908	5	606.39	0.03	4.21	Keratin, type II cytoskeletal 2 epidermal	7.93E+04	1.88E+04
P01009	8	479.04	0.04	1.48	Alpha-1-antitrypsin	9.45E+05	6.40E+05
Q06033	7	407.35	0.01	1.75	Inter-alpha-trypsin inhibitor heavy chain H3	2.23E+05	1.27E+05
P51884	5	335.57	0.01	2.06	Lumican	2.87E+05	1.39E+05
P10643	4	283.97	0.02	2.26	Complement component C7	8.63E+05	3.81E+05
Q15848	3	265.93	0.02	1.81	Adiponectin	2.57E+06	1.42E+06
P07357	3	170.49	0.006	1.39	Complement component C8 alpha chain	9.01E+04	6.50E+04
P02671	2	165.21	0.03	1.63	Fibrinogen alpha chain	9.25E+04	1.51E+05
P04220	2	134.48	0.02	16.64	Ig mu heavy chain disease protein	2.01E+03	3.35E+04

Table 15. Differentially expressed proteins in autoimmune versus control samples. Control sample DS-39 was used as reference run.

Appendix D

Metabolomics serum study raw data

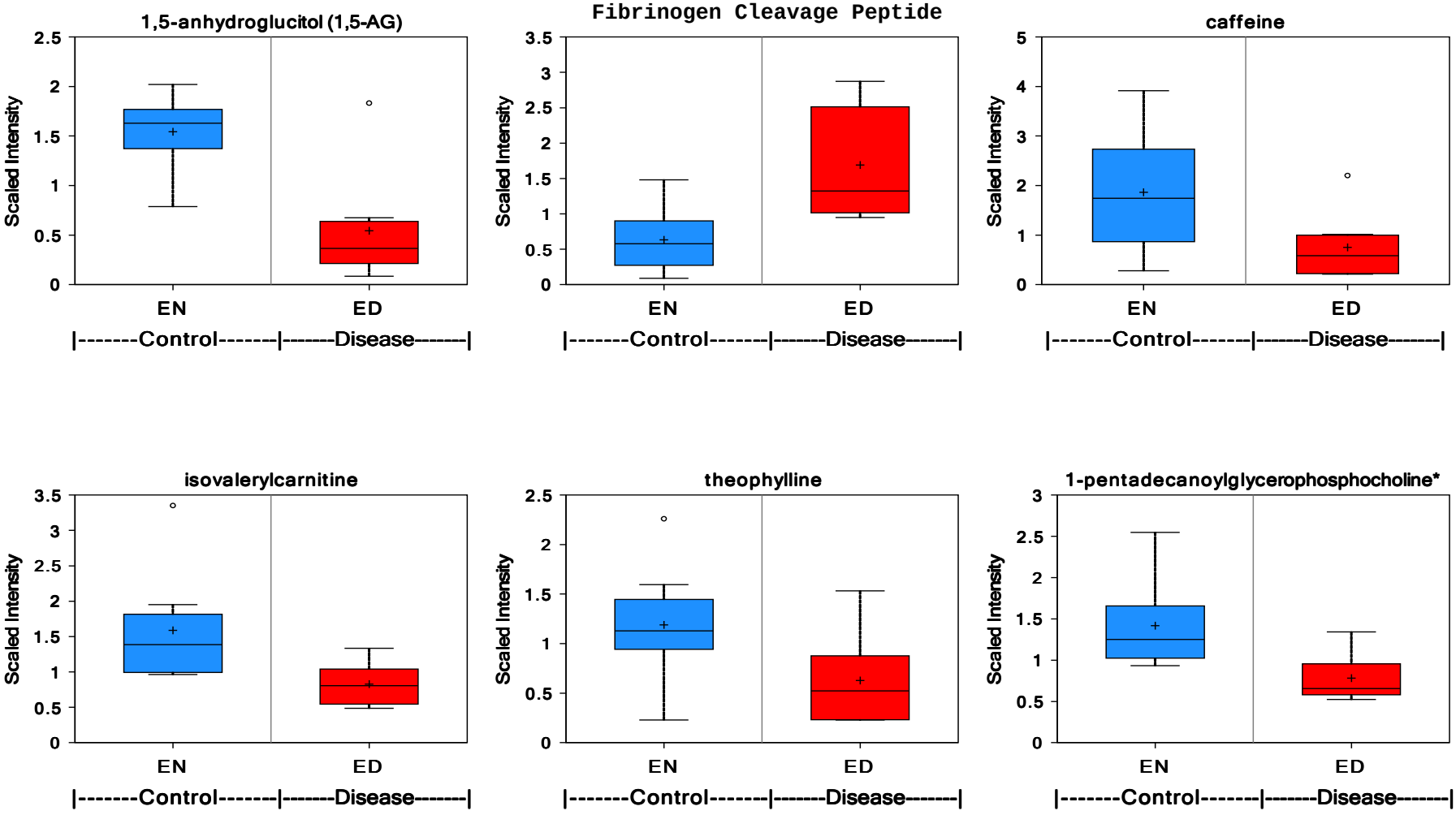
1,5-anhydroglucitol (1,5-AG)
Fibrinogen Cleavage Peptide
caffeine
isovalerylcarnitine
theophylline
1-pentadecanoylglycerophosphocholine*
Scaled Intensity
EN
ED
|-------Control-------|-------Disease-------|

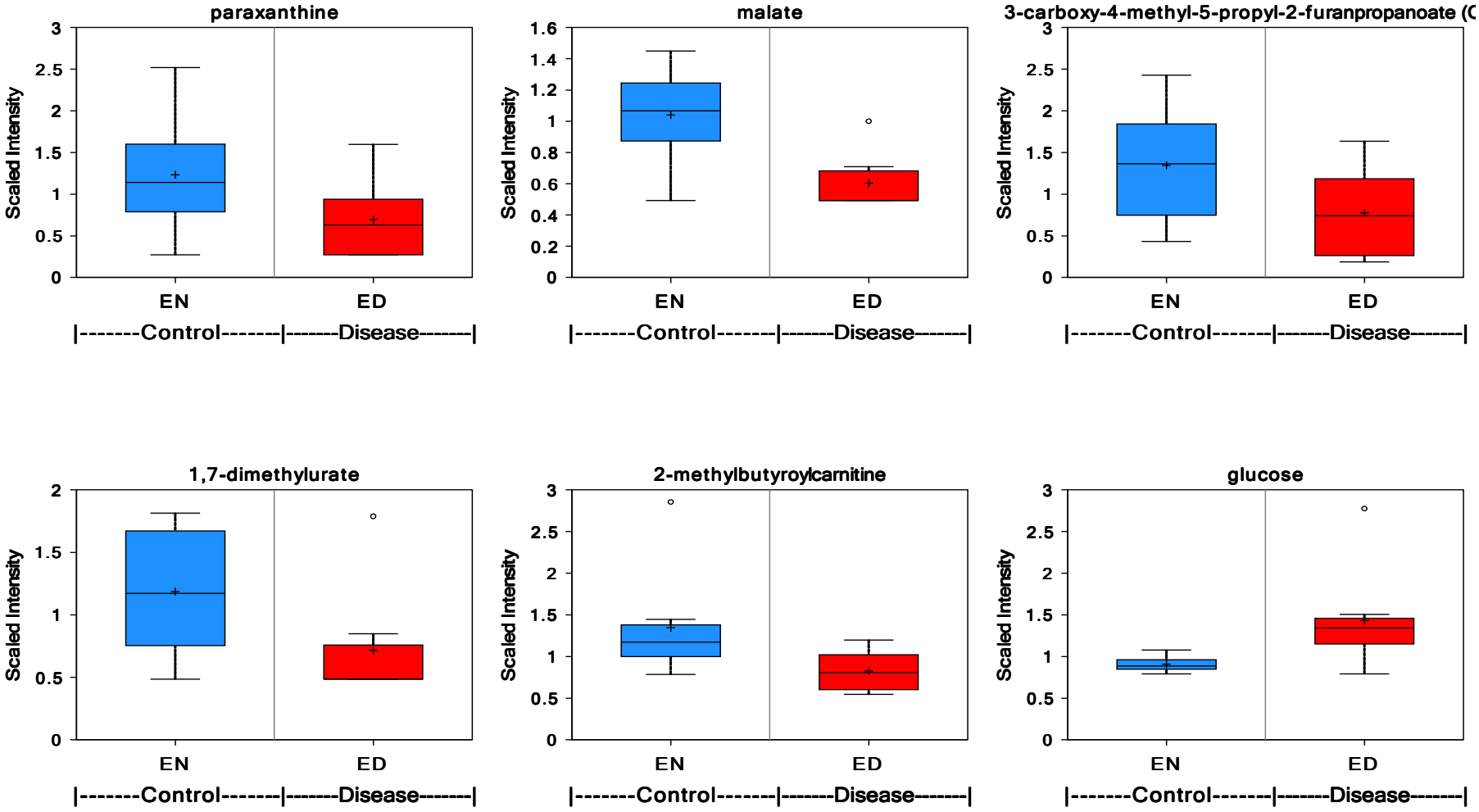
paraxanthine
malate
3-carboxy-4-methyl-5-propyl-2-furanpropanoate (C
1,7-dimethylurate
2-methylbutyroylcarnitine
glucose
Scaled Intensity
EN
ED
|-------Control-------|-------Disease-------|

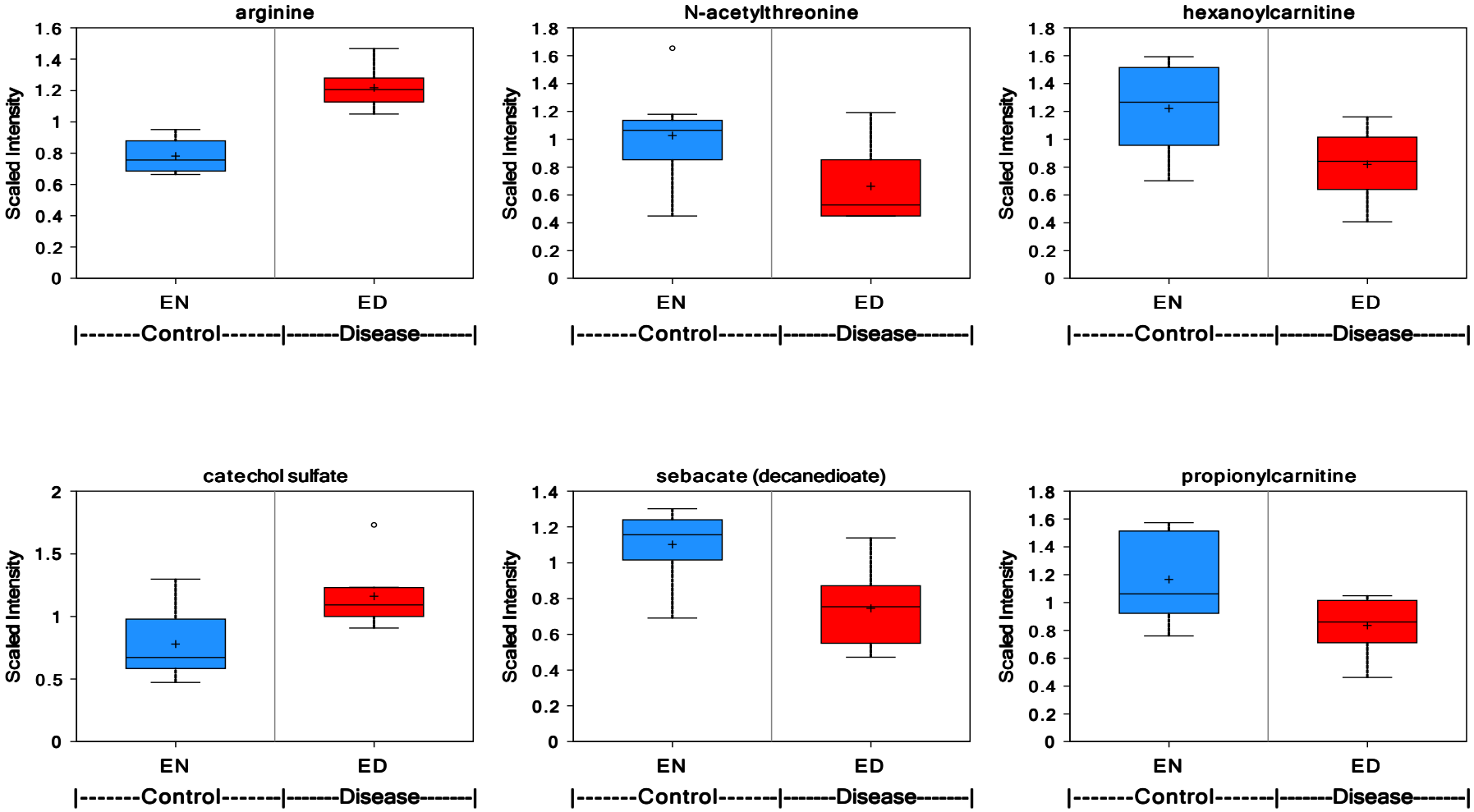
arginine
Scaled Intensity
1.6
1.4
1.2
1
0.8
0.6
0.4
0.2
0
EN
ED
|-------Control-------|-------Disease-------|
N-acetylthreonine
Scaled Intensity
1.8
1.6
1.4
1.2
1
0.8
0.6
0.4
0.2
0
EN
ED
|-------Control-------|-------Disease-------|
hexanoylcarnitine
Scaled Intensity
1.8
1.6
1.4
1.2
1
0.8
0.6
0.4
0.2
0
EN
ED
|-------Control-------|-------Disease-------|
catechol sulfate
Scaled Intensity
2
1.5
1
0.5
0
EN
ED
|-------Control-------|-------Disease-------|
sebacate (decanedioate)
Scaled Intensity
1.4
1.2
1
0.8
0.6
0.4
0.2
0
EN
ED
|-------Control-------|-------Disease-------|
propionylcarnitine
Scaled Intensity
1.8
1.6
1.4
1.2
1
0.8
0.6
0.4
0.2
0
EN
ED
|-------Control-------|-------Disease-------|

CV

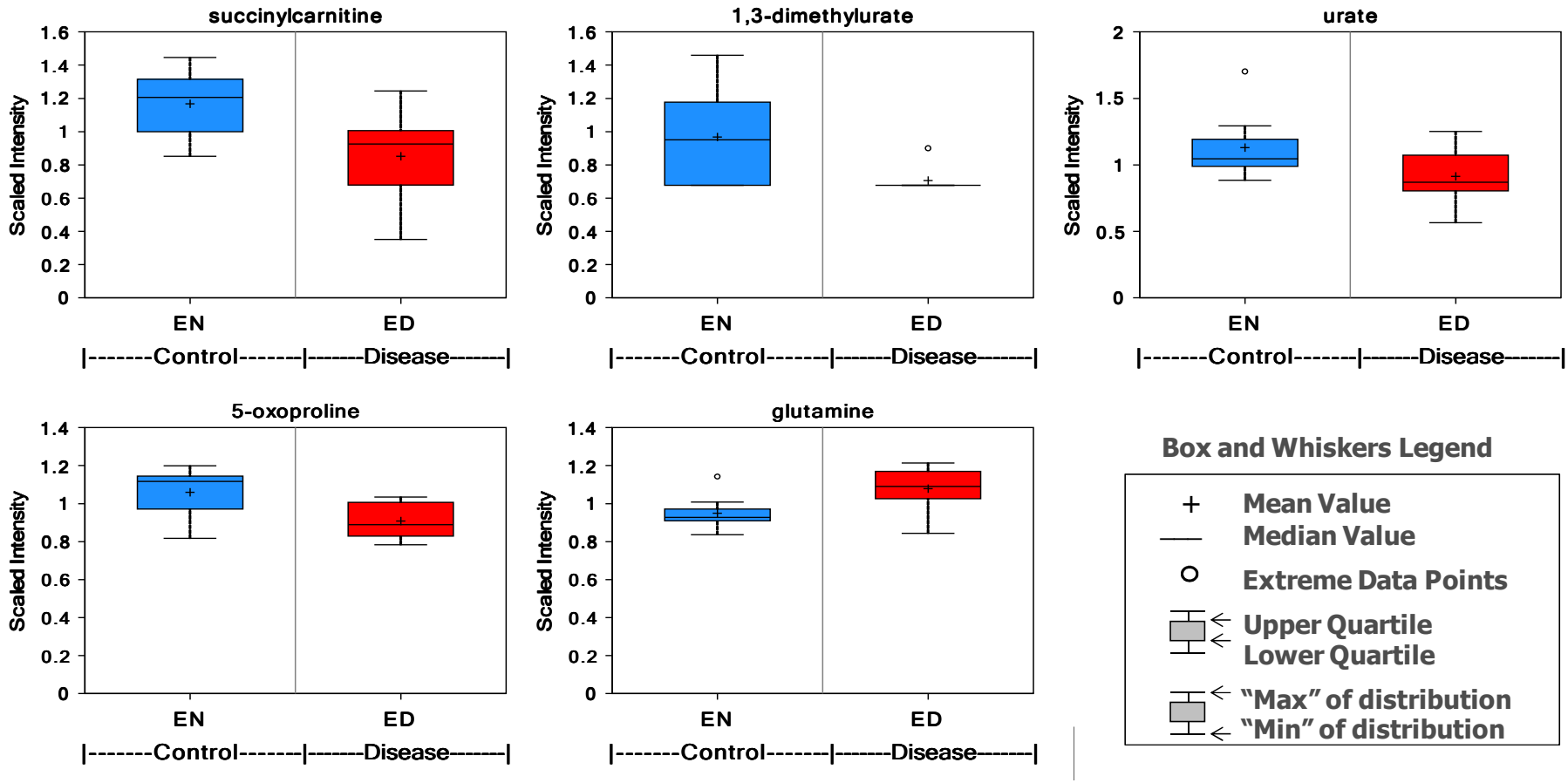

Figure 1. Box and whisker plots of all significantly different biochemicals in disease- newly diagnosed type 1 diabetes, compared to control- healthy specimens. Box and whisker plots show the distribution of the dataset. The median indicates the middle of the data, with 50% of the data being above and 50% below this value. Upper quartile indicates 25% of the data is above this value, while the lower quartile indicates that 25% of the data is below this value.

Appendix E

Publications

Publications:

Journal Articles:

- **Hennessy E.,** Clynes M., Jeppesen P.B., O'Driscoll L. 2010 **Identification of microRNAs with a role in glucose stimulated insulin secretion by expression profiling of MIN6 cells**. BBRC 396(2):457-62
- **Hennessy E.,** O'Driscoll L. 2008. **Molecular medicine of microRNAs: structure, function and implications for diabetes**. Expert Rev Mol Med 10:e24

Book Chapters:

- **Hennessy E.,** O'Driscoll L. 2011 **MicroRNA expression analysis: Techniques suitable for Studies of Intercellular and Extracellular MicroRNAs**. Methods Mol Biol 784:99-107

Conference presentations:

- **Hennessy E.,** Doolan P., Aherne S., Clarke C., Clynes M., O'Sullivan F. **Gene expression changes associated with differentiation of human iPS cells to definitive endoderm in 3D culture**. Stem cells in development and disease 11-14 September 2011 Max-Delbruck-Center, Berlin-Buch, Germany.
- **Hennessy E.,** Clynes M., O'Driscoll L. **MicroRNAs involved in glucose stimulated insulin secretion in MIN6 pancreatic beta cells**. CASH 05 June 2009. Tallaght Institute of Technology, Dublin Ireland.
- **Hennessy E.,** Clynes M., O'Driscoll L. **MicroRNA expression profile changes between glucose responsive and non-responsive MIN6 pancreatic beta cells.** RNAi2008: Functions and applications of non-coding RNAs 13-14 March 2008 St Anne's College, Oxford, UK.